SLITHERING THROUGH SPACE AND TIME: UNCOILING THE ROLES OF ECOLOGY AND PHYLOGENY ON MORPHOLOGICAL VARIATION IN FOSSIL AND EXTANT NORTH AMERICAN SNAKES ACROSS TAXONOMIC, TEMPORAL, AND SPATIAL SCALES

A Dissertation

by

JOHN JOSEPH JACISIN III

Submitted to the Graduate and Professional School of
Texas A&M University
in partial fulfillment of the requirements for the degree of

DOCTOR OF PHILOSOPHY

Chair of Committee,	A. Michelle Lawing
Committee Members,	Claudio Casola
	Darryl J. de Ruiter
	Lee A. Fitzgerald
Head of Department,	Kirk O. Winemiller

December 2021

Major Subject: Ecology and Conservation Biology

ABSTRACT

Anthropogenic effects on the environment are an irrefutable actuality. Understanding how environmental changes affect organismal fitness, ecology, morphology, and evolution is critical for managing natural systems and conserving organisms through these changes. The study of morphological variation in skeletal elements provides an integrative route to bridge the gap between the past and the present of organism-environment interactions over long time scales. In this dissertation, I focus on snake morphological variation and its implications for taxonomy, phylogeny, ecology, and environmental change across space and time. I show that describing fossil snakes can be useful for understanding paleoenvironment, biogeography, and evolutionary patterns, epitomized by addressing a temporal gap for North American snakes, using vertebral morphology to identify taxa, and using proxy congenerics with climate data to estimate paleoclimate. The fossils and models support a hypothesis of gradual modernization in North American snakes occurring as Miocene environments grew drier and cooler in the Great Plains. I assess variation in snake middle trunk vertebrae with geometric morphometrics as a method for assigning snake vertebrae to taxon. Applying geometric morphometrics at multiple taxonomic levels indicated that a stepwise method may maximize the ability to identify snakes through vertebrae without diagnostic expertise. I demonstrate how combining external and skeletal morphological data with geographic, climatic, sex, and dietary data in the Western massasauga shows that morphological change within a species is better identified by combining the

variation in both datasets, as variation gradated between the Southwest and Northeast. Finally, I construct a modern functional trait-environment framework for North American snakes using middle trunk vertebrae. I demonstrate that several aspects of shape variation are related to temperature-related variables and ecological province, and that combining multiple aspects produces better maximum likelihood models than any single aspect. My dissertation contributes to qualitative and quantitative methods to assess snakes and their interactions with the environment through time. This opens new avenues to append deep time data to our understanding of how snakes are functionally related to their environments, and what actions we can take to conserve and manage snakes in potential environmental futures.

DEDICATION

This one is for Frolic and me.

To all the family, friends, and colleagues that sustained me across space and through time, I pass onto you the words of Billy Mills: “Ultimately, every dream has its passion, and every passion has its destiny.” Thank you all for supporting me in mine.

ACKNOWLEDGEMENTS

I would like to thank my committee chair (and favorite advisor), Michelle Lawing, for her endless positivity, support, mentorship, patience, and friendship throughout this dissertation. I am thankful for our many discussions and ideas, and look forward to many more years of research and collaboration together. I would also like to thank my committee, Claudio Casola, Darryl de Ruiter, and Lee Fitzgerald, for their encouragement, constructive input, and support throughout this process.

I am most grateful to my family, and especially to my father, John, my mother, Cheryl, and my brother, Logan, for their unending support throughout my career. From the earliest dinosaur movies, to museum visits, to camping, hunting, and fishing, they have always done what they could to expose me to the natural world. They have always backed my career, even when I first chose it around the age of two. The sacrifices they've made along the way have not gone unnoticed, and the experiences they gave me are the reason I have achieved the goals I set so long ago. Their love and support despite the distance and time will stay with me wherever I go.

I have been lucky enough to have the support of some fantastic friends in addition to my family. While it is impossible to list everyone here, I would especially like to recognize my closest friends, confidants, and cheerleaders over the years. From the Ironwood crew: Casey Jarocki, Alison Smith, Elizabeth Perkis, and Aubre and Ron Hoeft have been helpful listeners when I've needed a boost. I consider the Perkis, Jarocki, Osier, and Radtke families an extended family who have supported me through

the years. From Albion: my former cross country and track and field teammates and coaches, especially William Ward, Carl Wharam, Aaron Croad and Michelle Burke, and Hayden and Penny Smith. They have always had my back, and Will has not only been my teammate and lab partner for those long geology labs, but has also enthusiastically supported me through all my trials and shared wisdom from his own. Chris and Cara Wardlaw, Greg Tovella, Annie Harb, Scott Boyse, Alex Cusma, Michael Eiten, Max Korzowski, and Kevin Gladstone have contributed countless hours of fun and support to me over the years, and have been with me throughout this journey. Finally, I am grateful to all my past lab mates at Albion, Oregon and Nebraska, and I am especially thankful for my labmates (and extended labmates) at Texas A&M: Rachel Short, Jeff Martin, James West, Leila Siciliano-Martina, Breann Richey, Peter Dorn, Louis Addae-Wireko, Chase Brooke, Beth Reinke, and Wesley Vermillion. They have provided insight and input on many aspects of this dissertation and in life, and made some of the long hours much easier.

Many colleagues, some of whom I also consider close friends, have provided excellent discussion and feedback over the years. I fear that I cannot name everyone here. William Bartels, Samantha Hopkins, Edward Davis, Jenny McGuire, Jason Moore, Jason Head, David Polly, Jim Mead, Julie Meachen, David Bapst, Christina Belanger, John Orcutt, Randall Irmis, and Jonathan Calede have all provided thoughtful discussion, feedback, mentorship, and opportunities for growth over the years. Kelsey Stilson, Selina Robson, Monya Anderson, James Proffitt, Natasha Vitek, Julia Schap, Ben Shipley, Nicholas Famoso, Kierstin Rosenbach, Julia Anderson, Meaghan Emery-

Wetherell, Win McLaughlin, and Elliott Smith have had their own journeys through graduate school intersect with mine, and I consider them valuable friends and colleagues. It has been a pleasure to work with Wade Ryberg, Danielle Walkup, Jesse Meik, Corey Fielder, Toby Hibbitts, and Michelle Lawing on the Western massasauga project, and they have provided useful suggestions and comments that resulted in Chapter 4 of this dissertation.

The data used in this dissertation would not be possible without the coordination and assistance of several people and museums. I would like to thank Michelle Lawing, Adrian Castellanos, Leila Siciliano-Martina, Rachel Short, James West, and Peter Dorn for their coding ideas and assistance during this dissertation. I would like the thank Toby Hibbitts and Heather Prestridge - Texas A&M University Biodiversity and Research Teaching Collections, George Corner and Ross Secord - University of Nebraska State Museum, and Chris Sagebiel, Christopher Bell, and Matthew Brown - University of Texas at Austin Vertebrate Paleontology Collections for allowing me access to their collections to collate data for Chapters 2, 3, and 5. I would further like to thank the following institutions for lending the specimens used in Chapter 4: Texas A&M University Biodiversity Research and Teaching Collections, University of Texas at Austin - Texas Natural History Collections, Natural History Museum of Los Angeles County, Carnegie Museum of Natural History, University of Kansas Biodiversity Institute, University of Colorado Museum of Natural History, Arizona State University Natural History Collections, Sam Noble Oklahoma Museum of Natural History, and Museum of Southwestern Biology.

Finally, I would like to recognize the professors that have provided the most mentorship to me through the years. William Bartels gave me my first opportunities in paleontological field and lab work as a college freshman, and his irreplaceable teachings and extensive knowledge were influential when I decided to focus on fossil and living reptiles and amphibians. Samantha Hopkins and Edward Davis helped me to find my place among fellow scientists, taught me key field and analytical skills, and were exemplary models for an early career scientist. Finally, Michelle Lawing helped me to improve in all aspects as a scientist, and added skills to my toolset I never expected I would use. Michelle's skills and ways of thinking about questions and research have been exceptionally complementary to my own, and I have benefitted greatly from combining our strengths. All these people have been invaluable to my growth as a scientist and a producer of knowledge, and have helped me direct my curiosity into research that can contribute to the world. Thank you!

CONTRIBUTORS AND FUNDING SOURCES

Contributors

This dissertation was completed under the supervision and guidance of a dissertation committee, consisting of Dr. A. Michelle Lawing (chair), Dr. Claudio Casola, and Dr. Lee Fitzgerald of the Department of Ecology and Conservation Biology, and Dr. Darryl de Ruiter of the Department of Anthropology, all at Texas A&M University.

My co-author for Chapter 2 is A. Michelle Lawing, Department of Ecology and Conservation Biology, Texas A&M University. George Corner (University of Nebraska State Museum) was my correspondent for the fossil specimen loan in Chapter 2, and provided official collection specimen numbers post-identification.

My co-author for Chapter 3 is A. Michelle Lawing, Department of Ecology and Conservation Biology, Texas A&M University.

My co-authors for Chapter 4 are Corey Fielder and A. Michelle Lawing – Department of Ecology and Conservation Biology, Texas A&M University; Wade Ryberg and Danielle Walkup – Natural Resources Institute, Texas A&M University, Toby Hibbitts – Department of Ecology and Conservation Biology and Natural Resources Institute, Texas A&M University, and Jesse Meik – Tarleton State University. Wade, Toby, Danielle and Corey obtained specimens and performed external measurements for this research. Corey also retrieved many snapshots of the skulls from the micro-CT data produced by Michelle and me.

My co-author for Chapter 5 is A. Michelle Lawing, Department of Ecology and Conservation Biology, Texas A&M University. All other work conducted for this dissertation was completed independently.

Funding Sources

My dissertation research was made possible by funding from Texas A&M University, including: the College of Agriculture and Life Sciences Graduate Merit Fellowship, the Department of Ecosystem Science and Management Henry Wayne Springfield Graduate Merit Fellowship, four Department of Ecosystem Science and Management Research and travel grants, and one Department of Ecology and Conservation Biology High Impact Grant. Research for Chapter four was supported by a National Fish and Wildlife Foundation grant awarded to Principal Investigators Wade Ryberg, co-PIs Michelle Lawing, Danielle Walkup, and Toby Hibbitts (Texas A&M University) for "Genomics and ecology of the massasauga in the Pecos." I received additional support through teaching assistantships for the Department of Ecology and Conservation Biology and the Department of Ecosystem Science and Management. I obtained additional travel support from the Society of Vertebrate Paleontology Jackson School of Geosciences Student Travel Grant. Each research chapter of this dissertation is in late stage preparation for submission to peer-reviewed journals. The contents of this dissertation are the responsibility of the author and do not represent endorsed views of the sources of funding.

TABLE OF CONTENTS

Page

LIST OF FIGURES

Page

LIST OF TABLES

Page

1. INTRODUCTION

"Every great story seems to begin with a snake." – Nicolas Cage

As Anthropogenic environmental change proceeds to alter Earth's habitat, understanding how environmental change and habitat alteration affects organismal ecology and evolution is becoming increasingly important for managing natural systems (Wake and Vredenburg, 2008; Barnosky et al., 2011; Alroy, 2015; Barnosky et al., 2017). Understanding the consequences of the ongoing changes in Earth's environments is difficult in that climate and habitat modeling based on what can be observed in the present is not enough to fully grasp the complexity of climate change's effects on Earth's biotic and geologic systems (Davis et al., 2014). As such, both the short- and long-term dynamics of climatic, biologic, and geologic history matter over temporal and spatial scales (Estes et al., 2011; Polly et al., 2011; Lawing et al., 2012). Efforts to predict and assess the effects of long-term environmental changes on organisms need a deep time perspective, as applying organismal responses to environmental change over long time scales improves forecasting models related to the behavior and survivability of living organisms facing present perils (Barnosky et al., 2017; Eronen et al., 2010). Unfortunately, our grasp of squamate faunal dynamics through deep time is limited, as fossil squamates (i.e., lizards, snakes, and amphisbaenians) are chronically understudied and subject to sampling and identification biases and outdated taxonomy (Hutchison,

1992; Holman, 2000; Parmley and Hunter, 2010; Smith, 2006; Smith, 2013). This impedes efforts to study habitat and climate change effects on squamate evolution, community assembly, ecology, biogeography, and extinction (Holman, 2000). To bridge the gap in knowledge, one must use data available for study through time; skeletal morphology is therefore key to addressing questions of the past and using deep time data to address biodiversity problems of the present and future.

In this dissertation, I examine the relationships between ecology, phylogeny, taxonomy, and morphology through the lens of variation in the snake skeleton. I uncoil this morphological variation through qualitative descriptions, traditional morphometric measurements, and geometric morphometrics at different geographic, phylogenetic, taxonomic and temporal scales. In doing so, I build the backbone for new or improved methods of taxonomic identification and assignment, paleoecological reconstruction, and trait-environment modeling for snakes.

Snakes are useful for studying biotic and abiotic changes as ectotherms that are sensitive to environmental perturbations (Root et al., 2003; McCallum, 2007; Böhm, 2013; Alroy, 2015). They have been recorded as part of the current global decline of herpetofauna populations (Gibbons et al., 2000; Lourenço-de-Moraes et al., 2020; Zipkin et al., 2020). Furthermore, snakes are of particular conservational, ecological, economic, social, and medical interest (Pimentel et al., 1997; Holman, 2000, 2006; Mullin and Siegel, 2009; Brooks et al., 2010), and are expected to exhibit significant responses to climate change and habitat alteration over the next century, as indicated by their

geographic responses to Quaternary climate cycles in North America (Lawing and Polly, 2011), ectothermic physiology (Head et al., 2009), global population declines (Reading et al., 2010), and trait-environment relationships (Head et al., 2009; Lawing and Polly, 2011; Lawing et al, 2012). It is unfortunate that older Cenozoic North American snake faunas have been chronically understudied and potentially misidentified (Bell et al., 2010), as the data on deep time interactions between snakes and their environments is currently underutilized. This is in spite of the interesting evolutionary history and dramatic radiation required to reach the current diversity of the suborder Serpentes (Parmley and Holman, 1995; Holman, 2000; Parmley and Hunter, 2010; Jacisin et al., 2015).

Limblessness has evolved repeatedly in vertebrates, but snake skeletons are somewhat unusual amongst limbless vertebrates (eels, caecilians, limbless lizards, and amphisbaenians) in that they have highly derived skulls and distinctive, complicated-looking vertebrae that are different enough to allow the identification of some isolated fossils to the genus- or species-level (Holman, 2000). The morphology of various skull bones, vertebrae, body shapes, sizes, and proportions have all been used to various degrees to explain function, but skeletal features have not commonly been used to relate functional traits to environmental conditions in snakes.

1.1. A snake in the grass? Integrative approaches to biotic-environmental relationships

Historical context provides information on natural variability through long term changes, and acts as a source of reference for the current and future impacts of climate change and habitat alteration. It helps approach the problem of what humans need to actively conserve, if we cannot conserve everything, and what methods of conservation and mitigation are historically "natural" enough to attempt (Eronen et al., 2010). Furthermore, climate and earth system dynamics are long-term historical processes, so using recent ecological data that extend back (at most) a few hundred years only provides a shallow perspective on the effects of long-term processes (Eronen et al., 2010, Davis et al., 2014; Polly et al., 2016). Deep time data on climate, habitat, and evolution can only be gained from paleontological, paleoecological, and geological studies (Willis and Birks, 2006), and is often better than appreciated (Fortelius et al., 2002; Eronen et al., 2010). Many methods used to study the past can also be applied to the present; these approaches, if used for both paleontological and modern ecological data, have great potential for improving our understanding and modeling of abiotic-biotic interactions through time and space (Eronen et al., 2010; Ceballos et al. 2015; Polly et al., 2016; Vermillion et al., 2018). Such interdisciplinary approaches to understand biotic-environmental relationships have therefore become progressively more important for biodiversity conservation, the management of natural systems and resources, and the consequences of change on biological, physical, and social

environments (Rosenzweig et al., 2007; Schneider et al., 2007; Eronen et al., 2010; Estes et al., 2011; Lawing et al., 2012).

Organismal functional traits represent one such integrative path forward, as these traits are selected upon by their environments, are clade-sorted, and are central to the disparity in fitness, reproductive success, and survivability of individuals in various environmental and geographic circumstances (Polly et al., 2011). Both paleontologists and ecologists have acknowledged the promise of using traits that are functionally related to an organism's biological (e.g., microvegetation), biologically mediated (e.g., microclimates below dense forest canopies), and physical (e.g., climate) environment. The functional-trait environmental relationship thus provides a unique opportunity to integrate modern and fossil data for the study of climate and habitat change biology (Eronen et al., 2010; Polly et al., 2011; Lawing et al., 2012; Burbrink et al., 2015; Ceballos et al., 2015; Dietl et al., 2015; Polly and Head, 2015; Lawing et al., 2016; Barnosky et al., 2017). In this dissertation, I use both qualitative and morphometric methods to examine morphological traits in snakes from family to intraspecific taxonomic levels. I identify variation explained by ecology, taxonomy, and phylogeny to construct both climate envelope and ecometric models that can be applied to the fossil record, as well as a new supplemental method for assigning vertebrae to taxa based on vertebral shape.

1.2. Slithering through the Neogene: Filling in a temporal gap and assessing snake modernization and paleoecology in the Central Great Plains

Fossil Cenozoic herpetofauna are potential tools for environmental reconstruction and understanding the effects of climate and habitat change, as the physiologies of extant reptiles and amphibians correlate strongly with habitat (Head et al., 2009; Lawing et al., 2012; Jacisin et al., 2015). The Neogene beds of Nebraska include a long, well-preserved record of fossil snakes that illuminates the history of richness, turnover, and modernization of snakes from the Central Great Plains (Holman, 2000; Jacisin et al., 2015). The snake fossil record of the Neogene provides an excellent series of natural experiments on how organisms have interacted with their environments over deep time, including periods of environmental change. Neogene snakes exhibit a wide geographic distribution and radiation overall in the North American fossil record; these fossils record a change in snake communities from booid-dominated to colubroid-dominated, along with the first appearances of many extant snake groups, and a number of snake ecologies (Holman, 1977; Holman, 2000; Parmley and Hunter, 2010). The processes involved in these changes appear to be related to drastic environmental changes through the Neogene (Parmley and Holman, 1995; Holman, 2000; Jacisin et al., 2015; Jacisin, 2016), and there are a significant number of snake fossils representing modern genera throughout museum collections in North America (Holman, 2000) that can be used to provide a deep time perspective for the conservation of modern snake groups.

Despite the excellent state of Nebraska's fossil snake record and an apparent peak of richness in the late Barstovian (Ba2, 14.75-12 Ma; Holman, 2000; Parmley and Hunter, 2010), a paucity of fossil material has resulted in a distinct scarcity of data on snake assemblages from the early Clarendonian (Cl1, 12.5-12 Ma). This temporal gap is present throughout most of North America and illuminates a glaring lack of knowledge about the scale of snake turnover and modernization immediately following the late Barstovian of Nebraska. The Penny Creek Local Fauna in southern Webster County, Nebraska is an early Clarendonian (Cl1; 12.5-12 Ma) fossil locality (UNSM Wt 13B) within the Ash Hollow Formation. Previously undescribed fossils from collected Penny Creek material represent the first record of snakes from the Cl1 time interval, and therefore confirm the presence of multiple taxa immediately following the Mid-Miocene Climatic Optimum.

In Chapter Two of this dissertation, I qualitatively describe the fossil snake vertebrae of the Penny Creek local fauna for systematic and taxonomic purposes, and compare it to other Neogene fossil snake assemblages in Nebraska in order to assess changes in known species richness, first and last occurrences, and biogeography. I apply climate envelope models using modern proxy taxa to predict a range of possible Mean Annual Temperature and Annual Precipitation values for paleoenvironmental reconstruction. This study provides the first account of snake fossils from this time interval, provides the most up-to-date assessment of the modernization of the North American snake fauna in the Central Great Plains, and makes use of climate envelope models for snakes in the Miocene. I expect the fauna to fill temporal gaps in the fossil

record for North American snakes and provide a blueprint for one type of paleoecological reconstruction using snakes and for future taxonomic qualitative descriptions of snake fossils.

1.3. Ophidian physique: using geometric morphometrics to investigate shape variation in snake trunk vertebrae

Taxonomic studies and descriptions of both living and fossil taxa commonly rely on detailed but subjective qualitative descriptions, sometimes additionally supported by DNA sequences or traditional linear morphometric measurements. While these methods are both typical and adequate for taxonomic studies, there are some challenges and limitations associated with these methods (Mayr, 1942; Nice and Shapiro, 1999; Baylac et al., 2003; Saez and Lozano, 2005; Kaila and Stahls, 2006; Bickford et al., 2007; Mutanen and Pretorius, 2007; Whitenack and Gottfried, 2010; Ruane, 2015). First, DNA sequences are not always applicable or effective in delimiting taxa. Both recent or ongoing gene flow or insufficient time for lineage sorting can produce a lack of genetic differentiation (Nice and Shapiro, 1999), and the sole use of some mtDNA fragment barcodes may be insufficient alone to recognize closely related species where traditional morphometrics and ecology can (Kaila and Stahls, 2006). Furthermore, molecular approaches often cannot be used for fossils or dry museum specimens (Baylac et al., 2003). Second, visual assessments can be gestalt in nature, biased by the subjective researcher, or lacking usefulness for phylogenetic inference, and therefore difficult to replicate without diagnostic expertise (Mayr, 1942; Bell et al., 2004, 2010; Ruane,

2015). Third, traditional linear morphometrics often describe variation in size more than shape, and may be unable to detect differences for taxa with high intraspecific variation or a limited number of autapomorphies (Ricklefs and Travis, 1980; Bookstein et al., 1985; Hutchison, 1997; Zelditch et al., 2004; Mutanen and Pretorius, 2007; Bell et al., 2010; Bell and Mead, 2014; Ruane 2015; Gray et al., 2017).

These methods are limited when applied to the fossil record, where DNA is usually unavailable and diagnostic characters are restricted to preserved skeletal elements (Hutchison, 1997; Baylac et al., 2003; Bell and Mead, 2014; Head, 2015; Head et al., 2016). This does not mean that morphology is uninformative; however, as the traditional methodologies used in previous studies can be supplemented by newer methods capable of detecting new or different aspects of morphological variation (Lawing and Polly, 2010; Ruane, 2015). One such innovative approach is geometric morphometrics.

Geometric morphometrics studies biological shape through a collection of shape-analysis techniques using Cartesian geometric coordinates, often in the form of homologous landmarks on biological structures (e.g., skull sutures and articular surfaces; Adams et al., 2004; Lawing and Polly, 2010). Because bones have shape – a truism, but vital to these methods – shapes can be quantified when combined with multivariate statistics to accurately differentiate phenotypic shape in structures, scaled to be independent of size, and is applicable to both extant and fossil organisms (Kendall, 1977; Rohlf, 1990; Rohlf and Marcus, 1993; Bookstein, 1996; Rohlf et al., 1996; Zelditch et al., 2004; Caumul and Polly, 2005; Mutanen and Pretorius, 2007; Polly,

2008; Lawing and Polly, 2010; Whitenack and Gottfried, 2010; Gray et al., 2017). Geometric morphometrics should therefore be useful as a simple, but effective, relatively objective tool for differentiating shape and delimiting taxa when applied to skeletal elements of function (e.g., teeth, skull shape, or elements involved in locomotion; Manier, 2004; Vincent et al., 2004; Ruane, 2015; Klaczko et al., 2016; Gray et al., 2017). Furthermore, these methods should be applicable across space and time (provided homologous structures are used for all taxa) for problems of taxonomic classification (Mutanen and Pretorius, 2007; Whitenack and Gottfried, 2010; Ruane, 2015; Klaczko et al., 2016; Gray et al., 2017), sexual dimorphism (Cardini et al., 2007; Wood et al., 2007; Huntley et al., 2021), functional morphology, modularity (Olson and Miller, 1958; Caumul and Polly, 2005), ecometrics (Lawing et al., 2012), and even taphonomic retrodeformation (Webster and Hughes, 1999; Angielczyk and Sheets, 2007; Lawing and Polly, 2010).

In Chapter Three of this dissertation, I build a framework of extant snake vertebral shape to explore the viability of using geometric morphometrics with quantitative methods to assign and identify fossil and living snake trunk vertebrae taxonomically and ecologically at higher to lower taxonomic levels. This study presents a new, easily replicable method to supplement typical qualitative morphological descriptions of taxa. It explores the success of this method for identifying taxa and ecologies for both an inclusive dataset and a taxonomically restricted dataset. I expect this study to become a commonly used method in studies of fossil snake assemblages with fair to excellent preservation for both identification and taxon-specific

paleoecological reconstruction. This method should allow non-expert diagnosticians to have more confidence in identifying fossil snakes, helping increase the number of snake fossils identified in museum collections. Furthermore, the results of this study may have future impacts on how methods such as ecometrics are applied to snakes, perhaps separating such studies to smaller taxonomic groups if it improves the ability to detect ecomorphology.

1.4. Striking the intraspecific morphological differences of the Western Massasauga

Studies of intraspecific geographic variation in snakes rarely link external and internal morphology. Understanding the relationship between ecological and morphological variation across populations and between sexes provides insight into both taxonomic distinctions and the functionality and performance of traits in different environments; this is vital for improving species identification, conservation, and management practices.

The Western massasauga, *Sistrurus tergeminus*, is a small (< 70 cm) rattlesnake that feeds primarily on small mammals and reptiles as an ambush predator (Holycross and Mackessy, 2002). Historically considered one of three subspecies of *Sistrurus catenatus*, subsequent phylogenetic studies suggested that *S.c. catenatus* was genetically distinct from both *S. tergeminus* and *S. edwardsii*, while more recently, Ryberg et al. (2015) found that populations of *S.t. tergeminus* and *S.t. edwardsii* were genetically indistinguishable, and likely represented a large and geographically contiguous assembly of populations that was more recently fragmented into several isolated populations.

Functionally, skeletal shape, body proportions, and soft-tissue morphologies are tied to snake feeding and locomotor ecologies. As such, species with wide geographic ranges may show morphological differences related the diet and locomotion between populations or sexes. In Chapter Four, I examine the intraspecific morphological variation in *S. tergeminus* using geometric morphometrics of skull shape, external head and body measurements, sex, diet, climate, habitat, and geographic distributions. I expect the use of both internal and external morphological data to be more informative on instraspecific morphological variation related to differences in ecology than either method alone. Using these methods together allows me to identify differences based on sex, diet, allometry, and bioclimatic factors.

1.5. Uncovering Ouroboros: an ecometric overview and a new shape-based ecometric using snake middle trunk vertebrae

Ecometrics are founded on the concept of functional traits, which organisms use to interact with their environments and fellow organisms. Each functional trait is mechanistically connected to the environment and is likely to perform better in some environments than others, thereby sorting organisms with similar traits into similar environments (Polly and Head, 2015). This means that functional traits that can be used as ecometrics play a role in community assembly via selection and geographic sorting. An ecometric trait has a functional relationship with at least one environmental or climatic factor at the community level, where environmental sorting is more visible than would be discernible at the species level (Eronen et al., 2010; Polly et al., 2011; Lawing

et al., 2016). Ecometric traits are therefore typically summarized as some measure (mean, median, range, skewness, or standard deviation) of trait value dispersion of species in a community (Polly and Head, 2015).

Ecometrics require three types of data – functional trait measurements, the abiotic factors of the environment, and the geographic ranges of the various species. If the ecometric is to be applicable to fossil specimens as well, I must include an addendum: the functional traits must also be measurable using skeletal material only. With the increase of online databases and global connectivity through the internet, the latter two types of data are more easily assembled than ever. Additionally, the improvement of analytical techniques and processing power allows for ever larger and improved models to perform complex analyses.

Ecometrics are also spatially inconstant, as the faunal composition and available traits in a community differ through geographic space. Perfect sorting of species would exhibit parallel details for environmental conditions and the linked functional traits. Both strong and weak ecometric correlations can be used to estimate the most likely environmental conditions for a given ecometric value via likelihood estimation or a transfer function, but the reconstruction would be more ambiguous with a weaker correlation (Vermillion et al., 2018; Short et al., 2021). As such, ecometrics can be considered taxon-free, insofar that the analysis has no need to have species, genus, or even family-level identifications to identify distinct ecological categories based purely on quantitative data (Polly and Head, 2015). These analyses are not truly taxon-free,

however, as they require the use of homologous structures to assess function, thereby limiting any analysis to taxa that have homologous functional features.

Ecometrics that quantify functional trait – environmental relationships exist for a number of different organisms, including plants, birds, mammals, and squamates. The majority of these measures require the analysis of pure shape (removing size, rotation, and orientation), density of structures, body mass estimates, or ratios. In vertebrates, measured traits most commonly come from teeth (Evans, 2013), limbs (Polly, 2010; Short and Lawing, 2021), or locomotion interfaces (e.g., relative tail length and vertebrae; Lawing et al., 2012). Table 1.1 summarizes some past ecometric methods used for organisms in terms of the functional traits and their paired environmental affiliations. Functional traits related to locomotion have been used for both mammals (Polly, 2010) and snakes (Lawing et al., 2012) in the past, with results suggesting close relationships between the organism's substrate interface (limbs in mammals, relative tail length in snakes).

Here, I discuss the progress of ecometric methodologies, and explore the potential of these methods for snakes specifically, and examine which methods would be most applicable to fossil material as well as extant material. If any of these methods exhibit differences in homologous functional traits related to locomotion, then it would be possible to identify which aspects of shape influence function and subsequently develop a methodology applicable to both fossil and living snake vertebrae using quick, less expensive methods. Furthermore, because snakes locomote with a high degree of body-to-surface contact, it is likely that environmental factors affecting those surfaces

(vegetation cover, temperature, precipitation, etc.) will influence the distributions of the various snake taxa. I hope to inspire the development of new ecometric methods and studies across a variety of organisms through these means, and to display how comprehensive these studies can become across organismal communities. First, I summarize previously established ecometric methods across multiple clades in this chapter. I then test the viability of a new potential ecometric, snake middle trunk vertebral shape, in Chapter Five. I investigate whether vertebral shape has both phylogenetic and ecological signal (in the form of substrate use). I assess Pearson's correlations for relationships between vertebral shape and environmental factors such as temperature- and precipitation-related bioclimatic variables, vegetation cover, ecological domain, ecological province, and altitude. I apply a maximum likelihood algorithm to community mean vertebral shape and Mean Annual Temperature to construct ecometric spaces and ecometric projection over geographic space. I expect this study to establish a new ecometric methods using snake vertebrae and Mean Annual Temperature, and for better predictions to result from combining more than one aspect of shape variation in snake vertebrae. With this new method, I can relate changes in snake faunas to changes in the environment through deep time, thereby improving both paleo-reconstructions and future projection models for snakes.

Table 1.1. Examples of established ecometrics in plants, birds, mammals, and squamates. Table summary modified from Polly et al., (2011) and Vermillion et al. (2018). Environmental factors include mean annual temperature (MAT), atmospheric carbon dioxide (pCO2), annual precipitation (AP), trophic position (TP), Ecological Province or Division (EP); dietary classification (DC), net primary productivity (NPP), and vegetative cover (VC).

Group	Functional Trait	Environmental Factor	Citation
Dicot Plants	Leaf Physiognomy	MAT; Water Stress	Wolf, 1990; Kowalski and Dilcher, 2003; Greenwood, 2005; Royer et al., 2005; Wing, 2005; Peppe et al., 2011
Seed Plants	Leaf Venation Density	MAT	Wolfe, 1979
Plants	Stomatal Density	pCO_2	Beerling et al., 2002
Birds	Body Mass	MAT	Meiri and Dayan, 2003
Mammals	Body Mass	MAT	Damuth et al., 1992
Mammals	Tooth Morphology	AP; TP; DC; NPP	Evans, 2013
Ungulates	Hypsodonty	AP; EP; VC	Janis and Fortelius, 1988; Fortelius et al., 2002; Schap et al., 2021; Short et al., 2021
Ungulates	Limb Proportion	AP; VC	Short and Lawing, 2021
Carnivorans	Limb Proportion	VC; MAT; AP	Polly, 2010
Squamates	Body Mass	MAT	Head et al., 2009; Head et al., 2013
Snakes	Relative Tail Length	VC	Lawing et al., 2012
Snakes	PC1 of Anterior Trunk Vertebral Shape	VC	Lawing et al., 2012
Snakes	Average Length to Width Ratio	VC	Lawing et al., 2012

1.5.1. Previously used and potential ecometrics in snakes

Previous studies have indicated several applicable ecometric tools for reconstructing past paleoclimate and paleoenvironment with snakes. Unfortunately, several other potential ecometrics related to locomotion, substrate, or feeding behavior such as whole-body vertebral counts (Lindell, 1994) or soft tissue morphology (such as keel of scales) are either rarely or never applicable to fossil snakes, and are therefore not available for a large portion of this study. Below, I outline both previously used and newly suggested ecometric relationships for snakes, as applicable to both fossil and modern samples. It is important to note here that the majority of snake fossils are isolated vertebrae or cranial elements (Rage, 1984; Holman, 2000); only rarely are even partially articulated skeletons discovered (Holman, 1977; Holman, 2000, Smith and Scanferla, 2016). As such, most, but not all, of the outlined or suggested ecometrics in this paper are those that can be accomplished via isolated skeletal elements. Beyond this section, I suggest a number of connections between functional traits and environmental factors; most of these are vertebral and related to substrate or vegetative cover (Fig. 1.1; Table 1.2).

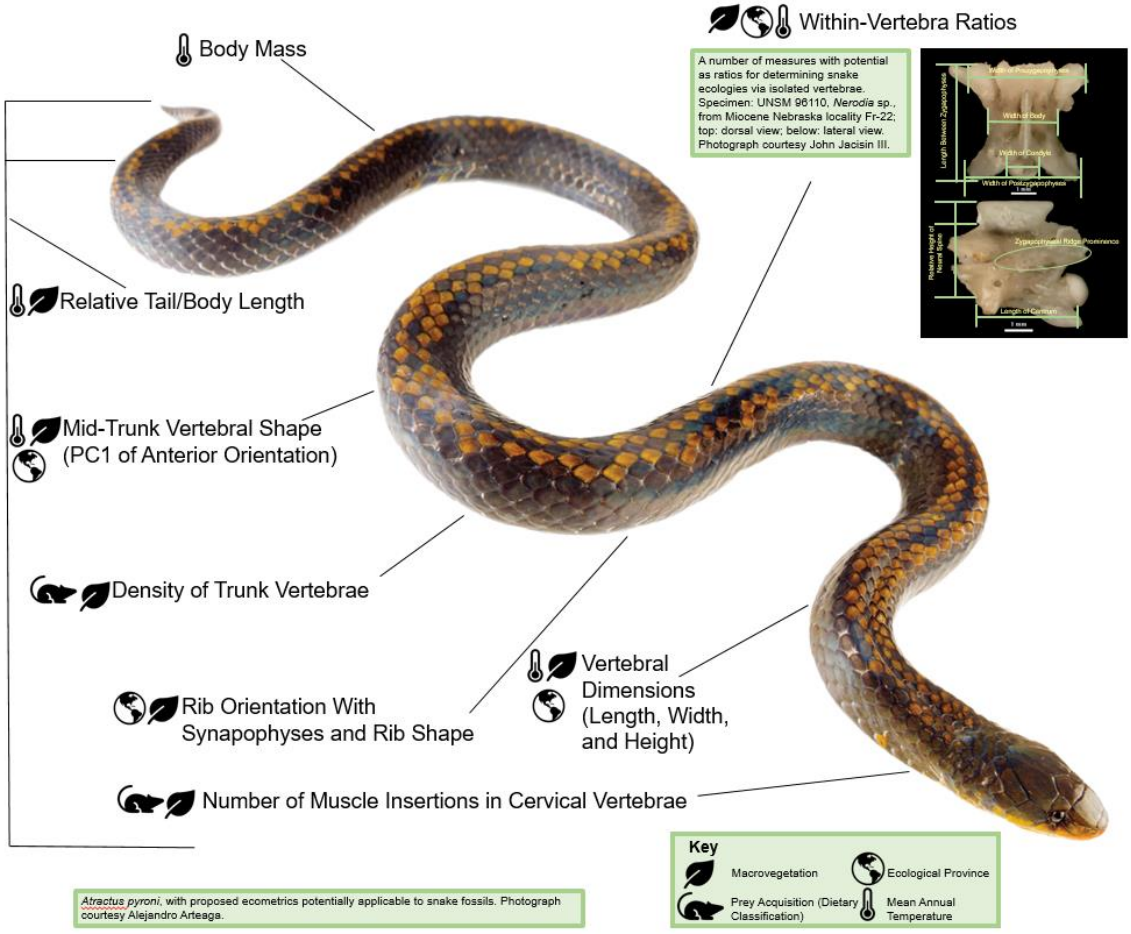

Figure 1.1. Diagram of potential snake ecometrics most applicable to the fossil record, with possible environmental relationships indicated symbolically.

Table 1.2. Examples of established and proposed snake ecometrics. Abbreviations: mean annual temperature (MAT), Annual Precipitation (AP) vegetative cover (VC), dietary classification/prey acquisition (DC), and ecological province (EP).

Functional Trait	Env. Factor	Argument	Citation
Body Mass	MAT	Mass-specific metabolic rate – temperature relationships	Head et al., 2009
Relative Tail/Body Length	VC	Locomotion Efficiency	Lawing et al., 2012
Dimensional Ratios of the Vertebral Column (Length, Width, and Height)	VC	Difference in main locomotive habit, body size, and needs for flexibility or rigidity in habitats	Lawing et al., 2012
Density of Trunk Vertebrae	VC, DC	Various requirements for behavior at depth underground or bottom of water column, and heavy-bodied striking	Houssaye et al., 2013
Mid-Trunk Vertebral Shape – Anterior, first Principal Component	VC	Muscle attachment site and vertebral articulation for locomotion	Lawing et al., 2012
Max. Width at PR vs. Max. Width at PO	VC	Different proportions for various needs of flexibility, torsion, rigidity, and cantilever abilities	Johnson, 1955; Lillywhite et al., 2000
Max. Width at PR vs. Max. Distance between PR and PO	VC	Different proportions for various needs of flexibility, torsion, rigidity, and cantilever abilities	Johnson, 1955; Lillywhite et al., 2000
Max. Width at PO vs. Least Width Dorsal Vertebra	VC	Different proportions for various needs of flexibility, torsion, rigidity, and cantilever abilities	Johnson, 1955; Lillywhite et al., 2000
Max. Width at PO vs. Max. Width of Condyle	VC	Different proportions for various needs of flexibility, torsion, rigidity, and cantilever abilities	Johnson, 1955; Lillywhite et al., 2000

Table 1.2. (continued)

Zygapophyseal Ridge Prominence	VC	Different proportions for various needs of flexibility, torsion, rigidity, and cantilever abilities	Johnson, 1955; Lillywhite et al., 2000
Zygosphene/Zygantrum Shape	VC	The articulation of these two vertebral structures may be indicative of the amount of torsion and flexibility allowed by the vertebrae when using muscles for locomotion.	Moon, 1999
Centrum Length vs. Neural Arch Width	VC	Various needs of agility and/or camouflage within habitat.	Meylan, 1982
Proportions of the Neural Spine	VC, MAT	Tall neural spines are often associated with body size and activity levels in extant snakes. Tall neural spines tend to be found on large, active snakes, while low spines tend to be associated with more secretive behaviors.	Holman, 2000
Space Between Ribs	VC, EP	Ribs may be closer together to aid musculature control that allows some snakes to depress the body on the vertical plane and increase contact area with a surface for more efficient locomotion.	Lillywhite, 2014
Rib Orientation	VC, EP	Ribs may be directly outward or downward in snakes, usually associated with a need to prevent downward displacement of muscle, such as when in the air between branches.	Lillywhite, 2014

Table 1.2. (continued)

No. of Muscle Insertions in Cervical Vertebrae	VC, DC	Strength and rigidity (or lack thereof for cantilever when moving across environmental gaps or striking prey	Lillywhite et al., 2000.
Tooth Morphology (Overall along the upper tooth row and individual tooth shape)	Microhabitat and Macrohabitat (VC), AP, seasonality,	Teeth can be specialized for certain prey types found only in certain environments (such as water) or for certain strategies (envenomation).	Meylan, 1982; Dwyer and Kaiser, 1997; Herrel et al., 2008; Alencar et al., 2013
Shape/Length of Jaws (pper and/or lower)	DC, VC	Jaws contribute to capturing various shapes of food, and may also contribute to certain behaviors (such as burrowing).	Meylan, 1982; Dwyer and Kaiser, 1997; Herrel et al., 2008
Relative Quadrate Length	DC, potential VC	Relative quadrate length is associated with the available gape of the skull, and therefore the shape and size of prey items. There are specializations for differently shaped types of prey found only in specific environments (such as fish in the water).	King, 2002; Vincent et al., 2009

Table 1.2. (continued)

Skull Shape (Brain Case and/or overall shape)	Prey Acquisition (DC), VC	Skull shape may vary depending on resistance forces encountered (such as into water or soil) or adaptations for feeding (such as large fangs or larger sensory organs).	Dwyer and Kaiser, 1997; Hibbits and Fitzgerald, 2005; Cundall and Irish, 2008
Skull thickness	Prey Acquisition (DC), VC	Skull thickness may vary depending on resistance forces encountered (such as into water or soil) or adaptations for feeding (such as large fangs or larger sensory organs).	Cundall and Irish, 2008

1.5.2. Body mass

Head et al. (2009) used the relationship between maximum size, ambient temperature, and mass-specific metabolic rate established by Makarieva et al. (2005) to determine mean annual temperature by comparing the body size and climate of giant fossil snakes like *Titanoboa* to extant anacondas, and has extended this tool to other fossil reptiles, including *Barbaturex* (Head et al., 2013) and living colubrids (Head et al., 2014). To estimate a range for body size, Head et al. (2009), regressed snout-vent length and total body length onto postzygapophyseal width for precloacal vertebrae between 60% and 65% intervals on the snake vertebral column. Body size has been used to examine the relationship between an organism and its environment, and is constrained by the mass-specific metabolic rate of the organism and ambient temperature (Head et al., 2009; Head, 2010; Lawing et al., 2012; Head et al., 2013; Head et al. 2014). Given this relationship, the body sizes of fossil taxa can be used to infer the paleotemperatures of an environment (Head et al., 2009; Head et al., 2013); however, this requires several fundamental assumptions of conservatism for metabolism and thermal ecology that may complicate the thermometric model, including the introduction of extreme ecological or physiological novelty (Head et al., 2014). Preliminary results presented by Head et al., (2014) from testing the thermometric model of cold-tolerant and heat-tolerant living colubroid taxa against fossil snakes from the middle Miocene (Clarendonian, ~12 Ma) Ashfall site of Nebraska (USA) indicated the necessity of a carefully selected model taxon for paleothermic reconstruction. Because the colubroid clade is extremely diverse, with a wide variety of substrate ecologies and a number of specializations (Rage, 1984;

Holman, 2000; Lawing et al., 2012; Vitt and Caldwell, 2014), it may be highly difficult to select a single colubroid taxon as a model. Probabilistic models that incorporate species distributions may assist in creating a more complete estimate of paleotemperature for fossil reptile faunas in future studies (Head et al., 2014).

1.5.3. Relative tail length

Lawing et al. (2012) explored the relationship between substrate use and three morphological snake traits (vertebral length-to width ratio, anterior vertebral shape, and relative tail length) to create a taxon-free proxy for paleoenvironmental reconstruction, then used relative tail length with North American snake communities to successfully relate morphology to vegetation cover, mean annual temperature, and ecological province.

Lawing et al., (2012) determined that the relative tail length (percentage of the length of the tail relative to the total body length) of snakes was more closely associated to substrate use and ecological province than the length/width ratio of trunk vertebrae or the first principal component of vertebral shape from an anterior view of a single trunk vertebrae. This is because snakes use their tails in different ways depending on substrate type and substrate temperature (Lillywhite, 2014). Unfortunately, while this ecometric is the most readily available and best correlated tool for living snakes, the application of this ecometric to the fossil record is limited to only a few rare specimens, as snake fossils are only rarely preserved as articulated skeletons with articulated tails (Lawing et al., 2012). Additionally, using the scale counts to calculate relative tail length is simply not possible for fossils.

1.5.4. Microanatomy

Very little has been done regarding the microanatomy of snake vertebrae. Houssaye et al. (2013) attempted to study the microanatomy of vertebrae taken at approximately one-third of the procloacal length and declared the vertebrae to be relatively homogenous despite size and proportion differences. They did find that taxa particularly specialized for certain ecologies with bone mass increased in many bottom-feeding aquatic snakes, fossorial snakes, and heavy-bodied strikers. Density was highest in fossorial snakes, lowest in fast terrestrial snakes, and intermediate for aquatic bottom-feeders. The study of Houssaye et al. (2013) is useful, but seems flawed in a few ways, however: (1) the use of centrum length as an estimate for size throughout many major snake families without taking into account that snakes have proportionately different centrum lengths and highly variable vertebral counts means that their size estimates may not be accurate; (2) their organization of habitat categories into fossorial and semi-fossorial, terrestrial and generalist, arboreal, semi-aquatic, and aquatic, with another analysis combining arboreal, generalist, and terrestrial snakes, and a third of aquatic and fossorial habitats and the rest of the taxa discriminated by their "body elongation", all seems to be a somewhat poor fit for arranging snake ecologies; and (3) using anterior trunk vertebrae is less likely to return a signal related to locomotion, as most locomotor types exhibited in snakes involve more posterior than anterior involvement (Lillywhite, 2014). Future work using a better fit of ecological habits (such as semifossorial), a larger sample size per species, or using caudal or posterior trunk vertebrae (imaged with micro-CT to prevent specimen damage) may produce a stronger ecologic signal for matching

phenotypes to local conditions in snake microanatomy in the future, as has been done for lizards (Houssaye et al., 2010).

1.5.5. Ribs

The long, curved ribs of snakes act to protect the inner organs and act as support for body structure as the organism utilizes its muscles for locomotion (Lillywhite, 2014). Snake ribs attach to the parapophysis and diapophysis (collectively, the synapophyses) of the trunk vertebrae via two facets and possess a prominence at the ventral end of the rib. These elements are present in the fossil record, but are usually not reliable for identification beyond the family level (Holman, 2000). It is unclear if this is because large scale analyses have never been done, or if there is not enough variation for identification to lower taxonomic levels. Nonetheless, I propose two potential metrics for ribs in snakes: (1) proximity of the tips of ribs; and (2) orientation of the ribs relative to the vertebral column. First, less space in between the ribs in snakes has been observed to be greater in sea snakes, and potentially in other aquatic snakes, therefore showing convergence of the trait and tying this observation to substrate use (Lillywhite et al., 2000). The function of this trait appears to be related to the tendency of aquatic snakes to depress the body and increase the area of contact between the snake and its environmental surface. If true, this arrangement is potentially useful for understanding ecological province and microvegetation in a community; however, this trait is less useful in for fossils, as even partially complete sections of articulated ribs and vertebrae are uncommon, and even if present, maybe be difficult to work with because of taphonomic deformation (Holman, 2000).

The orientation of the trunk ribs relative to the vertebra may have been observed to be direct downwards for arboreal snakes, rather than outwards as in most snakes (Lillywhite, 2014). The projection of ribs at a downward angle appears to be related to deep but slender body forms, which may improve the cantilever ability of snakes that need to cross spatial gaps, such as between branches (Lillywhite et al., 2000; Lillywhite, 2014). As such, the orientation of the ribs may be indicative of locomotion on specific substrates. Additionally, if the change in orientation in ribs begins at the articulation of with the synapophyses, the orientation of these structures on trunk vertebrae may also have potential use as an ecometric, for the same reasons. I suggest this method as the more likely and more useful approach for combining fossil and modern data via snake ribs.

1.5.6. Skull, jaws and teeth

Snakes have evolved a diverse set of skull morphologies and structures, most of which are related to prey selection and capture (Dwyer and Kaiser, 1997; Hibbitts and Fitzgerald, 2005; Cundall and Irish, 2008), but some of which also have some connection to traveling through a substrate (Hibbitts and Fitzgerald, 2005; Cundall and Irish, 2008). For example, the thickness and the relative width of the braincase form a wedge or cone-like shape in some fossorial snakes that is meant to counter the longitudinal pressure and other demands of burrowing into substrates on the skull (Cundall and Irish, 2008). In another example, Hibbitts and Fitzgerald (2005) noted an elongation of the snout in two different natricine genera associated with reducing drag while capturing their prey (fish) in fast-moving streams. These relationships may not be

especially useful for fossil in most cases, as features may not all be visible on isolated cranial elements, but some may exhibit enough details for ecometric interpretations with more detail investigation. Otherwise, these relationships, and any others related to specialized feeding or substrate type, may be useable for modern snakes and rare fossil skulls (in whole or in part).

I have found published information on potential ecometric uses in several isolated skull elements: the quadrate, the bones of the upper and lower jaws, and the teeth. The quadrate and jaw bones are both associated with the size of the gape in snakes, which is directly related to the size and/or size of prey they can capture. For example, Vincent et al. (2009) discovered a strong positive correlation between quadrate length and orientation and the speed of swallowing large fish prey. Adaptations for swallowing specific prey types such in that example implies at least a partial relationship with the environment of that animal; thus, a predominantly piscatorial diet requires at least a semi-aquatic ecology. It is important to note that the bones of the jaw may also exhibit various robustness or length; this may be related to prey capture, or even burrowing in some snakes (Cundall and Irish, 2008).

Similar to the jaw bones themselves, the morphology of the teeth, number of teeth, and shape of tooth row (especially on the upper jaw) all show specializations for specific prey types in some snakes (Cundall and Irish, 2008; Lillywhite, 2014). For example, the genus *Regina* is specialized for feeding on crayfish, and thus has short, stout, somewhat blunt teeth (Meylan, 1982); specialization in eating aquatic creatures implies aquatic affinities for the snakes, as mentioned before. As such, specialization

towards specific prey organisms can be connected to microhabitat and macrohabitat. In rare cases, prey type may also have implications for the degree of water availability.

1.5.7. Vertebral ratios – length, width, and height

Lawing et al., (2012) collected length and width measurements for all vertebrae of a single specimen per species (29 species), averaged the measurements over the entire species, and calculated the length/width ratio. They found that arboreal snakes (including semi-arboreal snakes were significantly different from all other snake groups. Notably, results from Lawing et al., (2012) suggest that plotting the mean length-to-width of vertebrae alongside vertebral shape (PC1) of living snakes should allow the separation of both arboreal and fossorial snakes, respectively, to stand out significantly enough for the identification of arboreal and fossorial habits in fossil vertebrae, when examined with the same ecometric tools. This method may be adjustable for use with both living and fossil snakes if one takes the average of all vertebral length-to-width ratios per fossil taxon in each locality, rather than averaging all the vertebrae from a single individual.

It is also worth considering the ratios of height-width and height-length in addition to length-width in snake fossils, as body shape has been shown to correlate with habitat type (Lillywhite, 2014). Various snakes show evidence of compression and elongation along different planes for traversing different habitat types (e.g., arboreal and aquatic; Lawing et al., 2012; Lillywhite, 2014).

1.5.8. Anterior-posterior vertebral articulation

Various authors have used different methods to quantify variation in the anterior-posterior articulations of snake vertebrae. Moon (1999) examined the degree and

capacity of torsion between vertebrae directly through video observation and freshly dissected snake segments, respectively. The latter method is of greater interest in this study, as it involves direct observation of vertebral limits; and can be applied to any fossils with at least two articulated vertebrae. With enough data or appropriate models, this method may be reduced to a handful of measurements that quantify the degree of torsion possible; this would be applicable to even individual fossil and modern elements, and would increase its utility as an ecometric for vegetative cover.

In this regard, the older work by Johnson (1955) may provide some hints on how to quantify the degree of torsion or rigidness in a single vertebra. Johnson (1955) observed that arboreal snake vertebrae tend to be elongate, with larger condyles relative to the postzygapophyses, short prezygapophyses that extend out at near-right angles, more robust zygantrums and zygosphenes, and a strong zygapophyseal ridge for muscle support. Johnson took vertebral ratios to avoid issues of size and identified characters of low intra-columnar variance for a variety of snakes. Finally, he chose characters that were translatable into functional requirements with mode-of-life attributes. He found twelve measurable characters for the dorsal and lateral orientations of trunk vertebrae and tested ratios on all possible combinations of the characters. Johnson (1955) found six instances where the ratios implied a difference in ecology, although a few also potentially carried a taxonomic signal: (1) greatest width of the prezygapophysis / greatest width of postzygapophysis (terrestrial vs. aquatic); (2) greatest width of postzygapophysis / greatest length of the condyle (terrestrial vs. aquatic); (3) greatest width of the prezygapophysis / greatest distance between pre- and postzygapophses

(terrestrial vs. arboreal); (4) greatest width of the postzygapophysis / least width of the dorsal body of the vertebra (terrestrial vs. fossorial); (5) greatest width of the prezygapophysis / greatest width of the postzygapophysis (aquatic vs. arboreal); and (6) greatest width of the prezygapophysis / greatest distance between pre- and postzygapophses (arboreal vs. fossorial). These results should certainly be checked with additional data, as this method appears to have the capability of separating out terrestrial, aquatic, arboreal, and fossorial snake vertebrae into four distinct groups.

1.5.9. Vertebral shape and geometric morphometrics

Most snake fossils are cranial elements or isolated vertebrae (Rage, 1984; Holman, 2000), so vertebral shape is a particularly viable source of fossil data for ecometric analyses (Head et al., 2009; Lawing et al., 2012). The procedure usually involves photographing isolated mid trunk vertebrae in multiple views, then applying geometric morphometrics to those images, before using quantitative methods on the ecometric values – derivations of the morphometric analyses – for inferences on the environment-trait relationship.

Quantifying morphological shape data can also help address questions of shape related to assigning a taxonomic identification to a specimen, differentiating between taxonomic groups (genera, species, even within species), identifying the causes of sexual dimorphism, and the causes of phenotypic differences that occur during speciation. Because bones have shape (a truism, but vital to these methods) and are used diagnostically to delimit species, geometric morphometrics can be used to analyze both living and fossil organisms – even on isolated elements such as vertebrae (Lawing et al.,

2012). These analyses quantify variation between, and even within, species, with the additional capability to analyze fossil specimens that have been deformed from their original shapes through taphonomic processes (Webster and Hughes, 1999). The utility of geometric morphometrics for both extant and fossil snakes, therefore, makes them ideal tools to test whether quantitative methods used on isolated snake vertebrae, which are commonly the only fossil material found for snakes, can be used to differentiate between North American genera (or even species) that have been classically difficult to describe or distinguish based on qualitative analysis alone (Lawing et al., 2012). Multivariate analysis of variance (MANOVA) and analysis of variance (ANOVA) calculations performed by Lawing et al. (2012) indicated that the first Principal Component (PC1) of anterior vertebral shape had a significant portion of its variation explained by substrate use (46%). The remainder of this paper expands on that method with a far more extensive dataset of snakes from the United States of America and Canada. Beyond this, certain structural relationships in snake vertebrae do not involve the anterior portion, or only include part of this view; these additional orientations are summarized in Table 1.2 and Figure 1.1 and are not used in this study.

This paper by no means claims to list all possible vertebral features with functional value and potential environmental correlations, but there are a couple more studies worth consideration. Meylan (1982) measured centrum length versus neural arch width, and found that both arboreal and fast terrestrial snakes stood out. This may imply a trend towards body and especially tail lengthening in those environments. Likewise, Holman (2000) mentions that low neural spines are more common in smaller, “secretive

snakes", while tall neural spines were more commonly associated with larger, "active" snakes.

1.5.10. The anatomy of a new snake-based ecometric method

Given the previously discussed state of the snake fossil record, vertebral shape and vertebral ratios are the most likely sources of fossil data for snake-based ecometric analyses (Head et al., 2009; Lawing et al., 2012). Snakes first appear in the Mesozoic fossil record and are geographically expansive by the Eocene in both the Old and New World (Rage, 1984; Holman, 2000). Various snakes show evidence of compression and elongation along different planes for traversing different habitat types (Johnson, 1955; Lawing et al., 2012; Lillywhite, 2014).

A number of the vertebral structures used in this study are functionally related to the environment and behavior of snakes. These structures may affect the ability of a snake to cantilever (extending the body out into space with no substrate for support), or to the flex and contort the body. The actions of cantilever and torsion are considered to be most related to the ability of a snake to extend the body out into space without substrate for support, or the rolling motion, three-dimensional movement, and flexion between vertebrae beneficial for underwater swimming, respectively (Johnson, 1955; Moon, 1999; Lillywhite et al., 2000; Lillywhite, 2014). In short, a number of these structures determine the relative rigidity a particular snake's vertebral column and musculature is capable of achieving. In the trunk region of the vertebral column, these structures should include the neural spine, prezygapophyses, prezygapophyseal articular facets, postzygapophyses, postzygapophyseal articular facets, zygapophyseal ridge,

zygosphene, zygantrum, condyle, and cotyle, in addition to the various ratios of length, width, and height (Johnson, 1955; Moon, 1999; Lillywhite et al., 2000).

Fully aquatic snakes (and perhaps some semiaquatic snakes) do not have cantilever capabilities (Lillywhite et al., 2000), suggesting a substrate-based relationship for that behavior. Cantilever abilities enable snakes to cross over spatial gaps without support, and/or to strike with force (Lillywhite et al., 2000). It is therefore unsurprising that both terrestrial and arboreal snakes have this ability; however, the extremes of this ability are observed only in specialized arboreal snakes (Johnson, 1955; Lillywhite et al., 2000).

Some active snakes swimming on, or especially under, the surface of the water, have exhibited an additional torsional and rolling motions in concurrence with typical aquatic undulation. This implies a higher degree of torsion or flexibility, as allowed by the previously mentioned articulations of the zygapophyses, the zygantrum-zygosphene, and the condyle/cotyle (Lillywhite, 2014). The relative size, shape, and orientations of these various structures apparently necessitate vertebral features on the opposite side of the spectrum compared to above (Johnson, 1995; Lillywhite et al., 2000).

Johnson (1955) observed that arboreal snake vertebrae tend to be elongate, with larger condyles relative to the postzygapophyses, short prezygapophyses that extend out at near-right angles, more robust zygantra and zygosphenes, and a strong zygapophyseal ridge for muscle support. Johnson (1955) took vertebral ratios to avoid issues of size and identified characters of low intra-columnar variance for a variety of snakes. Finally, he chose characters that were translatable into functional requirements with mode-of-life

attributes. He found twelve measurable characters for the dorsal and lateral orientations of trunk vertebrae and tested ratios on all possible combinations of the characters. Johnson (1955) found six instances where the ratios implied a difference in ecology, although a few also potentially carried a taxonomic signal: (1) greatest width of the prezygapophysis / greatest width of postzygapophysis (terrestrial vs. aquatic); (2) greatest width of postzygapophysis / greatest length of the condyle (terrestrial vs. aquatic); (3) greatest width of the prezygapophysis / greatest distance between pre- and postzygapophyses (terrestrial vs. arboreal); (4) greatest width of the postzygapophysis / least width of the dorsal body of the vertebra (terrestrial vs. fossorial); (5) greatest width of the prezygapophysis / greatest width of the postzygapophysis (aquatic vs. arboreal); and (6) greatest width of the prezygapophysis / greatest distance between pre- and postzygapophyses (arboreal vs. fossorial).

Additional vertebral structures suggested to be indicative of locomotive functionality relate to the ribs. The long, curved ribs of snakes act to protect the inner organs and act as support for body structure as the organism utilizes its muscles for locomotion (Lillywhite, 2014). Snake ribs attach to the parapophysis and diapophysis (collectively, the synapophyses) of the trunk vertebrae via two facets and possess a prominence at the ventral end of the rib. Rib elements are present in the fossil record, but are not usually considered reliable for identification beyond the family level (Holman, 2000). It is unclear if this is because large scale analyses have never been done, or if there is not enough variation for identification to lower taxonomic levels. Nonetheless, previous research indicates that the proximity of the tips of ribs and the orientation of the

ribs relative to the vertebral column may be indicative of different snake ecologies; these differences can be captures in the more commonly found vertebrae through the size and orientation of the synapophyses.

Less space in between the ribs in snakes is greater in sea snakes and potentially in other aquatic snakes relative to nonaquatic snakes, therefore showing convergence of the trait and tying this observation to substrate use (Lillywhite et al., 2000). The function of this trait appears to be related to the tendency of aquatic snakes to depress the body and increase the area of contact between the snake and its environmental surface. If true, this arrangement is potentially useful for understanding ecological province and microvegetation in a community. This trait is less useful for fossils, as even partially complete sections of articulated ribs and vertebrae are uncommon, and even if present, maybe be difficult to work with because of taphonomic deformation (Holman, 2000).

Likewise, the orientation of the trunk ribs relative to the vertebra is directed downwards for arboreal snakes, rather than outwards as in most snakes (Lillywhite, 2014). The projection of ribs at a downward angle appears to be related to deep but slender body forms, which may improve the cantilever ability of snakes that need to cross spatial gaps, such as between branches (Lillywhite et al., 2000; Lillywhite, 2014). As such the orientation of the ribs may be indicative of locomotion on specific substrates. Additionally, if the change in orientation in ribs begins at the articulation of with the synapophyses, the orientation and size of these structures on trunk vertebrae may also have potential use in ecometrics, for the same reasons. This method is likely the more useful approach for combining fossil and modern data via snake ribs.

1.5.11. A new twist on studying snake skeletal morphology: uncoiling the implications

In this dissertation, I investigate the nexus of morphological variation, taxonomy, phylogeny, and the environment in specific, functionally relevant parts of the snake skeleton. I highlight these interactions qualitatively and quantitatively at different taxonomic levels, geographic ranges, and temporal intervals. Further, I assess the potential of novel methodologies (e.g., an ecometric using geometric morphometrics) or apply established methodologies in novel ways (e.g., geometric morphometrics for step-wise taxonomic assignment using snake trunk vertebrae). These methods connect fossil and modern data by focusing on the skeletal elements commonly found in the fossil record of snakes. Critically, contributing deep time data on snake communities and evolution through environmental change will improve projections of the effects of present and future environmental perturbations for this ecologically important group. Though the path forward towards the conservation of environmentally sensitive species is difficult, it is possible to help mitigate of the effects of environmental alteration on biodiversity through integrative methods like those applied in this dissertation.

1.6. References

Adams, D. C., F. J. Rohlf, and D. E. Slice. 2004. Geometric morphometrics: ten years of progress following the “revolution”. Ital. J. Zool. 71: 5-16.

Alencar, L. R., M. P. Gaiarsa, and M. Martins, 2013. The evolution of diet and microhabitat use in pseudoboine snakes. *South American Journal of Herpetology*, *8*(1), pp.60-66.

Alroy, J. 2015. Current extinction rates of reptiles and amphibians. PNAS 112: 13003-13008.

Angielczyk, K. D. and H. D. Sheets. 2007. Investigation of simulated tectonic deformation in fossils using geometric morphometrics. Paleobiology 33: 125-148.

Barnosky, A. D., N. Matzke, S. Tomiya, G. O. Wogan, B. Swartz, T. B. Quental, C. Marshall, J. L. McGuire, E. L. Lindsey, and K. C. Maguire. 2011. Has the Earth's sixth mass extinction already arrived? Nature 471:51–57.

Barnosky, A. D., E. A. Hadly, P. Gonzalez, *et al*. 2017. Merging paleobiology with conservation biology to guide the future of terrestrial ecosystems. Science, 355(6325).

Baylac, M. C., C. Villemant, and G. Simbolotti. 2003. Combining geometric morphometrics with pattern recognition for the investigation of species complexes. Biological Journal of the LinneanSociety, 80:89–98.

Beerling, D., B. Lomax, D. Royer, G. Upchurch, & L. Kump. 2002. An atmospheric pCO2 reconstruction across the Cretaceous-Tertiary boundary from leaf

megafossils. Proceedings of the National Academy of Sciences of the United States of America, 99, 7836–7840.

Bell, C. J., J. J. Head, and J. I. Mead. 2004. Synopsis of the herpetofauna from Porcupine Cave, p. 117-126. In Barnosky, A.D. (ed.), Biodiversity Response to Climate Change in the Middle Pleistocene. The Porcupine Cave Fauna from Colorado. Berkeley: University of California Press.

Bell, C. J., J. A. Gauthier; and G. S. Bever. 2010. Covert biases, circularity, and apomorphies: A critical look at the North American Quaternary Herpetofaunal Stability Hypothesis. Quaternary International 217: 30-36.

Bell, C. J., and J. I. Mead. 2014. Not enough skeletons in the closet: collections-based anatomical research in an age of conservation conscience. Anatomical Record 297:344–348.

Bickford, D., D. J. Lohman, N. S. Sodhi, P. K. L. Ng, R. Meier, K. Winker, K. K. Ingram, and I. Das. 2007. Cryptic species as a window on diversity and conservation. Trends in Ecology & Evolution 22: 148–155.

Böhm, M., et al. 2013. The conservation status of the world's reptiles. Biol Conserv 157: 372–385.

Bookstein, F. L., B. Chernoff, R. Elder, J. Humphries, G. Smith. and R. Strauss, 1985. Morphometrics in evolutionary biology. Special Publication 15. Academy of Natural Sciences, Philadelphia, 277.

Bookstein, F.L. 1996. Biometrics, biomathematics and the morphometric synthesis. Bulletin of mathematical biology, 58:313.

Brooks, S. E., E. H. Allison, J. A. Gill, and J. D. Reynolds. 2010. Snake prices and crocodile appetites: aquatic wildlife supply and demand on Tonle Sap Lake, Cambodia. Biological Conservations 143:2127-2135.

Burbrink, F. T. and E. A. Myers. 2015. Both traits and phylogenetic history influence community structure in snakes over steep environmental gradients. *Ecography*, *38*:1036-1048.

Cardini, A., A. -U. Jansson, and S. Elton. 2007. A geometric morphometric approach to the study of ecogeographical and clinal variation in vervet monkeys. Journal of Biogeography 34: 1663-1678.

Caumul, R. and P. D. Polly. 2005. Phylogenetic and environmental components of morphological variation: skull, mandible, and molar shape in marmots (Marmota, Rodentia). Evolution 59: 2460-2472.

Ceballos, G., P. R. Ehrlich, A. D. Barnosky, A. García, R. M. Pringle, & T. M. Palmer. 2015. Accelerated modern human-induced species losses: Entering the sixth mass extinction. Science Advances, 1:1–5.

Cundall, D. and F. Irish, 2008. The snake skull. *Biology of the Reptilia*, *20*, pp.349-692.

Damuth, J. D., D. Jablonski, R. M. Harris, R. Potts, R. K. Stucky, H. D. Sues, & D. B. Weishampel. 1992. Taxon-free characterization of animal communities. In A. K. Beherensmeyer, J. D. Damuth, W. A. diMichele, R. Potts, H. D. Sues, & S. L. Wing (Eds.) Terrestrial Ecosystems Through Time: Evolutionary Paleoecology of Terrestrial Plants and Animals (pp. 183-203). Chicago: University of Chicago Press.

Davis, E. B., J. L. McGuire, and J. D. Orcutt. 2014. Ecological niche models of mammalian glacial refugia show consistent bias. Ecography 37: 1133-1138.

Dietl, G. P., S. M. Kidwell, M. Brenner, D. A. Burney, K. W. Flessa, S. T. Jackson, & P. L. Koch. 2015. Conservation paleobiology: Leveraging knowledge of the past to inform conservation and restoration. Annual Review of Earth and Planetary Sciences, 43:79–103.

Dwyer, C. M. and H. Kaiser. 1997. Relationship between skull form and prey selection in the thamnophiine snake genera Nerodia and Regina. *Journal of Herpetology*, pp.463-475.

Eronen, J. T., P. D. Polly, M. Fred, *et al*. 2010. Ecometrics: The traits that bind the past and present together. Int. Zoo. 5:88-101.

Estes, J. A., et al. 2011. Trophic Downgrading of Planet Earth. Science 15: 301-306.

Evans, A. R. 2013. Shape descriptors as ecometrics in dental ecology. Hystrix, 24:133–140.

Fortelius, M., J. Eronen, J. Jernvall, L. P. Liu, D. Pushkina, J. Rinne, A. Tesakov, I. Vislobokova, Z. Q. Zhang, and L. P. Zhou. 2002. Fossil mammals resolve regional patterns of Eurasian climate change over 20 million years. Evol Ecol Res 4:1005–1016.

Gibbons, D. E., et al. 2000. The global decline of reptiles, déjà vu amphibians. *Bioscience* 50: 653-666.

Gray, J. A., M. C. McDowell, M. N. Hutchinson, and M. E. Jones. 2017. Geometric morphometrics provides an alternative approach for interpreting the affinity of fossil lizard jaws. Journal of Herpetology, 51:375-382.

Greenwood, D. R. 2005. Leaf margin analysis: taphonomic constraints. *Palaios*, *20*:498-505.

Head, J. J., J. I. Bloch, A. K. Hastings, J. R. Bourque, E. A. Cadena, F. A. Herrera, P. D. Polly, and C. A. Jaramillo. 2009. Giant boid snake from the Palaeocene neotropics reveals hotter past equatorial temperatures. Nature 457:715-718.

Head, J. J. 2010. Climatic inferences from extant and fossil reptiles: toward a metabolic paleothermometer. AGU fall meeting abstracts, vol #B51F-0412.

Head, J. J., G. F. Gunnell, P. A. Holroyd, J. H. Hutchison, and R. L. Ciochon. 2013. "Giant lizards occupied herbivorous mammalian ecospace during the Paleogene greenhouse in Southeast Asia". Proceedings of the Royal Society B: Biological Sciences 280: 20130665.

Head, J. J., A. M. Lawing, and P. D. Polly. 2014. Herpetometrics: testing size-based metabolic thermometry of recent and fossil colubroid snakes across North America. SVP 74th annual meeting abstracts 146.

Head, J. J. 2015. Fossil calibration dates for molecular phylogenetic analysis of snakes 1: Serpentes, Alethinophidia, Boidae, Pythonidae. Palaeontologia Electronica, 18:1-17.

Head, J. J., K. Mahlow, and J. Mueller. 2016. Fossil calibration dates for molecular phylogenetic analysis of snakes 2: Caenophidia, Colubroidea, Elapoidea, Colubridae. Palaeontologia Electronica, 19(2FC):1-21.

Herrel, A., S. E. Vincent, M. E. Alfaro, S. Van Wassenbergh, B. Vanhooydonck, and D. J. Irschick, 2008. Morphological convergence as a consequence of extreme functional demands: examples from the feeding system of natricine snakes. Journal of evolutionary biology, 21:438-1448.

Hibbitts, T. J. and L. A. Fitzgerald. 2005. Morphological and ecological convergence in two natricine snakes. Biological Journal of the Linnean Society, 85:363-371.

Holman, J. A. 1977. Upper Miocene snakes (Reptilia, Serpentes) from southeastern Nebraska. Journal of Herpetology. 11:323-335.

Holman, J. A. 2000. Fossil snakes of North America: Origin, evolution, distribution, paleoecology. Bloomington: Indiana University Press.

Holman, J. A. 2006. Fossil Salamanders of North America. Bloomington: Indiana University Press. 233pp.

Holycross, A. T. and S. P. Mackessy, 2002. Variation in the diet of Sistrurus catenatus (Massasauga), with emphasis on Sistrurus catenatus edwardsii (Desert Massasauga). Journal of Herpetology, 36:454-464

Houssaye, A., A. Mazurier, A. Herrel, V. Volpato, P. Tafforeau, R. Boistel, V. de Buffrénil. 2010. Vertebral microanatomy in squamates: structure, growth and ecological correlates. J Anat 217:715–727.

Houssaye, A., R. Boistel, W. Böhme, A. Herrel. 2013. Jack-of-all-trades master of all? Snake vertebrae have a generalist inner organization. Naturwissenchaften 100: 997-1006.

Huntley, L. C., D. J. Gower, F. L. Sampaio, E. S. Collins, A. Goswami, and A. C. Fabre. 2021. Intraspecific morphological variation in the shieldtail snake *Rhinophis philippinus* (Serpentes: Uropeltidae), with particular reference to tail-shield and cranial 3D geometric morphometrics. Journal of Zoological Systematics and Evolutionary Research, 59:1357-1370.

Hutchison, J. H. 1992. Western North American reptile and amphibian record across the Eocene/Oligocene boundary and its climatic implications, p. 451-463. *In* Prothero, D.R. and Berggren, W.A. (eds.), Eocene-Oligocene Biotic and Climatic Evolution. Princeton University Press.

Hutchinson, M. N. 1997. The first fossil pygopod (Squamata: Gekkota) and a review of mandibular variation in living species. Memoirs of the Queensland Museum 41:355–366.

Jacisin III, J. J., E. T. Whiting, A. Ricker, J. Wallace, and J. J. Head. 2015. Neogene herpetofaunas from the Central Great Plains: diversity, modernization, and relationships to climate change. 75th Annual Meeting of the Society of Vertebrate Paleontology, Dallas, Texas, U.S.A.

Jacisin III, J. J. 2016. The first early Clarendonian snake assemblage from the Penny Creek Local Fauna, Webster County, Nebraska. 76th Annual Meeting of the Society of Vertebrate Paleontology, Salt Lake City, Utah, U.S.A.

Janis, C. M. & M. Fortelius. 1988. On the means whereby mammals achieve increased functional durability of their dentitions, with special reference to limiting factors. Biological Reviews of the Cambridge Philosophical Society, 63, 197-230.

Johnson, R. G. 1955. The adaptive and phylogenetic significance of vertebral form in snakes. Evolution 9:367–388.

Kaila, L. and G. Ståhls. 2006. DNA barcodes: Evaluating the potential of COI to diffentiate closely related species of Elachista (Lepidoptera: Gelechioidea: Elachistidae) from Australia. Zootaxa, 1170:1-26.

Kendall, D. G. 1977. The diffusion of shape. Advances in applied probability, 9:428-430.

King, R. B. 2002. Predicted and observed maximum prey size – snake size allometry. Functional Ecology 16:766-772.

Klaczko, J., E. Sherratt, and E. Z. Setz. 2016. Are diet preferences associated to skulls shape diversification in xenodontine snakes?. PloS one, 11, p.e0148375.

Kowalski, E. A. and D. L. Dilcher. 2003. Warmer paleotemperatures for terrestrial ecosystems. *Proceedings of the National academy of Sciences*, *100*:167-170.

Lawing, A. M. and P. D. Polly. 2010. Geometric morphometrics: recent applications to the study of evolution and development. Journal of Zoology 280:1-7.

Lawing, A. M. and P. D. Polly. 2011. Pleistocene climate, phylogeny, and climate envelope models: an integrative approach to better understand species' response to climate change. PLoS One 16:e28554.

Lawing, A. M., J. J. Head, and P. D. Polly. 2012. The ecology of morphology: the ecometrics of locomotion and macroenvironment in North American snakes. Pp. 117-146 in J. Louys (ed.), Palaeontology in Ecology and Conservation. Springer-Verlag, Berlin and Heidelberg.

Lawing, A. M., P. D. Polly, D. K. Hews, and E. P. Martins. 2016. Including fossils in phylogenetic climate reconstructions: A deep time perspective on the climatic niche evolution and diversification of spiny lizards (*Sceloporus*). The American Naturalist 188:133-148.

Lillywhite, H. B., J. R. LaFrentz, Y. C. Lin, and M. C. Tu. 2000. The cantilever abilities of snakes. Journal of Herpetology, 523-528.

Lillywhite, H. B. 2014. How snakes work: structure, function and behavior of the world's snakes. Oxford University Press.

Lindell, L. E. 1994. The evolution of vertebral number and body size in snakes. Functional Ecology, 708-719.

Lourenço-de-Moraes, R., F. S. Campos, R. B. Ferreira, K. H. Beard, M. Solé, G. A. Llorente, and R. P. Bastos. 2020. Functional traits explain amphibian distribution in the Brazilian Atlantic Forest. Journal of biogeography, 47:275-287.

Makarieva, A. M., V. G. Gorshkov, B. L. Li. 2005. Gigantism, temperature, and metabolic rate in terrestrial poikilotherms. Proc R Soc B Biol Sci 272:2325-2328.

Manier, M. K. 2004. Geographic variation in the long-nosed snake, Rhinocheilus lecontei (Colubridae): beyond the subspecies debate. Biological Journal of the Linnean Society 83: 65–85.

Mayr, E. 1942. Systematics and the origin of species, from the viewpoint of a zoologist. Cambridge, MA: Harvard University Press.

McCallum, M. L. 2007. Amphibian decline or extinction? Current declines dwarf background extinction rate. J Herptol 41:483–491.

Meiri, S. and T. Dayan. 2003. On the validity of Bergmann's rule. Journal of biogeography, *30*:331-351.

Meylan, P. A. 1982. The squamate reptiles of the Inglis IA Fauna (Irvingtonian: Citrus County, Florida). Bull. Florida State Mus. Biol. Ser. 27:1-85.

Moon, B. R. 1999. Testing an inference of function from structure: snake vertebrae do the twist. Journal of Morphology, 241:217-225.

Mullin, S. J., R.A. Siegel. 2009. Snakes: ecology and conservation. Cornell University Press Ithaca.

Mutanen, M. and E. Pretorius. 2007. Subjective visual evaluation vs. traditional and geometric morphometrics in species delimitation: a comparison of moth genitalia. Systematic Entomology 32:371–386.

Nice, C. C. and A. M. Shapiro. 1999. Molecular and morphological divergence in the butterfly genus Lycaeides (Lepidoptera: Lycaenidae) in North America: evidence of recent speciation. Journal of Evolutionary Biology, 12:936–950.

Olson, E. C. and R. L. Miller. 1958. Morphological integration. Chicago: University of Chicago Press.

Parmley, D. and J. A. Holman. 1995. Hemphillian (Late Miocene) snakes from Nebraska, with comments on Arikareean through Blancan snakes of midcontinental North America. Journal of Vertebrate Paleontology 15:79-95.

Parmley, D. & K. B. Hunter. 2010. Fossil Snakes of the Clarendonian (Late Miocene) Pratt Slide Local Fauna of Nebraska, with the description of a new natricine colubrid. J. of Herpetology 44:526-543.

Peppe, D. J., D. L. Royer, B. Cariglino, S. Y. Oliver, S. Newman, E. Leight, G. Enikolopov, M. Fernandez-Burgos, F. Herrera, J. M. Adams, and E. Correa. 2011. Sensitivity of leaf size and shape to climate: global patterns and paleoclimatic applications. New phytologist, 190:724-739.

Pimentel, D., et al. 1997. Economic and Environmental Benefits of Biodiversity. BioScience 47:747-757.

Polly, P. D. 2008. Developmental dynamics and G-matrices: can morphometric spaces be used to model phenotypic evolution? Evol. Biol. 35:1–20.

Polly, P. D. 2010. Tiptoeing through the trophics: geographic variation in carnivoran locomotor ecomorphology in relation to environment. – In: Goswami, A. and A. Friscia (eds), Carnivoran evolution: new views on phylogeny, form, and function. Cambridge University Press, pp. 374-410.

Polly, P. D., J. T. Eronen, M. Fred, G. P. Dietl, V. Mosbrugger, C. Scheidegger, D. C. Frank, J. Damuth, N. C. Stenseth, and M. Fortelius. 2011. History Matters: ecometrics and integrative climate change biology. – Proc. R. Soc. B 278: 1121-1130.

Polly, P. D., and J. J. Head. 2015. Measuring Earth-life transitions: Ecometric analysis of functional traits from late Cenozoic vertebrates. In P. D. Polly, J. J. Head, & D. L. Fox (Eds.), Earth-life transitions: Paleobiology in the context of earth system evolution The Paleontological Society 21:21–46.

Polly, P. D., A. M. Lawing, J. T. Eronen, & J. Schnitzler. 2016. Processes of ecometric patterning: modeling functional traits, environments, and clade dynamics in deep time. Biological Journal of the Linnaean Society, 118:39-63.

Rage, J.-C. 1984. Serpentes. Part 11. Handbuch der Palae¨oherpetologie. Gustav Fisher Verlag, Stuttgart, Germany. 80 pp.

Reading, C. J., L. M. Luiselli, G. C. Akani, X. Bonet, G. Amori, J. M. Ballouard, E. Filippi, G. Naulleau, D. Pearson, and L. Rugiero. 2010. Are snake populations in widespread decline? Biol Lett 6:777-780.

Ricklefs, R. E. and J. Travis. 1980. A morphological approach to the study of avian community organization. Auk, 97:321–338.

Rohlf, F. J. 1990. Morphometrics. Annu. Rev. Ecol. Syst. 21:299–316.

Rohlf, F. J. & L. Marcus. 1993. A revolution in morphometrics. Trends Ecol. Evol. 8:129–132.

Rohlf, F. J., A. Loy, and M. Corti. 1996. Morphometric analysis of old world Talpidae (Mammalia, Insectivora) using partial-warp scores. Systematic Biology 45:344–362.

Root, T. L. et al. 2003. Fingerprints of global warming on wild animals and plants. *Nature* 421, 57-60.

Rosenzweig C., G. Casassa, D. J. Karoly, et al. 2007. Assessment of observed changes and responses in natural and managed systems. In: IPCC. Climate Change 2007: Impacts, Adaptation and Vulnerability. Contribution of Working Group II to the Fourth Assessment Report of the Intergovernmental Panel on Climate Change. Cambridge University Press, Cambridge, UK, pp. 79–131.

Royer, D. L., P. Wilf, D. A. Janesko, E. A. Kowalski & D. L. Dilcher. 2005. Correlations of climate and plant ecology to leaf size and shape: potential proxies for the fossil record. American Journal of Botany, 92:1141-1151.

Ruane, S. 2015. Using geometric morphometrics for integrative taxonomy: An examination of head shapes of milksnakes (genus *Lampropeltis*). Zoological Journal of the Linnean Society, 174:394-413.

Ryberg, W. A., J. A. Harvey, A. Blick, T. J. Hibbitts, and G. Voelker. 2015. Genetic structure is inconsistent with subspecies designations in the western massasauga Sistrurus tergeminus. Journal of Fish and Wildlife Management, 6:350-359.

Saez, A. G. and E. Lozano. 2005. Body doubles. Nature 433:111.

Schneider, S. H., S. Semenov, A. Patwardhan, et al. 2007. Assessing key vulnerabilities and the risk from climate change. In: IPCC. Climate Change 2007: Impacts, Adaptation and Vulnerability. Contribution of Working Group II to the Fourth Assessment Report of the Intergovernmental Panel on Climate Change. Cambridge University Press, Cambridge, UK, pp. 779–810.

Schap, J. A., J. X. Samuels, and T. A. Joyner. 2021. Ecometric estimation of present and past climate of North America using crown heights of rodents and lagomorphs. Palaeogeography, Palaeoclimatology, Palaeoecology, 562:110144.

Short, R. A. and A. M. Lawing. 2021. Geography of artiodactyl locomotor morphology as an environmental predictor. Diversity and Distributions, 27:1818-1831.

Short, R. A., K. Pinson, and A. M. Lawing. 2021. Comparison of environmental inference approaches for ecometric analyses: Using hypsodonty to estimate precipitation. Ecology and evolution, 11:587-598.

Smith, K. T. 2006. A diverse new assemblage of late Eocene squamates (Reptilia) from the Chadron Formation of North Dakota, U.S.A. Palaeontologia Electronica 9.

Smith, K. T. 2013. New constraints on the evolution of the snake clades Ungaliophiinae, Loxocemidae and Colubridae (Serpentes), with comments on the fossil history of erycine boids in North America. Zoologischer Anzeiger, 252:157-182.

Smith, K. T. and A. Scanferla. 2016. Fossil snake preserving three trophic levels and evidence for an ontogenetic dietary shift. Palaeobiodiversity and Palaeoenvironments, 96:589-599.

Vermillion, W. A., P. D. Polly, J. J. Head, J. T. Eronen, and A. M. Lawing. 2018. Ecometrics: A trait-based approach to paleoclimate and paleoenvironmental reconstruction. *In* D. A. Croft, D. Su, & S. W. Simpson (Eds.), Methods in Paleoecology: Reconstructing Cenozoic terrestrial environments and ecological communities (pp. 373–394). Springer.

Vincent, S. E., A. Herrel, and D. J. Irschick. 2004. Sexual dimorphism in head shape and diet in the cottonmouth snake (Agkistrodon piscivorus). Journal of Zoology, 264:53-59.

Vincent, S. E., M. C. Brandley, A. Herrel, and M. E. Alfaro. 2009. Convergence in trophic morphology and feeding performance among piscivorous natricine snakes. Journal of evolutionary biology, 22:1203-1211.

Vitt, L. J., and J. P. Caldwell. 2014. Herpetology: An Introductory Biology of Amphibians and Reptiles, fourth ed. Academic Press, San Diego.

Wake D. B., V. T. Vredenburg. 2008. Colloquium paper: Are we in the midst of the sixth mass extinction? A view from the world of amphibians. Proc Natl Acad Sci USA 105 (Suppl 1):11466–11473.

Webster, M. and N. C. Hughes. 1999. Compaction-related deformation in Cambrian olenelloid trilobites and its implications for fossil morphometry. Journal of Paleontology 73: 355-371.

Whitenack, L. B. and M. D. Gottfried. 2010. A morphometric approach for addressing tooth-based species delimitation in fossil mako sharks, *Isurus* (Elasmobranchii: Lamniformes). Journal of Vertebrate Paleontology, 30:17-25.

Willis, K. J., L. Gillson, T. M. Brncic, and B. L., Figueroa-Rangel. 2005. Providing baselines for biodiversity measurement. Trends Ecol Evol 20:107-108.

Wing, S. L., G. L. Harrington, F. A. Smith, J. I. Bloch, D. M. Boyer & K. H. Freeman. 2005. Transient floral change and rapid global warming at the Paleoeocene-Eocene boundary. Science, 310:993-996.

Wolfe, J. A. 1979. Temperature parameters of humid to mesic forests of eastern Asia and relation to forests of other regions of the northern hemisphere and Australasia. Geological Survey Professional Paper, 1106.e.

Wolf, J. A., 1990. Palaeobotanical evidence for a marked temperature increase following the Cretaceous/Tertiary boundary. *Nature, 343*:153-156.

Wood, A. R., M. L. Zelditch, A. N. Rountrey, T. P. Eiting, H. D. Sheets, and P. D. Gingerich. 2007. Multivariate stasis in the dental morphology of the Paleocene-Eocene condylarth *Ectocion*. Paleobiology 33:248-260.

Zelditch, M. L., D. L. Swiderski, H. D. Sheets, and W. L. Fink. 2004. Geometric morphometrics for biologists: a primer. Amsterdam: Elsevier.

Zipkin, E. F., G. V. DiRenzo, J. M. Ray, S. Rossman, and K. R. Lips. 2020. Tropical snake diversity collapses after widespread amphibian loss. Science, 367:814-816.

2. FOSSIL SNAKES OF THE PENNY CREEK LOCAL FAUNA OF WEBSTER COUNTY, NEBRASKA, AND THE FIRST RECORD OF SNAKES FROM THE EARLY CLARENDONIAN (12.5-12 MA) OF NORTH AMERICA

"There is nothing like geology; the pleasure of the first day's partridge shooting or first day's hunting cannot be compared to finding a fine group of fossil bones, which tell their story of former times with almost a living tongue."

– Charles Darwin, letter to his sister Catherine, 1934

2.1. Introduction

Fossil Cenozoic herpetofauna are potential tools for environmental reconstruction and investigating the long-term biotic effects of climate change, as the physiologies of extant reptiles and amphibians are strongly associated with habitat (Webb and Shine, 1998; Head et al., 2009; Sinervo et al., 2010; Muthoni, 2010; Huey et al., 2012; Dupoue´ et al., 2017). Snakes have a longstanding, wide geographic distribution in the Cenozoic fossil record, with many modern North American groups first appearing in the Miocene of North America (Rage, 1984; Parmley and Holman, 1995; Holman 2000). Unfortunately, many Cenozoic North American snake faunas are chronically understudied and specimens misidentified, thereby hindering opportunities to apply a deep time perspective to investigate the effects of environmental change on snake communities (Bell et al., 2010). Further complicating matters is the difficulty of

identifying unique taxa based on isolated cranial and vertebral elements that may be weathered or otherwise damaged during or after the death of an organism (Rage, 1984).

While a relatively small number of mostly diminutive fossil snakes from the Paleogene of the Central Great Plains (South Dakota, Nebraska, Kansas, and Oklahoma) have been described, the Neogene beds of the Central Great Plains – specifically Nebraska – include a comparatively long, well-preserved record of fossil snakes that is unparalleled in illustrating the history of richness, turnover, and modernization of snake assemblages in North America (Holman, 2000; Parmley and Holman, 2007; Parmley and Hunter, 2010; Jacisin et al., 2015). Within the changing environments leading up to, then following the Mid-Miocene Climatic Optimum (MMCO), the "archaic" booid-dominated faunas represented by *Ogmophis*, *Calamagras*, and *Geringophis* gradually gave way to colubroid-dominated faunas (Parmley and Holman, 1995; Parmley and Hunter, 2010). The first recognized appearances of extant genera occur in the early Neogene of the Central Great Plains; these genera include *Lampropeltis*, *Pantherophis* (*Elaphe*), *Salvadora*, *Heterodon*, *Nerodia*, *Thamnophis*, *Crotalus*, *Sistrurus*, and *Charina* (Parmley and Holman, 1995; Parmley and Holman, 2007; Parmley and Hunter, 2010; Jacisin et al., 2015).

Despite the excellent state of the Central Great Plains' fossil snake record and apparent peaks of genus-level richness in the late Barstovian and late Clarendonian (Ba2, 14.75-12.5 Ma and Cl3, 10.0 Ma- 9.0 Ma; Holman, 2000; Parmley and Hunter, 2010; Jacisin et al., 2015), a paucity of fossil material has resulted in a knowledge gap on

snake assemblages from the earliest Clarendonian (Cl1, 12.5-12 Ma). This temporal gap in the snake fossil record is present throughout North America and highlights a glaring lack of knowledge about the scale of turnover and modernization of snake assemblages immediately following the late Barstovian (including the MMCO) of the Central Great Plains. While the description of snake taxa from a single locality of this age is not a comprehensive representation of which snakes were extirpated from the area by the early Clarendonian, locality Wt 13B does substantiate the presence of the taxa discussed in this study.

Here, I report the first known early Clarendonian snake assemblage in North America from locality Wt 13B of the Penny Creek Local Fauna, southern Webster County, Nebraska (Fig. 2.1). This fossil material allows me to confirm for the first time the presence of a number of snake taxa in Nebraska and the Central Great Plains during the Cl1, providing evidence to support previous geological and biological interpretations of the local paleoenvironment, and allowing for a more complete understanding of the modernization of North American snake faunas. While unidentified fossil reptiles were reported from this locality, previous focus was primarily given to the geology and the mammalian assemblages (Turner, 1972; Voorhies 1987, 1990; Corner, 2014). This is therefore the first study to explore the differences between Nebraska's latest Barstovian and earliest Clarendonian herpetofaunas, and the initial transition into a post-MMCO snake assemblage (Zachos et al., 2001; Song et al. 2018).

2.1.1. Institutional abbreviations

Collections — **UNSM**, University of Nebraska State Museum; **TCWC**, Texas A&M University Biodiversity and Research Teaching Collections; and **TMM,** University of Texas at Austin Vertebrate Paleontology Collections.

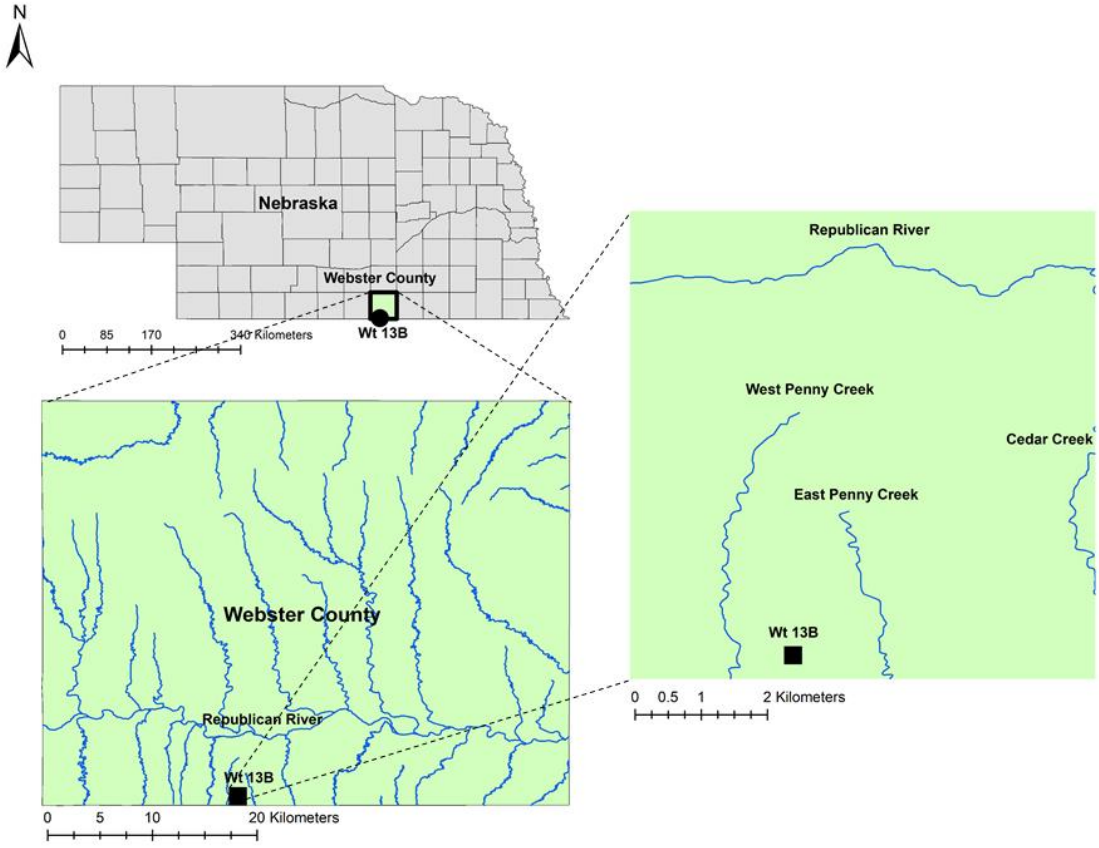

Figure 2.1. Map showing the geographic position of UNSM locality Wt 13B from the Penny Creek Local Fauna at state (A), county (B), and local (C) scales. The locality is represented by a solid black circle.

2.2. Geologic Setting

In general, the Ash Hollow Formation is composed of poorly sorted, heterogeneous sediments (Diffendal et al., 1996). The basal Ash Hollow Fm. of the Ogallala Group is a cross-bedded conglomerate composed of partially rounded concretions pulled from the underlying Whitney Member of the Brule Formation and is mostly composed of stream-transported and stream-deposited sediments (Diffendal et al. 1996). Boellstorff (1978) first assigned a Miocene age for the formation based on the dates returned during the study of fission tracks in volcanic ash shards. This conglomerate is variable in thickness, and sequences upward into unstratified, massive pebbly sands and calcite-cemented pebbly sandstones (Diffendal et al., 1996; also known as *pudding sands* via Lueninghoener, 1934). These massive sandstones tend to form massive ledges with the underlying conglomeratic layer. At the type locality of the Ash Hollow Fm., the conglomeratic unit lies upon an erosional surface developed on top of a Whitney Member (Brule Fm.) concretion zone to form an unconformity. Overlying the Ash Hollow Fm. are coarse, stream-deposited sands and gravels that represent the Pliocene Broadwater Formation (Fig. 2.1). While much of the Ash Hollow Fm. is epiclastic, it does contain several diatomite and ash beds (Thomasson, 1980), the latter of which includes the infamous Ashfall Fossil Beds located in Antelope County, Nebraska, although these beds are younger than the locality examined within this study (Voorhies, 1992; Diffendal et al., 1996).

In Webster County, Nebraska, Turner (1972) first reported granitic sand and gravel with cross-bedding indicative of a braided stream fluvial environment for several Nebraska localities collectively named the Penny Creek Local Fauna; this included locality Wt 13B, from which the fossils of this study were collected (Fig.2.1). She assigned an early Clarendonian age to those localities based on the mammalian fauna. Research by Voorhies (1987, 1990) and Corner (2014) confirmed this assessment for the locality, and provided additional knowledge on the geology, vertebrate biostratigraphy, and mammalian fossils of Wt 13B as part of larger studies. They concluded that the sediments belonged to the Ogallala Group's Ash Hollow Fm. and were earliest Clarendonian (middle Miocene) in age, or slightly older than the famous Ashfall Fossil Beds of northeastern Nebraska (Fig. 2.1). They also noted that the sediments of the Penny Creek local fauna, and the Ogallala sediments as a whole, were predominantly epiclastic, as opposed to the volcaniclastic sediments of the underlying Arikaree and White River Group rocks in Nebraska (Voorhies, 1990).

2.3. Materials and Methods

The fossils assessed in this study were collected from a single locality (Wt 13B), accessioned to the University of Nebraska State Museum's (UNSM's) collections, and are part of a diverse assemblage dubbed the "Penny Creek Local Fauna", consisting of several other Webster County localities (Wt 11, Wt 12, Wt 13A, and Wt 15B; Turner, 1972; Voorhies et al., 1987; Corner, 2014). These localities were collected extensively, especially in the 1960's and early 1970's, under the supervision of the UNSM. Wt 13B

was quarried annually for several years by students from the Red Cloud Community Schools under the supervision of J. L. Fitzgibbon (Voorhies et al., 1987). Collection methods included surface prospecting, quarrying, and screenwashing during these years (Corner, 2014).

I used a binocular dissecting microscope to examine the snake fossils from Wt 13B, which were predominantly pre-cloacal trunk vertebrae and a small number of caudal vertebrae. Apomorphic characters (such as the presence of a hypapophysis on mid-trunk vertebrae; Holman, 2000) capable of uniquely identifying different snake groups (e.g., natricine vs. colubrine snakes) were used for fossil identification following the recommendations of Bell and colleagues (Bell et al., 2004; Bell et al, 2010). Character tables suggested by Holman (2000) and modified by Ikeda (2007) assisted in the process through generalized descriptions of the range of shape variation for the neural arch, prezygapophyseal articular facets in dorsal view, postzygapophyseal articular facets in ventral view, anterior edge of the zygosphene in anterior and dorsal views, zygosphenal articular facets in lateral view, anterior and posterior edges of the neural spine in lateral view, hypapophysis, hemal keel, cotyl, condyle, prezygapophyseal accessory processes in ventral view, developmental degree of the parapophyses, prezygapophyseal accessory processes, interzygapophyseal ridge in lateral view, and subcentral ridge in lateral view (Fig. 2.2). In addition, I made personal observations using comparative methods with available modern and fossil specimens at the University of Nebraska State Museum (UNSM), the Texas A&M University Biodiversity and Research Teaching Collections (TCWC), and the University of Texas at Austin

Vertebrate Paleontology collections (TMM) collections, as well as previously published literature and figures.

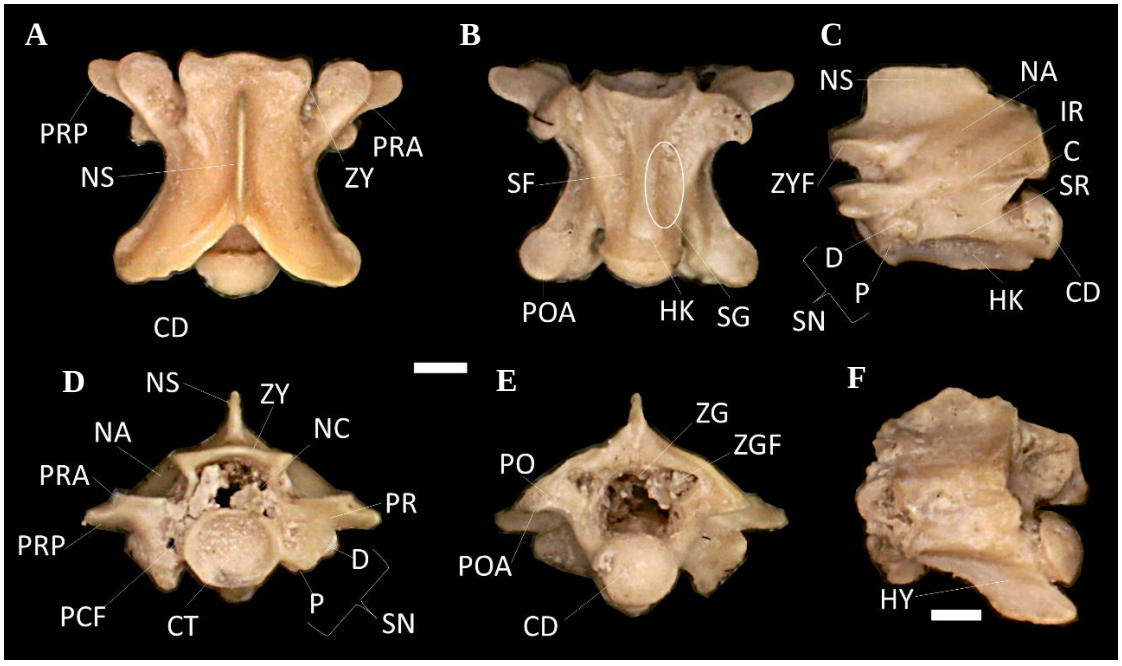

Figure 2.2. Basic units of snake trunk vertebrae. A-E are from a fossil colubrine, and F is from a fossil natricine. A: trunk vertebra in dorsal view. B: trunk vertebra in ventral view. C: trunk vertebra in left lateral view. D: trunk vertebra in anterior view. E: trunk vertebra in posterior view. F: trunk vertebrae in left lateral view. Abbreviations: C, centrum; CD, condyle; CT, cotyle; D, diapophysis; HE, hemapophysis; HK, hemal keel; HY, hypapophysis; IR interzygapophyseal ridge; LY, lymphapophyses; NA, neural arch; NC, neural canal; NS, neural spine; P, parapophysis; PCF, paracotylar foramen; PLE, pleurapophysis; PO, postzygapophysis; POA, postzygapophyseal articular facet; PR, prezygapophysis; PRA, prezygapophyseal articular facet; PRP, prezygapophyseal accessory process; SF, subcentral foramen; SG, subcentral groove; SN, synapophyses; SR, subcentral ridge; ZG, zygantrum; ZGF, zygantral articular facet; ZY, zygosphene; ZYF, zygosphenal articular facet.

I collected presence-absence data for snakes from 19 Barstovian through Blancan sites in the state of Nebraska in order to examine first and last occurrences and the transition to a more modern snake assemblage by examining the similarity of the snake

assemblages identified for those sites through time (Fig. 2.3). It is important to note that using presence-absence data in any estimate or comparison of biodiversity is biased in that absences may be representative of true absence, a lack of data or errors in identification. As such, true absences are exceptionally difficult or impossible to distinguish from false absences, especially when considering communities with numerous rare or difficult to distinguish species (Boulinier et al., 1998). Given that this research addresses small vertebrates, I expect detection to be relatively low, making it important to acknowledge potential detection bias in the presence-absence data. Nonetheless, it is important to use presence-absence data in order to estimate the composition of snake communities and distributions through time.

Beyond identifying the presence or absence of taxa at each location, I visualized the similarity between assemblages at these sites by constructing a Euclidean distance matrix and using a principal coordinates analysis (PCoA), a multidimensional scaling method that explores and displays the structure of the dissimilarities for the Nebraska localities. I also used this distance matrix to perform a hierarchical cluster analysis (HCA) with the complete-linkage method to distinguish groupings of localities that may suggest major shifts in the snake assemblages of Nebraska. Agglomerative HCA is a "bottom-up" analysis where each observation starts in its own cluster, and pairs of clusters are merged as the hierarchy is built up. The complete-linkage or farthest neighbor clustering method forms compact clusters of near-equal diameters and avoids forcing clusters together based on single elements being close. Complete-link clustering

builds clusters where the similarity of two clusters is the similarity of their most dissimilar members (thus, “farthest neighbor”).

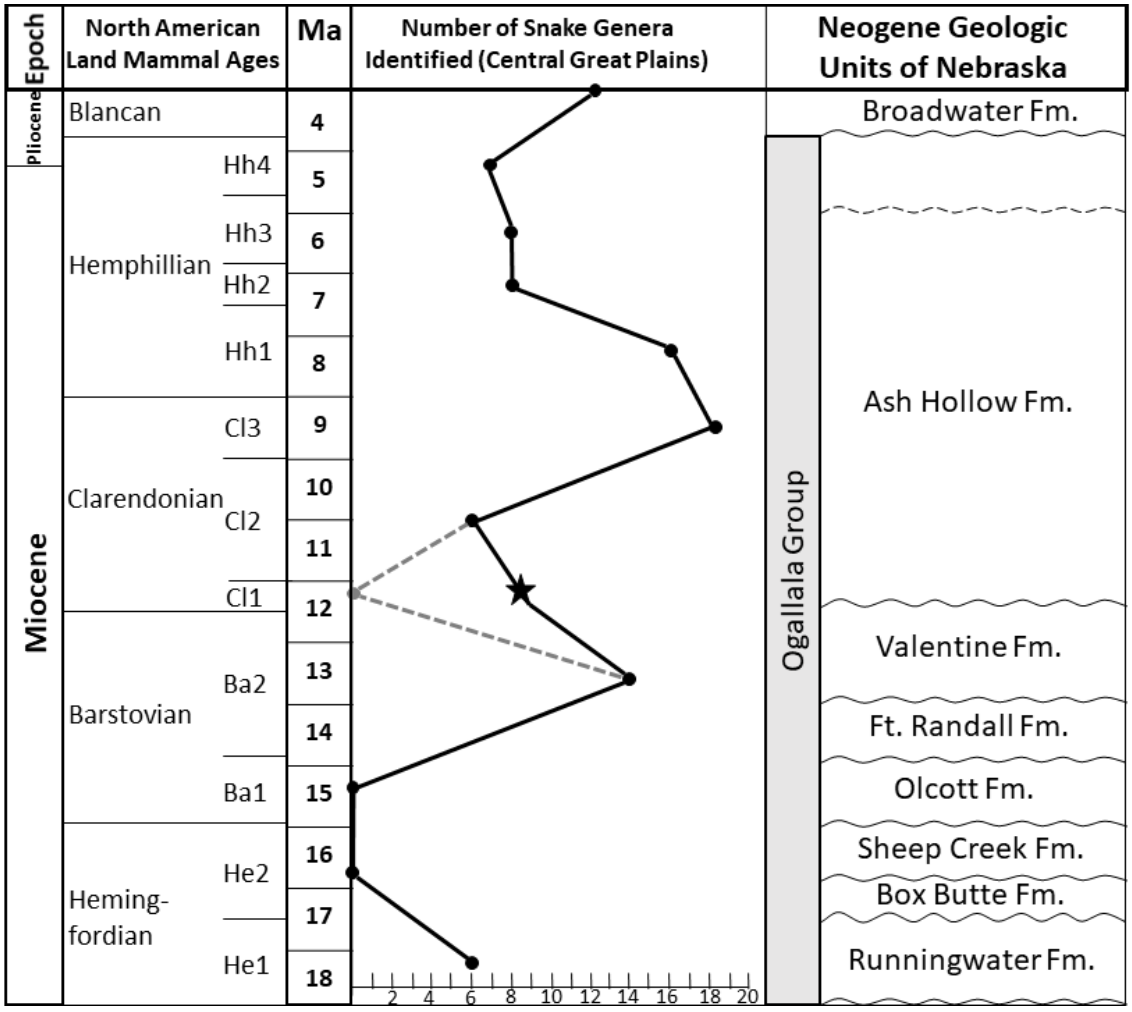

Figure 2.3. Composite time-stratigraphic chart of the Neogene of Nebraska, correlated with the number of snake genera presently identified from the Central Great Plains for each NALMA substage. Each point on the snake richness chart is summarized for each substage at that substage’s midpoint, and does not necessarily correlate with a particular rock unit on the right. The star represents the data from this study, which updates the previous lack of data from Cl1 across North America (represented by the gray hashed line). NALMAs and substages are correlated with time based on data and figures from Tedford et al. (2004). Rock Units are adapted from Joeckel et al. (2017) and Tedford et al. (2004). Snake generic richness is modified and updated from Jacisin et al., 2015).

Snake ectothermic physiology is highly dependent on ambient temperature and is therefore a practical choice for examining terrestrial climates of the past. To further examine the potential climate of the Penny Creek local fauna, I identified area of overlap in climate envelope models for the snake assemblage of the Penny Creek local fauna. Climate envelope models characterize a set of suitable climates for a species or group of species derived from their location in climate space. While these models are constructed from the associations between the geographic location of a species and its climate without consideration of biotic interactions, dispersal, or evolutionary change, past review has suggested that climate envelope models are capable of producing useful initial approximations of the dynamics of species to climate interactions at appropriate scales (Lawing, 2021). Climate envelope models have been used to evaluate impacts of climate associated changes in the projected geographic distributions of squamates through time to model both the past and future dispersal of a clade (Lawing and Polly, 2011; Lawing et al., 2016).

To create climate envelope models for the Penny Creek snake assemblage, I selected representative congenerics of presumed closely related living species for each of the fossil taxa (see Appendix Table A1 for list of congenerics used for each fossil taxon). I obtained geographic range maps of those congenerics from the IUCN Redlist (IUCN, 2021). Climate data for Mean Annual Temperature (MAT; climatic variable 1) and Annual Precipitation (AP; climatic variable 12) variables from the Worldclim database Version 2.1 (Fick and Hijmans, 2017) at 10-minute resolution were extracted from the polygon overlap of the congeneric species. The two variables described the mean of

temperature and sum of precipitation on an annual basis. All congeneric species were combined into a genus-level dataset to decrease the influence of specific-level difference. Finally, I produced density plot histograms to identify the area of overlap for all generic level models across taxa of the Penny Creek local fauna. I used the area of overlap to infer the potential climate envelope of the depositional setting of Penny Creek.

2.4. Systematic Paleontology

Class Reptilia Laurenti, 1768

Order Squamata Oppel, 1811

Suborder Serpentes Linnaeus, 1758

Infraorder Alethinophidia Nopsca, 1923

Superfamily Booidea Gray, 1825

Remarks — There are not many vertebral characters defining the diverse group of booid snakes; the most commonly cited characters include the absence of paracotylar foramina, the presence of lateral foramina, and higher neural arches than those found in Anilioidea (Holman, 2000; modified from Rage, 1984; supported by Ikeda, 2007). In comparison to Colubroidea, booid vertebrae are generally less slender and elongate, and

tend to have shorter and broader neural spines, at least in North American species (Holman, 2000; Smith, 2013).

Family Charinidae Gray, 1849

Remarks — The following vertebral osteological characters are modified from Brattstrom (1958), Kluge (1993), Bell and Mead (1996), and Holman (2000) to fit the current nomenclature for boiform snakes (Reynolds et al., 2014). The vertebrae possess a flattened neural arch. The neural spines are low, and in the caudal vertebrae are expanded, exhibiting a somewhat distended or distally lobate appearance relative to pre-caudal neural spines (Head, 2015). Prezygapophyseal accessory processes are reduced. Caudal vertebrae are very short, with a variety of processes giving them a complex appearance (with the exception of the genus *Lichanura*).

Snakes of the Charinidae are typically small to medium in size, robust in body form, with short tails and small eyes, all of which assist them in a semifossorial lifestyle (Holman, 2000). Many North American fossil booids, including extant genera *Charina* and *Lichanura*, were previously assigned to the Erycinae, which are generally similar in body form, vertebral morphology, and lifestyle. Under the most recent taxonomy, North American subfamilies Charininae Gray, 1849 (*Charina* and *Lichanura*) and Ungaliophiinae McDowell, 1987 (*Exiliboa* and *Ungaliophis*) are now grouped within the Charinidae (Pyron et al. 2014; Head, 2015). This further complicates the fossil record of older North American snakes not found in Penny Creek in that genera such as *Calamagras*, *Ogmophis*, *Geringophis*, *Pterygoboa*, and others are left with a

somewhat uncertain taxonomic status, although some research has suggested that the fossil species *Ogmophis compactus* and *Calamagras weigeli* may represent loxocemid and ungaliophiine snakes, respectively (Smith, 2013). An extensive apomorphy-based redescription and reorganization of the older fossil taxa may be necessary to determine if it is possible to morphologically differentiate them at the species or genus level given the newer taxonomy of extant booids (Bell et al. 2010; Pyron et al., 2014; Head, 2015).

Genus *Charina* Gray, 1849

Charina cf. *Charina prebottae* Brattstrom, 1958

Referred specimens — UNSM 139981 (1 posterior middle trunk vertebra).

Diagnosis and description — The vertebra appears near square in shape from dorsal view, but is slightly wider at the prezygapophyses than the postzygapophyses (Fig. 2.4). The postzygapophyses are rounded, while the prezygapophyses are moderately pointed with reduced accessory processes, and are raised antero-laterally. The neural spine is low, broad, and is longer than it is tall or wide. The top of the neural spine is broken, but this does not appear to affect the overall shape of the neural spine in dorsal view. The neural spine tapers in width anteriorly and is slightly incised posteriorly. The zygosphene is dorsally flat and v-shaped overall, with somewhat rounded lateral edges that extend slightly forward on the anterior face. In anterior view, the zygosphene is concave. The neural arch is somewhat flattened and deeply incised posteriorly. The cotyl is round and mildly angled ventrally, with the dorsal edge

extending more anteriorly and the ventral edge extending more posteriorly. The subcentral keel is wide, flat, and smooth, ending just before reaching the condylar head. It is bordered laterally by a flat indentation, primarily on the anterior end.

Remarks — The fossils described above are similar in size and morphology to known species of *Charina* and are most similar to *Charina prebottae* specimens from other Nebraska localities. The longer neural spine, the V-shaped (dorsal), strongly concave (anterior) zygosphene, and the depressed neural arch with an incised posterior edge suggest that these vertebrae do not belong to the genus *Lichanura*, however, it should be noted that Bell and Mead (1996) have observed some intraspecific variation in these characters. As in Parmley and Walker (2003), I instead attribute this fossil to the genus *Charina* based on the relative length of the neural spine, which is greater than that of *Lichanura*, and the lack of juvenile characteristics despite being relatively small in size. Parmley and Walker (2003) have observed that *Lichanura* of a similar size show juvenile characteristics such as a short, high overall morphology, thin neural arch, thin and highly arched zygosphene, exceptionally short neural spine, enlarged neural canal, and a condyle that appears too large for the centrum, none of which are visible in this specimen. *Charina prebottae* also exhibits notable variation across a wide geographic area throughout the Miocene (Holman, 2000). Previous literature suggests that *C. prebottae* may be a catch-all taxon for multiple species, as Brattstrom's (1958) un-illustrated account and subsequent illustrated accounts do not completely match (Bell and Mead, 1996). This warrants further study (Bell and Mead, 1996; Holman, 2000). Because this vertebra is badly weathered and missing the extreme parts of several of its

structures but shows no break of the slope of the neural spine as it descends onto the zygosphene (Brattstrom, 1958), and because the vertebra compares favorably to latter descriptions of *C. prebottae* (Holman, 2000), I confer this vertebra to *C. prebottae* until the taxon is more comprehensively assessed and re-diagnosed.

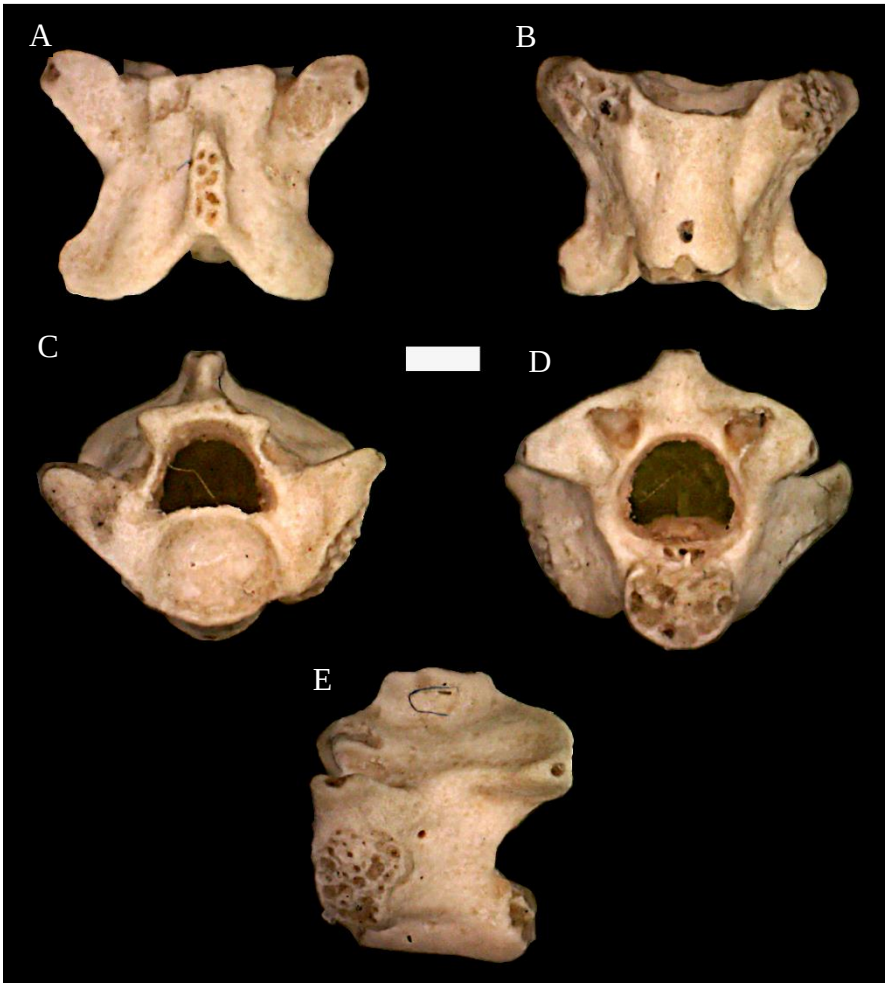

Figure 2.4. Trunk vertebra of *Charina* cf. *Charina prebottae* from the Penny Creek local fauna. From top left: dorsal, ventral, anterior, posterior, and lateral views (anterior to the left). Scale bar = 1 mm

Superfamily Colubroidea Oppel, 1811

Diagnosis and description — Vertebrae within the superfamily Colubroidea are typically longer than wide and lightly built. The neural spines are thin and long when compared to other groups, the zygosphenal and zygantral areas are less massive than in booids, and the synapophyses are distinctly divided into parapophyseal and diapophyseal processes (Holman, 2000). When present, trunk vertebral hypapophyses are relatively long and often pointed. Rage (1984), later supported in Ikeda (2007), noted that both paracotylar and lateral foramina are present throughout colubroids.

Remarks — There is some disparity in what constitutes the defining characters of colubroid vertebrae because of the vast diversity of the group. As such, I saw it fitting to summarize known defining characters in this study. Rage (1984) and Ikeda (2007) identified the presence of both paracotylar and lateral foramina together on the vertebrae as consistent throughout the group. Holman (2000) provided a number of additional characters, but some of the proposed characters describe only some groups of colubroids, and as such, are not included in the diagnosis of the group at this time. These disputed characters include the lack of hypapophyses beyond the cervical region in several groups, and possibly the presence of well-developed prezygapophyseal accessory processes, which Ikeda (2007) was unable to find in several Asian viperids. However, it should be noted that Holman (2000) focused only on North America colubroids, and therefore may have defined the group primarily for North American taxa.

Family Colubridae Oppel, 1811

Diagnosis and description —The trunk vertebrae are lightly built and longer than wide. The neural spines are long and thin, and are as high as or higher than they are long. The subcentral ridges are prominent. Prezygapophyseal accessory processes are present and may be accompanied by epizygapophyseal spines extending posteriorly from the postzygapophyses (Holman, 2000). The hemal keel is relatively thin and may appear similar to one of three types: hemal keels present without parapophyseal process development, both hypapophysis and parapophyseal processes present, and hemal keel thin with somewhat round prezygapophyseal articular processes (Ikeda, 2007).

Remarks — The defining characters for colubrids are complicated by the diversity and degree of variation within the group, and are partially dependent on whether groups such as the natricines are included within (as they are here). Post-cervical hypapophyseal characters would seem to be inappropriate for defining colubrids as a whole as long as natricines are included because, as noted in Ikeda (2007), several studies have pointed out that some natricines lack hypapophyses on their trunk vertebrae, while a small number of non-natricine homalopsine snakes exhibit prominent hypapophyses on their trunk vertebrae.

Subfamily Colubrinae Oppel, 1811

Diagnosis and description — Holman (2000) outlined some general osteological characters for colubrine snakes. The trunk vertebrae are typically longer than wide,

lightly built, and lack hypapophyses. The neural spines are somewhat thin, tall, and project posteriorly over adjacent vertebrae. The prezygapophyseal accessory processes are prominent. The hemal keels are thin and well-produced from the centrum, and the subcentral ridges and grooves are distinct. Epizygapophyseal spines may or may not be present in colubrines.

Remarks — While Holman's (2000) diagnosis of colubrines appears to fit North American taxa, Ikeda (2007) noted that lightly built vertebrae and relatively thin hemal keels are not features consistent with some non-North American taxa, as these features show various states amongst extant species. These characters may only be consistently useful for North American taxa, and should not preclude taxa from being assigned to the subfamily Colubrinae if those characters are not present as described in Holman (2000).

Genus *Lampropeltis* Fitzinger, 1843

Lampropeltis similis Holman, 1964

Referred specimens — UNSM 139982 (14 pre-cloacal trunk vertebrae).

Diagnosis and description — In anterior view, the neural arch is moderately vaulted (Fig. 2.5). The cotyl is a depressed oval bordered by deeply excavated pits, and is slightly larger than the ventrally restricted, inverted U-shaped neural canal. The zygosphene curves dorsally, and the prezygapophyseal articular facets tilt slightly upward. The diapophyses and parapophyses are distinct elements of the parapophyses,

with the latter portion more distally pointed than the former; however, they are not as clearly separated as in most other colubrids.

In dorsal view, the vertebrae are approximately as long as they are wide at the prezygapophyses, and the width at the well-developed, rounded prezygapophyseal accessory processes is greater than it is long through the zygapophyses. The neural spine tilts slightly ventrally in its anterior portion. The prezygapophyseal articular facets are oval to ovoid and slightly tilted upward. The epizygapophyseal spines are absent. The anterior edge of the zygosphene is slightly convex to slightly sinuate; the posterior notch of the zygosphene is V-shaped.

In lateral view, the neural spine is significantly longer than it is tall, and dips slightly downward cranially. The hemal keel is visible and quite strong. In posterior view, the neural arch is moderately vaulted, and the condyle is a dorso-ventrally depressed oval.

In ventral view, the strong hemal keel is spatulate or oblong in shape, but not wide throughout most of its length. Subcentral ridges are present and concave from below, but not exceptionally developed. The postzygapophyseal articular facets are ovoid.

Remarks — Holman (2000) suggested that *Lampropeltis* vertebrae are more easily diagnosed on a species-by-species basis, as there are greater differences among some species of *Lampropeltis* than there are among some other colubrine genera (such as

Coluber and *Masticophis*). This idea was reexamined and discussed in Parmley and Hunter (2010). *Lampropeltis alterna* and the *Lampropeltis pyromelana-zonata* grouping have diagnostic vertebral characters distinct from each other and from the rest of the genus, while *Lampropeltis getula*, *Lampropeltis calligaster*, and *Lampropeltis triangulum* form a discernable *L. getula* complex. Where exactly the known fossil species of *Lampropeltis* fall within the genus could therefore be dependent on the ability to discern between these three main morphospaces on a case-by-case basis. A better understanding of these morphospaces and the morphology of fossil species could also help determine when the genus started exploring the various morphologies associated with these groupings.

These vertebrae in particular appear to be more similar to the general morphology of the kingsnake *Lampropeltis calligaster* or the milksnakes of the *Lampropeltis triangulum* complex as opposed to the *L. alterna* or *L. pyromelana-zonata* groupings. They possess long neural spines, moderately depressed neural arches, distinct hemal keels with deep subcentral grooves, and robust, distinct subcentral ridges (Parmley, 1990; Parmley and Hunter, 2010). More specifically, *L. similis* has previously been described as similar in appearance to *L. triangulum*; however, *L. similis* possesses a less depressed neural arch in the trunk region with an inverse U-shaped rather than depressed ovoid-shaped neural canal, a thinner hemal keel, and a neural arch more similar to that of *L. calligaster*. Holman (2000) also stated a centrum that "is not as triangular from below" as an additional apomorphy for *L. similis*, but I am unable to confirm this as a consistent character throughout the vertebral column of the species.

Figure 2.5. Trunk vertebra of *Lampropeltis similis* from the Penny Creek local fauna. From top left: dorsal, ventral, anterior, posterior, and lateral views (anterior to the left). Scale bar = 1 mm.

Genus *Pantherophis* Fitzinger, 1843

Diagnosis and description — The vertebrae of North American *Pantherophis* are relatively short, but robustly built compared to most of their contemporary colubrids. The vertebrae have wide, high neural spines and broad hemal keels, but lack epizygapophyseal spines (Holman, 2000; Parmley and Hunter, 2010). The parapophyseal process is poorly developed on either side, and the interzygapophyseal ridge is straight in lateral view (Ikeda, 2007).

Remarks — The vertebrae of North American *Pantherophis* are similar to some species of other large-bodied colubrine genera. In North America, the vertebrae of *Pantherophis* differ from those of New World *Masticophis* and *Coluber* in that they are relatively shorter and more robustly built, have higher and wider neural spines, have wider hemal keels, and lack epizygapophyseal spines (Holman, 2000). *Pantherophis* generally differs from *Lampropeltis* in possessing a higher, more vaulted neural arch, a higher neural spine (compared to at least some species of *Lampropeltis*), less defined subcentral ridges, and less robust vertebrae (Holman, 2000; Parmley and Hunter, 2010). *Pantherophis* differs from *Pituophis* in having a lower neural spine and a zygosphene that is rarely or never concave (Auffenberg, 1963). There has been no work to definitively separate the skeletal morphology of *Pantherophis* and *Elaphe*, in part because their reclassification as separate genera have not been morphologically defined since their separation in Utiger et al. (2002).

Pantherophis kansensis Gilmore, 1938

Referred specimens. — UNSM 139983 (21 pre-cloacal trunk vertebrae).

Diagnosis and description. — In anterior view, the neural spine is relatively low for a colubrid, the neural arch is moderately vaulted, and the zygosphene is convex dorsally. The zygosphenal articular facets are strongly tilted dorso-ventrally. The neural canal is rounded and slightly smaller than the cotyl, which is also round. The prezygapophyseal articular facets tilt slightly upward, and the diapophyses and parapophyses are rounded, distinct sections of the synapophyses.

In dorsal view, the neural spine is long and located in the middle of the vertebra. The anterior edge of the zygosphene is concave. The prezygapophyseal accessory processes are moderately pointed, the prezygapophyseal articular facets are rounded to oval and tilted slightly upward, and the epizygapophyseal spines are absent. The posterior edge of the neural arch in dorsal view is slightly rounded.

In lateral view, the neural spine is approximately twice as long as it is high. The condyle is tilted slightly forward. The hemal keel is distinct from the centrum, and the synapophyses can clearly be divided into diapophyseal and parapophyseal sections. The interzygapophyseal ridge is bowed downward, and the subcentral ridge is bowed upward.

In posterior view, the neural arch is somewhat vaulted. The condyle is round and approximately the same size as the neural canal, which is an inverted U-shape. The

zygosphenal articular facets and the postzygapophyseal articular facets are all tilted sharply upward. The diapophyses and parapophyses are distinct parts of the synapophyses.

In ventral view, the centrum is triangular and bordered by visible subcentral ridges. The hemal keel is well developed, moderately wide, and constricted in the middle relative to the ends. The prezygapophyseal accessory processes are distinct, oblique, and directed anterolaterally. As in other views, the synapophyses are distinctly divided into the diapophyses and parapophyses.

Remarks. — *Pantherophis kansensis* has vertebrae with a lower neural spine and more anterolaterally directed prezygapophyseal accessory processes than any other known species of *Pantherophis* or *Bogertophis*. This neural spine is relatively taller in some specimens, and is proportionally more similar to *Pantherophis obsoletus* in that regard; these vertebrae appear to be from a more anterior portion of the vertebral column.

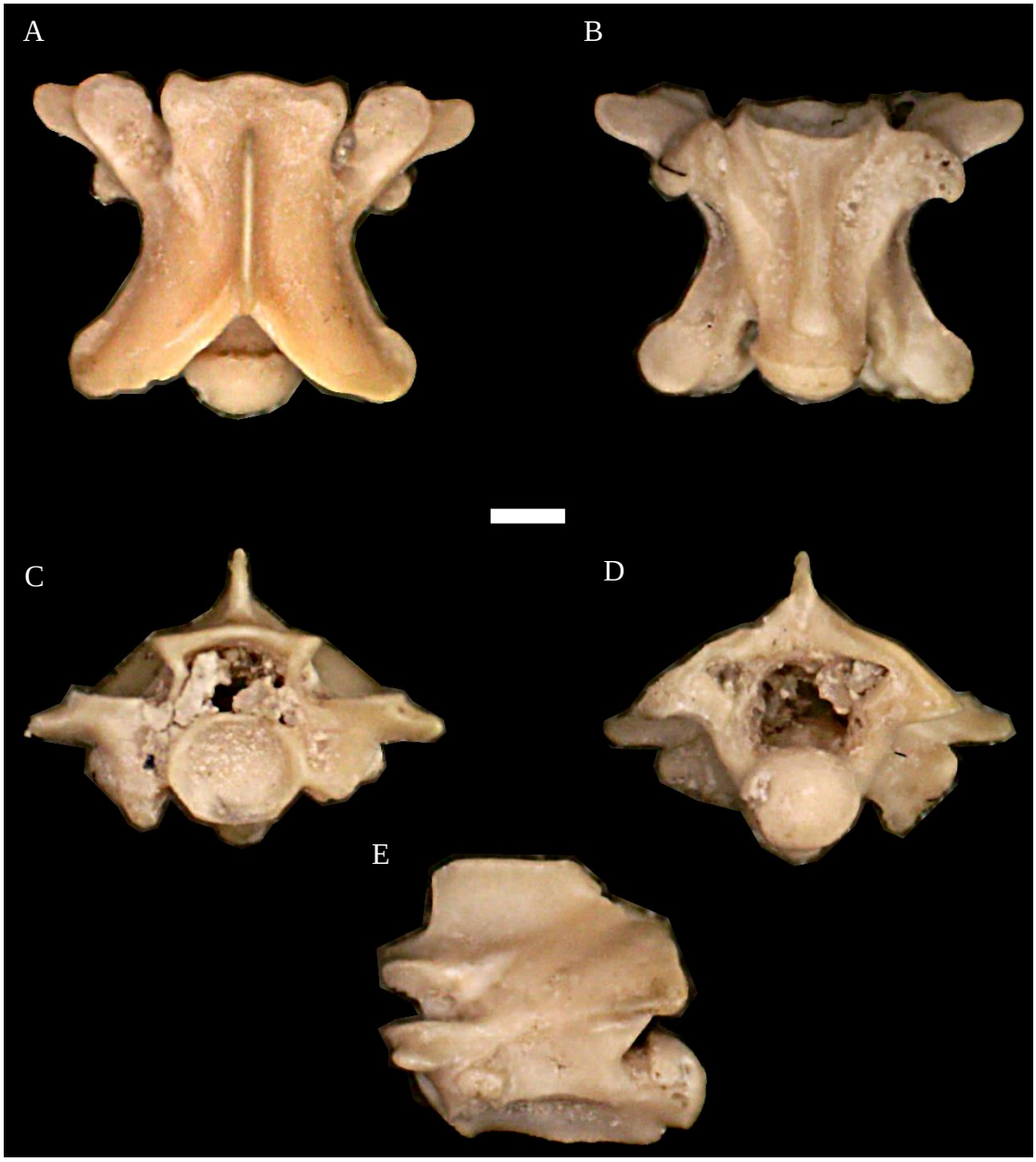

Figure 2.6. Trunk vertebra of *Pantherophis kansensis* from the Penny Creek local fauna. From top left: dorsal, ventral, anterior, posterior, and lateral views (anterior to the left). Scale bar = 1 mm.

Genus *Salvadora* Baird and Girard, 1853

Diagnosis and description — Generally, *Salvadora* can be identified by the combination of the following characters: (1) a thin, relatively low neural spine that gets shorter posteriorly through the trunk region; (2) obsolete to absent epizygapophyseal spines; (3) vertebrae that are approximately as wide as they are long; and (4) dorsally convex subcentral ridge in lateral view (Holman, 1973).

Remarks — The delicate neural spine and invariably thin hemal keel is similar to that found in other North American colubrids such as *Coluber* or *Masticophis*. However, *Salvadora* can be identified separately from those taxa on the basis of a proportionally shorter vertebra that appears to be nearly as wide as it is long, whereas the other two taxa appear elongate, possess more dorsally convex subcentral ridges, and have obsolete to absent epizygapophyseal spines.

Salvadora paleolineata Holman, 1973

Referred specimens — UNSM 139984 (8 pre-cloacal trunk vertebrae).

Diagnosis and description — The description is similar to Holman (2000) unless otherwise noted. In anterior view, the cotyl is a slightly depressed oval bookmarked by relatively large paracotylar foramen to each side (Fig. 2.7). The neural canal is similar in size to the cotyl and is an inverted U-shape with medially convex sides to the neural arch. The zygosphene is dorsally convex in this view. The prezygapophyses are tilted slightly upward, and the prezygapophyseal accessory processes are well developed.

In dorsal view, the vertebra is approximately as wide as it is long. The neural spine is thin and slightly overhangs the neural arch posteriorly. The zygosphene is slightly convex anteriorly. The prezygapophyseal articular facets are subrounded, and the prezygapophyseal accessory processes are approximately two-thirds as long as the width of the prezygapophyseal articular facets, are well-developed, and are moderately pointed. The diapophyses are only somewhat directed laterally and are barely visible from this orientation.

In lateral view, the neural spine is delicate and is low, over three times as long as it is tall, with a slight anterior and posterior overhang. The subcentral groove is relatively deep, with dorsally convex subcentral ridges and a clear, uniform hemal keel. The condyle is tilted somewhat postero-dorsally, while the cotyl is oriented slightly antero-ventrally. The lateral foramen are positioned near the center of the vertebrae in this orientation, just below the interzygapophyseal ridge. Epizygapophyseal spines are absent.

In posterior view, the subcentral ridges are well developed and narrow, and the hemal keel is strongly developed and uniformly thin. The postzygapophyseal articular facets are subrounded. The condyle is a slightly depressed oval. Epizygapophyseal spines are absent, as also seen in the lateral orientation.

In ventral view, the zygosphene is slightly convex anteriorly. The prezygapophyseal accessory processes are well developed. The hemal keel is uniformly

thin. Both the cotyl and the condyle are oval in shape and the condyle extends to be approximately even with the postzygapophyseal articular facets.

Remarks. — According to Holman (2000) and my own comparisons, the vertebrae from Penny Creek assigned to *S. paleolineata* are primarily from the middle trunk region, as noted by neural spines somewhat taller than in the type specimen and the larger condylar-cotylar articulation. As in Holman's description, none of the specimens appear to have epizygapophyseal spines; as such, taxonomic assignment to *S. paleolineata* is possible. *S. paleolineata* is suggested as an ancestral species to modern *Salvadora* species, which appear to be quite similar, but possess obsolete epizygapophyseal spines (Holman, 1973). It is possible that, as in *Heterodon* and other similar cases, there may be greater morphological differences in the elements of the skull, should they ever be found for this species.

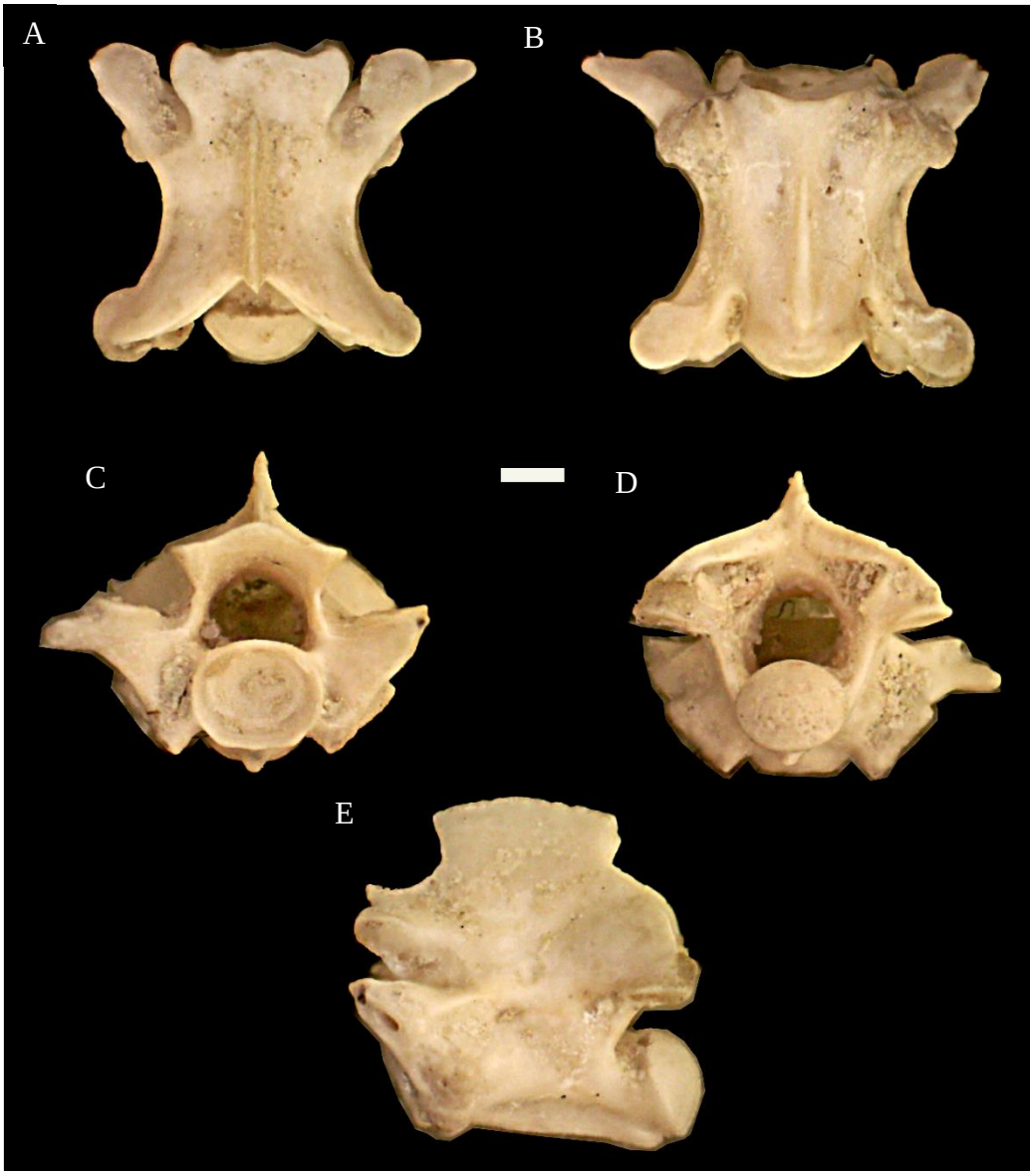

Figure 2.7. Posterior trunk vertebra of *Salvadora paleolineata* from the Penny Creek local fauna. From top left: dorsal, ventral, anterior, posterior, and left lateral views. Scale bar = 1 mm.

Subfamily Dipsadinae Bonaparte, 1838

Genus *Heterodon* Latreille, 1801 (in Sonnini and Latreille, 1801)

Referred specimens — UNSM 139985 (12 pre-cloacal trunk vertebrae).

Diagnosis and description — The trunk vertebrae of *Heterodon* can exhibit a very depressed to slightly vaulted neural arch, a neural spine that is longer than it is high, and a wide, but flattened (or even absent) hemal keel (Holman, 2000). The vertebrae are short and wide, giving them a somewhat squarish appearance (Fig. 2.8).

In dorsal view, the vertebrae of *Heterodon* are nearly square to slightly longer than wide. The anterior edge of the zygosphene is convex, and the prezygapophyseal facets, when preserved, are ovoid in shape. The prezygapophyseal accessory processes are well-developed and the tips are moderately pointed to obtuse. Epizygapophyseal spines are absent. The postzygapophyseal accessory processes are ovoid in shape.

In anterior view, both articular facets are visible on the synapophyses. The cotyl is mostly round, but sometimes slightly taller than wide. The neural arch is depressed. The neural canal is similar in shape to a ventrally restricted semi-cylinder, even somewhat squarish, and similar in size to the cotyl. The cotyl is somewhat dorso-ventrally compressed, with well-excavated pits on either side.

In lateral view, the neural spine is longer than it is tall, somewhat depressed, and is typically more undercut posteriorly than anteriorly. In posterior view, the shape of the condyle is a dorso-ventrally compressed oval, and similar overall to the cotyl.

In ventral view, the hemal keel generally is weak, wide, and oblong, and very depressed to flat. In some specimens, the hemal keel is slightly more distinct, and is slightly constricted between the synapophyses, indicating a more anterior trunk position for these vertebrae. The subcentral ridges are indistinct. The centrum itself is longer than it is wide.

Remarks — Though it is not typically difficult to identify trunk vertebrae at the generic level for *Heterodon*, individual vertebrae of this genus are difficult to distinguish at the species level. They share most diagnostic features with the genus *Farancia*, but the vertebrae of *Farancia* generally exhibit a more vaulted neural arch and a neural spine that is undercut both anteriorly and posteriorly (Holman, 2000).

The somewhat vaulted nature of the neural arch in the specimens from Wt 13B when compared to extant *Heterodon* vertebrae would previously have suggested that these fossils belong to *Heterodon* (or *Paleoheterodon*) *tiheni*, a species that is more easily determined based on skull morphology, rather than vertebral morphology (Holman, 1964; Holman, 2000; Parmley and Hunter, 2010). However, Parmley and Hunter (2010) determined that this neural arch character showed considerable and overlapping variation in specimens assigned to *Paleoheterodon* and *Heterodon*, and that vertebral characters are not sufficient to differentiate between the two taxa.

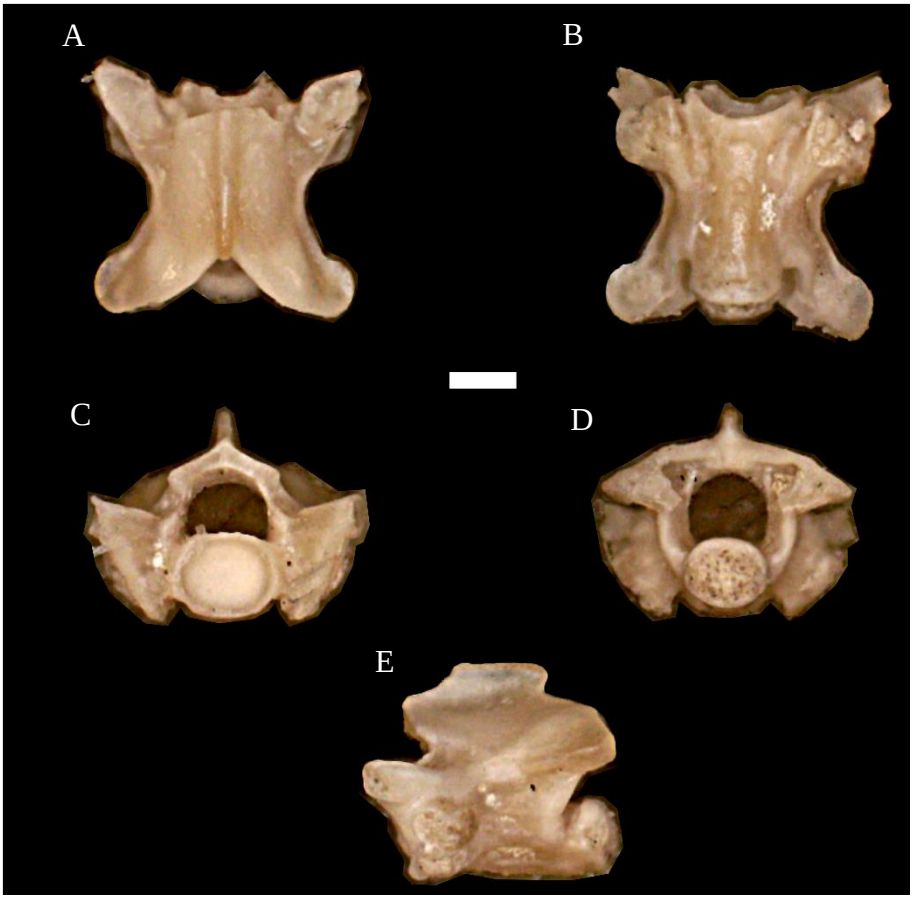

Figure 2.8. Middle trunk vertebra of *Heterodon* from the Penny Creek local fauna. From top left: dorsal, ventral, anterior, posterior, and lateral views (anterior to the left). Scale bar = 1 mm.

Subfamily Natricinae Bonaparte, 1840

Diagnosis and description — North American natricine vertebrae have well-developed, pointed hypapophyses directed posteriorly on the trunk vertebrae (Holman, 2000). These hypapophyses are usually sigmoid in shape (Szyndlar, 1991). The vertebrae overall are lightly built and elongate, with long centra, strong subcentral

ridges, posteriorly vaulted neural arches, and somewhat short parapophyseal processes (Szyndlar, 1991).

Remarks — Szyndlar (1991) differentiated natricine snakes from other snake groups known to possess hypapophyses on their trunk vertebrae. Natricines differ from viperids in exhibiting hypapophyses that are somewhat sigmoidal in shape, and in possessing relatively longer centra, posteriorly vaulted neural arches, and shorter parapophyseal processes. They differ from elapids in being more lightly built overall, with much longer centra and prominent subcentral ridges.

Despite the hypapophyses being presented as a definitive character for natricines as a whole, Ikeda (2007) showed that there are a few Asian exceptions to this rule, possibly representing a loss of this character later in the evolution of those species.

Genus *Neonatrix* Holman, 1973

Diagnosis and description — *Neonatrix* trunk vertebrae are most easily characterized by very short hypapophyses that strongly project posteriorly, are ventrally beveled in most North American species (except *Neonatrix elongata*) but are weakly developed, terminally rounded, and do not extend beyond the end of the condyle. Furthermore, they are relatively small and distinctly longer than wide. The neural spines of *Neonatrix* are much longer (up to 4x) than wide (Holman, 1973, 2000; Parmley and Hunter, 2010), with reduced or absent hooked projections at each terminal end.

Remarks — The hypapophyses of North American species of *Neonatrix* are less well-developed than the reported species from Europe (Holman, 1973, 1982, 1996; Rage and Holman, 1984) and shorter than in any other natricine genus (Holman, 1973, 2000).

Neonatrix elongata Holman, 1973

Referred specimen. — UNSM 139986 (17 pre-cloacal trunk vertebrae).

Diagnosis. — The diagnosis follows that of Holman (2000) and is only modified where otherwise noted. *Neonatrix elongata* trunk vertebrae are longer than wide, with a neural spine that is drastically longer than it is tall or wide (Fig. 2.9). The vertebrae possess poorly developed hypapophyses reaching only the posterior portion of the centrum, and unbeveled neural spines that end just short of the posterior end of the cotyle.

In anterior view, the neural canal is shaped like a ventrally restricted semi-cylinder, is medially convex at the sides, and is slightly narrower than the round cotyl. The zygosphene is convex dorsally. The synapophysis is developed. For the first time in this genus and species, I confirm the presence of paracotylar foramina in anterior view, adjacent to the cotyle on each side, approximately half-way down the cotyle. Previous descriptions exhibited excavated cavities on either side of the cotyle, but could not observe any foramina based on the specimens available.

In dorsal view, the centrum is longer than wide. The prezygapophyseal articular facets are ovoid in shape. This is a correction of Holman (2000), which appears to have

mistakenly labeled the prezygapophyseal processes as ovoid, rather than the articular facets. The prezygapophyseal processes are long and somewhat pointed on the anterior end. The diapophyses only slightly extend out laterally. The epizygapophysel spines are absent or obsolete.

In lateral view, the vertebrae are elongate. The neural spine is over two times as long as it is high. The neural spine is rarely preserved at the ends in Penny Creek fossils and in *Neonatrix* throughout the fossil record, and so is difficult to observe, but a few mostly preserved neural spines from Penny Creek material allow me to determine the absence of an anterior projection, and an extremely reduced to absent – typically absent – posterior overhang. The subcentral ridge is convex dorsally. The prezygapophyses tilt somewhat dorsally. The hypapophysis is short and ends short of the posterior-most part of the condyle; I find that it is does not extend past even the anterior-most part of that articulation in these specimens.

In posterior view, I find that the condyle is nearly circular, but is slightly depressed and closer to an oval shape in some vertebrae. The neural arch is vaulted, steeply incised by the zygantral articular facets, and similar in size to the condyle. The hypapophysis is visible below the condyle around one-half of the condyle's height when undamaged. The postzygapophyses tilt slightly upward, just as in the prezygapophyses. In ventral view, the centrum is long and narrow. The subcentral grooves are shallow, and the hemal keel narrows slightly anteriorly to the robust but truncated hypapophysis.

Remarks. — Like other species of North American *Neonatrix, N. elongata* have less well-developed hypapophyses that do not extend as far posteriorly (relative to the condyle) as seen in the European species (Rage and Holman, 1984). *Neonatrix elongata* occurs earlier than other North American species of *Neonatrix* and is known to occur more broadly in a temporal and geographic manner throughout the Miocene. In the Penny Creek specimens, the unbeveled neural spine and unbeveled hypapophysis that ends just short of the posterior end of the cotyl indicate that these fossils belong to *N. elongata*, as opposed to other known species of *Neonatrix*. There is some variation on how rounded (or pointed) the posterior tips of the hypapophyses are, likely indicating a small amount of intracolumnar variation in the hypapophyseal morphology of the species (LaDuke, 1991; McCartney, 2015). Nonetheless, I have not observed more variation within an individual taxon than between species, and the morphology is generally consistent with what is described above. *Neonatrix elongata* is typically smaller than *Neonatrix magna* and *Neonatrix infera,* but the taxon's relative length and neural spine height are intermediate between the other two species, which are either more elongate with a shorter neural spine (*N. infera*) or less elongate with a taller neural spine (*N. magna;* Holman, 2000). It is noteworthy that these specimens show some measure of variation in terms of the neural spine height and the shape of the hypapophyses, some of which appear similar to some morphologies known in the other North American species. Given that *N. elongata* was considered to have "intermediate" morphologies by Holman (2000), it may be necessary to further study the intracolumnar

variation with *Neonatrix* for additional definitive characters and consider potential changes to the taxonomy of the species within.

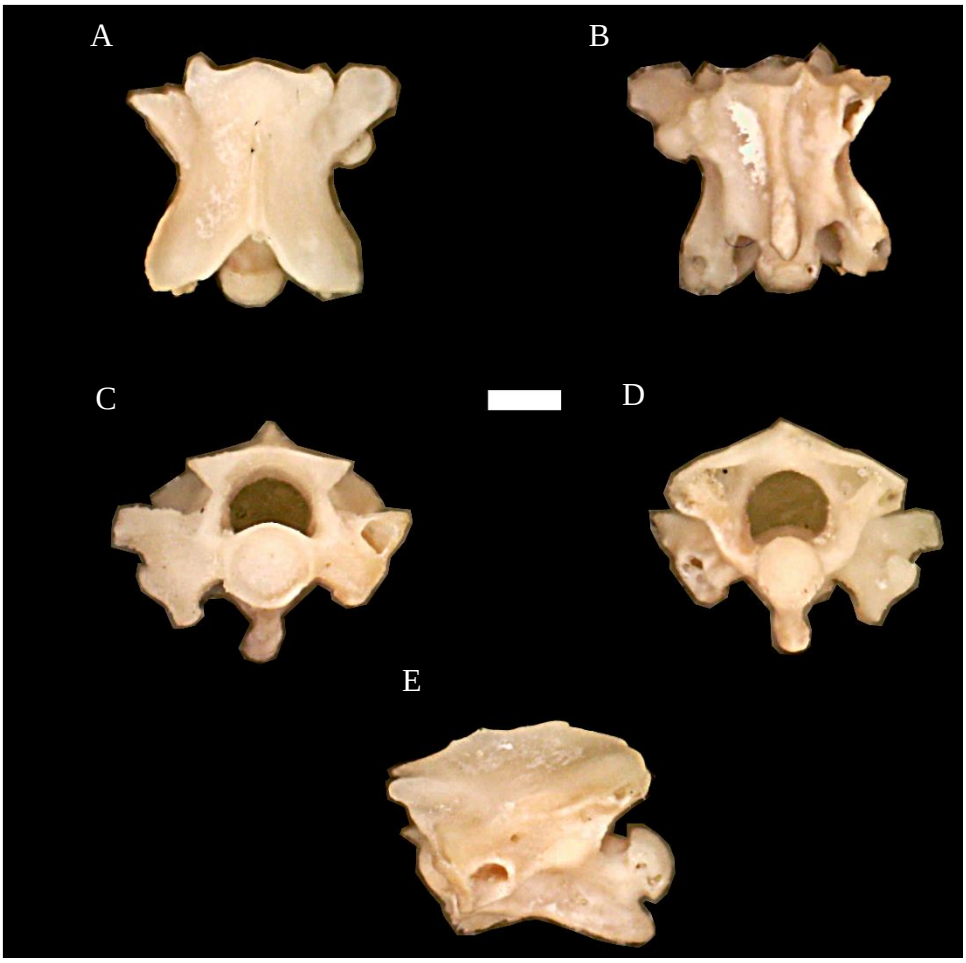

Figure 2.9. Posterior trunk vertebra of *Neonatrix elongata* from the Penny Creek local fauna. From top left: dorsal, ventral, anterior, posterior, and lateral views (anterior to the left). Scale bar = 1 mm.

Neonatrix magna Holman, 1982

Referred specimens. — UNSM 139987 (8 pre-cloacal trunk vertebrae).

Diagnosis. — The diagnosis is based on that of Holman (2000) but is modified where noted. The vertebrae are mainly distinguished by (1) a very poorly developed hypapophysis that typically terminates near the posterior part of the centrum; (2) ventral portion of the hypapophysis beveled and ending well anterior to the condyle; (3) vertebral size relatively large (at least relative to other North American *Neonatrix* at >5mm); (4) vertebrae nearly the same width and length; and (5) neural spine near same height and length (Fig. 2.10).

In anterior view, the cotyl is round and similar in size to the neural canal, which is an inverted U-shape with slightly convex lateral sides. The zygosphene is dorsally straight. The prezygapophyses are slightly tilted dorsally. Short excavations with single, centered paracotylar foramen border each side of the cotyl. I observe that the synapophyses that are missing from previous descriptions are moderately well developed and differentiated.

In dorsal view, the centrum's length and width are similar. The prezygapophyses are ovoid. The neural spine is somewhat thick and slightly overhangs posteriorly when preserved. Epizygapophyseal spines are absent. The zygosphene is slightly convex anteriorly. The diapophyses are produced laterally enough to be seen from the dorsal orientation.

In lateral view, the vertebra is only slightly elongate. The neural spines are not completely preserved but appear as though they are similar in height and length. There is a slight overhang on the posterior border of the neural spine. The hypapophysis is beveled ventrally, about as tall as it is long, and ends anterior to the condyle, but appears to have rounded rather than the pointed tips observed by Holman (1982; 2000).

In posterior view, the neural arch is significantly vaulted. I observed that the condyle is mostly round and slightly compressed, rather than truly oval, and is similar in size to the neural canal. The hypapophysis strongly projects ventrally and is clearly visible below the condyle.

In ventral view, the hypapophysis is somewhat narrow, ends clearly anterior to the anterior end of the condyle, and is beveled on the ventral surface. The subcentral ridges are well developed.

Remarks. — *Neonatrix magna* has the shortest relative length and widest appearance, the highest neural spine, and most anteriorly terminating hypapophyses of any species of *Neonatrix* in North America or Europe. It also has somewhat less strongly developed subcentral ridges and deeper subcentral groups than *N. elongata* or *N. infera*.

Several of my observations contribute to or differ slightly from previous descriptions of the species. I observe that the synapophyses are moderately developed. The hypapophyses of the specimens have rounded rather than pointed tips, and the condyle, while slightly depressed, is better described as round rather than oval.

Comparison with specimens of *N. elongata* and examination of intracolumnar differences in vertebral morphology in extant natricine snakes suggest that the hypapophysis does change shape along the column; however, the differences in the hypapophysis alone between the two species described from fossils seems to be greater than generally seen in other natricines, except between anterior or middle trunk vertebrae and precloacal vertebrae. Given other morphological differences discussed above and the observation that *N. magna* is not smaller but would appear to have a morphology more similar to the smaller posterior trunk and precloacal vertebrae, I do not believe that these vertebrae represent the same species. Nonetheless, little is known about the intracolumnar variation of *Neonatrix* at this time, as preserved elements are mainly trunk vertebrae; this would seem to warrant a more complete investigation, as also suggested by Jasinski and Moscato (2017).

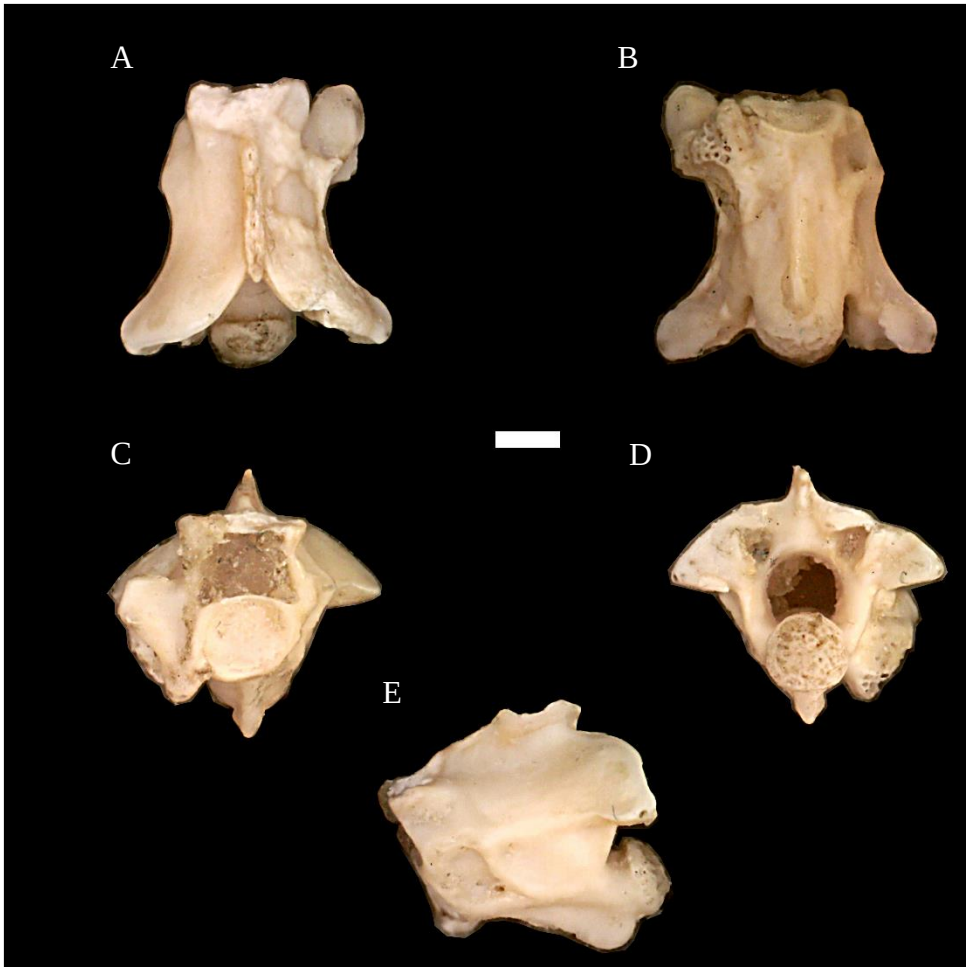

Figure 2.10. Trunk vertebra of *Neonatrix magna* from the Penny Creek local fauna. From top left: dorsal, ventral, anterior, posterior, and lateral views (anterior to the left). Scale bar = 1 mm.

Genus *Nerodia* Baird and Girard, 1853

Nerodia sp. indet.

Referred specimens. — UNSM 139988 (24 pre-cloacal trunk vertebrae).

Diagnosis. — The trunk vertebrae of *Nerodia* are large in size and relatively short and wide (Fig. 2.11). The neural spine is tall, but rarely preserved in its entirety. The hypapophyses on each precaudal vertebra are well-developed, laterally compressed, directed posteriorly, and usually end in a somewhat pointed tip. The hypapophysis extends beyond the condylar head, although the degree to which it does so differs between some taxa, and perhaps between individuals, though this has not been extensively studied at this time.

Remarks. — The trunk vertebrae of *Nerodia* relative to other North American natricines are typically medium to large in size and relatively short and wide, with a high neural spine. *Nerodia* vertebrae are typically less elongate than *Thamnophis* vertebrae, with a more ventrally-oriented hypapophysis. They possess higher neural spines than *Storeria*, *Tropidoclonion*, and *Virginia*, and the hypapophyses are longer and less squared in shape when compared to *Regina* (Holman, 2000). The only other concurrent species during the Miocene is *Nerodia hillmani* and an indeterminate species from the Pratt Slide (Bw 123) locality, which is ~10.5-9.5 Ma (Clarendonian 3). Based on the larger size, longer hypapophysis, and longer prezygapophyseal articular facets, the *Nerodia* fossils described here are more similar to the unnamed Pratt Slide species than to *N. hillmani*.

Comparison to more specimens, extant *Nerodia sipedon* and the somewhat younger *Nerodia hibbardi* from the Pliocene of Idaho and possibly Texas (Holman, 1968; Holman, 2000) may be necessary before assigning a species-level classification to these fossils.

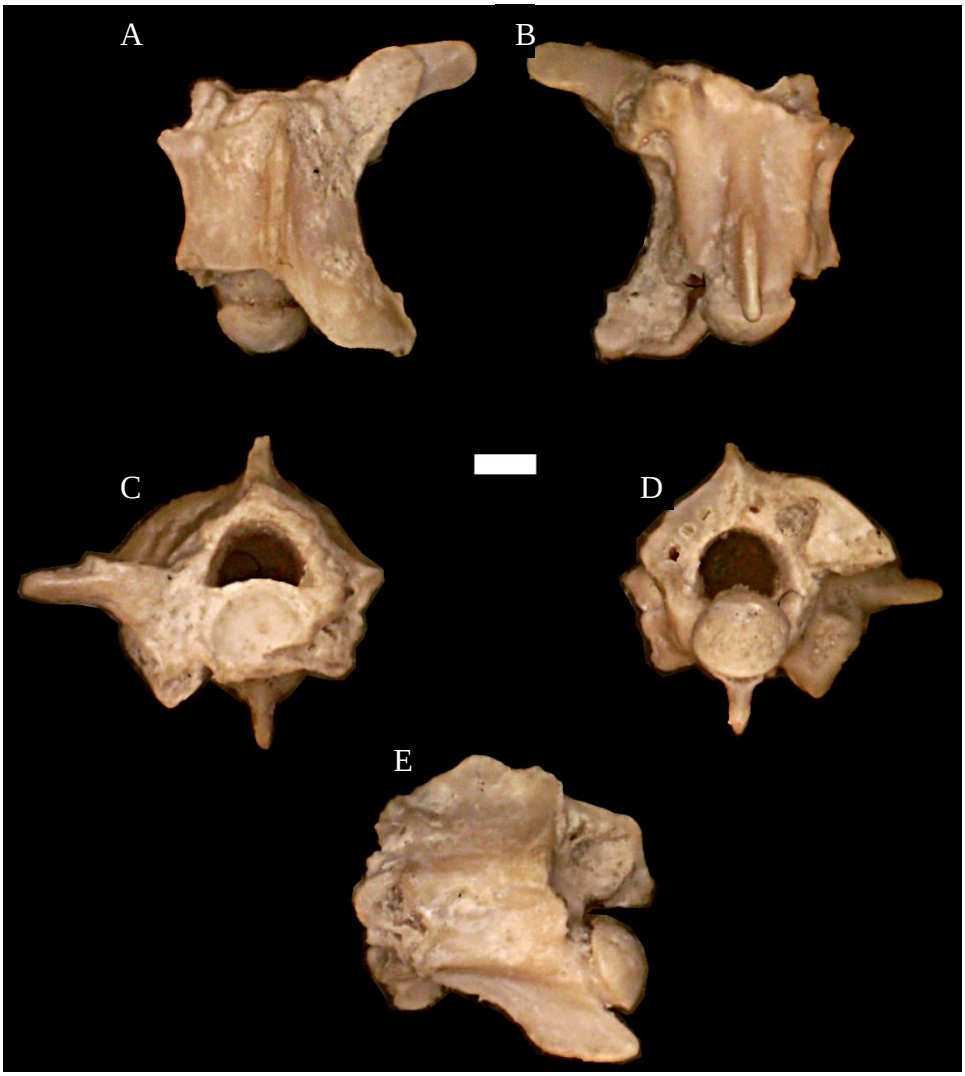

Figure 2.11. Posterior middle trunk vertebra of *Nerodia* sp., from the Penny Creek local fauna. From top left: dorsal, ventral, anterior, posterior, and lateral views (anterior to the left). Scale bar = 1 mm.

2.5. Results and Discussion

The Neogene fossil record of the Central Great Plains has produced the most significant and continuous record of the evolution and modernization of snakes in North America (Fig. 2.3). While the number of taxa represented in Penny Creek locality Wt 13B is low when compared to some other Nebraska localities, such as the older Late Barstovian Myers Farm Local Fauna or the younger Late Clarendonian Pratt Slide Local Fauna (Holman, 1977; Parmley and Hunter, 2010), the Penny Creek snake assemblage is a crucial piece of evidence to understand diversification and modernization of North American snake faunas. As the only described snake assemblage from the earliest Clarendonian (12.5-12.0 Ma), the presence of the snake species identified here can now be confirmed as having been present in the area, whereas the presence (or absence) of these taxa could previously only be assumed based on bracketing snake assemblages from older and younger localities (Fig. .2). Furthermore, the snakes of Wt 13B represent a case of non-testudine reptiles documented in a period temporally bracketed by the earlier peak of reptilian diversity in the warmer, more humid, and likely more closed environments of the Late Barstovian of the Central Great Plains (Holman, 1977; Jacisin et al., 2015) and the later Yellowstone hotspot eruption that preserved the Ashfall Fossil Beds lagerstätten in an opening, cooler, and more arid northeastern Nebraska (Voorhies, 1992).

Of the eight taxa identified at Penny Creek, all taxa described to the species level are extinct; however, only *Neonatrix* is extinct at the genus level. *Charina*, which still

persists in western North America, and *Salvadora*, which persists in the southwestern United States and Mexico, are extirpated from Nebraska and the Central Great Plains. All other genera described from Penny Creek currently persist in the Central Great Plains. Thus, approximately 88.9% of this assemblage can be considered taxonomically "modern" or extant at the genus level. Furthermore, the low abundance of booid snakes – represented here by a single taxon (*Charina*) – relative to colubroid snakes bridges the previous temporal gap in the transitional modernization of North American snake assemblages.

The lack of identified material for other previously common booids such as *Calamagras*, *Geringophis*, *Ogmophis*, *Pterygoboa*, and *Tregophis* does not reject the possibility of these taxa persisting over a wide geographic range in the post-Barstovian Central Great Plains, but their absence (or relative rarity) at both this locality and nearly all other published younger Miocene localities in the Central Great Plains is notable. Only two documented younger Clarendonian localities in the Central Great Plains have identified booids not attributable to *Charina* or *Lichanura*, and these localities are associated with environmental settings that differ from similarly-aged localities in the same region. The WaKeeney local fauna may preserve a "small stream-filled basin" depositional environment with vegetation and climate apparently comparable to present-day southeastern Texas during the Middle Clarendonian (Holman, 1975). One vertebra each – both of which represent the type specimens for both taxa – of *Tregophis brevirachis* and *Ogmophis pliocompactus* were described out of 1230 total snake vertebrae, an exceptionally low occurrence rate for the total number of snake fossils,

although 1230 vertebrae are unlikely to represent 1230 individuals (Holman, 1975). The Pratt Slide local fauna has been suggested as a wooded valley occupied by a riparian stream that is adjacent to a savanna landscape; this idea is supported by geological, paleontological, and isotopic data and differs from other localities of the Late Clarendonian in Nebraska (Rudnick, 1994; Parmley and Hunter, 2010; Parmley et al., 2015; Kita et al., 2014). This assemblage contains *Calamagras* sp. indet. or *Ogmophis* sp. indet., along with the second documented occurrence of *Tregophis brevirachis*. Both taxa are represented at Pratt Slide by three identifiable vertebrae each. As far as I am currently able to determine based on known occurrences and the above information, it seems possible that the state of the North American booid fossil record represents a true decline in extinct booid taxa in terms of both geographic range and relative abundance, rather than a lack of preservation during the Clarendonian and later. In broader terms, it is possible that the Clarendonian of North America represents a near-complete decline (but not necessarily complete loss) of now-extinct booid taxa as soon as the Central Great Plains began transitioning to a more open, arid, cooler, and seasonal environment from more closed, humid Barstovian environments. If that is the case, then the aforementioned examples above may represent a few persistent pockets containing relatively rare holdovers, where environmental conditions were more reminiscent of those in the Late Barstovian of the same region.

The transition away from extinct colubroids, for the most part, appears more prolonged. Starting with the Late Barstovian, *Dakotaophis* makes its last appearance in the Bijou Hills local fauna of South Dakota (Holman, 1978), and *Micrurus* is extirpated

from the region (Holman, 1977), and then does not reappear until the Early Pleistocene (Irvingtonian I) Inglis IA site of Florida and the Middle to Late Pleistocene (Irvingtonian 2) Fyllan Cave Fauna of Texas (Meylan, 1982; Holman and Winkler, 1987). As in the booids above, *Texasophis* and *Ameiseophis* make their final appearances at the unique Wakeeney, Ashfall, and Pratt Slide localities in the Middle and Late Clarendonian of the Central Great Plains (Parmley and Hunter, 2010). *Paracoluber* and *Nebraskophis* last appear in the Hemphillian (Late Miocene) Lemoyne Quarry of Nebraska; and *Salvadora* is extirpated from the region following the Hemphillian. Finally, *Neonatrix* makes its last known appearance in the Central Great Plains at Lemoyne Quarry, but may potentially be present in the Hemphillian Mio-Pliocene Gray Fossil Site of Northeastern Tennessee as well (Parmley and Holman, 1995; Jasinski and Moscato, 2017).

The PCoA and complete-linkage HCA produced similar results regarding the dissimilarity of the 19 selected fossil localities from Nebraska. The PCoA illustrates that axes 1 and 2, which represented 29.7% and 14.6% (44.3% total) of the variation in the dataset, indicate that the loss of "archaic" booids and colubroids (particularly natricines) and the introduction of "modern" colubroids – including more diverse crotaline and colubrine elements – lead to the separation of the localities into multiple groups (Fig. 2.12). The HCA further clarifies these clusters based on a dissimilarity matrix of the presence/absence data of each locality (Fig. 2.12). The Pratt Slide local fauna (Bw 123) was an outlier for the localities and forms the first main cluster. This is likely because of its high genus-level richness, which includes an uncommon combination of extinct, novel, and extant taxa. The second main cluster contains the ten other localities from the

Barstovian through the Clarendonian, with the addition of the Hemphillian Cn 106b, which only has *Thamnophis* and indeterminate colubrines identified. All other localities in this cluster seem to be defined by the presence of now extinct or extirpated taxa, including taxa such as *Neonatrix* and *Pterygoboa*. The third and final cluster includes all seven remaining Hemphillian through Blancan snake assemblages, with appearances from extant taxa such as *Regina*, *Storeria*, and *Rhinocheilus*, and more consistent identifications of extant crotaline genera. These results imply that the major compositional shift of the Central Great Plains occurred through the Clarendonian and the snake fauna was functionally a group of near extant assemblages by the Hemphillian.

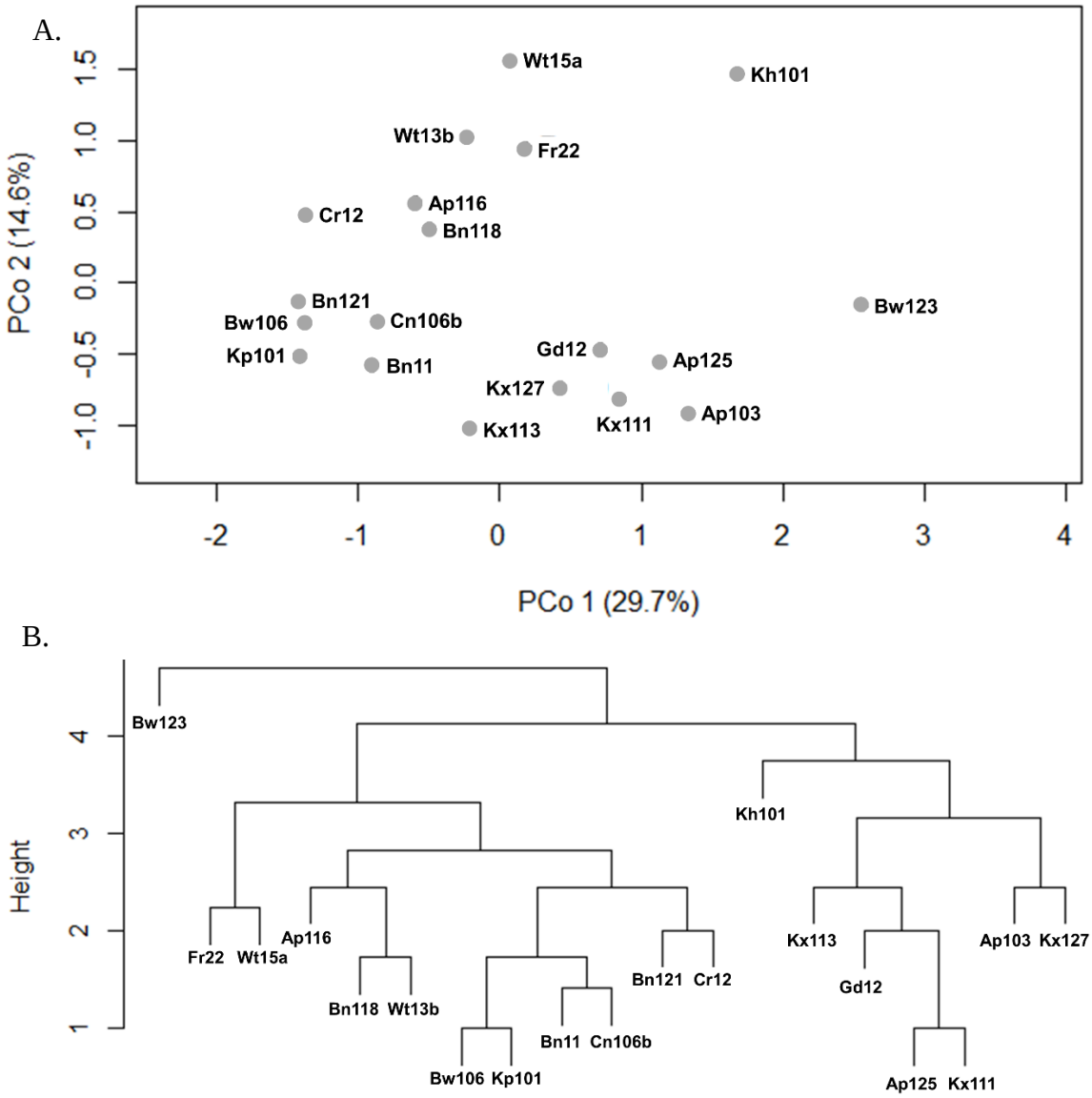

Figure 2.12. Relative similarity of snake assemblages from 19 Barstovian-Blancan localities in Nebraska based on presence-absence. A: Principal coordinates analysis; B: Complete-linkage hierarchical cluster analysis. Three major clusters are visible. From the left, the first cluster contains only Bw 123, the unique Pratt Slide local fauna; the second cluster contains all Barstovian and Clarendonian faunas minus Bw 123, but with the addition of Hemphillian Cn 106b (Thamnophis + Colubrinae indet.); and the third cluster contains all Hemphillian through Blancan sites except Cn 106b.

The climate envelope models using congenerics produced clear ranges of overlap, with differences on which specific congenerics provided the upper and lower bounds for MAT and AP estimates (Fig. 2.13). The MAT variable (Fig. 2.13a) suggests that the lowest overlapping values are bounded by *Salvadora*, while the highest overlapping values are bounded by *Charina*, as these taxa respectively have higher minimum MAT and lower maximum MAT tolerances today. The overlapping MAT values range from just below 5°C to 16°C, with a maximum density between 11°C-12°C. The maximum density of the area of overlap may suggest that MAT in the earliest Clarendonian of Webster Co., NE was higher than the present (~10.55°C); however, the range of projections could indicate higher or lower temperatures. Additionally, this would suggest that MAT in the early Clarendonian of the Penny Creek local fauna was lower than proposed for the older Late Barstovian Myers Farm local fauna, which has been considered warm and temperate to sub-tropical (Holman, 1977; Holman, 2000; Corner, 2014). The MAT climate envelope models therefore support an overall cooling climate in the early Clarendonian. The AP variable (Fig. 2.13b) is bounded at the lower values by *Nerodia* and at the higher values by both *Charina* and *Salvadora*, although *Nerodia* and *Charina* respectively occupy the lower and upper limits at peak density. The overlapping AP values range from approximately 200 mm to 1100 mm, with maximum density at 550-600 mm. While these values range from well-below to well-above the present AP of Webster Co., the maximum density suggests a slightly drier environment in the earliest Clarendonian, again indicating a more open, temperate, and cooler environment after the MMCO. The combined MAT and AP values suggest that

the most likely biome of the Penny Creek local fauna was a shrubland/woodland (Bailey, 1998; 2005), especially given the maximum density values for each. Slightly less likely biomes based on maximum and minimum values of MAT and AP include temperate grassland/cold desert (lower AP) or temperate seasonal forest (higher AP); however, the majority of MAT and AP combinations suggest the shrubland/woodland biome.

The results of the climate envelope models are supported by previous research using phytoliths (Stromberg 2004, 2006, 2011), vertebrate faunal composition (Turner, 1972; Corner, 2014; this study), mammal hypsodonty (Janis et al., 2000, 2002, 2004; Stromberg, 2006), paleosols (Retallack, 1997), carbonate isotopes (Fox and Koch, 2004), and isotope values for mammalian teeth from the late Miocene (Wang et al., 1994; Kita et al., 2014), as well as the snakes in this study. Interestingly, *Charina* and *Salvadora* impose opposing limits for MAT, but share much of the upper limit for AP in the climate envelope models. While both snakes are presently located in western North America and overlap somewhat in the southwestern United States today, *Charina* is adapted to cooler temperatures and *Salvadora* to warmer temperatures compared to all other congenerics in this analysis, thus limiting the overlap area of MAT. The shared upper limit of AP composed of *Charina* and *Salvadora* likely reflects the high degree of drier biomes occupied by those taxa; the long tail of *Charina*'s data in AP when compared to *Salvadora*'s signifies the former's presence in the Pacific Northwest of the United States and Canada. Conspicuously, both taxa were the only genera from this assemblage to be extirpated from Nebraska to the West and South during the Neogene, likely during the Hemphillian based on the last appearance datum for each (Jacisin et al.,

2015). *Nerodia*, on the other hand, is typically found near permanent sources of water, which likely imposes a lower limit on AP in the plots. It should be noted that the results of the climate envelope models are slightly complicated by the lack of extant species identified from the Penny Creek material. By choosing closely related congeneric species from the present, I assume that the fossil species share similar ecologies and ecomorphologies to their extant relatives, as suggested by niche conservatism. It is possible that directional trends of evolution related to climate are not detected when fossils are not included, as seen in other squamates such as *Sceloporus* (Lawing et al., 2016). Stronger predictions can be made by incorporating the entire known fossil record of a group in these models, but that is beyond the scope of this study.

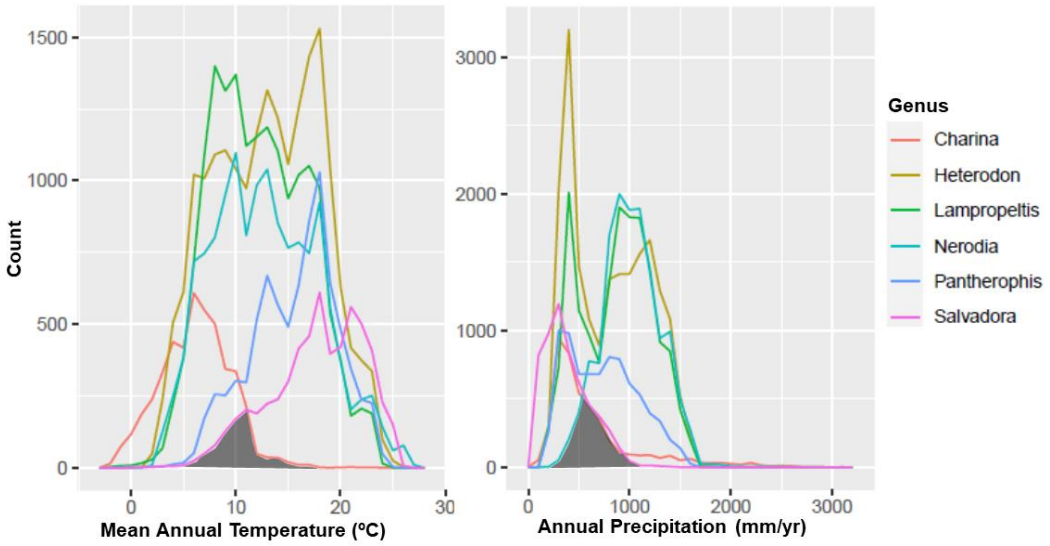

Figure 2.13. Climate envelope models of MAT and AP based on the congenerics of the Penny Creek local fauna snake assemblage. The gray-filled spaces signify the areas of overlap for all taxa included in the models.

Based on the ecologies of extant relatives for the taxa present at Penny Creek, the recovery of *Charina*, *Lampropeltis, Pantherophis, Heterodon,* and multiple natricine genera allows me to make a few assumptions about the past conditions of the Penny Creek environment. Extant *Charina, Heterodon, Lampropeltis,* and *Salvadora* all prefer loose substrates such as sandy soils, along with areas with plenty of ground-level cover (Holman, 1977; St. Clair, 1999; Plummer and Mills, 2000; Pyron and Burbrink, 2009, Davis and LaDuc, 2018). *Nerodia, Thamnophis* and some species of *Lampropeltis* generally prefer to reside near permanent sources of water and the surrounding grassy areas (Holman, 1977; Holman, 1991, McVay et al., 2015). Finally, the presence of *Charina* may indicate a relatively mild, temperate-to-semi-arid environment, as extant members of that genus are relatively cold-adapted booids (St. Clair, 1999; Holman, 2000; Rodriguez-Robles et al., 2001). Most of these snakes, including *Pantherophis* and crotaline viperids, are found across wide geographic swaths of North America today. The majority of the taxa would today be consistent with a transitional or mosaic woodland and shrubland ecotone, making it somewhat similar to the Barstovian Egelhoff fauna (Holman, 1987); however, there is notably less amphibian and turtle material presently known from Wt 13b. This difference suggests a permanent stream or river as a local water source, instead of a pond or lake. Furthermore, the severely weathered state of the fossil vertebrates at Wt 13B additionally suggest a high energy fluvial source as a depositional environment.

The interpretation of a somewhat open, permanent fluvial environment surrounded by a transitional or mosaic shrubland and woodland is consistent with

previous studies focused on the geology and mammalian paleoecology of the Penny Creek Local Fauna (Turner, 1972; Voorhies 1987, 1990). Furthermore, the Penny Creek fossil snakes represent the only presently described snake assemblage from 12.5-12.0 Ma in North America, providing us with an initial glimpse into the Clarendonian 1 NALMA for small herpetofauna. The description of the Penny Creek fossil snakes confirms the persistence of multiple taxa across the MMCO and contributes to our understanding of the interactions between post-MMCO environmental changes and the gradual modernization and evolution of North American snakes. Extensive future work is a requirement to better understand the modernization of the North American snake fauna – particularly in time intervals with sparse material and in regions outside of the Central Great Plains – but Penny Creek is a significant step towards filling the gap of knowledge in our present understanding of ophidian history.

2.6. References

Auffenberg, W. 1963. The fossil snakes of Florida. Tulane Studies in Zoology 10:131-216.

Bailey, R. G. 1998. Ecoregions map of North America. U.S. Forest Serv. Misc. Publ. 1548:1–10.

Bailey R. G. 2005. Identifying ecoregion boundaries. Environ Manage. 34:S14–S16.

Baird S. F. and C. Girard. 1853. Catalogue of North American Reptiles in the Museum of the Smithsonian Institution. Part I. – Serpentes. Smithson. Misc. Coll. 2:V-xvi + 172 p.

Bell, C. J., J. J. Head, and J. I. Mead. 2004. Synopsis of the herpetofauna from Porcupine Cave, p. 117-126. In Barnosky, A.D. (ed.), Biodiversity Response to Climate Change in the Middle Pleistocene. The Porcupine Cave Fauna from Colorado. Berkeley: University of California Press.

Bell, C. J., J. A. Gauthier; and G. S. Bever. 2010. Covert biases, circularity, and apomorphies: A critical look at the North American Quaternary Herpetofaunal Stability Hypothesis. Quaternary International 217: 30-36.

Boellstorff, J. 1978. Chronology of some late Cenozoic deposits from the central United States and the Ice Ages: Nebraska Academy of Sciences Transactions, 6: 35-49.

Bolinier, T., J. D. Nichols, J. R. Sauer, J. E. Hines, and K. H. Pollock. 1998. Estimating species richness: the importance of heterogeneity in species detectability. Ecology 79: 1018-1028.

Bonaparte, C. L. 1838. Amphibiorum tabula analytica. Nuovi Ann. Sci. Nat. 1: 391-393.

Bonaparte, C. L. 1840. Amphibia europaea ad systema nostrum vertebratorum ordinate. Memorie della Reale Accademia delle Scienze di Torino, 2: 385-456.

Brattstrom, B. H. 1958. New records of Cenozoic amphibians and reptiles from California. Bulletin of the Southern California Academy of Sciences 57: 5-12.

Corner, G. R. 2014. Newly acquired vertebrates from Webster County, South-Central Nebraska, USA. Abstract. 48th Annual Meeting of the Geological Society of America, North-Central Section.

Davis, D. R. and T. J. LaDuc. 2018. Amphibians and reptiles of C.E. Miller Ranch and the Sierra Vieja, Chihuahuan Desert, Texas, USA. Zookeys 735: 97-130.

Diffendal, R. F. Jr., R. K. Pabian, and J. R. Thomasson. 1996. Geologic history of Ash Hollow Park, Nebraska.Conservation and Survey Division, Institute of Agriculture and Natural Resources, University of Nebraska, Educational Circular 5, 33 pp.

Dupoue´, A., A. Rutschmann, J. F. Le Galliard, J. Clobert, F. Angelier, C. Marciau, S. Ruault, D. Miles, and S. Meylan. 2017. Shorter telomeres precede population extinction in wild lizards. Scientific Reports 7: 1-8.

Fick, S. E. and R. J. Hijmans, 2017. WorldClim 2: new 1km spatial resolution climate surfaces for global land areas. International Journal of Climatology 37:4302-4315.

Fitzinger, L. 1843. Systema reptilium. Fasciculus primus. Amblyglossae. Vindobonae. 1-106.

Fox, D. L. and P. L. Koch. 2004. Carbon and oxygen isotopic variability in Neogene paleosol carbonates: constraints on the evolution of the C4-grasslands of the Great Plains, USA. Palaeogeogr. Palaeoclimatol. Palaeoecol. 207: 305-329.

Gilmore, C. W. 1938. Fossil snakes of North America. Geological Society of North America Special Paper 9: 1-96.

Gray, J. E. 1825. A synopsis of the genera of Reptilia and Amphibia. Annals of Philosophy 10: 193-217.

Gray, J. E. 1849. Catalogue of the Specimens of Snakes in the Collection of the British Museum. Printed by order of the Trustees, 125 pp.

Head, J. J., J. I. Bloch, A. K. Hastings, J. R. Bourque, E. A. Cadena, F. A. Herrera, P. D. Polly, and C. A. Jaramillo. 2009. Giant boid snake from the Palaeocene neotropics reveals hotter past equatorial temperatures. Nature 457: 715-718.

Holman, J. A. 1964. Fossil snakes from the Valentine Formation of Nebraska. Copeia 1964: 631-637.

Holman, J. A. 1973. Reptiles of the Egelhoff local fauna (upper Miocene) of Nebraska. Contributions of the Museum of Paleontology, University of Michigan 24:125-134.

Holman, J. A. 1977. Upper Miocene snakes (Reptilia, Serpentes) from southeastern Nebraska. Journal of Herpetology. 11: 323-335.

Holman, J. A. 1978. Herpetofauna of the Bijou Hills Local Fauna (Late Miocene: Barstovian) of South Dakota. Herpetologica 34: 253-257.

Holman, J. A. 1982. A fossil snake (Elaphe vulpina) from a Pliocene ash bed in Nebraska. Transactions of the Nebraska Academy of Science, 10:37-42.

Holman, J. A. 1987. Herpetofauna of the Egelhoff Site (Miocene: Barstovian) of north-central Nebraska. Journal of Vertebrate Paleontology 7: 109-120.

Holman, J. A. and A. J. Winkler. 1987. A mid-Pleistocene (Irvingtonian) herpetofauna from a cave in southcentral Texas. *Pearce-Sellards Series*, Texas Memorial Museum, The University of Texas at Austin 44:1-17.

Holman, J. A. and M. E. Schroeder. 1991. Fossil herpetofauna of the Lisco C quarries (Pliocene: Early Blancan) of Nebraska. Transactions of the Nebraska Academy of Sciences, XVIII: 19-29.

Holman, J. A. 1996. Herpetofauna of the Trinity River local fauna (Miocene: Early Barstovian, San Jacinto County, Texas, USA. Tertiary Research 17: 5-10.

Holman, J. A. 2000. Fossil snakes of North America: Origin, evolution, distribution, paleoecology. Bloomington: Indiana University Press. 357 pp.

Huey, R. B., M. R. Kearney, A. Krockenberger, J. A. Holtum, M. Jess, and S. E. Williams. 2012. Predicting organismal vulnerability to climate warming: roles of

behaviour, physiology and adaptation. Philosophical Transactions of the Royal Society B: Biological Sciences, 367: 1665-1679.

Ikeda, T. 2007. A comparative morphological study of the vertebrae of snakes occurring in Japan and adjacent regions. Current Herpetology 26: 13-34.

IUCN. 2021. *The IUCN Red List of Threatened Species. Version 2021-1*. https://www.iucnredlist.org. Downloaded on 10 June 2021.

Jacisin III, J. J., E. T. Whiting, A. Ricker, J. Wallace, and J. J. Head. 2015. Neogene herpetofaunas from the Central Great Plains: diversity, modernization, and relationships to climate change. 75th Annual Meeting of the Society of Vertebrate Paleontology, Dallas, Texas, U.S.A.

Janis, C. M., J. Damuth, and J. M. Theodor. 2000. Miocene ungulates and terrestrial primary productivity: where have all the browsers gone? Proc. Natl. Acad. Sci., 97:899.

Janis, C. M., J. Damuth, and J. M. Theodor. 2002. The origins and evolution of the North American grassland biome: the story from the hoofed mammals. Palaeogeogr. Palaeoclimatol. Palaeoecol. 177: 183-198.

Janis, C. M., J. Damuth, and J. M. Theodor. 2004. The species richness of Miocene browsers, and implications for habitat type and primary productivity in the North American grassland biome. Palaeogeogr. Palaeoclimatol. Palaeoecol. 207: 371-398.

Jasinski, S. E., and D. A. Moscato. 2017. Late Hemphillian Colubrid Snakes (Serpentes, Colubridae) from the Gray Fossil Site of Northeastern Tennessee. Journal of Herpetology, 51: 245-257.

Joeckel, R. M., S. T. Tucker, and L. M. Howard. 2017. Geology and Paleontology Along Part of the Niobrara River in Northern Nebraska. Lincoln, NE: University of Nebraska, Conservation and Survey Division. pp. 52.

Kita, Z. A., R. Secord, and G. S. Boardman. 2014. A new stable isotope record of Neogene paleoenvironments and mammalian paleoecologies in the western Great Plains during the expansion of C4 grasslands. Palaeogeography, Palaeoclimatology, Palaeoecology 399:160-172.

Kluge, A. G. 1993. *Calabaria* and the phylogeny of erycine snakes. Zoological Journal of the Linnaean Society 107: 293-351.

LaDuke, T. C. 1991. The fossil snakes of Pit 91, Racho La Brea, California. Natural History Museum of Los Angeles County Contributions in Science 424: 1-28.

Laurenti, J. N. 1768. Specimen medicum, exhibens synopsin Reptilium emendatam cum experimentis circa venena et antidota Reptilium austriacorum. Viennae, Joan. Thom. Nob. de Trattnern, i–ii + 1–215, pl. 1–5.

Lawing A. M. and P. D. Polly. 2011. Pleistocene climate, phylogeny, and climate envelope models: an integrative approach to better understand species' response to climate change. PLoSOne 16:e28554.

Lawing, A. M., J. J. Head, and P. D. Polly. 2012. The ecology of morphology: the ecometrics of locomotion and macroenvironment in North American snakes. Pp. 117-146 in J. Louys (ed.), Palaeontology in Ecology and Conservation. Springer-Verlag, Berlin and Heidelberg.

Lawing, A. M., P. D. Polly, D. K. Hews, and E. P. Martins. 2016. Including fossils in phylogenetic climate reconstructions: A deep time perspective on the climatic niche evolution and diversification of spiny lizards (*Sceloporus*). The American Naturalist 188: 133-148.

Lawing, A. M. 2021. The geography of phylogenetic paleoecology: integrating data and methods to better understand biotic response to climate change. Paleobiology, 47:178-197.

Linnaeus, C. 1758. Systema Naturae per Regna Tria Naturae, Secundum Classes, Ordines, Genera, Species cum Characteribus, Differentiis, Synony-mis, Locis. 10th ed. Laurenti Salvi, Stockholm.

Lueninghoener, G. C. 1934. A lithologic study of some typical exposures of the Ogallala Formation in western Nebraska: Lincoln, Nebraska, University of Nebraska, unpublished M.S. thesis, 55 p.

McCartney, J. 2015. Morphology and function of the ophidian vertebral column: implications for the paleobiology of fossil snakes. Stony Brook, NY: The Graduate School, Stony Brook University.

McDowell, S. B. 1987. Systematics. p. 3–50. In: J.T. Collins, S. S. Novak, and R. A. Seigel. (eds.), Snakes: Ecology and Evolutionary Biology. McGraw-Hill Publ. Co., New York.

McVay, J. D., O. Flores-Villela, and B. Carstens. 2015. Diversification of North American natricine snakes. Biological Journal of the Linnaen Society 116: 1-12.

Meylan, P. A. 1982. The squamate reptiles of the Inglis IA fauna (Irvingtonian: Citrus County, Florida). Bulletin of the Florida State Museum, Biological Sciences 27:1-85.

Nopsca, F. 1923. Eidolosaurus und Pachyophis. Zwei neue Neocom-Reptilien. Palaeontographica, 65: 97–154.

Oppel, M. 1811. Die Ordnungen, Familien und Gattungen der Reptilien als Prodom einer Naturgeschichte derselben. Joseph Lindauer Verlag, Mu¨nchen.

Parmley, D. 1990. Late Pleistocene snakes from Fowlkes Cave, Culberson County, Texas. Journal of Herpetology 24:266–274.

Parmley, D. and J. A. Holman. 1995. Hemphillian (Late Miocene) snakes from Nebraska, with comments on Arikareean through Blancan snakes of midcontinental North America. Journal of Vertebrate Paleontology 15: 79-95.

Parmley, D. and J. A. Holman. 2007. Earliest fossil record of a pigmy rattlesnake (Viperidae: Sistrurus Garman). Journal of Herpetology, 41:141-144.

Parmley, D. and K. B. Hunter. 2010. Fossil Snakes of the Clarendonian (Late Miocene) Pratt Slide Local Fauna of Nebraska, with the description of a new natricine colubrid. Journal of Herpetology 44: 526-543.

Parmley, D., R. Chandler, and L. Chandler. 2015. Fossil frogs of the late Clarendonian (late Miocene) Pratt slide local fauna of Nebraska, with the description of a new genus. Journal of Herpetology, 49: 143-149.

Plummer, M. V. and N. E. Mills. 2000. Spatial ecology and survivorship of resident and translocated hognose snakes (*Heterodon platirhinos*). Journal of Herpetology 34: 565-575.

Pyron, R. A. and F. T. Burbrink. 2009. Lineage diversification in a widespread species: roles for niche divergence and conservatism in the common kingsnake, *Lampropeltis getula*. Molecular Ecology 18: 3443-3457.

Rage, J. -C. 1984. Serpentes. Part 11. Handbuch der Pala¨oherpetologie. Gustav Fisher Verlag, Stuttgart, Germany. 80 pp.

Rage, J. -C. and J. A. Holman. 1984. Des serpents (Reptilia, Squamata) de type nord-américain dans le Miocène Français. Évolution parallèle ou dispersion? Geobios, 17:89-104.

Reynolds, R. G., M. L. Niemiller, and L. J. Revell. 2014. Towards a Tree-of-Life for the boas and pythons: multilocus species-level phylogeny with unprecedented taxon sampling. Molecular Phylogenetics and Evolution, 71: 201-213.

Retallack, G. J. 2007. Cenozoic paleoclimate on land in North America. The Journal of Geology, 115: 271-294.

Rodriguez-Robles J. A., G. R. Stewart, and T. J. Papenfuss. 2001. Mitochondrial DNA-based phylogeography of North American rubber boas, Charina bottae (Serpentes: Boidae). Molecular Phylogenetics and Evolution 18: 227–237.

Rudnick, C. E. 1994. Insectivores from the Late Clarendonian (Miocene) Pratt Slide, North Central Nebraska. Unpublished master's thesis. University of Nebraska. Lincoln.

Sinervo, B., F. Mendez-De-La-Cruz, D. B. Miles, B. Heulin, E. Bastiaans, M. Villagrán-Santa Cruz, et al. 2010. Erosion of lizard diversity by climate change and altered thermal niches. Science 328: 894-899.

Smith, K. T. 2013. New constraints of the evolution of the snake clades Ungaliophiinae, Loxocemidae and Colubridae (Serpentes), with comments of the fossil history of erycine boids in North America. Zoologischer Anzeiger 252: 157-182.

Song Y., Q. Wang, Z. An, X. Qiang, J. Dong, H. Chang, M. Zhang, and X. Guo. 2018. Mid-Miocene climatic optimum: Clay mineral evidence from the red clay succession, Longzhong Basin, Northern China. Palaeogeography, Palaeoclimatology, Palaeoecology 512: 46-55.

Sonnini de Manoncourt, C. N. S. and P. A. Latreille. 1801. Histoire naturelle des reptiles, avec figures dessinees d'apres nature. Chez Deter- ville, Paris. 3: 1-335, 6 pls.; 4: 1-410, 13 pls.

St. Clair, R. C. 1999. Identifying critical habitats for a vulnerable snake species, the rubber boa. Report to Columbia Basin Fish and Wildlife Compensation Program, BC Hydro, Nelson, British Columbia.

Strömberg, C. A. E. 2004. Using phytolith assemblages to reconstruct the origin and spread of grass-dominated habitats in the Great Plains during the late Eocene to early Miocene Palaeogeogr. Palaeoclimatol. Palaeoecol. 207:239-275.

Strömberg, C. A. E. 2006. Evolution of hypsodonty in equids: testing a hypothesis of adaptation. Paleobiology 32:236-258.

Strömberg, C. A. E. 2011. Evolution of grasses and grassland ecosystems. Annu. Rev. Earth Planet. Sci., 39:517-544.

Szyndlar, Z. 1991. A review of Neogene and Quaternary snakes of central and Eastern Europe. Part II: Natricinae, Elapidae, Viperidae. Estudios Geol. 47: 237-266.

Tedford, R. H., B. Albright III, A. D. Barnosky, I. Ferrusquia-Villafranca, R. M. Hunt, Jr., J. E. Storer, C. C. Swisher III, M. R. Voorhies, S. D. Webb, and D. P. Whistler. 2004. Mammalian Biochronology of the Arikareean Through Hemphillian Interval (Late Oligocene Through Early Pliocene Epochs), p. 169-231. In Woodburne, M.O. (ed.), Late Cretaceous and Cenozoic Mammals of North America: Biostratigraphy and Geochronology. Columbia University Press, New York.

Thomasson, J. R. 1980. *Archaeoleersia nebraskensis* gen. et sp. nov. (Gramineae-Oryzeae), a new fossil grass from the Late Tertiary of Nebraska: American Journal of Botany 67: 876-882.

Turner, M. A. 1972. A faunal assemblage from the Lower Ash Hollow Formation (Neogene) of southern Nebraska. Master of Science Thesis, University of Nebraska-Lincoln. 88pp.

Utiger, U., N. Helfenberger, B. Schätti, C. Schmidt, M. Ruf, and V. Ziswiler. 2002. Molecular systematics and phylogeny of Old and New World Rat Snakes, *Elaphe* Auct., and related genera (Reptilia, Squamata, Colubridae). Russian Journal of Herpetology 9: 105-124.

Voorhies, M. R., R. G. Corner, J. L. Fitzgibbon. 1987. *Calippus regulus* (Mammalia: Equidae) in the Penny Creek Local Fauna (Clarendonian), Webster County, Nebraska. Transactions of the Nebraska Academy of Sciences and Affiliated Societies. Paper 206.

Voorhies, M. R. 1990. Vertebrate biostratigraphy of the Ogallala Group in Nebraska. In T. C. Gustavson (ed.), Geologic Framework and Regional Hydrology Upper Cenozoic Blackwater Draw and Ogallala Formation, Great Plains, pp. 115–151. Bureau of Economic Geology, University of Texas, Austin.

Voorhies, M. R. 1992. Ashfall: life and death at a Nebraska waterhole ten million years ago. University of Nebraska State Museum, Museum Notes 81: 1-4.

Wang, Y., T. E. Cerling, and B. J. MacFadden. 1994. Fossil horses and carbon isotopes: new evidence for Cenozoic dietary, habitat, and ecosystem changes in North America. Palaeogeogr. Palaeoclimatol. Palaeoecol. 107:269-279.

Webb, J. K., and R. Shine. 1998. Using thermal ecology to predict retreat-site selection by an endangered snake species. Biological Conservation, 86: 233-242.

Zachos, J., M. Pagani, L. Sloan, E. Thomas, K. Billups. 2001. Trends, rhythms, and aberrations in global climate 65 Ma to present. Science 292, 686–693.

3. THE CAPACITY OF MID-TRUNK VERTEBRAL SHAPE FOR QUANTITATIVE TAXONOMIC DELIMITATION IN SNAKES

"Taxonomy is described sometimes as a science and sometimes as an art, but really it's a battleground." – Bill Bryson, *A Short History of Nearly Everything*

3.1. Introduction

Snakes are amongst the most specialized vertebrates in history, equipped with evolutionary innovations for sensing the environment, feeding, and diverse modes of locomotion. While snakes are not the only limbless vertebrates, the morphology of their vertebrae is more complex and efficient than their limbless vertebrate compatriots (Holman, 2000). The elongate body form, skull specialization, and lack of appendages in snakes combine to result in impressive locomotive adaptability and oft-overlooked morphological complexity in the vertebral column (Johnson, 1955; Savitzky, 1980; Holman, 2000; Lillywhite et al., 2000; Jayne, 2020; Jurestovsky et al., 2020). In fact, at least 11 locomotive gaits for traveling across various substrates have been identified in snakes thus far, with recent research suggesting that rectilinear and sidewinding locomotion are unique gaits, but that lateral undulation and concertina categories can be further divided into five and four distinct motor patterns for specific needs to traverse on, across, or through different mediums (Jayne, 2020). In cases where characters based on

color pattern, scale counts, linear measurements, head shape, and molecular data as typically used are impossible, such as in the fossil record or in dry museum specimens, vertebral morphology has been used to implicate both taxonomy and ecology (Gilmore, 1938; Johnson, 1955; Meylan, 1982; Holman, 2000; Lillywhite et al., 2000; Shine et al., 2002; Fabien et al., 2004; Manier, 2004; Vincent et al., 2004; Klein et al., 2021).

Snake trunk vertebrae are the most common snake fossil elements in North America, but diagnosing and interpreting vertebral morphology in both living and fossil snakes based on apomorphies is limited to relatively few expert diagnosticians (Rage, 1984; Holman, 2000; Bell et al., 2010; Parmley and Hunter, 2010; Smith, 2013). The difficulty in these endeavors lies in discerning minute but complex differences in overall shape, proportion, and the effects of an exceptionally elaborate system of axial muscles and vertebral articulations, which substitute for the lack of appendicular appendages and allow for extreme locomotive behaviors (e.g., cantilevering, tying their bodies in knots, and spinning; Cundall, 1987; Holman, 2000; Jayne, 2020). As a result of this difficulty, fossil snakes (much like other fossil squamates) are not well studied in comparison with coeval mammalian counterparts despite samples being available in many localities. Detecting identifiable morphological features or patterns in vertebrae inherent to groups of snakes is useful for describing and assigning taxa and ecological relationships through time.

Snake vertebrae are usually identified via qualitative descriptions of morphological traits (e.g., Auffenberg, 1963; Szyndlar, 1984; LaDuke, 1991; Holman, 2000) that are occasionally supplemented by quantified linear measurements and ratios

(e.g., Johnson, 1955; Meylan, 1982; Jasinski and Moscato, 2017; Klein et al., 2021). Unfortunately, the dearth of spectacular specimens and the difficulty of identifying and describing snake elements in a scientifically replicable way has long hindered progress in research of the snake skeleton and in snake fossils. Attempts to identify between (e.g., *Coluber* and *Masticophis*) or within (e.g., crotalines) some snake groups at various taxonomic levels are often onerous and hindered by a lack of comparative methods and a poor understanding of snake osteology (Holman, 2000). In particularly complex cases, new, easily applicable methods are necessary to improve the processes of description, differentiation, and identification of snake skeletal material for both expert and inexperienced diagnosticians. Geometric morphometrics is one such methodology with excellent potential to assist in the process of assigning snake vertebrae to taxon and ecology. The implementation of geometric morphometrics would therefore provide a wealth of previously unexplored data on snake fossils and the snake skeleton.

Snake vertebrae are historically overlooked or ignored completely in samples and museum collections (Holman, 2000), inhibiting the accurate representation of snake richness and functional diversity in many taxonomic and paleoecological interpretations. Geometric morphometrics present an alternative, shape-based, and quantitative approach for comparing and depicting snake vertebrae. While these methods have not been widely applied to snake vertebrae, or even to snakes in general (e.g., Gentilli et al., 2009; Lawing and Polly, 2011; Lawing et al., 2012; Ruane, 2015; Huntley et al., 2021), some studies have shown that geometric morphometrics can detect morphological differences that support molecular taxonomic hypotheses at clade and even subspecies levels

(Gentilli et al., 2009; Lawing and Polly, 2011; Meik et al., 2012; Jacisin, 2021). The ability of geometric morphometric techniques to work on isolated elements such as snake trunk vertebrae would additionally provide a path forward to shape-based studies relating morphology to functional trait-environment relationships at individual to community levels, as in ecometrics, as well as skeletal studies of sexual dimorphism, allometry, and inter- or intraspecies variation.

Here, I evaluate the separation of anterior trunk vertebral shape among taxonomic categories using geometric morphometrics and additional multivariate analyses as a method of specimen assignment and shape differentiation. This methodology is applied across a vast array of extant snake groups and a large number of individuals. In doing so, I seek to create a methodological framework using extant snake taxa to answer the following questions: 1) can shape detected via geometric morphometrics act as a supplement to visual descriptions for assigning, identifying and describing taxa and their ecologies; 2) what shape changes explain the most variation in the anterior aspect of snake trunk vertebrae; and 3) how well do the observed differences in shape associate with taxa at the family, subfamily, genus, and species levels? If there are differences in shape related to phylogeny, I can expect greater morphological differences, and therefore increased predictive capacity, at higher levels of the taxonomic hierarchy. Furthermore, if these methods are capable of taxonomic delimitation, then two-dimensional geometric morphometrics stands as a relatively simple – but powerful – tool for identifying both extant and fossil material based solely

on vertebral shape, while requiring less anatomical expertise than more traditional methods.

3.2. Methods

I used geometric morphometrics to explore the viability of quantitative shape analysis as a method for assigning recent and fossil snake trunk vertebrae to already described and delimited species. I photographed the anterior view of 504 extant snake middle trunk vertebrae, ranging from one to three vertebrae per individual, one to ten individuals per species, and one to fifteen species per genus. Photographs were taken of material from the Texas A&M University Biodiversity Research and Teaching Collections (TCWC), the Texas Vertebrate Paleontology Collections (TMM), the University of Texas at Arlington (UTA), the William R. Adams Zooarcheology Lab, Indiana University (WRA), the University of Nebraska State Museum (UNSM), and the Smithsonian National Museum of Natural History (USNM). I used a DinoLite Edge digital microscope or a Canon EOS Rebel SX camera with a Canon Zoom EF-S lens (18-55 mm) for all photographs. The vertebrae comprised 11 families, 16 subfamilies, 89 genera, and 189 species from around the world, but primarily from North America (62%), based on availability of museum skeletal material with isolated trunk vertebrae. Each isolated vertebra was secured such that the anterior surface of the vertebra was as planar as possible, perpendicular and centered below the camera lens in order to minimize distortion from the curvature of the camera lens as recommended by Head et al. (2005). I used TPSUTIL, version 1.74 to build a TPS file from the photographs. I also

ordered a Microsoft Excel file with the classification information for each specimen for use in RStudio.

I described the shape for the anterior view of snake middle trunk vertebrae by digitizing 23 homologous landmarks in the TPSDIG2, version 2.30 application. This landmark scheme is based on the landmark scheme of Lawing et al. (2012), as I landmarked both lateral sides of the anterior vertebral aspect. All landmarks selected are homologous, clear on all specimens used, and best represent the anterior aspect of the vertebra (Fig. 3.1; Table 3.1). I selected the anterior aspect because it contains the most information on overall shape and articular surfaces on a single plane, and is therefore most ideal for capturing variation related to function and locomotive behaviors in two dimensions (Lawing et al., 2012).

To remove shape differences related to absolute size, orientation, and location, I used Procrustes superimposed landmarks (Zelditch et al., 2004; Lawing and Polly, 2010). Elimination of non-shape variation through superimposition differentiates geometric morphometrics from traditional morphometric methods, which are linear and capture size information better than shape information (Rohlf and Marcas, 1993). The overall arrangement of landmarks across all specimens and the centroids for each landmark can be viewed in Fig. 3.1. I then produced outlier plots for each of the 23 landmarks to ensure that the landmarks were properly ordered across all specimens in the data, as well as to find any outliers potentially indicative of a misdiagnosis a vertebra as belonging to the middle trunk region (Appendix Fig. B1). The proper order of

landmarks across all specimens was ensured and outliers were examined and addressed as necessary.

I performed a principal component analysis (PCA) on the middle trunk vertebral shape data using the *geomorph* package (Adams and Otarola-Castillo, 2013) in Rstudio (www.rstudio.com/products/rstudio/download2/) to examine the morphological space of the specimens and quantify independent differences in vertebral shape represented by the PC axes. The maximum variance within the dataset as determined by the PCA is effectively the linear combination of variables after the landmark arrangements are fitted around a mean shape constellation through Procrustes superimposition (Rohlf and Slice, 1990). I also took a subset of the data within a single subfamily, the Crotalinae, and ran a second PCA to investigate differences in the morphological changes representing the most variation within different taxonomic levels. I selected the Crotalinae because it had the best sample size at the subfamily level in the dataset.

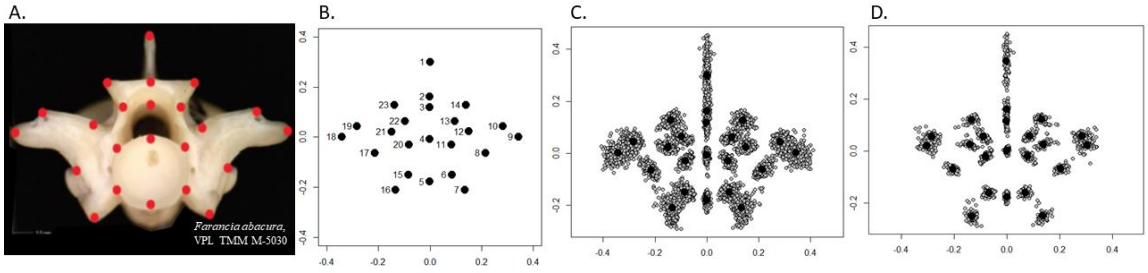

Figure 3.1. Overall landmark distributions of the data after implementing Procrustes superimposition. A: a photograph of the anterior aspect of a middle trunk vertebra with landmarks placed; B: the landmarks numbered in order of placement for each vertebra; C: Procrustes superimposed landmarks for vertebrae among all snake families in this study; and D: Procrustes superimposed landmarks for vertebrae for the Crotalinae-only dataset. Centroid values of each landmark are represented by large black circles.

In order to graphically illustrate and visually examine the variation in shape for each PC axis, I produced vector plots of the shape variation along each PC axis for both the all-group analysis and the Crotalinae-only analysis. These vector plots show the direction and degree of change at each individual landmark from three negative standard deviations to three positive standard deviations along a given axis. I chose the first six PCs for further analysis based on the results of the PCA, as the first six PCs combined to explain >80% of variance in both datasets.

Table 3.1. List of 23 vertebral landmarks used for anterior shape in this study.

Landmark	Description
1	Dorsal edge of neural spine
2	Midline dorsal edge of neural arch
3	Midline ventral edge of neural arch
4	Midline dorsal edge of centrum
5	Midline ventral edge of centrum
6	Right ventrolateral contact between apophysis & centrum
7	Right ventromedial edge of parapophysis
8	Right dorsomedial edge of diapophysis
9	Right lateral edge of prezygapophyseal body
10	Right dorsolateral edge of prezygapophyseal articular facet
11	Right medial contact between centrum & neural arch
12	Right ventromedial edge of prezygapophyseal articular facet
13	Right ventrolateral contact between zygosphene & neural canal
14	Right dorsolateral edge of zygophene
15	Left ventrolateral contact between apophysis & centrum
16	Left ventromedial edge of parapophysis
17	Left dorsomedial edge of diapophysis
18	Left lateral edge of prezygapophyseal body
19	Left dorsolateral edge of prezygapophyseal articular facet
20	Left medial contact between centrum & neural arch
21	Left ventromedial edge of prezygapophyseal articular facet
22	Left ventrolateral contact between zygosphene & neural canal
23	Left dorsolateral edge of zygosphene

To assess morphological differences between taxonomic groups, I used multivariate analyses of variance (MANOVAs) on the PCs of shape change for vertebrae at each taxonomic level, first for all groups, then for the Crotalinae-only group. The results of these analyses revealed which axes of shape change represented systematic (non-random) factors useful for assigning taxonomic identities. I also administered a post hoc Tukey's test in order to determine which specific groups comprised most of the variation at the family and subfamily levels. Finally, to determine whether already delimited species have shape differences that can be used to assign extant and fossil taxa, I used discriminant function analyses (DFAs) at the family, subfamily, genus, and species levels for the all-group dataset and at the genus and species levels for the Crotalinae-only dataset. The DFA classified all individuals included in the study into different groups a priori based on the combined morphological characters represented by the PC axes of shape variation. Application of DFA to both the all-group and the Crotalinae-only dataset allowed me to investigate if the discriminatory ability of lower taxonomic levels improves when using the shape variation present within a single, smaller group rather than across all groups. DFA has been shown to be more robust in the accuracy of its classifications and is relatively unaffected in its values with larger sample sizes when compared to methods such as cluster analysis (Jaiswara et al., 2013). I excluded all groups with a sample size of one (n = 1) from these analyses.

3.3. Results

3.3.1. Shape Variation Among Snake Families

Most of the shape variation was contained in the first few dimensions of the 46 principal components (PC). Specifically, the first six orthogonal PCs accounted for 84.5% of all observed variation in anterior vertebral shape captured by the landmark scheme (Figs. 3.2, 3.3, Appendix Fig. B2). Vector plots depicting shape change along each of the first six PC axes in the all-group analysis revealed that most shape variation was explained by differences in seven different locations: the neural spine, the zygosphene, the neural canal, the cotyl, the parapophyses, the diapophyses, and the prezygapophyses (with associated articular facets) (Fig. 3.4). These seven locations are all associated with articulations in the vertebrae and the overall proportions of height and width, and provide important information on taxonomic and ecological differences. PC1 accounted for 39.8% of the overall variation, and describes shape differences involving the neural spine and parapophyses, and therefore, the relative dorso-ventral height of the vertebra (Fig. 3.4A). Shapes ranged from proportionally tall vertebrae with long neural spines and parapophyses, but relatively narrower prezygapophyses in the terrestrial viperid *Sistrurus tergeminus* to the dorso-ventrally compressed, relatively wider vertebrae of the fossorial leptotyphlopid *Rena humilis*.

PC2 represented 20.4% of explained variation, and indicated that this variation was mainly in the orientation of the laterally located structures of the vertebrae (Fig. 3.4B). Shapes range from more ventrally located diapophyses and more ventrally oriented prezygapophyses with shorter prezygapophyseal articular facets in the aquatic

elapid sea snake, *Pelamis platura*, to more dorsally located diapophyses and dorsally oriented prezygapophyses with relatively wider prezygapophyseal articular facets in the semifossorial charinid rubber boa, *Charina bottae*. These differences were also associated with taller and shorter neural spines, respectively, and a ventral shift in the cotyl and parapophyses. Notably, PC1 and PC2 exhibited clearly visible separation of several snake clades, including the viperids, boids, charinids, and leptotyphlopids, while colubrids and elapids filled similar spaces in the two axes of variation (Fig 3.2A, 3.2B; Fig. 3.3).

PC3, which represented 11.6% of the overall variation, was mostly explained by variation in the dorsal region of the vertebrae, including the overall width of the vertebrae and the width of both the lateral and medial articular surfaces (Fig. 3.4C). Shapes for PC3 vary from relatively wider prezygapophyses and prezygapophyseal articular facets but narrower, thinner neural arches and narrower zygosphenes in the semifossorial dipsadinine colubrid, *Heterodon platirhinos*, to shorter prezygapophyses and prezygapophyseal facets but wide, convex neural arches and wide zygosphenes in the arboreal boid, *Corallus annulatus*.

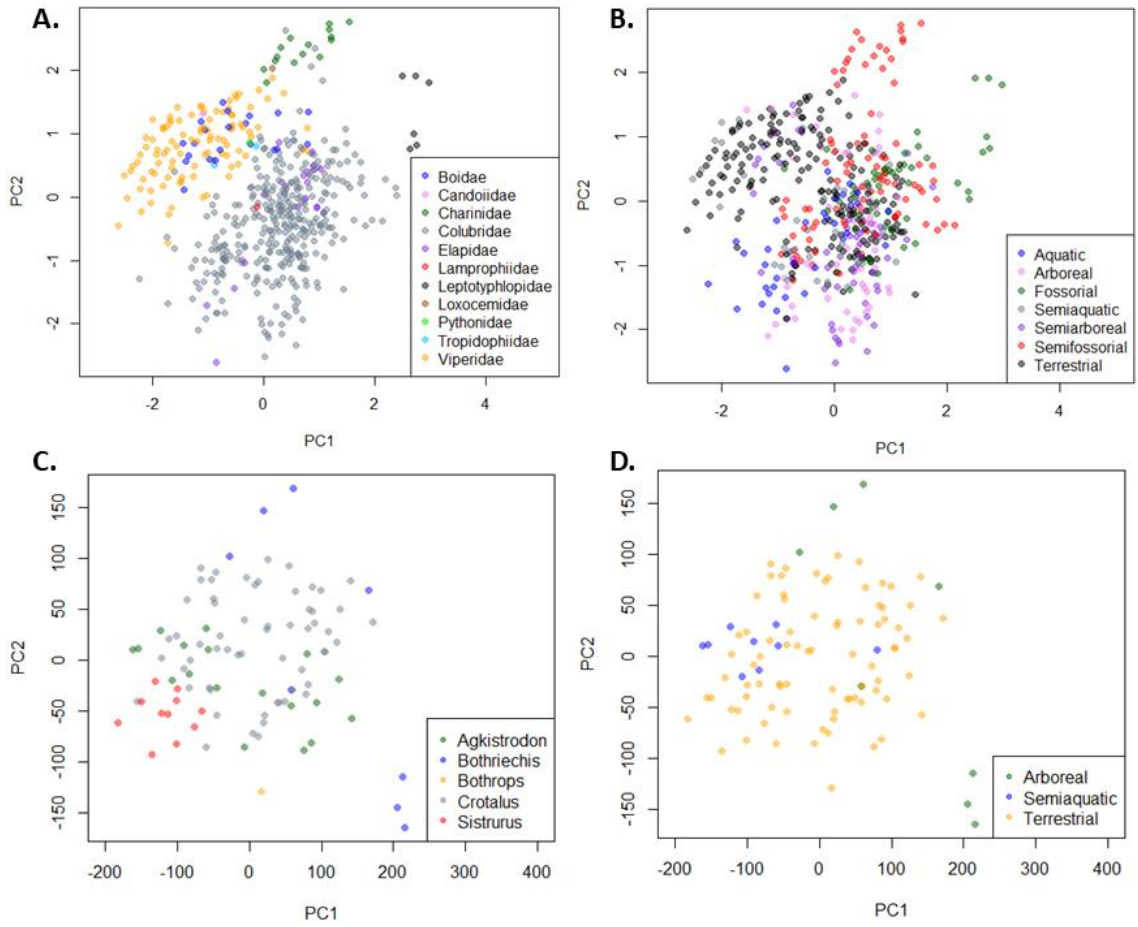

Figure 3.2 PCA plots of PC1 (x-axis) and PC2 (y-axis) for the all-group (A, B) and Crotalinae (C, D) analyses. Plots A and C are colored by family and genus, respectively, while plots B and D are colored by primary foraging habitat.

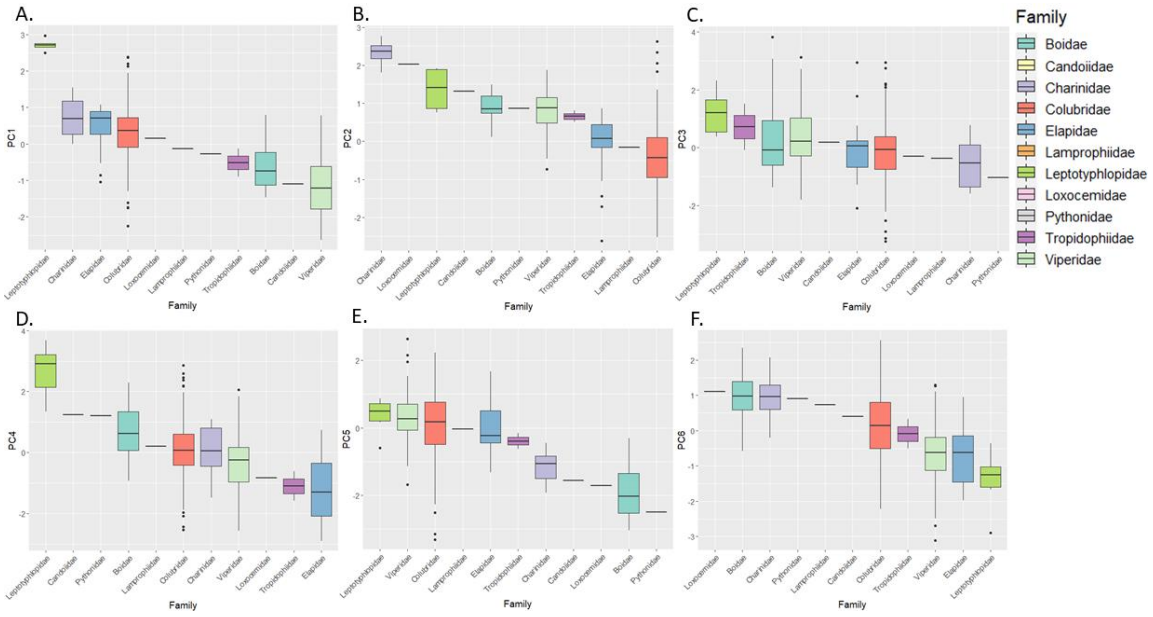

Figure 3.3. Box and whisker plots of PCs 1-6 in the all-group analysis by family. Colors represent family association. Lines within boxes represent median values, black circles are outliers. Single black lines without boxes are sample sizes of n=1.

PC4 represented 5.4% of the total variation and is attributable to changes in the ventral portion of the vertebrae, particularly cotylar shape and the orientation of the synapophyses (Fig. 3.4D). This ranges from the taller, circular cotyl and ventrally projecting synapophyses of the aquatic natricine *Liodytes pygaea*, to the wider, ellipsoidal cotyl and more laterally orientated synapophyses of the fossorial leptotyphlopid *Rena humilis*.

PC5 accounted for only 3.9% of the total variation, but exhibited important shape differences in the dorsal and ventral regions of the vertebrae (Fig. 3.4E). Shapes in PC5 ranged from a wider, lower, and thinner zygosphene associated with shorter parapophyses, narrower prezygapophyses, and wider prezygapophyseal articular facets in the terrestrial viperid, *Crotalus cerastes*, to a taller and thicker zygosphene associated

with longer parapophyses, wider prezygapophyses, and narrower prezygapophyseal articular facets in the semiarboreal boid, *Boa constrictor*.

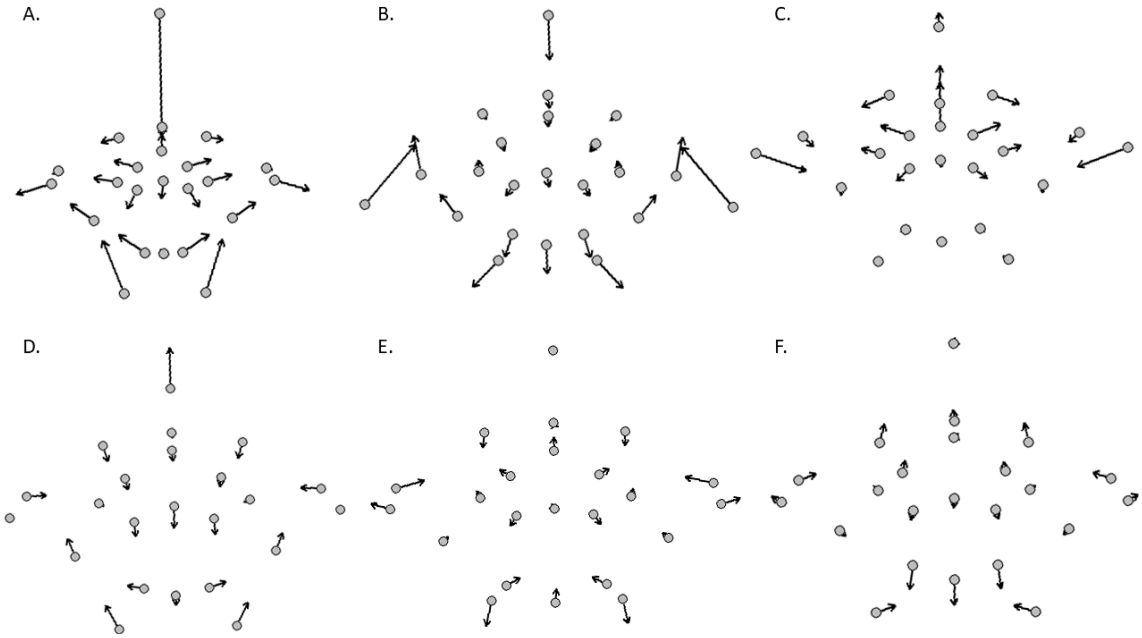

Figure 3.4. Vector plots for PCs 1-6 of the all-group analysis. The gray circles represent the negative standard deviations of the mean shape, while the arrows indicate shape change along each axis, ending at three positive standard deviations of mean shape.

Finally, PC6 is mainly explained by the distance between the bottom of the cotyl and the synapophyses, as well as the relative height of the prezygapophyseal articular facets and the top of the zygosphene (Fig. 3.4F). This ranges from longer parapophyses projecting ventrally away from the cotyl, with a more ventrally located zygosphene and prezygapophyseal articular facets in the arboreal viperid *Bothriechis nigroviridis*, to a relatively lower cotyl and shorter, medially located parapophyses with a more dorsally

located zygosphene and prezygapophyseal articular facets in the semifossorial natricine *Tropidoclonion lineatum*.

3.3.2. Shape Variation Within Crotalinae

In the Crotalinae-only analysis, results differed somewhat overall, both in the amount of variance explained by PC and in the morphological changes themselves. The first six PCs explained 81.9% of all variation in Crotalinae (Figs. 3.2C, 3.2D; Fig. 3.5). A plot of all PC percentages for the Crotalinae-only analysis is available in Appendix Fig. B2.

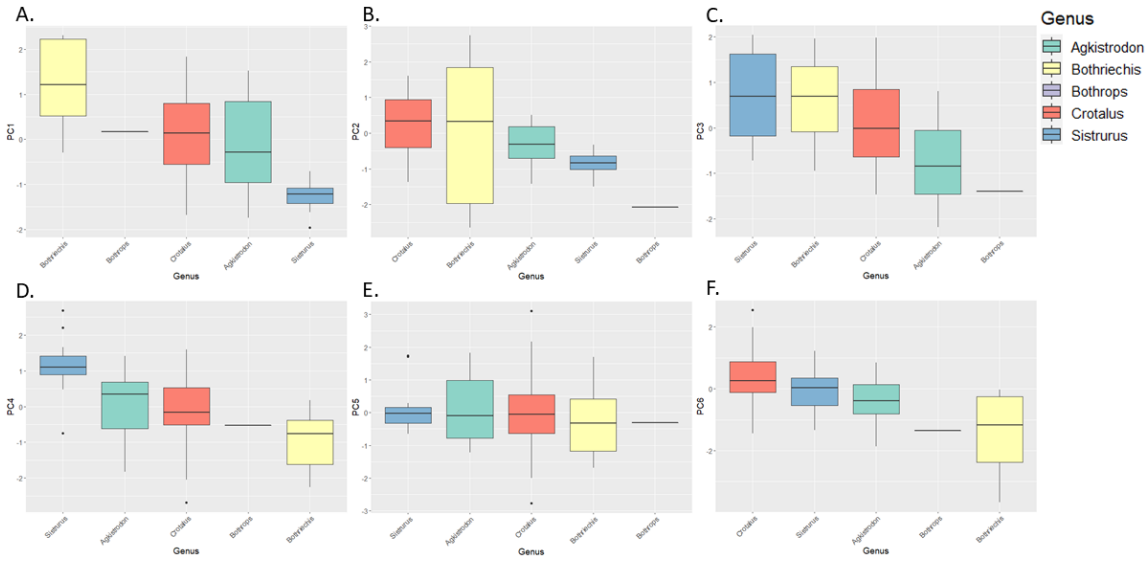

Figure 3.5. Box and whisker plots of PCs 1-6 (in numerical order) for the Crotalinae-only analysis by genus. Colors represent genus association. Lines within boxes represent median values, black circles are outliers. Single black lines without boxes represent sample sizes of n = 1.

PC1 explained 44.1 % of total variance and was similar to that of the previous analysis in that most of the variation is in the relative height of the vertebrae, composed primarily of neural spine and parapophyseal height (Fig. 3.6A). Unlike the previous analysis, the relative width was determined less by the prezygapophyses specifically, and was distributed more evenly throughout the vertebrae at each landmark. End members include terrestrial *Sistrurus miliarius* (negative) and arboreal *Bothriechis schlegelii* (positive). Beyond PC1, however, most of the PCs showed marked differences in the crotaline analysis compared to the all-group analysis.

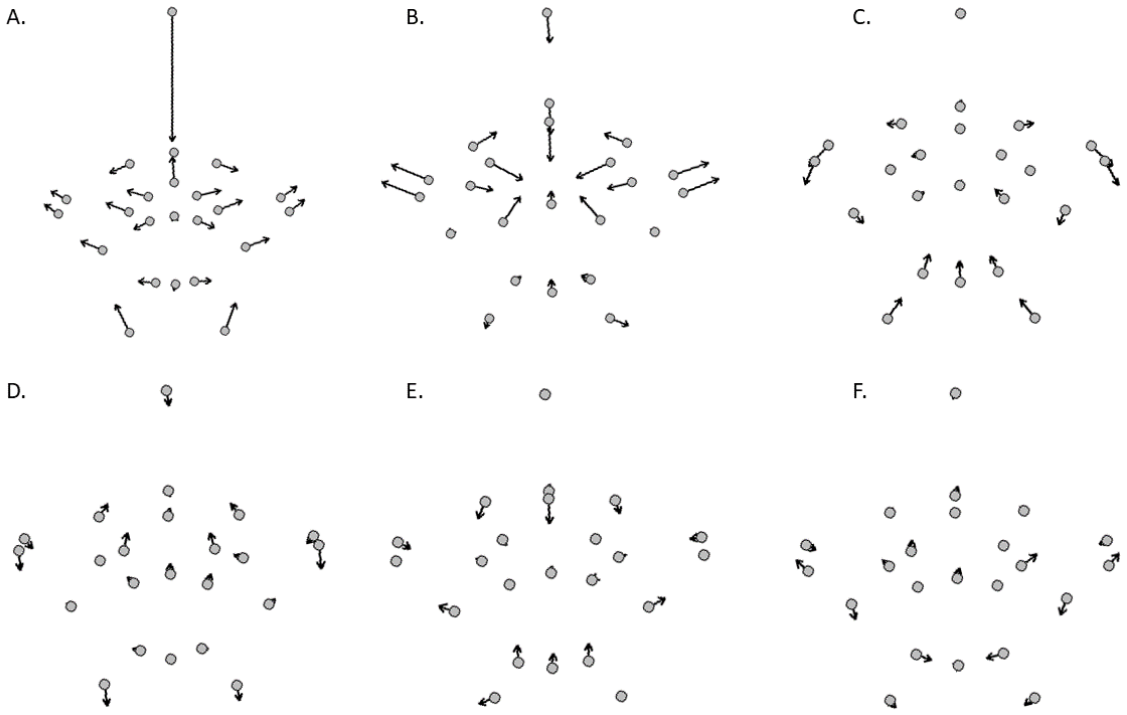

Figure 3.6. Vector plots for PCs 1-6 of the Crotalinae-only analysis (in numerical order). The gray circles represent the negative standard deviations of the mean shape, while the arrows indicate shape change along each axis, ending at three positive standard deviations of mean shape.

PC2 represented 19.5% of the total variation and was almost entirely explained by dorso-ventral compression and widening in the dorsal region of the vertebrae, where the prezygapophyses and associated articular facets would widen in parallel to the compression of the neural spine, zygosphene, and neural canal (Fig. 3.6B). The end members of PC2 include arboreal *Bothriechis schlegelii* (negative) and arboreal *Bothriechis nigroviridis* (positive).

PC3 explained 7.3% of the total variation, and intriguingly showed changes of the landmarks opposite to those of PC2 (Fig. 3.6C). Whereas PC2 explained relative width at the prezygapophyses and associated articular facets, PC3 explained the relative heights of those same structures. Similarly, while PC2 explained variation in the dorsal region of the vertebrae, PC3 explained variation in the ventral part of the vertebrae. Lower prezygapophyses and prezygapophyseal articular facets were associated with a smaller, rounder cotyl and shorter parapophyses in arboreal *Bothriechis schlegelii* (positive), and vice versa in terrestrial *Agkistrodon contortrix* (negative).

Beyond PC3, shape variation was much lower overall. PC4 represented 4.2% of variance and was attributable to the shape of the zygosphene and neural canal (Fig. 3.6D). Narrower, thinner zygosphenes were associated with taller neural canals in terrestrial *Sisturus miliarius* (positive), while terrestrial *Crotalus ruber* (negative) exhibited the opposing shape along this axis.

PC5 was 3.7% of total variation and showed a difference between the synapophyses compared to all other vertebral articulations (Fig. 3.6E). As the zygosphene, cotyl, and parapophyseal articular facets moved towards the center of the

vertebrae, the parapophyses and diapophyses migrated laterally away from the center of the vertebrae. End members include terrestrial *Crotalus molossus* (negative) and terrestrial *Crotalus cerastes* (positive).

Finally, PC6 represented 3.1% of shape variation and is explained by minor differences in the orientation of the prezygapophyses and associated articular facets, as well as the orientation of the diapophyses and shape of the cotyl (Fig. 3.6F). Dorsally oriented prezygapophyses were associated with slightly narrower prezygapophyseal articular facets, more ventrally located diapophyses, and a narrower but slightly taller cotyl in terrestrial *Crotalus cerastes* (positive) and vice versa in arboreal *Bothriechis schlegelii* (negative).

3.3.3. Multivariate Analyses of Snake Taxonomy

The Analysis of Variance (ANOVA) was different from zero variance explained ($p < 0.05$) for each of the first six selected PCs at the family, subfamily, genus, and species taxonomic levels in the all-group data and for the genus and species levels in the Crotalinae-only data (Appendix Tables B2-B9). Additionally, the F-values suggest that the variation among the group means at each taxonomic level were greater than would be expected by chance. For the all-group data, Tukey's tests at the family level suggested that much of the variation is found in the boids, charinids, leptotyphlopids, and viperids, although low sample sizes in some groups, such as in the loxocemids, may be obscuring some comparisons (Appendix Table B10). At the subfamily level, a second Tukey's test indicated that a large number of subfamilies, including boas, sea snakes, other elapids, leptotyphlopids, vipers, and several different colubrid subfamilies, varied

notably from at least one other group (Appendix Table B11). In the Crotalinae-only group, a genus-level Tukey's test most commonly indicated differences in *Sistrurus* and *Bothriechis* from other crotalines (Appendix Table B13). *Agkistrodon* commonly differed from both those two genera and occasionally from *Crotalus*, while *Bothrops* was poorly represented in the sample, and did not allow for thorough exploration.

A discriminant function analysis was applied to all PCs to classify individuals into certain groups, and performed best at higher taxonomic levels. The overall accuracy of the discriminant function analysis was 96.0% at the family level, 85.8% at the subfamily level, 68.2% at the genus level, 58.3% at the species level, and 57.1% for primary foraging habitat in the all-group data (Appendix Tables B10-B12). In the Crotalinae-only data, percentages increased to 82.3% at the genus level, 63.3% at the species level, and 89.7% for primary foraging habitat (Appendix Tables B13, B14).

3.4. Discussion

Geometric morphometrics have been used with increasing prevalence to examine isolated elements in both modern and fossil data (Lawing and Polly, 2010). The addition of geometric morphometrics for snake vertebral shape across a wide variety of snake species is a much-needed addition to the geometric morphometric body of literature. It opens new, replicable avenues for examining the evolution, ecology, and taxonomy of snakes in the fossil record as well as in the present. This study is the first to assess the ability of geometric morphometrics to delimit snake species using trunk vertebrae, and uses a large number of individuals and taxa from different clades. Overall, the analyses

suggest that there is a strong relationship between middle trunk vertebral shape and taxonomy, with differences between groups at family to species levels. The taxonomic groups can be separated in shape space and through discriminant functions; however, groups with smaller sample sizes and at lower taxonomic levels were more difficult to delimit, as predicted.

The PCA revealed a few important patterns of vertebral morphology in snakes. Throughout all the axes of variation considered in this study, specific structures of the vertebrae were consistently notable, some of which also contributed to the relative height and width of the vertebrae: the neural spine, the prezygapophyses, and the articular surfaces – including the prezygapophyseal articular facets on the distal regions of the vertebrae, the zygosphene and cotyl on the proximal region of the vertebrae, and the rib articulations at the synapophyses and diapophyses (Figs. 3.4, 3.6). In each of these cases, the relative shape, size, and orientation of the structures produced notable variation in the total shape of the vertebra.

The plot of PC1 and PC2 for the all-group data shows distinct groupings of proportionally heavy-bodied snakes, consisting of mainly booids and viperids on the upper left (tall neural spines, more dorsally oriented prezygapophyses and diapophyses, and wider prezygapophyseal articular facets), with more slender, agile snakes, primarily consisting of colubrines towards the bottom right of the plot (Fig. 3.2a). Tall neural spines tend to be found on large, active snakes, while low neural spines are found on snakes that exhibit more secretive behaviors and dorso-ventrally flatten the body for tight spaces, such as in the charinids, leptotyphlopids, and some dipsadinines (Holman,

2000). The position of the diapophyses and parapophyses is indicative of the general orientation of the ribs, which is associated with the need, or lack thereof, to prevent downward displacement of muscle when performing behaviors such as cantilevering (Lillywhite, 2014). Larger prezygapophyseal articular facets with more anteriorly oriented prezygapophyses indicate different proportions and uses for axial musculature when using their primary mode of locomotion and when procuring and feeding on prey (Johnson, 1955; Lillywhite et al., 2000; Lillywhite, 2014). Finally, the anterior to posterior articulations of the cotyl to the condyle and the zygosphene to the zygantrum are indicative of the amount of torsion and flexibility allowed by the vertebrae when using muscles for movement (Johnson, 1955; Moon, 1999; Lillywhite et al., 2000).

Along each PC axis, at least one of the maximum or minimum shapes were occupied by individuals possessing a specialized behavior for procuring and feeding on prey (e.g., viperid striking) or locomotion (e.g., leptotyphlopid burrowing) in the larger dataset. Furthermore, the individuals occupying the extremes of each axis of variation belonged to different families of snakes. Within the Crotalinae-only dataset, this pattern did not remain; however, as in the larger dataset, the terrestrial taxa occupy the majority of shape space, obscuring the clearer differences in shape between ecological specialties – something clearer in the crotalines alone than when examining all snakes at once. When primary foraging habitats were examined within the dataset and along the axes of shape variation, different spaces were occupied by different foraging habitat preferences both overall and within taxonomic groups at the family level, albeit with some degree of overlap.

The plot of PC1 and PC2 shows that fossorial and semifossorial taxa occupied spaces from the highest to medial values along both axes one and two; fossorial generally occupied values higher than semifossorial taxa on axis one, but lower values than semifossorial taxa on axis two (Fig. 3.2). Terrestrial taxa primarily occupied medial to low value spaces along axis one, and medial areas of PC2. Arboreal and semiarboreal taxa occupied medial values to low values on axes one and two, but extended to lower values than terrestrial, fossorial, and semifossorial taxa along axis two; specifically, semiarboreal taxa did not extend as far as arboreal taxa along axis one, but reached lower values than arboreal taxa along axis two. Finally, aquatic and semiaquatic taxa filled medial to low values on axes one and two, but reached lower values than all non-terrestrial taxa on axis one and lower values than all non-arboreal or semiarboreal taxa along axis two.

Remarkably, while there was generally more overlap between primary foraging habitats than between clades, similar convergent shifts in shape occurred within clades where these habitats were concerned (e.g., the shifts between arboreal and terrestrial colubrids and boids and the differences between semiaquatic and arboreal crotalines and semiaquatic and arboreal snakes overall). These results match qualitative (Lillywhite et al., 2000), linear (Johnson, 1955), and preliminary geometric morphometric (Lawing et al., 2012) results in much smaller datasets, and suggest that vertebral shape is influenced by both phylogeny and functional demands for different ecologies. Despite what is often considered a “generalized” body form across all snakes, snake trunk vertebral

morphology plays a locomotion-related functional role similar to that of limb bone proportions in mammals (Polly, 2010; Lawing et al., 2012; Short and Lawing, 2021).

Although the primary signal is taxonomic, primary foraging habitats still showed differences from the mean for all six PCs; likewise, the DFA for primary foraging habitat was similar to that of the DFA for species at 56.4% overall accuracy. Furthermore, both the PCA and the DFA showed stronger ecological differentiation when the resolution was changed to study within a specific subfamily, as in the crotaline example. This evidence suggests that snake vertebral morphology may have initially been influenced by adopting different types of predominant locomotor strategies when moving through different habitats or when using different prey capture methods. In this scenario, snakes would have then subsequently branched into other environments independently within their clades, eventually exhibiting a convergence of some shape alterations for specific primary foraging habitats. The separation of booids from most colubroids, the convergence of heavy-bodied booids and viperids in PC1 the all-group analyses, and the results of the crotaline DFA for PC1 and primary foraging habitat specifically support this interpretation.

A few considerations regarding the use of the geometric morphometric methods are necessary when interpreting results. The all-group dataset framework is best used for differentiating at higher taxonomic levels when including such a large sample and variety of groups. Similarly, the axes of shape change noted as responsible for the largest amounts of variation in the dataset are important at the scale of this study, but this may not be true for smaller analyses, such as within a single subfamily or genus. This is

exemplified well in the Crotalinae-only analyses, which showed different shape variations across PC axes and better delimitation at the genus and species level as well as for primary foraging habitat in the DFA. It may therefore be necessary to run the analysis separately within smaller scales, dependent upon the goal of the study using these methods (e.g., including only the genera within a subfamily or species within a genus, as done in some other geometric morphometric papers for taxonomic delimitation).

There are several important future directions for work related to the morphometrics of snake vertebral shape. Increasing the sample size with both more taxa from around the world and with more total vertebrae per taxon would allow statistical analysis of all the groups that I was unable to include in this study. This would also allow for the identification of any changes in shape variation among different geographic regions of the world.

As one of the main purposes of this study was to create a geometric morphometric framework for use with the fossil record, implementing these analyses with the addition of fossil vertebrae is a logical step forward. Doing so will allow for objective, quantitative support for fossil identifications, will produce insights on the evolutionary relationships and ecologies of fossil snakes, and will allow for the detection of any specific changes in morphological regimes (e.g., the shift from booid- to colubroid-dominated snake assemblages in the Neogene of North America; Holman, 2000; Parmley and Hunter, 2010; Jacisin et al., 2015). Furthermore, these techniques

should work when comparing fossil vertebrae whenever the homologous landmarks can be captured.

It is unlikely, based on both visual descriptions and linear measurements, that the anterior aspect of trunk vertebrae captures all diagnostic morphological variation in snakes. As such, the inclusion of other two-dimensional orientations for snake trunk vertebrae will likely produce additional information on shape variation in snakes that will improve these methods when combined with the anterior aspect. Finally, while the goal of this study was to create a simple, accessible method to improve taxonomic delimitation using snake vertebrae, I expect three-dimensional morphometrics to become more accessible and affordable in the future. As online databases of three-dimensional biological data continue to grow, techniques such as micro-computed tomography – and the programs with which to work on such data – will become more common and affordable. Three-dimensional morphometrics, then, will likely become a more commonly used, powerful tool on scales comparable to this study.

These results do not imply that geometric morphometrics should be used in lieu of gestalt and subjective visual identifications or traditional quantitative morphometrics and linear measurements, but rather as a more objective supplement to help build support for identifications in both extant and fossil skeletal material. Previous studies using geometric morphometrics for taxonomic delimitation on smaller scales have reached similar conclusions: the best results are likely to be achieved by combining morphometric shape data from homologous landmarks, traditional size morphometrics, and visual qualitative descriptions (Mutanen and Pretorius, 2007; Whitenack and

Gottfried, 2010; Meik et al., 2012; Ruane, 2015). The vector plots produced practical, objective visualizations of diagnostic shape differences between taxa at specific landmarks. These methods are more effective at describing shape variation as opposed to size variation, where qualitative descriptions and numerical measurements may be more appropriate.

In conclusion, shape space of this study provides a new blueprint that can be referenced to assist in taxonomic identification and delimitation in both extant and fossil snakes using middle trunk vertebrae. Shape variation in snake trunk vertebrae show both phylogenetic and ecomorphological signals, which has implications for both the evolution of morphology between and within snake clades, and for the potential of methods such as ecometrics to be utilized in future studies. While geometric morphometrics is a powerful suite of tools with the capacity to assist in the delimitation of recent and fossil snake vertebrae, it is not yet precise enough alone with the dataset of this study to provide high confidence delimitation for some groups when analyzed for all snake groups simultaneously. Qualitative descriptions should continue to be used alongside shape analysis to identify and describe snake vertebrae in future studies.

3.5. References

Adams, D. C., and E. Otarola-Castillo. 2013. Geomorph: an R package for the collection and analysis of geometric morphometric shape data. Methods in Ecology and Evolution 4:393–399.

Angielczyk, K. D. and H. D. Sheets. 2007. Investigation of simulated tectonic deformation in fossils using geometric morphometrics. Paleobiology 33: 125-148.

Auffenberg, W. 1963. The fossil snakes of Florida. Tulane Studies in Zoology 10:131-216.

Baylac, M. C., C. Villemant, and G. Simbolotti. 2003. Combining geometric morphometrics with pattern recognition for the investigation of species complexes. Biological Journal of the Linnean Society, 80:89–98.

Bell, C. J., J. J. Head, and J. I. Mead. 2004. Synopsis of the herpetofauna from Porcupine Cave. *In* A.D. Barnosky (Ed.), Biodiversity Response to Climate Change in the Middle Pleistocene: the Porcupine Cave Fauna from Colorado, University of California Press, Berkeley, California pp. 117-126.

Bell, C. J., J. A. Gauthier; and G. S. Bever. 2010. Covert biases, circularity, and apomorphies: A critical look at the North American Quaternary Herpetofaunal Stability Hypothesis. Quaternary International 217: 30-36.

Bell, C. J., and J. I. Mead. 2014. Not enough skeletons in the closet: collections-based anatomical research in an age of conservation conscience. Anatomical Record 297:344–348.

Bickford D., D. J. Lohman, N. S. Sodhi, P. K. L. Ng, R. Meier, K. Winker, K. K. Ingram, and I. Das. 2007. Cryptic species as a window on diversity and conservation. Trends in Ecology & Evolution 22: 148–155.

Bookstein, F. L., B. Chernoff, R. Elder, J. Humphries, G. Smith, and R. Strauss. 1985. Morphometrics in evolutionary biology. Special Publication 15. Academy of Natural Sciences, Philadelphia, 277.

Bookstein, F. L., 1996. Biometrics, biomathematics and the morphometric synthesis. Bulletin of mathematical biology, 58:313.

Burbrink F. T., R. Lawson, and J. B. Slowinski. 2000. Mitochondrial DNA phylogeography of the polytypic North American rat snake (Elaphe obsoleta): a critique of the subspecies concept. Evolution 54: 2107–2118.

Cardini, A., A. -U. Jansson, and S. Elton. 2007. A geometric morphometric approach to the study of ecogeographical and clinal variation in vervet monkeys. Journal of Biogeography 34: 1663-1678.

Caumul, R. and P. D. Polly. 2005. Phylogenetic and environmental components of morphological variation: skull, mandible, and molar shape in marmots (Marmota, Rodentia). Evolution 59: 2460-2472.

Cundall, D. 1987. Functional morphology. In ‘Snakes: Ecology and Evolutionary biology. (Eds RA Seigel, JT Collins and SS Novak.) pp. 106–142.

Fabien, A., S. Maumelat, D. Bradshaw, T. Schwaner, and X. Bonnet. 2004. Diet divergence, jaw size and scale counts in two neighbouring populations of tiger snakes (Notechis scutatus). Amphibia-Reptilia 25: 9–17.

Gentilli A., A. Cardini, D. Fontanetto, and M. A. L. Zuffi. 2009. The phylogenetic signal in cranial morphology of Vipera aspis: a contribution from geometric morphometrics. Herpetological Journal 19: 69–77.

Gilmore, C. W. 1938. Fossil snakes of North America (Vol. 9). Geological Society of America.

Gray, J. A., M. C. McDowell, M. N. Hutchinson, and M. E. Jones. 2017. Geometric morphometrics provides an alternative approach for interpreting the affinity of fossil lizard jaws. Journal of Herpetology, 51:375-382.

Head, J. J. 2015. Fossil calibration dates for molecular phylogenetic analysis of snakes 1: Serpentes, Alethinophidia, Boidae, Pythonidae. Palaeontologia Electronica, 18:1-17.

Head, J. J., K. Mahlow, and J. Mueller. 2016. Fossil calibration dates for molecular phylogenetic analysis of snakes 2: Caenophidia, Colubroidea, Elapoidea, Colubridae. Palaeontologia Electronica, 19:1-21.

Holman, J. A. 2000. Fossil snakes of North America: Origin, evolution, distribution, paleoecology. Bloomington: Indiana University Press.

Huntley, L. C., D. J. Gower, F. L. Sampaio, E. S. Collins, A. Goswami, and A. C. Fabre. 2021. Intraspecific morphological variation in the shieldtail snake Rhinophis philippinus (Serpentes: Uropeltidae), with particular reference to tail-shield and cranial 3D geometric morphometrics. Journal of Zoological Systematics and Evolutionary Research, 59:357-1370.

Hutchinson, M. N. 1997. The first fossil pygopod (Squamata: Gekkota) and a review of mandibular variation in living species. Memoirs of the Queensland Museum 41:355–366.

Jaiswara, R., D. Nandi, and R. Balakrishnan. 2013. Examining the effectiveness of discriminant function analysis and cluster analysis in species identification of male field crickets based on their calling songs. PloS one, 8, p.e75930.

Jasinski, S. E., and D. A. Moscato. 2017. Late Hemphillian Colubrid Snakes (Serpentes, Colubridae) from the Gray Fossil Site of Northeastern Tennessee. Journal of Herpetology, 51: 245-257.

Jayne, B. C. 2020. What defines different modes of snake locomotion?. Integrative and comparative biology, 60:156-170.

Johnson, R. G. 1955. The adaptive and phylogenetic significance of vertebral form in snakes. Evolution 9:367–388.

Jurestovsky, D. J., B. C. Jayne, and H. C. Astley. 2020. Experimental modification of morphology reveals the effects of the zygosphene–zygantrum joint on the range of motion of snake vertebrae. Journal of Experimental Biology, 223:jeb216531.

Kaila, L. and G. Ståhls. 2006. DNA barcodes: Evaluating the potential of COI to diffentiate closely related species of Elachista (Lepidoptera: Gelechioidea: Elachistidae) from Australia. Zootaxa, 1170:1-26.

Kendall, D. G. 1977. The diffusion of shape. Advances in applied probability, 9:428-430.

Klaczko, J., E. Sherratt, and E. Z. Setz. 2016. Are diet preferences associated to skulls shape diversification in xenodontine snakes? *PloS one*, *11*(2), p.e0148375.

Klein, C. G., D. Pisani, D. J. Field, R. Lakin, M. A. Wills, and N. R. Longrich. 2021. Evolution and dispersal of snakes across the Cretaceous-Paleogene mass extinction. Nature Communications, 12:1-9.

LaDuke, T. C. 1991. The fossil snakes of Pit 91, Racho La Brea, California. Natural History Museum of Los Angeles County Contributions in Science 424: 1-28.

Lawing, A. M. and P. D. Polly. 2010. Geometric morphometrics: recent applications to the study of evolution and development. Journal of Zoology 280: 1-7.

Lawing, A. M. and P. D. Polly. 2011. Pleistocene climate, phylogeny, and climate envelope models: an integrative approach to better understand species' response to climate change. PLoS One 16:e28554.

Lawing, A. M., J. J. Head, and P. D. Polly. 2012. The ecology of morphology: the ecometrics of locomotion and macroenvironment in North American snakes. Pp. 117-146 in J. Louys (ed.), Palaeontology in Ecology and Conservation. Springer-Verlag, Berlin and Heidelberg.

Lillywhite, H. B. and R. W. Henderson. 1993. Behavioral and functional ecology of arboreal snakes. In: Seigel RA, Collins JT, eds Snakes: Ecology and Behavior. New York: McGraw-Hill, 1–48.

Lillywhite, H. B., J. R. LaFrentz, Y. C. Lin, and M. C. Tu. 2000. The cantilever abilities of snakes. Journal of Herpetology, pp.523-528.

Lillywhite, H. B. 2014. How snakes work: structure, function and behavior of the world's snakes. Oxford University Press.

Manier, M. K. 2004. Geographic variation in the long-nosed snake, *Rhinocheilus lecontei* (Colubridae): beyond the subspecies debate. Biological Journal of the Linnean Society 83: 65–85.

Mayr, E. 1942. Systematics and the origin of species, from the viewpoint of a zoologist. Cambridge, MA: Harvard University Press.

Meik, J. M., K. Setser, E. Mocino-Deloya, and A. M. Lawing. 2012. Sexual differences in head form and diet in a population of Mexican lance-headed rattlesnakes, Crotalus polystictus. Biological Journal of the Linnean Society, 106:633-640.

Meylan, P. A. 1982. The squamate reptiles of the Inglis IA fauna (Irvingtonian: Citrus County, Florida). Bulletin of the Florida State Museum, Biological Sciences 27:1-85.

Mutanen, M. and E. Pretorius. 2007. Subjective visual evaluation vs. traditional and geometric morphometrics in species delimitation: a comparison of moth genitalia. Systematic Entomology 32:371–386.

Nice, C. C. and A. M. Shapiro. 1999. Molecular and morphological divergence in the butterfly genus Lycaeides (Lepidoptera: Lycaenidae) in North America: evidence of recent speciation. Journal of Evolutionary Biology, 12:936–950.

Olson, E. C. and R. L. Miller. 1958. Morphological integration. Chicago: University of Chicago Press.

Parmley, D. and K. B. Hunter. 2010. Fossil Snakes of the Clarendonian (Late Miocene) Pratt Slide Local Fauna of Nebraska, with the description of a new natricine colubrid. Journal of Herpetology 44:526-543.

Polly, P. D. 2008. Developmental dynamics and G-matrices: can morphometric spaces be used to model phenotypic evolution? Evol. Biol. 35:1–20. (Online DOI 10.1007/s11692-008-9020-0).

Rage, J. -C. 1984. Encyclopedia of Paleoherpetology, part 11, Serpentes. Gustav Fischer Verlag, Stuttgart.

Ricklefs, R. E. and J. Travis. 1980. A morphological approach to the study of avian community organization. Auk, 97:321–338.

Rohlf, F. J. 1990. Morphometrics. Annu. Rev. Ecol. Syst. 21:299–316.

Rohlf, F. J. and L. Marcus. 1993. A revolution in morphometrics. Trends Ecol. Evol. 8:129–132.

Rohlf F. J. and D. Slice. 1990. Extentions of the Procrustes method for the optimal superimposition of landmarks. Syst Zool 39:40–59.

Rohlf, F. J., A. Loy, and M. Corti. 1996. Morphometric analysis of old world Talpidae (Mammalia, Insectivora) using partial-warp scores. Systematic Biology 45:344–362.

Ruane, S. 2015. Using geometric morphometrics for integrative taxonomy: An examination of head shapes of milksnakes (genus *Lampropeltis*). Zoological Journal of the Linnean Society, 174:394-413.

Saez, A. G. and E. Lozano. 2005. Body doubles. Nature 433:111.

Savitzky, A. H. 1980. The role of venom delivery strategies in snake evolution. Evolution 34:1194–1204.Shine, R., Reed, R., Shetty, S. and Cogger, H. 2002.

Relationships between sexual dimorphism and niche partitioning within a clade of sea-snakes (Laticaudinae). Oecologia 133: 45–53.

Smith, K. T. 2013. New constraints on the evolution of the snake clades Ungaliophiinae, Loxocemidae and Colubridae (Serpentes), with comments on the fossil history of erycine boids in North America. Zoologischer Anzeiger-A Journal of Comparative Zoology, 252:157-182.

Szyndlar, Z., 1984. Fossil snakes from Poland. Acta zoologica cracoviensia, 28:1.

Vincent, S. E., A. Herrel, and D. J. Irschik. 2004. Ontogeny of intersexual head shape and prey selection in the pitviper *Agkistrodon piscivorus*. Biological Journal of the Linnean Society 81:151–159.

Webster, M. and N. C. Hughes. 1999. Compaction-related deformation in Cambrian olenelloid trilobites and its implications for fossil morphometry. Journal of Paleontology 73: 355-371.

Whitenack, L. B. and M. D. Gottfried. 2010. A morphometric approach for addressing tooth-based species delimitation in fossil mako sharks, Isurus (Elasmobranchii: Lamniformes). Journal of Vertebrate Paleontology, 30:17-25.

Wood, A. R., M. L. Zelditch, A. N. Rountrey, T. P. Eiting, H. D. Sheets, and P. D. Gingerich. 2007. Multivariate stasis in the dental morphology of the Paleocene-Eocene condylarth *Ectocion*. Paleobiology 33:248-260.

Zelditch, M. L., D. L. Swiderski, H. D. Sheets, and W. L. Fink. 2004. Geometric morphometrics for biologists: a primer. Amsterdam: Elsevier.

4. LINKING BIOGEOGRAPHY AND INTRASPECIFIC MORPHOLOGICAL VARIATION OF SKULL SHAPE AND BODY MEASUREMENTS IN THE WESTERN MASSASAUGA, *SISTRURUS TERGEMINUS* (SAY, 1823)

"Try to learn something about everything and everything about something." –

Thomas Henry Huxley

4.1. Introduction

Anthropogenic activity can cause natural populations to experience rapid trait change, extirpation, or extinction (Myers et al., 2000; Pimm and Raven, 2000; Barnosky et al., 2011). Under these conditions, species' traits will partly determine whether species will move, adapt, or perish. The distributions of such functional traits are controlled by both abiotic (e.g., temperature, precipitation, and other climate-related variables) and biotic (e.g., predation, competition, food availability) environmental factors, as well as the interactions among different functional traits, biotic factors, and abiotic variables (Polly et al., 2011). The intraspecific variation of these traits in particular can reveal the potential of a species to survive changing environments when directly or indirectly linked to diet or environmental factors such as climate or vegetation cover (Smith et al., 1995; Lawing and Polly, 2010; McGuire, 2010; Polly et al., 2011; Mimura et al., 2017; Herrando-Pérez et al., 2019; McGuire and Lauer, 2020; Huntley et al., 2021). While higher variation generally indicates larger population sizes (Mimura et

al., 2017) with higher potential for adapting to change (Herrando-Pérez et al., 2019), the mobility, distribution, and type of variation also play vital roles in determining adaptability in a species (McGuire and Lauer, 2020). However, few studies have examined intraspecific trait variation from the perspective of both internal and external morphology within a single, geographically widespread species; this is especially true for snakes.

Understanding both internal and external morphological variation is important from a fitness perspective, as both phenotypic plasticity and morphological adaptation can be influenced by environmental conditions (Polly et al., 2011; Lawing et al., 2012), social interaction (Håkansson and Jensen, 2005), diet and nutrition (O'Regan and Kitchener et al., 2005), and cognitive exercise (Carducci and Jakob, 2000). External and internal morphological changes may differ in magnitude or direction to each of these pressures, or subtle changes in one may mask greater changes in the other (O'Regan and Kitchener et al., 2005; Courtney Jones et al., 2018). Changes in these factors typically lead to changes in external morphological traits (e.g., body shape between populations of the spotted mackerel *Scomber australasicus* and head shape between sexes in the Mexican lance-headed snake *Crotalus polystictus*; Tzeng, 2004; Meik et al., 2012) or skeletal traits (e.g., cranial morphology in canids and between captive and wild mammals; Siciliano-Martina et al., 2021a, 2021b). In the face of the current climate crisis and its effects on the environment, understanding intraspecific changes as they relate specifically to ecomorphology is important for understanding how a species will handle changes for any of the habitats in which it presently resides.

Ecomorphology describes the relationships between morphological adaptations, developmental plasticity, and trait variation within and between species, and the ecological role of those traits as it relates to climate and environment (Ricklefs and Miles, 1994, Norton et al., 1995; Courtney Jones et al., 2018). Understanding the correspondence between ecological and morphological variation across populations provides insight into the functionality and performance of traits in different environments, and is paramount for developing better species conservation and management practices. For example, head shape, along with body proportions, body size, and many aspects of external soft-tissue morphologies, are functionally tied to feeding and locomotor ecologies in snakes (Dwyer and Kaiser, 1997; Hibbitts and Fitzgerald, 2005; Cundall and Irish, 2008; Head et al., 2009; Lawing et al., 2012). Head and skull shape in gape-limited predators can be implicative of prey size and shape (Hibbitts and Fitzgerald, 2005; Herrel et al., 2008; Vincent et al., 2009), which may sometimes also be related to sexual dimorphism (Meik et al., 2012; Klaczko et al., 2016; Watanabe et al., 2019). Similarly, the way snakes locomote and camouflage through their environments is influenced by their overall body proportions (Lawing et al., 2012) and vegetation cover or substrate (Harvey and Weatherhead, 2011), respectively. Higher numbers of labial and mid body dorsal scale rows (representing measures of girth) may be associated with both larger body size, increased flexibility, and larger prey size among populations of the same snake species (Fabien et al., 2004).

In this study, I describe intraspecific external and internal (skeletal) morphological variation the Western massasauga *Sistrurus tergeminus*, a snake species

known to be geographically expansive and exposed to different habitats, climate conditions, and primary prey types. *Sistrurus tergeminus* is a small (< 70 cm) rattlesnake known to feed primarily on small mammals, reptiles, and invertebrates as an ambush predator (Holycross and Mackessy, 2002). It was historically considered one of three subspecies of *Sistrurus catenatus*, along with the Eastern massasauga (*S.c. catenatus*) and the desert massasauga (previously, *S.c. edwardsii*, then *S.t. edwardsii*) based on limited studies of morphological variation within its widespread distribution (reviewed in Ryberg et al., 2015). Phylogenetic studies suggested that *S.c. catenatus* was genetically distinct from both *S.c. tergeminus* and *S.c. edwardsii*, further separating them into *S. catenatus, S.t. tergeminus*, and *S.t. edwardsii* (Kubatko et al., 2011; Gibbs et al., 2011; Crother et al., 2011; Crother et al., 2012). While the split between *S. catenatus* and *S. tergeminus* was well supported by these analyses, the distinction between *S.t. tergeminus* and *S.t. edwardsii* was weaker, either the result of overlapping distributions in north-central Texas (Campbell et al., 2004; Dixon, 2013), or the result of incomplete sampling (Ryberg et al., 2015). A newer study by Ryberg et al. (2015) found that populations of *S.t. tergeminus* and *S.t. edwardsii* as presently defined were genetically indistinguishable, and that historically, *S. tergeminus* likely represented a large and geographically contiguous assembly of populations that were more recently fragmented into several isolated populations.

Dietary differences have been observed both between species of massasaugas (*S. catenatus* and *S. tergeminus*) and between populations of *S. tergeminus* (Holycross and Mackessy, 2002); these dietary differences have resulted in allelic differences in snake

venom genes for specialization on mammalian (*S. catenatus*) or mixed mammalian and ectothermic prey (*S. tergeminus*; Gibbs and Rossiter, 2008). Holycross and Mackessy (2002) also found that while diet was similar within populations and between sexes in *Sistrurus*, juveniles generally consumed fewer mammals than adults. Furthermore, *Sistrurus* showed significant geographic variation in diet correlating with differences in ecological variation across its range. Eastern populations favored mesic environments and small mammalian prey, supplemented by occasional snakes or lizards, and western populations favored xeric grasslands and lizard prey, supplemented by small mammals and centipedes (Holycross and Mackessy, 2002). As such, an examination of these morphological aspects – vital to the functionality of diet and locomotion – is necessary for a holistic understanding of the habitat associations, diet, and ecology of *S. tergeminus*. Additionally, studying the morphological variation in these skeletal and external elements should be useful in investigating sex-specific morphological differences within and among populations.

Here, I examine the head squamation and skull morphology for over 100 individuals of *S. tergeminus* across 10 populations in the United States and Mexico, in order to test for detectable intraspecific morphological variation among populations of *S. tergeminus* (Fig. 4.1). I report data collection and analysis to address the following questions: (1) do populations of *S. tergeminus* differ in external morphometrics, squamation, and skull morphometrics across their range; and (2) do these differences vary with populations, sex, and environmental variables in a coordinated manner? I use geometric morphometrics, external measurements, and scale counts to approach the

study quantitatively for differences related to diet, sex, environmental variables, or some combination of those factors. I test the hypothesis that variation in skull shape and external morphology across 10 populations of *S. tergeminus* are associated with differences in diet, sex, and/or bioclimatic factors. I assess the collection of differences in skull shape and external morphology that associate with specific changes in prey selection and availability, sex, and temperature- and precipitation-related variables. I discuss whether these factors are likely to be direct or indirect drivers of intraspecific morphological variation. Reconciling the observed shallow genetic structure with known, but not well-resolved, morphological variation in light of the environmental gradients across widespread populations is key to understanding the evolutionary history of this species – and likely its future – under anthropogenic change.

4.2. Methods

To examine morphological variation of squamation and of cranial and external traits across the geographic distribution of *S. tergeminus* populations, I performed micro-computed tomography (micro-CT) scans of 130 wet-preserved full-body museum specimens. The data consisted of 52 adult females and 78 adult males across 10 populations of the U.S. and Mexico for use in the morphological studies (Fig. 4.1). The populations were assigned by state and country and selected to match the mtDNA clades of Ryberg et al. (2015), plus two additional localities in the western Texas and Coahuila, Mexico areas. The populations include Coahuila, Mexico (MX), Arizona (AZ), Colorado (CO), New Mexico (NM), South Texas (ST), West Texas (WT), North Texas (NT),

Oklahoma (OK), Kansas (KS), and Missouri (MO). Where diet is considered as a potential cause for morphological differences among populations, I refer to Holycross and Mackessy (2002), who described percentages of different prey items for several populations of *Sistrurus*.

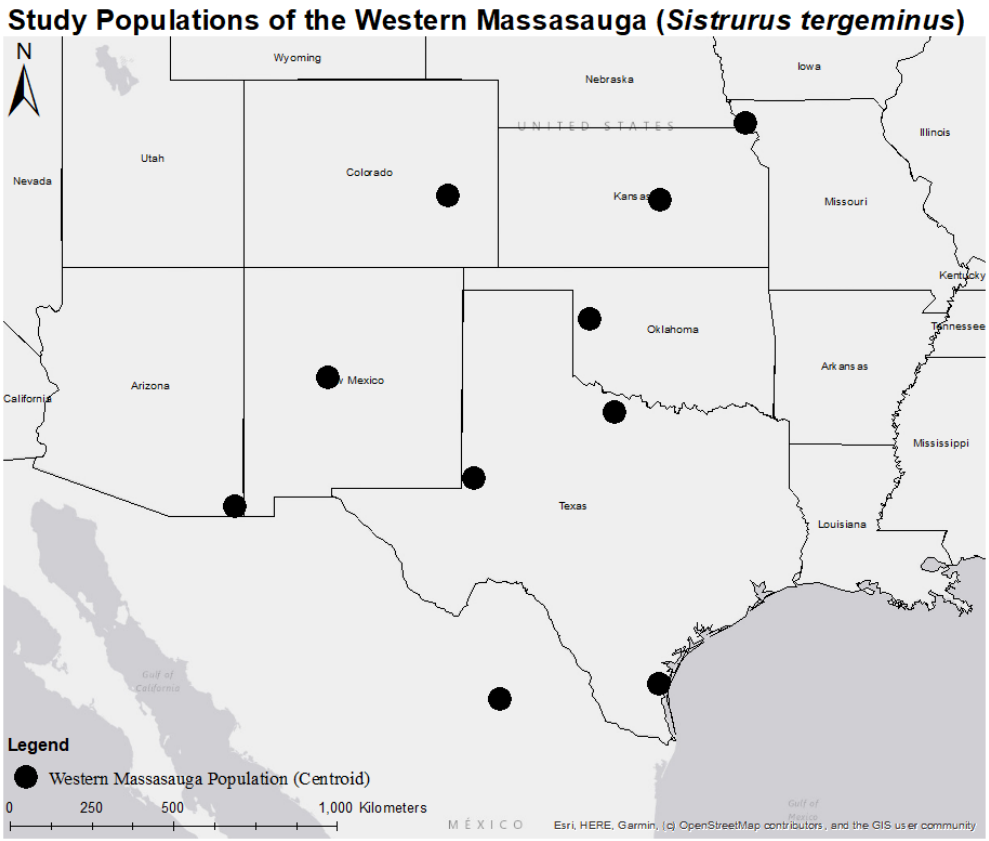

Figure 4.1. Centroid locations of all Western massasauga populations included in this study (n = 10).

To obtain the micro-CT scans, I coordinated with multiple museums to receive loaned specimens that represent geographic variation in this species. Collections included those from the Texas A&M University Biodiversity Research and Teaching

Collections, the University of Texas at Austin - Texas Natural History Collections, the Natural History Museum of Los Angeles County, the Carnegie Museum of Natural History, the University of Kansas Biodiversity Institute, the University of Colorado Museum of Natural History, the Arizona State University Natural History Collections, the Sam Noble Oklahoma Museum of Natural History, and the Museum of Southwestern Biology. I used a Brubaker Skyscan 1173 micro-CT scanner with a 1 mm Aluminum filter at 65 kV and 123 uA at Friday Harbor Laboratories on San Juan Island, Washington. I reconstructed the scans using the program NRecon, and preliminary models and 2D snapshots were taken in CTvox. All reconstructed scans were uploaded to and made available through the oVert: UW – CT Scan all Fishes project.

I further processed the skulls of these individuals to assess geographic variation and address skull-related ecological associations such as prey base and diet. Of the scanned individuals, 113 skulls in dorsal view (46 females and 67 males) and 102 skulls in left lateral view (42 females and 60 males) were suitable for the 2D geometric morphometric analyses. I excluded the remaining specimens from the original 130 individuals, as some images were unusable, and some skulls were damaged in specific orientations or were partially decalcified from long-term storage in formalin.

I developed landmark schemes of 20 and 22 fixed landmarks for the 2D images of the dorsal and left lateral orientations, respectively, that capture major aspects of skull shape and account for the kinetic nature of the snake skull (Tables 4.1 and 4.2; Fig. 4.2). The overall landmark schemes are based on those used for Xenodontinae in Klaczko et al. (2016), but are heavily modified and expanded for the skull morphology of

Crotalinae. As in other studies, I only digitized landmarks on one side of the skull, as the focus was not on the possible asymmetry of skull shape (Lawing and Polly, 2011; Klaczko et al., 2016). Landmarks were additionally split into one of three groups in each view in order to account for the hyperkinetic nature of snake skulls, with each group representing a portion of the skull that functions as a separately when feeding (Fig. 4.2; Watanabe et al., 2019). The groups were selected based on prior observations of the feeding mechanism in snakes, and how different parts of the skull behave during the feeding process (Gans, 1961; Klaczko et al., 2016; Watanabe et al., 2019; Rhoda et al., 2020). I collected and landmarked the 2D snapshots using the TPS suite programs TPSUtil and TPSdig2, then uploaded the TPS files to R (Rohlf, 2010). I then used Generalized Procrustes analysis to translate, rotate, and scale the schemes, thus removing the effects of size, orientation, and location differences in the images and superimposing landmarks onto a common coordinate system (Rohlf and Slice, 1990). Generalized Procrustes analysis removes size by scaling configurations to a common unit size through dividing by centroid size.

I ordinated the landmarks with a principal component analysis (PCA) for each landmark group to quantify and summarize the variations in skull shape (Dryden and Mardia, 1998; Klaczko et al., 2016). These variations are represented by individual PC axes of landmark configurations. I used linear discriminant functions with PC axes representing the most variation in each group for each orientation to test the reliability of population- and sex-based assignments. To examine the changes in skull morphology for each PC, I constructed vector plots and thin plate splines of skulls that best represented

the variation in shape along each PC axis for each landmark group (Fig. 3, Appendix Fig. C1; Rohlf, 1993; Lawing et al., 2012; Klaczko et al., 2016). These diagrams show the degree of variation between specimens and what landmark or combination of landmarks are most involved in that variance. To evaluate large scale spatial patterns of skull shape, I compared each PC axis of shape variation to the latitudes and longitudes associated with each specimen for all populations. Latitudes and longitudes of collection localities were obtained from museum records for each specimen. I used univariate analysis of variance tests (ANOVAs) to test for significant relationships among populations, sexes, and the axes of shape variation from the PCAs. I used ANOVAs to compare the morphological variables with bioclimatic variables from WorldClim, using individual records of latitude and longitude associated with each specimen to determine the geographic extent of the bioclimatic data (Fick and Hijmans, 2017).

I scored eight aspects of squamation for all 130 individuals and made 15 additional measurements, including 11 linear measurements and four measurements of coloration pattern, in order to compare variation in squamation, body size, body proportions, and skin pattern across *S. tergeminus* populations (Table 4.3; Meik et al., 2012). I summarized which measurements explained the greatest amount of external morphological variation in *S. tergeminus* with a PCA of the external phenotypic variables only, then constructed a correlation matrix to compare the relationships and covariance between the external measurements and the axes of skull shape. Finally, I again ran a series of ANOVAs to test for significant relationships between bioclimatic variables and the external measurements.

Table 4.1. Dorsal landmark identification numbers, subgroups, and definitions.

ID	Subgroup	Dorsal View Landmark Definitions
1	A	Midline point on the premaxilla at the inferior tip of the bony septum
2	A	Tip of the palatine process on the premaxilla
3	A	Tip of the nasal process on the premaxilla
4	B	Anterior-midline of nasal
5	B	Lateral tip of nasal
6	B	Tip of the frontal process on the nasal
7	B	Posterior-midline of nasal
8	C	Anterior-midline of frontal
9	C	Anterior frontal-prefrontal suture
10	C	Posterior frontal-prefrontal suture
11	C	Frontal-parietal lateral suture
12	C	Frontal-parietal midline suture
13	C	Anterior postorbital-parietal suture
14	C	Posterior postorbital-parietal suture
15	C	Parietal-supraoccipital suture, midline
16	C	Supraoccipital-exoccipital suture, midline
17	C	Supraoccipital-exoccipital suture, lateral
18	C	Exoccipital posterior tip, midline
19	C	Anteriormost tip of supratemporal
20	C	Posteriormost tip of supratemporal

Table 4.2. List of lateral view landmark identification numbers, subgroups, and definitions.

ID	Subgroup	Lateral View Landmark Definitions
1	A	Midline point on premaxilla at the inferior tip of the bony septum
2	A	Tip of the palatine process on the premaxilla
3	A	Tip of the nasal process on the premaxilla
4	A	Anterior tip of nasal
5	B	Nasal-frontal suture
6	B	Anterior frontal-prefrontal suture
7	B	Antero-ventral frontal-prefrontal suture
8	B	Anterior prefrontal-maxilla suture
9	B	Posterior prefrontal-maxilla suture
10	B	Posterior frontal-prefrontal suture
11	B	Anterior postorbital-parietal suture
12	B	Posterior postorbital-parietal suture
13	B	Parietal-supraoccipital suture, midline
14	B	Antero-ventral suture of the prootic with the basisphenoid
15	B	Anterior tip of supratemporal
16	B	Posterior tip of supratemporal at quadrate articulation
17	C	Anterior tip of maxilla
18	C	Posterior tip of the maxilla
19	C	Anterior tip of ectopterygoid
20	C	Posterior tip of ectopterygoid
21	C	Anterior tip of pterygoid
22	C	Posterior of pterygoid

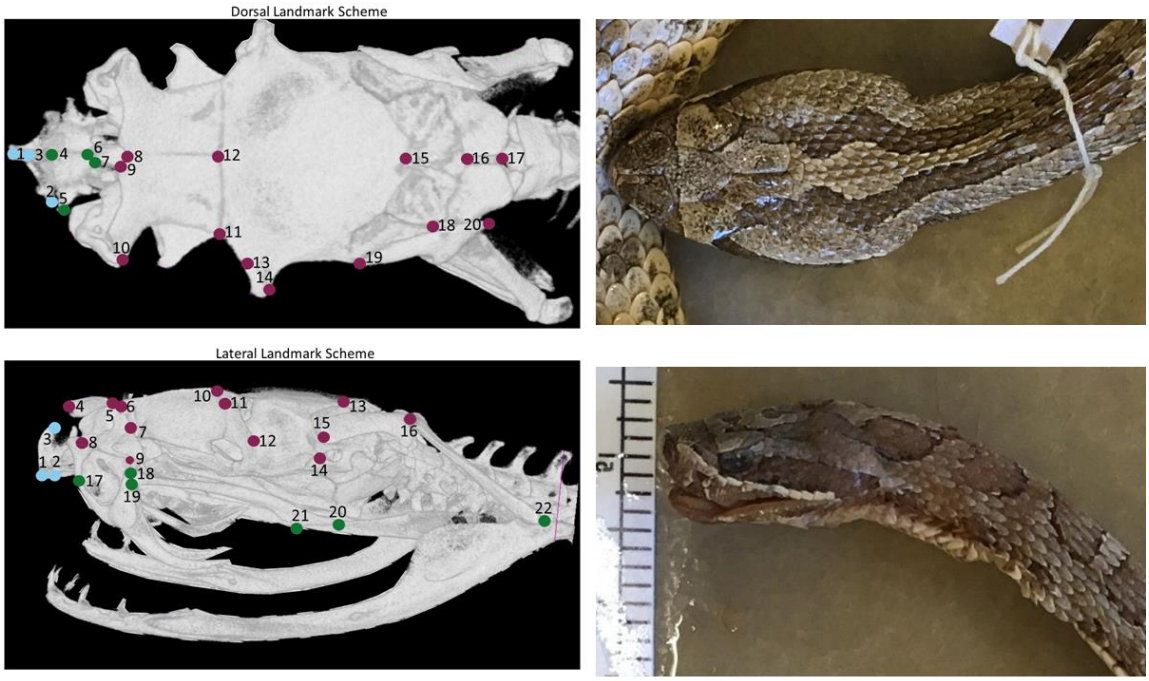

Figure 4.2. Dorsal (A) and lateral (B) landmark schemes used in this study. The landmark colors denote subgroup affiliation. A. On the dorsal landmark scheme the blue subgroup is associated with A, the green subgroup is associated with B, and the magenta subgroup is associated with C in Table 4.1. B. On the lateral landmark scheme the blue subgroup is associated with A, the green subgroup is associated with B, and the magenta subgroup is associated with C in Table 4.2.

Table 4.3. Measurement type, codes (abbreviations), and descriptions of each external morphology measurement included in this study.

Trait Type	Code	Measurement Description
Continuous	SVL	Body length from Snout-Vent (to mm)
Continuous	Tail	Tail length (to mm)
Continuous	HL	Head length from face of the rostral to the angle of the quadrate and mandible (to 0.1 mm)
Continuous	HW	Head width at widest point (to 0.1 mm)
Continuous	SL	Snout length from anterior edge of eye to center of rostral plate (to 0.1 mm)
Continuous	EPD	Eye-to-pit distance from the shortest distance between anterior edge of eye to posterior edge of pit organ (to 0.1mm)
Continuous	ISD	Intersupraocular distance from lateral edge of each supraocular scaled (to 0.1mm)
Continuous	EYE	Eye diameter along the midline of the eye from anterior to posterior (to 0.1mm)
Continuous	BRW	Width of the basal rattle segment along dorsal-ventral axis of rattle (to 0.1mm)
Continuous	MBL	Middle blotch length from anterior to posterior border of the middle dorsal blotch along vertebral line (to 0.1mm)
Continuous	MBI	Posterior middle blotch interspace measured as the length of the interspace immediately posterior to the middle dorsal blotch along vertebral line (to 0.1mm)
Meristic	VENT	Number of ventral scales
Meristic	SUBC	Number of subcaudal scales
Meristic	DSRN	Number of dorsal scale rows at neck (~3cm posterior from head)
Meristic	DSRM	Number of dorsal scale rows at midbody
Meristic	DSRC	Number of dorsal scale rows at end of body (~3cm anterior to vent)
Meristic	RFS	Number of rattle-fringe scales
Meristic	SLAB	Average number of supralabial scales on the left and right side of the head
Meristic	ILAB	Average number of infralabial scales on the left and right side of the head
Meristic	DBB	Number of dorsal body blotches – interconnected counted as 1 except for 3 or more were counted separately; divided (2 adjacent to midline) counted as 1
Meristic	TB	Number of tail blotches – interconnected counted as 1 except for 3 or more were counted separately; divided blotches (2 adjacent to midline) counted as 1
Threshold	SBB	Condition of dorsal blotch borders – described as distinct, indistinct, or absent
Percent	VPAT	% of melanistic color on ventral scales – from the body midpoint, count 5 ventral scales in both directions, over those 10 scales estimate the % of melanistic coloration

4.3. Results

Procrustes superimposed landmarks showed Gaussian or normally-distributed variation in both dorsal and lateral landmarks. Landmarks 1 and 12 also exhibited dorso-ventral variation in their distributions. Plotting these landmarks allowed for the visual inspection of landmark placements and the identification of any major outliers. Although there were some outlying landmarks, review of the specimens and landmarks revealed that there was not error in the digitization process of placing the landmarks.

4.3.1. Dorsal skull shape

The dorsal aspect landmark scheme was divided into three groups to accommodate regionalized kinetic behaviors in the skull (Fig. 4.2; Fig. 4.3A; Appendix Figs. C 1-C 4). In Group A, the first two PCs explained 98.1% of the shape variation; in Group B, the first two PCs explained 86.5% of the variation; and in Group C, the first three PCs explained 62.9% of the variation. Group A PC1 (82.2%) varied from a shorter (at the midpoint), wider premaxilla to a longer, narrower premaxilla. Group A PC2 (15.9%) varied in the angle and width of the premaxilla from the midline to the tip of the nasal process on the premaxilla, from a shorter angle with a wider premaxilla to a more obtuse angle with a narrower premaxilla. Group B PC1 (59.1%) varied from a narrower to a wider nasal throughout, with narrower nasals coinciding with an elongate midline of the element. Group B PC2 (27.4%) varied from short and wide nasals to long and narrow nasals, with greater change anteriorly in the group. Group C PC1 (34.4%) varied in the shape and size of frontal and parietal, with a longer supraoccipital when the frontal was

shorter and both the frontal and parietal were narrower. Group C PC2 (15.4%) showed a larger orbital region with a larger frontal coinciding with a shorter parietal, and vice versa. Lastly, Group C PC3 (13.1%) varied in the length of the parietal compared to the length and width of the supraoccipital and exoccipital.

I applied ANOVAs for all selected PCs from each dorsal group in order to distinguish statistically significant ($p < 0.05$) differences in mean values between the axes of shape by population or sex. While Group A showed no significant differences in mean factor scores between shape variation, population, and sex across all PCs, all other groups had at least one PC of shape variation that was significant. For those PCs, we used Tukey's test to determine where the greatest differences occurred. Group B PC1 revealed differences in population shapes, primarily between the Arizona and Oklahoma populations, as well as the North Texas and West Texas females when populations are also divided by sex. Group C PC1 showed a difference between males and females overall, and the Arizona population differed in mean shape from the New Mexico, Oklahoma, Kansas, and Missouri populations. Group C PC 2 differences were also present between sexes and populations individually. New Mexico differed from Arizona, Colorado, Kansas, and Missouri, while West Texas differed from Arizona and Missouri. Group C PC3 differed for populations, with the greatest difference in mean values occurring between the New Mexico and Missouri populations.

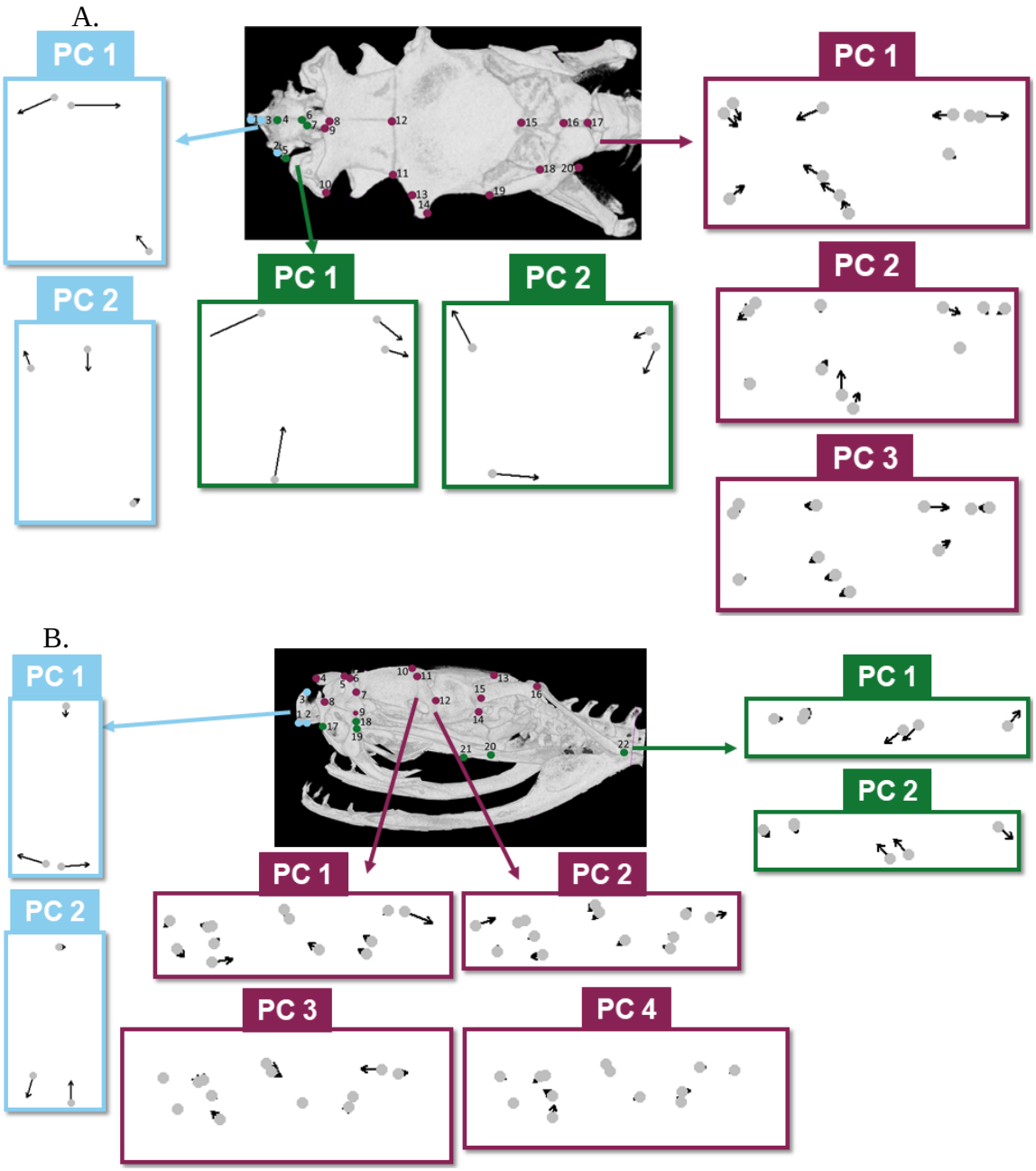

Figure 4.3. Shape grids for PCs in each orientation. Arrows indicate PC axis direction, colors indicate group, and grids indicate representative shapes from negative to positive scores along the axes. A: Dorsal shape extremes for Groups A (blue), B (green) and C (magenta). B: Lateral shape extremes for Groups A (blue), B (magenta), and C (green).

To assess overall geographic patterns of shape change in *S. tergeminus*, I examined plots of longitude and latitude against PCs of shape change for all individuals in dorsal orientation (Fig. 4.4). Overall, as longitude increased, Dorsal Group A PC1 and PC2, Group B PC2, and Group C PC 1 and PC2 decreased, while Group B PC1 and Group C PC3 increased along the PC axes. This suggests that as longitude increases, the following morphological trends occur overall: A) a shorter and wider premaxilla with a more acute angle from the midline of the nasal process; B) a shorter and wider nasal; and C) a shorter but narrower frontal and parietal and longer suproccipital. As latitude increases, there is a similar pattern except for the MX and ST populations, and for Group B PC2 and Group C PC3. Morphologically, the pattern differs in that the shape of the nasal shows little change latitudinally, the parietal increases in length, and the supraoccipital and exocciptal decrease in length and width.

I grouped *S. tergeminus* by population and sex designations for discriminant functions. (Fig. 4.5A; Fig. 4.6A). Discriminant functions of dorsal view classified populations with varying accuracy by group and as a whole. Overall accuracy using only Group A was 21.2%, Group B was 30.1%, and Group C was 33.6%. Using the complete landmark scheme was 40.7% accurate overall. Discriminant functions performed better when classifying individuals as female or male, however, as overall accuracy for predicting sex was generally higher for all groups individually (A: 55.8%, B: 53.1%, C: 72.6%) and combined (69.9%).

4.3.2. Lateral skull shape

The landmark scheme in lateral view was divided into three groups to account for the kinetic skull (Fig. 4.2; Fig. 4.3B; Appendix Fig. C1- C4). In Group A, the first two PCs explained 99.2% of shape variation; in Group B, the first four PCs explained 56.5% of variation; and in Group C, the first two PCs explained 80.3% of variation. Group A PC1 (60.3%) was the antero-posterior length vs dorso-ventral height of the premaxilla, which were inversely correlated; Group A PC2 (38.9%) changed the overall shape of the premaxilla, where the midline point of the premaxilla at the inferior tip of the bony septum and palatine process of the premaxilla shifted in opposite directions dorso-ventrally. Group B PC1 (20.9%) varied from a more anteriorly oriented nasal, prefrontal, and frontal (relative to the maxilla) with a longer frontal and shorter parietal, to the opposite. Group B PC2 (15.5%) varied in antero-posterior proportions, where a shorter prefrontal and frontal with a more posteriorly located nasal is associated with a longer parietal and supratemporal. Group B PC3 (11.5%) varied in the overall length of the skull and the compactness of the nasal and prefrontal to accommodate the maxillary fang. Similarly, Group B PC4 (8.6%) associated a smaller prefrontal with a shorter nasal, larger orbital region, and more posteriorly located parietal. Group C PC1 (44.2%) showed opposite trends in the length of the ectopterygoid and pterygoid, with both dorso-ventral and antero-posterior shifts of the ventral quadrate; Group C PC2 (36.1%) varied in the dorso-ventral straightness of the maxilla through pterygoid series, with a straighter series associated with a more antero-dorsally located ectopterygoid-pterygoid articulation and postero-ventrally located ventral quadrate.

The ANOVAs for the selected PCs in lateral orientation were also tested for relationships with population and sex (Fig. 4.5B; Fig. 4.6B). All lateral groups had at least one PC of shape variation that was significantly different for population, sex, or both except for Group C. Group A PC1 was significant for population, especially between North Texas, Colorado, Oklahoma, and Kansas. Group A PC2 was especially significant for the New Mexico population when compared to the South Texas, North Texas, Oklahoma, and Kansas populations. Group B PC1 was mostly explained by differences between the Missouri population and South Texas, West Texas, and Colorado; Colorado was also different from the North Texas and Kansas populations. Group B PC2 and PC3 were significantly different for sex, especially for the Oklahoma population in PC3. Finally, Group B PC4 was significant for population, especially between the Kansas and Arizona populations.

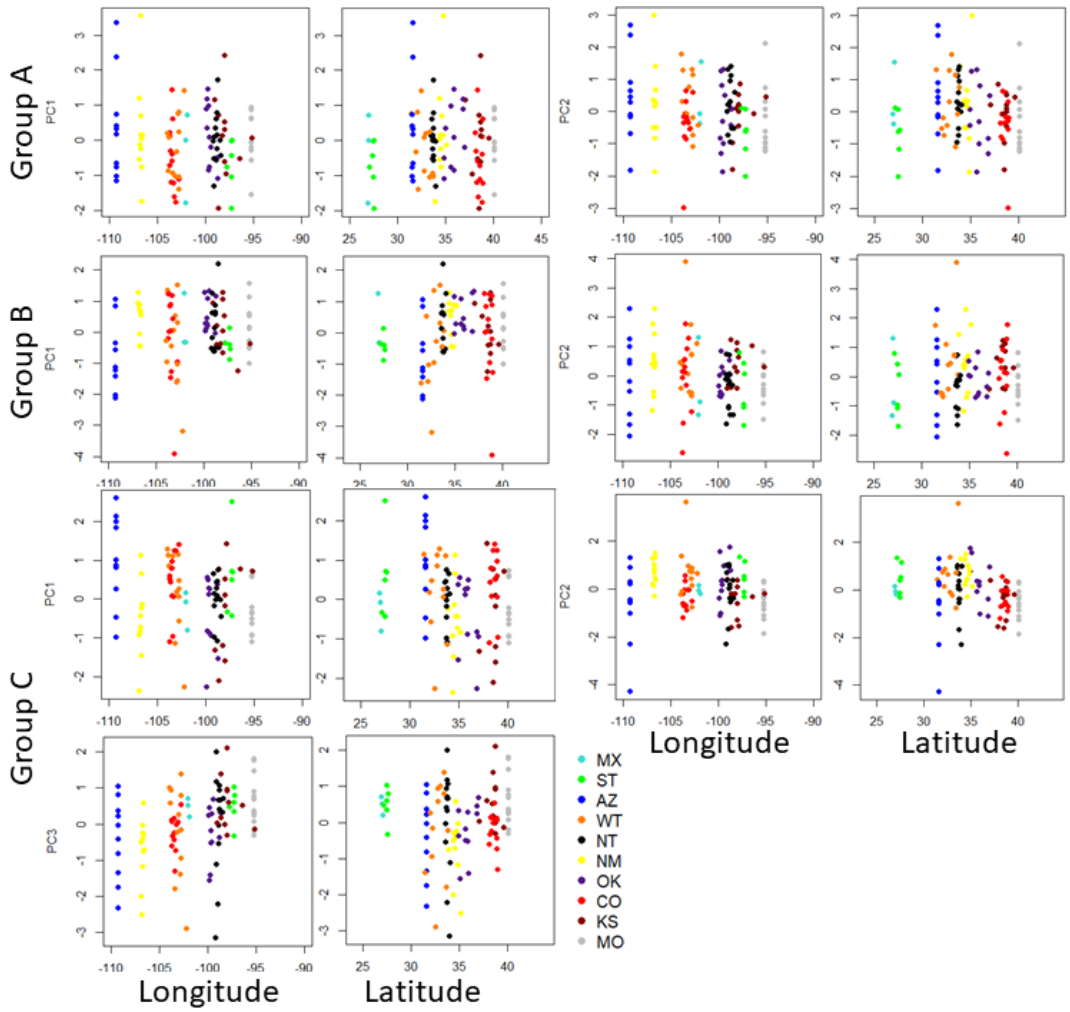

Figure 4.4. Plots of longitude and latitude for all species by population along selected PC axes in dorsal view. PC number increases from left to right, while longitude and latitude alternate for each PC. Group C includes three PCs.

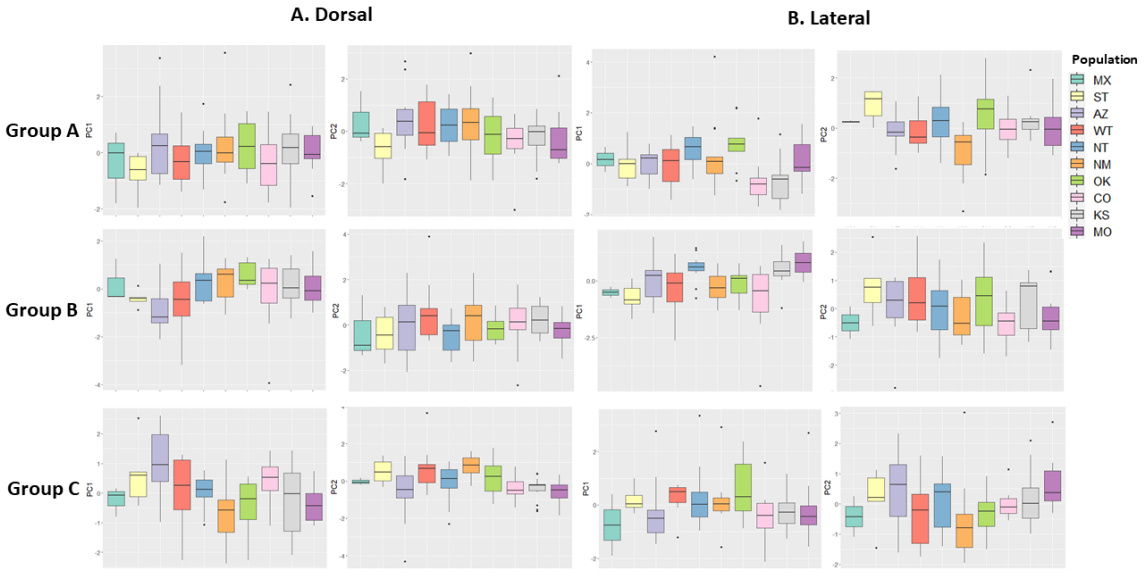

Figure 4.5. Box plots for selected PCs from each group in dorsal (A.) and lateral (B.) orientations, separated by population. The list of populations from top to bottom in the legend run left to right on the x-axis of each box plot.

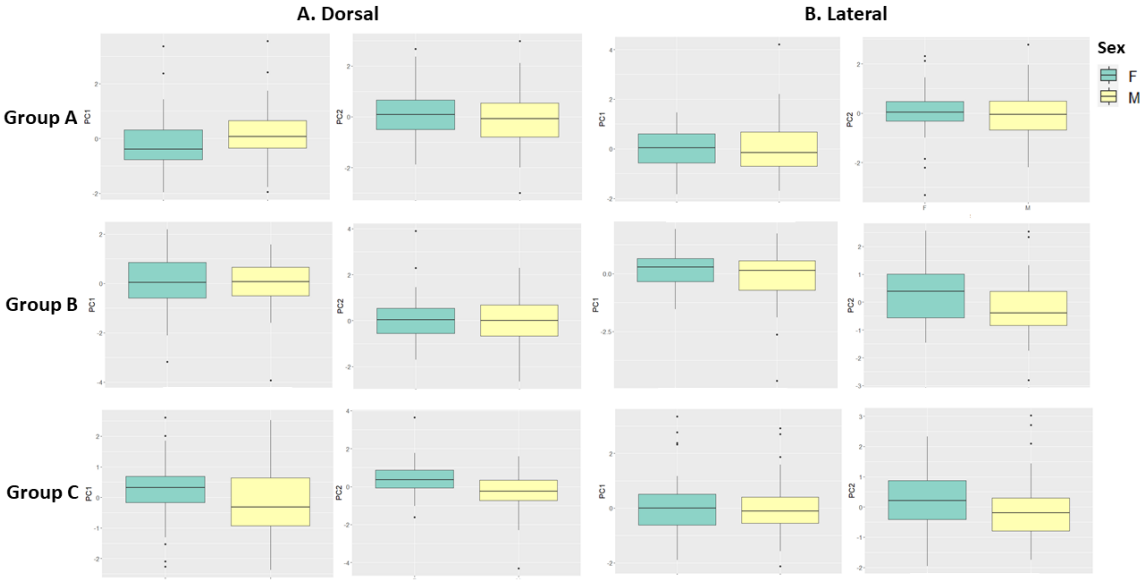

Figure 4.6. Box plots for selected PCs from each group in dorsal (A.) and lateral (B.) orientations, separated by sex.

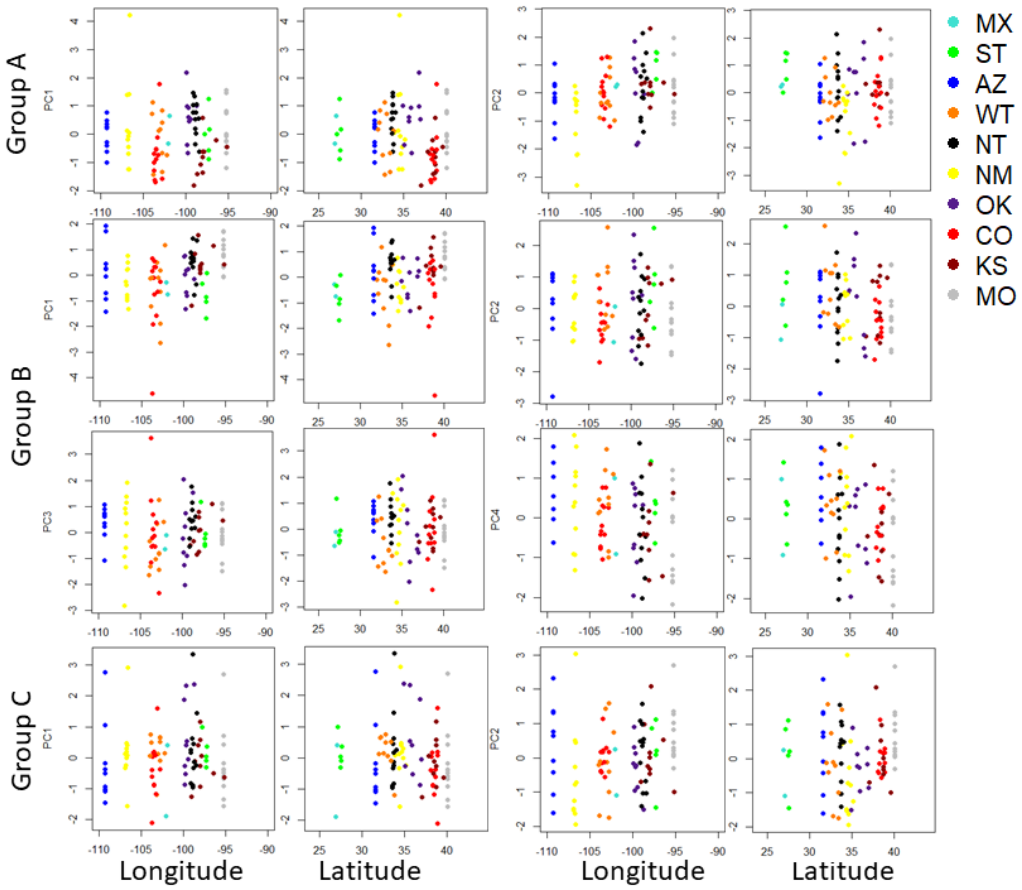

Figure 4.7. Plots of longitude and latitude for all species by population along selected PC axes in lateral view. PC number increases from left to right, while longitude and latitude alternate for each PC. Group B includes four PCs.

I also examined plots of longitude and latitude against PCs of shape change for all individuals in lateral orientation (Fig. 4.7). As longitude increased, Group A PC1 and PC2, Group B PC1, and Group C PC2 increased, while Group B PC2-PC4 and Group C PC1 decreased along the PC axis. However, the Arizona and New Mexico populations did not follow these trends, especially for Group B PC1 and PC3 and Group C PC1 and PC2. Outside of these exceptions, however, the following morphological trends occur as longitude increases: A) a longer, but lower premaxilla with a steeper angle between the

bony septum and palatine process; B) a more posterior orientation of the nasal, prefrontal, frontal and parietal relative to the maxilla, a shorter frontal and longer parietal, a less compact prefrontal and nasal to accommodate a larger maxillary fang insertion, and a smaller orbital region; and C) a shorter pterygoid and longer ectopterygoid, with a straighter series along the articulations of those elements. At Group B PC3, most of the decrease between AZ and NM compared to the other populations. In addition, as latitude increases, all PCs decreased except for Group B PC1 and Group C PC2, and in the NM and ST populations for Group B PC3. Morphologically, the pattern differs from the longitudinal trends in that the premaxilla becomes shorter but taller, with a shallower angle between the bony septum and palatine process.

Discriminant functions of lateral view generally produced better results when distinguishing sex rather than population assignment, except when all groups are combined into the overall landmark scheme. Overall accuracy for Group A was 34.4 % for population and 58.8% for sex. Similarly, Group B had an overall accuracy of 33.3% for population and 58.8% for sex. Group C's overall accuracy was 26.5% for population and 57.8% for sex. Finally, the overall accuracy of the full landmark scheme was 49.0% for population and 48.1% for sex.

4.3.3. External morphology

As in the landmark schemes, I used ANOVAs to detect significant variation related to morphology, population assignment, and sex. I primarily found at least population-level differences in external measurements of the morphology in *S.*

tergeminus. I documented a large amount of variation in measurements related to size and proportionality of head and tail (Table 4.4, 4.5). Measurement descriptions and abbreviations are listed in Table 4.3. The interaction between sexual dimorphism and population itself was only significant for DSRM. The relationships between morphological variation and both population and sex were significant for SVL, TAIL, HL, HW, SL, ISD, EYE, BRW, MBL, VENT, SubC, SLAB, and TB. The relationship was significant in regard to population only for EPD, MBI, DSRN, DSRC, RFS, ILAB, and DBB. A principal component analysis of all continuous and meristic measurements except for head width, which could not be measured in nine individuals, identified several measurements of particular interest in the first four PCs. These PCs represented ~64.7% of explained variation in the data (Fig. 4.8). PC 1 (~40.2% explained variation) identified SVL, HL, SL, BRW, EYE, Vpat, EPD, and ISD as major measurement variations along this axis, all towards the negative direction. PC 2 (~10.3% explained variation) identified TB and SubC in the negative direction, and VENT, DBB, and DSRC in the positive direction as the major measurement variations. PC 3 (~8.5% explained variation) is primarily allocated to TB, DSRN, DSRM, Slab, TAIL, and SubC in the positive direction, and MBI, MBL, SVL, and – to some extent – other body and head size measurements in the negative direction as the primary varying measurements. PC 4 (~5.8% explained variation) is primarily explained by RFS and Vpat in the positive direction and DSRC in the negative direction. Discriminant functions of the external measurements identified individuals as female and male at 76.6% and 88.7% accuracy,

respectively (83.9% overall accuracy). Classification to population was at 43.2% overall accuracy.

Table 4.4. Summary of means (standard deviation) for continuous measurements (in mm) taken, organized by population.

	AZ	CO	KS	MO	MX	NM	NT	OK	ST	WT
SVL	324.93 (±37.12)	353.20 (±48.54)	490.43 (±74.90)	565.38 (±49.17)	376.25 (±69.61)	364.86 (±38.33)	477.47 (±70.22)	404.77 (±97.82)	376.78 (±74.03)	364.71 (±60.51)
Tail	43.27 (±7.69)	43.27 (±6.50)	58.43 (±16.34)	69.38 (±10.40)	52.00 (±12.70)	50.86 (±13.88)	56.8 (±14.38)	50.69 (±15.00)	49.78 (±14.75)	47.71 (±13.76)
HL	19.99 (±1.29)	21.01 (±2.28)	27.37 (±3.77)	30.78 (±2.13)	22.47 (±2.93)	19.50 (±1.51)	27.82 (±3.22)	24.12 (±4.33)	22.60 (±3.44)	20.24 (±2.01)
HW	12.99 (±1.80)	13.49 (±1.87)	17.41 (±2.60)	18.67 (±1.75)	15.67 (±2.03)	12.93 (±1.02)	17.31 (±2.03)	15.82 (±3.39)	14.96 (±1.92)	13.17 (±1.85)
SL	6.16 (±0.64)	6.15 (±0.70)	8.46 (±1.21)	9.17 (±0.72)	7.09 (±0.81)	5.90 (±0.53)	8.16 (±1.09)	7.04 (±1.26)	6.87 (±1.14)	6.15 (±0.59)
EPD	1.62 (±0.20)	1.47 (±0.37)	2.23 (±0.43)	2.68 (±0.40)	1.69 (±0.23)	1.59 (±0.32)	2.23 (±0.35)	1.94 (±0.50)	1.74 (±0.42)	1.62 (±0.25)
ISD	9.06 (±1.00)	9.19 (±1.14)	11.92 (±1.49)	12.88 (±0.93)	9.88 (±1.20)	9.17 (±0.68)	11.27 (±1.43)	10.43 (±1.69)	9.73 (±0.87)	9.37 (±1.01)
Eye	3.00 (±0.35)	3.03 (±0.48)	3.63 (±0.47)	3.75 (±0.40)	3.47 (±0.68)	2.63 (±0.37)	3.35 (±0.46)	3.10 (±0.57)	3.20 (±0.36)	3.01 (±0.41)
BRW	5.13 (±0.84)	5.42 (±0.90)	7.11 (±1.22)	8.13 (±1.04)	6.16 (±0.81)	4.92 (±0.51)	7.65 (±1.19)	6.17 (±1.64)	5.32 (±0.82)	5.17 (±0.99)
MBL	6.31 (±1.19)	7.39 (±2.26)	9.74 (±2.19)	14.16 (±4.19)	8.78 (±2.56)	7.65 (±1.76)	9.51 (±5.24)	7.95 (±2.60)	7.62 (±3.26)	7.79 (±3.30)
MBI	3.86 (±0.96)	3.66 (±1.38)	4.07 (±1.08)	5.36 (±1.71)	5.50 (±1.75)	4.63 (±1.03)	4.19 (±1.29)	4.12 (±1.48)	4.50 (±0.68)	3.65 (±1.09)

Table 4.4. Summary of medians and modes (range) for meristic measurements taken, organized by population.

	AZ	CO	KS	MO	MX	NM	NT	OK	ST	WT
Vent	142, 146 (133-149)	142, 143 (138-145)	149, 143 (142-160)	146, 150 (139-152)	142, n/a (137-147)	143, 142 (139-158)	146, 145 (134-153)	145, 146 (138-156)	146, 141 (141-153)	145, 148 (132-159)
SubC	26, 27 (24-30)	27, 27 (22-31)	28, 28 (21-33)	29, 29 (23-32)	28.5, n/a (26-31)	31, 31 (25-33)	27, 30 (22-34)	28, 25 (24-31)	29, 32 (25-33)	29, 30 (22-32)
DSRN	21, 21 (17-23)	22, 21 (19-23)	22, 22 (19-27)	24, 23 (21-26)	21, 21 (20-22)	21, 20 (19-23)	23, 23 (17-25)	23, 25 (21-25)	22, 19 (19-27)	23, 23 (21-25)
DSRM	23, 23 (22-25)	23, 23 (22-25)	24, 24 (22-26)	25, 25 (23-28)	23, 23 (22-24)	23, 23 (21-24)	25, 25 (23-27)	25, 25 (23-25)	24, 25 (22-25)	23, 23 (22-25)
DSRC	17, 17 (15-20)	19, 19 (17-21)	19, 19 (16-20)	19, 19 (15-19)	18, 17 (17-19)	18, 17 (17-20)	19, 19 (17-20)	19, 19 (17-20)	19, 19 (18-19)	19, 19 (17-22)
RFS	10, 10 (10-11)	10, 10 (9-12)	11, 11 (10-13)	11, 12 (10-12)	11, 11 (10-12)	11, 11 (10-12)	11, 11 (10-12)	11, 11 (10-12)	11, 12 (10-12)	10, 10 (10-12)
Slab	11, 11 (10-13)	11, 11 (10-13)	12, 12 (10-12)	12, 12 (10-12)	11, 11 (11-12)	11, 11 (10-12)	12, 12 (10-13)	12, 11 (10-13)	12, 12 (11-13)	12, 12 (10-13)
ILab	11, 11 (9-12)	11, 11 (10-13)	11, 11 (10-14)	12, 12 (11-13)	11, n/a (10-13)	11, 11 (10-12)	12, 12 (11-13)	11, 11 (10-12)	12, 11.5 (11-13)	11, 11 (10-12)
DBB	36, 38 (33-38)	36, 37 (25-43)	38, 36 (32-44)	37, 37 (32-45)	30, n/a (24-37)	34, 33 (32-38)	36, 36 (31-45)	36, 36 (32-43)	37, 37 (30-41)	35, 36 (28-39)
TB	8, 7 (6-9)	7, 7 (6-10)	7, 7 (5-9)	8, 8 (6-10)	5.5, 5 (5-7)	8, 8 (7-11)	7, 6 (6-9)	7, 7 (5-11)	9, 9 (6-9)	7, 6 (4-10)

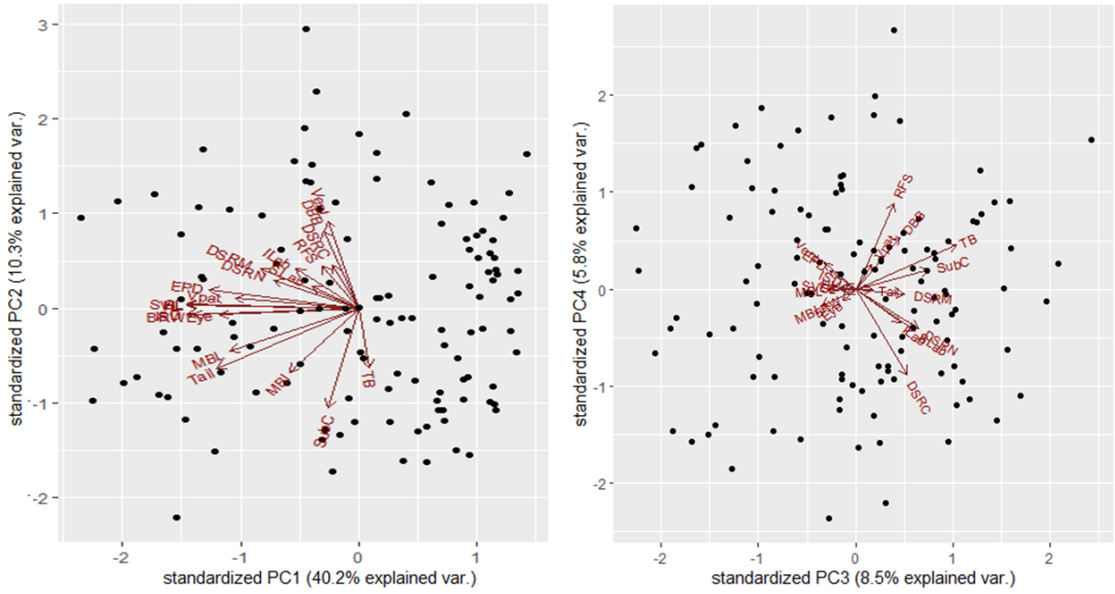

Figure 4.8. Plot of PCs 1-4 of external morphology measurements. Labeled red arrows indicate vectors of change in a specific measurement in the ordination space.

To consider linear correlations between internal and external morphological factors, I used Pearson's correlation coefficient on all of the external measurements and the selected PCs from the landmark schemes (Fig. 4.9). The strongest relationships were primarily positive correlations related to body and head size, including dorsal scale rows and, interestingly, the percent of melanistic coloration on ventral scales. The dorsal landmark scheme revealed several negative correlations with size, particularly for Group A PC2 and Group C PC1 and PC2. Group C PC3 showed a moderate positive correlation with those same measurements. The lateral landmark scheme revealed somewhat stronger correlations with external measurements, including positive correlations from Group A PC2, Group B PC1, and Group C PC2, and negative correlations from Group B PC2 and Group B PC4. Comparison between the two landmark schemes showed mixed results of mostly moderate correlations, although Dorsal Group C PC1 and Lateral Group B PC2 showed a strong positive relationship. These correlations reveal a pattern of allometry such that increased body size and cranial measurements are associated with: A) a wider premaxilla; B) a wider nasal; and C) a larger frontal but shorter parietal, shorter supraoccipital and exoccipital, and more anteriorly oriented orbital region in dorsal view. This results in an overall pattern of a wider anterior region, wider and longer medial region, and shorter posterior region of the skull in larger snakes. Similarly, increased body size and cranial measurements are associated with: A) a deeper premaxilla; B) a more posteriorly oriented and longer nasal, prefrontal, and frontal relative to the maxilla; and C) an upper jaw series with a more anteriorly located ectopterygoid-pterygoid articulation, a posteriorly located ventral quadrate, and a longer

pterygoid. This results in an overall pattern of a deeper skull with a wider gape size as body and head size increase.

4.3.4. Bioclimatic variables

I compared internal and external morphology to bioclimatic variables by selecting the external measurements and the relevant PCs of the landmark schemes, then using linear correlations of those schemes with bioclimatic variables to see which morphologies may show patterns related to environmental differences over geographic space. I selected bioclimatic variables through a PCA, which revealed that PC1 dominated the explained variance (97.2%) and was primarily explained by temperature-related variables; the majority of that variation is controlled by temperature seasonality (Appendix Tables C7-C8). Dorsal Group C PC1 and PC2, lateral Group B PC1, SVL, TAIL, HL, HW, SL, EPD, ISD, EYE, BRW, MBL, VENT, DSRN, DSRM, ILAB, DBB, SBB, and Vpat were all significant for temperature seasonality. PC2 (2.6%) was mostly explained by precipitation-related bioclimatic variables, but especially by annual precipitation. Dorsal Group PC3, Lateral Group A PC2 and Group B PC1, SVL, TAIL, HL, HW, SL, EPD, ISD, EYE, BRW, MBL, VENT, DSRN, DSRM, DSRC, RFS, SLAB, ILAB, DBB, SBB, and Vpat were all significant for annual precipitation. The mean annual temperature, mean diurnal range, minimum temperature of coldest month, temperature annual range, mean temp of driest quarter, mean temperature of coldest quarter, precipitation of wettest quarter, and precipitation of warmest quarter variables also contributed to bioclimatic variation. Nearly every bioclimatic factor showed a correlation to at least one morphological variable.

4.4. Discussion

The results show that combining external measurements and skeletal shape to inform the understanding of morphology can be more informative for ecology, sexual dimorphism, and allometry than either method alone. Morphology changes detectably in relation to different environments, prey types, body size, and other environmental factors at the intraspecific level just as it does on larger scales, as also seen in some other vertebrates (Figs. 4.2-4.7; Foote, 1993; Norton et al., 1995; Smith et al., 1995; McGuire, 2010; Herrando-Pérez et al., 2019; McGuire and Lauer, 2020). The associations between skull morphology, snake external morphology, diet, sex, and population differences have rarely been explored on an intraspecific level to this degree in snakes, as most studies analyzing these factors are typically broadly applied to clades or families, and rarely go beyond a genus-level description when skeletal elements are included (Vincent et al., 2006; Alencar et al., 2013; Klaczko et al., 2016; Huntley et al., 2021).

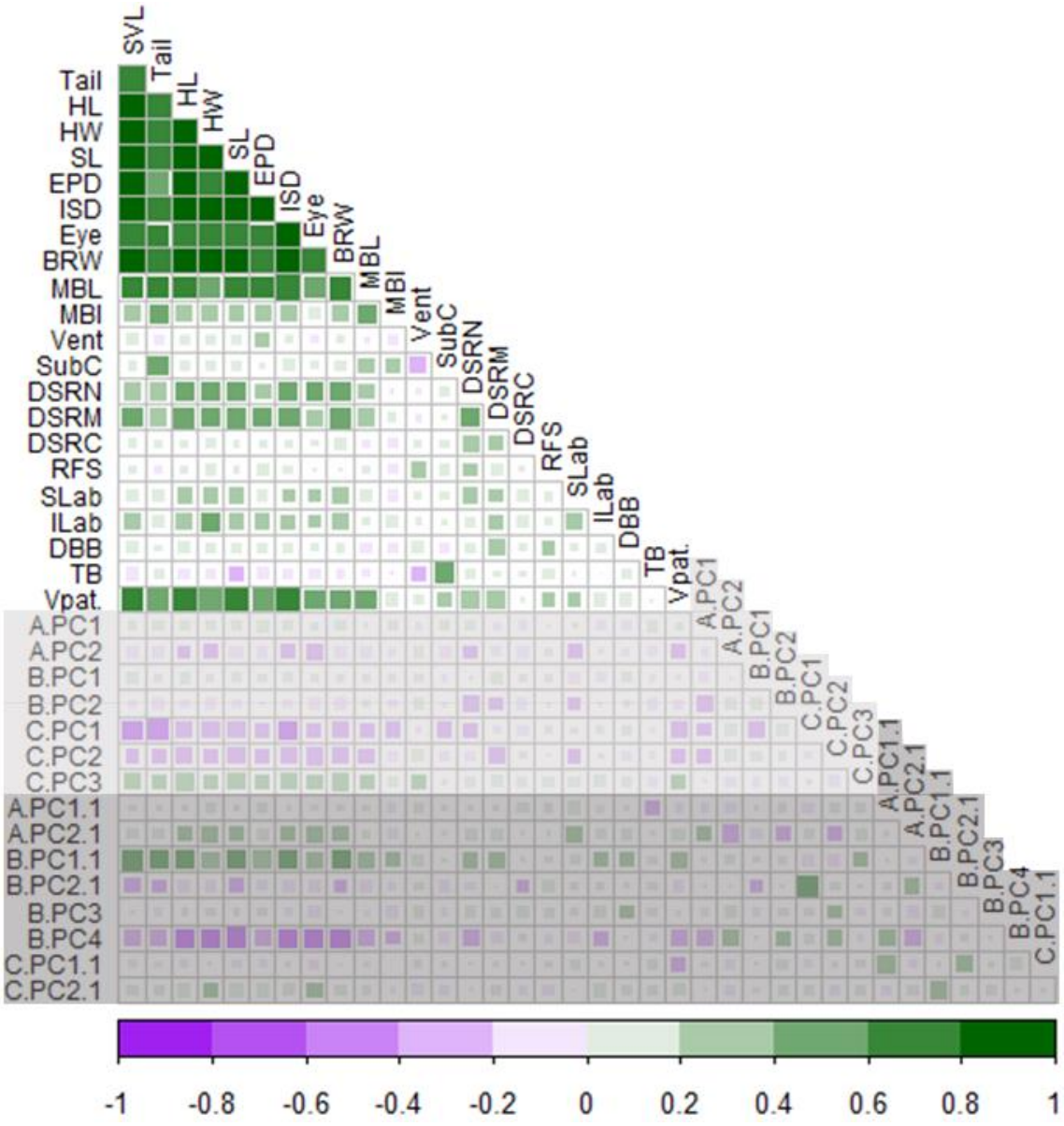

Figure 4.9. Correlation plot of all measurements and selected PCs of shape in this study. The areas and darkness of color of the squares reflect the absolute value of the corresponding correlation coefficients. Light gray shading indicates dorsal PCs and dark gray shading indicates lateral PCs.

Overall, I found that there is some congruence in the morphological differences among populations and between sexes. The groups from the dorsal landmark orientation suggest a pattern of premaxilla and nasal compression associated with an elongation of the occipital and braincase regions of the skull (and vice versa; Fig. 4.3A). Based on the correlation matrix and the differences by population (Fig. 4.5A; Fig. 4.9), this pattern is likely both allometric and dietary between populations, and between sexes within some populations. Additionally, lengthening of the supratemporal bone is associated with a more anteriorly oriented orbital region in more northern populations. This alteration to part of the viperid jaw, and therefore the striking and feeding mechanisms of the snake, likely points to differences in diet, with a different primary prey item (Gans, 1961; Dwyer and Kaiser, 1997; Queral-Regil and King, 1998; Cundall and Greene, 2000; Herrel et al., 2008; Britt et al., 2009; Klaczko et al., 2016).

The groups from the lateral landmark orientation indicate that a more dorso-ventrally compressed skull, particularly in the postorbital, parietal, and supraoccipital elements, may coincide with a slightly longer quadrate but slightly shorter supratemporal (Fig. 4.3B). These changes directly affect both the possible angles and the proportions of the lever system in the jaw and should therefore have a direct effect on the prey sizes available to an individual. Additionally, larger maxilla size coincides with an overall antero-dorsal shift in all other skull elements besides the nasal and premaxilla, which shift antero-ventrally. This may be to accommodate for the difference in the relative size of the maxilla in both form and function or may be indicative of allometric body size differences. The maxilla in vipers contains the maxillary fang, and so the size difference

in this element may be attributable to a larger fang size in an individual. If this pattern is persistent within populations and different among them, it could indicate preferred prey of deeper body type or could record a difference in overall skull or body size (Klauber, 1939; Gans, 1961; Cundall and Greene, 2000; Vincent et al., 2006; Knox and Jackson, 2010). In both dorsal Group C and lateral Group B, which contain the most landmarks and incorporate the largest areas of the skull in their respective views, the PCA explains a lower level of variation with respect to the other groups. This suggests that the middle and posterior portions of the skull are less integrated, as they incorporate more elements and require a greater number of landmarks and PCs to explain the variance in shape.

The external measurements show that most of variation (PC1) is attributable to overall body size and the size of the head, including measurements such as SVL, HL, SL, and ISD (Fig. 4.9). Furthermore, major variation in factors such as TB, DBB, SUBC, VENT, MBI, and TAIL (PC2) indicate that there is an aspect of variation related to scalation, scale pattern and tail length that is divorced from overall body size, which may be suggestive of sexual dimorphism (Meik et al., 2012), variation in locomotor habits (Wiens et al., 2006; Lawing et al., 2012), or camouflage for differences in vegetation cover (Guyer and Donnelly, 1990; Lindell, 1994; Martins et al., 2001; King, 1989). The interplay between the TB, SLAB, DSRN, DSRC, SUBC, and MBL as primary varying measurements (PC3) is related to the circumference of different regions of the body and colorations, perhaps indicative of potential predators or prey that the snakes must remain hidden from or sexual dimorphism (Harvey and Weatherhead, 2011). Because the PCA of external morphology grouped males and females, it is likely

that axes two and three reflected differences in sexual dimorphism, but I was unable to refute the possible influences of locomotor habit or cryptic coloration. Finally, the number of RFS and DSRC (PC4) are both posterior measurements that are near each end of the caudal region and record tail circumference, and may be relevant to locomotion, size, and perhaps age (Martins et al., 2001; Wiens et al., 2006; Lawing et al., 2012). Variation over the geographic range in *S. tergeminus* likely signifies sexual (Shine, 1986, 1991; Camilleri and Shine, 1990; Meik et al., 2012), ecological (e.g., diet, vegetation and substrate, bioclimatic factors; Bonnet et al., 2001; Dwyer and Kaiser, 1997; Shine et al., 2002; Vincent et al., 2004; Hampton, 2011; Lawing et al., 2012; Klaczko et al., 2016), and/or allometric differences across that range (or some combination of these factors; LaDuc, 2003; Meik et al., 2012).

While it is yet unclear as to whether the sexual dimorphism noted in this study is more strongly related to ecological niche divergence or sexual selection, correlations between sexual divergence in diet and head morphology in snakes have been demonstrated previously in numerous studies (Shine, 1986; Camilleri and Shine, 1990; Shine et al., 2002; Vincent et al., 2004; Meik et al., 2012). Morphologies I found especially prominent for sex included Dorsal Group C PC1 and PC2, Lateral Group B PC2 and PC3, and external measurements SVL, TAIL, HL, HW, SL, ISD, EYE, BRW, MBL, VENT, SubC, SLAB, and TB, and DSRM. Notably, the majority of the measurements and axes of shape variation suggest that the size and shape of the head around the frontal and parietal are especially important, along with the overall length of the skull and size of the body. While there is little prior evidence of sexual differences in

diet for rattlesnakes, Glaudas et al. (2008) presented evidence of longer heads and proportionally fewer lizards in the diets of male *Crotalus lutosus*, and Meik et al. (2012) found intersexual niche divergence in the head shape of *Crotalus polystictus*, with male head shapes allometrically growing wider and shorter in correlation to increased proportions of larger mammalian prey. Much as in these studies, it appears that when *S. tergeminus* grows in size, the proportions of the skull change allometrically.

Geographically, there are both longitudinal and latitudinal trends exhibited in the data that may be indicative of dietary differences. As longitude increases, the dorsal part of the skull becomes wider, but individual elements become shorter in the medial region and longer in the posterior region of the skull. Meanwhile, the lateral aspect shifts posteriorly relative to the maxilla, is shorter in the medial region and longer in the posterior region of the skull, is less compact around the maxillary fang, and shifts the proportions of the upper jaw such that the ectopterygoid is relatively longer. As latitude increases, the dorsal aspect differs from the longitudinal trend in that the medial portion of the skull is antero-posteriorly longer while the posterior part of the skull is shorter; the lateral aspect simultaneously exhibits increased depth in the front of the skull. This southwest-to-northeast trend of increased space for the maxillary fang, greater robustness and depth (shorter and wider) in the medial region of the skull, and more elongation in the posterior region of the skull suggests that populations to the north and east tend to feed on prey with deep bodies and potentially greater body mass. This is supported by the dietary observations of Holycross and Mackessey (2002), who found a

higher proportion of mammalian prey in adults for eastern populations, but more lizards and centipedes in the adult diet of western populations.

While there appear to be some differences in skull proportions and body measurements between sexes that are better captured in the Discriminant Function Analysis, the differences between populations are clearer in the ANOVAs. Most notably, populations at the southwestern and northeastern edges of the range of *S. tergeminus* are often more different from other populations, and are not necessarily similar to adjacent populations. This supports the previous study of Ryberg et al. (2015), which suggests that *S. tergeminus* is a single species composed of fragmented populations, rather than of two distinct subspecies. There is also support for a correlation between dietary and morphological differences by population. As previously mentioned, Holycross and Mackessy (2002) found that populations in Arizona, Colorado, and New Mexico differ from populations in Texas and Missouri in their greater dependence on lizards and centipedes as prey (along with small mammals), while the other populations consume mostly mammals once reaching adulthood. Similarly, the Arizona, New Mexico, and Colorado populations are often different from other populations and from each other. In these populations, both the prey type or variety and the environment (xeric-grassland as opposed to mesic environments) differ, producing a greater number of both internal and external changes. Arizona and New Mexico additionally show the greatest amount of variation overall in the dataset; although some populations, such as Coahuila, Mexico, suffer from small sample sizes.

Nearly all of the measurements and PC axes were correlated with population-level differences, except for Dorsal Group A and Lateral Group C, which both had few landmarks and were potentially vulnerable to warping and damage both before and after collection. The discriminant functions had moderate success in predicting groups overall. In all three collections of measurements (dorsal, lateral, and external), predictions were more accurate by percentage for sex than for population. This may be because of the differences in sample size for each group, as I used two categories for sex, but ten categories for population; across all of the ANOVAs and Tukey's tests, population was significant for a greater number of morphological factors.

While many of the axes of skull shape variation and external measurements were found to be significant for several bioclimatic factors, these relationships were not exceptionally linear. This implies a more indirect relationship between ecomorphology and climate, such as through ecological province or vegetation cover; such a relationship has previously been observed for other aspects of snake morphology (Lawing et al., 2012). Furthermore, the most important bioclimatic factors in this study match well with those of previous studies using habitat distribution models for *S. tergeminus*. A recent study by Walkup et al. (In Review) found that temperature seasonality and precipitation of the coldest quarter were the most important variables, and that *S. tergeminus* has slowly migrated northward over time as the environment changed. The bioclimatic factors of the study and that of Walkup et al. (In Review) indicate that *S. tergeminus* may undergo both morphological and geographic change as climate continues to shift. The morphological changes discussed throughout this study suggest that such a move

would cause a shift in traits related to both diet and vegetation cover, as the prey items and vegetation cover are altered in their own ways by the same climatic processes. The exact nature of these changes may depend especially on the effects climate change have on prey items, as snakes in less seasonal, drier environments also feed on fewer mammals and have shallower, more compact skulls.

Although both are exceptionally important to an organism's fitness, internal (skeletal) and external morphology are rarely considered together when examining intraspecific variation in snakes. Many studies typically investigate one or the other, many of which also investigate larger taxonomic groups (Dwyer and Kaiser, 1997; Hibbitts and Fitzgerald, 2005; Meik et al., 2012; Klaczko et al., 2016; Watanabe et al., 2019). However, including both is important at intraspecific levels for understanding patterns of morphologic change and adaptability as they relate to differences in diet, climate, sex, and location, thus revealing information on species' potential to survive changing environment (Lawing and Polly, 2011; Lawing et al., 2012, Mimura et al., 2017; Herrando-Perez et al., 2019). The findings demonstrate that both the internal morphology of the skull and the external morphology of the body are significantly different in their assemblage of morphological traits between different populations and between sexes. Furthermore, these differences are relatable to differences in the environment and diet of the ten populations of *S. tergeminus* in this study. The relationships among these morphological traits and between the traits and the bioclimatic factors indicate a strong ecomorphological relationship in *S. tergeminus* populations across their range. More detailed work, including 3D morphometrics and skeletal

morphometrics throughout the rest of the body, more dietary work, and greater sample sizes for less strongly sampled populations, will produce greater clarity on the extent of these trait-environment relationships. These morphological analyses will help determine what changes to expect in *S. tergeminus* – and what measures to take to conserve and protect Western massasauga populations.

4.5. References

Alencar, L. R., M. P. Gaiarsa, and M. Martins. 2013. The evolution of diet and microhabitat use in pseudoboine snakes. South American Journal of Herpetology 8:60-66.

Barnosky, A. D., N. Matzke, S. Tomiya, G. O. Wogan, B. Swartz, T. B. Quental, C. Marshall, J. L. McGuire, E. L. Lindsey, K. C. Maguire, and B. Mersey. 2011. Has the Earth's sixth mass extinction already arrived? Nature 471(7336), pp.51-57.

Bonnet, X., R. Shine, G. Naulleau, and C. Thiburce. 2001. Plastic vipers: influence of food intake on the size and shape of Gaboon vipers (*Bitis gabonica*). Journal of Zoology 255:341-351.

Britt, E. J., A. J. Clark, and A. F. Bennett. 2009. Dental morphologies in gartersnakes (*Thamnophis*) and their connection to dietary preferences. Journal of Herpetology pp.252-259.

Camilleri, C. and R. Shine. 1990**.** Sexual dimorphism and dietary divergence: differences in trophic morphology between male and female snakes. Copeia 1990**:**649–658.

Campbell, J. A., W. W. Lamar, and E. D. Brodie. 2004. The venomous reptiles of the western hemisphere (Vol. 1, No. 2). Ithaca [NY]: Comstock Pub. Associates.

Carducci, J. P. and E. M. Jakob. 2000. Rearing environment affects behaviour of jumping spiders. Animal Behaviour 59:39-46.

Courtney Jones, S. K., A. J. Munn, and P. G. Byrne. 2018. Effect of captivity on morphology: negligible changes in external morphology mask significant changes in internal morphology. Royal Society open science 5:172470.

Crother, B. I., J. M. Savage, and A. T. Holycross. 2011. Case 3571 *Crotalinus catenatus* Rafinesque, 1818 (currently *Sistrurus catenatus*) and *Crotalus tergeminus* Say in James, 1822 (currently *Sistrurus tergeminus*; Reptilia, Serpentes): proposed conservation of usage by designation of neotypes for both species. Bulletin of Zoological Nomenclature 68:271–274.

Crother, B. I., J. M. Savage, A. T. Holycross. 2012. Comment on the proposed conservation of *Crotalinus catenatus* Rafinesque, 1818 (currently *Sistrurus catenatus*) and *Crotalus tergeminus* (currently *Sistrurus tergeminus*; Reptilia, Serpentes) by designation of neotypes for both species, Case 3571. Bulletin of Zoological Nomenclature 69:62–63.

Cundall, D. and H. W. Greene, 2000. Feeding in snakes. Feeding: form, function, and evolution in tetrapod vertebrates. Academic Press, San Diego, CA.

Cundall, D. and F. Irish. 2008. The snake skull. Biology of the Reptilia, 20:349-692.

Dixon, J. R. 2013. Amphibians and reptiles of Texas: with keys, taxonomic synopses, bibliography, and distribution maps. College Station: Texas A&M University Press.

Dryden, I. L., and K. V. Mardia. 1998. Statistical analysis of shape. New York, NY: John Wiley.

Dwyer, C. M. and H. Kaiser. 1997. Relationship between skull form and prey selection in the thamnophiine snake genera *Nerodia* and *Regina*. Journal of Herpetology pp.463-475.

Fabien, A., X. Bonnet, S. Maumelat, D. Bradshaw, and T. Schwaner. 2004. Diet divergence, jaw size and scale counts in two neighbouring populations of tiger snakes (*Notechis scutatus*). Amphibia-Reptilia 25:9-17.

Fick, S. E. and R. J. Hijmans. 2017. WorldClim 2: new 1-km spatial resolution climate surfaces for global land areas. International journal of climatology 37:4302-4315.

Foote, M., 1993. Contributions of individual taxa to overall morphological disparity. Paleobiology 19:403-419.

Gans, C., 1961. The feeding mechanism of snakes and its possible evolution. American Zoologist pp.217-227.

Gibbs, H. L. and W. Rossiter. 2008. Rapid evolution by positive selection and gene gain and loss: PLA 2 venom genes in closely related *Sistrurus* rattlesnakes with divergent diets. Journal of molecular evolution 66:151-166.

Gibbs H. L., M. Murphy, and J. E. Chiucchi. 2011. Genetic identity of endangered massasauga rattlesnakes (*Sistrurus* sp.) in Missouri. Conservation Genetics 12:433–439. doi:10.1007/s10592-010-0151-3.

Glaudas, X., T. Jezkova, and J. A. Rodriguez-Robles. 2008. Feeding ecology of the Great Basin rattlesnake (*Crotalus lutosus*, Viperidae). Canadian Journal of Zoology 86:723-734.

Guyer, C. and M. A. Donnelly. 1990. Length-mass relationships among an assemblage of tropical snakes in Costa Rica. Journal of Tropical Ecology 6:65-76.

Håkansson, J. and P. Jensen. 2005. Behavioural and morphological variation between captive populations of red junglefowl (*Gallus gallus*)–possible implications for conservation. Biological conservation 122:431-439.

Hampton, P. M. 2011. Comparison of cranial form and function in association with diet in natricine snakes. Journal of Morphology 272:1435-1443.

Harvey, D. S. and P. J. Weatherhead. 2011. Thermal ecology of massasauga rattlesnakes (Sistrurus catenatus) near their northern range limit. Canadian Journal of Zoology 89:60-68.

Head, J. J., J. I. Bloch, A. K. Hastings, J. R. Bourque, E. A. Cadena, F. A. Herrera, P. D. Polly, and C. A. Jaramillo. 2009. Giant boid snake from the Palaeocene neotropics reveals hotter past equatorial temperatures. Nature 457:715-717.

Herrando-Pérez, S., F. Ferri-Yáñez, C. Monasterio, W. Beukema, V. Gomes, J. Belliure, S. L. Chown, D. R. Vieites, and M. B. Araújo. 2019. Intraspecific variation in

lizard heat tolerance alters estimates of climate impact. Journal of Animal Ecology 88:247-257.

Herrel, A., S. E. Vincent, M. E. Alfaro, S. Van Wassenbergh, B. Vanhooydonck, and D. J. Irschick. 2008. Morphological convergence as a consequence of extreme functional demands: examples from the feeding system of natricine snakes. Journal of evolutionary biology 21:1438-1448.

Hibbitts, T. J. and L. A. Fitzgerald. 2005. Morphological and ecological convergence in two natricine snakes. Biological Journal of the Linnean Society 85:363-371.

Holycross, A. T. and S. P. Mackessy. 2002. Variation in the diet of *Sistrurus catenatus* (Massasauga), with emphasis on *Sistrurus catenatus edwardsii* (Desert Massasauga). Journal of Herpetology 36:454-464.

Huntley, L. C., D. J. Gower, F. L. Sampaio, E. S. Collins, A. Goswami, and A. C. Fabre. 2021. Intraspecific morphological variation in the shieldtail snake *Rhinophis philippinus* (Serpentes: Uropeltidae), with particular reference to tail-shield and cranial 3D geometric morphometrics. Journal of Zoological Systematics and Evolutionary Research 59:1357-1370.

King, R. B. 1989. Sexual dimorphism in snake tail length: sexual selection, natural selection, or morphological constraint? Biological Journal of the Linnean Society 38:133-154.

Klaczko, J., E. Sherratt, and E. Z. Setz. 2016. Are diet preferences associated to skulls shape diversification in xenodontine snakes? PloS one 11(2), p.e0148375.

Klauber, L. M. 1939. A Statistical Study of Rattlesnakes. VI, Fangs. San Diego Soc. Nat. Hist. Occasional Papers. San Diego.

Knox, A. and K. Jackson. 2010. Ecological and phylogenetic influences on maxillary dentition in snakes. Phyllomedusa: Journal of Herpetology 9:121-131.

Kubatko L. S., H. L. Gibbs, E. W. Bloomquist. 2011. Inferring species-level phylogenies and taxonomic distinctiveness using multilocus data in *Sistrurus* rattlesnakes. Systematic Biology 60:393–409.

LaDuc, T. J. 2003. Allometry and size evolution in the rattlesnake, with emphasis on predatory strike performance. The University of Texas at Austin.

Lawing, A. M. and P. D. Polly. 2010. Geometric morphometrics: recent applications to the study of evolution and development. Journal of Zoology 280:1-7.

Lawing, A. M. and P. D. Polly. 2011. Pleistocene climate, phylogeny, and climate envelope models: an integrative approach to better understand species' response to climate change. PloS one, 6(12), p.e28554.

Lawing, A. M., J. J. Head, and P. D. Polly. 2012. The ecology of morphology: the ecometrics of locomotion and macroenvironment in North American snakes. In Paleontology in ecology and conservation (pp. 117-146). Springer, Berlin, Heidelberg.

Lindell, L. E. 1994. The evolution of vertebral number and body size in snakes. Functional Ecology pp.708-719.

Martins, M., M. S. Araujo, R. J. Sawaya, and R. Nunes. 2001. Diversity and evolution of macrohabitat use, body size and morphology in a monophyletic group of Neotropical pitvipers (*Bothrops*). Journal of Zoology 254:529-538.

McGuire, J. L. 2010. Geometric morphometrics of vole (*Microtus californicus*) dentition as a new paleoclimate proxy: Shape change along geographic and climatic clines. Quaternary international 212:198-205.

McGuire, J. L. and D. A. Lauer. 2020. Linking patterns of intraspecific morphology to changing climates. Journal of Biogeography 47:2417-2425.

Meik, J. M., K. Setser, E. Mocino-Deloya, and A. M. Lawing. 2012. Sexual differences in head form and diet in a population of Mexican lance-headed rattlesnakes, *Crotalus polystictus*. Biological Journal of the Linnean Society 106:633-640.

Mimura, M., T. Yahara, D. P. Faith, E. Vázquez-Domínguez, R. I. Colautti, H. Araki, F. Javadi, J. Núñez-Farfán, A. S. Mori, S. Zhou, and P. M. Hollingsworth. 2017. Understanding and monitoring the consequences of human impacts on intraspecific variation. Evolutionary applications 10:121-139.

Myers, N., R. A. Mittermeier, C. G. Mittermeier, G. A. Da Fonseca, and J. Kent. 2000. Biodiversity hotspots for conservation priorities. Nature 403:853.

Norton, S. F., J. J. Luczkovich, and P. J. Motta. 1995. The role of ecomorphological studies in the comparative biology of fishes. In Ecomorphology of fishes (pp. 287-304). Springer, Dordrecht.

O'Regan, H. J. and A. C. Kitchener. 2005. The effects of captivity on the morphology of captive, domesticated and feral mammals. Mammal Review 35:215-230.

Pimm, S. L., and P. Raven. 2000. Extinction by numbers. Nature 403:843–845.

Polly, P. D., J. T. Eronen, M. Fred, G. P. Dietl, V. Mosbrugger, C. Scheidegger, D. C. Frank, J. Damuth, N. C. Stenseth, and M. Fortelius. 2011. History matters: ecometrics and integrative climate change biology. Proceedings of the Royal Society B: Biological Sciences 278:1131-1140.

Queral-Regil, A. and R. B. King. 1998. Evidence for phenotypic plasticity in snake body size and relative head dimensions in response to amount and size of prey. Copeia pp.423-429.

Rhoda, D., P. D. Polly, C. Raxworthy, and M. Segall. 2021. Morphological integration and modularity in the hyperkinetic feeding system of aquatic-foraging snakes. Evolution 75:56-72.

Ricklefs, R.E. and D. B. Miles. 1994. Ecological and evolutionary inferences from morphology: an ecological perspective. Ecological morphology: integrative organismal biology 1:13-41.

Rohlf, F. J. and D. Slice. 1990. Extensions of the Procrustes method for the optimal superimposition of landmarks. Systematic biology 39:40-59.

Rohlf, F. J. 1993. Relative warp analysis and an example of its application to mosquito wings. Contributions to morphometrics 8:131-159.

Rohlf F. J. 2010. tpsDIG2. Available at: http://life.bio.sunysb.edu/morph/index.html.

Ryberg, W. A., J. A. Harvey, A. Blick, T. J. Hibbitts, and G. Voelker. 2015. Genetic structure is inconsistent with subspecies designations in the western massasauga Sistrurus tergeminus. Journal of Fish and Wildlife Management 6:350-359.

Siciliano-Martina, L., J. E. Light, and A. M. Lawing. 2021a. Changes in canid cranial morphology induced by captivity and conservation implications. Biological Conservation 257:109143.

Siciliano-Martina, L., J. E. Light, and A. M. Lawing. 2021b. Cranial morphology of captive mammals: a meta-analysis. Frontiers in zoology 18:1-13.

Shine, R. 1986. Sexual differences in morphology and niche utilization in an aquatic snake, *Acrochordus arafurae*. Oecologia 69:260-267.

Shine, R. 1991. Why do larger snakes eat larger prey items? Functional Ecology pp.493-502.

Shine, R., R. Reed, S. Shetty, and H. Cogger. 2002. Relationships between sexual dimorphism and niche partitioning within a clade of sea-snakes (Laticaudinae). Oecologia 133:45-53.

Smith, F. A., J. L. Betancourt, and J. H. Brown. 1995. Evolution of body size in the woodrat over the past 25,000 years of climate change. Science, 270:2012-2014.

Tzeng, T. D., 2004. Morphological variation between populations of spotted mackerel (*Scomber australasicus*) off Taiwan. Fisheries Research 68:45-55.

Vincent, S. E., A. Herrel, and D. J. Irschick. 2004. Sexual dimorphism in head shape and diet in the cottonmouth snake (*Agkistrodon piscivorus*). Journal of Zoology 264:53-59.

Vincent, S. E., P. D. Dang, A. Herrel, and N. J. Kley. 2006. Morphological integration and adaptation in the snake feeding system: a comparative phylogenetic study. Journal of Evolutionary Biology 19:1545-1554.

Vincent, S. E., M. C. Brandley, A. Herrel, and M. E. Alfaro. 2009. Convergence in trophic morphology and feeding performance among piscivorous natricine snakes. Journal of evolutionary biology 22:1203-1211.

Walkup, D. K., A. M. Lawing, T. J. Hibbitts, and W. A. Ryberg. Biogeographic consequences of shifting climate in *Sistrurus tergeminus* (western massasauga). *In Review* at Diversity and Distributions.

Watanabe, A., A. C. Fabre, R. N. Felice, J. A. Maisano, J. Müller, A. Herrel, and A. Goswami. 2019. Ecomorphological diversification in squamates from conserved pattern of cranial integration. Proceedings of the National Academy of Sciences 116:14688-14697.

Wiens, J. J., M. C. Brandley, and T. W. Reeder. 2006. Why does a trait evolve multiple times within a clade? Repeated evolution of snakeline body form in squamate reptiles. Evolution 60:123-141.

5. BUILDING A BACKBONE FOR SNAKE ECOMETRICS USING ANTERIOR MORPHOLOGY IN MIDDLE TRUNK VERTEBRAE

"The philosophical study of nature endeavors, in the vicissitudes of phenomena, to connect the present with the past." – Alexander von Humboldt

5.1. Introduction

Anthropogenic environmental change threatens to overwhelm the ability of ecosystems and species to sustain historical function (Myers et al., 2000; Pimm and Raven, 2000; Brook et al., 2003; Thomas et al., 2004; Barnosky et al., 2011; Barnosky et al., 2017). Integrative science merging conservation biology, paleontology, and Earth sciences is vital to accessing information on deep time data for historical function, equipping it to secure the future of Earth's organisms, resources, and natural systems (Eronen et al., 2010; Polly et al., 2011; Barnosky et al., 2017). Efforts to predict and assess the effects of long-term environmental changes on organisms need a deep time perspective, as applying organismal responses to environmental change over long time scales improves forecasting models related to the behavior and survivability of living organisms facing present perils (McGuire and Davis, 2013; Davis et al., 2014; Badgley et al., 2017; Lima-Ribeiro et al., 2017; Rivera et al., 2020). One way to connect the present to the past is through functional traits – measurable features that influence the interaction between the organism and its environment (Eronen et al., 2010; Polly et al., 2011). At the community level, these functional traits are potentially strong indicators of

climates (e.g., mean annual temperature) or environments (e.g., vegetation cover) spanning space and time. This enables access to the deep time data capable of anticipatory models of potential range shifts and extinctions, thus improving our understanding of how organisms have interacted with their environments through periods of past environmental change (Polly, 2010; Lawing et al., 2012; Enquist et al., 2015).

The field of *ecometrics* examines the community-level relationships between organismal functional traits and environmental factors across geographic and temporal scales (Eronen et al., 2010; Polly 2010; Polly et al., 2011; Lawing et al., 2012; Polly and Head, 2015; Vermillion et al., 2018). Each functional trait is mechanistically connected to the environment and is likely to perform better in some environments than others, thereby sorting organisms with similar traits into similar environments and playing a role in community assembly via selection and geographic sorting (Polly and Head, 2015).

Ecometrics has been applied to examine a plethora of ecological and paleoecological questions, which makes it possible to understand biodiversity responses to changes in different environmental factors (e.g., temperature, precipation, or vegetation cover). For example, ecometrics has been used to expand the synthesis of conservation biology and paleobiology, (i.e., conservation paleobiology; Eronen et al., 2010; Polly et al., 2011; Lawing et al., 2012; Polly and Head, 2015; Barnosky et al., 2017). Ecometrics that quantify functional trait – environmental relationships exist for a number of different organisms. Some of these relationships include leaf physiognomy and mean annual temperature (Peppe et al., 2011); hypsodonty in ungulates, rodents, and

lagomorphs and annual precipitation (Fortelius et al., 2002, 2016; Evans, 2013; Schap et al., 2021; Short et al., 2021); limb proportions in carnivorans for vegetation cover, mean annual temperature, and annual precipitation (Polly, 2010; Polly et al., 2017) and ungulates for ecoregion division, vegetation cover, and annual precipitation (Short and Lawing, 2021); squamate body mass and physiology and mean annual temperature (Head, 2010; Headet al., 2009, 2013), and snake relative tail length and ecological province, vegetation cover, and mean annual temperature. (Lawing et al., 2012). Polly and Sarwar (2014) used ecometrics to assess extinction, extirpation, and exotic introductions on continental scales. Polly and Head (2015) evaluated the how vulnerable communities were to environmental change, and were followed by Barnosky et al. (2017) in that endeavor. Lawing et al. (2017) sought to comprehend how non-ecological processes effected patterns of biodiversity, and a number of papers have been used to reconstruct paleoenvironment and paleoclimate (Fortelius et al., 2016; Vermillion et al., 2018; Faith et al., 2019; Polly, 2020; Schap et al., 2021; Short et al., 2021). As such, ecometric methods are increasingly useful integrative tools for reconstructing past environments and understanding geologically short- and long-term organismal dynamics in the face of environmental perturbations.

With a long history of extant groups appearing back in the Miocene fossil record of North America (Holman, 2000), snakes are excellent candidates for developing an ecometric method applicable to modern and paleontological datasets alike. Snakes in particular are of conservational, ecological, economic, and medical interest (Holman, 2000; Mullin and Siegel, 2009; Brooks et al., 2010), and are expected to exhibit

significant responses to climate change over the next century, as indicated by their geographic responses to Quaternary climate cycles in North America (Lawing and Polly, 2011), ectothermic physiology (Head et al., 2009), global population declines (Gibbons et al., 2000; Reading et al., 2010), and ecometric relationships (Head et al., 2009; Lawing et al, 2012). Furthermore, because snakes locomote with a high degree of body-to-surface contact, it is likely that environmental factors affecting those surfaces (vegetation cover, temperature, precipitation, etc.) will influence the distributions of the various snake taxa. Whereas the locomotor morphology of mammals is primarily captured through limb bone proportions (Polly, 2010; Short and Lawing, 2021), snakes mainly employ their vertebrae as the primary skeletal element to pursue prey and move through myriad environments. As such, it has been suggested that snake vertebrae may show functional ecomorphology related to locomotion, especially in regard to body elasticity or rigidity, much as limb bone proportions do in mammals (Johnson, 1955; Meylan, 1982; Moon, 1999; Holman, 2000; Lillywhite et al., 2000; Lawing et al., 2012; Lillywhite, 2014). Because middle trunk vertebrae are the most common snake skeletal elements in the North American fossil record (Holman, 2000), vertebral shape shows great potential as an ecometric.

Creating new models and combining multiple ecometrics will likely provide more complete reconstructions of paleoenvironments and organismal dynamics. While ecometrics are well-established and have been successfully applied to interpret the relationships between functional morphology and environment for some plant and mammal communities, we know less about functional trait-environment relationships

across other groups of organisms. Foundational work on squamate ecometrics established maximum squamate body mass and ecothermic physiology as a paleothermometer (Head et al. 2009, Head et al. 2013). Lawing et al. (2012) established relative tail length of snakes, functionally tied to locomotion, as an indicator of vegetation cover, ecological province, and mean annual temperature. However, few snake fossils are preserved as articulated skeletons, so establishing other ecometric traits in snakes would be useful to make better use of the many disarticulated snake vertebrae preserved in the fossil record. Lawing et al. (2012) also investigated vertebral shape and vertebral length-to-width ratios and found ecomorphological signal, so both of these aspects of morphology serve as good candidates to develop into ecometric traits with the collection of more trait data. This serves as an excellent opportunity to develop ecometric methods that are applicable to reptile communities through both space and deep time.

Here, I construct a framework to investigate vertebral shape in snakes as an ecometric tool using geometric morphometrics. In constructing this ecometric framework, I aim to 1) describe ecomorphological signal in the anterior aspect of vertebral shape; 2) explore the relationships between the community-level geography of morphology and environmental factors to produce ecometric models; 3) evaluate the ecometric models by both calculating the anomaly between maximum likelihood predictions and actual environmental values and by examining case studies of communities with documented environmental shifts through space and time. I examine the anterior aspect of the snake trunk vertebrae in two dimensions. I select two-

dimensional geometric morphometrics in order to create an easily reproducible and accessible method of capturing shape without the effects of size, and I select anterior view because it contains the most information on vertebral articular surfaces compared to other aspects on a single plane. This makes the anterior aspect ideal for capturing variation related to function and locomotion. If the anterior aspect of snake middle trunk vertebrae exhibits differences in homologous functional traits related to locomotion, then it would be possible to identify which aspects of vertebral shape influence function and subsequently develop a methodology applicable to both fossil and living snake vertebrae. When compared to methods such as CT-scanning, photogrammetry, or taking multiple linear measurements, this method should also be less time-intensive and monetarily expensive.

5.2. Materials and methods

5.2.1. Data Collection

I examined snake vertebral shape with geometric morphometric methods to evaluate the potential of a shape-based ecometric using snake middle trunk vertebrae. I then explored several methods and selected potential ecometric indices based on the distribution of community vertebral shape. I photographed the anterior view of 396 middle trunk vertebrae from disarticulated skeletal material for 119 North American snake species, representing >99% of extant snake genera and >85% of extant snake species in the United States of America and Canada (Appendix Table D5). I took all photographs with a DinoLite Edge digital microscope or a Canon EOS Rebel SX camera

with a Canon Zoom EF-S Lens (18-55mm). Because I did not have the same number of vertebrae photographed for each species (one to ten vertebrae per species; one to three individuals per species), and wished to have each species weighted evenly for the analyses, I took the mean shape of the vertebrae for each species as representatives of the 119 taxa to use in the analyses. In doing this, I assume that the interspecific difference in the morphometric shape of middle trunk vertebrae overwhelms the intraspecific and inter-individual variation in snakes – an assumption also made in previous studies (Holman, 2000; Parmley and Walker, 2003; Lawing and Polly, 2010; Lawing et al., 2012). I collected data from disarticulated skeletal material in vertebrate zoology or vertebrate paleontology collections and assigned each species a substrate lifestyle category (aquatic, semiaquatic, arboreal, semiarboreal, fossorial, semifossorial, and terrestrial), that best describes the typical locomotor behavior of a species (Catalogue of American Amphibians and Reptiles; Lawing et al., 2012 Online Supplemental Data).

5.2.2. Quantitative methods

I described the shape of the anterior view of a middle trunk vertebra in an individual snake by developing a landmark scheme with 23 homologous landmarks (Fig. 5.1A, Table 5.1; see Appendix Fig. D1 for the distributions at each landmark) using the tpsDig2 application. These landmarks are selected to capture both the overall anterior shape of the vertebrae as well as the anterior shape of the major articulations associated with the snake vertebral column. I chose the anterior aspect because it contains the most information on overall shape and articular surfaces on a single plane compared to other

aspects; this makes the anterior view more useful for capturing variation related to function and locomotive behaviors in two dimensions. This landmark scheme is based on the landmark scheme of Lawing et al. (2012). I did not include any landmarks that are not present in the middle trunk vertebrae of all species in the data (e.g., no landmarks for the hypophysis). I removed size, orientation, and location effects in landmark data by Procrustes superimposing landmarks to scale, rotate, and translate the data for analysis using a least-squares algorithm on the overall dataset of 396 specimens (Fig. 1B), then used Procrustes superimposition again after reducing that dataset to the mean vertebral shapes of the 119 species in the study (Fig. 1C; Sneath 1967; Gower 1975; Rohlf and Slice 1990; Lawing and Polly 2010).

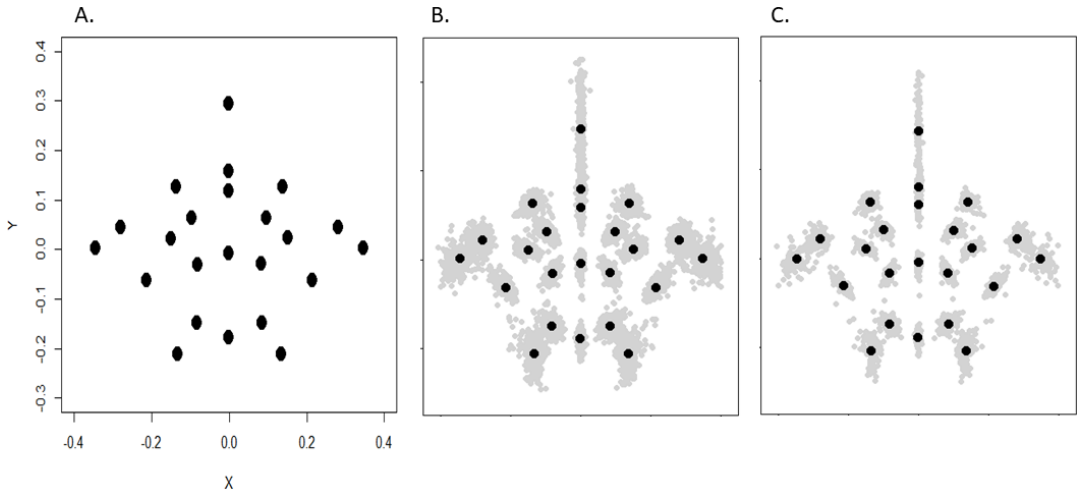

Figure 5.1. A.: Hypothetical snake vertebra represented by a 23-landmark scheme. B.: Distribution of landmarks (gray) around centroid landmark values (black) for all 396 snakes in the data after Procrustes superimposition. C.: Distribution of landmarks (gray) around centroid landmark values (black) for 119 snakes species represented by mean shapes for each species.

I implemented a Principal Component Analysis (PCA) on the superimposed landmarks to quantify independent differences in vertebral shape represented by PC axes. While phylogenetic principal components analysis (pPCA), which ordinates multivariate data while taking into account phylogenetic non-independence among species means, is an option for producing a shape space that preserves Procrustes distance, this method also produces scores that are 1) correlated with each other and 2) have variances that do not correspond to the eigenvalues on phylogenetically corrected axes (Polly et al., 2013). I therefore elected to apply an ordinary PCA in order to have independent axes of shape variation for a phylogenetically informed Multivariate Analysis of Variance (MANOVA). I then used the phylogenetically informed MANOVA on the Principal Components (PCs), with substrate use as the factor, to determine if differences in aspects of vertebral shape explained variation in substrate use. Traits and phylogeny have been shown to interact together in relation to environmental factors, also known as clade sorting, so ecometric relationships could result from underlying mechanisms of speciation, adaptation, and geographic sorting (Polly et al., 2017). I used the maximum-likelihood phylogeny of extant snakes by Figueroa et al., (2016), as it is one of the few large-scale species-level phylogenies focusing solely on snakes available. Based on the results of the MANOVA and Analyses of Variance (ANOVAs) of individual PCs, I selected the PCs that described the greatest amount of variance and exhibited significant relationships with substrate use. I then constructed vector plots of the vertebrae along each PC axis – in this case, the shape three standard deviations away from the mean in each direction on the selected PC axes

in the dataset – and examined them to determine what morphological changes best explained the most variation in snake middle trunk vertebrae. Based on the results, I chose the first six PCs (~89% of total variation explained) for the vector plots and ecometric analyses.

Table 5.1. Landmark definitions of the 23-landmark configuration for this study.

Landmark No.	Description
1	Dorsal edge of neural spine
2	Midline dorsal edge of neural arch
3	Midline ventral edge of neural arch
4	Midline dorsal edge of centrum
5	Midline ventral edge of centrum
6	Right ventrolateral contact between apophysis & centrum
7	Right ventromedial edge of parapophysis
8	Right dorsomedial edge of diapophysis
9	Right lateral edge of prezygapophyseal body
10	Right dorsolateral edge of prezygapophyseal articular facet
11	Right medial contact between centrum & neural arch
12	Right ventromedial edge of prezygapophyseal articular facet
13	Right ventrolateral contact between zygosphene & neural canal
14	Right dorsolateral edge of zygophene
15	Left ventrolateral contact between apophysis & centrum
16	Left ventromedial edge of parapophysis
17	Left dorsomedial edge of diapophysis
18	Left lateral edge of prezygapophyseal body
19	Left dorsolateral edge of prezygapophyseal articular facet
20	Left medial contact between centrum & neural arch
21	Left ventromedial edge of prezygapophyseal articular facet
22	Left ventrolateral contact between zygosphene & neural canal
23	Left dorsolateral edge of zygosphene

5.2.3. Models

I investigated the relationships between the geographic distribution of community vertebral shape and mean annual temperature (Willmott and Legates 1998), annual precipitation (Willmott and Legates 1998), vegetation cover (Matthews 1983, 1984), and ecoregion province (Bailey 1998; 2005; Hijmans et al., 2005). I sampled climate, environment, and snake assemblages from the U.S. and Canadian landscape using 50 km equidistant points (sampling scheme derived from Polly, 2010). This resulted in 4572 geographic sampling points. Snake assemblages were sampled by extracting a list of snakes that occur at each point based on range maps that overlap with each other at each sample point (Polly 2010). This scale is appropriate for measuring patterns for the fossil record, as it is similar in scale to the geographic mixing that often occurs in fossil assemblages (Fortelius et al. 2002; Polly 2010; Polly and Sarwar 2014). To understand the geography of morphology – or the variation in shape of the functional trait represented by each PC – I mapped the amount of variation at each sampling point.

I used two methods to model the relationship between the traits and climate, vegetation cover, and ecoregion province: 1) the coefficient of determination (R^2) of the linear relationships between the PCs and environmental factors, and 2) a maximum likelihood estimation of environment given the community-level distribution of traits. I extracted the amount of explained variance from the R^2 values and used that to inform which trait-environment relationships I should model with the maximum likelihood approach. For the maximum likelihood method, I created an ecometric space for each environmental parameter by calculating the means and standard deviations of vertebral

shape, represented by PCs, at each sampling point and recording the respective environmental parameters or categories. I then binned the means and standard deviations into a 25-by-25 cell bivariate plot. In each cell, I tallied the frequency of the environmental value, and used those to develop a maximum likelihood surface to quantify the expected value or category specified by the mean and standard deviation of a given assemblage of traits. Finally, I plotted the maximum likelihood estimate of environments from the traits over the geographic surface of the U.S. and Canada. I also plotted the difference between the actual Mean Annual Temperature (MAT) values and the maximum likelihood model projections over geographic space to create an anomaly map visualizing any mismatched predictions, and used Pearson's correlation coefficient to calculate the proportion of variance represented by the projections compared to actual values. All analyses were performed in R, and scripts are available via the Appendix D.

5.2.4. Case studies

I use five sites in the United States of America to test if the PCs accurately identify MAT and potential changes in MAT through time (four sites) and space (one site). Here, I also assess case study sites that have shown detectable changes for other ecometrics – as well as two new sites – to distinguish detectable changes in the mean and standard deviation of snake vertebral shape related to environmental change and alterations to the snake faunas. These case studies were plotted in the ecometric spaces by the means and standard deviations of their community trunk vertebral shape values. The five case study sites are further described below.

Brodman et al. (2002) described herpetofaunal changes at the Jackson-Pulaski Fish and Wildlife Refuge in Indiana from 1931 to 1994 that included a decrease from 13 to 10 snake species. During that time, drained, agriculturally-allocated wetlands, marsh, and dry prairie transitioned to homogenized, closed-canopy oak woodlands (Lawing et al., 2012). Lawing et al. (2012) identified an ecometric shift for relative tail length between the historical and modern snake faunas related to vegetation cover.

Fort Riley, Kansas, is a grassland reported by Busby and Parmelee (1996) to have suffered a decline from 22 to 17 snake species between 1930 and 1996, likely as a result of agriculture and land development altering the river valleys. Lawing et al. (2012) were able to detect a small change in relative tail length, likely related to the decrease in snake taxonomic richness.

The University of Kansas Natural History Reservation in Lawrence, Kansas is located in a grassland-deciduous forest ecotone. From 1947-2006, the reservation has reverted from tall-grass prairie and agricultural land to a grassland-deciduous forest mosaic environment; during this same period, snakes suffered a severe decline from ten to six species, with additional decreases in abundance for four additional species (Fitch, 2006). Lawing et al. (2012) were able to detect both the change in the snake fauna and the change in vegetation type with their relative tail length ecometric.

The Middle Rio Grande riparian forest of New Mexico was monitored by Bateman et al. (2009) from 2000-2006 and compared with previous surveys from 1984, 1995, 1996, and georeferenced records from the Museum of Southwestern Biology in order to determine the effects of non-native plant and fuel removal on snake species

richness and abundance. Compared to historical records, Bateman et al., (2009) found four fewer taxa, some of which may be attributable to the loss of off-channel semi-aquatic habitats in the area.

The fifth case study documents change in a snake fauna attributable to environmental differences across space, rather than through time. Ford et al. (1991) recorded species richness and abundance in adjacent areas of Sheff's Wood in Eastern Texas, where trees in the reserve had not been disturbed for 45 years, and grazing had not been allowed for 20 years at the time of the study's publication. Ford et al. (1991) selected three distinct habitats of equal size to evaluate for differences in the snake assemblage between adjacent environments. They found 15 species in a lowland floodplain, 17 species in an upland deciduous woodland, and 10 species in an upland coniferous woodland. Detecting vertebral shape differences and changes in MAT for adjacent snake faunas as well as in historical to modern snake faunas would suggest that these methods could be used to compare modern, historical, and fossil localities of similar or dissimilar ages regardless of how near the sites are to each other – provided the necessary material is available.

5.3. Results

5.3.1. Characterization of shape space

The results of the phylogenetically informed Multivariate Analysis of Variance (MANOVA) on the PCs indicate that five of the first six PCs (excluding PC4) show a significant difference ($p < 0.05$) from mean shape for at least one ecological category (Table 5.2). Figure 5.2 shows the PCA plots for the first six PCs, with associated box-

and-whisker plots in Figure 5.3. I selected the first six PCs because they represented >85% of shape variation in the data, at 88.8% total variance explained. A plot of the distribution of variation across all 46 PCs by percentage is included in Appendix Figure D2.

Table 5.2. Summary of statistics for phylogenetically informed MANOVA and correlation coefficients for substrate-use ecology and the first six PCs.

	Lambda	Delta	Kappa	Df	Sum of Sq.	Mean Sq.	F	Pr (>F)	Mult. R^2	Adj. R^2
PC1-PC6	0.90	1.00	1.00	6	5.64	0.94	2.82	0.01	0.15	0.10
PC1	0.99	1.00	1.00	6	0.51	0.09	2.75	0.02	0.15	0.09
PC2	1.00	1.00	1.00	6	0.92	0.15	3.81	<0.01	0.19	0.14
PC3	0.59	1.00	1.00	6	0.60	0.10	2.22	0.05	0.12	0.07
PC4	0.99	1.00	1.00	6	0.26	0.04	0.57	0.75	0.03	-0.03
PC5	0.79	1.00	1.00	6	1.03	0.17	3.10	0.01	0.16	0.11
PC6	0.91	1.00	1.00	6	0.61	0.10	2.27	0.04	0.12	0.07

Examination of vector plots for three standard deviations in both the negative and positive directions for PC1-PC6 (on each individual PC axis) provided important information about how shape varied in snake mid-trunk vertebrae and across environments (Fig. 5.4). The lambda, F-value, p-value, and R^2 statistics are summarized in Table 5.2, while t-values and p-values for individual substrate use ecologies are summarized in Appendix Table D1. The relative height of the vertebrae, particularly at the neural spine and the parapophyses, best explain shape change along the PC1 axis (48.1% of total variation), with *Crotalus tigris* (terrestrial) and *Rena humilis* (fossorial) representing the terminal members at each end of the axis. Along this axis of shape variation, vertebrae with longer neural spines also tend to have longer, ventrally oriented

parapophyses, and vice versa. PC1 found that shape differences were explained by both phylogeny (lambda = 0.90) and ecology ($R^2 = 0.09$, $p < 0.05$) in shape mainly for the assigned fossorial, semifossorial, and terrestrial substrate use categories when the effects of phylogeny were considered. Substrate use categories with shorter neural spines and parapophyses primarily included arboreal, semiarboreal, fossorial, and semifossorial groups, while aquatic, semiaquatic, and terrestrial groups generally had longer neural spines and parapophyses. Additionally, each "semi-" category falls between and/or within their more specialized counterparts and terrestrial shape values, confirming that for at least this axis of shape change, the substrate use categories work well.

The relative length and orientation of the prezygapophyses, and therefore the relative width of the vertebrae at the prezygapophyses, best explain shape change along the PC2 axis (~18.7% of total variation), with *Masticophis bilineatus* (semiarboreal) and *Charina bottae* (semifossorial) representing the end members. Longer prezygapophyses are generally more ventrally oriented in this axis of shape variation, whereas shorter prezygapophyses are typically more dorsally oriented. These differences were also associated with smaller changes in the length of the parapophyses, the height of the cotyl, and the lateral extent of the prezygapophyseal articular facets. PC2 found significant differences ($R^2 = 0.14$, $p < 0.05$) for the fossorial and semifossorial categories when the effects of phylogeny were considered. Fossorial, semifossorial, and terrestrial groups generally possess more dorsally oriented and relatively shorter prezygapophyses than aquatic, arboreal, and semiarboreal groups, while semiaquatic snakes are near the

mean shape. Again, most “semi-” categories fall in-between or overlap with their more specialized counterparts and the terrestrial category.

The overall shape of the vertebra dorsal to the cotyl best explains shape change along the PC3 axis (~10.9 % of total variation), with *Lampropeltis alterna* (terrestrial) and *Regina grahamii* (aquatic) representing the terminal members. These changes include the shape and wdith of the zygosphene and neural canal and the overall width at the prezygapophyses. Generally, this axis of shape variation ranges from wide, depressed neural arches with wider neural canals to narrower, vaulted neural arches and less wide neural canals. PC3 found a significant difference ($R^2 = 0.07$, $p < 0.05$) when the effects of phylogeny were considered, but for no specific ecologies. Generally, semifossorial and semiaquatic groups tend to have narrower neural arches and depressed neural canals, the terrestrial group falls in the middle, and fossorial, semiarboreal, aquatic, and arboreal groups have progressively more vaulted neural arches and slightly more open neural canals.

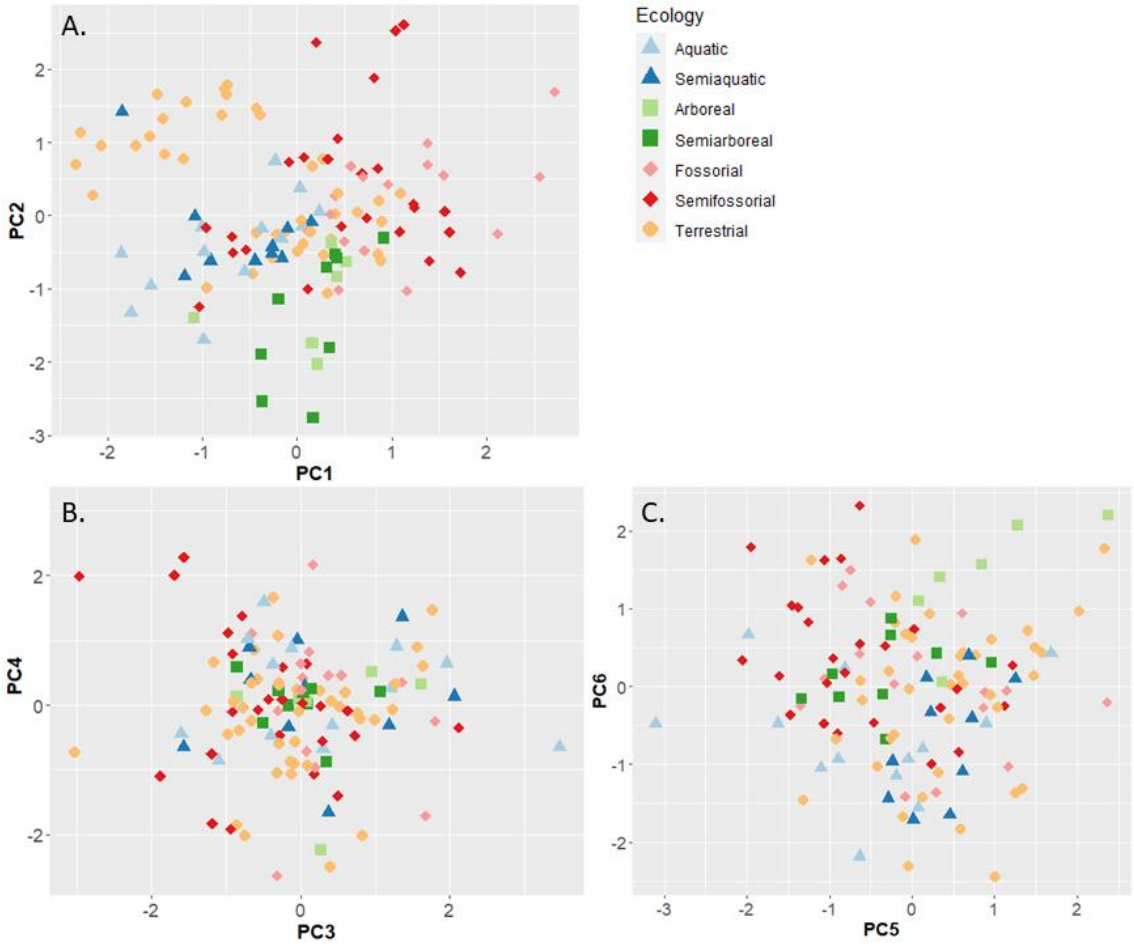

Figure 5.2. PCA plots for PC1-PC6. Colors and shapes represent different primary foraging habitat. A. is PC1-PC2, B. is PC3-PC4, and C. is PC5-PC6.

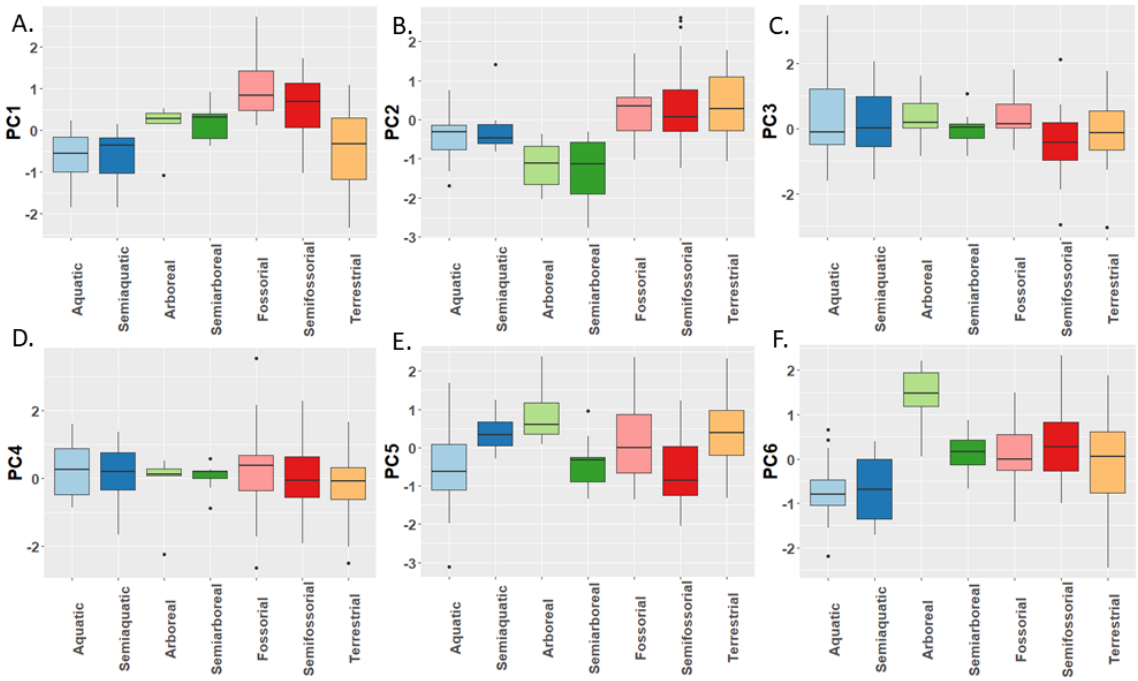

Figure 5.3. Box-and-whisker plots for PC1-PC6. Colors represent different primary foraging habitats, and lines within boxes represent median values. Ecologies from top-to-bottom in the legend run left-to-right in the plots. A. is PC1, B. is PC2, C. is PC3, D. is PC4, E. is PC5, and D. is PC6.

PC4 (~5.8% of total variation) did not show any significant relationship to any ecological category, and may be predominantly explained by phylogeny, with each landmark moving a small amount, but the relative length of the parapophyses changing the most. The variation of PC4 is represented by end members *Micrurus fulvius* (fossorial) and *Rena humilis* (fossorial), and shape space is dominated by the unusual vertebral morphologies of the latter. If the leptotyphlopids are removed, the shape changes are similar, but to a lesser degree and nearly equally across all landmarks. Along this axis of shape variation, relatively wide prezygapophyseal articular facets are generally associated with larger and rounder cotyl, and shorter, more laterally located

parapophyses; the opposite is true on the other extreme of this axis, with slightly dorso-ventrally depressed cotyl and narrower prezygapophyseal articular facets. This differentiates PC4 from PC1, where the observed shape change along the PC1 axis remains large even if the leptotyphlopids are removed, and the lengths of the neural spine and parapophyses are positively correlated. All ecological categories overlap along this axis of shape change, though the general trend of "semi-" categories occupying ranges near their specialist counterparts and the terrestrial category appears to continue.

The relative width and orientation of the prezygapophyseal articular facets, which grow longer as the prezygapophyses and neural canal constrict and the cotyl dorso-ventrally flattens, best explain shape change along the PC5 axis (~2.8% of total variation), with *Nerodia harteri* (aquatic) and *Oxybelis aeneus* (arboreal) representing the terminal members. On one end of this axis of shape variation, relatively wide prezygapophyseal articular facets coincide with shorter prezygapophyses, dorso-ventrally compressed cotyls, and constricted neural canals, while the other side exhibits the opposite shape associations. PC5 found significant differences ($R^2 = 0.11$, $p < 0.05$; Table 5.2) when the effects of phylogeny were considered, but for no specific ecologies, although the subaquatic category was near the p-value threshold (Appendix Table D1). Generally, the arboreal and terrestrial categories have relatively longer prezygapophyses on this axis of shape variation.

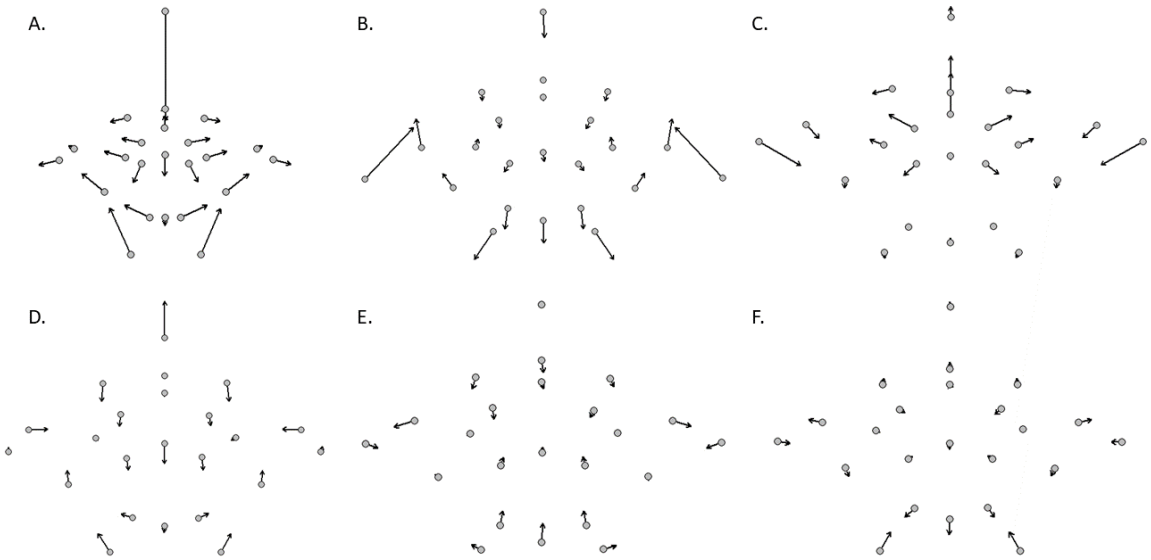

Figure 5.4. Vector plots for PC1-PC6. The gray circles represent three negative standard deviations of the mean shape, while the arrows indicate shape change along each axis, ending at three positive standard deviations of mean shape. A. is PC1, B. is PC2, C. is PC3, D. is PC4, E. is PC5, and F is PC6.

The overall proportion of the lateral and ventral articulations compared to the overall compactness of the vertebrae best explain shape change along the PC6 axis (~2.5% of total variation), with *Thamnophis butleri* (terrestrial) and *Lichanura roseofusca* (semifossorial) representing the terminal members. Relatively larger articulations are associated with a constriction of both overall height and width, with taller cotyls and shorter parapophyses, while relatively smaller articulations are associated with longer parapophyses, slightly shorter diapophyses, and a round cotyl on this axis of shape variation. PC6 found significant differences ($R^2 = 0.07$, $p < 0.05$; Table 5.2) when the effects of phylogeny were considered, but for no specific ecologies, although both aquatic and arboreal ecologies were near the p-value threshold (Appendix Table D1). The aquatic, semiaquatic, and terrestrial categories generally exhibit less

compact shapes with longer prezygapophyses, a taller cotyle, longer parapophyses, and relatively small prezygapophyseal articular facets, while the fossorial category falls near the medial part of the axis, and all other categories show more compact vertebral forms with larger prezygapophyseal facets. At the latter extreme, some vertebrae also show the anterior-most portion of an interzygapophyseal "shelf" that assists in cantilevering behavior. For each of the first six PCs besides PC4, evidence from examining the PCA and box-and-whisker plots suggest that additional ecologies become significant when phylogenetic effects are not considered separately (Fig. 5.2, Fig. 5.3).

5.3.2. Geography of morphology

The projection of taxonomic richness across the geographic space of the continental United States and Canada shows a latitudinal gradient that is similar to that of MAT over the same area, where the highest taxonomic richness and highest MAT are in the southern United States, and the lowest taxonomic richness and lowest MAT are in central to northern Canada (Fig. 5.5). It is important to note that taxonomic diversity is not necessarily equivalent to morphological diversity, and that the mean values of shape can be reached through multiple combinations of shape values from the PCA. A higher taxonomic diversity may therefore have a high, low, or central shape value depending on the combination of vertebral shapes present in any given location. I refer to the community-level morphology across space as the "geography of morphology."

The differences between taxonomic richness and mean vertebral shape values is clear beginning with the geography of morphology for PC1, where much of the southeastern United states is at or near zero, or moderate, shape values (Fig. 5.6). The

mean vertebral shape of PC1 trends towards shorter neural spines and/or shorter parapophyses across much of the country, except in the Rocky Mountains, where the opposite trend occurs. The highest mean vertebral shape values occur primarily in the West, Southwest, and Northeast, while the lowest values occur in the Rocky Mountains and Southeast, including the coast around the Gulf of Mexico.

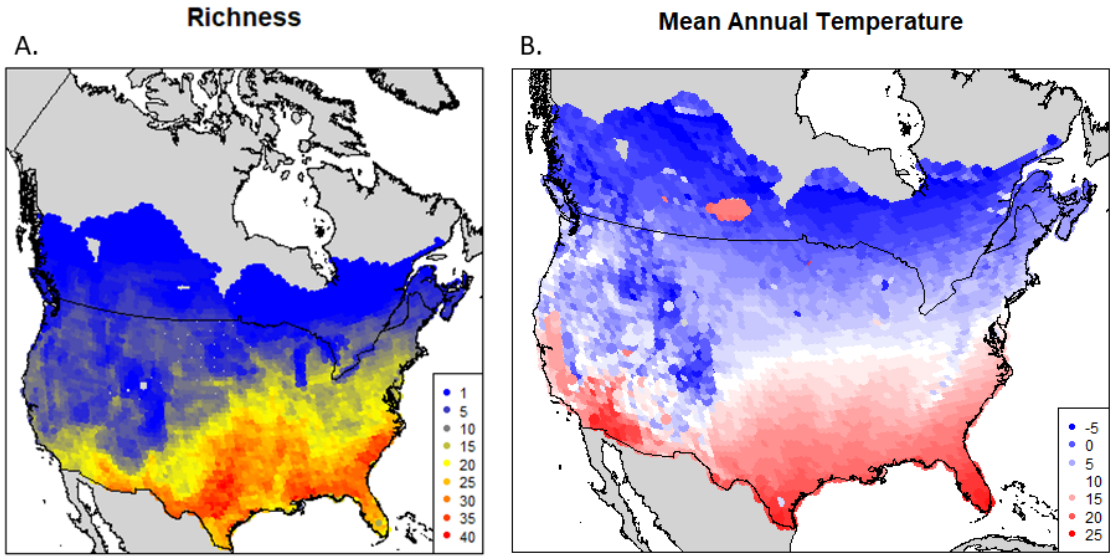

Figure 5.5. Maps of snake species richness (A) and Mean Annual temperature (B) over the regions of the continental United States and Canada that contain snakes.

In PC2, the majority of mean shape values are negative or near zero, with lowest mean values in the North, the southern Rocky Mountains, and near the Great Lakes, and highest mean values in the Columbia Plateau. Morphologically, prezygapophyses are generally longer and more ventrally oriented in areas with lower mean values, and generally shorter and more dorsally oriented in areas with higher values.

The mean vertebral shape values of PC3 are also mostly negative or near zero, where higher values indicated wider, depressed zygosphenes with wider neural canals, and lower values indicate narrower, vaulted zygosphenes and less wide neural canals. The highest mean shape values are located in the southern Midwest, the Great Basin, and south-central Canada, while the lowest mean values are mostly located in the Rocky Mountains.

The lowest mean vertebral shape values of PC4, where the mean shape is relatively wide prezygapophyseal articular facets, larger centra, and short, laterally located parapophyses are found from the Pacific coast to the western Rocky Mountains, whereas the highest mean values exhibiting the opposite morphological trends are in the northern Central Great Plains.

In PC5, mean morphologies are predominantly at or near the middle of the axis of shape variation. The mean values are lower, coinciding with relatively wide prezygapophyseal articular facets, less wide prezygapophyses, larger cotyls, constricted neural canals, and taller neural spines in areas of higher elevation such as the Rocky Mountains, Cascade Range, Sierra Nevada Range, and the Appalachian Mountains, and generally show the opposite trend in areas of lower elevation and in the northernmost parts of the study area.

There is a clear latitudinal gradient for the mean vertebral morphology of PC6, with highest values coinciding with relatively larger articulations and ventrally constricted, taller zygosphenes in the southernmost extent of the data and lowest values with relatively smaller articulations and wider, shorter zygosphenes in the northernmost

extent of the data. There is also a slight East-West gradient, with higher values in the Southwest and lower values in the Northeast.

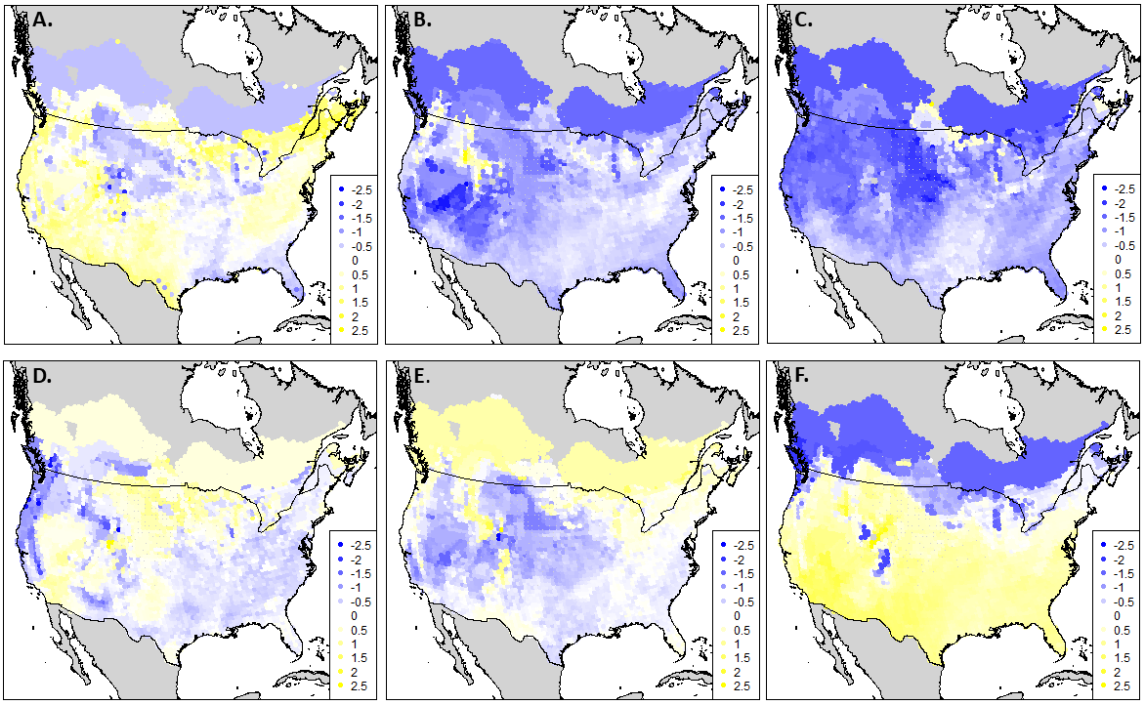

Figure 5.6. The geography of morphology for PC1-PC6. Values represent the community mean vertebral shape values along each PC axis, plotted for snake communities at each 50 km grid point throughout the study region. A. shows PC1 values of the snake communities, B. shows PC2, C. shows PC3, D. shows PC4, E. shows PC5, and F shows PC6. Values range from -2.5 (blue) to 2.5 (yellow).

5.3.3. Linear correlations

I used Pearson's correlation coefficients to determine the coefficient of determination (or proportion of variance), primarily to inform on which functional trait-environmental relationships to prioritize with the maximum likelihood approach, as well as to highlight several potential relationships worth considering. A summary of the statistics for the 19 bioclimatic variables can be found in Appendix Table D2.

Notably, combining the six PCs resulted in higher R^2 values for all 19 bioclimatic variables when compared to any individual PC. All bioclimatic variables were significantly different from the mean ($p < 0.05$) for the combined PCs. For many of the environmental factors, however, low R^2 values imply that, although significant, some environmental factors explain little trait variation. Amongst all environmental factors, the greatest R^2 values were temperature-related and included Mean Annual Temperature ($R^2 = 0.68$, $F_{6,4565} = 1629$, $p < 0.05$), Isothermality ($R^2 = 0.59$, $F_{6,4565} = 1103.00$, $p < 0.05$), Maximum Temperature of Warmest Month ($R^2 = 0.71$, $F_{6,4565} = 1838.00$, $p < 0.05$), Minimum Temperature of Coldest Month ($R^2 = 0.65$, $F_{6,4565} = 1386.00$, $p < 0.05$), Mean Temperature of Warmest Quarter ($R^2 = 0.61$, $F_{6,4565} = 1200$, $p < 0.05$), and Mean Temperature of Coldest Quarter ($R^2 = 0.68$, $F_{6,4565} = 1627.00$, $p < 0.05$). Precipitation-related bioclimatic factors had much lower values, with the highest R^2 values for log Annual Precipitation ($R^2 = 0.32$, $F_{6,4565} = 367.50$, $p < 0.05$). For individual PCs, PC6 performed the best overall for temperature-related variables, followed by PC3 and PC5. In the precipitation-related variables, PC4, PC2, and PC5 performed the best overall. Individual PCs showed similar patterns to the combined PC results, with higher R^2 values for temperature-related bioclimatic variables than precipitation bioclimatic variables, but significant differences from the mean ($p < 0.05$) for many variables regardless of the R^2 value.

Beyond the temperature- and precipitation-related bioclimatic variables, I investigated individual PCs and Matthew's vegetation cover, Bailey's ecoregions, and altitude. A summary of the statistics for altitude, ecological domain, ecological province,

and vegetation cover can be found in Appendix Table D3. Altitude only had low R^2 values for PCs within the p-value threshold, with PC2 showing the highest value ($R^2 = 0.01$, $F_{1,4390} = 21.09$, $p < 0.05$). The highest values for ecoregion domain were PC6 ($R^2 = 0.21$, $F_{3,4388} = 400.50$, $p < 0.05$) and PC3 ($R^2 = 0.16$, $F_{3,4388} = 280.50$, $p < 0.05$). Ecoregion province showed the strongest correlations for individual PCs outside of some of the temperature-related bioclimatic variables, particularly for PC6 ($R^2 = 0.57$, $F_{48,4343} = 120.60$, $p < 0.05$), PC5 ($R^2 = 0.37$, $F_{48,4343} = 53.66$, $p < 0.05$), and PC3 ($R^2 = 0.24$, $F_{48,4343} = 30.11$, $p < 0.05$). Vegetation cover was most strongly correlated with PC6 ($R^2 = 0.31$, $F_{21,4370} = 94.79$, $p < 0.05$), and PC3 ($R^2 = 0.17$, $F_{21,4370} = 44.94$, $p < 0.05$). Much like the temperature-related bioclimatic variables, PC6, PC3, and PC5 showed the strongest correlations to any environmental factor. Because of its strong relationship with community mean trunk vertebral shape and its usefulness for both reconstructing past environments and making future predictions, I selected Mean Annual Temperature as a variable for further investigation and to produce ecometric spaces.

5.3.4. Ecometric space

Ecometric space, which summarizes the relationship between a community functional trait and an environmental factor, produces a bivariate histogram of 25 x 25 cells by binning the means and standard deviations of vertebral shape, then calculating the most likely environmental condition (e.g., vegetation type or mean annual temperature value) for a given community mean and standard deviation. Because of the close correlation between community mean trunk vertebral shape and Mean Annual Temperature (MAT), an expectation exists that particular combinations of means and

standard deviations of shape will indicate specific ranges of MAT. As PC3 and PC6 showed the strongest relationships to MAT, I discuss the ecometric spaces of those two PCs below. Ecometric spaces for all six PCs can be found in Figure 5.7.

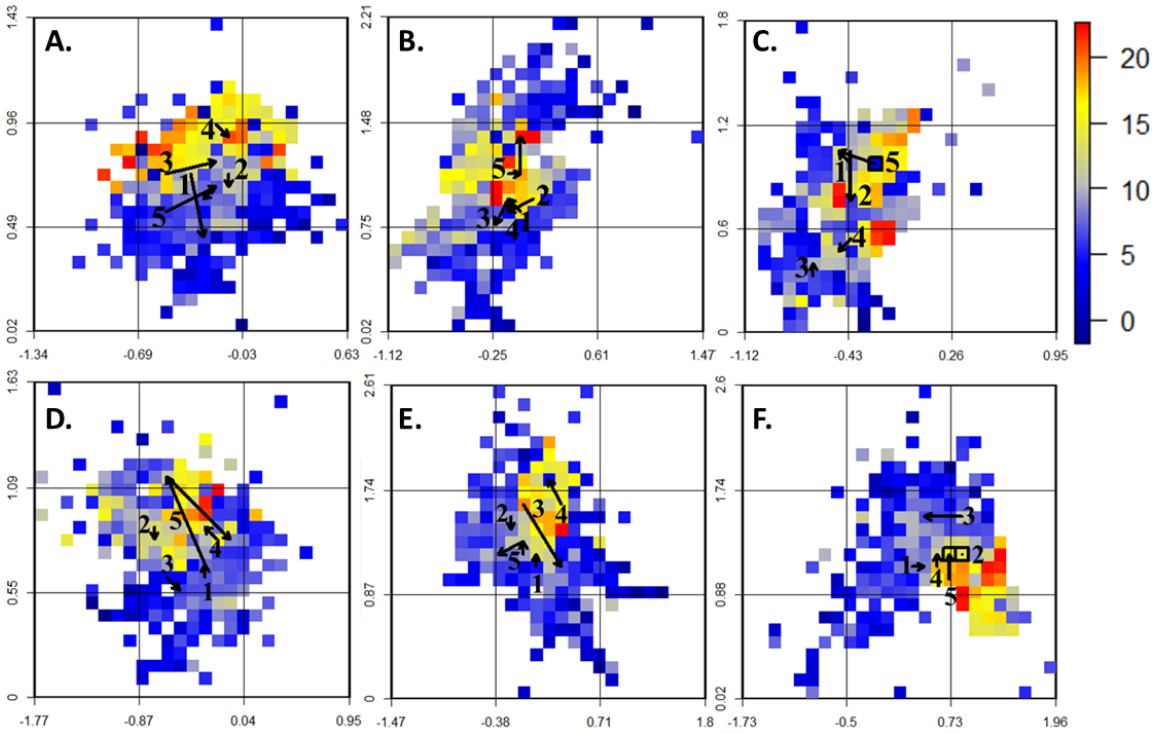

Figure 5.7. Ecometric spaces for PC1 and PC6. Each grid cell is colored by the maximum likelihood MAT prediction based on a given mean and standard deviation of vertebral shape in a snake community. A is PC1, B is PC2, C is PC3, D is PC4, E is PC5, and F is PC6. In order, the numbered case studies are: 1) Jackson-Pulaski Fish and Wildlife Refuge, Indiana; 2) Fort Riley, Kansas; 3) University of Kansas Natural History Reservation, Lawrence, Kansas; 4) Middle Rio Grande riparian forest, New Mexico; and 5) Sheff's Wood, Eastern Texas. The arrows indicate the direction of change through time (1-4) or geographic space (5). The black boxes indicated that the mean and standard deviation values did not change over time or space. The Texas case study moves from the lowland floodplain to the upland deciduous woodland, then to the upland coniferous woodland.

The relatively cool, temperate conditions of the continental United States and Canada are clear based on the ecometric spaces produced, with most grid cells predicting the MAT to be $\leq$15ºC. The ecometric space for PC3 exhibits an overall trend of higher MAT predictions coinciding with moderate to high mean and standard deviation values for community shape; however, lower MAT predictions occur along the full spectrum of standard deviation values for PC3 and at both the highest and lowest mean values. Therefore, communities appear to separate primarily along mean trait values for this aspect of shape change. Higher mean shape values typically associate with higher predicted MAT and increases as standard deviation increases, but may follow a parabolic pattern, where high or low means predict lower temperatures, but moderate to high mean values predict higher temperatures. The appearance of cold temperatures predicted for both high and low standard deviation values is likely a derivative of taxonomic richness, where there are few taxa present at higher latitudes in North America. With fewer taxa, the standard deviation may vary greatly based on the composition of individual communities. In contrast, the shift in mean values in the ecometric space is more likely to represent a larger change in general community composition, as the mean values generally increase with temperature, suggesting that additional taxa are introduced and/or some taxa reach their range limits.

The ecometric space for PC6, which represents a different type of variation in vertebral shape than PC3, shows separation of mean trait values such that lower mean values are associated with lower MAT and higher mean values are associated with higher MAT. The standard deviation in PC6 predicts high standard deviation to correlate

with cooler temperatures overall, but low and moderate standard deviations exist across the spectrum of MAT. As in PC3, taxonomic richness likely has a strong effect on the standard deviation values, with low richness in cooler areas resulting fewer community members to contribute to the range of values. Community mean values again show a more linear relationship to temperature than standard deviation, with low mean values predicting low MAT, and high mean values predicting high MAT.

5.3.5. Projection of maximum likelihood onto geographic space

To get maximum likelihood predictions of MAT across the continental United States and Canada, I projected the ecometric spaces across the 50-km grid of geographic space to make MAT predictions based on the ecometric (Fig. 5.8A-C). I then created anomaly maps by calculating the difference between the ecometrically-predicted MAT values and actual MAT values in order to see how well the ecometric models predicted MAT, and where those models were most and least accurate (Fig. 5.8 D-I). I calculated R^2 values for each model to evaluate the fit of the maximum likelihood models to actual MAT data, and found that PC1 ($R^2 = 0.53$) and PC6 ($R^2 = 0.68$) performed the best individually, followed by PC5 ($R^2 = 0.49$), PC3 ($R^2 = 0.47$), PC2 ($R^2 = 0.46$) and PC4 ($R^2 = 0.35$). Because the results of the linear models suggested that combining the PCs representing different aspects of shape variation in snake trunk vertebrae will produce better results than any individual PC, I also combined PC6 with one other individual PC for each of the other five PCs. In the combined models, PC3 and PC6 was the best fitting model ($R^2 = 0.91$), and PC1 and PC6 ($R^2 = 0.90$) performed nearly as well (Fig. 5.9).

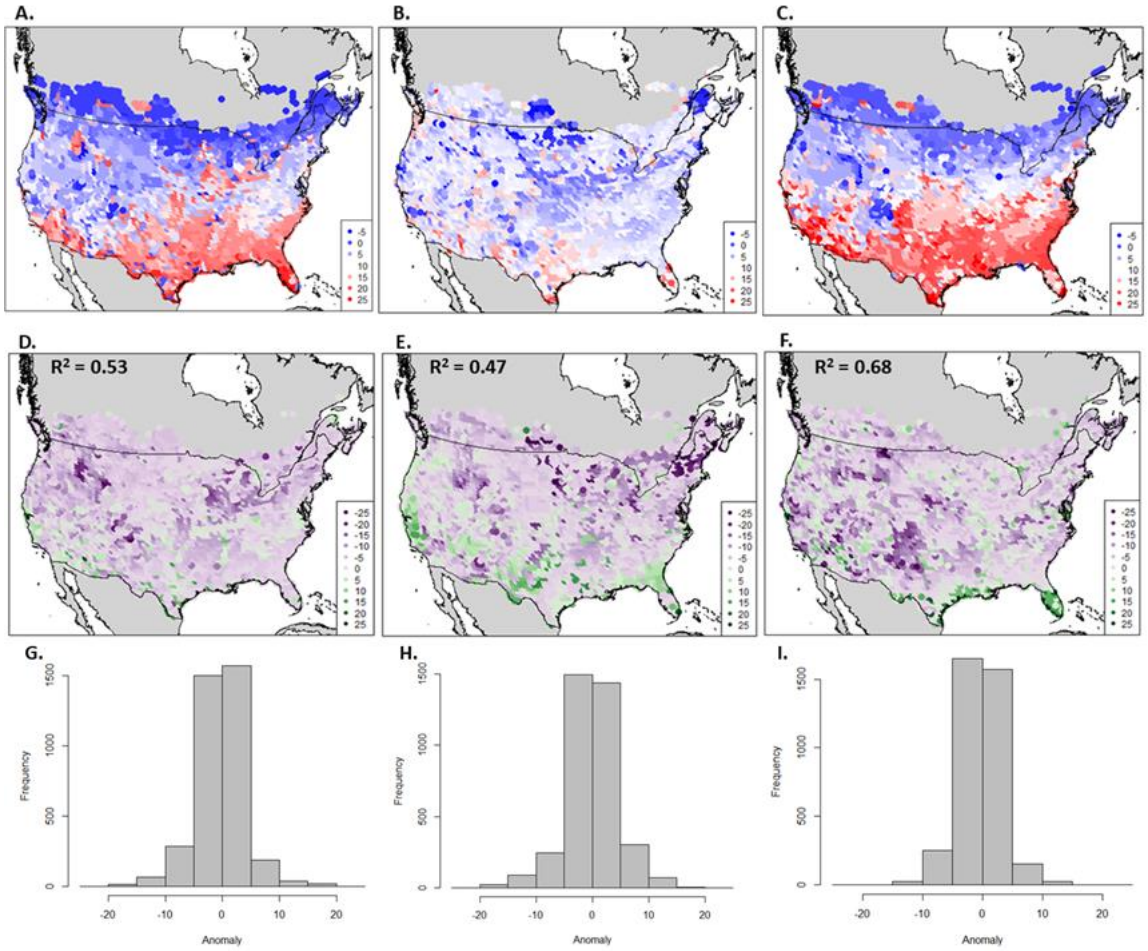

Figure 5.8. Maximum likelihood projections of PC1, PC3, and PC6 over geographic space, anomaly maps with associated R^2 values, and histograms of anomaly frequency at intervals of 5ºC.

The maximum likelihood model of MAT for PC1 projects a latitudinal temperature gradient similar to that of actual MAT overall; however, the gradient is less clear in the ecometric projection. Mean Annual Temperatures are projected to be highest in the southern United States, especially bordering the Gulf of Mexico, in the Southeastern deserts and in part of the Great Basin, while lowest MAT is predicted to be in the Rocky Mountains and from the northern United States into Canada; however, the

ecometric model for PC1 appears to underestimate MAT in some warmer areas and overestimate MAT in some cooler areas. This observation is supported in the anomaly map for PC1, where the largest anomalies occur in the Northern Midwest, Northeast, and Rocky Mountains (15ºC to 20ºC difference) and Southwest and Central Great Plains regions (15ºC to 20ºC difference) of the study area.

The model for PC3 makes a greater number of underpredictions for MAT overall than in PC1, especially along the coast of the Gulf of Mexico, the Southwestern border of the United States, and the coast of Southern California (5ºC to 20ºC difference). The PC3 model also overpredicts MAT in the North-Central and Northeast of the study area, especially near the Atlantic Coast, the Great Lakes, and the Northern Great Plains (5ºC to 20ºC difference).

Compared to PC1 and PC3, PC6 fairs better overall when predicting MAT. While showing a latitudinal gradient overall, the PC6 projection overpredicts how far areas with the hottest and coldest MAT extend spatially. Areas of particular note include the Great Plains and Rocky Mountains, where temperatures are overpredicted (5ºC to 15ºC difference), and the southernmost United States in the Southwest, Texas, and Florida, where temperatures are underpredicted (10ºC to 15ºC difference).

Combining PC3 and PC6 produces the best predictions when projected onto geographic space, with only few areas not accurately predicting near the actual MAT values (Fig. 5.9). The anomaly map best exhibits the minor differences between the combined projection and actual MAT values, with a general trend of temperature underpredictions by <5ºC except in a few locations along the Gulf Coast, Rocky

Mountains, Great Plains, and the far Northeast of the study area (<10ºC). The model combining PC1 and PC6 shows a similar trend overall, but makes larger overpredictions (<15ºC) across the central U.S. and west of the Rocky Mountains.

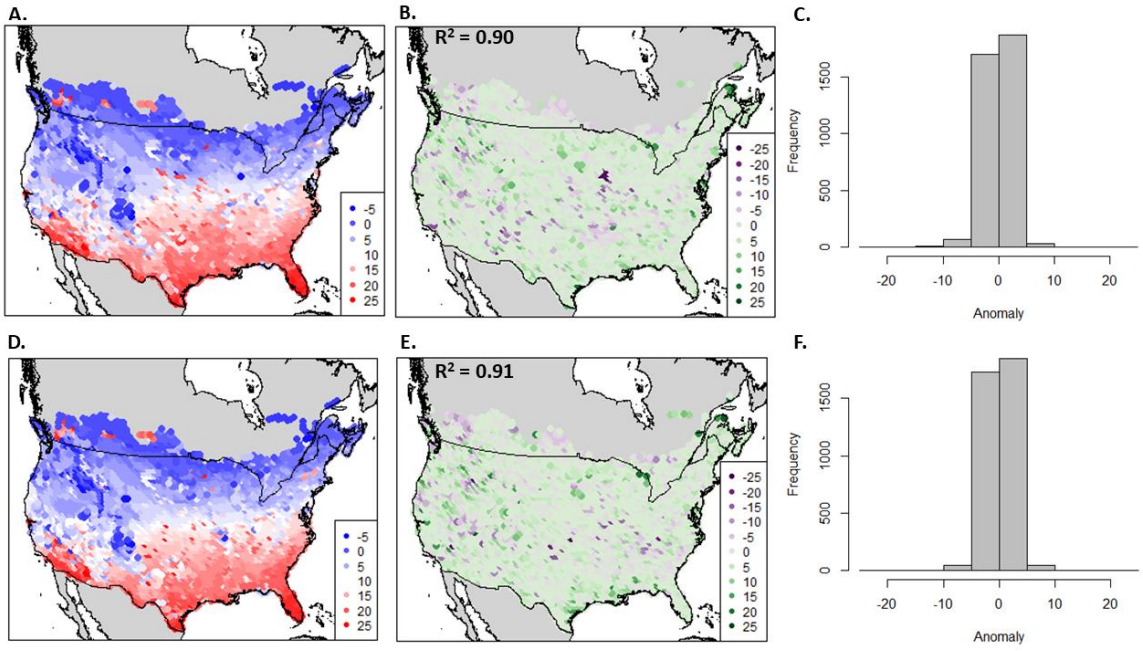

Figure 5.9. Maximum likelihood projection of PC1 + PC6 (A) and PC3 + PC6 (D) over geographic space, anomaly maps with associated R2 values (B and E), and histograms showing the frequency of anomalous values for each 50-km grid point at intervals of 5ºC (C and F).

5.3.6. Case studies

The ecometric spaces constructed from PC1-PC6 produce varying results for each case study (Fig. 5.7). At the Jackson-Pulaski Fish and Wildlife Refuge, most PCs suggest that the standard deviation of shape changed as much as or more than mean shape (except for in PC6). PC1, PC3, and PC6 suggest a decrease in MAT over time, PC2 and PC4 suggest similar MAT, and PC5 suggests an increase in MAT. At the Fort

Riley Military Reservation, a decrease in standard deviation over time resulted in most train bin shifts except for in PC2, where mean values also contributed to the shift, and PC6, which did not shift bins. PC1, PC4, and PC6 suggested little to no change in MAT over time, while PC2, PC3, and PC5 suggested a decrease in MAT over time. At the University of Kansas Natural History Reservation, both shape means and standard deviations were responsible for shifting trait bins in ecometric space except for in PC3, which was standard deviation only, and PC6, which was mean shape only. In this case study, PC1, PC2, PC5, and PC6 suggested a decrease in MAT over time, while PC3 and PC4 suggest an increase in MAT over time. In central New Mexico, both changes in mean and standard deviation values resulted in shifting trait bins, although standard deviation contributed more or was solely responsible for the changes in PC1-PC5, with the mean values resulting in the shift of PC6 ecometric space. PC1 and PC2 indicated an increase MAT over time for this case study, while PC3, PC5, and PC6 indicated a decrease and PC4 indicated little or no change. Finally, in eastern Texas, both mean and standard deviation contributed changes in ecometric space except for in PC6, where only standard deviation shifted the bin. From the lowland floodplain to the deciduous woodland, PC1, PC2, PC4, and PC5 suggested an increase in MAT, PC6 suggested a decrease, and PC3 suggested no change. From the deciduous woodland to the coniferous woodland, PC2 and PC3 suggested and increase in MAT, PC4 and PC5 suggested a decrease in MAT, and PC1 and PC6 suggested no change.

The five sites here hale from different parts of the United States, with Texas and New Mexico in the South, both Kansas locations in the Central Great Plains near the

center of the country, and Indiana furthest north in the Midwest region. In terms of ecological province, eastern Texas is a humid temperate climate of prairies and mixed forest. Central New Mexico is a dry mosaic of montane semidesert, open woodland, coniferous forest, and alpine meadow. The Fort Riley Military Reservation is a dry grassland prairie, while the University of Kansas Natural History Reservation falls on an ecotone of temperate eastern deciduous forest and dry tall-grass prairie. Finally, the Jackson-Pulaski Fish and Wildlife Refuge in Indiana is also located near the temperate eastern deciduous forest and dry prairie ecotone, and has transitioned to a homogenized, closed-canopy eastern broadleaf forest from agricultural land (that in turn was once a mosaic of marsh, wetlands, and dry prairie).

5.4. Discussion

Here, I discuss the value of snake middle trunk vertebrae as an ecometric through quantifying the relationship between community mean vertebral shape and MAT. Furthermore, I discuss the connectivity of vertebral shape, substrate use, and phylogeny. The vertebra of a snake is directly related to the primary locomotion strategy of the snake, and is therefore indirectly affected by the environment in which the animal lives. As large portions of a snake's body is in constant contact with any surface over which it locomotes, the poikilothermic physiology of the snake also comes into play – through interactions with surface and air temperatures – without limbs to rise up on. As shown in this study, there are strong relationships between middle trunk vertebral shape and

phylogeny, temperature-related environmental variables, and ecological province (Tables 2-5).

5.4.1. Aspects of shape variation and substrate use

The axes of middle trunk vertebral shape variation reveal several ecomorphological trends that support the investigation of a shape-based ecometric in this study. Several of the PCs were also significant for phylogeny, with high lambda values in the phylogenetically informed MANOVA. This supports the concept that clade-level trait-based sorting has a strong impact on community-level distributions (see Table 5.2, Appendix Table D1; Polly, 2010; Lawing et al., 2012; Polly et al., 2017). The taxa included in this study are generally sorted by clade first, then by substrate use when both are significant; this is supported further by the end members of each PC discussed in the study, as end members along any given axis share neither substrate use ecology nor subfamily except for in PC4, which is not significant for substrate use ecology. As such, clade membership interacts with both environment and vertebral shape to assemble community mean vertebral shape in snakes.

In addition to the expected association between morphology and phylogeny across taxa (Table 5.2, Appendix Table D1; Lawing et al., 2012), both dominant substrate use and body size appear to contribute to shape variation in snake trunk vertebral shape. Although Procrustes superimposition removed differences in size for analysis, the effects of body mass, body shape, and bone density on vertebral shape are not removed as part of that process. This is best seen when examining PC1 and PC2, where there is a clear division between heavier-bodied or “robust” taxa on the upper left

and more slender taxa to the bottom right (Fig 5.2A). In fact, the changes in shape represented by the first two PC axes encapsulate relative height and relative width as part of those morphological variations (Fig. 5.4A-B). As such, it is likely that the shape variations along those axes are exhibiting the coincidental effects of phylogeny, body size, and dominant substrate use.

Lawing et al., (2012) showed that the mean vertebral length-to-width ratio was significantly correlated with substrate use, regardless of phylogenetic considerations. This is partially captured and supported by the analyses of shape, and relative lengths and widths are an integral part of forming various morphologies. Unlike in Lawing et al., (2012), vertebral shape in the dataset showed significant relationships between vertebral shape represented by each of the first six PCs except for PC4, as well as all six of the PCs together. This is likely attributable in part to the larger sample size (119 species) compared to the previous study (60 species). The first PC in Lawing et al., (2012) and this study also describe a similar axis of shape variation, although this study also shows a comparatively larger change in parapophyseal length and orientation along with the change in neural spine height observed in the dorso-ventral flattening of vertebrae in both studies.

The division of groups into separate ecologies (e.g., terrestrial, fossorial, arboreal, and aquatic, etc.) must be carefully done and made clear in every test. The differences in results between Lawing et al. (2012), which grouped “semi-” ecologies with specialized ecologies, and this study, which did not, suggest that there are strengths and weaknesses to using a greater or lesser number of ecological assignments for snakes.

As such, it is worth using a more diverse set of categories upon first testing hypotheses, then decreasing the group sizes in order to find the best natural fit. A tendency in some cases may be to group semi-aquatic organisms with fully aquatic ones, semi-fossorial organisms with fully fossorial organisms, and semi-arboreal organisms with fully arboreal organisms; however, are those associations the most accurate for the organisms being studied? As seen in the data, the "semi-" category taxa often, but not always, fell somewhere between terrestrial and the more specialized ecology (Fig. 5.2, Fig. 5.3). Many snakes employ multiple substrates and/or locomotive types both during development and as adults, and such groupings may require case-by-case decisions for assigning groups, or even the addition of new groups. I suspect that taxa currently assigned to the "semi-" groups may each have one of two tendencies: 1) to be more similar to whichever major substrate ecology the taxon spends the most time using; in some cases, this may make the terrestrial substrate ecology the best assignment, in others, it may be the non-terrestrial substrate ecology; or 2) to truly fall between two "main" ecologies in shape space, possessing some aspects of shape closer to one ecology and other aspects of shape closer to the other. As such, ecological assignments may explain too much or too little, but are almost certainly subjective to some degree.

Each of the PCs in this study represent a different type of shape variation in the vertebrae; however, most of the shape changes relevant to substrate use and the bioclimatic variables involve changes in the size, shape, and orientation of the articular surfaces on the vertebrae. This is most likely related to the specific needs of taxa for locomotion through specific substrates (e.g., serpentine, rectilinear, etc.), increased

torsion or rigidity for specific movements such as cantilevering or swimming, and predatory habit (e.g., striking, constricting, thrashing, and active hunting). As articular surfaces represent locations of muscle attachment and interactions between different parts of the skeleton, the way these articular surfaces are assembled can result in different strengths and weaknesses in different environments, much like relative tail length in snakes (Lawing et al., 2012) or carnivoran limb proportions (Polly, 2010). As such, each of the PCs show different patterns of mean shape values across geographic space, dependent on which aspect of shape variation is examined. Furthermore, because multiple PCs capture different aspects of shape change through different environments, combining relevant PCs produced improved accuracy in both the linear and maximum likelihood models.

5.4.2. Implications of the geography of morphology

Each PC in this study represents a different aspect of vertebral shape variation; these PCs each produce a unique geographic structure in relation to the environment and climate. In PC1, it appears that the presence of fossorial/semifossorial and arboreal taxa are major drivers of mean shape; in areas with more fossorial taxa, mean shape tends to show more dorso-ventrally flattened morphologies. This also generally coincides with patterns of richness, temperature, and precipitation, as regions with high species richness and low precipitation also exhibit “shorter” mean shape values. In PC2, patterns of mean vertebral shape suggest influences from colder temperatures, richness, and perhaps ecological domain. Areas with lower temperatures such as the Rocky Mountains, parts of the Great Lakes region of the United States, and much of Canada have both lower

richness and lower temperatures overall, and coincide with shorter, more dorsally oriented prezygapophyses, which are most often present in fossorial, semifossorial, and terrestrial snakes compared to other substrate ecologies. PC3, which was only significant for semifossorial snakes, may capture some aspect of vegetation cover or precipitation, as areas with more heterogeneous environments and vegetation types have higher mean values (narrower, vaulted neural arches and narrower neural canals), and arid environments with limited vegetation types have low to moderate mean values (wider, depressed neural arches and wider neural canals). While PC4 was not significant for substrate use, it was significant with low R^2 values with multiple other environmental factors, suggesting weak or indirect relationships with those factors, particularly in precipitation-related variables (Appendix Table D2. Appendix Table D3). The geography of morphology for PC4 suggests a potential relationship with ecosystem subdivisions such as ecological domain or ecological province, particularly along the Pacific coast to the Rocky Mountains and in the Northeast. In terms of morphology, mean values are highest along the Pacific Coast and lowest in the Northeast. In PC5, mean values mostly fall near the middle, with a few exceptions such as part of the Rocky Mountains (high values) and the Great Lakes region (low values). While it is unclear if the former result is attributable to an environmental factor such as temperature or altitude or sampling bias, the latter result is most likely attributable to decreased richness and temperature. Finally, PC6 shows a strong geographic structure that varies similarly to species richness, MAT, and ecological province, with both a latitudinal gradient of

shape and an east-west division into separate mean value patterns. Overall, proportionally wider articulations are found in the south when compared to the north.

As shown in previously established ecometrics (e.g., mean gear ratio in carnivorans and artiodactyls; Polly, 2010; Short and Lawing, 2021), communities of low species richness result in mean vertebral shapes that occur across the range of values, while communities with high species richness tend to have medial mean values. In communities of low richness, mean values differ depending on where they occur: For example, the Rocky Mountains produce similar mean values to the northern United States and Canada for PC1, PC3, PC5, and PC6, while for the other PCs, they produce mean values that differ greatly. These differences are certainly driven by differences in species composition, with a greater number of colubrine, dipsadinine, and crotaline taxa as well as fossorial substrate use ecologies further south in North America. In the North, taxonomic composition is likely altered by lower MAT and winter temperatures, resulting in communities with cold-adapted snakes only; at its extreme, snake communities are composed only of *Thamnophis sirtalis*.

Conversely, areas of high richness tend to show more moderate mean vertebral shape values overall; albeit with differences between the eastern and western parts of the study area, as most clearly seen in the geography of morphology for PC6. The moderate mean values are consistent with what is found for more rich communities in other ecometrics (Polly, 2010; Lawing et al., 2012; Short and Lawing, 2021). The division between the eastern and western United States suggests a factor other than temperature playing a role in the distribution of snake species with different morphologies; this

division is similar to that of ecosystem domains, with the eastern division and Pacific Coast comprised primarily of humid temperate ecosystems (and humid tropic ecosystems in southern Florida), while the western division excepting the Pacific Coast is composed of various dry ecosystems. These divisions are also likely indicative of vegetation cover and precipitation differences having some effect on snake communities in the study area, both of which are significant and most closely correlated with PC6.

5.4.3. Ecometric Space and Maximum Likelihood

Because there is a close correlation between several of the PCs and MAT (Appendix Table D2, Fig. 5.8, Fig. 5.9), a specific range of MAT values is expected for a given mean and standard deviation of trunk vertebral shape in snakes and vice versa. Ecometric spaces, then, are constructed through the most frequent MAT associated with means and standard deviations of snake vertebral shapes. Because each PC in the study constructed a unique ecometric space, I can confirm that each aspect of shape variation is also unique across the study area, with their own maximum likelihood predictions and trait bins based on the trait-environment relationship. While I selected PC1, PC3, PC6, and MAT based on their respective geographies of morphology and on the high correlations between the PCs and the bioclimatic factor, this does not preclude any other community trait-environment relationships that may affect the predictions, nor does it mean that other PCs may not be useful as ecometrics. Future work to address these topics will be necessary steps forward in understanding these community trait-environment relationships.

PC1 and PC6 both showed anomalies primarily centered around zero – evidence that the predictions are accurate over the majority of the geographic surface. The maximum likelihood ecometric models overpredicted temperature in some cold areas and underpredicted temperature in some warmer areas. These trends are likely the combined result of maximum likelihood as a method and of the effects of other significant environmental factors. Maximum likelihood uses the most frequent MAT of the communities in a given trait bin to predict MAT for *all* communities in that trait bin. While this pushes ecometric model predictions towards the mean, Short et al. (2021) showed that maximum likelihood produced the most accurate estimates consistently.

Unlike mammals, snakes are poikilothermic and are therefore more reliant and vulnerable to changes in temperature (Lawing and Polly, 2011). Geographic ranges for snake taxa are therefore reliant on both mean temperature and minimum and maximum temperatures for survival. This will necessarily drive overpredictions of MAT in cold areas and underpredictions of MAT in hot areas towards the mean as minimum temperatures (cold areas) and maximum temperatures (hot areas) exceed the thermal tolerances of the variegated snake species. This is supported by the linear correlations, which show high correlations similar in value to MAT for maximum temperature of warmest month, minimum temperature of coldest month, mean temperature of warmest quarter, and mean temperature of coldest quarter, as well as other temperature-related variables such as isothermality, and environmental variables such as ecological province. These results are further supported by past work that primarily examined the relationships between species richness and environmental variables in squamates

(Lawing et al., 2012; Burbrink and Myer, 2015; Whiting and Fox, 2020). Additionally, over- and underpredictions may be areas of concern in regard to environmental change, with snake faunas, and therefore community trait values, lagging behind as a relict of past environmental conditions. Evidence shows that at least some snakes do not adapt as fast as climate can change, and that those environmental changes may initially drive geographic change over evolutionary change (Lawing and Polly, 2011). In the future, snake species may have to move greater distances more quickly than in the past in order to escape extinction (Lawing and Polly, 2011).

5.4.4. Case studies and conservation

Although the results vary for the five case studies across the six PCs (Fig. 5.7), the R^2 values indicating how well each model fits reality (from highest to lowest: PC6, PC1, PC5, PC3, PC2, and PC4) allowed for additional interpretation of these results. The trait bin predictions for the recent values at each site mostly coincided geographically with the anomaly between the maximum likelihood models and actual MAT; possible reasons for the under- and overpredictions are discussed in the previous section. The better-fitting models (higher R^2) may also indicate which ecometric spaces are the better predictors of change over time and across space for case studies. Following this logic, PC6 would be the best supported model for MAT overall, while PC4 would be the least supported model; thus, PC6 is more likely to make the correct prediction for changes in MAT for each case study (followed by PC1, etc.).

The most likely change (as predicted on local scales) for the Jackson-Pulaski Fish and Wildlife Refuge is an overall decrease in MAT. The drastic transformation of

this natural reserve from marsh/wetland/dry prairie to agricultural land prior to 1800, then from agricultural land to a homogenized closed-canopy oak woodland after the 1930s, likely had an effect on both the MAT and the snake assemblage's composition. Increased woodland cover would like decrease temperature locally, resulting in a different snake fauna than would be found in more open agricultural land. At the Fort Riley Military Reservation, vegetation cover was consistently a dry prairie grassland for both historic and recent snake communities, and this is reflected in the maximum likelihood models, which show either no change in MAT over time, or a small decrease in MAT over time. For the Middle Rio Grande riparian forest in New Mexico, most models show a decrease in MAT. Not only did the removal of non-native vegetation and accumulated fuel reduce fire risk (Bateman et al., 2009), but it also likely improved flow rate and the health of the riparian vegetation, both of which are known to cause local cooling (Abdi et al., 2020). Finally, the case study of Sheff's Wood in Eastern Texas recorded differences in geographic space rather than through time in the form of three adjacent habitats. The ecometric space maximum likelihood models mostly indicated an increase in MAT from the lowland floodplain to the upper deciduous woodland, and most commonly indicated either similar MAT between the two woodland environments or a slight increase in MAT when moving into the upper coniferous woodland. This prediction is corroborated by the reported temperature differences in Ford et al., (1991).

It is imperative to note here that weighing mean values to account for relative abundance may change the predictions for these models and additionally allow for case

studies where only abundance, rather than taxonomic composition, change. Abundance and ecometrics are discussed further in a later section of this study.

5.4.5. Challenges and limitations

There are several potential methodological stumbling points when utilizing snake ecometrics. First, while ecometric methods have been considered a taxon-free method, this is only within the group being studied at the community level (Polly and Head, 2015). As such, long evolutionary histories between two branches of a group and their most recent common ancestor may direct the groups towards vastly different trajectories. Thus, while the overall arrangement of a bone or group of bones stays the same, long periods since divergence may indicate different starting and ending points for the evolution of the same trait. For example, measuring limb proportions in carnivores and artiodactyls together would produce two different distributions of data based on the same metric; while overall trends towards convergence for the lengthening of limbs and increased speed in open habitats may be the same, the two groups of mammals took different evolutionary paths to get there.

Booids and Pan-Caenophidia (which includes Colubroids) likely diverged 72.1-66 Ma, in the Cretaceous (Head et al., 2016), and thus have different starting and ending points for the evolution and diversification of their morphologies today. Thus, while similar patterns and convergence of certain traits in both groups do occur, their vastly different evolutionary histories since their divergence may skew or hide trends when analyzed together. In these cases, it may be better to examine the groups both together and separate when using ecometrics. Similarly, the inclusion of extreme morphologies

such as the leptotyphlopids in this study had a clear influence on the overall distributions along certain shape axes. While this is not in itself a reason for concern, it is important to recognize the potential for data to be skewed by such groups and check the data both with and without them to ascertain whether the observed variation is true across the whole dataset. These precautions are especially important when dealing with limited sample sizes.

Second, ecometric methods are limited by the datasets they use. The collection of trait data is limited in multiple ways, including the availability of museum specimens, completeness of the fossil record on small to large geographic and temporal scales, the condition of fossil or modern bones, and previously published data. While Polly and Sarwar (2014) have indicated that only 25% of species in a community are required to predict ecometric relationships accurately in mammals, and Short and Lawing (2021) have shown that community trait values are not sensitive to decreased richness in mammals, the same may not be true for other ecometrics. Additionally, because modern range maps tend to overestimate species distributions, this bias extends to the trait values of communities (Chen, 2013). Finally, this study specifically notes a lack of even decadal-scale survey data for snake community case studies. The solution to these issues is likely to come through an increased availability of geographic range and trait data in databases and publications (Short and Lawing, 2021).

Another caveat of this study is that I use one average vertebral shape per species to test the potential of snake trunk vertebral shape as an ecometric and identify potential environmental relationships; however, instraspecific variation is not accounted for

equally across all species, and the analyses do not represent true snake faunas at the community level. While variation within species is presumed to be less than between species for vertebral shape (Holman, 2000; Parmley and Walker, 2003; Lawing and Polly, 2011; Lawing et al., 2012), the dataset is vulnerable to potential misidentifications of vertebral column placement or unusual specimens, and does not necessarily capture the morphological variation for all 119 species, especially for the taxa that only had one specimen or vertebra in the dataset. While this is unlikely to affect the ecometric patterns identified in this study, there is a chance that individual community means and standard deviations could be altered. Furthermore, neither relative abundance nor fossil assemblage sample size are addressed with the current dataset; both are likely to have some effect on ecometric means and could possibly skew environmental inferences for individual communities (Faith et al., 2019). To address such sampling issues, Faith et al. (2019) recommended taking approaches to weight ecometric means through approaches such as taxonomic abundance. Unfortunately, abundance data may be missing from present, historical, and fossil datasets alike. As with other dataset limitations, increased availability and access to data will help resolve this issue.

An additional factor to consider is that the current framework only covers taxa from the United States and Canada. As such, the ecometric framework and specific shape changes on continental and smaller scales may not be applicable at larger scales. Some morphological features described for snake taxonomic groups may vary on larger geographic scales (Holman, 2000; Ikeda, 2007). Furthermore, little is known about the potential effects of sexual dimorphism on vertebral shape in snakes. Understanding any

possible morphological differences related to sexual dimorphism that could alter the values recorded for the taxa in the dataset, therefore potentially changing community mean values, is important for specimen selection. On a similar, but larger scale, exposure to different combinations of environmental factors across the globe may result in multiple different morphological on continental or smaller scales, thus shifting the aspects of shape change explaining the most variation, and their impact on the models. While the models have not been tested to predict globally based on the North American-only dataset, the addition of data from other regions of the world is likely needed to produce multicontinental or global models.

Ecometrics can be used to compare no-analog communities (species are all extant today, but not together in the same communities as in the past; Williams and Jackson, 2007), novel ecosystems (ecosystems heavily influenced by humans but not under human management; Marris, 2009), and fossil communities and environments to modern communities and environments through the ecometric spaces trait values (Vermillion et al, 2017; Short and Lawing, 2021). Short and Lawing (2021) caution, however, that using maximum likelihood for such communities may be limited if the trait compositions of such communities do not exist within the context of a constructed ecometric space's trait bins.

5.4.6. Future work

While I have considered this new ecometric primarily in the context of a relationship between MAT and community mean vertebral shape, there is both potential and a need to examine potential correlations between other environmental factors and

community mean vertebral shape. Several of the areas that overpredicted or underpredicted MAT in the models may be attributable to the influence of other factors, including environmental change, maximum temperatures, minimum temperatures, ecological province, annual precipitation, and vegetation cover, on the overall composition of snake faunas. This is supported both by analyses in this study and by previous work done be Burbrink and Myers (2015), who found positive relationships between precipitation, temperature, and species richness with trait means (size, diet, parity, and habitat preference), and negative relationships for precipitation and temperature with trait variability. In this study, that hypothesis is supported by the general trends of the models underpredicting MAT in warmer areas and overpredicting MAT in colder areas, and through the linear correlations, which suggest strong relationships with several other temperature-related environmental factors, ecological province, and to a lesser extent, annual precipitation and vegetation cover (Appendix Table D2, D3).

Non-native animals provide a puzzling issue for community trait composition through several avenues. First, snakes are often at risk from introduced predators such as feral cats, which are capable to killing even some of the larger and more venomous snake species (Whitaker and Shine, 2000). Second, the accidental or intentional introduction of non-native snake species, such as Burmese pythons in southern Florida (Harvey et al., 2008; Willson, 2017) or brown treesnakes in Guam (Rodda and Savidge, 2007), may outcompete or prey upon native fauna and/or fill new ecological roles. The

effects of these non-native species on ecometric relationships in communities is not known, and should be a target for future investigation.

As discussed previously, in order to assess this new ecometric more completely, I must examine it on various geographic and temporal scales. As such, in addition to expanding the ecometric framework of community mean vertebral shape to include data from regions outside of the United States and Canada, the addition of more case studies from current, historical, and fossil communities across the current geographic extent is necessary for testing 1) predictions from different areas within the study area; 2) the ability of this ecometric to be used with the fossil record of snakes; and 3) the temporal and taxonomic limits of this ecometric through time. Finally, weighting the ecometric means of the case studies based on the relative abundance of those communities should provide more accurate values, and therefore, more accurate maximum likelihood models.

5.5. Conclusions

I found that multiple aspects of the mean shape of snake trunk vertebrae, a proxy for locomotor specialization, body mass, and perhaps predatory habit, is geographically sorted at a regional scale in snake communities. The sorting of these shapes at the community level is most strongly correlated with temperature-related bioclimatic variables such as MAT and ecological province. Increasing MAT is associated with greater changes in community mean shape values, especially in warmer, more taxonomically rich southern areas, but both mean and standard deviation increase for cooler, less taxonomically rich northern areas in the selected ecometric PCs. While

maximum likelihood models perform well overall with the ecometrics, ecotones, high elevation montane regions, and areas with extreme seasonal temperatures likely have an effect on taxonomic composition that is not predicted through MAT alone, as the geographic distributions of poikilotherms such as snakes are dependent on surviving extreme temperatures as well as mean temperatures in any given area. An additional benefit of this ecometric is its applicability to the fossil record. The use of middle trunk vertebrae, which are the most common snake fossils, is more commonly applicable to fossil assemblages than relative tail length, which is difficult to obtain for fossils.

Ecometrics have vast potential as a taxon-free method of studying and predicting community-level functional trait-environmental relationships through space and time. As such, these methods have much to offer towards understanding faunal dynamics in the fossil record, as well as during historical, present, and future environmental change. As such, ecometrics can help create better-informed conservation strategies based on both long- and short-term processes. The strong association between community mean vertebral shape and environmental factors (such as MAT and ecological province) provide a new ecometric method to integrate paleontological analyses of faunal dynamics in changing environments with geographically large-scale analyses of those relationships through the present and into the future.

5.6. References

Abdi, R., T. Endreny, and D. Nowak. 2020. A model to integrate urban river thermal cooling in river restoration. Journal of environmental management 258:110023.

Badgley, C., T. M. Smiley, R. Terry, E. B. Davis, L. R. DeSantis, D. L. Fox, S. S. B. Hopkins, T. Jezkova, M. D. Matocq, N. Matzke, and J. L. McGuire. 2017. Biodiversity and topographic complexity: modern and geohistorical perspectives. Trends in Ecology & Evolution 32:211-226.

Bailey, R. G. 1998. Ecoregions map of North America. US Forest Serv Misc Publ. 1548:1–10.

Bailey, R. G. 2005. Identifying ecoregion boundaries. Environ Manage 34:S14–S16.

Barnosky, A. D., N. Matzke, S. Tomiya, G. O. Wogan, B. Swartz, T. B. Quental, C. Marshall, J. L. McGuire, E. L. Lindsey, and K. C. Maguire. 2011. Has the Earth's sixth mass extinction already arrived? Nature 471:51–57.

Barnosky, A. D., E. A. Hadly, P. Gonzalez, J. J. Head, P. D. Polly, A. M. Lawing, … Z. Zhang. 2017. Merging paleobiology with conservation biology to guide the future of terrestrial ecosystems. Science 355(6325) eaah4787. https://doi.org/10.1126/science.aah4787

Bateman, H. L., A. Chung-MacCoubrey, H. L. Snell, and D. M. Finch. 2009. Abundance and species richness of snakes along the Middle Rio Grande riparian forest in New Mexico. Herpetological Conservation and Biology 4:1-8.

Brodman R., S. Cortwright, and A. Resetar. 2002. Historical changes of reptiles and amphibians of northwest Indiana fish and wildlife properties. Am Midl Nat 147:135–144.

Brook, B. W., N. S. Sodhi, and P. K. Ng. 2003. Catastrophic extinctions follow deforestation in Singapore. Nature 424:420–423.

Brooks, S. E., E. H. Allison, J. A. Gill, and J. D. Reynolds. 2010. Snake prices and crocodile appetites: aquatic wildlife supply and demand on Tonle Sap Lake, Cambodia. Biological Conservations 143:2127-2135.

Burbrink, F. T. and E. A. Myers. 2015. Both traits and phylogenetic history influence community structure in snakes over steep environmental gradients. Ecography 38:1036-1048.

Busby, W. H. and J. R. Parmelee. 1996. Historical changes in a herpetofaunal assemblage in the Flint Hills of Kansas. Am Midl Nat 135:81–91.

Chen, Y. 2013. Species-area relationship is overestimated using distributional range maps. Theoretical Biology Forum, 106:17–21.

Davis, E. B., J. L. McGuire, and J. D. Orcutt. 2014. Ecological niche models of mammalian glacial refugia show consistent bias. Ecography 37:1133-1138.

Enquist, B. J., J. Norberg, S. P. Bonser, C. Violle, C. T. Webb, A. Henderson, and V. M. Savage. 2015. Scaling from traits to ecosystems: Developing a general trait driver theory via integrating trait-based and metabolic scaling theories. Advances in Ecological Research 52:249–318.

Eronen, J. T., P. D. Polly, M. Fred, J. Damuth, D. C. Frank, V. Mosbrugger, C. Scheidegger, N. C. Stenseth, and M. Fortelius. 2010. Ecometrics: The traits that bind the past and present together. Integrative Zoology 5: 88-101.

Evans, A. R. 2013. Shape descriptors as ecometrics in dental ecology. Hystrix 24:133–140.

Faith, J. T., A. Du, and J. Rowan. 2019. Addressing the effects of sampling on ecometric-based paleoenvironmental reconstructions. Palaeogeography, Palaeoclimatology, Palaeoecology 528:175-185.

Figueroa, A., A. D. McKelvy, L. L. Grismer, C. D. Bell, and S. P. Lailvaux. 2016. A species-level phylogeny of extant snakes with description of a new colubrid subfamily and genus. PloS one 11(9), p.e0161070.

Fitch, H. S. 2006. Collapse of a fauna: reptiles and turtles of the University of Kansas natural history reservation. J Kans Herpetol 17:10–13.

Ford, N. B., V. A. Cobb, and J. Stout. 1991. Species diversity and seasonal abundance of snakes in a mixed pine-hardwood forest of eastern Texas. The Southwestern Naturalist pp.171-177.

Fortelius, M., J. Eronen, J. Jernvall, L. P. Liu, D. Pushkina, J. Rinne, A. Tesakov, I. Vislobokova, Z. Q. Zhang, L. P. Zhou. 2002. Fossil mammals resolve regional patterns of Eurasian climate change over 20 million years. Evol Ecol Res 4:1005–1016.

Fortelius, M., I. Žliobaitė, F. Kaya, F. Bibi, R. Bobe, L. Leakey, D. Patterson, J. Rannikko, and L. Werdelin. 2016. An ecometric analysis of the fossil mammal

record of the Turkana Basin. Philosophical Transactions of the Royal Society B: Biological Sciences 371(1698), 20150232. https://doi.org/10.1098/rstb.2015.0232.

Gibbons, D. E., et al. 2000. The global decline of reptiles, déjà vu amphibians. Bioscience 50: 653-666.

Gower, J. C. 1975. Generalized Procrustes analysis. Psychometrika 40:33–51.

Harvey, R. G., M. L. Brien, M. S. Cherkiss, M. Dorcas, M. Rochford, R. W. Snow, and F. J. Mazzotti. 2008. Burmese Pythons in South Florida: scientific support for invasive species management. EDIS 2008(4).

Head, J. J. 2010. Climatic inferences from extant and fossil reptiles: toward a metabolic paleothermometer. AGU fall meeting abstracts, vol #B51F-0412. Smithsonian/NASA Astrophysics Data System

Head, J. J., J. I. Bloch, A. K. Hastings, J. R. Bourque, E. A. Cadena, F. A. Herrera, P. D. Polly, C. A. Jaramillo. 2009. Giant boid snake from the Palaeocene neotropics reveals hotter past equatorial temperatures. Nature 457: 715-718.

Head, J. J., G. F. Gunnell, P. A. Holroyd, J. H. Hutchison, R. L. Ciochon. 2013. Giant lizards occupied herbivorous mammalian ecospace during the Paleogene greenhouse in Southeast Asia. Proceedings of the Royal Society B: Biological Sciences 280 (1763): 20130665.

Head, J. J., A. M. Lawing, and P. D. Polly. 2014. Herpetometrics: testing size-based metabolic thermometry of recent and fossil colubroid snakes across North America. SVP annual meeting Abstracts: 146.

Head, J. J., K. Mahlow, and J. Mueller. 2016. Fossil calibration dates for molecular phylogenetic analysis of snakes 2: Caenophidia, Colubroidea, Elapoidea, Colubridae. Palaeontologia Electronica 19(2FC):1-21.

Hijmans, R. J., S. E. Cameron, J. L. Parra, P. G. Jones, and A. Jarvis. 2005. Very high resolution interpolated climate surfaces for global land areas. International Journal of Climatology 25:1965-1978.

Holman, J. A. 2000. Fossil snakes of North America: Origin, evolution, distribution, paleoecology. Bloomington: Indiana University Press.

Ikeda, T. 2007. A comparative morphological study of the vertebrae of snakes occurring in Japan and adjacent regions. Current Herpetology *26*:13-34.

Johnson, R. G. 1955. The adaptive and phylogenetic significance of vertebral form in snakes. Evolution 9:367–388.

Lawing, A. M. and P. D. Polly. 2010. Geometric morphometrics: recent applications to the study of evolution and development. Journal of Zoology 280:1-7.

Lawing, A. M. and P. D. Polly. 2011. Pleistocene climate, phylogeny, and climate envelope models: an integrative approach to better understand species' response to climate change. PLoS One 16:e28554.

Lawing, A. M., J. J. Head, P. D. Polly. 2012. The ecology of morphology: the ecometrics of locomotion and macroenvironment in North American snakes. Pp. 117-146 in J. Louys (ed.), Palaeontology in Ecology and Conservation. Springer-Verlag, Berlin and Heidelberg.

Lawing, A. M., J. T. Eronen, J. L. Blois, C. H. Graham, and P. D. Polly. 2017. Community functional trait composition at the continental scale: The effects of non-ecological processes. Ecography 40:651–663.

Lillywhite, H. B., J. R. LaFrentz, Y. C. Lin, and M. C. Tu. 2000. The cantilever abilities of snakes. Journal of Herpetology pp.523-528.

Lillywhite, H. B. 2014. How snakes work: structure, function and behavior of the world's snakes. Oxford University Press.

Lima-Ribeiro, M. S., A. K. M. Moreno, L. C. Terribile, C. T. Caten, R. Loyola, T. F. Rangel, and J. A. F. Diniz-Filho. 2017. Fossil record improves biodiversity risk assessment under future climate change scenarios. Diversity and Distributions 23:922-933.

Marris, E. 2009. Ecology: ragamuffin earth. Nature News 460:450-453.

Matthews, E. 1983. Global vegetation and land use: new high-resolution data bases for climate studies. J Clim Appl Meteorol 22:474–487.

Matthews, E. 1984. Prescription of land-surface boundary conditions in GISS GCM II: a simple method based on high-resolution vegetation datasets NASA TM-86096. National Aeronautics and Space Administration, Washington, DC.

McGill, B. J., B. J. Enquist, E. Weiher, and M. Westoby. 2006. Rebuilding community ecology from functional traits. Trends in Ecology and Evolution 21:178–185.

McGuire, J. L. and E. B. Davis. 2013. Using the palaeontological record of Microtus to test species distribution models and reveal responses to climate change. Journal of Biogeography, 40:1490-1500.

Meylan, P. A. 1982. The squamate reptiles of the Inglis IA Fauna (Irvingtonian: Citrus County, Florida). Bull. Florida State Mus. Biol. Ser. 27:1-85.

Moon, B. R. 1999. Testing an inference of function from structure: snake vertebrae do the twist. Journal of Morphology 241:217-225.

Mullin, S. J. and R. A. Siegel. 2009. Snakes: ecology and conservation. Cornell University Press Ithaca.

Myers, N., R. A. Mittermeier, C. G. Mittermeier, G. A. Da Fonseca, and J. Kent. 2000. Biodiversity hotspots for conservation priorities. Nature 403:853.

Parmley, D. and D. Walker, 2003. Snakes of the Pliocene Taunton local fauna of Adams County, Washington with the description of a new colubrid. Journal of Herpetology, 37:235-244.

Peppe, D. J., D. L. Royer, B. Cariglino, S. Y. Oliver, S. Newman, E. Leight, G. Enikolopov, M. Fernandez-Burgos, F. Herrera, J. M. Adams, and E. Correa. 2011. Sensitivity of leaf size and shape to climate: global patterns and paleoclimatic applications. New phytologist 190:724-739.

Pimm, S. L., and P. Raven. 2000. Extinction by numbers. Nature 403:843–845.

Polly, P. D. 2010. Tiptoeing through the trophics: geographic variation in carnivoran locomotor ecomorphology in relation to environment. – In: Goswami, A. and A. Friscia (eds), Carnivoran evolution: new views on phylogeny, form, and function. Cambridge University Press, pp. 374-410.

Polly, P. D., J. T. Eronen, M. Fred, G. P. Dietl, V. Mosbrugger, C. Scheidegger, D. C. Frank, J. Damuth, N. C. Stenseth, and M. Fortelius. 2011. History Matters:

ecometrics and integrative climate change biology. – Proc. R. Soc. B 278: 1121-1130.

Polly P. D. and S. Sarwar. 2014. Extinction, extirpation, and exotics: effects of the correlation between traits and environment at the continental level. – Ann. Zool. Fenn. 51: 209-226.

Polly, P. D., and J. J. Head. 2015. Measuring Earth-life transitions: Ecometric analysis of functional traits from late Cenozoic vertebrates. In P. D. Polly, J. J. Head, & D. L. Fox (Eds.), Earth-life transitions: Paleobiology in the context of earth system evolution The Paleontological Society 21:21–46.

Polly, P. D., J. Fuentes-Gonzalez, A. M. Lawing, A. K. Bormet, and R. G. Dundas. 2017. Clade sorting has a greater effect than local adaptation on ecometric patterns in Carnivora. Evolutionary Ecology Research 18:61–95.

Polly, P. D. 2020. Functional tradeoffs carry phenotypes across the valley of the shadow of death. Integrative and Comparative Biology 60:1268-1282.

Reading, C. J., L. M. Luiselli, G. C. Akani, X. Bonet, G. Amori, J. M. Ballouard, E. Filippi, G. Naulleau, D. Pearson, and L. Rugiero. 2010. Are snake populations in widespread decline? Biol Lett 6:777-780.

Rivera, J. A., A. M. Lawing, and E. P. Martins. 2020. Reconstructing historical shifts in suitable habitat of Sceloporus lineages using phylogenetic niche modelling. Journal of Biogeography 47:2117-2128.

Rodda, G. H. and J. A. Savidge. 2007. Biology and impacts of Pacific island invasive species. 2. *Boiga irregularis*, the brown tree snake (Reptilia: colubridae) 1. Pacific Science 61:307-324.

Rohlf F. J. and D. Slice. 1990. Extensions of the Procrustes method for the optimal superimposition of landmarks. Syst Zool 39:40–59.

Schap, J. A., J. X. Samuels, and T. A. Joyner. 2021. Ecometric estimation of present and past climate of North America using crown heights of rodents and lagomorphs. Palaeogeography, Palaeoclimatology, Palaeoecology 562, p.110144.

Short, R. A. and A. M. Lawing. 2021. Geography of artiodactyl locomotor morphology as an environmental predictor. Diversity and Distributions 27:1818-1831.

Short, R. A., K. Pinson, and A. M. Lawing. 2021. Comparison of environmental inference approaches for ecometric analyses: Using hypsodonty to estimate precipitation. Ecology and evolution 11:587-598

Sneath, P. H. 1967. Trend-surface analysis of transformation grids. J Zool 151:65–122

Thomas, J. A., M. Telfer, D. B. Roy, C. D. Preston, J. Greenwood, J. Asher, R. Fox, R. Clarke, and J. Lawton. 2004. Comparative losses of British butterflies, birds, and plants and the global extinction crisis. Science 303:1879–1881.

Vermillion, W. A., P. D. Polly, J. J. Head, J. T. Eronen, and A. M. Lawing. 2018. Ecometrics: A trait-based approach to paleoclimate and paleoenvironmental reconstruction. *In* D.A. Croft, D. Su, & S.W. Simpson (Eds.), Methods in Paleoecology: Reconstructing Cenozoic terrestrial environments and ecological communities (pp. 373–394). Springer.

Violle, C., M. L. Navas, D. Vile, E. Kazakou, C. Fortunel, I. Hummel, and E. Garnier. 2007. Let the concept of traits be functional! Oikos 116:882–892.

Whitaker, P. B. and R. Shine. 2000. Sources of mortality of large elapid snakes in an agricultural landscape. Journal of Herpetology 34:121-128.

Whiting, E. T. and D. L. Fox. 2021. Latitudinal and environmental patterns of species richness in lizards and snakes across continental North America. Journal of Biogeography 48:291-304.

Williams, J. W. and S. T. Jackson. 2007. Novel climates, no-analog communities, and ecological surprises. Frontiers in Ecology and the Environment 5:475–482.

Willmott, K. M. and D. R. Legates. 1998. Global air temperature and precipitation: regridded monthly and annual climatologies (version 2.01). Center for Climatic Research, University of Delaware, Newark.

Willson, J. D. 2017. Indirect effects of invasive Burmese pythons on ecosystems in southern Florida. Journal of Applied Ecology, 54:1251-1258.

6. CONCLUSIONS

"Just as a snake sheds its skin, we must shed our past over and over again."

– Gautama Buddha

6.1. Implications

This dissertation contributes to scientific efforts by: 1) Contributing qualitative apomorphic identifications to a previous temporal gap in the North American snake fossil record, allowing for deep time comparisons of species richness; 2) investigating the viability of geometric morphometrics as an consistently reproducible method to assist in assigning extant or fossil vertebrae to taxa at several taxonomic scales; 3) examining the roles of geography, climate, sex, and diet in intraspecific variation for a geographically fragmented but widespread snake species; and 4) building the framework for a new shape-based ecometric analysis by establishing a trait-environment relationship in snakes. Examining both the causes and the results of morphological variation at various scales is important for understanding how species respond to changes in their environments through time. This comprehensive assessment is possible through interdisciplinary building blocks from comparative anatomy, paleontology, ecology, biogeography, quantitative methods, climate science, and geology. While all chapters of this dissertation investigate morphological variation, the methodology, scale, and purpose of these chapters differ. For example, Chapters Two and Three used different methods to identify snake vertebrae; Chapters Two and Five used models to

predict climatic conditions using taxon and shape, respectively; Chapters Three and Four used geometric morphometrics to assess morphological variation at different taxonomic scales; and Chapters Three, Four, and Five used geometric morphometrics to examine ecomorphological patterns at different geographic scales.

In Chapter Two, I used qualitative observations and anatomical comparisons to describe and identify snake fossils from 12.5-12 mya. The use of apomorphies allowed me to identify the more complete fossil snakes to the genus or species level. The impact of this study goes beyond the identification of fossils, however, as these specimens are the first sample for a previously unknown time interval in the evolutionary history of North American snakes, immediately following what had been a peak in species richness for snakes and the early stages of aridification and cooling in the Central Great Plains. The existence of this snake fauna allowed me to make comparisons to other snake fossils through time in the Central Great Plains and provided support for a stepwise, rather than sudden, modernization of the North American snake fauna, as suggested in previous studies (Holman, 2000; Parmley and Hunter, 2010). Furthermore, I was able to use the identifications of these fossil snakes to select extant congeneric proxies for the construction of climate envelope models, which suggested a shrubland woodland environment near a permanent body of water based on estimates of MAT and AP. These models are backed by data from phytoliths, fossil mammals, isotopes, paleosols, and sedimentary geology (Turner, 1972; Retallack, 1997; Fox and Koch, 2004; Janis et al., 2004; Strömberg, 2011; Kita et al., 2014). As a result, I expect the use of climate envelope models and similar paleophylogeographic models to expand quickly in the

study of fossil herpetofaunas, and for an increase in apomorphy-based descriptions combined with methods such as traditional and geometric morphometrics.

In Chapter Three, I used geometric morphometrics with quantitative methods to determine how well shape variation in middle trunk vertebrae could correctly assign taxon and ecology at different taxonomic levels without qualitative assessments. I compared datasets of two different sizes to assess how well these methods performed within different taxonomic ranks. First, a dataset composed of 11 different snake families performed well at the family and subfamily level, but struggled with classification despite identifying differences for genus, species and ecology. This dataset also indicated that behavioral differences in locomotion and feeding strategy as well as body mass may have roles in morphological differences across and within snake groups. This has been suggested qualitatively or with traditional measurements in previous works (Johnson, 1955; Lillywhite et al., 2000; Lillywhite, 2014; Holman, 2000), but has been tested neither with geometric morphometrics nor with this numerically large or taxonomically expansive of a dataset. Second, a dataset using only crotaline taxa showed drastic improvement for classifying genus and ecology, but marginal improvement for classifying species, suggesting that investigating within smaller groups may have more success in classifying snakes to finer taxonomic levels and in differentiating ecologies.

Also notable was the nature of shape changes when assessing the two datasets: while some of the selected shape variations were consistent between analyses, this was not true for all principal components (or at least, not in the same order). This suggests that some variations in shape are consistent across many groups, but others are group-

specific in terms of importance. Furthermore, trends for specialized (non-terrestrial generalist) ecologies appeared to follow a similar pattern across different snake groups in the first two PCs. This research establishes a new and easily reproducible method for assigning extant or fossil snake vertebrae to taxon and is a useful supplement to more traditional qualitative descriptions for identifying specimens and ecologies. Additionally, this method may help increase the number of fossil snakes that are described and improve classification confidence from those that are not expert diagnosticians of snake fossils.

I used a combination of traditional, external morphometric measurements and internal geometric morphometric skull shape in two orientations to assess *S. tergeminus* across geographic space for ten assigned populations. In doing so, I identified shape differences that were associated with diet, sex, location, climate, and allometry; these changes are not independent, as in the dietary shift towards lizards and invertebrates (noted in Holycross and Mackessy, 2002) in the western range of the species producing different morphologies in populations from Arizona and New Mexico. Few studies have used a large dataset combining both skeletal and external morphologies when describing intraspecific variation, especially in snakes. The results of this study suggest that more information relevant to the morphology, variation, and distribution of a species can be captured by doing so, and will impact our understanding of adaptability, and therefore survivability, within a species regarding diet, climate, and location as environments continue to change in response to anthropogenic behaviors (Lawing and Polly, 2011; Lawing et al., 2012, Mimura et al., 2017; Herrando-Perez et al., 2019).

In Chapter Five, I found the community mean shape of middle trunk vertebrae in North American snakes to correlate with a number of environmental variables. While these correlations were strongest for temperature-related variables and ecological province, differences were still noticeable for Annual Precipitation and Vegetation Cover. Quantitative assessment of vertebral shape and substrate use ecology revealed that both phylogeny and ecology play important roles in driving shape variation for five of the first six PCs. The ecometrics spaces revealed that mean shape typically increases more with MAT, and that together, the maximum likelihood predictions of MAT detected changes in local environments for the case studies both through time and across adjacent geographic spaces. Projection of maximum likelihood predictions onto geographic spaces revealed that several types of shape change could make good predictions of MAT across the U.S. and Canada, and that combining multiple types of shape change to make predictions improved projections to explain as much as 91% based on MAT. This interdisciplinary research not only establishes a framework for a new geometric morphometric-based ecometric, but is also an important link between ecological and fossil data with strong predictions for MAT in North America. While ecometrics for snakes have been established previously (Head et al., 2009; Lawing et al., 2012), this method is especially applicable to the fossil record as it is based on the most common fossil snake element: the vertebra.

An additional contribution of this dissertation comes from data and methodology. Large datasets including code for geometric morphometrics, quantitative methods, climate envelope models, and ecometrics are included in the Appendices in numerical

order. This code includes the newly established geometric morphometric method for taxonomic assignment and the new ecometric method using snake vertebrae. Data tables of measurements and quantitative methods are included in each chapter of the dissertation. Finally, because there have not been snakes described for the earliest Clarendonian of North America, that data provides an entirely new temporal sample of snakes to the field of paleontology.

6.2. Recommendations

As indicated throughout this dissertation, snakes are often considered difficult to work with in the fossil record and are generally understudied. While this has improved in recent years, the introduction of good methods for identification and the addition of new uses for snake vertebrae will highlight the value of snake fossils for paleoecological and paleoclimatic reconstructions and faunal assessments through time. The application of geometric morphometrics to the snake skeleton and the combination of snake skeletal shape data with external measurements will improve our understanding of the interface between functional traits and the environment. Furthermore, such methods should also be able to enhance studies of sexual dimorphism, ontogeny, and intracolumnar variation. Finally, all these featured topics contribute to conservation paleobiology. Conservation paleobiology aims to combine the deep time data of the fossil record with historical and modern data to provide long-term information on species responses to climate change (Barnosky et al., 2017). This, in turn, will help improve the ability of researchers to anticipate the potential responses of species to present environmental alterations. The

addition of a new ecometric (Chapter Five) that is easily transferrable to fossils from a group as geographically expanse and species rich as snakes is beneficial to the field of conservation paleobiology. I therefore recommend its application to future studies. Any methods that can contribute to our understanding of taxonomy and identification through skeletal materials (Chapter Two; Chapter Three) will contribute to both our understanding of the past and two our ability to apply techniques like this ecometric. Finally, much of what we know about the past life comes from our understanding of the life around us today. Each of these chapters contributes to this understanding at different scales, and Chapter Four shows how skeletal data can be combined with more typical means of understanding the present to enhance our ability to identify variation.

Snake vertebrae have much to reveal about the evolutionary history of the group and their interactions with the ecosystems they slither through. The most important and encompassing contribution of this dissertation is to the study of morphological variation. I highlight the nexus of ecological, paleontological, taxonomic, phylogenetic, geographic, and environmental interactions with skeletal morphology, and how these influences manipulate the variation we see through time. The expansion of data and methodologies to address questions of morphological variation improves our understanding of organisms at multiple spatial, temporal, and taxonomic scales and will lead to improvement on biases related to each of those factors. More robust information will lead to a better understanding of snakes in their entirety, and hopefully lead to a greater appreciation for how truly unique their vertebrae are within the animal kingdom. Finally, the contributions made possible by this uniqueness have the potential to

influence and inform conservation and management of snake species, and to help them persist into the future.

6.3. References

Barnosky, A. D., E. A. Hadly, P. Gonzalez, J. J. Head, P. D. Polly, A. M. Lawing, …, Z. Zhang. 2017. Merging paleobiology with conservation biology to guide the future of terrestrial ecosystems. Science 355, eaah4787. https://doi.org/10.1126/science.aah4787.

Fox, D. L. and P. L. Koch. 2004. Carbon and oxygen isotopic variability in Neogene paleosol carbonates: constraints on the evolution of the C4-grasslands of the Great Plains, USA. Palaeogeogr. Palaeoclimatol. Palaeoecol. 207:305-329.

Head, J. J., J. I. Bloch, A. K. Hastings, J. R. Bourque, E. A. Cadena, F. A. Herrera, P. D. Polly, and C. A. Jaramillo. 2009. Giant boid snake from the Palaeocene neotropics reveals hotter past equatorial temperatures. Nature 457:715-718.

Herrando-Pérez, S., F. Ferri-Yáñez, C. Monasterio, W. Beukema, V. Gomes, J. Belliure, S. L. Chown, D. R. Vieites, and M. B. Araújo. 2019. Intraspecific variation in lizard heat tolerance alters estimates of climate impact. Journal of Animal Ecology 88:247-257.

Holman, J. A. 2000. Fossil snakes of North America: Origin, evolution, distribution, paleoecology. Bloomington: Indiana University Press. 357 pp.

Holycross, A. T. and S. P. Mackessy. 2002. Variation in the diet of *Sistrurus catenatus* (Massasauga), with emphasis on *Sistrurus catenatus edwardsii* (Desert Massasauga). Journal of Herpetology 36:454-464.

Janis, C. M., J. Damuth, and J. M. Theodor. 2004. The species richness of Miocene browsers, and implications for habitat type and primary productivity in the North American grassland biome. Palaeogeogr. Palaeoclimatol. Palaeoecol. 207:371-398.

Johnson, R. G. 1955. The adaptive and phylogenetic significance of vertebral form in snakes. Evolution 9:367–388.

Kita, Z. A., R. Secord, and G. S. Boardman. 2014. A new stable isotope record of Neogene paleoenvironments and mammalian paleoecologies in the western Great Plains during the expansion of C4 grasslands. Palaeogeography, Palaeoclimatology, Palaeoecology 399:160-172.

Lawing A. M. and P. D. Polly. 2011. Pleistocene climate, phylogeny, and climate envelope models: an integrative approach to better understand species' response to climate change. PLoSOne 16:e28554.

Lawing, A. M., J. J. Head, and P. D. Polly. 2012. The ecology of morphology: the ecometrics of locomotion and macroenvironment in North American snakes. Pp. 117-146 in J. Louys (ed.), Palaeontology in Ecology and Conservation. Springer-Verlag, Berlin and Heidelberg.

Lillywhite, H. B., J. R. LaFrentz, Y. C. Lin, and M. C. Tu. 2000. The cantilever abilities of snakes. Journal of Herpetology 523-528.

Lillywhite, H. B., 2014. How snakes work: structure, function and behavior of the world's snakes. Oxford University Press.

Mimura, M., T. Yahara, D. P. Faith, E. Vázquez-Domínguez, R. I. Colautti, H. Araki, F. Javadi, J. Núñez-Farfán, A. S. Mori, S. Zhou, and P. M. Hollingsworth. 2017. Understanding and monitoring the consequences of human impacts on intraspecific variation. Evolutionary applications 10:121-139.

Parmley, D. and K. B. Hunter. 2010. Fossil Snakes of the Clarendonian (Late Miocene) Pratt Slide Local Fauna of Nebraska, with the description of a new natricine colubrid. Journal of Herpetology 44: 526-543.

Retallack, G. J. 2007. Cenozoic paleoclimate on land in North America. The Journal of Geology 115: 271-294.

Strömberg, C. A. E. 2011. Evolution of grasses and grassland ecosystems. Annu. Rev. Earth Planet. Sci. 39:517-544.

Turner, M. A. 1972. A faunal assemblage from the Lower Ash Hollow Formation (Neogene) of southern Nebraska. Master of Science Thesis, University of Nebraska-Lincoln. 88pp.

APPENDIX A

SUPPLEMENTAL MATERIAL FOR CHAPTER 2

"Snakes! Why did it have to be snakes?"

– Dr. Henry Walton "Indiana" Jones, *Raiders of the Lost Ark*

Appendix A contents:

Table A1. List of congenerics used for climate envelope models, grouped by genus.

Charina	*Lampropeltis*	*Pantherophis*	*Salvadora*	*Heterodon*	*Nerodia*
Charina bottae	*Lampropeltis calligaster*	*Pantherophis emoryi*	*Salvadora grahamiae*	*Heterodon nasicus*	*Nerodia cyclopion*
Charina umbratica	*Lampropeltis getula*	*Pantherophis obsoletus*	*Salvadora hexalepis*	*Heterodon platirhinos*	*Nerodia rhombifer*
	Lampropeltis holbrooki	*Pantherophis ramspotti*		*Heterodon simus*	*Nerodia sipedon*
	Lampropeltis Triangulum				

Code A1. This code uses fossil presence/absence data to perform a PCO analysis as well as a hierarchical cluster analysis, visualized with a scatterplot and dendrogram, respectively.

```
#make sure to install required packages
library(geomorph)
library(shapes)
library(reshape2)
library(rgdal)
library(raster)
library(rer)
library(rgeos)
library(dplyr)
library(sp)
library(car)
library(phytools)
library(picante)
library(RColorBrewer)
library(ggplot2)
getwd()
setwd("D:/Data/Manuscripts/Jacisin_Lawing_PennyCreekLF")

lmfossil<-read.csv("LM_fossils.csv", header=T)
head(lmfossil)

flandmarks<-readland.tps("Combined3.TPS")
flandmarks<-flandmarks[-15,,]

plot(flandmarks[,,1], xlim = c(0,1000), ylim = c(0,1000), cex=2)

for(i in 2:length(flandmarks[1,1,])){
  points(flandmarks[,,i], col=i, cex=2)
}


lmfossil$Family=as.factor(lmfossil$Family)
lmfossil$Subfamily=as.factor(lmfossil$Subfamily)
lmfossil$Genus=as.factor(lmfossil$Genus)
lmfossil$Locality=as.factor(lmfossil$Locality)

PCAfos <- procGPA(flandmarks)
par(cex=1)
par(pch=16)
```

```
cols = c("blue", "violet", "darkgreen", "slategray", "blueviolet", "red", "black",
"chocolate4", "green2", "deepskyblue" , "orange", "yellow", "maroon")
plot(PCAfos$stdscores[,1], PCAfos$stdscores[,2], xlim = c(-4, 4), ylim = c(-4, 4), xlab =
"PC1", ylab= "PC2", col= alpha(cols[lmfossil$Genus], 0.5))
text(PCAfos$stdscores[,1], PCAfos$stdscores[,2], cex= 0.75, labels = lmfossil$Number)
legend('bottomright', legend=levels(lmfossil$Subfamily), col =
alpha(cols[seq_along(lmfossil$Locality)], 0.5), cex=1, pch=20)

library(mclust)
PC123 <- cbind(PCAfos$stdscores[, 1:3])
SM <- Mclust(PC123[,1:3])
summary(SM)
BIC <- SM$BIC
plot(SM, what = "BIC")

hclustfunc <- function(x) hclust(x, method="complete")
distfunc <- function(x) as.dist((1-cor(t(x)))/2)
d <- dist(PC123, method = "euclidean")
fit <- hclustfunc(d)
plot(fit, cex = 0.5)

sites<-read.csv("flipped.csv", header=T)
head(sites)
sites$Genus = as.factor(sites$Genus)
head(sites)
summary(sites)

dis.euc <- dist(sites[,2:38], method = "euclidean")
dis.manh <- dist(sites[,2:38], method = "manhattan")
dis.bin <- dist(sites[,2:38], method = "binary")
dis.mink <- dist(sites[,2:38], method = "minkowski")


euc.pco <- pcoa(dis.euc, correction="none", rn=NULL)
colnames(euc.pco$vectors)[1:2] <- c("PCo 1 (29.7%)", "PCo 2 (14.6%)")
biplot(euc.pco, plot.axes = (c(1,2)), col = "gray", xlab = "PCo 1 (29.7%)",ylab = "PCo 2
(14.6%)")
biplot(euc.pco, plot.axes = (c(3,4)))

hclustfunc2 <- function(x) hclust(x, method="complete")
distfunc2 <- function(x) as.dist((1-cor(t(x)))/2)
fit2 <- hclustfunc2(dis.euc)
plot(fit2, cex = 0.5)
```

Code A2. This code uses extant congenerics of fossil taxa and associated climate data with those species to extract annual precipitation and mean annual temperature and create climate envelope models for the Penny Creek fossil snake assemblage.

```
#####################################################################
#Code to extract AP and MAT for Penny Creek Snakes
#####################################################################
library(maps)
library(maptools)
library(raster)
library(rgdal)
library(ggplot2)
library(ggpubr)
setwd("F:/climate_envelopes/climate_envelopes")
#####################################################################
# Charina bottae and umbratica
#####################################################################

#read in polygons
cbo <- readOGR("data/redlist_species_data_Cbo", layer = "data_0")
cum <- readOGR("data/redlist_species_data_Cum", layer = "data_0")
charina <- rbind(cbo,cum)

################################
# Climate data
################################

bioclim_10 <- getData(name = "worldclim", var = "bio", res = 10, path = "data/")

bio1_10 <- crop(bioclim_10[[1]], charina)
charina_r <- rasterize(charina, bio1_10, field = 1)

plot(bio1_10/10)

plot(charina_r, add =T, col = "red", legend = F)

bio1_10_mask <- mask(bio1_10, charina_r)

hist(bio1_10_mask/10, breaks = 50, main = "", xlab = "Mean Annual Temperature (C)")
```

```
bio12_10 <- crop(bioclim_10[[12]], charina_r)

plot(bio12_10)

plot(charina_r, add =T, col = "red", legend = F)

bio12_10_mask <- mask(bio12_10, charina_r)

hist(bio12_10_mask, breaks = 50, xlim = c(0,6000), main = "", xlab = "Annual
Precipitation (mm)")

charina_data <- data.frame("MAT" = na.omit(bio1_10_mask@data@values), "AP" =
na.omit(bio12_10_mask@data@values))

write.csv(charina_data, file = "data/charina_data.csv")

################################
# Heterodon x3
################################

#read in polygons
Hpl <- readOGR("data/redlist_species_data_Hpl", layer = "data_0")
Hna <- readOGR("data/redlist_species_data_Hna", layer = "data_0")
Hsi <- readOGR("data/redlist_species_data_Hsi", layer = "data_0")

Heterodon <- rbind(Hpl, Hna, Hsi)

################################
# Climate data
################################

bio1_10 <- crop(bioclim_10[[1]], Heterodon)

Heterodon_r <- rasterize(Heterodon, bio1_10, field = 1)

plot(bio1_10/10)

plot(Heterodon_r, add =T, col = "red", legend = F)

bio1_10_mask <- mask(bio1_10, Heterodon_r)

hist(bio1_10_mask/10, breaks = 50, main = "", xlab = "Mean Annual Temperature (C)")

bio12_10 <- crop(bioclim_10[[12]], Heterodon)
```

```
plot(bio12_10)

plot(Heterodon_r, add =T, col = "red", legend = F)

bio12_10_mask <- mask(bio12_10, Heterodon_r)

hist(bio12_10_mask, breaks = 50, main = "", xlab = "Annual Precipitation (mm)")

Heterodon_data <- data.frame("MAT" = na.omit(bio1_10_mask@data@values), "AP" =
na.omit(bio12_10_mask@data@values))


write.csv(Heterodon_data, file = "data/heterodon_data.csv")

################################
# Pantherophis x 3
################################

#read in polygons
Pem <- readOGR("data/redlist_species_data_Pem", layer = "data_0")
Pob <- readOGR("data/redlist_species_data_Pob", layer = "data_0")
Pra <- readOGR("data/redlist_species_data_Pra", layer = "data_0")
Pantherophis <- rbind(Pem, Pob, Pra)

################################
# Climate data
################################

bio1_10 <- crop(bioclim_10[[1]], Pantherophis)

Pantherophis_r <- rasterize(Pantherophis, bio1_10, field = 1)

plot(bio1_10/10)

plot(Pantherophis_r, add =T, col = "red", legend = F)

bio1_10_mask <- mask(bio1_10, Pantherophis_r)

hist(bio1_10_mask/10, breaks = 50, main = "", xlab = "Mean Annual Temperature (C)")

bio12_10 <- crop(bioclim_10[[12]], Pantherophis_r)

plot(bio12_10)
```

```
plot(Pantherophis_r, add =T, col = "red", legend = F)

bio12_10_mask <- mask(bio12_10, Pantherophis_r)

hist(bio12_10_mask, breaks = 50, main = "", xlab = "Annual Precipitation (mm)")

Pantherophis_data <- data.frame("MAT" = na.omit(bio1_10_mask@data@values),
"AP" = na.omit(bio12_10_mask@data@values))

write.csv(Pantherophis_data, file = "data/pantherophis_data")
```

APPENDIX B

SUPPLEMENTAL MATERIAL FOR CHAPTER 3

Appendix B contents:

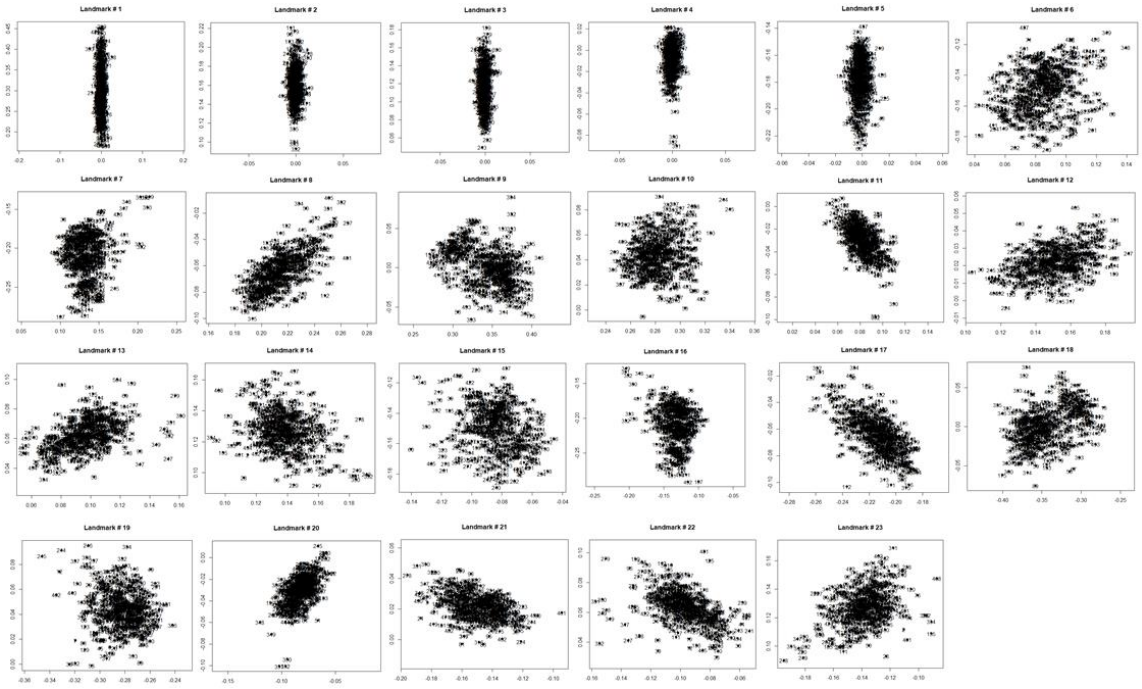

Figure B1. Outlier plots for each of the 23 landmarks used in this study (in numerical order).

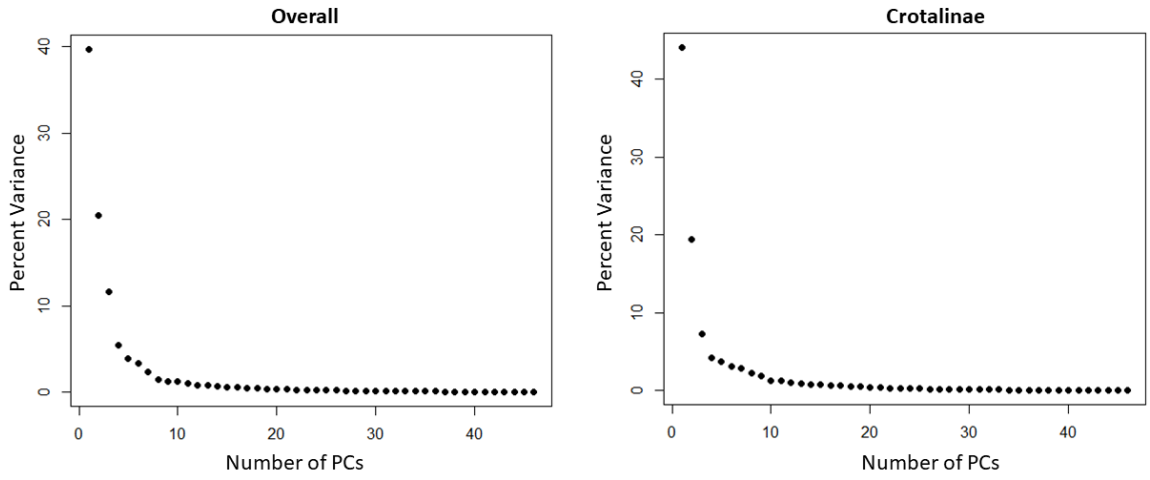

Figure B2. Plot of the percent of morphological variation represented by each PC in from the whole group (left) and Crotalinae-only (right) PCA analyses.

Table B1. List of taxa, including family, subfamily, genus, species, and primary foraging habitat.

ID	Genus	Species	Family	Subfamily	Substrate
1	*Agkistrodon*	*contortrix*	Viperidae	Crotalinae	Terrestrial
2	*Agkistrodon*	*piscivorus*	Viperidae	Crotalinae	Semiaquatic
3	*Alsophis*	*antillensis*	Colubridae	Dipsadinae	Terrestrial
4	*Alsophis*	*cantherigerus*	Colubridae	Dipsadinae	Terrestrial
5	*Alsophis*	*portoricensis*	Colubridae	Dipsadinae	Terrestrial
6	*Alsophis*	*vudii*	Colubridae	Dipsadinae	Terrestrial
7	*Antillophis*	*parvifrons*	Colubridae	Dipsadinae	Terrestrial
8	*Atractus*	*trilineatus*	Colubridae	Dipsadinae	Semifossorial
9	*Boa*	*constrictor*	Boidae	Boinae	Semiarboreal
10	*Bogertophis*	*subocularis*	Colubridae	Colubrinae	Terrestrial
11	*Bothriechis*	*nigroviridis*	Viperidae	Crotalinae	Arboreal
12	*Bothriechis*	*schlegelii*	Viperidae	Crotalinae	Arboreal
13	*Bothrops*	*asper*	Viperidae	Crotalinae	Terrestrial
14	*Candoia*	*carinata*	Candoiidae	Candoiinae	Terrestrial
15	*Carphophis*	*amoenus*	Colubridae	Dipsadinae	Fossorial
16	*Cemophora*	*coccinea*	Colubridae	Colubrinae	Fossorial
17	*Charina*	*bottae*	Charinidae	Charininae	Semifossorial
18	*Chilomeniscus*	*stramineus*	Colubridae	Colubrinae	Fossorial
19	*Chironius*	*carinatus*	Colubridae	Colubrinae	Arboreal
20	*Chironius*	*scurrulus*	Colubridae	Colubrinae	Arboreal
21	*Clelia*	*clelia*	Colubridae	Dipsadinae	Terrestrial
22	*Coluber*	*constrictor*	Colubridae	Colubrinae	Semiarboreal
23	*Conophis*	*pulcher*	Colubridae	Dipsadinae	Terrestrial
24	*Contia*	*tenuis*	Colubridae	Dipsadinae	Semifossorial
25	*Crotalus*	*adamanteus*	Viperidae	Crotalinae	Terrestrial
26	*Crotalus*	*atrox*	Viperidae	Crotalinae	Terrestrial
27	*Crotalus*	*cerastes*	Viperidae	Crotalinae	Terrestrial
28	*Crotalus*	*enyo*	Viperidae	Crotalinae	Terrestrial
29	*Crotalus*	*horridus*	Viperidae	Crotalinae	Terrestrial
30	*Crotalus*	*mitchellii*	Viperidae	Crotalinae	Terrestrial
31	*Crotalus*	*molossus*	Viperidae	Crotalinae	Terrestrial
32	*Crotalus*	*ravus*	Viperidae	Crotalinae	Terrestrial
33	*Crotalus*	*ruber*	Viperidae	Crotalinae	Terrestrial
34	*Crotalus*	*scutulatus*	Viperidae	Crotalinae	Terrestrial

Table B1. (continued)

35	*Crotalus*	*viridis*	Viperidae	Crotalinae	Terrestrial
36	*Dendrophidion*	*vinitor*	Colubridae	Colubrinae	Semiarboreal
37	*Diadophis*	*punctatus*	Colubridae	Dipsadinae	Semifossorial
38	*Dipsas*	*articulata*	Colubridae	Dipsadinae	Arboreal
39	*Dipsas*	*variegata*	Colubridae	Dipsadinae	Arboreal
40	*Drymarchon*	*corais*	Colubridae	Colubrinae	Terrestrial
41	*Chilabothrus*	*angulifer*	Boidae	Boinae	Arboreal
42	*Epicrates*	*cenchria*	Boidae	Boinae	Terrestrial
43	*Chilabothrus*	*striatus*	Boidae	Boinae	Terrestrial
44	*Chilabothrus*	*subflavus*	Boidae	Boinae	Arboreal
45	*Erythrolamprus*	*aesculapii*	Colubridae	Dipsadinae	Terrestrial
46	*Erythrolamprus*	*ocellatus*	Colubridae	Dipsadinae	Terrestrial
47	*Farancia*	*abacura*	Colubridae	Dipsadinae	Semiaquatic
48	*Farancia*	*erytrogramma*	Colubridae	Dipsadinae	Aquatic
49	*Heterodon*	*nasicus*	Colubridae	Dipsadinae	Semifossorial
50	*Heterodon*	*platirhinos*	Colubridae	Dipsadinae	Semifossorial
51	*Heterodon*	*simus*	Colubridae	Dipsadinae	Semifossorial
52	*Hypsirhynchus*	*ferox*	Colubridae	Dipsadinae	Terrestrial
53	*Imantodes*	*cenchoa*	Colubridae	Dipsadinae	Arboreal
54	*Lampropeltis*	*calligaster*	Colubridae	Colubrinae	Semifossorial
55	*Lampropeltis*	*extenuata*	Colubridae	Colubrinae	Fossorial
56	*Lampropeltis*	*getula*	Colubridae	Colubrinae	Terrestrial
57	*Lampropeltis*	*triangulum*	Colubridae	Colubrinae	Semifossorial
58	*Leptodeira*	*annulata*	Colubridae	Dipsadinae	Semiaquatic
59	*Leptophis*	*ahaetulla*	Colubridae	Colubrinae	Arboreal
60	*Lichanura*	*trivirgata*	Charinidae	Charininae	Semifossorial
61	*Erythrolamprus*	*cobella*	Colubridae	Dipsadinae	Semiaquatic
62	*Erythrolamprus*	*melanotus*	Colubridae	Dipsadinae	Semiaquatic
63	*Erythrolamprus*	*reginae*	Colubridae	Dipsadinae	Aquatic
64	*Loxocemus*	*bicolor*	Loxocemidae	Loxoceminae	Semifossorial
65	*Masticophis*	*flagellum*	Colubridae	Colubrinae	Semiarboreal
66	*Masticophis*	*taeniatus*	Colubridae	Colubrinae	Arboreal
67	*Mastigodryas*	*pleei*	Colubridae	Colubrinae	Arboreal
68	*Micruroides*	*euryxanthus*	Elapidae	Elapinae	Fossorial
69	*Micrurus*	*diastema*	Elapidae	Elapinae	Terrestrial
70	*Micrurus*	*fulvius*	Elapidae	Elapinae	Fossorial
71	*Micrurus*	*psyches*	Elapidae	Elapinae	Fossorial

Table B1. (continued)

72	*Nerodia*	*cyclopion*	Colubridae	Natricinae	Aquatic
73	*Nerodia*	*erythrogaster*	Colubridae	Natricinae	Semiaquatic
74	*Nerodia*	*fasciata*	Colubridae	Natricinae	Aquatic
75	*Nerodia*	*floridana*	Colubridae	Natricinae	Aquatic
76	*Nerodia*	*rhombifer*	Colubridae	Natricinae	Semiaquatic
77	*Nerodia*	*sipedon*	Colubridae	Natricinae	Aquatic
78	*Nerodia*	*taxispilota*	Colubridae	Natricinae	Aquatic
79	*Ninia*	*atrata*	Colubridae	Dipsadinae	Semifossorial
80	*Opheodrys*	*aestivus*	Colubridae	Colubrinae	Arboreal
81	*Opheodrys*	*vernalis*	Colubridae	Colubrinae	Semiarboreal
82	*Oxybelis*	*aeneus*	Colubridae	Colubrinae	Arboreal
83	*Oxybelis*	*brevirostris*	Colubridae	Colubrinae	Arboreal
84	*Oxybelis*	*fulgidus*	Colubridae	Colubrinae	Arboreal
85	*Oxyrhopus*	*petolarius*	Colubridae	Dipsadinae	Terrestrial
86	*Pantherophis*	*guttatus*	Colubridae	Colubrinae	Terrestrial
87	*Pantherophis*	*obsoletus*	Colubridae	Colubrinae	Arboreal
88	*Pantherophis*	*vulpinus*	Colubridae	Colubrinae	Terrestrial
89	*Pelamis*	*platura*	Elapidae	Hydrophiinae	Aquatic
90	*Phyllorhynchus*	*decurtatus*	Colubridae	Colubrinae	Fossorial
91	*Pituophis*	*catenifer*	Colubridae	Colubrinae	Semifossorial
92	*Pituophis*	*deppei*	Colubridae	Colubrinae	Semifossorial
93	*Pituophis*	*melanoleucus*	Colubridae	Colubrinae	Semifossorial
94	*Phrynonax*	*poecilonotus*	Colubridae	Colubrinae	Semiarboreal
95	*Spilotes*	*sulphureus*	Colubridae	Colubrinae	Semiarboreal
96	*Regina*	*grahami*	Colubridae	Natricinae	Aquatic
97	*Regina*	*septemvittata*	Colubridae	Natricinae	Semiaquatic
98	*Rhadinaea*	*flavilata*	Colubridae	Colubrinae	Terrestrial
99	*Rhinocheilus*	*lecontei*	Colubridae	Colubrinae	Semifossorial
100	*Salvadora*	*grahamiae*	Colubridae	Colubrinae	Semiarboreal
101	*Salvadora*	*hexalepis*	Colubridae	Colubrinae	Semiarboreal
102	*Salvadora*	*intermedia*	Colubridae	Colubrinae	Semiarboreal
103	*Seminatrix*	*pygaea*	Colubridae	Natricinae	Aquatic
104	*Sibon*	*anthracops*	Colubridae	Dipsadinae	Arboreal
105	*Sibon*	*nebulatus*	Colubridae	Dipsadinae	Arboreal
106	*Sistrurus*	*catenatus*	Viperidae	Crotalinae	Terrestrial
107	*Sistrurus*	*miliarius*	Viperidae	Crotalinae	Terrestrial
108	*Spilotes*	*pullatus*	Colubridae	Colubrinae	Semiarboreal

Table B15. (continued)

109	*Stenorrhina*	*degenhardtii*	Colubridae	Colubrinae	Terrestrial
110	*Storeria*	*dekayi*	Colubridae	Natricinae	Terrestrial
111	*Storeria*	*occipitomaculata*	Colubridae	Natricinae	Terrestrial
112	*Tantilla*	*relicta*	Colubridae	Colubrinae	Fossorial
113	*Thamnophis*	*brachystoma*	Colubridae	Natricinae	Terrestrial
114	*Thamnophis*	*butleri*	Colubridae	Natricinae	Terrestrial
115	*Thamnophis*	*cyrtopsis*	Colubridae	Natricinae	Terrestrial
116	*Thamnophis*	*elegans*	Colubridae	Natricinae	Terrestrial
117	*Thamnophis*	*eques*	Colubridae	Natricinae	Terrestrial
118	*Thamnophis*	*marcianus*	Colubridae	Natricinae	Semiaquatic
119	*Thamnophis*	*proximus*	Colubridae	Natricinae	Semiaquatic
120	*Thamnophis*	*radix*	Colubridae	Natricinae	Terrestrial
121	*Thamnophis*	*sauritus*	Colubridae	Natricinae	Semiaquatic
122	*Thamnophis*	*sirtalis*	Colubridae	Natricinae	Semiaquatic
123	*Trimorphodon*	*biscutatus*	Colubridae	Colubrinae	Terrestrial
124	*Siphlophis*	*compressus*	Colubridae	Dipsadinae	Terrestrial
125	*Tropidoclonion*	*lineatum*	Colubridae	Natricinae	Semifossorial
126	*Tropidophis*	*canus*	Tropidophiidae	Tropidophiinae	Fossorial
127	*Tropidophis*	*haetianus*	Tropidophiidae	Tropidophiinae	Fossorial
128	*Uromacer*	*catesbyi*	Colubridae	Dipsadinae	Arboreal
129	*Uromacer*	*oxyrhynchus*	Colubridae	Dipsadinae	Arboreal
130	*Virginia*	*valeriae*	Colubridae	Natricinae	Semifossorial
131	*Nerodia*	*harteri*	Colubridae	Natricinae	Aquatic
132	*Heterodon*	*nasicus*	Colubridae	Dipsadinae	Semifossorial
133	*Heterodon*	*nasicus*	Colubridae	Dipsadinae	Semifossorial
134	*Agkistrodon*	*piscivorus*	Viperidae	Crotalinae	Semiaquatic
135	*Crotalus*	*atrox*	Viperidae	Crotalinae	Terrestrial
136	*Crotalus*	*atrox*	Viperidae	Crotalinae	Terrestrial
137	*Crotalus*	*atrox*	Viperidae	Crotalinae	Terrestrial
138	*Agkistrodon*	*piscivorus*	Viperidae	Crotalinae	Semiaquatic
139	*Agkistrodon*	*piscivorus*	Viperidae	Crotalinae	Semiaquatic
140	*Agkistrodon*	*piscivorus*	Viperidae	Crotalinae	Semiaquatic
141	*Nerodia*	*rhombifer*	Colubridae	Natricinae	Semiaquatic
142	*Nerodia*	*rhombifer*	Colubridae	Natricinae	Semiaquatic
143	*Nerodia*	*rhombifer*	Colubridae	Natricinae	Semiaquatic
144	*Heterodon*	*nasicus*	Colubridae	Dipsadinae	Semifossorial
145	*Heterodon*	*nasicus*	Colubridae	Dipsadinae	Semifossorial

Table B16. (continued)

146	*Heterodon*	*nasicus*	Colubridae	Dipsadinae	Semifossorial
147	*Crotalus*	*atrox*	Viperidae	Crotalinae	Terrestrial
148	*Crotalus*	*atrox*	Viperidae	Crotalinae	Terrestrial
149	*Crotalus*	*atrox*	Viperidae	Crotalinae	Terrestrial
150	*Crotalus*	*molossus*	Viperidae	Crotalinae	Terrestrial
151	*Pantherophis*	*obsoletus*	Colubridae	Colubrinae	Arboreal
152	*Pantherophis*	*obsoletus*	Colubridae	Colubrinae	Arboreal
153	*Pantherophis*	*obsoletus*	Colubridae	Colubrinae	Arboreal
154	*Pantherophis*	*obsoletus*	Colubridae	Colubrinae	Arboreal
155	*Nerodia*	*rhombifer*	Colubridae	Natricinae	Semiaquatic
156	*Crotalus*	*lepidus*	Viperidae	Crotalinae	Terrestrial
157	*Crotalus*	*scutulatus*	Viperidae	Crotalinae	Terrestrial
158	*Crotalus*	*tigris*	Viperidae	Crotalinae	Terrestrial
159	*Micruroides*	*euryxanthus*	Elapidae	Elapinae	Fossorial
160	*Arizona*	*elegans*	Colubridae	Colubrinae	Semifossorial
161	*Chionactis*	*occipitalis*	Colubridae	Colubrinae	Fossorial
162	*Chilomeniscus*	*stramineus*	Colubridae	Colubrinae	Fossorial
163	*Diadophis*	*punctatus*	Colubridae	Dipsadinae	Semifossorial
164	*Senticolis*	*triaspis*	Colubridae	Colubrinae	Semiarboreal
165	*Senticolis*	*triaspis*	Colubridae	Colubrinae	Semiarboreal
166	*Bogertophis*	*subocularis*	Colubridae	Colubrinae	Terrestrial
167	*Hypsiglena*	*torquata*	Colubridae	Dipsadinae	Terrestrial
168	*Lampropeltis*	*pyromelana*	Colubridae	Colubrinae	Terrestrial
169	*Lampropeltis*	*pyromelana*	Colubridae	Colubrinae	Terrestrial
170	*Lampropeltis*	*pyromelana*	Colubridae	Colubrinae	Terrestrial
171	*Lampropeltis*	*triangulum*	Colubridae	Colubrinae	Semifossorial
172	*Lampropeltis*	*triangulum*	Colubridae	Colubrinae	Semifossorial
173	*Lampropeltis*	*triangulum*	Colubridae	Colubrinae	Semifossorial
174	*Lampropeltis*	*triangulum*	Colubridae	Colubrinae	Semifossorial
175	*Masticophis*	*bilineatus*	Colubridae	Colubrinae	Semiarboreal
176	*Masticophis*	*flagellum*	Colubridae	Colubrinae	Semiarboreal
177	*Nerodia*	*erythrogaster*	Colubridae	Natricinae	Semiaquatic
178	*Nerodia*	*fasciata*	Colubridae	Natricinae	Aquatic
179	*Nerodia*	*rhombifer*	Colubridae	Natricinae	Semiaquatic
180	*Nerodia*	*sipedon*	Colubridae	Natricinae	Aquatic
181	*Opheodrys*	*aestivus*	Colubridae	Colubrinae	Arboreal
182	*Phyllorhynchus*	*decurtatus*	Colubridae	Colubrinae	Fossorial

Table B1. (continued)

183	*Rhinocheilus*	*lecontei*	Colubridae	Colubrinae	Semifossorial
184	*Salvadora*	*hexalepis*	Colubridae	Colubrinae	Semiarboreal
185	*Trimorphodon*	*lambda*	Colubridae	Colubrinae	Terrestrial
186	*Trimorphodon*	*biscutatus*	Colubridae	Colubrinae	Terrestrial
187	*Thamnophis*	*cyrtopsis*	Colubridae	Natricinae	Terrestrial
188	*Thamnophis*	*elegans*	Colubridae	Natricinae	Terrestrial
189	*Thamnophis*	*eques*	Colubridae	Natricinae	Terrestrial
190	*Thamnophis*	*marcianus*	Colubridae	Natricinae	Semiaquatic
191	*Thamnophis*	*marcianus*	Colubridae	Natricinae	Semiaquatic
192	*Thamnophis*	*proximus*	Colubridae	Natricinae	Semiaquatic
193	*Thamnophis*	*rufipunctatus*	Colubridae	Natricinae	Aquatic
194	*Thamnophis*	*sirtalis*	Colubridae	Natricinae	Semiaquatic
195	*Agkistrodon*	*contortrix*	Viperidae	Crotalinae	Terrestrial
196	*Agkistrodon*	*contortrix*	Viperidae	Crotalinae	Terrestrial
197	*Agkistrodon*	*contortrix*	Viperidae	Crotalinae	Terrestrial
198	*Agkistrodon*	*contortrix*	Viperidae	Crotalinae	Terrestrial
199	*Agkistrodon*	*contortrix*	Viperidae	Crotalinae	Terrestrial
200	*Agkistrodon*	*contortrix*	Viperidae	Crotalinae	Terrestrial
201	*Agkistrodon*	*contortrix*	Viperidae	Crotalinae	Terrestrial
202	*Agkistrodon*	*contortrix*	Viperidae	Crotalinae	Terrestrial
203	*Pantherophis*	*guttatus*	Colubridae	Colubrinae	Terrestrial
204	*Pantherophis*	*emoryi*	Colubridae	Colubrinae	Terrestrial
205	*Pantherophis*	*emoryi*	Colubridae	Colubrinae	Terrestrial
206	*Pantherophis*	*emoryi*	Colubridae	Colubrinae	Terrestrial
207	*Pantherophis*	*emoryi*	Colubridae	Colubrinae	Terrestrial
208	*Pantherophis*	*emoryi*	Colubridae	Colubrinae	Terrestrial
209	*Pantherophis*	*emoryi*	Colubridae	Colubrinae	Terrestrial
210	*Pantherophis*	*emoryi*	Colubridae	Colubrinae	Terrestrial
211	*Pantherophis*	*guttatus*	Colubridae	Colubrinae	Terrestrial
212	*Pantherophis*	*guttatus*	Colubridae	Colubrinae	Terrestrial
213	*Pantherophis*	*guttatus*	Colubridae	Colubrinae	Terrestrial
214	*Pantherophis*	*guttatus*	Colubridae	Colubrinae	Terrestrial
215	*Micrurus*	*tener*	Elapidae	Elapinae	Fossorial
216	*Micrurus*	*tener*	Elapidae	Elapinae	Fossorial
217	*Micrurus*	*tener*	Elapidae	Elapinae	Fossorial
218	*Micrurus*	*tener*	Elapidae	Elapinae	Fossorial
219	*Phyllorhynchus*	*sp*	Colubridae	Colubrinae	Fossorial

Table B1. (continued)

220	*Phyllorhynchus*	*sp*	Colubridae	Colubrinae	Fossorial
221	*Lampropeltis*	*calligaster*	Colubridae	Colubrinae	Semifossorial
222	*Lampropeltis*	*calligaster*	Colubridae	Colubrinae	Semifossorial
223	*Lampropeltis*	*calligaster*	Colubridae	Colubrinae	Semifossorial
224	*Drymarchon*	*couperi*	Colubridae	Colubrinae	Terrestrial
225	*Sonora*	*semiannulata*	Colubridae	Colubrinae	Semifossorial
226	*Sonora*	*semiannulata*	Colubridae	Colubrinae	Semifossorial
227	*Crotalus*	*molossus*	Viperidae	Crotalinae	Terrestrial
228	*Crotalus*	*molossus*	Viperidae	Crotalinae	Terrestrial
229	*Crotalus*	*molossus*	Viperidae	Crotalinae	Terrestrial
230	*Crotalus*	*molossus*	Viperidae	Crotalinae	Terrestrial
231	*Crotalus*	*molossus*	Viperidae	Crotalinae	Terrestrial
232	*Arizona*	*elegans*	Colubridae	Colubrinae	Semifossorial
233	*Arizona*	*elegans*	Colubridae	Colubrinae	Semifossorial
234	*Arizona*	*elegans*	Colubridae	Colubrinae	Semifossorial
235	*Arizona*	*elegans*	Colubridae	Colubrinae	Semifossorial
236	*Arizona*	*elegans*	Colubridae	Colubrinae	Semifossorial
237	*Arizona*	*elegans*	Colubridae	Colubrinae	Semifossorial
238	*Boa*	*constrictor*	Boidae	Boinae	Semiarboreal
239	*Boa*	*constrictor*	Boidae	Boinae	Semiarboreal
240	*Boa*	*constrictor*	Boidae	Boinae	Semiarboreal
241	*Boa*	*constrictor*	Boidae	Boinae	Semiarboreal
242	*Boa*	*constrictor*	Boidae	Boinae	Semiarboreal
243	*Boa*	*constrictor*	Boidae	Boinae	Semiarboreal
244	*Bothriechis*	*nigroviridis*	Viperidae	Crotalinae	Arboreal
245	*Bothriechis*	*nigroviridis*	Viperidae	Crotalinae	Arboreal
246	*Bothriechis*	*nigroviridis*	Viperidae	Crotalinae	Arboreal
247	*Bothriechis*	*schlegelii*	Viperidae	Crotalinae	Arboreal
248	*Bothriechis*	*schlegelii*	Viperidae	Crotalinae	Arboreal
249	*Bothriechis*	*schlegelii*	Viperidae	Crotalinae	Arboreal
250	*Carphophis*	*amoenus*	Colubridae	Dipsadinae	Fossorial
251	*Carphophis*	*amoenus*	Colubridae	Dipsadinae	Fossorial
252	*Carphophis*	*amoenus*	Colubridae	Dipsadinae	Fossorial
253	*Cemophora*	*coccinea*	Colubridae	Colubrinae	Fossorial
254	*Cemophora*	*coccinea*	Colubridae	Colubrinae	Fossorial
255	*Cemophora*	*coccinea*	Colubridae	Colubrinae	Fossorial
256	*Charina*	*bottae*	Charinidae	Charininae	Semifossorial

Table B1. (continued)

257	*Charina*	*bottae*	Charinidae	Charininae	Semifossorial
258	*Charina*	*bottae*	Charinidae	Charininae	Semifossorial
259	*Lichanura*	*trivirgata*	Charinidae	Charininae	Semifossorial
260	*Lichanura*	*trivirgata*	Charinidae	Charininae	Semifossorial
261	*Lichanura*	*trivirgata*	Charinidae	Charininae	Semifossorial
262	*Chilomeniscus*	*stramineus*	Colubridae	Colubrinae	Fossorial
263	*Chilomeniscus*	*stramineus*	Colubridae	Colubrinae	Fossorial
264	*Chilomeniscus*	*stramineus*	Colubridae	Colubrinae	Fossorial
265	*Chilomeniscus*	*stramineus*	Colubridae	Colubrinae	Fossorial
266	*Chilomeniscus*	*stramineus*	Colubridae	Colubrinae	Fossorial
267	*Chilomeniscus*	*stramineus*	Colubridae	Colubrinae	Fossorial
268	*Chilomeniscus*	*stramineus*	Colubridae	Colubrinae	Fossorial
269	*Chilomeniscus*	*stramineus*	Colubridae	Colubrinae	Fossorial
270	*Chrysopelea*	*ornata*	Colubridae	Ahaetuliinae	Arboreal
271	*Coluber*	*constrictor*	Colubridae	Colubrinae	Semiarboreal
272	*Coluber*	*constrictor*	Colubridae	Colubrinae	Semiarboreal
273	*Coluber*	*constrictor*	Colubridae	Colubrinae	Semiarboreal
274	*Coluber*	*constrictor*	Colubridae	Colubrinae	Semiarboreal
275	*Coluber*	*constrictor*	Colubridae	Colubrinae	Semiarboreal
276	*Coluber*	*constrictor*	Colubridae	Colubrinae	Semiarboreal
277	*Corallus*	*annulatus*	Boidae	Boinae	Arboreal
278	*Corallus*	*annulatus*	Boidae	Boinae	Arboreal
279	*Corallus*	*annulatus*	Boidae	Boinae	Arboreal
280	*Crotalus*	*adamanteus*	Viperidae	Crotalinae	Terrestrial
281	*Crotalus*	*adamanteus*	Viperidae	Crotalinae	Terrestrial
282	*Crotalus*	*adamanteus*	Viperidae	Crotalinae	Terrestrial
283	*Crotalus*	*cerastes*	Viperidae	Crotalinae	Terrestrial
284	*Crotalus*	*cerastes*	Viperidae	Crotalinae	Terrestrial
285	*Crotalus*	*cerastes*	Viperidae	Crotalinae	Terrestrial
286	*Crotalus*	*cerastes*	Viperidae	Crotalinae	Terrestrial
287	*Crotalus*	*cerastes*	Viperidae	Crotalinae	Terrestrial
288	*Crotalus*	*cerastes*	Viperidae	Crotalinae	Terrestrial
289	*Crotalus*	*enyo*	Viperidae	Crotalinae	Terrestrial
290	*Crotalus*	*enyo*	Viperidae	Crotalinae	Terrestrial
291	*Crotalus*	*enyo*	Viperidae	Crotalinae	Terrestrial
292	*Crotalus*	*horridus*	Viperidae	Crotalinae	Terrestrial
293	*Crotalus*	*horridus*	Viperidae	Crotalinae	Terrestrial

Table B1. (continued)

294	*Crotalus*	*horridus*	Viperidae	Crotalinae	Terrestrial
295	*Crotalus*	*horridus*	Viperidae	Crotalinae	Terrestrial
296	*Crotalus*	*mitchellii*	Viperidae	Crotalinae	Terrestrial
297	*Crotalus*	*mitchellii*	Viperidae	Crotalinae	Terrestrial
298	*Crotalus*	*mitchellii*	Viperidae	Crotalinae	Terrestrial
299	*Crotalus*	*mitchellii*	Viperidae	Crotalinae	Terrestrial
300	*Crotalus*	*mitchellii*	Viperidae	Crotalinae	Terrestrial
301	*Crotalus*	*mitchellii*	Viperidae	Crotalinae	Terrestrial
302	*Crotalus*	*oreganus*	Viperidae	Crotalinae	Terrestrial
303	*Crotalus*	*oreganus*	Viperidae	Crotalinae	Terrestrial
304	*Crotalus*	*oreganus*	Viperidae	Crotalinae	Terrestrial
305	*Crotalus*	*oreganus*	Viperidae	Crotalinae	Terrestrial
306	*Crotalus*	*oreganus*	Viperidae	Crotalinae	Terrestrial
307	*Crotalus*	*oreganus*	Viperidae	Crotalinae	Terrestrial
308	*Crotalus*	*viridis*	Viperidae	Crotalinae	Terrestrial
309	*Crotalus*	*viridis*	Viperidae	Crotalinae	Terrestrial
310	*Crotalus*	*viridis*	Viperidae	Crotalinae	Terrestrial
311	*Drymarchon*	*corais*	Colubridae	Colubrinae	Terrestrial
312	*Drymarchon*	*corais*	Colubridae	Colubrinae	Terrestrial
313	*Drymarchon*	*corais*	Colubridae	Colubrinae	Terrestrial
314	*Drymobius*	*margaritiferus*	Colubridae	Colubrinae	Arboreal
315	*Ahaetulla*	*nasutus*	Colubridae	Ahaetuliinae	Arboreal
316	*Ahaetulla*	*nasutus*	Colubridae	Ahaetuliinae	Arboreal
317	*Ahaetulla*	*nasutus*	Colubridae	Ahaetuliinae	Arboreal
318	*Pantherophis*	*bairdi*	Colubridae	Colubrinae	Arboreal
319	*Pantherophis*	*bairdi*	Colubridae	Colubrinae	Arboreal
320	*Pantherophis*	*bairdi*	Colubridae	Colubrinae	Arboreal
321	*Epicrates*	*cenchria*	Boidae	Boinae	Terrestrial
322	*Epicrates*	*cenchria*	Boidae	Boinae	Terrestrial
323	*Epicrates*	*cenchria*	Boidae	Boinae	Terrestrial
324	*Epicrates*	*cenchria*	Boidae	Boinae	Terrestrial
325	*Eunectes*	*murinus*	Boidae	Boinae	Semiaquatic
326	*Farancia*	*abacura*	Colubridae	Dipsadinae	Semiaquatic
327	*Farancia*	*abacura*	Colubridae	Dipsadinae	Semiaquatic
328	*Farancia*	*abacura*	Colubridae	Dipsadinae	Semiaquatic
329	*Haldea*	*striatula*	Colubridae	Natricinae	Semifossorial
330	*Haldea*	*striatula*	Colubridae	Natricinae	Semifossorial

Table B1. (continued)

331	*Haldea*	*striatula*	Colubridae	Natricinae	Semifossorial
332	*Heterodon*	*platirhinos*	Colubridae	Dipsadinae	Semifossorial
333	*Heterodon*	*platirhinos*	Colubridae	Dipsadinae	Semifossorial
334	*Heterodon*	*platirhinos*	Colubridae	Dipsadinae	Semifossorial
335	*Lampropeltis*	*alterna*	Colubridae	Colubrinae	Terrestrial
336	*Lampropeltis*	*getula*	Colubridae	Colubrinae	Terrestrial
337	*Lampropeltis*	*getula*	Colubridae	Colubrinae	Terrestrial
338	*Lampropeltis*	*getula*	Colubridae	Colubrinae	Terrestrial
339	*Lampropeltis*	*getula*	Colubridae	Colubrinae	Terrestrial
340	*Lampropeltis*	*getula*	Colubridae	Colubrinae	Terrestrial
341	*Lampropeltis*	*getula*	Colubridae	Colubrinae	Terrestrial
342	*Lampropeltis*	*getula*	Colubridae	Colubrinae	Terrestrial
343	*Lampropeltis*	*zonata*	Colubridae	Colubrinae	Terrestrial
344	*Lampropeltis*	*zonata*	Colubridae	Colubrinae	Terrestrial
345	*Lampropeltis*	*zonata*	Colubridae	Colubrinae	Terrestrial
346	*Laticauda*	*colubrina*	Elapidae	Hydrophiinae	Aquatic
347	*Rena*	*dulcis*	Leptotyphlopidae	Leptotyphlopinae	Fossorial
348	*Rena*	*dulcis*	Leptotyphlopidae	Leptotyphlopinae	Fossorial
349	*Rena*	*dulcis*	Leptotyphlopidae	Leptotyphlopinae	Fossorial
350	*Rena*	*humilis*	Leptotyphlopidae	Leptotyphlopinae	Fossorial
351	*Rena*	*humilis*	Leptotyphlopidae	Leptotyphlopinae	Fossorial
352	*Rena*	*humilis*	Leptotyphlopidae	Leptotyphlopinae	Fossorial
353	*Lichanura*	*trivirgata*	Charinidae	Charininae	Semifossorial
354	*Lichanura*	*trivirgata*	Charinidae	Charininae	Semifossorial
355	*Lichanura*	*trivirgata*	Charinidae	Charininae	Semifossorial
356	*Lichanura*	*trivirgata*	Charinidae	Charininae	Semifossorial
357	*Lichanura*	*trivirgata*	Charinidae	Charininae	Semifossorial
358	*Lichanura*	*trivirgata*	Charinidae	Charininae	Semifossorial
359	*Masticophis*	*fuliginosus*	Colubridae	Colubrinae	Semiarboreal
360	*Masticophis*	*fuliginosus*	Colubridae	Colubrinae	Semiarboreal
361	*Masticophis*	*fuliginosus*	Colubridae	Colubrinae	Semiarboreal
362	*Masticophis*	*flagellum*	Colubridae	Colubrinae	Semiarboreal
363	*Masticophis*	*flagellum*	Colubridae	Colubrinae	Semiarboreal
364	*Masticophis*	*flagellum*	Colubridae	Colubrinae	Semiarboreal
365	*Masticophis*	*lateralis*	Colubridae	Colubrinae	Semiarboreal
366	*Masticophis*	*lateralis*	Colubridae	Colubrinae	Semiarboreal
367	*Masticophis*	*lateralis*	Colubridae	Colubrinae	Semiarboreal

Table B1. (continued)

368	*Masticophis*	*lateralis*	Colubridae	Colubrinae	Semiarboreal
369	*Masticophis*	*lateralis*	Colubridae	Colubrinae	Semiarboreal
370	*Masticophis*	*lateralis*	Colubridae	Colubrinae	Semiarboreal
371	*Masticophis*	*taeniatus*	Colubridae	Colubrinae	Arboreal
372	*Masticophis*	*taeniatus*	Colubridae	Colubrinae	Arboreal
373	*Masticophis*	*taeniatus*	Colubridae	Colubrinae	Arboreal
374	*Masticophis*	*taeniatus*	Colubridae	Colubrinae	Arboreal
375	*Micrurus*	*fulvius*	Elapidae	Elapinae	Fossorial
376	*Micrurus*	*fulvius*	Elapidae	Elapinae	Fossorial
377	*Micrurus*	*fulvius*	Elapidae	Elapinae	Fossorial
378	*Micrurus*	*spixii*	Elapidae	Elapinae	Fossorial
379	*Naja*	*naja*	Elapidae	Elapinae	Terrestrial
380	*Nerodia*	*cyclopion*	Colubridae	Natricinae	Aquatic
381	*Nerodia*	*cyclopion*	Colubridae	Natricinae	Aquatic
382	*Nerodia*	*cyclopion*	Colubridae	Natricinae	Aquatic
383	*Nerodia*	*taxispilota*	Colubridae	Natricinae	Aquatic
384	*Nerodia*	*taxispilota*	Colubridae	Natricinae	Aquatic
385	*Nerodia*	*taxispilota*	Colubridae	Natricinae	Aquatic
386	*Opheodrys*	*vernalis*	Colubridae	Colubrinae	Semiarboreal
387	*Opheodrys*	*vernalis*	Colubridae	Colubrinae	Semiarboreal
388	*Oxybelis*	*sp*	Colubridae	Colubrinae	Arboreal
389	*Oxybelis*	*sp*	Colubridae	Colubrinae	Arboreal
390	*Oxybelis*	*sp*	Colubridae	Colubrinae	Arboreal
391	*Pelamis*	*platura*	Elapidae	Hydrophiinae	Aquatic
392	*Pelamis*	*platura*	Elapidae	Hydrophiinae	Aquatic
393	*Pelamis*	*platura*	Elapidae	Hydrophiinae	Aquatic
394	*Phyllorhynchus*	*browni*	Colubridae	Colubrinae	Fossorial
395	*Phyllorhynchus*	*browni*	Colubridae	Colubrinae	Fossorial
396	*Phyllorhynchus*	*browni*	Colubridae	Colubrinae	Fossorial
397	*Pituophis*	*catenifer*	Colubridae	Colubrinae	Semifossorial
398	*Pituophis*	*catenifer*	Colubridae	Colubrinae	Semifossorial
399	*Pituophis*	*catenifer*	Colubridae	Colubrinae	Semifossorial
400	*Pituophis*	*catenifer*	Colubridae	Colubrinae	Semifossorial
401	*Pituophis*	*melanoleucas*	Colubridae	Colubrinae	Semifossorial
402	*Pituophis*	*melanoleucas*	Colubridae	Colubrinae	Semifossorial
403	*Pituophis*	*melanoleucas*	Colubridae	Colubrinae	Semifossorial
404	*Pituophis*	*sayi*	Colubridae	Colubrinae	Semifossorial

Table B1. (continued)

405	*Pituophis*	*sayi*	Colubridae	Colubrinae	Semifossorial
406	*Pituophis*	*sayi*	Colubridae	Colubrinae	Semifossorial
407	*Malayopython*	*reticulatus*	Pythonidae	Pythoninae	Terrestrial
408	*Salvadora*	*lineata*	Colubridae	Colubrinae	Semiarboreal
409	*Salvadora*	*lineata*	Colubridae	Colubrinae	Semiarboreal
410	*Salvadora*	*lineata*	Colubridae	Colubrinae	Semiarboreal
411	*Sistrurus*	*catenatus*	Viperidae	Crotalinae	Terrestrial
412	*Sistrurus*	*catenatus*	Viperidae	Crotalinae	Terrestrial
413	*Sistrurus*	*catenatus*	Viperidae	Crotalinae	Terrestrial
414	*Sistrurus*	*miliarus*	Viperidae	Crotalinae	Terrestrial
415	*Sistrurus*	*miliarus*	Viperidae	Crotalinae	Terrestrial
416	*Sistrurus*	*miliarus*	Viperidae	Crotalinae	Terrestrial
417	*Sistrurus*	*miliarus*	Viperidae	Crotalinae	Terrestrial
418	*Storeria*	*dekayi*	Colubridae	Natricinae	Terrestrial
419	*Storeria*	*dekayi*	Colubridae	Natricinae	Terrestrial
420	*Storeria*	*dekayi*	Colubridae	Natricinae	Terrestrial
421	*Tantilla*	*coronata*	Colubridae	Colubrinae	Semifossorial
422	*Tantilla*	*coronata*	Colubridae	Colubrinae	Semifossorial
423	*Tantilla*	*coronata*	Colubridae	Colubrinae	Semifossorial
424	*Tantilla*	*planiceps*	Colubridae	Colubrinae	Fossorial
425	*Tantilla*	*planiceps*	Colubridae	Colubrinae	Fossorial
426	*Tantilla*	*planiceps*	Colubridae	Colubrinae	Fossorial
427	*Thamnophis*	*hammondii*	Colubridae	Natricinae	Aquatic
428	*Thamnophis*	*hammondii*	Colubridae	Natricinae	Aquatic
429	*Thamnophis*	*hammondii*	Colubridae	Natricinae	Aquatic
430	*Thamnophis*	*ordinoides*	Colubridae	Natricinae	Terrestrial
431	*Thamnophis*	*ordinoides*	Colubridae	Natricinae	Terrestrial
432	*Thamnophis*	*ordinoides*	Colubridae	Natricinae	Terrestrial
433	*Thamnophis*	*radix*	Colubridae	Natricinae	Terrestrial
434	*Thamnophis*	*radix*	Colubridae	Natricinae	Terrestrial
435	*Thamnophis*	*radix*	Colubridae	Natricinae	Terrestrial
436	*Thamnophis*	*radix*	Colubridae	Natricinae	Terrestrial
437	*Thamnophis*	*radix*	Colubridae	Natricinae	Terrestrial
438	*Thamnophis*	*radix*	Colubridae	Natricinae	Terrestrial
439	*Tropidoclonion*	*lineatum*	Colubridae	Natricinae	Semifossorial
440	*Tropidoclonion*	*lineatum*	Colubridae	Natricinae	Semifossorial
441	*Tropidoclonion*	*lineatum*	Colubridae	Natricinae	Semifossorial

Table B1. (continued)

442	*Crotalus*	*willardi*	Viperidae	Crotalinae	Terrestrial
443	*Ficimia*	*streckeri*	Colubridae	Colubrinae	Fossorial
444	*Gyalopion*	*canum*	Colubridae	Colubrinae	Fossorial
445	*Hypsiglena*	*torquata*	Colubridae	Dipsadinae	Terrestrial
446	*Nerodia*	*paucimaculata*	Colubridae	Natricinae	Aquatic
447	*Tantilla*	*gracilis*	Colubridae	Colubrinae	Semifossorial
448	*Tantilla*	*hobartsmithi*	Colubridae	Colubrinae	Semifossorial
449	*Tantilla*	*nigriceps*	Colubridae	Colubrinae	Semifossorial
450	*Agkistrodon*	*bilineatus*	Viperidae	Crotalinae	Semiaquatic
451	*Agkistrodon*	*bilineatus*	Viperidae	Crotalinae	Semiaquatic
452	*Agkistrodon*	*piscivorus*	Viperidae	Crotalinae	Semiaquatic
453	*Agkistrodon*	*piscivorus*	Viperidae	Crotalinae	Semiaquatic
454	*Bitis*	*arietans*	Viperidae	Viperinae	Terrestrial
455	*Bitis*	*gabonica*	Viperidae	Viperinae	Terrestrial
456	*Boa*	*constrictor*	Boidae	Boinae	Semiarboreal
457	*Carphophis*	*amoenus*	Colubridae	Dipsadinae	Fossorial
458	*Charina*	*bottae*	Charinidae	Charininae	Semifossorial
459	*Chrysopelea*	*pelias*	Colubridae	Ahaetuliinae	Arboreal
460	*Coluber*	*constrictor*	Colubridae	Colubrinae	Semiarboreal
461	*Crotalus*	*adamanteus*	Viperidae	Crotalinae	Terrestrial
462	*Chilabothrus*	*angulifer*	Boidae	Boinae	Arboreal
463	*Farancia*	*abacura*	Colubridae	Dipsadinae	Semiaquatic
464	*Virginia*	*valeriae*	Colubridae	Natricinae	Semifossorial
465	*Heterodon*	*platirhinos*	Colubridae	Dipsadinae	Semifossorial
466	*Lampropeltis*	*calligaster*	Colubridae	Colubrinae	Semifossorial
467	*Lampropeltis*	*triangulum*	Colubridae	Colubrinae	Semifossorial
468	*Lampropeltis*	*getula*	Colubridae	Colubrinae	Terrestrial
469	*Lampropeltis*	*nigra*	Colubridae	Colubrinae	Terrestrial
470	*Lampropeltis*	*elapsoides*	Colubridae	Colubrinae	Semifossorial
471	*Leptodeira*	*annulata*	Colubridae	Dipsadinae	Semiaquatic
472	*Micrurus*	*fulvius*	Elapidae	Elapinae	Fossorial
473	*Naja*	*naja*	Elapidae	Elapinae	Terrestrial
474	*Nerodia*	*cyclopion*	Colubridae	Natricinae	Aquatic
475	*Nerodia*	*erythrogaster*	Colubridae	Natricinae	Semiaquatic
476	*Clonophis*	*kirtlandi*	Colubridae	Natricinae	Semiaquatic
477	*Natrix*	*natrix*	Colubridae	Natricinae	Aquatic
478	*Nerodia*	*rhombifera*	Colubridae	Natricinae	Semiaquatic

Table B1. (continued)

479	*Nerodia*	*taxispilota*	Colubridae	Natricinae	Aquatic
480	*Natrix*	*tessellata*	Colubridae	Natricinae	Aquatic
481	*Opheodrys*	*vernalis*	Colubridae	Colubrinae	Semiarboreal
482	*Oxybelis*	*aeneus*	Colubridae	Colubrinae	Arboreal
483	*Oxybelis*	*fulgidus*	Colubridae	Colubrinae	Arboreal
484	*Phyllorhynchus*	*decurtatus*	Colubridae	Colubrinae	Fossorial
485	*Pituophis*	*catenifer*	Colubridae	Colubrinae	Semifossorial
486	*Pituophis*	*melanoleucas*	Colubridae	Colubrinae	Semifossorial
487	*Pituophis*	*sayi*	Colubridae	Colubrinae	Semifossorial
488	*Pseudaspis*	*cana*	Lamprophiidae	Pseudaspidinae	Fossorial
489	*Rhinocheilus*	*lecontei*	Colubridae	Colubrinae	Semifossorial
490	*Rhadinaea*	*flavilata*	Colubridae	Dipsadinae	Terrestrial
491	*Liodytes*	*pygaea*	Colubridae	Natricinae	Aquatic
492	*Sistrurus*	*catenatus*	Viperidae	Crotalinae	Terrestrial
493	*Sistrurus*	*miliarus*	Viperidae	Crotalinae	Terrestrial
494	*Sonora*	*semiannulata*	Colubridae	Colubrinae	Semifossorial
495	*Spilotes*	*pullatus*	Colubridae	Colubrinae	Arboreal
496	*Storeria*	*dekayi*	Colubridae	Natricinae	Terrestrial
497	*Thamnophis*	*elegans*	Colubridae	Natricinae	Terrestrial
498	*Thamnophis*	*marcianus*	Colubridae	Natricinae	Semiaquatic
499	*Thamnophis*	*ordinoides*	Colubridae	Natricinae	Terrestrial
500	*Thamnophis*	*radix*	Colubridae	Natricinae	Terrestrial
501	*Thamnophis*	*sauritus*	Colubridae	Natricinae	Semiaquatic
502	*Thamnophis*	*sirtalis*	Colubridae	Natricinae	Semiaquatic
503	*Thamnophis*	*sirtalis*	Colubridae	Natricinae	Semiaquatic
504	*Virginia*	*valeriae*	Colubridae	Natricinae	Semifossorial

Table B2. ANOVA results for families within all groups.

	Df	Sum Sq	Mean Sq	F value	Pr(>F)
PC1					
Family	1<0.01	236.09	23.61	43.61	<0.05
Residuals	493.00	266.90	0.54		
PC2					
Family	1<0.01	247.44	24.74	47.73	<0.05
Residuals	493.00	255.56	0.52		
PC3					
Family	1<0.01	30.88	3.09	3.22	<0.05
Residuals	493.00	472.12	0.96		
PC4					
Family	1<0.01	103.36	10.34	12.75	<0.05
Residuals	493.00	399.64	0.81		
PC5					
Family	1<0.01	128.18	12.82	16.86	<0.05
Residuals	493.00	374.82	0.76		
PC6					
Family	1<0.01	112.52	11.25	14.21	<0.05
Residuals	493.00	390.48	0.79		

Table B17. ANOVA results for subfamilies within all groups.

	Df	Sum Sq	Mean Sq	F	Pr(>F)
PC1					
Subfamily	15.00	268.88	17.93	37.36	<0.05
Residuals	488.00	234.12	0.48		
PC2					
Subfamily	15.00	279.02	18.60	40.53	<0.05
Residuals	488.00	223.98	0.46		
PC3					
Subfamily	15.00	37.11	2.47	2.59	<0.05
Residuals	488.00	465.89	0.95		
PC4					
Subfamily	15.00	140.33	9.36	12.59	<0.05
Residuals	488.00	362.67	0.74		
PC5					
Subfamily	15.00	223.15	14.88	25.94	<0.05
Residuals	488.00	279.85	0.57		
PC6					
Subfamily	15.00	140.79	9.39	12.65	<0.05
Residuals	488.00	362.21	0.74		

Table B4. ANOVA results for genera within all groups.

	Df	Sum Sq	Mean Sq	F	Pr(>F)
PC1					
Genus	88.00	408.01	4.64	20.26	<0.05
Residuals	415.00	94.99	0.23		
PC2					
Genus	88.00	413.03	4.69	21.65	<0.05
Residuals	415.00	89.97	0.22		
PC3					
Genus	88.00	261.39	2.97	5.10	<0.05
Residuals	415.00	241.61	0.58		
PC4					
Genus	88.00	296.07	3.36	6.75	<0.05
Residuals	415.00	206.93	0.50		
PC5					
Genus	88.00	367.97	4.18	12.85	<0.05
Residuals	415.00	135.03	0.33		
PC6					
Genus	88.00	268.88	3.06	5.42	<0.05
Residuals	415.00	234.12	0.56		

Table B5. ANOVA results for species within all groups.

	Df	Sum Sq	Mean Sq	F	Pr(>F)
PC1					
Species	188.00	450.56	2.40	14.40	<0.05
Residuals	315.00	52.44	0.17		
PC2					
Species	188.00	437.08	2.32	11.11	<0.05
Residuals	315.00	65.92	0.21		
PC3					
Species	188.00	373.55	1.99	4.84	<0.05
Residuals	315.00	129.45	0.41		
PC4					
Species	188.00	377.82	2.01	5.06	<0.05
Residuals	315.00	125.18	0.40		
PC5					
Species	188.00	375.30	2.00	4.92	<0.05
Residuals	315.00	127.70	0.41		
PC6					
Species	188.00	362.78	1.93	4.34	<0.05
Residuals	315.00	140.22	0.45		

Table B6. ANOVA results for primary foraging habitats within all groups.

	Df	Sum Sq	Mean Sq	F	Pr(>F)
PC1					
Substrate	6.00	137.41	22.90	31.13	<0.05
Residuals	497.00	365.59	0.74		
PC2					
Substrate	6.00	98.36	16.39	20.13	<0.05
Residuals	497.00	404.64	0.81		
PC3					
Substrate	6.00	45.35	7.56	8.21	<0.05
Residuals	497.00	457.65	0.92		
PC4					
Substrate	6.00	15.82	2.64	2.69	<0.05
Residuals	497.00	487.18	0.98		
PC5					
Substrate	6.00	119.87	19.98	25.92	<0.05
Residuals	497.00	383.13	0.77		
PC6					
Substrate	6.00	110.39	18.40	23.29	<0.05
Residuals	497.00	392.61	0.79		

Table B7. ANOVA results for genera within Crotalinae.

	Df	Sum Sq	Mean Sq	F value	Pr(>F)
PC1					
Crotalinae	4	30.06	7.51	10.48	<0.05
Residuals	92	65.94	0.72		
PC2					
Crotalinae	4	19.66	4.91	5.92	<0.05
Residuals	92	76.34	0.83		
PC3					
Crotalinae	4	21.01	5.25	6.44	<0.05
Residuals	92	74.99	0.82		
PC4					
Crotalinae	4	22.12	5.53	6.88	<0.05
Residuals	92	73.89	0.80		
PC5					
Crotalinae	4	1.02	0.25	0.25	0.91
Residuals	92	94.98	1.03		
PC6					
Crotalinae	4	27.00	6.75	9.00	<0.05
Residuals	92	69.00	0.75		

Table B8. ANOVA results for species within Crotalinae.

	Df	Sum Sq	Mean Sq	F value	Pr(>F)
PC1					
Crotalinae	23.00	71.13	3.09	9.08	<0.05
Residuals	73.00	24.88	0.34		
PC2					
Crotalinae	23.00	56.22	2.44	4.49	<0.05
Residuals	73.00	39.78	0.54		
PC3					
Crotalinae	23.00	53.66	2.33	4.02	<0.05
Residuals	73.00	42.34	0.58		
PC4					
Crotalinae	23.00	62.19	2.70	5.84	<0.05
Residuals	73.00	33.81	0.46		
PC5					
Crotalinae	23.00	59.82	2.60	5.25	<0.05
Residuals	73.00	36.18	0.50		
PC6					
Crotalinae	23.00	45.61	1.98	2.87	<0.05
Residuals	73.00	50.39	0.69		

Table B9. ANOVA results for primary foraging ecology within Crotalinae.

	Df	Sum Sq	Mean Sq	F value	Pr(>F)
PC1					
Crotalinae	2.00	19.35	9.68	11.87	<0.05
Residuals	94.00	76.65	0.82		
PC2					
Crotalinae	2.00	0.30	0.15	0.15	0.86
Residuals	94.00	95.70	1.02		
PC3					
Crotalinae	2.00	6.14	3.07	3.21	<0.05
Residuals	94.00	89.86	0.96		
PC4					
Crotalinae	2.00	16.10	8.05	9.47	<0.05
Residuals	94.00	79.90	0.85		
PC5					
Crotalinae	2.00	6.36	3.18	3.33	<0.05
Residuals	94.00	89.64	0.95		
PC6					
Crotalinae	2.00	19.70	9.85	12.13	<0.05
Residuals	94.00	76.31	0.81		

Table B10. Tukey's test results of family-level taxonomy for PCs 1-6 of the all-groups data.

PC1 All	diff	lwr	upr	p adj
Candoiidae-Boidae	-0.50	-2.94	1.93	1.00
Charinidae-Boidae	1.30	0.49	2.10	<0.01
Colubridae-Boidae	0.88	0.35	1.42	<0.01
Elapidae-Boidae	1.03	0.29	1.76	<0.01
Lamprophiidae-Boidae	0.47	-1.97	2.90	1.00
Leptotyphlopidae-Boidae	3.31	2.21	4.41	<0.01
Loxocemidae-Boidae	0.74	-1.70	3.17	1.00
Pythonidae-Boidae	0.32	-2.11	2.76	1.00
Tropidophiidae-Boidae	0.07	-1.69	1.84	1.00
Viperidae-Boidae	-0.61	-1.18	-0.04	0.03
Charinidae-Candoiidae	1.80	-0.66	4.26	0.39
Colubridae-Candoiidae	1.38	-1.00	3.76	0.73
Elapidae-Candoiidae	1.53	-0.91	3.96	0.63
Lamprophiidae-Candoiidae	0.97	-2.40	4.33	1.00
Leptotyphlopidae-Candoiidae	3.81	1.24	6.38	<0.01
Loxocemidae-Candoiidae	1.24	-2.13	4.60	0.98
Pythonidae-Candoiidae	0.82	-2.54	4.19	1.00
Tropidophiidae-Candoiidae	0.57	-2.34	3.49	1.00
Viperidae-Candoiidae	-0.11	-2.50	2.28	1.00
Colubridae-Charinidae	-0.42	-1.05	0.21	0.54
Elapidae-Charinidae	-0.27	-1.08	0.53	0.99
Lamprophiidae-Charinidae	-0.83	-3.29	1.62	0.99
Leptotyphlopidae-Charinidae	2.01	0.86	3.16	<0.01
Loxocemidae-Charinidae	-0.56	-3.02	1.90	1.00
Pythonidae-Charinidae	-0.97	-3.43	1.48	0.97
Tropidophiidae-Charinidae	-1.22	-3.02	0.57	0.50
Viperidae-Charinidae	-1.91	-2.57	-1.25	<0.01
Elapidae-Colubridae	0.14	-0.39	0.68	1.00
Lamprophiidae-Colubridae	-0.42	-2.80	1.97	1.00
Leptotyphlopidae-Colubridae	2.43	1.45	3.41	<0.01
Loxocemidae-Colubridae	-0.14	-2.53	2.24	1.00
Pythonidae-Colubridae	-0.56	-2.94	1.83	1.00
Tropidophiidae-Colubridae	-0.81	-2.49	0.88	0.90
Viperidae-Colubridae	-1.49	-1.76	-1.22	<0.01
Lamprophiidae-Elapidae	-0.56	-3.00	1.88	1.00
Leptotyphlopidae-Elapidae	2.28	1.18	3.38	<0.01

Table B10. (continued)

Loxocemidae-Elapidae	-0.29	-2.72	2.15	1.00
Pythonidae-Elapidae	-0.70	-3.14	1.73	1.00
Tropidophiidae-Elapidae	-0.95	-2.71	0.81	0.81
Viperidae-Elapidae	-1.64	-2.21	-1.06	<0.01
Leptotyphlopidae-Lamprophiidae	2.84	0.27	5.41	0.02
Loxocemidae-Lamprophiidae	0.27	-3.09	3.64	1.00
Pythonidae-Lamprophiidae	-0.14	-3.51	3.22	1.00
Tropidophiidae-Lamprophiidae	-0.39	-3.31	2.52	1.00
Viperidae-Lamprophiidae	-1.08	-3.47	1.32	0.93
Loxocemidae-Leptotyphlopidae	-2.57	-5.14	<0.01	0.05
Pythonidae-Leptotyphlopidae	-2.98	-5.55	-0.41	0.01
Tropidophiidae-Leptotyphlopidae	-3.23	-5.18	-1.29	<0.01
Viperidae-Leptotyphlopidae	-3.92	-4.92	-2.92	<0.01
Pythonidae-Loxocemidae	-0.41	-3.78	2.95	1.00
Tropidophiidae-Loxocemidae	-0.66	-3.58	2.25	1.00
Viperidae-Loxocemidae	-1.35	-3.74	1.04	0.77
Tropidophiidae-Pythonidae	-0.25	-3.16	2.66	1.00
Viperidae-Pythonidae	-0.93	-3.33	1.46	0.97
Viperidae-Tropidophiidae	-0.68	-2.38	1.02	0.97
PC2 All				
Candoiidae-Boidae	0.39	-1.99	2.77	1.00
Charinidae-Boidae	1.42	0.64	2.21	<0.01
Colubridae-Boidae	-1.36	-1.88	-0.83	<0.01
Elapidae-Boidae	-1.04	-1.76	-0.33	<0.01
Lamprophiidae-Boidae	-1.08	-3.46	1.30	0.93
Leptotyphlopidae-Boidae	0.44	-0.63	1.52	0.96
Loxocemidae-Boidae	1.10	-1.28	3.48	0.92
Pythonidae-Boidae	-0.06	-2.44	2.33	1.00
Tropidophiidae-Boidae	-0.27	-1.99	1.45	1.00
Viperidae-Boidae	-0.12	-0.67	0.44	1.00
Charinidae-Candoiidae	1.03	-1.37	3.44	0.95
Colubridae-Candoiidae	-1.75	-4.08	0.58	0.35
Elapidae-Candoiidae	-1.44	-3.82	0.95	0.68
Lamprophiidae-Candoiidae	-1.47	-4.76	1.82	0.94
Leptotyphlopidae-Candoiidae	0.05	-2.46	2.57	1.00
Loxocemidae-Candoiidae	0.71	-2.59	4.00	1.00
Pythonidae-Candoiidae	-0.45	-3.74	2.85	1.00

Table B10. (continued)

Tropidophiidae-Candoiidae	-0.66	-3.51	2.19	1.00
Viperidae-Candoiidae	-0.51	-2.85	1.83	1.00
Colubridae-Charinidae	-2.78	-3.39	-2.17	<0.01
Elapidae-Charinidae	-2.47	-3.25	-1.68	<0.01
Lamprophiidae-Charinidae	-2.50	-4.91	-0.10	0.03
Leptotyphlopidae-Charinidae	-0.98	-2.10	0.15	0.16
Loxocemidae-Charinidae	-0.32	-2.73	2.08	1.00
Pythonidae-Charinidae	-1.48	-3.88	0.93	0.66
Tropidophiidae-Charinidae	-1.69	-3.45	0.06	0.07
Viperidae-Charinidae	-1.54	-2.18	-0.89	<0.01
Elapidae-Colubridae	0.31	-0.21	0.84	0.69
Lamprophiidae-Colubridae	0.28	-2.05	2.61	1.00
Leptotyphlopidae-Colubridae	1.80	0.84	2.76	<0.01
Loxocemidae-Colubridae	2.46	0.12	4.79	0.03
Pythonidae-Colubridae	1.30	-1.03	3.63	0.78
Tropidophiidae-Colubridae	1.09	-0.56	2.74	0.56
Viperidae-Colubridae	1.24	0.98	1.51	<0.01
Lamprophiidae-Elapidae	-0.03	-2.42	2.35	1.00
Leptotyphlopidae-Elapidae	1.49	0.41	2.57	<0.01
Loxocemidae-Elapidae	2.14	-0.24	4.53	0.12
Pythonidae-Elapidae	0.99	-1.39	3.37	0.96
Tropidophiidae-Elapidae	0.77	-0.95	2.50	0.93
Viperidae-Elapidae	0.93	0.37	1.49	<0.01
Leptotyphlopidae-Lamprophiidae	1.52	-0.99	4.04	0.68
Loxocemidae-Lamprophiidae	2.18	-1.11	5.47	0.55
Pythonidae-Lamprophiidae	1.02	-2.27	4.32	1.00
Tropidophiidae-Lamprophiidae	0.81	-2.04	3.66	1.00
Viperidae-Lamprophiidae	0.96	-1.38	3.30	0.96
Loxocemidae-Leptotyphlopidae	0.65	-1.86	3.17	1.00
Pythonidae-Leptotyphlopidae	-0.50	-3.01	2.02	1.00
Tropidophiidae-Leptotyphlopidae	-0.71	-2.62	1.19	0.98
Viperidae-Leptotyphlopidae	-0.56	-1.54	0.42	0.75
Pythonidae-Loxocemidae	-1.15	-4.45	2.14	0.99
Tropidophiidae-Loxocemidae	-1.37	-4.22	1.48	0.90
Viperidae-Loxocemidae	-1.21	-3.55	1.13	0.85
Tropidophiidae-Pythonidae	-0.21	-3.07	2.64	1.00
Viperidae-Pythonidae	-0.06	-2.40	2.28	1.00

Table B10. (continued)

Viperidae-Tropidophiidae	0.15	-1.51	1.82	1.00
PC3 All				
Candoiidae-Boidae	-0.18	-3.42	3.06	1.00
Charinidae-Boidae	-0.93	-2.00	0.14	0.15
Colubridae-Boidae	-0.48	-1.19	0.24	0.53
Elapidae-Boidae	-0.40	-1.38	0.57	0.96
Lamprophiidae-Boidae	-0.75	-3.99	2.49	1.00
Leptotyphlopidae-Boidae	0.83	-0.64	2.29	0.76
Loxocemidae-Boidae	-0.67	-3.91	2.57	1.00
Pythonidae-Boidae	-1.42	-4.66	1.82	0.94
Tropidophiidae-Boidae	0.34	-2.00	2.68	1.00
Viperidae-Boidae	-0.08	-0.84	0.68	1.00
Charinidae-Candoiidae	-0.75	-4.02	2.52	1.00
Colubridae-Candoiidae	-0.29	-3.46	2.88	1.00
Elapidae-Candoiidae	-0.22	-3.46	3.02	1.00
Lamprophiidae-Candoiidae	-0.57	-5.04	3.91	1.00
Leptotyphlopidae-Candoiidae	1.01	-2.40	4.43	1.00
Loxocemidae-Candoiidae	-0.48	-4.96	3.99	1.00
Pythonidae-Candoiidae	-1.23	-5.71	3.24	1.00
Tropidophiidae-Candoiidae	0.52	-3.35	4.40	1.00
Viperidae-Candoiidae	0.11	-3.08	3.29	1.00
Colubridae-Charinidae	0.46	-0.38	1.29	0.80
Elapidae-Charinidae	0.53	-0.54	1.60	0.88
Lamprophiidae-Charinidae	0.18	-3.09	3.45	1.00
Leptotyphlopidae-Charinidae	1.76	0.23	3.29	0.01
Loxocemidae-Charinidae	0.27	-3.00	3.54	1.00
Pythonidae-Charinidae	-0.48	-3.75	2.78	1.00
Tropidophiidae-Charinidae	1.27	-1.11	3.66	0.82
Viperidae-Charinidae	0.86	-0.02	1.73	0.06
Elapidae-Colubridae	0.07	-0.64	0.78	1.00
Lamprophiidae-Colubridae	-0.28	-3.45	2.89	1.00
Leptotyphlopidae-Colubridae	1.31	<0.01	2.61	0.05
Loxocemidae-Colubridae	-0.19	-3.36	2.98	1.00
Pythonidae-Colubridae	-0.94	-4.11	2.23	1.00
Tropidophiidae-Colubridae	0.82	-1.43	3.06	0.98
Viperidae-Colubridae	0.40	0.04	0.76	0.02
Lamprophiidae-Elapidae	-0.35	-3.59	2.89	1.00

Table B10. (continued)

Leptotyphlopidae-Elapidae	1.23	-0.23	2.70	0.19
PC4 All				
Candoiidae-Boidae	0.59	-2.39	3.57	1.00
Charinidae-Boidae	-0.62	-1.60	0.37	0.63
Colubridae-Boidae	-0.56	-1.21	0.10	0.18
Elapidae-Boidae	-1.85	-2.75	-0.96	<0.01
Lamprophiidae-Boidae	-0.45	-3.43	2.53	1.00
Leptotyphlopidae-Boidae	2.02	0.67	3.37	<0.01
Loxocemidae-Boidae	-1.49	-4.47	1.49	0.88
Pythonidae-Boidae	0.55	-2.43	3.53	1.00
Tropidophiidae-Boidae	-1.75	-3.91	0.40	0.24
Viperidae-Boidae	-1.00	-1.70	-0.30	<0.01
Charinidae-Candoiidae	-1.21	-4.22	1.80	0.97
Colubridae-Candoiidae	-1.15	-4.07	1.77	0.97
Elapidae-Candoiidae	-2.45	-5.43	0.54	0.22
Lamprophiidae-Candoiidae	-1.04	-5.16	3.08	1.00
Leptotyphlopidae-Candoiidae	1.43	-1.72	4.57	0.93
Loxocemidae-Candoiidae	-2.08	-6.19	2.04	0.87
Pythonidae-Candoiidae	-0.04	-4.16	4.08	1.00
Tropidophiidae-Candoiidae	-2.34	-5.91	1.22	0.56
Viperidae-Candoiidae	-1.59	-4.52	1.33	0.80
Colubridae-Charinidae	0.06	-0.71	0.83	1.00
Elapidae-Charinidae	-1.23	-2.22	-0.25	<0.01
Lamprophiidae-Charinidae	0.17	-2.83	3.18	1.00
Leptotyphlopidae-Charinidae	2.64	1.23	4.05	<0.01
Loxocemidae-Charinidae	-0.87	-3.87	2.14	1.00
Pythonidae-Charinidae	1.17	-1.84	4.18	0.98
Tropidophiidae-Charinidae	-1.13	-3.33	1.06	0.85
Viperidae-Charinidae	-0.38	-1.19	0.42	0.91
Elapidae-Colubridae	-1.29	-1.95	-0.64	<0.01
Lamprophiidae-Colubridae	0.11	-2.80	3.03	1.00
Leptotyphlopidae-Colubridae	2.58	1.38	3.78	<0.01
Loxocemidae-Colubridae	-0.93	-3.84	1.99	0.99
Pythonidae-Colubridae	1.11	-1.81	4.02	0.98
Tropidophiidae-Colubridae	-1.19	-3.26	0.87	0.74
Viperidae-Colubridae	-0.44	-0.78	-0.11	<0.01
Lamprophiidae-Elapidae	1.41	-1.57	4.39	0.91

Table B10. (continued)

Leptotyphlopidae-Elapidae	3.87	2.53	5.22	<0.01
Loxocemidae-Elapidae	0.37	-2.61	3.35	1.00
Pythonidae-Elapidae	2.40	-0.58	5.38	0.25
Tropidophiidae-Elapidae	0.10	-2.05	2.26	1.00
Viperidae-Elapidae	0.85	0.15	1.55	<0.01
Leptotyphlopidae-Lamprophiidae	2.47	-0.68	5.61	0.29
Loxocemidae-Lamprophiidae	-1.04	-5.16	3.08	1.00
Pythonidae-Lamprophiidae	1.00	-3.12	5.11	1.00
Tropidophiidae-Lamprophiidae	-1.31	-4.87	2.26	0.98
Viperidae-Lamprophiidae	-0.56	-3.48	2.37	1.00
Loxocemidae-Leptotyphlopidae	-3.50	-6.65	-0.36	0.02
Pythonidae-Leptotyphlopidae	-1.47	-4.61	1.68	0.92
Tropidophiidae-Leptotyphlopidae	-3.77	-6.15	-1.40	<0.01
Viperidae-Leptotyphlopidae	-3.02	-4.25	-1.80	<0.01
Pythonidae-Loxocemidae	2.04	-2.08	6.15	0.88
Tropidophiidae-Loxocemidae	-0.27	-3.83	3.30	1.00
Viperidae-Loxocemidae	0.48	-2.44	3.41	1.00
Tropidophiidae-Pythonidae	-2.30	-5.87	1.26	0.59
Viperidae-Pythonidae	-1.55	-4.48	1.37	0.83
Viperidae-Tropidophiidae	0.75	-1.33	2.83	0.99
PC5 All				
Candoiidae-Boidae	0.40	-2.49	3.29	1.00
Charinidae-Boidae	0.79	-0.16	1.74	0.21
Colubridae-Boidae	2.07	1.43	2.70	<0.01
Elapidae-Boidae	1.92	1.05	2.79	<0.01
Lamprophiidae-Boidae	1.94	-0.95	4.82	0.53
Leptotyphlopidae-Boidae	2.33	1.02	3.63	<0.01
Loxocemidae-Boidae	0.25	-2.64	3.13	1.00
Pythonidae-Boidae	-0.53	-3.42	2.35	1.00
Tropidophiidae-Boidae	1.57	-0.51	3.66	0.35
Viperidae-Boidae	2.28	1.61	2.96	<0.01
Charinidae-Candoiidae	0.39	-2.52	3.30	1.00
Colubridae-Candoiidae	1.67	-1.16	4.49	0.71
Elapidae-Candoiidae	1.52	-1.37	4.41	0.83
Lamprophiidae-Candoiidae	1.54	-2.45	5.52	0.98
Leptotyphlopidae-Candoiidae	1.93	-1.12	4.97	0.62
Loxocemidae-Candoiidae	-0.15	-4.14	3.83	1.00

Table B10. (continued)

Pythonidae-Candoiidae	-0.93	-4.92	3.05	1.00
Tropidophiidae-Candoiidae	1.17	-2.28	4.63	0.99
Viperidae-Candoiidae	1.88	-0.95	4.72	0.54
Colubridae-Charinidae	1.28	0.53	2.02	<0.01
Elapidae-Charinidae	1.13	0.18	2.08	0.01
Lamprophiidae-Charinidae	1.15	-1.77	4.06	0.97
Leptotyphlopidae-Charinidae	1.54	0.17	2.90	0.01
Loxocemidae-Charinidae	-0.54	-3.46	2.37	1.00
Pythonidae-Charinidae	-1.32	-4.24	1.59	0.93
Tropidophiidae-Charinidae	0.78	-1.34	2.90	0.98
Viperidae-Charinidae	1.49	0.71	2.28	<0.01
Elapidae-Colubridae	-0.15	-0.78	0.49	1.00
Lamprophiidae-Colubridae	-0.13	-2.95	2.69	1.00
Leptotyphlopidae-Colubridae	0.26	-0.90	1.42	1.00
Loxocemidae-Colubridae	-1.82	-4.64	1.00	0.59
Pythonidae-Colubridae	-2.60	-5.43	0.22	0.10
Tropidophiidae-Colubridae	-0.49	-2.49	1.50	1.00
Viperidae-Colubridae	0.22	-0.10	0.54	0.51
Lamprophiidae-Elapidae	0.02	-2.87	2.90	1.00
Leptotyphlopidae-Elapidae	0.41	-0.90	1.71	1.00
Loxocemidae-Elapidae	-1.67	-4.56	1.21	0.73
Pythonidae-Elapidae	-2.45	-5.34	0.43	0.18
Tropidophiidae-Elapidae	-0.35	-2.43	1.74	1.00
Viperidae-Elapidae	0.37	-0.31	1.04	0.81
Leptotyphlopidae-Lamprophiidae	0.39	-2.66	3.44	1.00
Loxocemidae-Lamprophiidae	-1.69	-5.68	2.30	0.95
Pythonidae-Lamprophiidae	-2.47	-6.46	1.52	0.65
Tropidophiidae-Lamprophiidae	-0.36	-3.82	3.09	1.00
Viperidae-Lamprophiidae	0.35	-2.49	3.18	1.00
Loxocemidae-Leptotyphlopidae	-2.08	-5.13	0.97	0.50
Pythonidae-Leptotyphlopidae	-2.86	-5.91	0.18	0.09
Tropidophiidae-Leptotyphlopidae	-0.76	-3.06	1.55	0.99
Viperidae-Leptotyphlopidae	-0.04	-1.23	1.14	1.00
Pythonidae-Loxocemidae	-0.78	-4.77	3.21	1.00
Tropidophiidae-Loxocemidae	1.33	-2.13	4.78	0.98
Viperidae-Loxocemidae	2.04	-0.80	4.87	0.42
Tropidophiidae-Pythonidae	2.11	-1.35	5.56	0.67

Table B10. (continued)

Viperidae-Pythonidae	2.82	-0.01	5.65	0.05
Viperidae-Tropidophiidae	0.71	-1.30	2.73	0.99
PC6 All				
Candoiidae-Boidae	-0.62	-3.57	2.33	1.00
Charinidae-Boidae	-0.03	-1.01	0.94	1.00
Colubridae-Boidae	-0.87	-1.52	-0.22	<0.01
Elapidae-Boidae	-1.77	-2.66	-0.88	<0.01
Lamprophiidae-Boidae	-0.29	-3.23	2.66	1.00
Leptotyphlopidae-Boidae	-2.42	-3.76	-1.09	<0.01
Loxocemidae-Boidae	0.09	-2.86	3.03	1.00
Pythonidae-Boidae	-0.11	-3.06	2.83	1.00
Tropidophiidae-Boidae	-1.11	-3.24	1.02	0.84
Viperidae-Boidae	-1.67	-2.36	-0.98	<0.01
Charinidae-Candoiidae	0.59	-2.38	3.56	1.00
Colubridae-Candoiidae	-0.25	-3.13	2.63	1.00
Elapidae-Candoiidae	-1.15	-4.10	1.80	0.97
Lamprophiidae-Candoiidae	0.33	-3.74	4.40	1.00
Leptotyphlopidae-Candoiidae	-1.80	-4.91	1.30	0.73
Loxocemidae-Candoiidae	0.71	-3.36	4.78	1.00
Pythonidae-Candoiidae	0.51	-3.56	4.58	1.00
Tropidophiidae-Candoiidae	-0.49	-4.01	3.04	1.00
Viperidae-Candoiidae	-1.05	-3.95	1.84	0.98
Colubridae-Charinidae	-0.84	-1.60	-0.08	0.02
Elapidae-Charinidae	-1.74	-2.71	-0.76	<0.01
Lamprophiidae-Charinidae	-0.25	-3.23	2.72	1.00
Leptotyphlopidae-Charinidae	-2.39	-3.78	-1.00	<0.01
Loxocemidae-Charinidae	0.12	-2.85	3.09	1.00
Pythonidae-Charinidae	-0.08	-3.05	2.89	1.00
Tropidophiidae-Charinidae	-1.08	-3.24	1.09	0.88
Viperidae-Charinidae	-1.64	-2.44	-0.84	<0.01
Elapidae-Colubridae	-0.90	-1.55	-0.25	<0.01
Lamprophiidae-Colubridae	0.58	-2.30	3.47	1.00
Leptotyphlopidae-Colubridae	-1.55	-2.74	-0.37	<0.01
Loxocemidae-Colubridae	0.96	-1.93	3.84	0.99
Pythonidae-Colubridae	0.76	-2.12	3.64	1.00
Tropidophiidae-Colubridae	-0.24	-2.28	1.80	1.00
Viperidae-Colubridae	-0.80	-1.13	-0.47	<0.01

Table B10. (continued)

Lamprophiidae-Elapidae	1.48	-1.46	4.43	0.87
Leptotyphlopidae-Elapidae	-0.65	-1.99	0.68	0.89
Loxocemidae-Elapidae	1.86	-1.09	4.80	0.62
Pythonidae-Elapidae	1.66	-1.29	4.60	0.77
Tropidophiidae-Elapidae	0.66	-1.47	2.79	1.00
Viperidae-Elapidae	0.10	-0.59	0.79	1.00
Leptotyphlopidae-Lamprophiidae	-2.14	-5.25	0.97	0.49
Loxocemidae-Lamprophiidae	0.37	-3.70	4.44	1.00
Pythonidae-Lamprophiidae	0.18	-3.90	4.25	1.00
Tropidophiidae-Lamprophiidae	-0.82	-4.35	2.70	1.00
Viperidae-Lamprophiidae	-1.39	-4.28	1.51	0.90
Loxocemidae-Leptotyphlopidae	2.51	-0.60	5.62	0.25
Pythonidae-Leptotyphlopidae	2.31	-0.80	5.42	0.37
Tropidophiidae-Leptotyphlopidae	1.31	-1.04	3.66	0.77
Viperidae-Leptotyphlopidae	0.75	-0.46	1.96	0.64
Pythonidae-Loxocemidae	-0.20	-4.27	3.87	1.00
Tropidophiidae-Loxocemidae	-1.20	-4.72	2.33	0.99
Viperidae-Loxocemidae	-1.76	-4.65	1.13	0.67
Tropidophiidae-Pythonidae	-1.00	-4.52	2.53	1.00
Viperidae-Pythonidae	-1.56	-4.45	1.33	0.81
Viperidae-Tropidophiidae	-0.56	-2.62	1.49	1.00

Table B11. Tukey's test results of subfamily taxonomy for PCs 1-6 for all groups.

PC1 All	diff	lwr	upr	p adj
Boinae-Ahaetuliinae	-1.19	-2.37	<0.01	0.05
Candoiinae-Ahaetuliinae	-1.69	-4.30	0.93	0.68
Charininae-Ahaetuliinae	0.11	-1.12	1.34	1.00
Colubrinae-Ahaetuliinae	-0.20	-1.28	0.88	1.00
Crotalinae-Ahaetuliinae	-1.79	-2.88	-0.69	<0.01
Dipsadinae-Ahaetuliinae	0.05	-1.07	1.16	1.00
Elapinae-Ahaetuliinae	0.09	-1.13	1.31	1.00
Hydrophiinae-Ahaetuliinae	-0.96	-2.47	0.55	0.71
Leptotyphlopinae-Ahaetuliinae	2.12	0.68	3.57	<0.01
Loxoceminae-Ahaetuliinae	-0.45	-3.06	2.16	1.00
Natricinae-Ahaetuliinae	-0.77	-1.87	0.33	0.53
Pseudaspidinae-Ahaetuliinae	-0.72	-3.33	1.89	1.00
Pythoninae-Ahaetuliinae	-0.86	-3.47	1.75	1.00
Tropidophiinae-Ahaetuliinae	-1.11	-3.11	0.88	0.87
Viperinae-Ahaetuliinae	-2.27	-4.26	-0.27	0.01
Candoiinae-Boinae	-0.50	-2.94	1.94	1.00
Charininae-Boinae	1.30	0.49	2.11	<0.01
Colubrinae-Boinae	0.99	0.44	1.53	<0.01
Crotalinae-Boinae	-0.60	-1.17	-0.03	0.03
Dipsadinae-Boinae	1.23	0.62	1.84	<0.01
Elapinae-Boinae	1.28	0.48	2.07	<0.01
Hydrophiinae-Boinae	0.23	-0.96	1.42	1.00
Leptotyphlopinae-Boinae	3.31	2.20	4.41	<0.01
Loxoceminae-Boinae	0.74	-1.70	3.18	1.00
Natricinae-Boinae	0.42	-0.16	1.00	0.50
Pseudaspidinae-Boinae	0.47	-1.98	2.91	1.00
Pythoninae-Boinae	0.32	-2.12	2.77	1.00
Tropidophiinae-Boinae	0.07	-1.69	1.84	1.00
Viperinae-Boinae	-1.08	-2.84	0.69	0.76
Charininae-Candoiinae	1.80	-0.66	4.26	0.46
Colubrinae-Candoiinae	1.49	-0.91	3.88	0.74
Crotalinae-Candoiinae	-0.10	-2.50	2.30	1.00
Dipsadinae-Candoiinae	1.73	-0.68	4.14	0.49
Elapinae-Candoiinae	1.78	-0.68	4.24	0.48
Hydrophiinae-Candoiinae	0.73	-1.88	3.34	1.00

Table B11. (continued)

Leptotyphlopinae-Candoiinae	3.81	1.23	6.38	<0.01
Loxoceminae-Candoiinae	1.24	-2.14	4.61	1.00
Natricinae-Candoiinae	0.92	-1.48	3.32	1.00
Pseudaspidinae-Candoiinae	0.97	-2.41	4.34	1.00
Pythoninae-Candoiinae	0.82	-2.55	4.20	1.00
Tropidophiinae-Candoiinae	0.57	-2.35	3.50	1.00
Viperinae-Candoiinae	-0.58	-3.50	2.34	1.00
Colubrinae-Charininae	-0.31	-0.95	0.33	0.95
Crotalinae-Charininae	-1.90	-2.56	-1.24	<0.01
Dipsadinae-Charininae	-0.07	-0.76	0.63	1.00
Elapinae-Charininae	-0.02	-0.88	0.83	1.00
Hydrophiinae-Charininae	-1.07	-2.30	0.16	0.18
Leptotyphlopinae-Charininae	2.01	0.86	3.16	<0.01
Loxoceminae-Charininae	-0.56	-3.03	1.90	1.00
Natricinae-Charininae	-0.88	-1.55	-0.22	<0.01
Pseudaspidinae-Charininae	-0.83	-3.30	1.63	1.00
Pythoninae-Charininae	-0.97	-3.44	1.49	0.99
Tropidophiinae-Charininae	-1.22	-3.02	0.57	0.59
Viperinae-Charininae	-2.38	-4.17	-0.58	<0.01
Crotalinae-Colubrinae	-1.59	-1.88	-1.29	<0.01
Dipsadinae-Colubrinae	0.24	-0.12	0.61	0.62
Elapinae-Colubrinae	0.29	-0.33	0.91	0.97
Hydrophiinae-Colubrinae	-0.76	-1.84	0.32	0.54
Leptotyphlopinae-Colubrinae	2.32	1.33	3.31	<0.01
Loxoceminae-Colubrinae	-0.25	-2.64	2.14	1.00
Natricinae-Colubrinae	-0.57	-0.88	-0.26	<0.01
Pseudaspidinae-Colubrinae	-0.52	-2.91	1.87	1.00
Pythoninae-Colubrinae	-0.66	-3.05	1.73	1.00
Tropidophiinae-Colubrinae	-0.91	-2.61	0.78	0.90
Viperinae-Colubrinae	-2.07	-3.76	-0.37	<0.01
Dipsadinae-Crotalinae	1.83	1.43	2.23	<0.01
Elapinae-Crotalinae	1.88	1.23	2.52	<0.01
Hydrophiinae-Crotalinae	0.83	-0.27	1.92	0.40
Leptotyphlopinae-Crotalinae	3.91	2.90	4.91	<0.01
Loxoceminae-Crotalinae	1.34	-1.06	3.74	0.87
Natricinae-Crotalinae	1.02	0.66	1.37	<0.01
Pseudaspidinae-Crotalinae	1.07	-1.33	3.46	0.98

Table B11. (continued)

Pythoninae-Crotalinae	0.92	-1.47	3.32	0.99
Tropidophiinae-Crotalinae	0.67	-1.03	2.38	0.99
Viperinae-Crotalinae	-0.48	-2.18	1.23	1.00
Elapinae-Dipsadinae	0.04	-0.63	0.72	1.00
Hydrophiinae-Dipsadinae	-1.00	-2.12	0.11	0.13
Leptotyphlopinae-Dipsadinae	2.08	1.05	3.10	<0.01
Loxoceminae-Dipsadinae	-0.49	-2.90	1.91	1.00
Natricinae-Dipsadinae	-0.82	-1.23	-0.40	<0.01
Pseudaspidinae-Dipsadinae	-0.76	-3.17	1.64	1.00
Pythoninae-Dipsadinae	-0.91	-3.31	1.50	1.00
Tropidophiinae-Dipsadinae	-1.16	-2.87	0.56	0.61
Viperinae-Dipsadinae	-2.31	-4.03	-0.59	<0.01
Hydrophiinae-Elapinae	-1.05	-2.27	0.17	0.19
Leptotyphlopinae-Elapinae	2.03	0.89	3.17	<0.01
Loxoceminae-Elapinae	-0.54	-3.00	1.92	1.00
Natricinae-Elapinae	-0.86	-1.51	-0.21	<0.01
Pseudaspidinae-Elapinae	-0.81	-3.27	1.65	1.00
Pythoninae-Elapinae	-0.95	-3.41	1.51	0.99
Tropidophiinae-Elapinae	-1.20	-2.99	0.59	0.61
Viperinae-Elapinae	-2.36	-4.14	-0.57	<0.01
Leptotyphlopinae-Hydrophiinae	3.08	1.63	4.52	<0.01
Loxoceminae-Hydrophiinae	0.51	-2.10	3.12	1.00
Natricinae-Hydrophiinae	0.19	-0.91	1.28	1.00
Pseudaspidinae-Hydrophiinae	0.24	-2.38	2.85	1.00
Pythoninae-Hydrophiinae	0.10	-2.52	2.71	1.00
Tropidophiinae-Hydrophiinae	-0.15	-2.15	1.84	1.00
Viperinae-Hydrophiinae	-1.31	-3.30	0.69	0.66
Loxoceminae-Leptotyphlopinae	-2.57	-5.15	0.01	0.05
Natricinae-Leptotyphlopinae	-2.89	-3.90	-1.88	<0.01
Pseudaspidinae-Leptotyphlopinae	-2.84	-5.42	-0.26	0.02
Pythoninae-Leptotyphlopinae	-2.98	-5.56	-0.41	0.01
Tropidophiinae-Leptotyphlopinae	-3.23	-5.18	-1.29	<0.01
Viperinae-Leptotyphlopinae	-4.39	-6.33	-2.44	<0.01
Natricinae-Loxoceminae	-0.32	-2.72	2.08	1.00

Table B11. (continued)

Pseudaspidinae-Loxoceminae	-0.27	-3.64	3.10	1.00
Pythoninae-Loxoceminae	-0.41	-3.79	2.96	1.00
Tropidophiinae-Loxoceminae	-0.66	-3.58	2.26	1.00
Viperinae-Loxoceminae	-1.82	-4.74	1.11	0.74
Pseudaspidinae-Natricinae	0.05	-2.35	2.45	1.00
Pythoninae-Natricinae	-0.09	-2.49	2.31	1.00
Tropidophiinae-Natricinae	-0.34	-2.05	1.36	1.00
Viperinae-Natricinae	-1.49	-3.20	0.21	0.17
Pythoninae-Pseudaspidinae	-0.14	-3.52	3.23	1.00
Tropidophiinae-Pseudaspidinae	-0.39	-3.31	2.53	1.00
Viperinae-Pseudaspidinae	-1.55	-4.47	1.38	0.91
Tropidophiinae-Pythoninae	-0.25	-3.17	2.67	1.00
Viperinae-Pythoninae	-1.40	-4.33	1.52	0.96
Viperinae-Tropidophiinae	-1.15	-3.54	1.23	0.95
PC2 All				
Boinae-Ahaetuliinae	2.38	1.21	3.54	<0.01
Candoiinae-Ahaetuliinae	2.77	0.21	5.32	0.02
Charininae-Ahaetuliinae	3.80	2.59	5.00	<0.01
Colubrinae-Ahaetuliinae	0.86	-0.20	1.92	0.27
Crotalinae-Ahaetuliinae	2.25	1.18	3.32	<0.01
Dipsadinae-Ahaetuliinae	1.43	0.34	2.52	<0.01
Elapinae-Ahaetuliinae	1.73	0.53	2.92	<0.01
Hydrophiinae-Ahaetuliinae	0.06	-1.42	1.53	1.00
Leptotyphlopinae-Ahaetuliinae	2.82	1.41	4.23	<0.01
Loxoceminae-Ahaetuliinae	3.47	0.92	6.03	<0.01
Natricinae-Ahaetuliinae	1.16	0.08	2.23	0.02
Pseudaspidinae-Ahaetuliinae	1.30	-1.26	3.85	0.93
Pythoninae-Ahaetuliinae	2.32	-0.24	4.88	0.13
Tropidophiinae-Ahaetuliinae	2.11	0.15	4.06	0.02
Viperinae-Ahaetuliinae	2.59	0.64	4.54	<0.01
Candoiinae-Boinae	0.39	-2.00	2.78	1.00
Charininae-Boinae	1.42	0.63	2.21	<0.01
Colubrinae-Boinae	-1.51	-2.05	-0.98	<0.01
Crotalinae-Boinae	-0.12	-0.68	0.44	1.00
Dipsadinae-Boinae	-0.95	-1.55	-0.35	<0.01
Elapinae-Boinae	-0.65	-1.42	0.13	0.23

Table B11. (continued)

Hydrophiinae-Boinae	-2.32	-3.48	-1.16	<0.01
Leptotyphlopinae-Boinae	0.44	-0.64	1.52	0.99
Loxoceminae-Boinae	1.10	-1.29	3.49	0.97
Natricinae-Boinae	-1.22	-1.79	-0.65	<0.01
Pseudaspidinae-Boinae	-1.08	-3.47	1.31	0.97
Pythoninae-Boinae	-0.06	-2.44	2.33	1.00
Tropidophiinae-Boinae	-0.27	-2.00	1.46	1.00
Viperinae-Boinae	0.21	-1.51	1.94	1.00
Charininae-Candoiinae	1.03	-1.38	3.44	0.99
Colubrinae-Candoiinae	-1.91	-4.25	0.43	0.27
Crotalinae-Candoiinae	-0.51	-2.86	1.83	1.00
Dipsadinae-Candoiinae	-1.34	-3.69	1.02	0.85
Elapinae-Candoiinae	-1.04	-3.44	1.37	0.98
Hydrophiinae-Candoiinae	-2.71	-5.26	-0.15	0.03
Leptotyphlopinae-Candoiinae	0.05	-2.47	2.57	1.00
Loxoceminae-Candoiinae	0.71	-2.59	4.01	1.00
Natricinae-Candoiinae	-1.61	-3.96	0.74	0.58
Pseudaspidinae-Candoiinae	-1.47	-4.77	1.83	0.98
Pythoninae-Candoiinae	-0.45	-3.75	2.85	1.00
Tropidophiinae-Candoiinae	-0.66	-3.52	2.20	1.00
Viperinae-Candoiinae	-0.18	-3.03	2.68	1.00
Colubrinae-Charininae	-2.94	-3.56	-2.31	<0.01
Crotalinae-Charininae	-1.54	-2.19	-0.90	<0.01
Dipsadinae-Charininae	-2.37	-3.05	-1.69	<0.01
Elapinae-Charininae	-2.07	-2.91	-1.23	<0.01
Hydrophiinae-Charininae	-3.74	-4.94	-2.53	<0.01
Leptotyphlopinae-Charininae	-0.98	-2.11	0.15	0.18
Loxoceminae-Charininae	-0.32	-2.73	2.09	1.00
Natricinae-Charininae	-2.64	-3.29	-1.99	<0.01
Pseudaspidinae-Charininae	-2.50	-4.91	-0.09	0.03
Pythoninae-Charininae	-1.48	-3.89	0.93	0.76
Tropidophiinae-Charininae	-1.69	-3.45	0.06	0.07
Viperinae-Charininae	-1.21	-2.96	0.55	0.57
Crotalinae-Colubrinae	1.39	1.10	1.68	<0.01
Dipsadinae-Colubrinae	0.57	0.21	0.92	<0.01
Elapinae-Colubrinae	0.87	0.26	1.47	<0.01
Hydrophiinae-Colubrinae	-0.80	-1.86	0.25	0.39

Table B11. (continued)

Leptotyphlopinae-Colubrinae	1.96	0.99	2.93	<0.01
Loxoceminae-Colubrinae	2.61	0.27	4.95	0.01
Natricinae-Colubrinae	0.30	-0.01	0.60	0.06
Pseudaspidinae-Colubrinae	0.44	-1.90	2.77	1.00
Pythoninae-Colubrinae	1.46	-0.88	3.80	0.73
Tropidophiinae-Colubrinae	1.24	-0.41	2.90	0.41
Viperinae-Colubrinae	1.73	0.07	3.39	0.03
Dipsadinae-Crotalinae	-0.83	-1.22	-0.43	<0.01
Elapinae-Crotalinae	-0.52	-1.15	0.11	0.23
Hydrophiinae-Crotalinae	-2.19	-3.26	-1.12	<0.01
Leptotyphlopinae-Crotalinae	0.57	-0.42	1.55	0.83
Loxoceminae-Crotalinae	1.22	-1.12	3.57	0.92
Natricinae-Crotalinae	-1.10	-1.44	-0.75	<0.01
Pseudaspidinae-Crotalinae	-0.96	-3.30	1.39	0.99
Pythoninae-Crotalinae	0.07	-2.28	2.41	1.00
Tropidophiinae-Crotalinae	-0.15	-1.81	1.52	1.00
Viperinae-Crotalinae	0.34	-1.33	2.00	1.00
Elapinae-Dipsadinae	0.30	-0.36	0.96	0.97
Hydrophiinae-Dipsadinae	-1.37	-2.46	-0.28	<0.01
Leptotyphlopinae-Dipsadinae	1.39	0.39	2.40	<0.01
Loxoceminae-Dipsadinae	2.05	-0.31	4.40	0.18
Natricinae-Dipsadinae	-0.27	-0.67	0.13	0.61
Pseudaspidinae-Dipsadinae	-0.13	-2.49	2.22	1.00
Pythoninae-Dipsadinae	0.89	-1.46	3.25	1.00
Tropidophiinae-Dipsadinae	0.68	-1.00	2.36	0.99
Viperinae-Dipsadinae	1.16	-0.52	2.84	0.56
Hydrophiinae-Elapinae	-1.67	-2.87	-0.47	<0.01
Leptotyphlopinae-Elapinae	1.09	-0.03	2.21	0.06
Loxoceminae-Elapinae	1.75	-0.66	4.15	0.47
Natricinae-Elapinae	-0.57	-1.21	0.06	0.13
Pseudaspidinae-Elapinae	-0.43	-2.84	1.97	1.00
Pythoninae-Elapinae	0.59	-1.81	3.00	1.00
Tropidophiinae-Elapinae	0.38	-1.37	2.13	1.00
Viperinae-Elapinae	0.86	-0.89	2.61	0.95
Leptotyphlopinae-Hydrophiinae	2.76	1.35	4.17	<0.01
Loxoceminae-Hydrophiinae	3.42	0.86	5.97	<0.01

Table B11. (continued)

Natricinae-Hydrophiinae	1.10	0.03	2.17	0.04
Pseudaspidinae-Hydrophiinae	1.24	-1.32	3.79	0.95
Pythoninae-Hydrophiinae	2.26	-0.29	4.82	0.15
Tropidophiinae-Hydrophiinae	2.05	0.09	4.00	0.03
Viperinae-Hydrophiinae	2.53	0.58	4.48	<0.01
Loxoceminae-Leptotyphlopinae	0.65	-1.87	3.18	1.00
Natricinae-Leptotyphlopinae	-1.66	-2.65	-0.68	<0.01
Pseudaspidinae-Leptotyphlopinae	-1.52	-4.04	1.00	0.78
Pythoninae-Leptotyphlopinae	-0.50	-3.02	2.02	1.00
Tropidophiinae-Leptotyphlopinae	-0.71	-2.62	1.19	1.00
Viperinae-Leptotyphlopinae	-0.23	-2.13	1.68	1.00
Natricinae-Loxoceminae	-2.32	-4.66	0.03	0.06
Pseudaspidinae-Loxoceminae	-2.18	-5.48	1.12	0.64
Pythoninae-Loxoceminae	-1.15	-4.45	2.15	1.00
Tropidophiinae-Loxoceminae	-1.37	-4.23	1.49	0.96
Viperinae-Loxoceminae	-0.88	-3.74	1.97	1.00
Pseudaspidinae-Natricinae	0.14	-2.21	2.49	1.00
Pythoninae-Natricinae	1.16	-1.18	3.51	0.94
Tropidophiinae-Natricinae	0.95	-0.72	2.62	0.85
Viperinae-Natricinae	1.43	-0.24	3.10	0.19
Pythoninae-Pseudaspidinae	1.02	-2.28	4.32	1.00
Tropidophiinae-Pseudaspidinae	0.81	-2.05	3.67	1.00
Viperinae-Pseudaspidinae	1.29	-1.56	4.15	0.97
Tropidophiinae-Pythoninae	-0.21	-3.07	2.64	1.00
Viperinae-Pythoninae	0.27	-2.59	3.13	1.00
Viperinae-Tropidophiinae	0.49	-1.85	2.82	1.00
PC3 All				
Boinae-Ahaetuliinae	-0.04	-1.71	1.64	1.00
Candoiinae-Ahaetuliinae	-0.22	-3.91	3.46	1.00
Charininae-Ahaetuliinae	-0.97	-2.71	0.76	0.86
Colubrinae-Ahaetuliinae	-0.47	-1.99	1.06	1.00
Crotalinae-Ahaetuliinae	-0.09	-1.64	1.45	1.00
Dipsadinae-Ahaetuliinae	-0.68	-2.25	0.89	0.98
Elapinae-Ahaetuliinae	-0.52	-2.24	1.20	1.00

Table B11. (continued)

Hydrophiinae-Ahaetuliinae	-0.20	-2.33	1.93	1.00
Leptotyphlopinae-Ahaetuliinae	0.79	-1.25	2.83	0.99
Loxoceminae-Ahaetuliinae	-0.71	-4.39	2.98	1.00
Natricinae-Ahaetuliinae	-0.55	-2.10	1.00	1.00
Pseudaspidinae-Ahaetuliinae	-0.79	-4.48	2.89	1.00
Pythoninae-Ahaetuliinae	-1.46	-5.14	2.23	0.99
Tropidophiinae-Ahaetuliinae	0.30	-2.52	3.12	1.00
Viperinae-Ahaetuliinae	-1.22	-4.04	1.59	0.98
Candoiinae-Boinae	-0.18	-3.63	3.26	1.00
Charininae-Boinae	-0.93	-2.07	0.20	0.26
Colubrinae-Boinae	-0.43	-1.20	0.35	0.87
Crotalinae-Boinae	-0.06	-0.87	0.75	1.00
Dipsadinae-Boinae	-0.64	-1.50	0.22	0.43
Elapinae-Boinae	-0.48	-1.60	0.64	0.98
Hydrophiinae-Boinae	-0.16	-1.84	1.51	1.00
Leptotyphlopinae-Boinae	0.83	-0.73	2.39	0.90
Loxoceminae-Boinae	-0.67	-4.11	2.78	1.00
Natricinae-Boinae	-0.51	-1.33	0.31	0.74
Pseudaspidinae-Boinae	-0.75	-4.20	2.69	1.00
Pythoninae-Boinae	-1.42	-4.86	2.03	0.99
Tropidophiinae-Boinae	0.34	-2.15	2.83	1.00
Viperinae-Boinae	-1.18	-3.67	1.31	0.96
Charininae-Candoiinae	-0.75	-4.23	2.73	1.00
Colubrinae-Candoiinae	-0.24	-3.62	3.13	1.00
Crotalinae-Candoiinae	0.13	-3.25	3.51	1.00
Dipsadinae-Candoiinae	-0.46	-3.85	2.94	1.00
Elapinae-Candoiinae	-0.30	-3.77	3.17	1.00
Hydrophiinae-Candoiinae	0.02	-3.67	3.71	1.00
Leptotyphlopinae-Candoiinae	1.01	-2.62	4.65	1.00
Loxoceminae-Candoiinae	-0.48	-5.24	4.28	1.00
Natricinae-Candoiinae	-0.32	-3.71	3.06	1.00
Pseudaspidinae-Candoiinae	-0.57	-5.33	4.19	1.00
Pythoninae-Candoiinae	-1.23	-5.99	3.52	1.00
Tropidophiinae-Candoiinae	0.52	-3.60	4.64	1.00
Viperinae-Candoiinae	-1.00	-5.12	3.12	1.00
Colubrinae-Charininae	0.51	-0.40	1.41	0.86

Table B11. (continued)

Crotalinae-Charininae	0.88	-0.06	1.81	0.09
Dipsadinae-Charininae	0.29	-0.69	1.27	1.00
Elapinae-Charininae	0.45	-0.76	1.66	1.00
Hydrophiinae-Charininae	0.77	-0.97	2.51	0.98
Leptotyphlopinae-Charininae	1.76	0.14	3.39	0.02
Loxoceminae-Charininae	0.27	-3.21	3.74	1.00
Natricinae-Charininae	0.43	-0.52	1.37	0.97
Pseudaspidinae-Charininae	0.18	-3.29	3.66	1.00
Pythoninae-Charininae	-0.48	-3.96	2.99	1.00
Tropidophiinae-Charininae	1.27	-1.26	3.81	0.94
Viperinae-Charininae	-0.25	-2.78	2.28	1.00
Crotalinae-Colubrinae	0.37	-0.05	0.79	0.15
Dipsadinae-Colubrinae	-0.21	-0.73	0.30	0.99
Elapinae-Colubrinae	-0.05	-0.93	0.82	1.00
Hydrophiinae-Colubrinae	0.26	-1.26	1.79	1.00
Leptotyphlopinae-Colubrinae	1.26	-0.14	2.65	0.13
Loxoceminae-Colubrinae	-0.24	-3.61	3.13	1.00
Natricinae-Colubrinae	-0.08	-0.52	0.35	1.00
Pseudaspidinae-Colubrinae	-0.33	-3.70	3.05	1.00
Pythoninae-Colubrinae	-0.99	-4.37	2.38	1.00
Tropidophiinae-Colubrinae	0.77	-1.63	3.16	1.00
Viperinae-Colubrinae	-0.76	-3.15	1.64	1.00
Dipsadinae-Crotalinae	-0.58	-1.15	-0.02	0.04
Elapinae-Crotalinae	-0.42	-1.33	0.48	0.97
Hydrophiinae-Crotalinae	-0.11	-1.65	1.44	1.00
Leptotyphlopinae-Crotalinae	0.89	-0.53	2.30	0.73
Loxoceminae-Crotalinae	-0.61	-3.99	2.77	1.00
Natricinae-Crotalinae	-0.45	-0.95	0.04	0.12
Pseudaspidinae-Crotalinae	-0.70	-4.08	2.69	1.00
Pythoninae-Crotalinae	-1.36	-4.75	2.02	0.99
Tropidophiinae-Crotalinae	0.40	-2.01	2.80	1.00
Viperinae-Crotalinae	-1.13	-3.53	1.28	0.96
Elapinae-Dipsadinae	0.16	-0.80	1.12	1.00
Hydrophiinae-Dipsadinae	0.48	-1.10	2.05	1.00
Leptotyphlopinae-Dipsadinae	1.47	0.02	2.92	0.04
Loxoceminae-Dipsadinae	-0.03	-3.42	3.37	1.00
Natricinae-Dipsadinae	0.13	-0.45	0.71	1.00

Table B11. (continued)

Pseudaspidinae-Dipsadinae	-0.11	-3.51	3.28	1.00
Pythoninae-Dipsadinae	-0.78	-4.17	2.62	1.00
Tropidophiinae-Dipsadinae	0.98	-1.44	3.40	0.99
Viperinae-Dipsadinae	-0.54	-2.97	1.88	1.00
Hydrophiinae-Elapinae	0.32	-1.41	2.04	1.00
Leptotyphlopinae-Elapinae	1.31	-0.30	2.92	0.27
Loxoceminae-Elapinae	-0.19	-3.66	3.28	1.00
Natricinae-Elapinae	-0.03	-0.94	0.89	1.00
Pseudaspidinae-Elapinae	-0.27	-3.74	3.20	1.00
Pythoninae-Elapinae	-0.94	-4.41	2.53	1.00
Tropidophiinae-Elapinae	0.82	-1.70	3.34	1.00
Viperinae-Elapinae	-0.70	-3.23	1.82	1.00
Leptotyphlopinae-Hydrophiinae	0.99	-1.04	3.03	0.95
Loxoceminae-Hydrophiinae	-0.50	-4.19	3.18	1.00
Natricinae-Hydrophiinae	-0.35	-1.89	1.20	1.00
Pseudaspidinae-Hydrophiinae	-0.59	-4.28	3.10	1.00
Pythoninae-Hydrophiinae	-1.26	-4.94	2.43	1.00
Tropidophiinae-Hydrophiinae	0.50	-2.31	3.32	1.00
Viperinae-Hydrophiinae	-1.02	-3.84	1.79	1.00
Loxoceminae-Leptotyphlopinae	-1.50	-5.13	2.14	0.99
Natricinae-Leptotyphlopinae	-1.34	-2.76	0.08	0.09
Pseudaspidinae-Leptotyphlopinae	-1.58	-5.22	2.05	0.98
Pythoninae-Leptotyphlopinae	-2.25	-5.88	1.39	0.74
Tropidophiinae-Leptotyphlopinae	-0.49	-3.24	2.26	1.00
Viperinae-Leptotyphlopinae	-2.01	-4.76	0.73	0.46
Natricinae-Loxoceminae	0.16	-3.23	3.54	1.00
Pseudaspidinae-Loxoceminae	-0.09	-4.85	4.67	1.00
Pythoninae-Loxoceminae	-0.75	-5.51	4.01	1.00
Tropidophiinae-Loxoceminae	1.01	-3.12	5.13	1.00
Viperinae-Loxoceminae	-0.52	-4.64	3.60	1.00
Pseudaspidinae-Natricinae	-0.24	-3.63	3.14	1.00
Pythoninae-Natricinae	-0.91	-4.29	2.47	1.00
Tropidophiinae-Natricinae	0.85	-1.56	3.25	1.00
Viperinae-Natricinae	-0.68	-3.08	1.73	1.00

Table B11. (continued)

Pythoninae-Pseudaspidinae	-0.67	-5.42	4.09	1.00
Tropidophiinae-Pseudaspidinae	1.09	-3.03	5.21	1.00
Viperinae-Pseudaspidinae	-0.43	-4.55	3.69	1.00
Tropidophiinae-Pythoninae	1.76	-2.36	5.88	0.99
Viperinae-Pythoninae	0.23	-3.89	4.36	1.00
Viperinae-Tropidophiinae	-1.52	-4.89	1.84	0.97
PC4 All				
Boinae-Ahaetuliinae	1.83	0.36	3.31	<0.01
Candoiinae-Ahaetuliinae	2.42	-0.83	5.68	0.42
Charininae-Ahaetuliinae	1.21	-0.32	2.75	0.32
Colubrinae-Ahaetuliinae	1.30	-0.05	2.64	0.07
Crotalinae-Ahaetuliinae	0.80	-0.56	2.16	0.81
Dipsadinae-Ahaetuliinae	1.70	0.31	3.09	<0.01
Elapinae-Ahaetuliinae	-0.39	-1.91	1.13	1.00
Hydrophiinae-Ahaetuliinae	1.15	-0.73	3.03	0.76
Leptotyphlopinae-Ahaetuliinae	3.85	2.05	5.65	<0.01
Loxoceminae-Ahaetuliinae	0.35	-2.90	3.60	1.00
Natricinae-Ahaetuliinae	1.03	-0.34	2.39	0.41
Pseudaspidinae-Ahaetuliinae	1.39	-1.87	4.64	0.99
Pythoninae-Ahaetuliinae	2.38	-0.87	5.64	0.46
Tropidophiinae-Ahaetuliinae	0.08	-2.40	2.56	1.00
Viperinae-Ahaetuliinae	2.29	-0.19	4.78	0.11
Candoiinae-Boinae	0.59	-2.45	3.63	1.00
Charininae-Boinae	-0.62	-1.62	0.38	0.75
Colubrinae-Boinae	-0.54	-1.22	0.15	0.33
Crotalinae-Boinae	-1.03	-1.75	-0.32	<0.01
Dipsadinae-Boinae	-0.13	-0.89	0.63	1.00
Elapinae-Boinae	-2.22	-3.20	-1.23	<0.01
Hydrophiinae-Boinae	-0.68	-2.16	0.79	0.97
Leptotyphlopinae-Boinae	2.02	0.65	3.39	<0.01
Loxoceminae-Boinae	-1.49	-4.52	1.55	0.95
Natricinae-Boinae	-0.81	-1.53	-0.08	0.01
Pseudaspidinae-Boinae	-0.45	-3.48	2.59	1.00
Pythoninae-Boinae	0.55	-2.49	3.59	1.00
Tropidophiinae-Boinae	-1.75	-3.95	0.44	0.30
Viperinae-Boinae	0.46	-1.74	2.66	1.00

Table B11. (continued)

Charininae-Candoiinae	-1.21	-4.28	1.86	0.99
Colubrinae-Candoiinae	-1.13	-4.10	1.85	1.00
Crotalinae-Candoiinae	-1.62	-4.61	1.36	0.89
Dipsadinae-Candoiinae	-0.72	-3.72	2.27	1.00
Elapinae-Candoiinae	-2.81	-5.87	0.25	0.11
Hydrophiinae-Candoiinae	-1.27	-4.53	1.98	0.99
Leptotyphlopinae-Candoiinae	1.43	-1.78	4.64	0.98
Loxoceminae-Candoiinae	-2.08	-6.28	2.12	0.95
Natricinae-Candoiinae	-1.40	-4.38	1.59	0.97
Pseudaspidinae-Candoiinae	-1.04	-5.24	3.16	1.00
Pythoninae-Candoiinae	-0.04	-4.24	4.16	1.00
Tropidophiinae-Candoiinae	-2.34	-5.98	1.29	0.68
Viperinae-Candoiinae	-0.13	-3.77	3.50	1.00
Colubrinae-Charininae	0.08	-0.71	0.88	1.00
Crotalinae-Charininae	-0.41	-1.24	0.41	0.94
Dipsadinae-Charininae	0.49	-0.38	1.35	0.86
Elapinae-Charininae	-1.60	-2.67	-0.53	<0.01
Hydrophiinae-Charininae	-0.06	-1.60	1.47	1.00
Leptotyphlopinae-Charininae	2.64	1.20	4.07	<0.01
Loxoceminae-Charininae	-0.87	-3.93	2.20	1.00
Natricinae-Charininae	-0.19	-1.02	0.64	1.00
Pseudaspidinae-Charininae	0.17	-2.89	3.24	1.00
Pythoninae-Charininae	1.17	-1.90	4.24	1.00
Tropidophiinae-Charininae	-1.13	-3.37	1.10	0.93
Viperinae-Charininae	1.08	-1.16	3.31	0.96
Crotalinae-Colubrinae	-0.50	-0.87	-0.13	<0.01
Dipsadinae-Colubrinae	0.40	-0.05	0.86	0.15
Elapinae-Colubrinae	-1.68	-2.46	-0.91	<0.01
Hydrophiinae-Colubrinae	-0.15	-1.49	1.20	1.00
Leptotyphlopinae-Colubrinae	2.56	1.32	3.79	<0.01
Loxoceminae-Colubrinae	-0.95	-3.93	2.03	1.00
Natricinae-Colubrinae	-0.27	-0.66	0.11	0.53
Pseudaspidinae-Colubrinae	0.09	-2.89	3.07	1.00
Pythoninae-Colubrinae	1.09	-1.89	4.06	1.00
Tropidophiinae-Colubrinae	-1.22	-3.33	0.89	0.83
Viperinae-Colubrinae	1.00	-1.12	3.11	0.96
Dipsadinae-Crotalinae	0.90	0.40	1.40	<0.01

Table B11. (continued)

Elapinae-Crotalinae	-1.19	-1.99	-0.39	<0.01
Hydrophiinae-Crotalinae	0.35	-1.01	1.71	1.00
Leptotyphlopinae-Crotalinae	3.05	1.80	4.30	<0.01
Loxoceminae-Crotalinae	-0.45	-3.44	2.53	1.00
Natricinae-Crotalinae	0.23	-0.21	0.67	0.92
Pseudaspidinae-Crotalinae	0.59	-2.40	3.57	1.00
Pythoninae-Crotalinae	1.58	-1.40	4.57	0.91
Tropidophiinae-Crotalinae	-0.72	-2.84	1.40	1.00
Viperinae-Crotalinae	1.49	-0.63	3.61	0.53
Elapinae-Dipsadinae	-2.09	-2.93	-1.24	<0.01
Hydrophiinae-Dipsadinae	-0.55	-1.94	0.84	0.99
Leptotyphlopinae-Dipsadinae	2.15	0.87	3.43	<0.01
Loxoceminae-Dipsadinae	-1.35	-4.35	1.64	0.97
Natricinae-Dipsadinae	-0.67	-1.19	-0.16	<0.01
Pseudaspidinae-Dipsadinae	-0.31	-3.31	2.68	1.00
Pythoninae-Dipsadinae	0.68	-2.31	3.68	1.00
Tropidophiinae-Dipsadinae	-1.62	-3.76	0.52	0.39
Viperinae-Dipsadinae	0.59	-1.55	2.73	1.00
Hydrophiinae-Elapinae	1.54	0.02	3.06	0.04
Leptotyphlopinae-Elapinae	4.24	2.82	5.66	<0.01
Loxoceminae-Elapinae	0.73	-2.33	3.79	1.00
Natricinae-Elapinae	1.41	0.61	2.22	<0.01
Pseudaspidinae-Elapinae	1.77	-1.29	4.83	0.83
Pythoninae-Elapinae	2.77	-0.29	5.83	0.13
Tropidophiinae-Elapinae	0.47	-1.76	2.69	1.00
Viperinae-Elapinae	2.68	0.45	4.91	<0.01
Leptotyphlopinae-Hydrophiinae	2.70	0.90	4.50	<0.01
Loxoceminae-Hydrophiinae	-0.80	-4.06	2.45	1.00
Natricinae-Hydrophiinae	-0.12	-1.49	1.24	1.00
Pseudaspidinae-Hydrophiinae	0.24	-3.02	3.49	1.00
Pythoninae-Hydrophiinae	1.23	-2.02	4.48	1.00
Tropidophiinae-Hydrophiinae	-1.07	-3.55	1.41	0.98
Viperinae-Hydrophiinae	1.14	-1.34	3.63	0.97
Loxoceminae-Leptotyphlopinae	-3.50	-6.71	-0.30	0.02
Natricinae-Leptotyphlopinae	-2.83	-4.08	-1.57	<0.01

Table B11. (continued)

Pseudaspidinae-Leptotyphlopinae	-2.47	-5.67	0.74	0.37
Pythoninae-Leptotyphlopinae	-1.47	-4.68	1.74	0.97
Tropidophiinae-Leptotyphlopinae	-3.77	-6.20	-1.35	<0.01
Viperinae-Leptotyphlopinae	-1.56	-3.98	0.86	0.69
Natricinae-Loxoceminae	0.68	-2.31	3.67	1.00
Pseudaspidinae-Loxoceminae	1.04	-3.16	5.24	1.00
Pythoninae-Loxoceminae	2.04	-2.16	6.23	0.95
Tropidophiinae-Loxoceminae	-0.27	-3.90	3.37	1.00
Viperinae-Loxoceminae	1.95	-1.69	5.58	0.90
Pseudaspidinae-Natricinae	0.36	-2.63	3.35	1.00
Pythoninae-Natricinae	1.36	-1.63	4.34	0.97
Tropidophiinae-Natricinae	-0.95	-3.07	1.18	0.98
Viperinae-Natricinae	1.27	-0.86	3.39	0.79
Pythoninae-Pseudaspidinae	1.00	-3.20	5.19	1.00
Tropidophiinae-Pseudaspidinae	-1.31	-4.94	2.33	1.00
Viperinae-Pseudaspidinae	0.91	-2.73	4.54	1.00
Tropidophiinae-Pythoninae	-2.30	-5.94	1.33	0.71
Viperinae-Pythoninae	-0.09	-3.73	3.55	1.00
Viperinae-Tropidophiinae	2.21	-0.76	5.18	0.42
PC5 All				
Boinae-Ahaetuliinae	-0.82	-2.12	0.47	0.71
Candoiinae-Ahaetuliinae	-0.42	-3.28	2.43	1.00
Charininae-Ahaetuliinae	-0.03	-1.38	1.31	1.00
Colubrinae-Ahaetuliinae	0.96	-0.22	2.14	0.27
Crotalinae-Ahaetuliinae	1.48	0.28	2.67	<0.01
Dipsadinae-Ahaetuliinae	0.94	-0.27	2.16	0.35
Elapinae-Ahaetuliinae	1.12	-0.22	2.45	0.23
Hydrophiinae-Ahaetuliinae	1.03	-0.62	2.68	0.73
Leptotyphlopinae-Ahaetuliinae	1.50	-0.08	3.08	0.08
Loxoceminae-Ahaetuliinae	-0.58	-3.43	2.28	1.00
Natricinae-Ahaetuliinae	2.11	0.92	3.31	<0.01
Pseudaspidinae-Ahaetuliinae	1.11	-1.74	3.97	0.99
Pythoninae-Ahaetuliinae	-1.36	-4.22	1.50	0.96
Tropidophiinae-Ahaetuliinae	0.75	-1.43	2.93	1.00

Table B11. (continued)

Viperinae-Ahaetuliinae	0.71	-1.48	2.89	1.00
Candoiinae-Boinae	0.40	-2.27	3.07	1.00
Charininae-Boinae	0.79	-0.09	1.67	0.14
Colubrinae-Boinae	1.79	1.19	2.39	<0.01
Crotalinae-Boinae	2.30	1.67	2.93	<0.01
Dipsadinae-Boinae	1.77	1.10	2.44	<0.01
Elapinae-Boinae	1.94	1.07	2.80	<0.01
Hydrophiinae-Boinae	1.86	0.56	3.16	<0.01
Leptotyphlopinae-Boinae	2.33	1.12	3.53	<0.01
Loxoceminae-Boinae	0.25	-2.42	2.92	1.00
Natricinae-Boinae	2.94	2.30	3.57	<0.01
Pseudaspidinae-Boinae	1.94	-0.73	4.61	0.47
Pythoninae-Boinae	-0.53	-3.20	2.14	1.00
Tropidophiinae-Boinae	1.57	-0.36	3.50	0.27
Viperinae-Boinae	1.53	-0.40	3.46	0.31
Charininae-Candoiinae	0.39	-2.30	3.08	1.00
Colubrinae-Candoiinae	1.38	-1.23	4.00	0.91
Crotalinae-Candoiinae	1.90	-0.72	4.52	0.48
Dipsadinae-Candoiinae	1.37	-1.26	4.00	0.92
Elapinae-Candoiinae	1.54	-1.15	4.23	0.84
Hydrophiinae-Candoiinae	1.46	-1.40	4.31	0.93
Leptotyphlopinae-Candoiinae	1.93	-0.89	4.74	0.58
Loxoceminae-Candoiinae	-0.15	-3.84	3.54	1.00
Natricinae-Candoiinae	2.54	-0.08	5.16	0.07
Pseudaspidinae-Candoiinae	1.54	-2.15	5.23	0.99
Pythoninae-Candoiinae	-0.93	-4.62	2.75	1.00
Tropidophiinae-Candoiinae	1.17	-2.02	4.37	1.00
Viperinae-Candoiinae	1.13	-2.06	4.32	1.00
Colubrinae-Charininae	0.99	0.30	1.69	<0.01
Crotalinae-Charininae	1.51	0.79	2.23	<0.01
Dipsadinae-Charininae	0.98	0.22	1.74	<0.01
Elapinae-Charininae	1.15	0.21	2.09	<0.01
Hydrophiinae-Charininae	1.07	-0.28	2.41	0.31
Leptotyphlopinae-Charininae	1.54	0.28	2.80	<0.01
Loxoceminae-Charininae	-0.54	-3.24	2.15	1.00
Natricinae-Charininae	2.15	1.42	2.88	<0.01
Pseudaspidinae-Charininae	1.15	-1.55	3.84	0.99

Table B11. (continued)

Pythoninae-Charininae	-1.32	-4.02	1.37	0.95
Tropidophiinae-Charininae	0.78	-1.18	2.75	0.99
Viperinae-Charininae	0.74	-1.22	2.70	1.00
Crotalinae-Colubrinae	0.52	0.19	0.84	<0.01
Dipsadinae-Colubrinae	-0.02	-0.42	0.38	1.00
Elapinae-Colubrinae	0.15	-0.52	0.83	1.00
Hydrophiinae-Colubrinae	0.07	-1.11	1.25	1.00
Leptotyphlopinae-Colubrinae	0.54	-0.54	1.62	0.94
Loxoceminae-Colubrinae	-1.54	-4.15	1.08	0.81
Natricinae-Colubrinae	1.15	0.82	1.49	<0.01
Pseudaspidinae-Colubrinae	0.15	-2.46	2.77	1.00
Pythoninae-Colubrinae	-2.32	-4.93	0.30	0.15
Tropidophiinae-Colubrinae	-0.21	-2.07	1.64	1.00
Viperinae-Colubrinae	-0.26	-2.11	1.60	1.00
Dipsadinae-Crotalinae	-0.53	-0.97	-0.09	<0.01
Elapinae-Crotalinae	-0.36	-1.07	0.34	0.93
Hydrophiinae-Crotalinae	-0.44	-1.64	0.75	1.00
Leptotyphlopinae-Crotalinae	0.03	-1.07	1.12	1.00
Loxoceminae-Crotalinae	-2.05	-4.68	0.57	0.33
Natricinae-Crotalinae	0.64	0.25	1.02	<0.01
Pseudaspidinae-Crotalinae	-0.36	-2.99	2.26	1.00
Pythoninae-Crotalinae	-2.83	-5.46	-0.21	0.02
Tropidophiinae-Crotalinae	-0.73	-2.59	1.13	0.99
Viperinae-Crotalinae	-0.77	-2.63	1.09	0.99
Elapinae-Dipsadinae	0.17	-0.57	0.91	1.00
Hydrophiinae-Dipsadinae	0.09	-1.13	1.31	1.00
Leptotyphlopinae-Dipsadinae	0.56	-0.56	1.68	0.94
Loxoceminae-Dipsadinae	-1.52	-4.15	1.11	0.83
Natricinae-Dipsadinae	1.17	0.72	1.62	<0.01
Pseudaspidinae-Dipsadinae	0.17	-2.46	2.80	1.00
Pythoninae-Dipsadinae	-2.30	-4.93	0.33	0.17
Tropidophiinae-Dipsadinae	-0.20	-2.07	1.68	1.00
Viperinae-Dipsadinae	-0.24	-2.12	1.64	1.00
Hydrophiinae-Elapinae	-0.08	-1.42	1.26	1.00
Leptotyphlopinae-Elapinae	0.39	-0.86	1.64	1.00
Loxoceminae-Elapinae	-1.69	-4.38	1.00	0.72
Natricinae-Elapinae	1.00	0.29	1.71	<0.01

Table B11. (continued)

Pseudaspidinae-Elapinae	<0.01	-2.69	2.69	1.00
Pythoninae-Elapinae	-2.47	-5.16	0.21	0.11
Tropidophiinae-Elapinae	-0.37	-2.32	1.59	1.00
Viperinae-Elapinae	-0.41	-2.37	1.55	1.00
Leptotyphlopinae-Hydrophiinae	0.47	-1.11	2.05	1.00
Loxoceminae-Hydrophiinae	-1.61	-4.47	1.25	0.85
Natricinae-Hydrophiinae	1.08	-0.12	2.28	0.13
Pseudaspidinae-Hydrophiinae	0.08	-2.78	2.94	1.00
Pythoninae-Hydrophiinae	-2.39	-5.25	0.46	0.23
Tropidophiinae-Hydrophiinae	-0.29	-2.47	1.90	1.00
Viperinae-Hydrophiinae	-0.33	-2.51	1.85	1.00
Loxoceminae-Leptotyphlopinae	-2.08	-4.90	0.74	0.44
Natricinae-Leptotyphlopinae	0.61	-0.49	1.71	0.87
Pseudaspidinae-Leptotyphlopinae	-0.39	-3.21	2.43	1.00
Pythoninae-Leptotyphlopinae	-2.86	-5.68	-0.04	0.04
Tropidophiinae-Leptotyphlopinae	-0.76	-2.88	1.37	1.00
Viperinae-Leptotyphlopinae	-0.80	-2.93	1.33	1.00
Natricinae-Loxoceminae	2.69	0.07	5.32	0.04
Pseudaspidinae-Loxoceminae	1.69	-2.00	5.38	0.97
Pythoninae-Loxoceminae	-0.78	-4.47	2.91	1.00
Tropidophiinae-Loxoceminae	1.33	-1.87	4.52	0.99
Viperinae-Loxoceminae	1.28	-1.91	4.48	0.99
Pseudaspidinae-Natricinae	-1.00	-3.63	1.62	1.00
Pythoninae-Natricinae	-3.47	-6.10	-0.85	<0.01
Tropidophiinae-Natricinae	-1.37	-3.23	0.50	0.46
Viperinae-Natricinae	-1.41	-3.27	0.46	0.40
Pythoninae-Pseudaspidinae	-2.47	-6.16	1.22	0.62
Tropidophiinae-Pseudaspidinae	-0.36	-3.56	2.83	1.00
Viperinae-Pseudaspidinae	-0.41	-3.60	2.79	1.00
Tropidophiinae-Pythoninae	2.11	-1.09	5.30	0.65
Viperinae-Pythoninae	2.06	-1.13	5.26	0.68
Viperinae-Tropidophiinae	-0.04	-2.65	2.57	1.00

Table B11. (continued)

PC6 All				
Boinae-Ahaetuliinae	1.63	0.16	3.11	0.01
Candoiinae-Ahaetuliinae	1.01	-2.24	4.26	1.00
Charininae-Ahaetuliinae	1.60	0.07	3.13	0.03
Colubrinae-Ahaetuliinae	1.00	-0.34	2.35	0.42
Crotalinae-Ahaetuliinae	-0.04	-1.40	1.32	1.00
Dipsadinae-Ahaetuliinae	0.33	-1.06	1.71	1.00
Elapinae-Ahaetuliinae	-0.21	-1.73	1.31	1.00
Hydrophiinae-Ahaetuliinae	0.09	-1.79	1.97	1.00
Leptotyphlopinae-Ahaetuliinae	-0.79	-2.59	1.01	0.98
Loxoceminae-Ahaetuliinae	1.72	-1.53	4.97	0.91
Natricinae-Ahaetuliinae	0.56	-0.80	1.93	0.99
Pseudaspidinae-Ahaetuliinae	1.35	-1.90	4.60	0.99
Pythoninae-Ahaetuliinae	1.52	-1.73	4.77	0.97
Tropidophiinae-Ahaetuliinae	0.52	-1.96	3.01	1.00
Viperinae-Ahaetuliinae	-0.01	-2.50	2.47	1.00
Candoiinae-Boinae	-0.62	-3.66	2.42	1.00
Charininae-Boinae	-0.03	-1.04	0.97	1.00
Colubrinae-Boinae	-0.63	-1.31	0.05	0.11
Crotalinae-Boinae	-1.67	-2.39	-0.96	<0.01
Dipsadinae-Boinae	-1.31	-2.07	-0.55	<0.01
Elapinae-Boinae	-1.84	-2.83	-0.86	<0.01
Hydrophiinae-Boinae	-1.54	-3.02	-0.07	0.03
Leptotyphlopinae-Boinae	-2.42	-3.80	-1.05	<0.01
Loxoceminae-Boinae	0.09	-2.95	3.12	1.00
Natricinae-Boinae	-1.07	-1.79	-0.35	<0.01
Pseudaspidinae-Boinae	-0.29	-3.32	2.75	1.00
Pythoninae-Boinae	-0.11	-3.15	2.92	1.00
Tropidophiinae-Boinae	-1.11	-3.31	1.09	0.93
Viperinae-Boinae	-1.65	-3.84	0.55	0.41
Charininae-Candoiinae	0.59	-2.48	3.65	1.00
Colubrinae-Candoiinae	-0.01	-2.99	2.96	1.00
Crotalinae-Candoiinae	-1.05	-4.04	1.93	1.00
Dipsadinae-Candoiinae	-0.69	-3.68	2.31	1.00
Elapinae-Candoiinae	-1.22	-4.28	1.84	0.99
Hydrophiinae-Candoiinae	-0.92	-4.17	2.33	1.00

Table B11. (continued)

Leptotyphlopinae-Candoiinae	-1.80	-5.01	1.40	0.86
Loxoceminae-Candoiinae	0.71	-3.49	4.90	1.00
Natricinae-Candoiinae	-0.45	-3.44	2.53	1.00
Pseudaspidinae-Candoiinae	0.33	-3.86	4.53	1.00
Pythoninae-Candoiinae	0.51	-3.69	4.70	1.00
Tropidophiinae-Candoiinae	-0.49	-4.12	3.14	1.00
Viperinae-Candoiinae	-1.03	-4.66	2.61	1.00
Colubrinae-Charininae	-0.60	-1.39	0.20	0.41
Crotalinae-Charininae	-1.64	-2.46	-0.82	<0.01
Dipsadinae-Charininae	-1.28	-2.14	-0.41	<0.01
Elapinae-Charininae	-1.81	-2.87	-0.74	<0.01
Hydrophiinae-Charininae	-1.51	-3.04	0.02	0.06
Leptotyphlopinae-Charininae	-2.39	-3.83	-0.96	<0.01
Loxoceminae-Charininae	0.12	-2.95	3.18	1.00
Natricinae-Charininae	-1.04	-1.87	-0.21	<0.01
Pseudaspidinae-Charininae	-0.25	-3.32	2.81	1.00
Pythoninae-Charininae	-0.08	-3.14	2.98	1.00
Tropidophiinae-Charininae	-1.08	-3.31	1.16	0.96
Viperinae-Charininae	-1.62	-3.85	0.62	0.48
Crotalinae-Colubrinae	-1.04	-1.41	-0.67	<0.01
Dipsadinae-Colubrinae	-0.68	-1.13	-0.22	<0.01
Elapinae-Colubrinae	-1.21	-1.98	-0.44	<0.01
Hydrophiinae-Colubrinae	-0.91	-2.26	0.43	0.59
Leptotyphlopinae-Colubrinae	-1.79	-3.02	-0.56	<0.01
Loxoceminae-Colubrinae	0.72	-2.26	3.69	1.00
Natricinae-Colubrinae	-0.44	-0.83	-0.06	0.01
Pseudaspidinae-Colubrinae	0.34	-2.63	3.32	1.00
Pythoninae-Colubrinae	0.52	-2.46	3.49	1.00
Tropidophiinae-Colubrinae	-0.48	-2.59	1.63	1.00
Viperinae-Colubrinae	-1.02	-3.13	1.09	0.96
Dipsadinae-Crotalinae	0.36	-0.14	0.86	0.47
Elapinae-Crotalinae	-0.17	-0.97	0.63	1.00
Hydrophiinae-Crotalinae	0.13	-1.23	1.49	1.00
Leptotyphlopinae-Crotalinae	-0.75	-2.00	0.50	0.78
Loxoceminae-Crotalinae	1.76	-1.22	4.74	0.81
Natricinae-Crotalinae	0.60	0.16	1.04	<0.01
Pseudaspidinae-Crotalinae	1.39	-1.60	4.37	0.97

Table B11. (continued)

Pythoninae-Crotalinae	1.56	-1.42	4.54	0.91
Tropidophiinae-Crotalinae	0.56	-1.56	2.68	1.00
Viperinae-Crotalinae	0.02	-2.10	2.14	1.00
Elapinae-Dipsadinae	-0.53	-1.37	0.31	0.72
Hydrophiinae-Dipsadinae	-0.24	-1.62	1.15	1.00
Leptotyphlopinae-Dipsadinae	-1.12	-2.39	0.16	0.17
Loxoceminae-Dipsadinae	1.40	-1.60	4.39	0.97
Natricinae-Dipsadinae	0.24	-0.27	0.75	0.97
Pseudaspidinae-Dipsadinae	1.02	-1.97	4.02	1.00
Pythoninae-Dipsadinae	1.20	-1.80	4.19	0.99
Tropidophiinae-Dipsadinae	0.20	-1.94	2.34	1.00
Viperinae-Dipsadinae	-0.34	-2.48	1.80	1.00
Hydrophiinae-Elapinae	0.30	-1.22	1.82	1.00
Leptotyphlopinae-Elapinae	-0.58	-2.00	0.84	0.99
Loxoceminae-Elapinae	1.93	-1.13	4.99	0.72
Natricinae-Elapinae	0.77	-0.04	1.58	0.08
Pseudaspidinae-Elapinae	1.55	-1.50	4.61	0.93
Pythoninae-Elapinae	1.73	-1.33	4.79	0.85
Tropidophiinae-Elapinae	0.73	-1.49	2.96	1.00
Viperinae-Elapinae	0.19	-2.03	2.42	1.00
Leptotyphlopinae-Hydrophiinae	-0.88	-2.68	0.92	0.95
Loxoceminae-Hydrophiinae	1.63	-1.62	4.88	0.94
Natricinae-Hydrophiinae	0.47	-0.89	1.84	1.00
Pseudaspidinae-Hydrophiinae	1.26	-1.99	4.51	0.99
Pythoninae-Hydrophiinae	1.43	-1.82	4.68	0.98
Tropidophiinae-Hydrophiinae	0.43	-2.05	2.92	1.00
Viperinae-Hydrophiinae	-0.10	-2.59	2.38	1.00
Loxoceminae-Leptotyphlopinae	2.51	-0.69	5.72	0.34
Natricinae-Leptotyphlopinae	1.35	0.10	2.60	0.02
Pseudaspidinae-Leptotyphlopinae	2.14	-1.07	5.34	0.63
Pythoninae-Leptotyphlopinae	2.31	-0.89	5.52	0.48
Tropidophiinae-Leptotyphlopinae	1.31	-1.11	3.74	0.89
Viperinae-Leptotyphlopinae	0.78	-1.65	3.20	1.00
Natricinae-Loxoceminae	-1.16	-4.14	1.83	0.99

Table B11. (continued)

Pseudaspidinae-Loxoceminae	-0.37	-4.57	3.82	1.00
Pythoninae-Loxoceminae	-0.20	-4.39	4.00	1.00
Tropidophiinae-Loxoceminae	-1.20	-4.83	2.44	1.00
Viperinae-Loxoceminae	-1.73	-5.37	1.90	0.96
Pseudaspidinae-Natricinae	0.79	-2.20	3.77	1.00
Pythoninae-Natricinae	0.96	-2.02	3.95	1.00
Tropidophiinae-Natricinae	-0.04	-2.16	2.09	1.00
Viperinae-Natricinae	-0.58	-2.70	1.55	1.00
Pythoninae-Pseudaspidinae	0.18	-4.02	4.37	1.00
Tropidophiinae-Pseudaspidinae	-0.82	-4.46	2.81	1.00
Viperinae-Pseudaspidinae	-1.36	-5.00	2.27	1.00
Tropidophiinae-Pythoninae	-1.00	-4.63	2.64	1.00
Viperinae-Pythoninae	-1.54	-5.17	2.10	0.99
Viperinae-Tropidophiinae	-0.54	-3.51	2.43	1.00

Table B12. Tukey's test results of primary foraging habitat for PCs 1-6 of the all-groups data.

PC1 All	diff	lwr	upr	p adj
Arboreal-Aquatic	0.71	0.15	1.27	<0.01
Fossorial-Aquatic	1.58	1.03	2.14	<0.01
Semiaquatic-Aquatic	0.03	-0.55	0.62	1.00
Semiarboreal-Aquatic	0.63	0.06	1.21	0.02
Semifossorial-Aquatic	1.04	0.52	1.56	<0.01
Terrestrial-Aquatic	0.13	-0.36	0.61	0.99
Fossorial-Arboreal	0.87	0.39	1.35	<0.01
Semiaquatic-Arboreal	-0.68	-1.20	-0.16	<0.01
Semiarboreal-Arboreal	-0.08	-0.58	0.42	1.00
Semifossorial-Arboreal	0.33	-0.11	0.76	0.28
Terrestrial-Arboreal	-0.59	-0.98	-0.20	<0.01
Semiaquatic-Fossorial	-1.55	-2.06	-1.03	<0.01
Semiarboreal-Fossorial	-0.95	-1.45	-0.45	<0.01
Semifossorial-Fossorial	-0.54	-0.97	-0.11	<0.01
Terrestrial-Fossorial	-1.46	-1.84	-1.07	<0.01
Semiarboreal-Semiaquatic	0.60	0.07	1.13	0.02
Semifossorial-Semiaquatic	1.01	0.53	1.48	<0.01
Terrestrial-Semiaquatic	0.09	-0.34	0.52	1.00
Semifossorial-Semiarboreal	0.41	-0.05	0.86	0.11
Terrestrial-Semiarboreal	-0.51	-0.92	-0.09	0.01
Terrestrial-Semifossorial	-0.91	-1.24	-0.58	<0.01
PC2 All				
Arboreal-Aquatic	0.23	-0.36	0.82	0.91
Fossorial-Aquatic	0.92	0.34	1.51	<0.01
Semiaquatic-Aquatic	0.61	-0.01	1.22	0.06
Semiarboreal-Aquatic	-0.03	-0.63	0.58	1.00
Semifossorial-Aquatic	1.27	0.72	1.81	<0.01
Terrestrial-Aquatic	0.98	0.47	1.49	<0.01
Fossorial-Arboreal	0.69	0.19	1.20	<0.01
Semiaquatic-Arboreal	0.38	-0.17	0.92	0.39
Semiarboreal-Arboreal	-0.26	-0.78	0.27	0.78
Semifossorial-Arboreal	1.04	0.58	1.49	<0.01
Terrestrial-Arboreal	0.75	0.34	1.16	<0.01
Semiaquatic-Fossorial	-0.32	-0.86	0.22	0.59
Semiarboreal-Fossorial	-0.95	-1.47	-0.42	<0.01
Semifossorial-Fossorial	0.34	-0.11	0.80	0.27
Terrestrial-Fossorial	0.06	-0.35	0.46	1.00

Table B12. (continued)

Semiarboreal-Semiaquatic	-0.63	-1.19	-0.07	0.02
Semifossorial-Semiaquatic	0.66	0.17	1.16	<0.01
Terrestrial-Semiaquatic	0.37	-0.08	0.83	0.19
Semifossorial-Semiarboreal	1.29	0.82	1.77	<0.01
Terrestrial-Semiarboreal	1.01	0.57	1.44	<0.01
Terrestrial-Semifossorial	-0.29	-0.63	0.06	0.18
PC3 All				
Arboreal-Aquatic	0.84	0.22	1.47	<0.01
Fossorial-Aquatic	0.54	-0.08	1.16	0.14
Semiaquatic-Aquatic	0.02	-0.64	0.68	1.00
Semiarboreal-Aquatic	0.07	-0.57	0.71	1.00
Semifossorial-Aquatic	-0.17	-0.75	0.41	0.98
Terrestrial-Aquatic	0.20	-0.34	0.74	0.93
Fossorial-Arboreal	-0.30	-0.84	0.23	0.63
Semiaquatic-Arboreal	-0.83	-1.41	-0.25	<0.01
Semiarboreal-Arboreal	-0.78	-1.34	-0.22	<0.01
Semifossorial-Arboreal	-1.01	-1.50	-0.53	<0.01
Terrestrial-Arboreal	-0.64	-1.08	-0.21	<0.01
Semiaquatic-Fossorial	-0.52	-1.10	0.05	0.10
Semiarboreal-Fossorial	-0.47	-1.03	0.08	0.16
Semifossorial-Fossorial	-0.71	-1.19	-0.23	<0.01
Terrestrial-Fossorial	-0.34	-0.77	0.09	0.23
Semiarboreal-Semiaquatic	0.05	-0.55	0.65	1.00
Semifossorial-Semiaquatic	-0.19	-0.71	0.34	0.94
Terrestrial-Semiaquatic	0.18	-0.30	0.67	0.92
Semifossorial-Semiarboreal	-0.24	-0.74	0.27	0.81
Terrestrial-Semiarboreal	0.13	-0.33	0.60	0.98
Terrestrial-Semifossorial	0.37	<0.01	0.74	0.05
PC4 All				
Arboreal-Aquatic	-0.23	-0.87	0.42	0.94
Fossorial-Aquatic	0.03	-0.61	0.67	1.00
Semiaquatic-Aquatic	0.05	-0.63	0.73	1.00
Semiarboreal-Aquatic	0.21	-0.45	0.88	0.96
Semifossorial-Aquatic	0.09	-0.51	0.68	1.00
Terrestrial-Aquatic	-0.27	-0.82	0.29	0.79
Fossorial-Arboreal	0.26	-0.29	0.81	0.81
Semiaquatic-Arboreal	0.28	-0.32	0.87	0.82

Table B12. (continued)

Semiarboreal-Arboreal	0.44	-0.14	1.02	0.26
Semifossorial-Arboreal	0.32	-0.18	0.82	0.50
Terrestrial-Arboreal	-0.04	-0.49	0.41	1.00
Semiaquatic-Fossorial	0.02	-0.58	0.61	1.00
Semiarboreal-Fossorial	0.18	-0.39	0.76	0.96
Semifossorial-Fossorial	0.06	-0.44	0.55	1.00
Terrestrial-Fossorial	-0.30	-0.75	0.15	0.43
Semiarboreal-Semiaquatic	0.17	-0.45	0.78	0.98
Semifossorial-Semiaquatic	0.04	-0.50	0.58	1.00
Terrestrial-Semiaquatic	-0.31	-0.81	0.18	0.50
Semifossorial-Semiarboreal	-0.13	-0.65	0.40	0.99
Terrestrial-Semiarboreal	-0.48	-0.96	-0.01	0.04
Terrestrial-Semifossorial	-0.36	-0.74	0.02	0.08
PC5 All				
Arboreal-Aquatic	-1.95	-2.52	-1.38	<0.01
Fossorial-Aquatic	-0.55	-1.12	0.02	0.07
Semiaquatic-Aquatic	-0.24	-0.84	0.36	0.90
Semiarboreal-Aquatic	-1.17	-1.76	-0.58	<0.01
Semifossorial-Aquatic	-0.82	-1.35	-0.29	<0.01
Terrestrial-Aquatic	-0.68	-1.17	-0.19	<0.01
Fossorial-Arboreal	1.40	0.91	1.89	<0.01
Semiaquatic-Arboreal	1.71	1.18	2.24	<0.01
Semiarboreal-Arboreal	0.78	0.26	1.29	<0.01
Semifossorial-Arboreal	1.13	0.68	1.57	<0.01
Terrestrial-Arboreal	1.27	0.87	1.67	<0.01
Semiaquatic-Fossorial	0.31	-0.21	0.84	0.58
Semiarboreal-Fossorial	-0.62	-1.13	-0.11	0.01
Semifossorial-Fossorial	-0.27	-0.71	0.17	0.54
Terrestrial-Fossorial	-0.13	-0.52	0.27	0.96
Semiarboreal-Semiaquatic	-0.93	-1.48	-0.39	<0.01
Semifossorial-Semiaquatic	-0.58	-1.06	-0.10	0.01
Terrestrial-Semiaquatic	-0.44	-0.88	<0.01	0.05
Semifossorial-Semiarboreal	0.35	-0.11	0.82	0.28
Terrestrial-Semiarboreal	0.49	0.07	0.91	0.01
Terrestrial-Semifossorial	0.14	-0.20	0.48	0.88

Table B12. (continued)

PC6 All				
Arboreal-Aquatic	-0.38	-0.96	0.20	0.47
Fossorial-Aquatic	-0.03	-0.61	0.55	1.00
Semiaquatic-Aquatic	-0.49	-1.09	0.12	0.22
Semiarboreal-Aquatic	0.66	0.06	1.25	0.02
Semifossorial-Aquatic	0.77	0.24	1.31	<0.01
Terrestrial-Aquatic	-0.32	-0.82	0.18	0.48
Fossorial-Arboreal	0.35	-0.15	0.84	0.38
Semiaquatic-Arboreal	-0.11	-0.64	0.43	1.00
Semiarboreal-Arboreal	1.03	0.51	1.55	<0.01
Semifossorial-Arboreal	1.15	0.70	1.60	<0.01
Terrestrial-Arboreal	0.06	-0.35	0.46	1.00
Semiaquatic-Fossorial	-0.45	-0.99	0.08	0.15
Semiarboreal-Fossorial	0.69	0.17	1.20	<0.01
Semifossorial-Fossorial	0.80	0.36	1.25	<0.01
Terrestrial-Fossorial	-0.29	-0.69	0.11	0.33
Semiarboreal-Semiaquatic	1.14	0.59	1.69	<0.01
Semifossorial-Semiaquatic	1.26	0.77	1.74	<0.01
Terrestrial-Semiaquatic	0.17	-0.28	0.61	0.93
Semifossorial-Semiarboreal	0.11	-0.36	0.58	0.99
Terrestrial-Semiarboreal	-0.98	-1.40	-0.55	<0.01
Terrestrial-Semifossorial	-1.09	-1.43	-0.75	<0.01

Table B13. Tukey's test results of genus-level taxonomy for PCs 1-6 of the Crotalinae-only data.

PC1 Crotalinae	diff	lwr	upr	p adj
Bothriechis-Agkistrodon	1.35	0.35	2.35	<0.01
Bothrops-Agkistrodon	0.30	-2.12	2.72	1.00
Crotalus-Agkistrodon	0.24	-0.40	0.87	0.84
Sistrurus-Agkistrodon	-1.12	-2.02	-0.22	0.01
Bothrops-Bothriechis	-1.05	-3.55	1.45	0.77
Crotalus-Bothriechis	-1.11	-2.00	-0.23	0.01
Sistrurus-Bothriechis	-2.47	-3.56	-1.37	<0.01
Crotalus-Bothrops	-0.07	-2.44	2.31	1.00
Sistrurus-Bothrops	-1.42	-3.88	1.04	0.50
Sistrurus-Crotalus	-1.35	-2.13	-0.58	<0.01
PC2 Crotalinae				
Bothriechis-Agkistrodon	0.43	-0.65	1.50	0.80
Bothrops-Agkistrodon	-1.73	-4.33	0.88	0.35
Crotalus-Agkistrodon	0.64	-0.04	1.32	0.08
Sistrurus-Agkistrodon	-0.51	-1.48	0.46	0.60
Bothrops-Bothriechis	-2.15	-4.84	0.54	0.18
Crotalus-Bothriechis	0.22	-0.74	1.17	0.97
Sistrurus-Bothriechis	-0.93	-2.11	0.24	0.19
Crotalus-Bothrops	2.37	-0.19	4.92	0.08
Sistrurus-Bothrops	1.22	-1.43	3.87	0.70
Sistrurus-Crotalus	-1.15	-1.98	-0.32	<0.01
PC3 Crotalinae				
Bothriechis-Agkistrodon	1.42	0.36	2.49	<0.01
Bothrops-Agkistrodon	-0.62	-3.20	1.96	0.96
Crotalus-Agkistrodon	0.84	0.16	1.52	0.01
Sistrurus-Agkistrodon	1.43	0.46	2.39	<0.01
Bothrops-Bothriechis	-2.04	-4.70	0.63	0.22
Crotalus-Bothriechis	-0.58	-1.53	0.37	0.43
Sistrurus-Bothriechis	<0.01	-1.16	1.17	1.00
Crotalus-Bothrops	1.46	-1.08	3.99	0.50
Sistrurus-Bothrops	2.04	-0.58	4.67	0.20
Sistrurus-Crotalus	0.58	-0.24	1.41	0.29

Table B13. (continued)

PC4 Crotalinae				
Bothriechis-Agkistrodon	-0.96	-2.02	0.10	0.10
Bothrops-Agkistrodon	-0.54	-3.10	2.03	0.98
Crotalus-Agkistrodon	-0.09	-0.76	0.59	1.00
Sistrurus-Agkistrodon	1.13	0.18	2.09	0.01
Bothrops-Bothriechis	0.42	-2.22	3.07	0.99
Crotalus-Bothriechis	0.87	-0.07	1.81	0.08
Sistrurus-Bothriechis	2.09	0.93	3.25	<0.01
Crotalus-Bothrops	0.45	-2.06	2.96	0.99
Sistrurus-Bothrops	1.67	-0.94	4.27	0.39
Sistrurus-Crotalus	1.22	0.40	2.04	<0.01
PC5 Crotalinae				
Bothriechis-Agkistrodon	-0.33	-1.53	0.87	0.94
Bothrops-Agkistrodon	-0.38	-3.29	2.52	1.00
Crotalus-Agkistrodon	-0.10	-0.86	0.66	1.00
Sistrurus-Agkistrodon	0.08	-1.00	1.17	1.00
Bothrops-Bothriechis	-0.06	-3.05	2.94	1.00
Crotalus-Bothriechis	0.23	-0.83	1.30	0.97
Sistrurus-Bothriechis	0.41	-0.90	1.73	0.91
Crotalus-Bothrops	0.29	-2.56	3.14	1.00
Sistrurus-Bothrops	0.47	-2.48	3.42	0.99
Sistrurus-Crotalus	0.18	-0.75	1.11	0.98
PC6 Crotalinae				
Bothriechis-Agkistrodon	-1.08	-2.10	-0.05	0.03
Bothrops-Agkistrodon	-1.01	-3.48	1.47	0.79
Crotalus-Agkistrodon	0.69	0.04	1.33	0.03
Sistrurus-Agkistrodon	0.30	-0.62	1.22	0.89
Bothrops-Bothriechis	0.07	-2.49	2.63	1.00
Crotalus-Bothriechis	1.76	0.85	2.67	<0.01
Sistrurus-Bothriechis	1.38	0.26	2.50	0.01
Crotalus-Bothrops	1.69	-0.74	4.12	0.31
Sistrurus-Bothrops	1.31	-1.21	3.82	0.60
Sistrurus-Crotalus	-0.39	-1.18	0.41	0.66

Table B14. Tukey's test results of primary foraging habitat for PCs 1-6 of the Crotalinae-only data.

PC1 Crotalinae				
Semiaquatic-Arboreal	-2.13	-3.17	-1.08	<0.01
Terrestrial-Arboreal	-1.24	-2.04	-0.44	<0.01
Terrestrial-Semiaquatic	0.89	0.13	1.64	0.02
PC2 Crotalinae				
Semiaquatic-Arboreal	0.07	-1.09	1.24	0.99
Terrestrial-Arboreal	-0.10	-0.99	0.79	0.96
Terrestrial-Semiaquatic	-0.18	-1.02	0.67	0.87
PC3 Crotalinae				
Semiaquatic-Arboreal	-1.20	-2.34	-0.07	0.03
Terrestrial-Arboreal	-0.64	-1.50	0.22	0.19
Terrestrial-Semiaquatic	0.57	-0.25	1.38	0.23
PC4 Crotalinae				
Semiaquatic-Arboreal	0.13	-0.94	1.19	0.96
Terrestrial-Arboreal	1.14	0.32	1.95	<0.01
Terrestrial-Semiaquatic	1.01	0.24	1.78	0.01
PC5 Crotalinae				
Semiaquatic-Arboreal	1.03	-0.10	2.16	0.08
Terrestrial-Arboreal	0.18	-0.68	1.05	0.87
Terrestrial-Semiaquatic	-0.85	-1.67	-0.03	0.04
PC6 Crotalinae				
Semiaquatic-Arboreal	1.12	0.08	2.17	0.03
Terrestrial-Arboreal	1.61	0.81	2.40	<0.01
Terrestrial-Semiaquatic	0.48	-0.27	1.24	0.28

Code B1. This code performs Procrustes superimposition on landmark data, and completes PCAs, Tukey Tests, and DFAs for that data.

```
#make sure to install required packages
library(geomorph)
library(shapes)
library(ggplot2)
library(reshape2)
library(rgdal)
library(raster)
library(rgeos)
library(dplyr)
library(sp)
library(car)
library(phytools)
library(picante)
library(RColorBrewer)
getwd()
setwd("D:/morphometricschapter/")

snakemorph<-read.csv("Delimit_Dissertation_Table.csv", header=T)
head(snakemorph)
dim(snakemorph)
#Vsnakemorph <- snakemorph[-c(),]
#Bsnakemorph <- snakemorph[-c(),]
#Csnakemorph <- snakemorph[-c(),]
#Esnakemorph <- snakemorph[-c(),]
#Nsnakemorph <- snakemorph[-c(),]

#where x = number of specimens; y = ???
landmarks<-readland.tps("fullantmorph.TPS")
landmarks<-landmarks[-24,,]
dim(landmarks)

#######
crotalinae_subset <- snakemorph %>%
  filter (Subfamily == "Crotalinae")
crotalinae_ID <- crotalinae_subset[,1]
crotalinae_lm <-
landmarks[,,c(1,2,11,12,13,25,26,27,28,29,30,31,32,33,34,35,106,107,134,135,136,137,
138,139, 140, 147, 148, 149, 150, 156, 157, 158, 195, 196, 197, 198, 199, 200, 201, 202,
227, 228, 229, 230, 231, 244, 245, 246, 247, 248, 249, 280, 281, 282,283, 284, 285, 286,
287, 288, 289, 290, 291, 292, 293, 294, 295, 296, 297, 298, 299, 300, 301, 302, 303,
304, 305, 306, 307, 308, 309, 310, 411, 412, 413, 414, 415, 416, 417, 442, 450, 451,
452, 453, 461, 492, 493)]
```

```
###########

plot(landmarks[,,1], xlim = c(0,3000), ylim = c(0,3000), cex=2)

for(i in 2:length(landmarks[1,1,])){
  points(landmarks[,,i], col=i, cex=2)
}

proc<-gpagen(landmarks)

PC_proc<-gm.prcomp(proc$coords)

crotalinae_proc<-gpagen(crotalinae_lm)

par(cex=1.0)
par(pch = 16)
par(col = "black", bg="white")
plot(proc)
plot(crotalinae_proc)


for(lm in 1:23){
  plot(proc$coords[lm,1,], proc$coords[lm,2,], xlim =
c(min(proc$coords[lm,1,]),max(proc$coords[lm,1,])), ylim =
c(min(proc$coords[lm,2,]),max(proc$coords[lm,2,])), main = paste("Landmark #", lm),
asp = 1)
  text(proc$coords[lm,1,], proc$coords[lm,2,], labels = 1:length(snakemorph$Genus))
}
par(pch=16)
par(cex=1.0)
par()

dev.off()
plot(proc$consensus, xlab="X", ylab="Y", xlim = c(-0.4, 0.4), ylim = c(-0.4, 0.4),
cex=2, pch=19)
text(proc$consensus,labels=1:23, pos = 2)


snakemorph$Family=as.factor(snakemorph$Family)
plot(proc)
snakemorph$Substrate=as.factor(snakemorph$Substrate)
#PCAF <- plotTangentSpace(proc$coords,axis1=1, axis2=2, label=T, groups =
snakemorph$Family, legend=F)
```

```
#PCAF$pc.summary
#PCAF$pc.scores[,1]
snakemorph$Substrate=as.factor(snakemorph$Substrate)

snakemorph$Subfamily=as.factor(snakemorph$Subfamily)

snakemorph$Genus=as.factor(snakemorph$Genus)

snakemorph$Species=as.factor(snakemorph$Species)

#exportpdf, 6x11 landscape for current window size xlim -3, 6 (PC1&2), -3, 7 (PC3&4)
altPCAF <- procGPA(landmarks)
par(cex=1)
par(pch=19)
cols = c("blue", "violet", "darkgreen", "slategray", "blueviolet", "red", "black",
"chocolate4", "green2", "deepskyblue" , "orange")
plot(altPCAF$stdscores[,1], altPCAF$stdscores[,2], xlim = c(-3.5, 3), xlab = "PC1",
ylab= "PC2", col= alpha(cols[snakemorph$Family], 0.5))
text(altPCAF$stdscores[,1], altPCAF$stdscores[,2], cex= 0.75, labels = snakemorph$ID)
legend('bottomright', legend=levels(snakemorph$Family), col =
alpha(cols[seq_along(snakemorph$Family)], 0.5), cex=1, pch=19)

altPCAF$percent
#write.csv(altPCAF$percent, file="PCAF_percent.csv")


crotalinae_subset$Substrate=as.factor(crotalinae_subset$Substrate)

crotalinae_subset$Subfamily=as.factor(crotalinae_subset$Subfamily)

crotalinae_subset$Genus=as.factor(crotalinae_subset$Genus)

crotalinae_subset$Species=as.factor(crotalinae_subset$Species)

crotalinae_PCA <- procGPA(crotalinae_lm)
par(cex=1)
par(pch=16)
cols = c("darkgreen", "blue", "orange", "slategray", "red")
plot(crotalinae_PCA$scores[,5], crotalinae_PCA$scores[,6], xlim = c(-100, 100),  xlab =
"PC5", ylab= "PC6", col= alpha(cols[crotalinae_subset$Substrate], 0.5))
text(crotalinae_PCA$scores[,5], crotalinae_PCA$scores[,6], cex= 0.75, labels =
crotalinae_subset$ID)
legend('bottomright', legend=levels(crotalinae_subset$Substrate), col =
alpha(cols[seq_along(crotalinae_subset$Substrate)], 0.5), cex=1, pch=20)
```

```
crotalinae_PCA$percent
#write.csv(crotalinae_PCA$percent, file="crotalinae_percent.csv")

#adjust the values below to show extremes of shape for different PCs
#PC1
#tpsgrid(proc$coords[,,37], proc$coords[,,60], mag = 1, cex = 2)
#tpsgrid(proc$coords[,,70], proc$coords[,,29], mag = 1, cex = 2)

pcaxis <- 1
sd_mag <- 1
plotRefToTarget(-sd_mag*sd(altPCAF$scores[,pcaxis])*altPCAF$pcar[,pcaxis] +
altPCAF$mshape, sd_mag*sd(altPCAF$scores[,pcaxis])*altPCAF$pcar[,pcaxis] +
altPCAF$mshape, method="vector")
plotRefToTarget(-sd_mag*sd(PC_proc$x[,pcaxis])*PC_proc$rotation[,pcaxis] +
proc$consensus, sd_mag*sd(PC_proc$x[,pcaxis])*PC_proc$rotation[,pcaxis] +
proc$consensus, method="vector")

pcaxis <- 6
sd_mag <- 1
plotRefToTarget(-
sd_mag*sd(crotalinae_PCA$scores[,pcaxis])*crotalinae_PCA$pcar[,pcaxis] +
crotalinae_PCA$mshape,
sd_mag*sd(crotalinae_PCA$scores[,pcaxis])*crotalinae_PCA$pcar[,pcaxis] +
crotalinae_PCA$mshape, method="vector")



tpsgrid(proc$consensus, proc$coords[,,107], col=1, mag =1, cex = 2.5) #bot
tpsgrid(proc$consensus, proc$coords[,,351], col=1, mag = 1, cex = 2.5) #top
tpsgrid(proc$coords[,,107], proc$coords[,,351], col=1, mag = 1, cex = 2.5)

#PC2

tpsgrid(proc$consensus, proc$coords[,,89], mag = 1, cex = 2.5) #bot
tpsgrid(proc$consensus, proc$coords[,,257], mag = 1, cex = 2.5) #top
tpsgrid(proc$coords[,,89], proc$coords[,,257], col=1, mag = 1, cex = 2.5)

#tpsgrid(proc$coords[,,91], proc$coords[,,103], mag = 1, cex = 2)
#tpsgrid(proc$coords[,,5], proc$coords[,,79], mag = 1, cex = 2)

#PC3
tpsgrid(proc$coords[,,279], proc$coords[,,334], col=1, mag = 1, cex = 2.5)
```

```
#PC4
tpsgrid(proc$coords[,,491], proc$coords[,,352], col=1, mag = 1, cex = 2.5) #bottop

#PC5
tpsgrid(proc$coords[,,285], proc$coords[,,242], col=1, mag = 1, cex = 2.5) #bottop


#do boxplots for for all six PC scores individually; add splines in illustrator


BXPLT <- cbind.data.frame(altPCAF$stdscores[, 1:6], Family = snakemorph$Family)
ggplot(data = BXPLT, aes(x = reorder(Family, -PC1), y = PC1)) +
scale_fill_brewer(palette="Set3") + geom_boxplot(aes(fill =
Family))+xlab("Family")+theme(text=element_text(size=14), axis.text.x =
element_text(angle=45, hjust=1))
ggplot(data = BXPLT, aes(x = reorder(Family, -PC2), y = PC2)) +
scale_fill_brewer(palette="Set3") + geom_boxplot(aes(fill =
Family))+xlab("Family")+theme(text=element_text(size=14), axis.text.x =
element_text(angle=45, hjust=1))
ggplot(data = BXPLT, aes(x = reorder(Family, -PC3), y = PC3)) +
scale_fill_brewer(palette="Set3") + geom_boxplot(aes(fill =
Family))+xlab("Family")+theme(text=element_text(size=14), axis.text.x =
element_text(angle=45, hjust=1))
ggplot(data = BXPLT, aes(x = reorder(Family, -PC4), y = PC4)) +
scale_fill_brewer(palette="Set3") + geom_boxplot(aes(fill =
Family))+xlab("Family")+theme(text=element_text(size=14), axis.text.x =
element_text(angle=45, hjust=1))
ggplot(data = BXPLT, aes(x = reorder(Family, -PC5), y = PC5)) +
scale_fill_brewer(palette="Set3") + geom_boxplot(aes(fill =
Family))+xlab("Family")+theme(text=element_text(size=14), axis.text.x =
element_text(angle=45, hjust=1))
ggplot(data = BXPLT, aes(x = reorder(Family, -PC6), y = PC6)) +
scale_fill_brewer(palette="Set3") + geom_boxplot(aes(fill =
Family))+xlab("Family")+theme(text=element_text(size=14), axis.text.x =
element_text(angle=45, hjust=1))

MLT <- melt(BXPLT, id.var = "Family")
ggplot(data = MLT, aes(x = reorder(Family, -value),y = value)) + geom_boxplot(aes(fill
= variable))

BXPLT <- cbind.data.frame(altPCAF$stdscores[, 1:6], ecology =
snakemorph$Substrate)
ggplot(data = BXPLT, aes(x = reorder(ecology, -PC1), y = PC1)) +
scale_fill_brewer(palette="Set3") + geom_boxplot(aes(fill =
```

```
ecology))+xlab("Ecology")+theme(text=element_text(size=14), axis.text.x =
element_text(angle=45, hjust=1))
ggplot(data = BXPLT, aes(x = reorder(ecology, -PC2), y = PC2)) +
scale_fill_brewer(palette="Set3") + geom_boxplot(aes(fill =
ecology))+xlab("Ecology")+theme(text=element_text(size=14), axis.text.x =
element_text(angle=45, hjust=1))
ggplot(data = BXPLT, aes(x = reorder(ecology, -PC3), y = PC3)) +
scale_fill_brewer(palette="Set3") + geom_boxplot(aes(fill =
ecology))+xlab("Ecology")+theme(text=element_text(size=14), axis.text.x =
element_text(angle=45, hjust=1))
ggplot(data = BXPLT, aes(x = reorder(ecology, -PC4), y = PC4)) +
scale_fill_brewer(palette="Set3") + geom_boxplot(aes(fill =
ecology))+xlab("Ecology")+theme(text=element_text(size=14), axis.text.x =
element_text(angle=45, hjust=1))
ggplot(data = BXPLT, aes(x = reorder(ecology, -PC5), y = PC5)) +
scale_fill_brewer(palette="Set3") + geom_boxplot(aes(fill =
ecology))+xlab("Ecology")+theme(text=element_text(size=14), axis.text.x =
element_text(angle=45, hjust=1))
ggplot(data = BXPLT, aes(x = reorder(ecology, -PC6), y = PC6)) +
scale_fill_brewer(palette="Set3") + geom_boxplot(aes(fill =
ecology))+xlab("Ecology")+theme(text=element_text(size=14), axis.text.x =
element_text(angle=45, hjust=1))

BXPLT <- cbind.data.frame(crotalinae_PCA$stdscores[, 1:6], Genus =
crotalinae_subset$Genus)
ggplot(data = BXPLT, aes(x = reorder(Genus, -PC1), y = PC1)) +
scale_fill_brewer(palette="Set3") + geom_boxplot(aes(fill =
Genus))+xlab("Genus")+theme(text=element_text(size=14), axis.text.x =
element_text(angle=45, hjust=1))
ggplot(data = BXPLT, aes(x = reorder(Genus, -PC2), y = PC2)) +
scale_fill_brewer(palette="Set3") + geom_boxplot(aes(fill =
Genus))+xlab("Genus")+theme(text=element_text(size=14), axis.text.x =
element_text(angle=45, hjust=1))
ggplot(data = BXPLT, aes(x = reorder(Genus, -PC3), y = PC3)) +
scale_fill_brewer(palette="Set3") + geom_boxplot(aes(fill =
Genus))+xlab("Genus")+theme(text=element_text(size=14), axis.text.x =
element_text(angle=45, hjust=1))
ggplot(data = BXPLT, aes(x = reorder(Genus, -PC4), y = PC4)) +
scale_fill_brewer(palette="Set3") + geom_boxplot(aes(fill =
Genus))+xlab("Genus")+theme(text=element_text(size=14), axis.text.x =
element_text(angle=45, hjust=1))
ggplot(data = BXPLT, aes(x = reorder(Genus, -PC5), y = PC5)) +
scale_fill_brewer(palette="Set3") + geom_boxplot(aes(fill =
```

```
Genus))+xlab("Genus")+theme(text=element_text(size=14), axis.text.x =
element_text(angle=45, hjust=1))
ggplot(data = BXPLT, aes(x = reorder(Genus, -PC6), y = PC6)) +
scale_fill_brewer(palette="Set3") + geom_boxplot(aes(fill =
Genus))+xlab("Genus")+theme(text=element_text(size=14), axis.text.x =
element_text(angle=45, hjust=1))

MLT <- melt(BXPLT, id.var = "Genus")
ggplot(data = MLT, aes(x = reorder(Genus, -value),y = value)) + geom_boxplot(aes(fill
= variable))

BXPLT <- cbind.data.frame(crotalinae_PCA$stdscores[, 1:6], ecology =
crotalinae_subset$Substrate)
ggplot(data = BXPLT, aes(x = reorder(ecology, -PC1), y = PC1)) +
scale_fill_brewer(palette="Set3") + geom_boxplot(aes(fill =
ecology))+xlab("Ecology")+theme(text=element_text(size=14), axis.text.x =
element_text(angle=45, hjust=1))
ggplot(data = BXPLT, aes(x = reorder(ecology, -PC2), y = PC2)) +
scale_fill_brewer(palette="Set3") + geom_boxplot(aes(fill =
ecology))+xlab("Ecology")+theme(text=element_text(size=14), axis.text.x =
element_text(angle=45, hjust=1))
ggplot(data = BXPLT, aes(x = reorder(ecology, -PC3), y = PC3)) +
scale_fill_brewer(palette="Set3") + geom_boxplot(aes(fill =
ecology))+xlab("Ecology")+theme(text=element_text(size=14), axis.text.x =
element_text(angle=45, hjust=1))
ggplot(data = BXPLT, aes(x = reorder(ecology, -PC4), y = PC4)) +
scale_fill_brewer(palette="Set3") + geom_boxplot(aes(fill =
ecology))+xlab("Ecology")+theme(text=element_text(size=14), axis.text.x =
element_text(angle=45, hjust=1))
ggplot(data = BXPLT, aes(x = reorder(ecology, -PC5), y = PC5)) +
scale_fill_brewer(palette="Set3") + geom_boxplot(aes(fill =
ecology))+xlab("Ecology")+theme(text=element_text(size=14), axis.text.x =
element_text(angle=45, hjust=1))
ggplot(data = BXPLT, aes(x = reorder(ecology, -PC6), y = PC6)) +
scale_fill_brewer(palette="Set3") + geom_boxplot(aes(fill =
ecology))+xlab("Ecology")+theme(text=element_text(size=14), axis.text.x =
element_text(angle=45, hjust=1))

##################
summary(aov(altPCAF$stdscores[,1]~snakemorph$Substrate*snakemorph$Family))
summary(aov(altPCAF$stdscores[,2]~snakemorph$Substrate*snakemorph$Family))
summary(aov(altPCAF$stdscores[,1]~snakemorph$Substrate*snakemorph$Family))
summary(aov(altPCAF$stdscores[,2]~snakemorph$Substrate*snakemorph$Family))
summary(aov(altPCAF$stdscores[,2]~snakemorph$Substrate*snakemorph$Family))
```

```
summary(aov(altPCAF$stdscores[,1]~snakemorph$Family)) #shape is different by
family
summary(aov(altPCAF$stdscores[,1]~snakemorph$Subfamily))
summary(aov(altPCAF$stdscores[,1]~snakemorph$Substrate))
summary(aov(altPCAF$stdscores[,1]~snakemorph$Genus))
summary(aov(altPCAF$stdscores[,1]~snakemorph$Species))

anova1 <- summary(aov(altPCAF$stdscores[,1:6]~snakemorph$Family))
anova2 <- summary(aov(altPCAF$stdscores[,1:6]~snakemorph$Subfamily))
anova3 <- summary(aov(altPCAF$stdscores[,1:6]~snakemorph$Substrate))
anova4 <- summary(aov(altPCAF$stdscores[,1:6]~snakemorph$Genus))
anova5 <- summary(aov(altPCAF$stdscores[,1:6]~snakemorph$Species))
#capture.output(anova5, file="species_anova")

C_anova1 <-
summary(aov(crotalinae_PCA$stdscores[,1:6]~crotalinae_subset$Substrate))
C_anova2 <- summary(aov(crotalinae_PCA$stdscores[,1:6]~crotalinae_subset$Genus))
C_anova3 <-
summary(aov(crotalinae_PCA$stdscores[,1:6]~crotalinae_subset$Species))
#capture.output(C_anova3, file="species_Canova")

summary(aov(altPCAF$stdscores[,2]~snakemorph$Family))
summary(aov(altPCAF$stdscores[,2]~snakemorph$Subfamily))
summary(aov(altPCAF$stdscores[,2]~snakemorph$Substrate))
summary(aov(altPCAF$stdscores[,2]~snakemorph$Genus))
summary(aov(altPCAF$stdscores[,2]~snakemorph$Species))

summary(aov(altPCAF$stdscores[,3]~snakemorph$Family))
summary(aov(altPCAF$stdscores[,3]~snakemorph$Subfamily))
summary(aov(altPCAF$stdscores[,3]~snakemorph$Substrate))
summary(aov(altPCAF$stdscores[,3]~snakemorph$Genus))
summary(aov(altPCAF$stdscores[,3]~snakemorph$Species))

summary(aov(altPCAF$stdscores[,4]~snakemorph$Family))
summary(aov(altPCAF$stdscores[,4]~snakemorph$Subfamily))
summary(aov(altPCAF$stdscores[,4]~snakemorph$Substrate))
summary(aov(altPCAF$stdscores[,4]~snakemorph$Genus))
summary(aov(altPCAF$stdscores[,4]~snakemorph$Species))

summary(aov(altPCAF$stdscores[,5]~snakemorph$Family))
summary(aov(altPCAF$stdscores[,5]~snakemorph$Subfamily))
summary(aov(altPCAF$stdscores[,5]~snakemorph$Substrate))
summary(aov(altPCAF$stdscores[,5]~snakemorph$Genus))
```

```
summary(aov(altPCAF$stdscores[,5]~snakemorph$Species))

tukey.test <- TukeyHSD(aov(altPCAF$stdscores[,6]~snakemorph$Subfamily))
tukey.test
write.csv(tukey.test$`snakemorph$Subfamily`, file="PC6tukeysubfam.csv")
#do 2 significant digits in excel file
plot(tukey.test)
summary(tukey.test)

tukey.test2 <- TukeyHSD(aov(crotalinae_PCA$stdscores[,2]~crotalinae_subset$Genus))
tukey.test2
write.csv(tukey.test2$`crotalinae_subset$Genus`, file="PC2crogen.csv")
plot(tukey.test2)
summary(tukey.test2)


#DFA stuff################################

#function for creating a confusion matrix for the DFA results
confusion <- function(actual, predicted, names = NULL, prinit = T, prior = NULL) {
  if(is.null(names)) names <- levels(actual)
  tab <- table(actual, predicted)
  acctab <- t(apply(tab, 1, function(x)x/sum(x)))
  dimnames(acctab) <- list(Actual = names, Predicted = names)
  if(is.null(prior)) {
    relnum <- table(actual)
    prior <- relnum /sum(relnum)
    acc <- sum(tab[row(tab)==col(tab)])/sum(tab)
  } else {
    acc <- sum(prior*diag(acctab))
    names(prior) <- names
  }
  if(prinit) print(round(c("Overall accuracy" = acc, "Prior frequency" = prior), 4))
  if(prinit) {
    cat("\nConfusion matrix", "\n")
    print(round(acctab, 4))
  }
  invisible(acctab)
}

#below grabs family info (switch or add whatever is needed) and pc scores up to about
the inflection point
getOption("max.print")
options(max.print = 10)
```

```
SVAL <- cbind.data.frame(family = snakemorph$Family, subfamily =
snakemorph$Subfamily, substrate = snakemorph$Substrate, altPCAF$scores[, 1:46])
DFA <- MASS::lda(droplevels(SVAL$family) ~ ., data = SVAL[,3:22], CV = T)
confusion(SVAL$family, DFA$class)

DFAS <- MASS::lda(SVAL$substrate ~ ., data = SVAL[,3:37], CV = T)
confusion(SVAL$substrate, DFAS$class)


#below grabs subfamily info (switch or add whatever is needed) and all pc scores
SVAL2 <- cbind.data.frame(subfamily = snakemorph$Subfamily, substrate =
snakemorph$Substrate, altPCAF$scores[, 1:46])
DFA2 <- MASS::lda(SVAL2$subfamily ~ ., data = SVAL2[,3:38], CV = T)
confusion(SVAL2$subfamily, DFA2$class)

#below grabs genus info (switch or add whatever is needed) and all pc scores
SVAL3 <- cbind.data.frame(genus = snakemorph$Genus, substrate =
snakemorph$Substrate, altPCAF$scores[, 1:46])
DFA3 <- MASS::lda(SVAL3$genus ~ ., data = SVAL3[,3:19], CV = T)
confusion3 <- confusion(SVAL3$genus, DFA3$class)

#below grabs species info (switch or add whatever is needed) and all pc scores
SVAL4 <- cbind.data.frame(species = snakemorph$Species, substrate =
snakemorph$Substrate, altPCAF$stdscores[, 1:46])
DFA4 <- MASS::lda(SVAL4$species ~ ., data = SVAL4[, 3:19], CV = T)
confusion(SVAL4$species, DFA4$class)



#below grabs genus info (switch or add whatever is needed) and all pc scores
crotal1 <- cbind.data.frame(genus = crotalinae_subset$Genus, substrate =
crotalinae_subset$Substrate, crotalinae_PCA$scores[, 1:46])
crotalDFA1 <- MASS::lda(crotal1$genus ~ ., data = crotal1[, 3:19], CV = T)
crotal_genus <- confusion(crotal1$genus, crotalDFA1$class)

#below grabs species info (switch or add whatever is needed) and all pc scores
crotal2 <- cbind.data.frame(species = crotalinae_subset$Species, substrate =
crotalinae_subset$Substrate, crotalinae_PCA$scores[, 1:46])
crotalDFA2 <- MASS::lda(crotal2$species ~ ., data = crotal2[, 3:30], CV = T)
confusion(crotal2$species, crotalDFA2$class)

crotalDFAS <- MASS::lda(crotal1$substrate ~ ., data = crotal1[,3:8], CV = T)
confusion(crotal1$substrate, crotalDFAS$class)
```

APPENDIX C

SUPPLEMENTAL MATERIAL FOR CHAPTER 4

Appendix C contents:

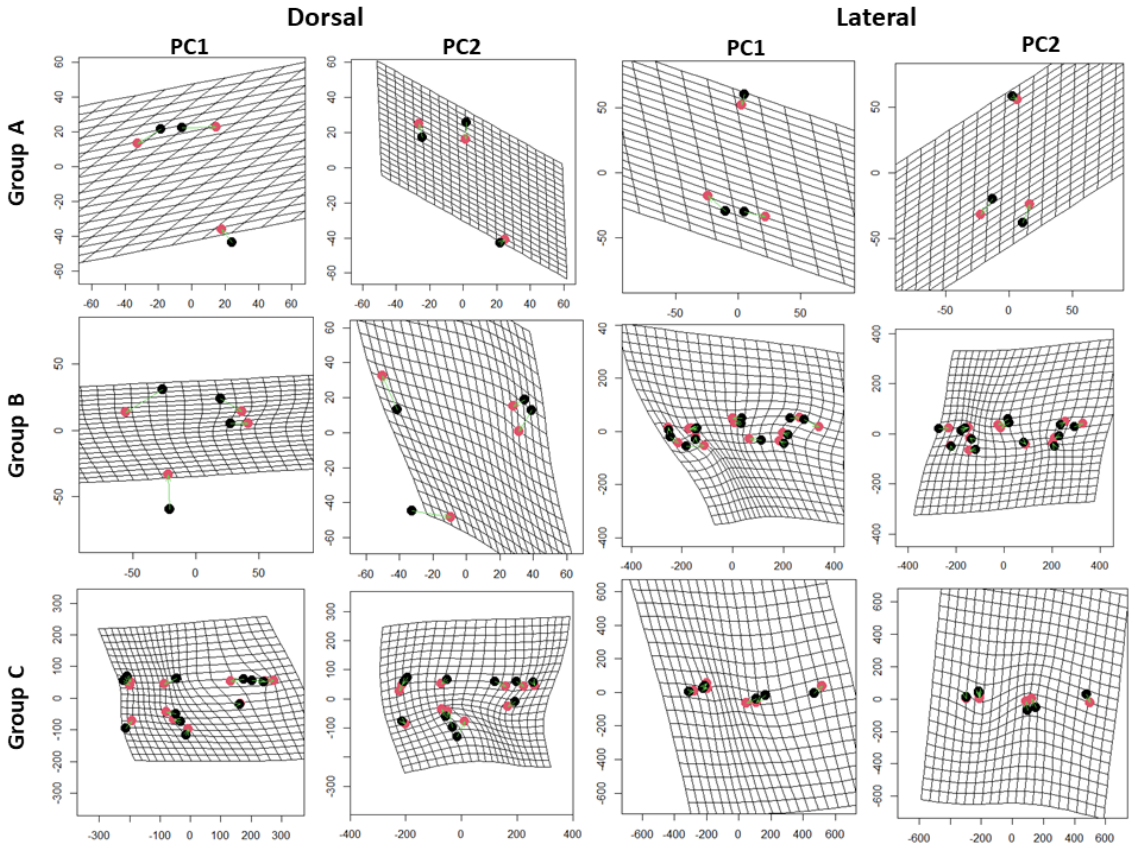

Figure C1. Thin plate spline deformation grids for all selected PCs from each group in the dorsal and lateral orientations. Green arrows indicate direction of change from shapes from negative (black circles) to positive (red circles) along the PC axis.

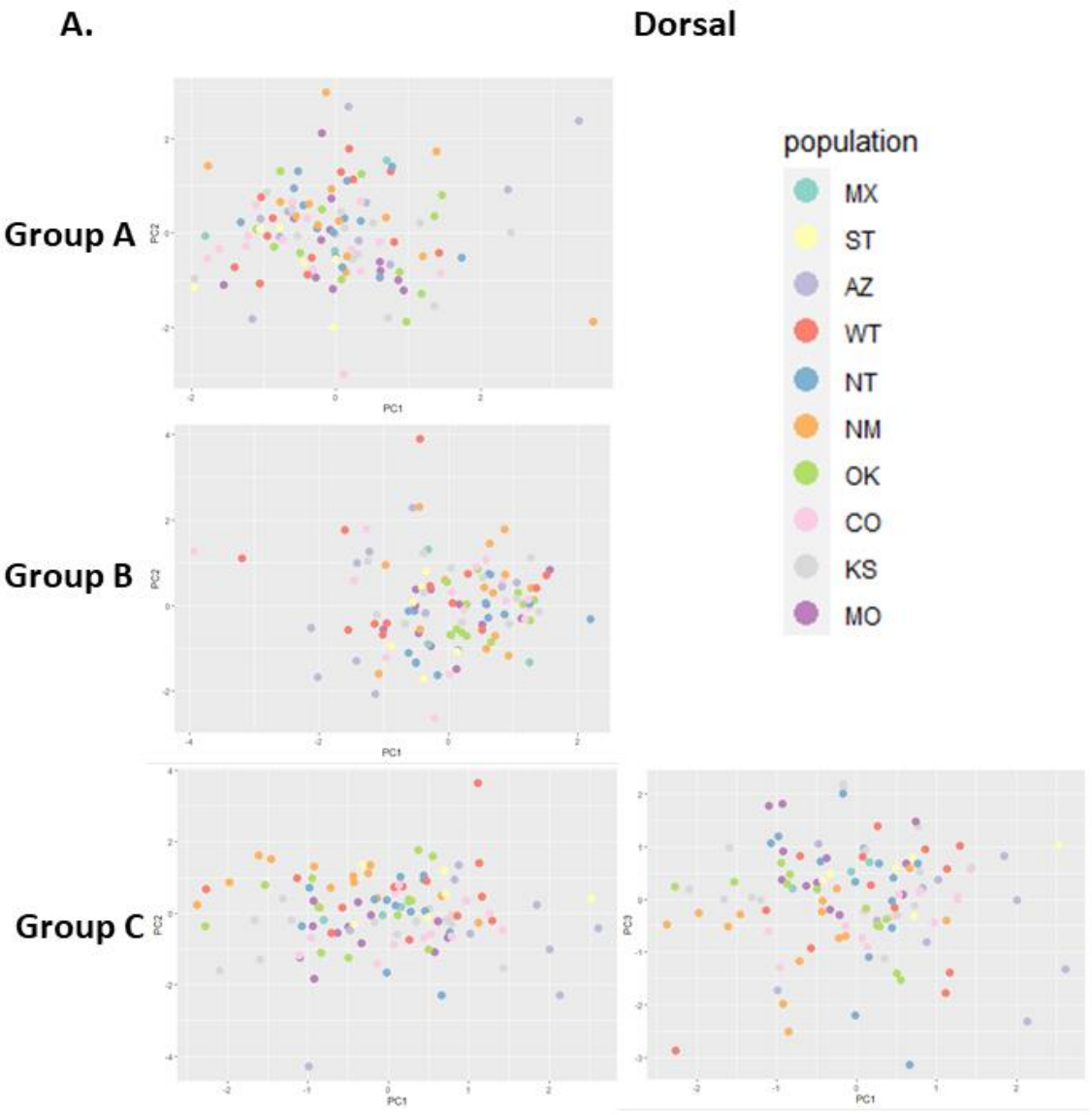

Figure C2. PC plots for each dorsal group, colored by population.

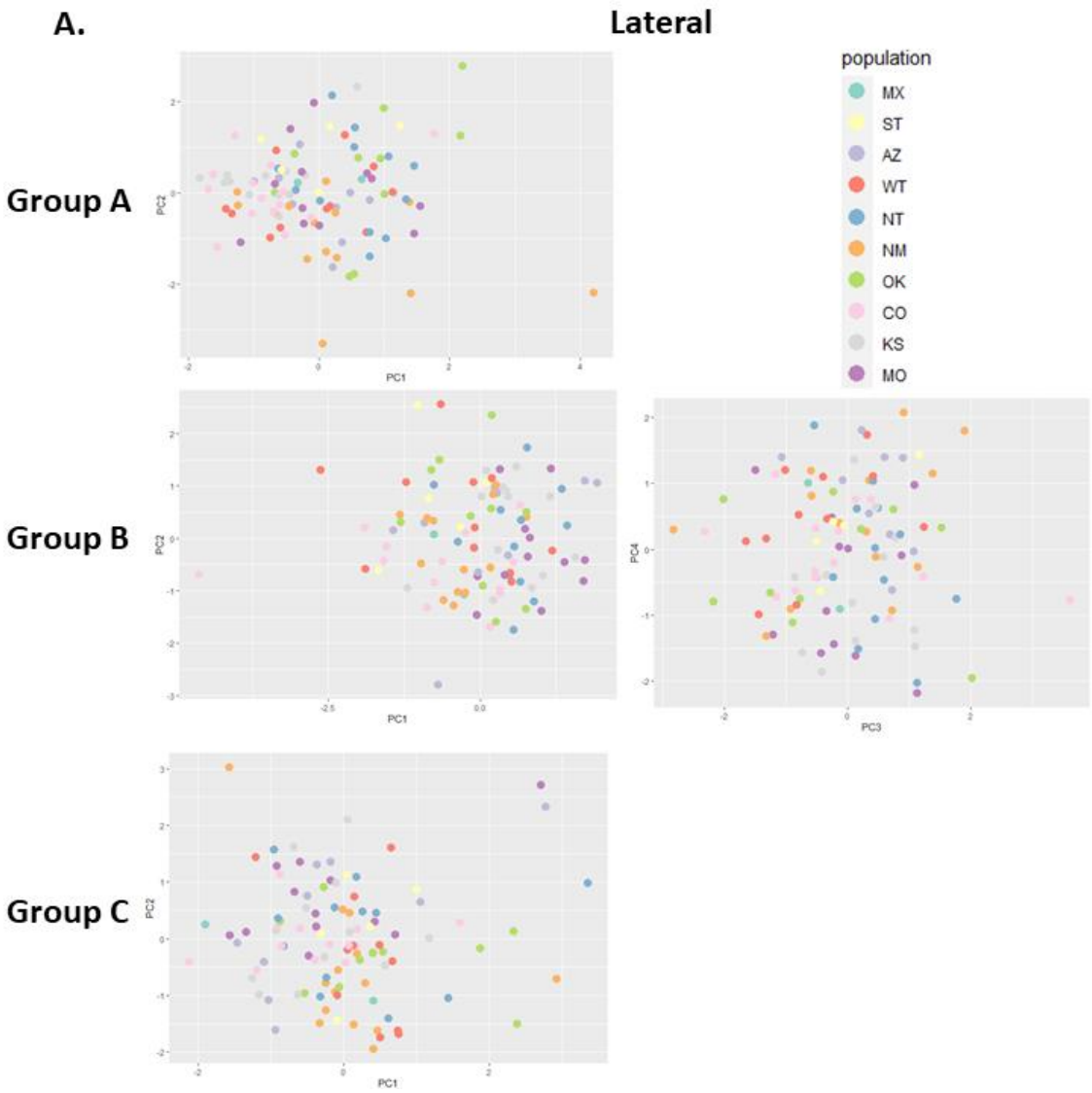

Figure C3. PC plots for each lateral group, colored by population.

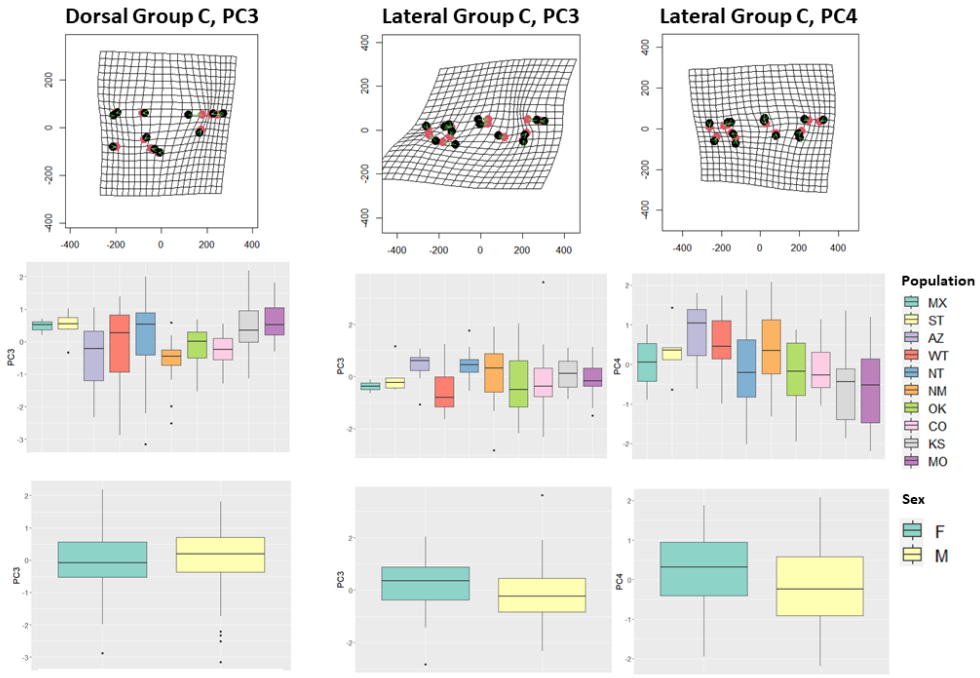

Figure C4. Thin plate splines and box plots for additional selected PCs from dorsal (Group C) and lateral (Group B) orientations. Box plots are separated by population (top) and sex (bottom).

Table C1. Tukey's test table for dorsal skull shape groups, between populations.

	diff	lwr	upr	p adj
Group A PC1				
ST-MX	-0.34	-2.56	1.88	1.00
AZ-MX	0.75	-1.32	2.82	0.98
WT-MX	0.18	-1.84	2.19	1.00
NT-MX	0.42	-1.58	2.42	1.00
NM-MX	0.60	-1.40	2.60	0.99
OK-MX	0.61	-1.42	2.64	0.99
CO-MX	-0.02	-2.01	1.97	1.00
KS-MX	0.57	-1.43	2.58	1.00
MO-MX	0.37	-1.66	2.40	1.00
AZ-ST	1.09	-0.54	2.71	0.49
WT-ST	0.52	-1.04	2.07	0.99
NT-ST	0.76	-0.78	2.29	0.84
NM-ST	0.94	-0.59	2.48	0.61
OK-ST	0.95	-0.62	2.52	0.63
CO-ST	0.32	-1.20	1.83	1.00
KS-ST	0.91	-0.62	2.45	0.65
MO-ST	0.71	-0.86	2.29	0.90
WT-AZ	-0.57	-1.89	0.75	0.93
NT-AZ	-0.33	-1.63	0.98	1.00
NM-AZ	-0.14	-1.44	1.16	1.00
OK-AZ	-0.13	-1.48	1.21	1.00
CO-AZ	-0.77	-2.05	0.51	0.64
KS-AZ	-0.17	-1.47	1.13	1.00
MO-AZ	-0.37	-1.72	0.97	1.00
NT-WT	0.24	-0.97	1.45	1.00
NM-WT	0.43	-0.78	1.64	0.98
OK-WT	0.43	-0.82	1.69	0.98
CO-WT	-0.20	-1.39	0.99	1.00
KS-WT	0.40	-0.81	1.61	0.99
MO-WT	0.20	-1.06	1.46	1.00
NM-NT	0.18	-1.00	1.37	1.00
OK-NT	0.19	-1.04	1.43	1.00
CO-NT	-0.44	-1.61	0.73	0.97
KS-NT	0.16	-1.03	1.34	1.00

Table C1. (continued)

MO-NT	-0.05	-1.28	1.19	1.00
OK-NM	0.01	-1.23	1.25	1.00
CO-NM	-0.63	-1.80	0.54	0.77
KS-NM	-0.03	-1.22	1.16	1.00
MO-NM	-0.23	-1.47	1.01	1.00
CO-OK	-0.64	-1.85	0.58	0.80
KS-OK	-0.04	-1.27	1.20	1.00
MO-OK	-0.24	-1.52	1.05	1.00
KS-CO	0.60	-0.57	1.77	0.82
MO-CO	0.40	-0.82	1.62	0.99
MO-KS	-0.20	-1.44	1.04	1.00
Group A PC2				
ST-MX	-1.05	-3.27	1.17	0.87
AZ-MX	0.10	-1.97	2.17	1.00
WT-MX	-0.15	-2.16	1.86	1.00
NT-MX	-0.11	-2.11	1.89	1.00
NM-MX	0.05	-1.95	2.05	1.00
OK-MX	-0.48	-2.51	1.55	1.00
CO-MX	-0.70	-2.69	1.28	0.98
KS-MX	-0.58	-2.58	1.42	0.99
MO-MX	-0.68	-2.70	1.35	0.99
AZ-ST	1.15	-0.47	2.77	0.40
WT-ST	0.90	-0.65	2.45	0.68
NT-ST	0.94	-0.59	2.47	0.60
NM-ST	1.10	-0.43	2.63	0.38
OK-ST	0.57	-1.00	2.14	0.97
CO-ST	0.35	-1.17	1.86	1.00
KS-ST	0.47	-1.06	2.00	0.99
MO-ST	0.38	-1.19	1.95	1.00
WT-AZ	-0.25	-1.57	1.07	1.00
NT-AZ	-0.21	-1.51	1.09	1.00
NM-AZ	-0.05	-1.35	1.25	1.00
OK-AZ	-0.58	-1.92	0.76	0.92
CO-AZ	-0.80	-2.08	0.48	0.58
KS-AZ	-0.68	-1.98	0.62	0.79
MO-AZ	-0.77	-2.12	0.57	0.69
NT-WT	0.04	-1.16	1.25	1.00

Table C1. (continued)

NM-WT	0.20	-1.01	1.41	1.00
OK-WT	-0.33	-1.58	0.93	1.00
CO-WT	-0.55	-1.74	0.64	0.89
KS-WT	-0.43	-1.64	0.78	0.98
MO-WT	-0.52	-1.78	0.74	0.94
NM-NT	0.16	-1.03	1.34	1.00
OK-NT	-0.37	-1.61	0.86	0.99
CO-NT	-0.59	-1.76	0.57	0.82
KS-NT	-0.47	-1.66	0.71	0.95
MO-NT	-0.57	-1.80	0.67	0.89
OK-NM	-0.53	-1.76	0.71	0.93
CO-NM	-0.75	-1.92	0.41	0.54
KS-NM	-0.63	-1.82	0.56	0.78
MO-NM	-0.72	-1.96	0.51	0.67
CO-OK	-0.22	-1.44	0.99	1.00
KS-OK	-0.10	-1.34	1.13	1.00
MO-OK	-0.19	-1.48	1.09	1.00
KS-CO	0.12	-1.04	1.29	1.00
MO-CO	0.03	-1.19	1.24	1.00
MO-KS	-0.09	-1.33	1.14	1.00
Group B PC1				
ST-MX	-0.61	-2.76	1.54	1.00
AZ-MX	-1.04	-3.05	0.96	0.80
WT-MX	-0.70	-2.65	1.25	0.98
NT-MX	0.08	-1.86	2.01	1.00
NM-MX	0.09	-1.85	2.02	1.00
OK-MX	0.36	-1.60	2.33	1.00
CO-MX	-0.28	-2.21	1.64	1.00
KS-MX	-0.11	-2.05	1.82	1.00
MO-MX	-0.12	-2.08	1.85	1.00
AZ-ST	-0.43	-2.00	1.14	1.00
WT-ST	-0.09	-1.59	1.42	1.00
NT-ST	0.69	-0.79	2.18	0.89
NM-ST	0.70	-0.78	2.19	0.88
OK-ST	0.97	-0.55	2.50	0.55
CO-ST	0.33	-1.14	1.80	1.00
KS-ST	0.50	-0.98	1.99	0.98

Table C1. (continued)

MO-ST	0.49	-1.03	2.02	0.99
WT-AZ	0.34	-0.94	1.62	1.00
NT-AZ	1.12	-0.14	2.38	0.12
NM-AZ	1.13	-0.13	2.39	0.12
OK-AZ	1.40	0.10	2.71	0.02
CO-AZ	0.76	-0.48	2.00	0.61
KS-AZ	0.93	-0.33	2.19	0.34
MO-AZ	0.92	-0.38	2.23	0.40
NT-WT	0.78	-0.40	1.95	0.50
NM-WT	0.79	-0.38	1.96	0.48
OK-WT	1.06	-0.16	2.28	0.14
CO-WT	0.42	-0.74	1.57	0.98
KS-WT	0.59	-0.59	1.76	0.83
MO-WT	0.58	-0.64	1.80	0.87
NM-NT	0.01	-1.14	1.16	1.00
OK-NT	0.28	-0.91	1.48	1.00
CO-NT	-0.36	-1.49	0.77	0.99
KS-NT	-0.19	-1.34	0.96	1.00
MO-NT	-0.20	-1.39	1.00	1.00
OK-NM	0.27	-0.92	1.47	1.00
CO-NM	-0.37	-1.50	0.76	0.99
KS-NM	-0.20	-1.35	0.95	1.00
MO-NM	-0.21	-1.40	0.99	1.00
CO-OK	-0.64	-1.82	0.53	0.75
KS-OK	-0.47	-1.67	0.72	0.96
MO-OK	-0.48	-1.72	0.76	0.96
KS-CO	0.17	-0.96	1.30	1.00
MO-CO	0.16	-1.01	1.34	1.00
MO-KS	-0.01	-1.20	1.19	1.00
Group B PC2				
ST-MX	-0.10	-2.36	2.16	1.00
AZ-MX	0.28	-1.82	2.38	1.00
WT-MX	0.80	-1.25	2.85	0.96
NT-MX	-0.12	-2.16	1.91	1.00
NM-MX	0.58	-1.46	2.61	1.00
OK-MX	0.14	-1.92	2.21	1.00
CO-MX	0.35	-1.67	2.37	1.00

Table C1. (continued)

KS-MX	0.54	-1.49	2.58	1.00
MO-MX	0.07	-1.99	2.14	1.00
AZ-ST	0.38	-1.27	2.03	1.00
WT-ST	0.90	-0.68	2.48	0.70
NT-ST	-0.02	-1.58	1.54	1.00
NM-ST	0.68	-0.88	2.24	0.92
OK-ST	0.25	-1.35	1.84	1.00
CO-ST	0.46	-1.09	2.00	0.99
KS-ST	0.65	-0.91	2.21	0.94
MO-ST	0.18	-1.42	1.77	1.00
WT-AZ	0.52	-0.82	1.87	0.96
NT-AZ	-0.40	-1.73	0.92	0.99
NM-AZ	0.30	-1.03	1.62	1.00
OK-AZ	-0.14	-1.51	1.23	1.00
CO-AZ	0.07	-1.23	1.38	1.00
KS-AZ	0.26	-1.06	1.59	1.00
MO-AZ	-0.21	-1.58	1.16	1.00
NT-WT	-0.92	-2.15	0.31	0.32
NM-WT	-0.22	-1.45	1.01	1.00
OK-WT	-0.66	-1.94	0.62	0.81
CO-WT	-0.45	-1.66	0.76	0.97
KS-WT	-0.26	-1.49	0.97	1.00
MO-WT	-0.73	-2.01	0.55	0.71
NM-NT	0.70	-0.51	1.91	0.68
OK-NT	0.27	-0.99	1.52	1.00
CO-NT	0.47	-0.71	1.66	0.95
KS-NT	0.67	-0.54	1.87	0.74
MO-NT	0.20	-1.06	1.45	1.00
OK-NM	-0.43	-1.69	0.82	0.98
CO-NM	-0.22	-1.41	0.96	1.00
KS-NM	-0.03	-1.24	1.17	1.00
MO-NM	-0.50	-1.76	0.75	0.95
CO-OK	0.21	-1.03	1.45	1.00
KS-OK	0.40	-0.86	1.66	0.99
MO-OK	-0.07	-1.37	1.24	1.00
KS-CO	0.19	-1.00	1.38	1.00
MO-CO	-0.28	-1.52	0.96	1.00

Table C1. (continued)

MO-KS	-0.47	-1.73	0.79	0.97
Group C PC1				
ST-MX	0.85	-1.26	2.97	0.95
AZ-MX	1.25	-0.72	3.22	0.56
WT-MX	0.38	-1.54	2.30	1.00
NT-MX	0.28	-1.63	2.18	1.00
NM-MX	-0.45	-2.35	1.46	1.00
OK-MX	-0.17	-2.10	1.76	1.00
CO-MX	0.65	-1.25	2.54	0.98
KS-MX	-0.01	-1.92	1.89	1.00
MO-MX	-0.10	-2.03	1.84	1.00
AZ-ST	0.40	-1.15	1.94	1.00
WT-ST	-0.47	-1.95	1.00	0.99
NT-ST	-0.57	-2.03	0.89	0.96
NM-ST	-1.30	-2.76	0.16	0.13
OK-ST	-1.02	-2.52	0.48	0.46
CO-ST	-0.21	-1.65	1.24	1.00
KS-ST	-0.87	-2.33	0.59	0.65
MO-ST	-0.95	-2.44	0.55	0.56
WT-AZ	-0.87	-2.13	0.39	0.44
NT-AZ	-0.97	-2.21	0.27	0.26
NM-AZ	-1.70	-2.93	-0.46	<0.01
OK-AZ	-1.42	-2.70	-0.14	0.02
CO-AZ	-0.60	-1.82	0.62	0.85
KS-AZ	-1.26	-2.50	-0.02	0.04
MO-AZ	-1.34	-2.63	-0.06	0.03
NT-WT	-0.10	-1.25	1.05	1.00
NM-WT	-0.83	-1.98	0.33	0.38
OK-WT	-0.55	-1.75	0.65	0.90
CO-WT	0.27	-0.87	1.40	1.00
KS-WT	-0.39	-1.55	0.76	0.98
MO-WT	-0.48	-1.67	0.72	0.95
NM-NT	-0.72	-1.86	0.41	0.55
OK-NT	-0.45	-1.62	0.73	0.97
CO-NT	0.37	-0.74	1.48	0.99
KS-NT	-0.29	-1.42	0.84	1.00
MO-NT	-0.37	-1.55	0.80	0.99

Table C1. (continued)

OK-NM	0.28	-0.90	1.46	1.00
CO-NM	1.09	-0.02	2.21	0.06
KS-NM	0.43	-0.70	1.56	0.96
MO-NM	0.35	-0.83	1.53	0.99
CO-OK	0.81	-0.34	1.97	0.41
KS-OK	0.15	-1.02	1.33	1.00
MO-OK	0.07	-1.15	1.29	1.00
KS-CO	-0.66	-1.77	0.45	0.65
MO-CO	-0.74	-1.90	0.42	0.55
MO-KS	-0.08	-1.26	1.10	1.00
Group C PC2				
ST-MX	0.54	-1.35	2.43	1.00
AZ-MX	-0.60	-2.36	1.16	0.98
WT-MX	0.65	-1.06	2.36	0.97
NT-MX	<0.01	-1.71	1.70	1.00
NM-MX	0.84	-0.86	2.54	0.85
OK-MX	0.21	-1.51	1.94	1.00
CO-MX	-0.31	-2.01	1.38	1.00
KS-MX	-0.37	-2.08	1.33	1.00
MO-MX	-0.53	-2.25	1.20	0.99
AZ-ST	-1.14	-2.52	0.24	0.20
WT-ST	0.11	-1.21	1.43	1.00
NT-ST	-0.54	-1.85	0.76	0.94
NM-ST	0.30	-1.01	1.60	1.00
OK-ST	-0.32	-1.66	1.01	1.00
CO-ST	-0.85	-2.15	0.44	0.50
KS-ST	-0.91	-2.22	0.39	0.42
MO-ST	-1.07	-2.40	0.27	0.24
WT-AZ	1.25	0.13	2.38	0.02
NT-AZ	0.59	-0.51	1.70	0.77
NM-AZ	1.44	0.33	2.54	<0.01
OK-AZ	0.81	-0.33	1.96	0.40
CO-AZ	0.28	-0.81	1.38	1.00
KS-AZ	0.22	-0.88	1.33	1.00
MO-AZ	0.07	-1.07	1.22	1.00
NT-WT	-0.66	-1.69	0.37	0.56
NM-WT	0.19	-0.84	1.22	1.00

Table C1. (continued)

OK-WT	-0.44	-1.51	0.63	0.95
CO-WT	-0.97	-1.98	0.05	0.08
KS-WT	-1.03	-2.06	<0.01	0.05
MO-WT	-1.18	-2.25	-0.11	0.02
NM-NT	0.84	-0.17	1.85	0.19
OK-NT	0.22	-0.83	1.27	1.00
CO-NT	-0.31	-1.30	0.68	0.99
KS-NT	-0.37	-1.38	0.64	0.97
MO-NT	-0.52	-1.57	0.53	0.84
OK-NM	-0.62	-1.68	0.43	0.65
CO-NM	-1.15	-2.15	-0.16	0.01
KS-NM	-1.21	-2.22	-0.20	0.01
MO-NM	-1.37	-2.42	-0.31	<0.01
CO-OK	-0.53	-1.56	0.51	0.82
KS-OK	-0.59	-1.64	0.46	0.73
MO-OK	-0.74	-1.83	0.35	0.46
KS-CO	-0.06	-1.05	0.93	1.00
MO-CO	-0.21	-1.25	0.82	1.00
MO-KS	-0.15	-1.20	0.90	1.00
Group C PC3				
ST-MX	0.01	-2.19	2.22	1.00
AZ-MX	-0.90	-2.95	1.16	0.92
WT-MX	-0.60	-2.60	1.40	0.99
NT-MX	-0.41	-2.39	1.58	1.00
NM-MX	-1.09	-3.08	0.90	0.75
OK-MX	-0.67	-2.68	1.35	0.99
CO-MX	-0.74	-2.72	1.24	0.97
KS-MX	0.05	-1.94	2.03	1.00
MO-MX	0.18	-1.83	2.20	1.00
AZ-ST	-0.91	-2.52	0.70	0.72
WT-ST	-0.61	-2.15	0.93	0.96
NT-ST	-0.42	-1.94	1.10	1.00
NM-ST	-1.10	-2.63	0.42	0.37
OK-ST	-0.68	-2.24	0.88	0.92
CO-ST	-0.75	-2.26	0.75	0.83
KS-ST	0.03	-1.49	1.56	1.00
MO-ST	0.17	-1.39	1.73	1.00

Table C1. (continued)

WT-AZ	0.30	-1.01	1.61	1.00
NT-AZ	0.49	-0.80	1.78	0.97
NM-AZ	-0.19	-1.49	1.10	1.00
OK-AZ	0.23	-1.11	1.56	1.00
CO-AZ	0.16	-1.12	1.43	1.00
KS-AZ	0.94	-0.35	2.24	0.36
MO-AZ	1.08	-0.26	2.42	0.22
NT-WT	0.19	-1.01	1.39	1.00
NM-WT	-0.49	-1.70	0.71	0.94
OK-WT	-0.07	-1.32	1.18	1.00
CO-WT	-0.14	-1.33	1.04	1.00
KS-WT	0.64	-0.56	1.85	0.77
MO-WT	0.78	-0.47	2.03	0.58
NM-NT	-0.68	-1.86	0.50	0.68
OK-NT	-0.26	-1.49	0.97	1.00
CO-NT	-0.33	-1.49	0.83	0.99
KS-NT	0.45	-0.73	1.63	0.96
MO-NT	0.59	-0.64	1.82	0.86
OK-NM	0.42	-0.81	1.65	0.98
CO-NM	0.35	-0.81	1.51	0.99
KS-NM	1.14	-0.04	2.32	0.07
MO-NM	1.27	0.05	2.50	0.04
CO-OK	-0.07	-1.28	1.14	1.00
KS-OK	0.72	-0.51	1.94	0.68
MO-OK	0.85	-0.42	2.13	0.48
KS-CO	0.79	-0.37	1.95	0.46
MO-CO	0.92	-0.28	2.13	0.29
MO-KS	0.14	-1.09	1.37	1.00

Table C2. Tukey's test table for dorsal skull shape groups, between sexes.

	diff	lwr	upr	p adj
Group A PC1				
M-F	0.29	-0.08	0.66	0.12
Group A PC2				
M-F	-0.11	-0.48	0.26	0.55
Group B PC1				
M-F	-0.03	-0.39	0.33	0.87
Group B PC2				
M-F	-0.10	-0.47	0.28	0.60
Group C PC1				
M-F	-0.25	-0.60	0.10	0.16
Group C PC2				
M-F	-0.74	-1.06	-0.43	<0.01
Group C PC3				
M-F	0.17	-0.20	0.54	0.36

Table C3. Tukey's test table for dorsal skull shape groups among sexes and populations.

	diff	lwr	upr	p adj
Group A PC1				
ST:F-MX:F	0.80	-3.29	4.89	1.00
AZ:F-MX:F	2.52	-1.30	6.34	0.66
WT:F-MX:F	1.56	-2.22	5.34	0.99
NT:F-MX:F	1.58	-2.20	5.37	0.99
NM:F-MX:F	0.78	-3.31	4.87	1.00
OK:F-MX:F	1.60	-2.28	5.48	0.99
CO:F-MX:F	1.46	-2.50	5.42	1.00
KS:F-MX:F	2.14	-1.61	5.90	0.86
MO:F-MX:F	1.48	-2.85	5.82	1.00
MX:M-MX:F	2.15	-2.19	6.48	0.95
ST:M-MX:F	1.39	-2.70	5.48	1.00
AZ:M-MX:F	1.67	-2.29	5.63	0.99
WT:M-MX:F	1.67	-2.16	5.49	0.99
NT:M-MX:F	2.12	-1.66	5.90	0.88
NM:M-MX:F	2.38	-1.32	6.08	0.70
OK:M-MX:F	2.36	-1.42	6.15	0.74
CO:M-MX:F	1.39	-2.31	5.09	1.00
KS:M-MX:F	1.83	-2.00	5.65	0.97
MO:M-MX:F	1.87	-1.84	5.58	0.95
AZ:F-ST:F	1.72	-0.78	4.22	0.58
WT:F-ST:F	0.76	-1.68	3.20	1.00
NT:F-ST:F	0.79	-1.66	3.23	1.00
NM:F-ST:F	-0.02	-2.91	2.87	1.00
OK:F-ST:F	0.80	-1.79	3.38	1.00
CO:F-ST:F	0.66	-2.04	3.36	1.00
KS:F-ST:F	1.34	-1.05	3.74	0.87
MO:F-ST:F	0.68	-2.55	3.91	1.00
MX:M-ST:F	1.35	-1.88	4.58	0.99
ST:M-ST:F	0.59	-2.30	3.48	1.00
AZ:M-ST:F	0.87	-1.83	3.57	1.00
WT:M-ST:F	0.87	-1.63	3.37	1.00
NT:M-ST:F	1.32	-1.12	3.76	0.91
NM:M-ST:F	1.58	-0.73	3.89	0.59

Table C3. (continued)

OK:M-ST:F	1.56	-0.88	4.01	0.71
CO:M-ST:F	0.59	-1.71	2.90	1.00
MO:M-ST:F	1.07	-1.26	3.40	0.98
WT:F-AZ:F	-0.96	-2.93	1.01	0.96
NT:F-AZ:F	-0.93	-2.90	1.03	0.97
NM:F-AZ:F	-1.74	-4.24	0.76	0.56
OK:F-AZ:F	-0.92	-3.06	1.22	0.99
CO:F-AZ:F	-1.06	-3.35	1.22	0.98
KS:F-AZ:F	-0.38	-2.29	1.54	1.00
MO:F-AZ:F	-1.04	-3.93	1.85	1.00
MX:M-AZ:F	-0.37	-3.26	2.52	1.00
ST:M-AZ:F	-1.13	-3.63	1.37	0.98
AZ:M-AZ:F	-0.85	-3.13	1.43	1.00
WT:M-AZ:F	-0.85	-2.90	1.19	0.99
NT:M-AZ:F	-0.40	-2.37	1.57	1.00
NM:M-AZ:F	-0.14	-1.94	1.66	1.00
OK:M-AZ:F	-0.16	-2.13	1.81	1.00
CO:M-AZ:F	-1.13	-2.92	0.67	0.74
KS:M-AZ:F	-0.69	-2.74	1.35	1.00
MO:M-AZ:F	-0.65	-2.48	1.18	1.00
NT:F-WT:F	0.02	-1.87	1.92	1.00
NM:F-WT:F	-0.78	-3.22	1.66	1.00
OK:F-WT:F	0.04	-2.03	2.11	1.00
CO:F-WT:F	-0.10	-2.32	2.12	1.00
KS:F-WT:F	0.58	-1.25	2.41	1.00
MO:F-WT:F	-0.08	-2.92	2.76	1.00
MX:M-WT:F	0.59	-2.25	3.43	1.00
ST:M-WT:F	-0.17	-2.61	2.27	1.00
AZ:M-WT:F	0.11	-2.11	2.33	1.00
WT:M-WT:F	0.11	-1.86	2.08	1.00
NT:M-WT:F	0.56	-1.33	2.45	1.00
NM:M-WT:F	0.82	-0.89	2.53	0.97
OK:M-WT:F	0.80	-1.09	2.69	0.99
CO:M-WT:F	-0.17	-1.88	1.54	1.00
KS:M-WT:F	0.27	-1.70	2.23	1.00
MO:M-WT:F	0.31	-1.43	2.06	1.00
NM:F-NT:F	-0.81	-3.25	1.64	1.00
OK:F-NT:F	0.01	-2.06	2.09	1.00

Table C3. (continued)

CO:F-NT:F	-0.13	-2.35	2.09	1.00
KS:F-NT:F	0.56	-1.27	2.39	1.00
MO:F-NT:F	-0.10	-2.94	2.74	1.00
MX:M-NT:F	0.56	-2.27	3.40	1.00
ST:M-NT:F	-0.20	-2.64	2.25	1.00
AZ:M-NT:F	0.08	-2.13	2.30	1.00
WT:M-NT:F	0.08	-1.89	2.05	1.00
NT:M-NT:F	0.53	-1.36	2.43	1.00
NM:M-NT:F	0.79	-0.92	2.51	0.98
OK:M-NT:F	0.78	-1.11	2.67	0.99
CO:M-NT:F	-0.19	-1.90	1.52	1.00
KS:M-NT:F	0.24	-1.73	2.21	1.00
MO:M-NT:F	0.29	-1.46	2.03	1.00
OK:F-NM:F	0.82	-1.77	3.40	1.00
CO:F-NM:F	0.68	-2.02	3.38	1.00
KS:F-NM:F	1.36	-1.03	3.76	0.86
MO:F-NM:F	0.70	-2.53	3.94	1.00
MX:M-NM:F	1.37	-1.86	4.60	0.99
ST:M-NM:F	0.61	-2.28	3.50	1.00
AZ:M-NM:F	0.89	-1.81	3.59	1.00
WT:M-NM:F	0.89	-1.61	3.39	1.00
NT:M-NM:F	1.34	-1.10	3.78	0.89
NM:M-NM:F	1.60	-0.71	3.91	0.56
OK:M-NM:F	1.58	-0.86	4.03	0.68
CO:M-NM:F	0.61	-1.69	2.92	1.00
KS:M-NM:F	1.05	-1.46	3.55	0.99
MO:M-NM:F	1.09	-1.24	3.42	0.97
CO:F-OK:F	-0.14	-2.51	2.23	1.00
KS:F-OK:F	0.54	-1.47	2.56	1.00
MO:F-OK:F	-0.12	-3.08	2.85	1.00
MX:M-OK:F	0.55	-2.41	3.51	1.00
ST:M-OK:F	-0.21	-2.80	2.37	1.00
AZ:M-OK:F	0.07	-2.30	2.44	1.00
WT:M-OK:F	0.07	-2.07	2.21	1.00
NT:M-OK:F	0.52	-1.55	2.59	1.00
NM:M-OK:F	0.78	-1.13	2.69	0.99

Table C3. (continued)

OK:M-OK:F	0.76	-1.31	2.84	1.00
CO:M-OK:F	-0.21	-2.12	1.70	1.00
KS:M-OK:F	0.23	-1.92	2.37	1.00
MO:M-OK:F	0.27	-1.67	2.21	1.00
KS:F-CO:F	0.69	-1.48	2.85	1.00
MO:F-CO:F	0.03	-3.04	3.09	1.00
MX:M-CO:F	0.69	-2.37	3.76	1.00
ST:M-CO:F	-0.07	-2.77	2.63	1.00
AZ:M-CO:F	0.21	-2.29	2.71	1.00
WT:M-CO:F	0.21	-2.08	2.49	1.00
NT:M-CO:F	0.66	-1.56	2.88	1.00
NM:M-CO:F	0.92	-1.15	2.99	0.98
OK:M-CO:F	0.91	-1.31	3.12	0.99
CO:M-CO:F	-0.07	-2.13	2.00	1.00
KS:M-CO:F	0.37	-1.92	2.65	1.00
MO:M-CO:F	0.41	-1.68	2.51	1.00
MO:F-KS:F	-0.66	-3.46	2.14	1.00
MX:M-KS:F	0.01	-2.79	2.80	1.00
ST:M-KS:F	-0.75	-3.15	1.64	1.00
AZ:M-KS:F	-0.47	-2.64	1.69	1.00
WT:M-KS:F	-0.48	-2.39	1.44	1.00
NT:M-KS:F	-0.02	-1.86	1.81	1.00
NM:M-KS:F	0.24	-1.41	1.88	1.00
OK:M-KS:F	0.22	-1.61	2.05	1.00
CO:M-KS:F	-0.75	-2.40	0.89	0.98
KS:M-KS:F	-0.32	-2.23	1.59	1.00
MO:M-KS:F	-0.27	-1.95	1.41	1.00
MX:M-MO:F	0.67	-2.87	4.21	1.00
ST:M-MO:F	-0.09	-3.33	3.14	1.00
AZ:M-MO:F	0.19	-2.88	3.25	1.00
WT:M-MO:F	0.18	-2.71	3.07	1.00
NT:M-MO:F	0.64	-2.20	3.47	1.00
NM:M-MO:F	0.90	-1.82	3.62	1.00
OK:M-MO:F	0.88	-1.96	3.72	1.00
CO:M-MO:F	-0.09	-2.81	2.63	1.00
KS:M-MO:F	0.34	-2.55	3.23	1.00

Table C3. (continued)

MO:M-MO:F	0.39	-2.35	3.13	1.00
ST:M-MX:M	-0.76	-3.99	2.47	1.00
AZ:M-MX:M	-0.48	-3.55	2.58	1.00
WT:M-MX:M	-0.48	-3.37	2.41	1.00
NT:M-MX:M	-0.03	-2.87	2.81	1.00
NM:M-MX:M	0.23	-2.49	2.95	1.00
OK:M-MX:M	0.21	-2.62	3.05	1.00
CO:M-MX:M	-0.76	-3.48	1.96	1.00
KS:M-MX:M	-0.32	-3.21	2.57	1.00
MO:M-MX:M	-0.28	-3.02	2.46	1.00
AZ:M-ST:M	0.28	-2.42	2.98	1.00
WT:M-ST:M	0.28	-2.22	2.78	1.00
NT:M-ST:M	0.73	-1.71	3.17	1.00
NM:M-ST:M	0.99	-1.31	3.30	0.99
OK:M-ST:M	0.97	-1.47	3.42	1.00
CO:M-ST:M	<0.01	-2.30	2.31	1.00
KS:M-ST:M	0.44	-2.07	2.94	1.00
MO:M-ST:M	0.48	-1.85	2.81	1.00
WT:M-AZ:M	<0.01	-2.29	2.28	1.00
NT:M-AZ:M	0.45	-1.77	2.67	1.00
NM:M-AZ:M	0.71	-1.36	2.78	1.00
OK:M-AZ:M	0.69	-1.52	2.91	1.00
CO:M-AZ:M	-0.28	-2.34	1.79	1.00
KS:M-AZ:M	0.16	-2.13	2.44	1.00
MO:M-AZ:M	0.20	-1.89	2.30	1.00
NT:M-WT:M	0.45	-1.52	2.42	1.00
NM:M-WT:M	0.71	-1.08	2.51	1.00
OK:M-WT:M	0.70	-1.27	2.66	1.00
CO:M-WT:M	-0.28	-2.07	1.52	1.00
KS:M-WT:M	0.16	-1.88	2.20	1.00
MO:M-WT:M	0.20	-1.62	2.03	1.00
NM:M-NT:M	0.26	-1.45	1.97	1.00
OK:M-NT:M	0.24	-1.65	2.14	1.00
CO:M-NT:M	-0.73	-2.44	0.98	0.99
KS:M-NT:M	-0.29	-2.26	1.68	1.00
MO:M-NT:M	-0.25	-1.99	1.50	1.00

Table C3. (continued)

OK:M-NM:M	-0.02	-1.73	1.69	1.00
CO:M-NM:M	-0.99	-2.50	0.52	0.67
KS:M-NM:M	-0.55	-2.35	1.24	1.00
MO:M-NM:M	-0.51	-2.05	1.04	1.00
CO:M-OK:M	-0.97	-2.68	0.74	0.86
KS:M-OK:M	-0.54	-2.51	1.43	1.00
MO:M-OK:M	-0.49	-2.24	1.25	1.00
KS:M-CO:M	0.43	-1.36	2.23	1.00
MO:M-CO:M	0.48	-1.07	2.03	1.00
MO:M-KS:M	0.05	-1.78	1.87	1.00
Group A PC2				
ST:F-MX:F	-0.48	-4.55	3.60	1.00
AZ:F-MX:F	0.71	-3.10	4.53	1.00
WT:F-MX:F	-0.29	-4.07	3.49	1.00
NT:F-MX:F	0.41	-3.36	4.19	1.00
NM:F-MX:F	0.88	-3.20	4.95	1.00
OK:F-MX:F	0.13	-3.74	4.00	1.00
CO:F-MX:F	0.44	-3.51	4.38	1.00
KS:F-MX:F	-0.34	-4.09	3.41	1.00
MO:F-MX:F	0.59	-3.73	4.92	1.00
MX:M-MX:F	0.64	-3.68	4.97	1.00
ST:M-MX:F	-0.77	-4.85	3.31	1.00
AZ:M-MX:F	0.25	-3.70	4.20	1.00
WT:M-MX:F	0.93	-2.88	4.75	1.00
NT:M-MX:F	0.22	-3.55	4.00	1.00
NM:M-MX:F	0.37	-3.32	4.06	1.00
OK:M-MX:F	-0.18	-3.96	3.59	1.00
CO:M-MX:F	-0.53	-4.22	3.16	1.00
KS:M-MX:F	0.10	-3.72	3.91	1.00
MO:M-MX:F	-0.42	-4.12	3.29	1.00
AZ:F-ST:F	1.19	-1.31	3.69	0.97
WT:F-ST:F	0.19	-2.25	2.62	1.00
NT:F-ST:F	0.89	-1.55	3.33	1.00
NM:F-ST:F	1.35	-1.53	4.24	0.97
OK:F-ST:F	0.61	-1.97	3.19	1.00
CO:F-ST:F	0.91	-1.79	3.61	1.00

Table C3. (continued)

KS:F-ST:F	0.14	-2.26	2.53	1.00
MO:F-ST:F	1.07	-2.16	4.29	1.00
MX:M-ST:F	1.12	-2.11	4.34	1.00
ST:M-ST:F	-0.29	-3.18	2.59	1.00
AZ:M-ST:F	0.72	-1.97	3.42	1.00
WT:M-ST:F	1.41	-1.09	3.91	0.87
NT:M-ST:F	0.70	-1.74	3.14	1.00
NM:M-ST:F	0.84	-1.46	3.14	1.00
OK:M-ST:F	0.29	-2.15	2.73	1.00
CO:M-ST:F	-0.06	-2.36	2.24	1.00
KS:M-ST:F	0.57	-1.92	3.07	1.00
MO:M-ST:F	0.06	-2.26	2.39	1.00
WT:F-AZ:F	-1.00	-2.97	0.96	0.94
NT:F-AZ:F	-0.30	-2.26	1.67	1.00
NM:F-AZ:F	0.16	-2.34	2.66	1.00
OK:F-AZ:F	-0.58	-2.72	1.56	1.00
CO:F-AZ:F	-0.28	-2.56	2.00	1.00
KS:F-AZ:F	-1.05	-2.96	0.85	0.89
MO:F-AZ:F	-0.12	-3.01	2.76	1.00
MX:M-AZ:F	-0.07	-2.96	2.81	1.00
ST:M-AZ:F	-1.48	-3.98	1.01	0.81
AZ:M-AZ:F	-0.47	-2.75	1.81	1.00
WT:M-AZ:F	0.22	-1.82	2.26	1.00
NT:M-AZ:F	-0.49	-2.46	1.47	1.00
NM:M-AZ:F	-0.35	-2.14	1.45	1.00
OK:M-AZ:F	-0.90	-2.86	1.07	0.98
CO:M-AZ:F	-1.25	-3.04	0.55	0.56
KS:M-AZ:F	-0.62	-2.66	1.42	1.00
MO:M-AZ:F	-1.13	-2.95	0.69	0.76
NT:F-WT:F	0.70	-1.18	2.59	1.00
NM:F-WT:F	1.16	-1.27	3.60	0.97
OK:F-WT:F	0.42	-1.65	2.49	1.00
CO:F-WT:F	0.72	-1.49	2.94	1.00
KS:F-WT:F	-0.05	-1.88	1.78	1.00
MO:F-WT:F	0.88	-1.95	3.71	1.00
MX:M-WT:F	0.93	-1.90	3.76	1.00

Table C3. (continued)

ST:M-WT:F	-0.48	-2.92	1.96	1.00
AZ:M-WT:F	0.54	-1.68	2.75	1.00
WT:M-WT:F	1.22	-0.74	3.19	0.75
NT:M-WT:F	0.51	-1.38	2.40	1.00
NM:M-WT:F	0.66	-1.05	2.36	1.00
OK:M-WT:F	0.10	-1.78	1.99	1.00
CO:M-WT:F	-0.24	-1.95	1.46	1.00
KS:M-WT:F	0.39	-1.58	2.35	1.00
MO:M-WT:F	-0.13	-1.87	1.61	1.00
NM:F-NT:F	0.46	-1.98	2.90	1.00
OK:F-NT:F	-0.28	-2.35	1.79	1.00
CO:F-NT:F	0.02	-2.19	2.23	1.00
KS:F-NT:F	-0.76	-2.58	1.07	0.99
MO:F-NT:F	0.18	-2.65	3.01	1.00
MX:M-NT:F	0.23	-2.60	3.06	1.00
ST:M-NT:F	-1.19	-3.62	1.25	0.96
AZ:M-NT:F	-0.17	-2.38	2.05	1.00
WT:M-NT:F	0.52	-1.45	2.48	1.00
NT:M-NT:F	-0.19	-2.08	1.70	1.00
NM:M-NT:F	-0.05	-1.75	1.66	1.00
OK:M-NT:F	-0.60	-2.49	1.29	1.00
CO:M-NT:F	-0.95	-2.66	0.76	0.88
KS:M-NT:F	-0.32	-2.28	1.65	1.00
MO:M-NT:F	-0.83	-2.57	0.91	0.97
OK:F-NM:F	-0.74	-3.32	1.84	1.00
CO:F-NM:F	-0.44	-3.14	2.26	1.00
KS:F-NM:F	-1.22	-3.61	1.18	0.94
MO:F-NM:F	-0.28	-3.51	2.94	1.00
MX:M-NM:F	-0.23	-3.46	2.99	1.00
ST:M-NM:F	-1.65	-4.53	1.24	0.86
AZ:M-NM:F	-0.63	-3.33	2.07	1.00
WT:M-NM:F	0.06	-2.44	2.55	1.00
NT:M-NM:F	-0.65	-3.09	1.78	1.00
NM:M-NM:F	-0.51	-2.81	1.79	1.00
OK:M-NM:F	-1.06	-3.50	1.38	0.99
CO:M-NM:F	-1.41	-3.71	0.89	0.77

Table C3. (continued)

KS:M-NM:F	-0.78	-3.28	1.72	1.00
MO:M-NM:F	-1.29	-3.62	1.03	0.88
CO:F-OK:F	0.30	-2.07	2.67	1.00
KS:F-OK:F	-0.47	-2.49	1.54	1.00
MO:F-OK:F	0.46	-2.50	3.42	1.00
MX:M-OK:F	0.51	-2.45	3.47	1.00
ST:M-OK:F	-0.90	-3.48	1.68	1.00
AZ:M-OK:F	0.12	-2.25	2.49	1.00
WT:M-OK:F	0.80	-1.34	2.94	1.00
NT:M-OK:F	0.09	-1.98	2.16	1.00
NM:M-OK:F	0.24	-1.67	2.14	1.00
OK:M-OK:F	-0.32	-2.39	1.75	1.00
CO:M-OK:F	-0.67	-2.57	1.24	1.00
KS:M-OK:F	-0.04	-2.17	2.10	1.00
MO:M-OK:F	-0.55	-2.48	1.39	1.00
KS:F-CO:F	-0.78	-2.94	1.39	1.00
MO:F-CO:F	0.16	-2.90	3.22	1.00
MX:M-CO:F	0.21	-2.85	3.27	1.00
ST:M-CO:F	-1.21	-3.90	1.49	0.98
AZ:M-CO:F	-0.19	-2.68	2.31	1.00
WT:M-CO:F	0.50	-1.78	2.78	1.00
NT:M-CO:F	-0.21	-2.43	2.00	1.00
NM:M-CO:F	-0.07	-2.13	2.00	1.00
OK:M-CO:F	-0.62	-2.83	1.59	1.00
CO:M-CO:F	-0.97	-3.03	1.09	0.97
KS:M-CO:F	-0.34	-2.62	1.94	1.00
MO:M-CO:F	-0.85	-2.94	1.24	0.99
MO:F-KS:F	0.93	-1.86	3.73	1.00
MX:M-KS:F	0.98	-1.81	3.78	1.00
ST:M-KS:F	-0.43	-2.82	1.96	1.00
AZ:M-KS:F	0.59	-1.57	2.75	1.00
WT:M-KS:F	1.27	-0.64	3.18	0.64
NT:M-KS:F	0.56	-1.26	2.39	1.00
NM:M-KS:F	0.71	-0.93	2.35	0.99
OK:M-KS:F	0.16	-1.67	1.98	1.00
CO:M-KS:F	-0.19	-1.83	1.45	1.00

Table C3. (continued)

KS:M-KS:F	0.44	-1.47	2.34	1.00
MO:M-KS:F	-0.07	-1.75	1.60	1.00
MX:M-MO:F	0.05	-3.48	3.58	1.00
ST:M-MO:F	-1.36	-4.59	1.86	0.99
AZ:M-MO:F	-0.34	-3.40	2.71	1.00
WT:M-MO:F	0.34	-2.54	3.22	1.00
NT:M-MO:F	-0.37	-3.20	2.46	1.00
NM:M-MO:F	-0.22	-2.94	2.49	1.00
OK:M-MO:F	-0.78	-3.61	2.06	1.00
CO:M-MO:F	-1.13	-3.84	1.59	0.99
KS:M-MO:F	-0.50	-3.38	2.39	1.00
MO:M-MO:F	-1.01	-3.74	1.73	1.00
ST:M-MX:M	-1.41	-4.64	1.81	0.99
AZ:M-MX:M	-0.39	-3.45	2.66	1.00
WT:M-MX:M	0.29	-2.59	3.17	1.00
NT:M-MX:M	-0.42	-3.25	2.41	1.00
NM:M-MX:M	-0.27	-2.99	2.44	1.00
OK:M-MX:M	-0.83	-3.66	2.00	1.00
CO:M-MX:M	-1.18	-3.89	1.54	0.99
KS:M-MX:M	-0.55	-3.43	2.34	1.00
MO:M-MX:M	-1.06	-3.79	1.68	1.00
AZ:M-ST:M	1.02	-1.68	3.72	1.00
WT:M-ST:M	1.70	-0.80	4.20	0.60
NT:M-ST:M	0.99	-1.44	3.43	0.99
NM:M-ST:M	1.14	-1.16	3.44	0.96
OK:M-ST:M	0.59	-1.85	3.02	1.00
CO:M-ST:M	0.24	-2.06	2.54	1.00
KS:M-ST:M	0.87	-1.63	3.36	1.00
MO:M-ST:M	0.36	-1.97	2.68	1.00
WT:M-AZ:M	0.68	-1.60	2.96	1.00
NT:M-AZ:M	-0.02	-2.24	2.19	1.00
NM:M-AZ:M	0.12	-1.94	2.18	1.00
OK:M-AZ:M	-0.43	-2.65	1.78	1.00
CO:M-AZ:M	-0.78	-2.84	1.28	1.00
KS:M-AZ:M	-0.15	-2.43	2.13	1.00
MO:M-AZ:M	-0.66	-2.75	1.43	1.00

Table C3. (continued)

NT:M-WT:M	-0.71	-2.67	1.26	1.00
NM:M-WT:M	-0.56	-2.36	1.23	1.00
OK:M-WT:M	-1.12	-3.08	0.85	0.86
CO:M-WT:M	-1.46	-3.26	0.33	0.26
KS:M-WT:M	-0.83	-2.87	1.20	0.99
MO:M-WT:M	-1.35	-3.17	0.48	0.45
NM:M-NT:M	0.14	-1.56	1.85	1.00
OK:M-NT:M	-0.41	-2.30	1.48	1.00
CO:M-NT:M	-0.76	-2.46	0.95	0.99
KS:M-NT:M	-0.13	-2.09	1.84	1.00
MO:M-NT:M	-0.64	-2.38	1.10	1.00
OK:M-NM:M	-0.55	-2.26	1.16	1.00
CO:M-NM:M	-0.90	-2.41	0.60	0.80
KS:M-NM:M	-0.27	-2.06	1.52	1.00
MO:M-NM:M	-0.78	-2.33	0.76	0.94
CO:M-OK:M	-0.35	-2.06	1.36	1.00
KS:M-OK:M	0.28	-1.68	2.25	1.00
MO:M-OK:M	-0.23	-1.97	1.51	1.00
KS:M-CO:M	0.63	-1.16	2.42	1.00
MO:M-CO:M	0.12	-1.43	1.66	1.00
MO:M-KS:M	-0.51	-2.34	1.31	1.00
Group B PC1				
ST:F-MX:F	-1.70	-5.65	2.25	0.99
AZ:F-MX:F	-1.92	-5.62	1.77	0.93
WT:F-MX:F	-2.36	-6.02	1.30	0.69
NT:F-MX:F	-0.53	-4.19	3.13	1.00
NM:F-MX:F	-0.76	-4.72	3.19	1.00
OK:F-MX:F	-0.70	-4.45	3.05	1.00
CO:F-MX:F	-0.94	-4.77	2.89	1.00
KS:F-MX:F	-1.35	-4.99	2.28	1.00
MO:F-MX:F	-1.33	-5.52	2.87	1.00
MX:M-MX:F	-1.57	-5.76	2.63	1.00
ST:M-MX:F	-1.62	-5.57	2.34	0.99
AZ:M-MX:F	-2.33	-6.16	1.49	0.78
WT:M-MX:F	-1.03	-4.72	2.67	1.00
NT:M-MX:F	-1.41	-5.07	2.25	1.00

Table C3. (continued)

NM:M-MX:F	-1.01	-4.58	2.57	1.00
OK:M-MX:F	-0.67	-4.33	2.99	1.00
CO:M-MX:F	-1.47	-5.05	2.11	0.99
KS:M-MX:F	-0.89	-4.59	2.80	1.00
MO:M-MX:F	-1.13	-4.72	2.46	1.00
AZ:F-ST:F	-0.22	-2.64	2.20	1.00
WT:F-ST:F	-0.66	-3.02	1.70	1.00
NT:F-ST:F	1.17	-1.19	3.54	0.95
NM:F-ST:F	0.94	-1.86	3.73	1.00
OK:F-ST:F	1.00	-1.50	3.50	1.00
CO:F-ST:F	0.76	-1.85	3.38	1.00
KS:F-ST:F	0.35	-1.97	2.67	1.00
MO:F-ST:F	0.37	-2.75	3.50	1.00
MX:M-ST:F	0.13	-2.99	3.26	1.00
ST:M-ST:F	0.08	-2.71	2.88	1.00
AZ:M-ST:F	-0.63	-3.25	1.98	1.00
WT:M-ST:F	0.67	-1.75	3.10	1.00
NT:M-ST:F	0.29	-2.07	2.66	1.00
NM:M-ST:F	0.69	-1.54	2.92	1.00
OK:M-ST:F	1.03	-1.33	3.39	0.99
CO:M-ST:F	0.23	-2.00	2.46	1.00
KS:M-ST:F	0.81	-1.62	3.23	1.00
MO:M-ST:F	0.57	-1.68	2.82	1.00
WT:F-AZ:F	-0.43	-2.34	1.47	1.00
NT:F-AZ:F	1.40	-0.51	3.30	0.46
NM:F-AZ:F	1.16	-1.26	3.58	0.97
OK:F-AZ:F	1.23	-0.85	3.30	0.82
CO:F-AZ:F	0.98	-1.23	3.20	0.98
KS:F-AZ:F	0.57	-1.28	2.42	1.00
MO:F-AZ:F	0.60	-2.20	3.39	1.00
MX:M-AZ:F	0.36	-2.44	3.15	1.00
ST:M-AZ:F	0.31	-2.11	2.73	1.00
AZ:M-AZ:F	-0.41	-2.62	1.80	1.00
WT:M-AZ:F	0.90	-1.08	2.88	0.98
NT:M-AZ:F	0.52	-1.39	2.42	1.00
NM:M-AZ:F	0.92	-0.82	2.65	0.92

Table C3. (continued)

OK:M-AZ:F	1.25	-0.65	3.16	0.66
CO:M-AZ:F	0.46	-1.28	2.19	1.00
KS:M-AZ:F	1.03	-0.95	3.01	0.93
MO:M-AZ:F	0.79	-0.97	2.56	0.98
NT:F-WT:F	1.83	<0.01	3.66	0.05
NM:F-WT:F	1.59	-0.77	3.96	0.62
OK:F-WT:F	1.66	-0.34	3.67	0.24
CO:F-WT:F	1.42	-0.73	3.57	0.65
KS:F-WT:F	1.01	-0.77	2.78	0.86
MO:F-WT:F	1.03	-1.72	3.78	1.00
MX:M-WT:F	0.79	-1.95	3.54	1.00
ST:M-WT:F	0.74	-1.62	3.11	1.00
AZ:M-WT:F	0.02	-2.12	2.17	1.00
WT:M-WT:F	1.33	-0.57	3.24	0.55
NT:M-WT:F	0.95	-0.88	2.78	0.93
NM:M-WT:F	1.35	-0.31	3.01	0.27
OK:M-WT:F	1.69	-0.14	3.52	0.11
CO:M-WT:F	0.89	-0.77	2.55	0.91
KS:M-WT:F	1.46	-0.44	3.37	0.37
MO:M-WT:F	1.23	-0.46	2.92	0.47
NM:F-NT:F	-0.24	-2.60	2.13	1.00
OK:F-NT:F	-0.17	-2.18	1.83	1.00
CO:F-NT:F	-0.41	-2.56	1.73	1.00
KS:F-NT:F	-0.83	-2.60	0.95	0.97
MO:F-NT:F	-0.80	-3.55	1.94	1.00
MX:M-NT:F	-1.04	-3.79	1.70	1.00
ST:M-NT:F	-1.09	-3.45	1.27	0.98
AZ:M-NT:F	-1.81	-3.95	0.34	0.22
WT:M-NT:F	-0.50	-2.40	1.41	1.00
NT:M-NT:F	-0.88	-2.71	0.95	0.97
NM:M-NT:F	-0.48	-2.14	1.17	1.00
OK:M-NT:F	-0.15	-1.98	1.68	1.00
CO:M-NT:F	-0.94	-2.60	0.71	0.86
KS:M-NT:F	-0.37	-2.27	1.54	1.00
MO:M-NT:F	-0.60	-2.29	1.08	1.00
OK:F-NM:F	0.07	-2.43	2.57	1.00

Table C3. (continued)

CO:F-NM:F	-0.18	-2.79	2.44	1.00
KS:F-NM:F	-0.59	-2.91	1.73	1.00
MO:F-NM:F	-0.56	-3.69	2.56	1.00
MX:M-NM:F	-0.80	-3.93	2.32	1.00
ST:M-NM:F	-0.85	-3.65	1.94	1.00
AZ:M-NM:F	-1.57	-4.19	1.05	0.80
WT:M-NM:F	-0.26	-2.68	2.16	1.00
NT:M-NM:F	-0.64	-3.01	1.72	1.00
NM:M-NM:F	-0.24	-2.47	1.99	1.00
OK:M-NM:F	0.09	-2.27	2.46	1.00
CO:M-NM:F	-0.70	-2.93	1.53	1.00
KS:M-NM:F	-0.13	-2.55	2.29	1.00
MO:M-NM:F	-0.37	-2.62	1.89	1.00
CO:F-OK:F	-0.24	-2.54	2.06	1.00
KS:F-OK:F	-0.65	-2.61	1.30	1.00
MO:F-OK:F	-0.63	-3.50	2.23	1.00
MX:M-OK:F	-0.87	-3.73	2.00	1.00
ST:M-OK:F	-0.92	-3.42	1.58	1.00
AZ:M-OK:F	-1.64	-3.93	0.66	0.52
WT:M-OK:F	-0.33	-2.40	1.75	1.00
NT:M-OK:F	-0.71	-2.71	1.30	1.00
NM:M-OK:F	-0.31	-2.16	1.54	1.00
OK:M-OK:F	0.03	-1.98	2.03	1.00
CO:M-OK:F	-0.77	-2.62	1.08	0.99
KS:M-OK:F	-0.20	-2.27	1.88	1.00
MO:M-OK:F	-0.43	-2.31	1.44	1.00
KS:F-CO:F	-0.41	-2.51	1.68	1.00
MO:F-CO:F	-0.39	-3.35	2.58	1.00
MX:M-CO:F	-0.63	-3.59	2.34	1.00
ST:M-CO:F	-0.68	-3.29	1.94	1.00
AZ:M-CO:F	-1.39	-3.82	1.03	0.85
WT:M-CO:F	-0.09	-2.30	2.12	1.00
NT:M-CO:F	-0.47	-2.61	1.68	1.00
NM:M-CO:F	-0.07	-2.07	1.93	1.00
OK:M-CO:F	0.27	-1.88	2.41	1.00
CO:M-CO:F	-0.53	-2.53	1.47	1.00

Table C3. (continued)

KS:M-CO:F	0.04	-2.17	2.26	1.00
MO:M-CO:F	-0.19	-2.22	1.83	1.00
MO:F-KS:F	0.02	-2.68	2.73	1.00
MX:M-KS:F	-0.21	-2.92	2.49	1.00
ST:M-KS:F	-0.26	-2.58	2.06	1.00
AZ:M-KS:F	-0.98	-3.08	1.12	0.97
WT:M-KS:F	0.33	-1.52	2.18	1.00
NT:M-KS:F	-0.05	-1.83	1.72	1.00
NM:M-KS:F	0.35	-1.25	1.94	1.00
OK:M-KS:F	0.68	-1.09	2.45	1.00
CO:M-KS:F	-0.11	-1.71	1.48	1.00
KS:M-KS:F	0.46	-1.39	2.31	1.00
MO:M-KS:F	0.22	-1.40	1.85	1.00
MX:M-MO:F	-0.24	-3.66	3.19	1.00
ST:M-MO:F	-0.29	-3.41	2.84	1.00
AZ:M-MO:F	-1.01	-3.97	1.96	1.00
WT:M-MO:F	0.30	-2.49	3.10	1.00
NT:M-MO:F	-0.08	-2.82	2.67	1.00
NM:M-MO:F	0.32	-2.31	2.95	1.00
OK:M-MO:F	0.66	-2.09	3.40	1.00
CO:M-MO:F	-0.14	-2.77	2.49	1.00
KS:M-MO:F	0.43	-2.36	3.23	1.00
MO:M-MO:F	0.20	-2.45	2.85	1.00
ST:M-MX:M	-0.05	-3.17	3.08	1.00
AZ:M-MX:M	-0.77	-3.73	2.20	1.00
WT:M-MX:M	0.54	-2.25	3.34	1.00
NT:M-MX:M	0.16	-2.59	2.91	1.00
NM:M-MX:M	0.56	-2.07	3.19	1.00
OK:M-MX:M	0.89	-1.85	3.64	1.00
CO:M-MX:M	0.10	-2.53	2.73	1.00
KS:M-MX:M	0.67	-2.12	3.47	1.00
MO:M-MX:M	0.44	-2.22	3.09	1.00
AZ:M-ST:M	-0.72	-3.33	1.90	1.00
WT:M-ST:M	0.59	-1.83	3.01	1.00
NT:M-ST:M	0.21	-2.16	2.57	1.00
NM:M-ST:M	0.61	-1.62	2.84	1.00

Table C3. (continued)

OK:M-ST:M	0.94	-1.42	3.31	1.00
CO:M-ST:M	0.15	-2.08	2.38	1.00
KS:M-ST:M	0.72	-1.70	3.14	1.00
MO:M-ST:M	0.49	-1.77	2.74	1.00
WT:M-AZ:M	1.31	-0.90	3.52	0.82
NT:M-AZ:M	0.93	-1.22	3.07	0.99
NM:M-AZ:M	1.33	-0.67	3.33	0.65
OK:M-AZ:M	1.66	-0.48	3.81	0.36
CO:M-AZ:M	0.87	-1.13	2.86	0.99
KS:M-AZ:M	1.44	-0.77	3.65	0.68
MO:M-AZ:M	1.20	-0.82	3.23	0.81
NT:M-WT:M	-0.38	-2.29	1.52	1.00
NM:M-WT:M	0.02	-1.72	1.76	1.00
OK:M-WT:M	0.35	-1.55	2.26	1.00
CO:M-WT:M	-0.44	-2.18	1.30	1.00
KS:M-WT:M	0.13	-1.85	2.11	1.00
MO:M-WT:M	-0.10	-1.87	1.66	1.00
NM:M-NT:M	0.40	-1.26	2.06	1.00
OK:M-NT:M	0.74	-1.09	2.57	1.00
CO:M-NT:M	-0.06	-1.72	1.59	1.00
KS:M-NT:M	0.51	-1.39	2.42	1.00
MO:M-NT:M	0.28	-1.41	1.96	1.00
OK:M-NM:M	0.34	-1.32	1.99	1.00
CO:M-NM:M	-0.46	-1.92	1.00	1.00
KS:M-NM:M	0.11	-1.62	1.85	1.00
MO:M-NM:M	-0.12	-1.62	1.37	1.00
CO:M-OK:M	-0.80	-2.45	0.86	0.97
KS:M-OK:M	-0.22	-2.13	1.68	1.00
MO:M-OK:M	-0.46	-2.15	1.23	1.00
KS:M-CO:M	0.57	-1.16	2.31	1.00
MO:M-CO:M	0.34	-1.16	1.83	1.00
MO:M-KS:M	-0.24	-2.00	1.53	1.00
Group B PC2				
ST:F-MX:F	0.93	-3.23	5.08	1.00
AZ:F-MX:F	0.88	-3.01	4.76	1.00
WT:F-MX:F	1.66	-2.19	5.51	0.99

Table C3. (continued)

NT:F-MX:F	1.01	-2.83	4.86	1.00
NM:F-MX:F	2.71	-1.44	6.87	0.67
OK:F-MX:F	1.36	-2.58	5.31	1.00
CO:F-MX:F	1.80	-2.23	5.82	0.98
KS:F-MX:F	1.73	-2.09	5.55	0.98
MO:F-MX:F	0.77	-3.64	5.17	1.00
MX:M-MX:F	1.54	-2.87	5.94	1.00
ST:M-MX:F	0.91	-3.24	5.07	1.00
AZ:M-MX:F	1.95	-2.08	5.97	0.96
WT:M-MX:F	2.02	-1.87	5.90	0.93
NT:M-MX:F	0.79	-3.06	4.63	1.00
NM:M-MX:F	1.30	-2.46	5.06	1.00
OK:M-MX:F	1.03	-2.82	4.87	1.00
CO:M-MX:F	1.22	-2.54	4.98	1.00
KS:M-MX:F	1.35	-2.54	5.24	1.00
MO:M-MX:F	1.16	-2.61	4.94	1.00
AZ:F-ST:F	-0.05	-2.60	2.49	1.00
WT:F-ST:F	0.73	-1.75	3.21	1.00
NT:F-ST:F	0.09	-2.40	2.57	1.00
NM:F-ST:F	1.78	-1.15	4.72	0.78
OK:F-ST:F	0.44	-2.19	3.06	1.00
CO:F-ST:F	0.87	-1.88	3.62	1.00
KS:F-ST:F	0.80	-1.63	3.24	1.00
MO:F-ST:F	-0.16	-3.45	3.12	1.00
MX:M-ST:F	0.61	-2.68	3.89	1.00
ST:M-ST:F	-0.01	-2.95	2.92	1.00
AZ:M-ST:F	1.02	-1.73	3.77	1.00
WT:M-ST:F	1.09	-1.46	3.63	0.99
NT:M-ST:F	-0.14	-2.62	2.34	1.00
NM:M-ST:F	0.37	-1.97	2.71	1.00
OK:M-ST:F	0.10	-2.39	2.58	1.00
CO:M-ST:F	0.29	-2.05	2.64	1.00
KS:M-ST:F	0.42	-2.12	2.97	1.00
MO:M-ST:F	0.24	-2.13	2.60	1.00
WT:F-AZ:F	0.78	-1.22	2.79	1.00
NT:F-AZ:F	0.14	-1.86	2.14	1.00

Table C3. (continued)

NM:F-AZ:F	1.84	-0.71	4.38	0.49
OK:F-AZ:F	0.49	-1.69	2.67	1.00
CO:F-AZ:F	0.92	-1.40	3.24	1.00
KS:F-AZ:F	0.85	-1.09	2.80	0.99
MO:F-AZ:F	-0.11	-3.05	2.83	1.00
MX:M-AZ:F	0.66	-2.28	3.60	1.00
ST:M-AZ:F	0.04	-2.51	2.58	1.00
AZ:M-AZ:F	1.07	-1.25	3.39	0.98
WT:M-AZ:F	1.14	-0.94	3.22	0.89
NT:M-AZ:F	-0.09	-2.09	1.91	1.00
NM:M-AZ:F	0.42	-1.40	2.25	1.00
OK:M-AZ:F	0.15	-1.85	2.15	1.00
CO:M-AZ:F	0.35	-1.48	2.17	1.00
KS:M-AZ:F	0.47	-1.60	2.55	1.00
MO:M-AZ:F	0.29	-1.57	2.15	1.00
NT:F-WT:F	-0.64	-2.57	1.28	1.00
NM:F-WT:F	1.05	-1.43	3.54	0.99
OK:F-WT:F	-0.29	-2.40	1.81	1.00
CO:F-WT:F	0.14	-2.12	2.39	1.00
KS:F-WT:F	0.07	-1.79	1.93	1.00
MO:F-WT:F	-0.89	-3.78	1.99	1.00
MX:M-WT:F	-0.12	-3.01	2.76	1.00
ST:M-WT:F	-0.74	-3.23	1.74	1.00
AZ:M-WT:F	0.29	-1.97	2.54	1.00
WT:M-WT:F	0.36	-1.65	2.36	1.00
NT:M-WT:F	-0.87	-2.79	1.05	0.98
NM:M-WT:F	-0.36	-2.10	1.38	1.00
OK:M-WT:F	-0.63	-2.56	1.29	1.00
CO:M-WT:F	-0.44	-2.18	1.30	1.00
KS:M-WT:F	-0.31	-2.31	1.69	1.00
MO:M-WT:F	-0.50	-2.27	1.28	1.00
NM:F-NT:F	1.70	-0.79	4.18	0.59
OK:F-NT:F	0.35	-1.76	2.46	1.00
CO:F-NT:F	0.78	-1.47	3.04	1.00
KS:F-NT:F	0.71	-1.15	2.58	1.00
MO:F-NT:F	-0.25	-3.13	2.64	1.00

Table C3. (continued)

MX:M-NT:F	0.52	-2.36	3.41	1.00
ST:M-NT:F	-0.10	-2.58	2.38	1.00
AZ:M-NT:F	0.93	-1.32	3.19	0.99
WT:M-NT:F	1.00	-1.00	3.00	0.95
NT:M-NT:F	-0.23	-2.15	1.70	1.00
NM:M-NT:F	0.28	-1.46	2.02	1.00
OK:M-NT:F	0.01	-1.91	1.93	1.00
CO:M-NT:F	0.21	-1.53	1.95	1.00
KS:M-NT:F	0.34	-1.67	2.34	1.00
MO:M-NT:F	0.15	-1.62	1.92	1.00
OK:F-NM:F	-1.35	-3.97	1.28	0.94
CO:F-NM:F	-0.91	-3.66	1.83	1.00
KS:F-NM:F	-0.98	-3.42	1.45	0.99
MO:F-NM:F	-1.95	-5.23	1.34	0.82
MX:M-NM:F	-1.18	-4.46	2.11	1.00
ST:M-NM:F	-1.80	-4.74	1.14	0.77
AZ:M-NM:F	-0.77	-3.51	1.98	1.00
WT:M-NM:F	-0.70	-3.24	1.85	1.00
NT:M-NM:F	-1.92	-4.41	0.56	0.36
NM:M-NM:F	-1.41	-3.76	0.93	0.79
OK:M-NM:F	-1.69	-4.17	0.80	0.60
CO:M-NM:F	-1.49	-3.83	0.86	0.72
KS:M-NM:F	-1.36	-3.91	1.18	0.91
MO:M-NM:F	-1.55	-3.92	0.82	0.67
CO:F-OK:F	0.43	-1.98	2.85	1.00
KS:F-OK:F	0.36	-1.69	2.42	1.00
MO:F-OK:F	-0.60	-3.61	2.41	1.00
MX:M-OK:F	0.17	-2.84	3.18	1.00
ST:M-OK:F	-0.45	-3.08	2.18	1.00
AZ:M-OK:F	0.58	-1.83	2.99	1.00
WT:M-OK:F	0.65	-1.53	2.83	1.00
NT:M-OK:F	-0.58	-2.68	1.53	1.00
NM:M-OK:F	-0.07	-2.01	1.87	1.00
OK:M-OK:F	-0.34	-2.45	1.77	1.00
CO:M-OK:F	-0.14	-2.08	1.80	1.00
KS:M-OK:F	-0.01	-2.19	2.16	1.00

Table C3. (continued)

MO:M-OK:F	-0.20	-2.17	1.77	1.00
KS:F-CO:F	-0.07	-2.27	2.14	1.00
MO:F-CO:F	-1.03	-4.15	2.08	1.00
MX:M-CO:F	-0.26	-3.38	2.85	1.00
ST:M-CO:F	-0.88	-3.63	1.86	1.00
AZ:M-CO:F	0.15	-2.40	2.69	1.00
WT:M-CO:F	0.22	-2.10	2.54	1.00
NT:M-CO:F	-1.01	-3.26	1.25	0.98
NM:M-CO:F	-0.50	-2.60	1.60	1.00
OK:M-CO:F	-0.77	-3.03	1.48	1.00
CO:M-CO:F	-0.57	-2.68	1.53	1.00
KS:M-CO:F	-0.45	-2.77	1.88	1.00
MO:M-CO:F	-0.63	-2.76	1.49	1.00
MO:F-KS:F	-0.96	-3.81	1.88	1.00
MX:M-KS:F	-0.19	-3.04	2.65	1.00
ST:M-KS:F	-0.82	-3.25	1.62	1.00
AZ:M-KS:F	0.22	-1.99	2.42	1.00
WT:M-KS:F	0.29	-1.66	2.23	1.00
NT:M-KS:F	-0.94	-2.80	0.92	0.95
NM:M-KS:F	-0.43	-2.10	1.24	1.00
OK:M-KS:F	-0.70	-2.57	1.16	1.00
CO:M-KS:F	-0.51	-2.18	1.17	1.00
KS:M-KS:F	-0.38	-2.32	1.56	1.00
MO:M-KS:F	-0.57	-2.27	1.14	1.00
MX:M-MO:F	0.77	-2.83	4.37	1.00
ST:M-MO:F	0.15	-3.14	3.43	1.00
AZ:M-MO:F	1.18	-1.94	4.30	1.00
WT:M-MO:F	1.25	-1.69	4.19	0.99
NT:M-MO:F	0.02	-2.86	2.91	1.00
NM:M-MO:F	0.53	-2.23	3.30	1.00
OK:M-MO:F	0.26	-2.63	3.14	1.00
CO:M-MO:F	0.46	-2.31	3.22	1.00
KS:M-MO:F	0.58	-2.35	3.52	1.00
MO:M-MO:F	0.40	-2.39	3.18	1.00
ST:M-MX:M	-0.62	-3.91	2.66	1.00
AZ:M-MX:M	0.41	-2.71	3.53	1.00

Table C3. (continued)

WT:M-MX:M	0.48	-2.46	3.42	1.00
NT:M-MX:M	-0.75	-3.63	2.14	1.00
NM:M-MX:M	-0.24	-3.00	2.53	1.00
OK:M-MX:M	-0.51	-3.40	2.38	1.00
CO:M-MX:M	-0.31	-3.08	2.45	1.00
KS:M-MX:M	-0.19	-3.12	2.75	1.00
MO:M-MX:M	-0.37	-3.16	2.42	1.00
AZ:M-ST:M	1.03	-1.72	3.78	1.00
WT:M-ST:M	1.10	-1.44	3.65	0.99
NT:M-ST:M	-0.13	-2.61	2.36	1.00
NM:M-ST:M	0.38	-1.96	2.73	1.00
OK:M-ST:M	0.11	-2.37	2.59	1.00
CO:M-ST:M	0.31	-2.03	2.65	1.00
KS:M-ST:M	0.44	-2.11	2.98	1.00
MO:M-ST:M	0.25	-2.12	2.62	1.00
WT:M-AZ:M	0.07	-2.25	2.39	1.00
NT:M-AZ:M	-1.16	-3.41	1.10	0.94
NM:M-AZ:M	-0.65	-2.75	1.45	1.00
OK:M-AZ:M	-0.92	-3.18	1.34	0.99
CO:M-AZ:M	-0.72	-2.82	1.38	1.00
KS:M-AZ:M	-0.60	-2.92	1.73	1.00
MO:M-AZ:M	-0.78	-2.91	1.35	1.00
NT:M-WT:M	-1.23	-3.23	0.77	0.77
NM:M-WT:M	-0.72	-2.54	1.11	1.00
OK:M-WT:M	-0.99	-2.99	1.01	0.96
CO:M-WT:M	-0.79	-2.62	1.03	0.99
KS:M-WT:M	-0.67	-2.74	1.41	1.00
MO:M-WT:M	-0.85	-2.71	1.01	0.98
NM:M-NT:M	0.51	-1.23	2.25	1.00
OK:M-NT:M	0.24	-1.69	2.16	1.00
CO:M-NT:M	0.43	-1.30	2.17	1.00
KS:M-NT:M	0.56	-1.44	2.56	1.00
MO:M-NT:M	0.38	-1.40	2.15	1.00
OK:M-NM:M	-0.27	-2.01	1.47	1.00
CO:M-NM:M	-0.07	-1.61	1.46	1.00
KS:M-NM:M	0.05	-1.77	1.88	1.00

Table C3. (continued)

MO:M-NM:M	-0.13	-1.71	1.44	1.00
CO:M-OK:M	0.20	-1.54	1.94	1.00
KS:M-OK:M	0.32	-1.68	2.33	1.00
MO:M-OK:M	0.14	-1.64	1.91	1.00
KS:M-CO:M	0.13	-1.70	1.95	1.00
MO:M-CO:M	-0.06	-1.63	1.51	1.00
MO:M-KS:M	-0.19	-2.04	1.67	1.00
Group C PC1				
ST:F-MX:F	0.48	-3.41	4.37	1.00
AZ:F-MX:F	1.28	-2.36	4.92	1.00
WT:F-MX:F	-0.25	-3.85	3.35	1.00
NT:F-MX:F	0.07	-3.53	3.67	1.00
NM:F-MX:F	-0.32	-4.20	3.57	1.00
OK:F-MX:F	-0.20	-3.89	3.49	1.00
CO:F-MX:F	0.27	-3.49	4.04	1.00
KS:F-MX:F	-0.33	-3.90	3.24	1.00
MO:F-MX:F	-0.45	-4.57	3.67	1.00
MX:M-MX:F	-0.59	-4.72	3.53	1.00
ST:M-MX:F	0.44	-3.45	4.32	1.00
AZ:M-MX:F	0.22	-3.55	3.98	1.00
WT:M-MX:F	0.26	-3.38	3.90	1.00
NT:M-MX:F	-0.30	-3.90	3.30	1.00
NM:M-MX:F	-0.98	-4.50	2.53	1.00
OK:M-MX:F	-0.82	-4.42	2.78	1.00
CO:M-MX:F	0.25	-3.27	3.76	1.00
KS:M-MX:F	-0.52	-4.15	3.12	1.00
MO:M-MX:F	-0.50	-4.03	3.03	1.00
AZ:F-ST:F	0.80	-1.58	3.18	1.00
WT:F-ST:F	-0.73	-3.05	1.59	1.00
NT:F-ST:F	-0.41	-2.73	1.91	1.00
NM:F-ST:F	-0.80	-3.55	1.95	1.00
OK:F-ST:F	-0.68	-3.14	1.78	1.00
CO:F-ST:F	-0.21	-2.78	2.37	1.00
KS:F-ST:F	-0.81	-3.09	1.47	1.00
MO:F-ST:F	-0.93	-4.00	2.14	1.00
MX:M-ST:F	-1.07	-4.15	2.00	1.00

Table C3. (continued)

ST:M-ST:F	-0.04	-2.79	2.70	1.00
AZ:M-ST:F	-0.26	-2.84	2.31	1.00
WT:M-ST:F	-0.22	-2.60	2.16	1.00
NT:M-ST:F	-0.78	-3.11	1.54	1.00
NM:M-ST:F	-1.46	-3.66	0.73	0.63
OK:M-ST:F	-1.30	-3.62	1.03	0.88
CO:M-ST:F	-0.23	-2.43	1.96	1.00
KS:M-ST:F	-1.00	-3.38	1.39	0.99
MO:M-ST:F	-0.98	-3.20	1.24	0.99
WT:F-AZ:F	-1.53	-3.40	0.34	0.27
NT:F-AZ:F	-1.21	-3.08	0.66	0.69
NM:F-AZ:F	-1.59	-3.98	0.79	0.63
OK:F-AZ:F	-1.48	-3.52	0.56	0.48
CO:F-AZ:F	-1.01	-3.18	1.17	0.98
KS:F-AZ:F	-1.61	-3.43	0.21	0.15
MO:F-AZ:F	-1.73	-4.48	1.02	0.73
MX:M-AZ:F	-1.87	-4.62	0.88	0.60
ST:M-AZ:F	-0.84	-3.23	1.54	1.00
AZ:M-AZ:F	-1.06	-3.24	1.11	0.96
WT:M-AZ:F	-1.02	-2.96	0.92	0.93
NT:M-AZ:F	-1.58	-3.45	0.29	0.22
NM:M-AZ:F	-2.26	-3.97	-0.55	<0.01
OK:M-AZ:F	-2.10	-3.97	-0.22	0.01
CO:M-AZ:F	-1.03	-2.74	0.67	0.79
KS:M-AZ:F	-1.79	-3.74	0.15	0.11
MO:M-AZ:F	-1.78	-3.52	-0.04	0.04
NT:F-WT:F	0.32	-1.48	2.12	1.00
NM:F-WT:F	-0.07	-2.39	2.26	1.00
OK:F-WT:F	0.05	-1.93	2.02	1.00
CO:F-WT:F	0.52	-1.59	2.63	1.00
KS:F-WT:F	-0.08	-1.82	1.66	1.00
MO:F-WT:F	-0.20	-2.90	2.50	1.00
MX:M-WT:F	-0.34	-3.04	2.36	1.00
ST:M-WT:F	0.68	-1.64	3.01	1.00
AZ:M-WT:F	0.47	-1.64	2.58	1.00
WT:M-WT:F	0.51	-1.36	2.38	1.00

Table C3. (continued)

NT:M-WT:F	-0.05	-1.85	1.75	1.00
NM:M-WT:F	-0.73	-2.36	0.89	0.98
OK:M-WT:F	-0.57	-2.37	1.23	1.00
CO:M-WT:F	0.49	-1.13	2.12	1.00
KS:M-WT:F	-0.27	-2.14	1.61	1.00
MO:M-WT:F	-0.25	-1.91	1.41	1.00
NM:F-NT:F	-0.38	-2.71	1.94	1.00
OK:F-NT:F	-0.27	-2.24	1.70	1.00
CO:F-NT:F	0.20	-1.91	2.31	1.00
KS:F-NT:F	-0.40	-2.14	1.34	1.00
MO:F-NT:F	-0.52	-3.22	2.18	1.00
MX:M-NT:F	-0.66	-3.36	2.04	1.00
ST:M-NT:F	0.37	-1.96	2.69	1.00
AZ:M-NT:F	0.15	-1.96	2.26	1.00
WT:M-NT:F	0.19	-1.68	2.06	1.00
NT:M-NT:F	-0.37	-2.17	1.43	1.00
NM:M-NT:F	-1.05	-2.68	0.57	0.69
OK:M-NT:F	-0.89	-2.69	0.91	0.96
CO:M-NT:F	0.18	-1.45	1.80	1.00
KS:M-NT:F	-0.58	-2.46	1.29	1.00
MO:M-NT:F	-0.57	-2.23	1.09	1.00
OK:F-NM:F	0.11	-2.35	2.57	1.00
CO:F-NM:F	0.59	-1.98	3.16	1.00
KS:F-NM:F	-0.01	-2.29	2.27	1.00
MO:F-NM:F	-0.13	-3.21	2.94	1.00
MX:M-NM:F	-0.28	-3.35	2.80	1.00
ST:M-NM:F	0.75	-2.00	3.50	1.00
AZ:M-NM:F	0.53	-2.04	3.10	1.00
WT:M-NM:F	0.57	-1.81	2.96	1.00
NT:M-NM:F	0.01	-2.31	2.34	1.00
NM:M-NM:F	-0.67	-2.86	1.53	1.00
OK:M-NM:F	-0.50	-2.83	1.82	1.00
CO:M-NM:F	0.56	-1.63	2.75	1.00
KS:M-NM:F	-0.20	-2.58	2.18	1.00
MO:M-NM:F	-0.18	-2.40	2.03	1.00
CO:F-OK:F	0.48	-1.78	2.74	1.00

Table C3. (continued)

KS:F-OK:F	-0.13	-2.05	1.79	1.00
MO:F-OK:F	-0.25	-3.06	2.57	1.00
MX:M-OK:F	-0.39	-3.21	2.43	1.00
ST:M-OK:F	0.64	-1.82	3.10	1.00
AZ:M-OK:F	0.42	-1.84	2.68	1.00
WT:M-OK:F	0.46	-1.58	2.50	1.00
NT:M-OK:F	-0.10	-2.07	1.87	1.00
NM:M-OK:F	-0.78	-2.60	1.04	0.99
OK:M-OK:F	-0.62	-2.59	1.36	1.00
CO:M-OK:F	0.45	-1.37	2.26	1.00
KS:M-OK:F	-0.31	-2.35	1.73	1.00
MO:M-OK:F	-0.30	-2.14	1.55	1.00
KS:F-CO:F	-0.60	-2.66	1.46	1.00
MO:F-CO:F	-0.72	-3.64	2.19	1.00
MX:M-CO:F	-0.86	-3.78	2.05	1.00
ST:M-CO:F	0.16	-2.41	2.73	1.00
AZ:M-CO:F	-0.06	-2.44	2.33	1.00
WT:M-CO:F	-0.01	-2.19	2.16	1.00
NT:M-CO:F	-0.57	-2.69	1.54	1.00
NM:M-CO:F	-1.26	-3.22	0.71	0.71
OK:M-CO:F	-1.09	-3.20	1.02	0.93
CO:M-CO:F	-0.03	-1.99	1.94	1.00
KS:M-CO:F	-0.79	-2.96	1.39	1.00
MO:M-CO:F	-0.77	-2.76	1.22	1.00
MO:F-KS:F	-0.12	-2.78	2.54	1.00
MX:M-KS:F	-0.26	-2.92	2.40	1.00
ST:M-KS:F	0.76	-1.52	3.04	1.00
AZ:M-KS:F	0.55	-1.52	2.61	1.00
WT:M-KS:F	0.59	-1.23	2.41	1.00
NT:M-KS:F	0.03	-1.72	1.77	1.00
NM:M-KS:F	-0.65	-2.22	0.91	0.99
OK:M-KS:F	-0.49	-2.23	1.25	1.00
CO:M-KS:F	0.57	-0.99	2.14	1.00
KS:M-KS:F	-0.19	-2.00	1.63	1.00
MO:M-KS:F	-0.17	-1.77	1.43	1.00
MX:M-MO:F	-0.14	-3.51	3.23	1.00

Table C3. (continued)

ST:M-MO:F	0.89	-2.19	3.96	1.00
AZ:M-MO:F	0.67	-2.25	3.58	1.00
WT:M-MO:F	0.71	-2.04	3.46	1.00
NT:M-MO:F	0.15	-2.55	2.85	1.00
NM:M-MO:F	-0.53	-3.12	2.05	1.00
OK:M-MO:F	-0.37	-3.07	2.33	1.00
CO:M-MO:F	0.70	-1.89	3.28	1.00
KS:M-MO:F	-0.07	-2.81	2.68	1.00
MO:M-MO:F	-0.05	-2.66	2.56	1.00
ST:M-MX:M	1.03	-2.05	4.10	1.00
AZ:M-MX:M	0.81	-2.11	3.73	1.00
WT:M-MX:M	0.85	-1.90	3.60	1.00
NT:M-MX:M	0.29	-2.41	2.99	1.00
NM:M-MX:M	-0.39	-2.98	2.20	1.00
OK:M-MX:M	-0.23	-2.93	2.47	1.00
CO:M-MX:M	0.84	-1.75	3.43	1.00
KS:M-MX:M	0.08	-2.67	2.83	1.00
MO:M-MX:M	0.09	-2.52	2.70	1.00
AZ:M-ST:M	-0.22	-2.79	2.35	1.00
WT:M-ST:M	-0.18	-2.56	2.21	1.00
NT:M-ST:M	-0.74	-3.06	1.59	1.00
NM:M-ST:M	-1.42	-3.61	0.77	0.69
OK:M-ST:M	-1.25	-3.58	1.07	0.91
CO:M-ST:M	-0.19	-2.38	2.00	1.00
KS:M-ST:M	-0.95	-3.33	1.43	1.00
MO:M-ST:M	-0.93	-3.15	1.28	0.99
WT:M-AZ:M	0.04	-2.13	2.22	1.00
NT:M-AZ:M	-0.52	-2.63	1.59	1.00
NM:M-AZ:M	-1.20	-3.17	0.77	0.78
OK:M-AZ:M	-1.04	-3.15	1.08	0.96
CO:M-AZ:M	0.03	-1.94	1.99	1.00
KS:M-AZ:M	-0.73	-2.91	1.44	1.00
MO:M-AZ:M	-0.72	-2.71	1.28	1.00
NT:M-WT:M	-0.56	-2.43	1.31	1.00
NM:M-WT:M	-1.24	-2.95	0.47	0.47
OK:M-WT:M	-1.08	-2.95	0.80	0.85

Table C3. (continued)

CO:M-WT:M	-0.01	-1.72	1.69	1.00
KS:M-WT:M	-0.77	-2.72	1.17	1.00
MO:M-WT:M	-0.76	-2.50	0.98	0.99
NM:M-NT:M	-0.68	-2.31	0.95	0.99
OK:M-NT:M	-0.52	-2.32	1.28	1.00
CO:M-NT:M	0.55	-1.08	2.17	1.00
KS:M-NT:M	-0.21	-2.09	1.66	1.00
MO:M-NT:M	-0.20	-1.86	1.46	1.00
OK:M-NM:M	0.17	-1.46	1.79	1.00
CO:M-NM:M	1.23	-0.21	2.66	0.20
KS:M-NM:M	0.47	-1.24	2.18	1.00
MO:M-NM:M	0.49	-0.99	1.96	1.00
CO:M-OK:M	1.06	-0.57	2.69	0.67
KS:M-OK:M	0.30	-1.57	2.18	1.00
MO:M-OK:M	0.32	-1.34	1.98	1.00
KS:M-CO:M	-0.76	-2.47	0.95	0.98
MO:M-CO:M	-0.74	-2.22	0.73	0.95
MO:M-KS:M	0.02	-1.72	1.76	1.00
Group C PC2				
ST:F-MX:F	0.37	-3.11	3.84	1.00
AZ:F-MX:F	-0.19	-3.45	3.06	1.00
WT:F-MX:F	0.82	-2.39	4.04	1.00
NT:F-MX:F	0.38	-2.84	3.60	1.00
NM:F-MX:F	0.87	-2.61	4.34	1.00
OK:F-MX:F	0.72	-2.58	4.02	1.00
CO:F-MX:F	0.11	-3.26	3.47	1.00
KS:F-MX:F	-0.38	-3.57	2.81	1.00
MO:F-MX:F	-0.05	-3.74	3.63	1.00
MX:M-MX:F	-0.30	-3.99	3.39	1.00
ST:M-MX:F	0.31	-3.16	3.79	1.00
AZ:M-MX:F	-1.70	-5.07	1.66	0.95
WT:M-MX:F	0.02	-3.23	3.27	1.00
NT:M-MX:F	-0.79	-4.01	2.43	1.00
NM:M-MX:F	0.58	-2.57	3.72	1.00
OK:M-MX:F	-0.49	-3.71	2.73	1.00
CO:M-MX:F	-0.74	-3.88	2.40	1.00

Table C3. (continued)

KS:M-MX:F	-0.83	-4.08	2.42	1.00
MO:M-MX:F	-0.86	-4.02	2.30	1.00
AZ:F-ST:F	-0.56	-2.69	1.57	1.00
WT:F-ST:F	0.46	-1.62	2.53	1.00
NT:F-ST:F	0.01	-2.06	2.09	1.00
NM:F-ST:F	0.50	-1.96	2.96	1.00
OK:F-ST:F	0.35	-1.84	2.55	1.00
CO:F-ST:F	-0.26	-2.56	2.04	1.00
KS:F-ST:F	-0.75	-2.78	1.29	1.00
MO:F-ST:F	-0.42	-3.17	2.33	1.00
MX:M-ST:F	-0.67	-3.41	2.08	1.00
ST:M-ST:F	-0.05	-2.51	2.40	1.00
AZ:M-ST:F	-2.07	-4.37	0.23	0.13
WT:M-ST:F	-0.35	-2.48	1.78	1.00
NT:M-ST:F	-1.15	-3.23	0.92	0.88
NM:M-ST:F	0.21	-1.75	2.17	1.00
OK:M-ST:F	-0.86	-2.93	1.22	0.99
CO:M-ST:F	-1.11	-3.07	0.85	0.87
KS:M-ST:F	-1.20	-3.33	0.93	0.87
MO:M-ST:F	-1.23	-3.21	0.75	0.75
WT:F-AZ:F	1.02	-0.66	2.69	0.78
NT:F-AZ:F	0.58	-1.10	2.25	1.00
NM:F-AZ:F	1.06	-1.07	3.19	0.95
OK:F-AZ:F	0.91	-0.91	2.74	0.95
CO:F-AZ:F	0.30	-1.64	2.25	1.00
KS:F-AZ:F	-0.19	-1.81	1.44	1.00
MO:F-AZ:F	0.14	-2.31	2.60	1.00
MX:M-AZ:F	-0.10	-2.56	2.35	1.00
ST:M-AZ:F	0.51	-1.62	2.63	1.00
AZ:M-AZ:F	-1.51	-3.45	0.43	0.35
WT:M-AZ:F	0.21	-1.53	1.95	1.00
NT:M-AZ:F	-0.59	-2.27	1.08	1.00
NM:M-AZ:F	0.77	-0.76	2.30	0.95
OK:M-AZ:F	-0.29	-1.97	1.38	1.00
CO:M-AZ:F	-0.55	-2.07	0.98	1.00
KS:M-AZ:F	-0.64	-2.38	1.10	1.00

Table C3. (continued)

MO:M-AZ:F	-0.67	-2.22	0.89	0.99
NT:F-WT:F	-0.44	-2.05	1.17	1.00
NM:F-WT:F	0.04	-2.03	2.12	1.00
OK:F-WT:F	-0.10	-1.87	1.66	1.00
CO:F-WT:F	-0.71	-2.60	1.17	1.00
KS:F-WT:F	-1.20	-2.76	0.35	0.36
MO:F-WT:F	-0.88	-3.29	1.54	1.00
MX:M-WT:F	-1.12	-3.54	1.29	0.98
ST:M-WT:F	-0.51	-2.59	1.56	1.00
AZ:M-WT:F	-2.53	-4.42	-0.64	<0.01
WT:M-WT:F	-0.81	-2.48	0.87	0.96
NT:M-WT:F	-1.61	-3.22	<0.01	0.05
NM:M-WT:F	-0.25	-1.70	1.21	1.00
OK:M-WT:F	-1.31	-2.92	0.29	0.27
CO:M-WT:F	-1.57	-3.02	-0.11	0.02
KS:M-WT:F	-1.66	-3.33	0.02	0.06
MO:M-WT:F	-1.69	-3.17	-0.20	0.01
NM:F-NT:F	0.49	-1.59	2.56	1.00
OK:F-NT:F	0.34	-1.42	2.10	1.00
CO:F-NT:F	-0.27	-2.16	1.62	1.00
KS:F-NT:F	-0.76	-2.32	0.80	0.96
MO:F-NT:F	-0.43	-2.85	1.98	1.00
MX:M-NT:F	-0.68	-3.09	1.73	1.00
ST:M-NT:F	-0.07	-2.15	2.01	1.00
AZ:M-NT:F	-2.09	-3.97	-0.20	0.02
WT:M-NT:F	-0.36	-2.04	1.31	1.00
NT:M-NT:F	-1.17	-2.78	0.44	0.48
NM:M-NT:F	0.20	-1.26	1.65	1.00
OK:M-NT:F	-0.87	-2.48	0.74	0.90
CO:M-NT:F	-1.12	-2.58	0.33	0.36
KS:M-NT:F	-1.21	-2.89	0.46	0.48
MO:M-NT:F	-1.24	-2.73	0.24	0.23
OK:F-NM:F	-0.15	-2.35	2.05	1.00
CO:F-NM:F	-0.76	-3.06	1.54	1.00
KS:F-NM:F	-1.25	-3.28	0.79	0.77
MO:F-NM:F	-0.92	-3.67	1.83	1.00

Table C3. (continued)

MX:M-NM:F	-1.17	-3.91	1.58	0.99
ST:M-NM:F	-0.56	-3.01	1.90	1.00
AZ:M-NM:F	-2.57	-4.87	-0.27	0.01
WT:M-NM:F	-0.85	-2.98	1.28	1.00
NT:M-NM:F	-1.66	-3.73	0.42	0.31
NM:M-NM:F	-0.29	-2.25	1.67	1.00
OK:M-NM:F	-1.36	-3.43	0.72	0.67
CO:M-NM:F	-1.61	-3.57	0.35	0.26
KS:M-NM:F	-1.70	-3.83	0.43	0.30
MO:M-NM:F	-1.73	-3.71	0.25	0.17
CO:F-OK:F	-0.61	-2.63	1.41	1.00
KS:F-OK:F	-1.10	-2.82	0.62	0.70
MO:F-OK:F	-0.77	-3.29	1.75	1.00
MX:M-OK:F	-1.02	-3.54	1.50	0.99
ST:M-OK:F	-0.41	-2.61	1.79	1.00
AZ:M-OK:F	-2.42	-4.44	-0.41	<0.01
WT:M-OK:F	-0.70	-2.53	1.12	1.00
NT:M-OK:F	-1.51	-3.27	0.25	0.20
NM:M-OK:F	-0.14	-1.77	1.48	1.00
OK:M-OK:F	-1.21	-2.97	0.55	0.58
CO:M-OK:F	-1.46	-3.08	0.16	0.13
KS:M-OK:F	-1.55	-3.38	0.27	0.20
MO:M-OK:F	-1.58	-3.23	0.07	0.08
KS:F-CO:F	-0.49	-2.33	1.35	1.00
MO:F-CO:F	-0.16	-2.77	2.45	1.00
MX:M-CO:F	-0.41	-3.02	2.20	1.00
ST:M-CO:F	0.20	-2.10	2.50	1.00
AZ:M-CO:F	-1.81	-3.94	0.31	0.20
WT:M-CO:F	-0.09	-2.04	1.85	1.00
NT:M-CO:F	-0.90	-2.78	0.99	0.97
NM:M-CO:F	0.47	-1.29	2.22	1.00
OK:M-CO:F	-0.60	-2.49	1.29	1.00
CO:M-CO:F	-0.85	-2.61	0.91	0.96
KS:M-CO:F	-0.94	-2.89	1.00	0.96
MO:M-CO:F	-0.97	-2.75	0.81	0.90
MO:F-KS:F	0.33	-2.05	2.71	1.00

Table C3. (continued)

MX:M-KS:F	0.08	-2.30	2.46	1.00
ST:M-KS:F	0.69	-1.35	2.73	1.00
AZ:M-KS:F	-1.32	-3.17	0.52	0.50
WT:M-KS:F	0.40	-1.23	2.02	1.00
NT:M-KS:F	-0.41	-1.97	1.15	1.00
NM:M-KS:F	0.96	-0.44	2.35	0.59
OK:M-KS:F	-0.11	-1.67	1.45	1.00
CO:M-KS:F	-0.36	-1.76	1.04	1.00
KS:M-KS:F	-0.45	-2.08	1.17	1.00
MO:M-KS:F	-0.48	-1.91	0.95	1.00
MX:M-MO:F	-0.25	-3.26	2.76	1.00
ST:M-MO:F	0.36	-2.38	3.11	1.00
AZ:M-MO:F	-1.65	-4.26	0.95	0.72
WT:M-MO:F	0.07	-2.39	2.53	1.00
NT:M-MO:F	-0.74	-3.15	1.68	1.00
NM:M-MO:F	0.63	-1.69	2.94	1.00
OK:M-MO:F	-0.44	-2.85	1.98	1.00
CO:M-MO:F	-0.69	-3.00	1.62	1.00
KS:M-MO:F	-0.78	-3.24	1.68	1.00
MO:M-MO:F	-0.81	-3.14	1.52	1.00
ST:M-MX:M	0.61	-2.14	3.36	1.00
AZ:M-MX:M	-1.41	-4.01	1.20	0.91
WT:M-MX:M	0.32	-2.14	2.77	1.00
NT:M-MX:M	-0.49	-2.90	1.92	1.00
NM:M-MX:M	0.88	-1.44	3.19	1.00
OK:M-MX:M	-0.19	-2.60	2.22	1.00
CO:M-MX:M	-0.44	-2.75	1.87	1.00
KS:M-MX:M	-0.53	-2.99	1.92	1.00
MO:M-MX:M	-0.56	-2.89	1.77	1.00
AZ:M-ST:M	-2.02	-4.32	0.28	0.16
WT:M-ST:M	-0.30	-2.42	1.83	1.00
NT:M-ST:M	-1.10	-3.18	0.98	0.92
NM:M-ST:M	0.26	-1.70	2.23	1.00
OK:M-ST:M	-0.80	-2.88	1.28	1.00
CO:M-ST:M	-1.05	-3.01	0.91	0.91
KS:M-ST:M	-1.14	-3.27	0.98	0.91

Table C3. (continued)

MO:M-ST:M	-1.17	-3.15	0.81	0.82
WT:M-AZ:M	1.72	-0.22	3.66	0.15
NT:M-AZ:M	0.92	-0.97	2.80	0.96
NM:M-AZ:M	2.28	0.52	4.04	<0.01
OK:M-AZ:M	1.22	-0.67	3.10	0.70
CO:M-AZ:M	0.96	-0.79	2.72	0.89
KS:M-AZ:M	0.87	-1.07	2.81	0.98
MO:M-AZ:M	0.84	-0.94	2.62	0.97
NT:M-WT:M	-0.80	-2.48	0.87	0.97
NM:M-WT:M	0.56	-0.97	2.09	1.00
OK:M-WT:M	-0.51	-2.18	1.17	1.00
CO:M-WT:M	-0.76	-2.28	0.77	0.95
KS:M-WT:M	-0.85	-2.59	0.89	0.96
MO:M-WT:M	-0.88	-2.43	0.68	0.87
NM:M-NT:M	1.37	-0.09	2.82	0.09
OK:M-NT:M	0.30	-1.31	1.91	1.00
CO:M-NT:M	0.05	-1.41	1.50	1.00
KS:M-NT:M	-0.04	-1.72	1.63	1.00
MO:M-NT:M	-0.07	-1.56	1.41	1.00
OK:M-NM:M	-1.07	-2.52	0.39	0.46
CO:M-NM:M	-1.32	-2.60	-0.03	0.04
KS:M-NM:M	-1.41	-2.94	0.12	0.11
MO:M-NM:M	-1.44	-2.75	-0.12	0.02
CO:M-OK:M	-0.25	-1.71	1.20	1.00
KS:M-OK:M	-0.34	-2.02	1.33	1.00
MO:M-OK:M	-0.37	-1.86	1.11	1.00
KS:M-CO:M	-0.09	-1.62	1.44	1.00
MO:M-CO:M	-0.12	-1.44	1.19	1.00
MO:M-KS:M	-0.03	-1.58	1.53	1.00
Group C PC3				
ST:F-MX:F	-0.35	-4.41	3.71	1.00
AZ:F-MX:F	-0.94	-4.74	2.86	1.00
WT:F-MX:F	-1.29	-5.05	2.47	1.00
NT:F-MX:F	-0.46	-4.21	3.30	1.00
NM:F-MX:F	-1.42	-5.48	2.64	1.00
OK:F-MX:F	-1.16	-5.01	2.69	1.00

Table C3. (continued)

CO:F-MX:F	-1.08	-5.01	2.85	1.00
KS:F-MX:F	-0.27	-4.00	3.45	1.00
MO:F-MX:F	-0.47	-4.77	3.84	1.00
MX:M-MX:F	-0.35	-4.65	3.96	1.00
ST:M-MX:F	-0.08	-4.14	3.98	1.00
AZ:M-MX:F	-1.41	-5.34	2.52	1.00
WT:M-MX:F	-0.28	-4.08	3.51	1.00
NT:M-MX:F	-0.82	-4.57	2.94	1.00
NM:M-MX:F	-1.29	-4.96	2.38	1.00
OK:M-MX:F	-0.71	-4.47	3.04	1.00
CO:M-MX:F	-0.93	-4.60	2.74	1.00
KS:M-MX:F	-0.06	-3.86	3.74	1.00
MO:M-MX:F	0.04	-3.65	3.73	1.00
AZ:F-ST:F	-0.59	-3.07	1.90	1.00
WT:F-ST:F	-0.94	-3.37	1.49	1.00
NT:F-ST:F	-0.11	-2.53	2.32	1.00
NM:F-ST:F	-1.07	-3.94	1.80	1.00
OK:F-ST:F	-0.81	-3.37	1.76	1.00
CO:F-ST:F	-0.73	-3.42	1.95	1.00
KS:F-ST:F	0.08	-2.30	2.46	1.00
MO:F-ST:F	-0.12	-3.33	3.09	1.00
MX:M-ST:F	<0.01	-3.20	3.21	1.00
ST:M-ST:F	0.27	-2.60	3.14	1.00
AZ:M-ST:F	-1.06	-3.74	1.63	1.00
WT:M-ST:F	0.07	-2.42	2.55	1.00
NT:M-ST:F	-0.47	-2.89	1.96	1.00
NM:M-ST:F	-0.94	-3.23	1.35	0.99
OK:M-ST:F	-0.36	-2.79	2.06	1.00
CO:M-ST:F	-0.58	-2.87	1.71	1.00
KS:M-ST:F	0.29	-2.20	2.77	1.00
MO:M-ST:F	0.39	-1.92	2.70	1.00
WT:F-AZ:F	-0.35	-2.31	1.60	1.00
NT:F-AZ:F	0.48	-1.47	2.44	1.00
NM:F-AZ:F	-0.48	-2.97	2.00	1.00
OK:F-AZ:F	-0.22	-2.35	1.91	1.00
CO:F-AZ:F	-0.14	-2.41	2.12	1.00

Table C3. (continued)

KS:F-AZ:F	0.67	-1.23	2.56	1.00
MO:F-AZ:F	0.47	-2.40	3.34	1.00
MX:M-AZ:F	0.59	-2.28	3.46	1.00
ST:M-AZ:F	0.86	-1.63	3.34	1.00
AZ:M-AZ:F	-0.47	-2.74	1.80	1.00
WT:M-AZ:F	0.65	-1.38	2.68	1.00
NT:M-AZ:F	0.12	-1.83	2.08	1.00
NM:M-AZ:F	-0.35	-2.14	1.43	1.00
OK:M-AZ:F	0.22	-1.73	2.18	1.00
CO:M-AZ:F	0.01	-1.77	1.79	1.00
KS:M-AZ:F	0.88	-1.15	2.91	0.99
MO:M-AZ:F	0.98	-0.84	2.79	0.91
NT:F-WT:F	0.83	-1.05	2.71	0.98
NM:F-WT:F	-0.13	-2.56	2.30	1.00
OK:F-WT:F	0.13	-1.93	2.19	1.00
CO:F-WT:F	0.21	-2.00	2.41	1.00
KS:F-WT:F	1.02	-0.80	2.84	0.88
MO:F-WT:F	0.82	-2.00	3.64	1.00
MX:M-WT:F	0.95	-1.87	3.76	1.00
ST:M-WT:F	1.21	-1.22	3.63	0.95
AZ:M-WT:F	-0.12	-2.32	2.09	1.00
WT:M-WT:F	1.01	-0.95	2.96	0.94
NT:M-WT:F	0.48	-1.40	2.35	1.00
NM:M-WT:F	<0.01	-1.70	1.70	1.00
OK:M-WT:F	0.58	-1.30	2.46	1.00
CO:M-WT:F	0.36	-1.34	2.06	1.00
KS:M-WT:F	1.23	-0.73	3.18	0.73
MO:M-WT:F	1.33	-0.40	3.06	0.37
NM:F-NT:F	-0.96	-3.39	1.46	1.00
OK:F-NT:F	-0.70	-2.76	1.36	1.00
CO:F-NT:F	-0.63	-2.83	1.58	1.00
KS:F-NT:F	0.18	-1.64	2.00	1.00
MO:F-NT:F	-0.01	-2.83	2.81	1.00
MX:M-NT:F	0.11	-2.71	2.93	1.00
ST:M-NT:F	0.37	-2.05	2.80	1.00
AZ:M-NT:F	-0.95	-3.15	1.25	0.99

Table C3. (continued)

WT:M-NT:F	0.17	-1.78	2.13	1.00
NT:M-NT:F	-0.36	-2.24	1.52	1.00
NM:M-NT:F	-0.84	-2.53	0.86	0.96
OK:M-NT:F	-0.26	-2.14	1.62	1.00
CO:M-NT:F	-0.47	-2.17	1.23	1.00
KS:M-NT:F	0.40	-1.56	2.35	1.00
MO:M-NT:F	0.50	-1.24	2.23	1.00
OK:F-NM:F	0.26	-2.30	2.83	1.00
CO:F-NM:F	0.34	-2.35	3.02	1.00
KS:F-NM:F	1.15	-1.23	3.53	0.97
MO:F-NM:F	0.95	-2.26	4.16	1.00
MX:M-NM:F	1.08	-2.13	4.28	1.00
ST:M-NM:F	1.34	-1.53	4.21	0.97
AZ:M-NM:F	0.01	-2.67	2.70	1.00
WT:M-NM:F	1.14	-1.35	3.62	0.98
NT:M-NM:F	0.61	-1.82	3.03	1.00
NM:M-NM:F	0.13	-2.16	2.42	1.00
OK:M-NM:F	0.71	-1.72	3.13	1.00
CO:M-NM:F	0.49	-1.80	2.78	1.00
KS:M-NM:F	1.36	-1.13	3.84	0.90
MO:M-NM:F	1.46	-0.85	3.77	0.73
CO:F-OK:F	0.07	-2.28	2.43	1.00
KS:F-OK:F	0.88	-1.12	2.89	0.99
MO:F-OK:F	0.69	-2.25	3.63	1.00
MX:M-OK:F	0.81	-2.13	3.75	1.00
ST:M-OK:F	1.08	-1.49	3.64	0.99
AZ:M-OK:F	-0.25	-2.61	2.11	1.00
WT:M-OK:F	0.87	-1.26	3.00	0.99
NT:M-OK:F	0.34	-1.72	2.40	1.00
NM:M-OK:F	-0.13	-2.03	1.76	1.00
OK:M-OK:F	0.44	-1.61	2.50	1.00
CO:M-OK:F	0.23	-1.67	2.12	1.00
KS:M-OK:F	1.10	-1.03	3.22	0.94
MO:M-OK:F	1.20	-0.73	3.12	0.75
KS:F-CO:F	0.81	-1.34	2.96	1.00
MO:F-CO:F	0.61	-2.43	3.66	1.00

Table C3. (continued)

MX:M-CO:F	0.74	-2.31	3.78	1.00
ST:M-CO:F	1.00	-1.68	3.69	1.00
AZ:M-CO:F	-0.32	-2.81	2.16	1.00
WT:M-CO:F	0.80	-1.47	3.07	1.00
NT:M-CO:F	0.27	-1.94	2.47	1.00
NM:M-CO:F	-0.21	-2.26	1.84	1.00
OK:M-CO:F	0.37	-1.83	2.57	1.00
CO:M-CO:F	0.15	-1.90	2.21	1.00
KS:M-CO:F	1.02	-1.25	3.29	0.98
MO:M-CO:F	1.12	-0.96	3.20	0.91
MO:F-KS:F	-0.19	-2.97	2.58	1.00
MX:M-KS:F	-0.07	-2.85	2.71	1.00
ST:M-KS:F	0.19	-2.19	2.57	1.00
AZ:M-KS:F	-1.13	-3.28	1.02	0.92
WT:M-KS:F	-0.01	-1.91	1.89	1.00
NT:M-KS:F	-0.54	-2.36	1.28	1.00
NM:M-KS:F	-1.02	-2.65	0.61	0.75
OK:M-KS:F	-0.44	-2.26	1.38	1.00
CO:M-KS:F	-0.66	-2.29	0.98	1.00
KS:M-KS:F	0.21	-1.69	2.11	1.00
MO:M-KS:F	0.31	-1.35	1.98	1.00
MX:M-MO:F	0.12	-3.39	3.64	1.00
ST:M-MO:F	0.39	-2.82	3.60	1.00
AZ:M-MO:F	-0.94	-3.98	2.11	1.00
WT:M-MO:F	0.18	-2.69	3.05	1.00
NT:M-MO:F	-0.35	-3.17	2.47	1.00
NM:M-MO:F	-0.82	-3.53	1.88	1.00
OK:M-MO:F	-0.25	-3.06	2.57	1.00
CO:M-MO:F	-0.46	-3.16	2.24	1.00
KS:M-MO:F	0.41	-2.46	3.28	1.00
MO:M-MO:F	0.51	-2.22	3.23	1.00
ST:M-MX:M	0.26	-2.95	3.47	1.00
AZ:M-MX:M	-1.06	-4.10	1.98	1.00
WT:M-MX:M	0.06	-2.81	2.93	1.00
NT:M-MX:M	-0.47	-3.29	2.35	1.00
NM:M-MX:M	-0.95	-3.65	1.76	1.00

Table C3. (continued)

OK:M-MX:M	-0.37	-3.19	2.45	1.00
CO:M-MX:M	-0.58	-3.29	2.12	1.00
KS:M-MX:M	0.28	-2.59	3.15	1.00
MO:M-MX:M	0.38	-2.34	3.11	1.00
AZ:M-ST:M	-1.32	-4.01	1.36	0.96
WT:M-ST:M	-0.20	-2.69	2.28	1.00
NT:M-ST:M	-0.73	-3.16	1.69	1.00
NM:M-ST:M	-1.21	-3.50	1.08	0.92
OK:M-ST:M	-0.63	-3.06	1.79	1.00
CO:M-ST:M	-0.85	-3.14	1.44	1.00
KS:M-ST:M	0.02	-2.46	2.51	1.00
MO:M-ST:M	0.12	-2.19	2.43	1.00
WT:M-AZ:M	1.12	-1.15	3.39	0.96
NT:M-AZ:M	0.59	-1.61	2.79	1.00
NM:M-AZ:M	0.11	-1.94	2.17	1.00
OK:M-AZ:M	0.69	-1.51	2.89	1.00
CO:M-AZ:M	0.48	-1.58	2.53	1.00
KS:M-AZ:M	1.34	-0.92	3.61	0.82
MO:M-AZ:M	1.44	-0.63	3.52	0.56
NT:M-WT:M	-0.53	-2.49	1.42	1.00
NM:M-WT:M	-1.01	-2.79	0.78	0.87
OK:M-WT:M	-0.43	-2.38	1.53	1.00
CO:M-WT:M	-0.65	-2.43	1.14	1.00
KS:M-WT:M	0.22	-1.81	2.25	1.00
MO:M-WT:M	0.32	-1.49	2.14	1.00
NM:M-NT:M	-0.48	-2.18	1.22	1.00
OK:M-NT:M	0.10	-1.78	1.98	1.00
CO:M-NT:M	-0.11	-1.81	1.59	1.00
KS:M-NT:M	0.75	-1.20	2.71	1.00
MO:M-NT:M	0.85	-0.88	2.59	0.96
OK:M-NM:M	0.58	-1.12	2.28	1.00
CO:M-NM:M	0.36	-1.14	1.86	1.00
KS:M-NM:M	1.23	-0.55	3.01	0.57
MO:M-NM:M	1.33	-0.20	2.87	0.18
CO:M-OK:M	-0.22	-1.92	1.48	1.00
KS:M-OK:M	0.65	-1.30	2.61	1.00

Table C3. (continued)

MO:M-OK:M	0.75	-0.98	2.49	0.99
KS:M-CO:M	0.87	-0.92	2.65	0.96
MO:M-CO:M	0.97	-0.57	2.50	0.73
MO:M-KS:M	0.10	-1.71	1.92	1.00

Table C4. Tukey's test table for lateral skull shape groups, between populations.

	diff	lwr	upr	p adj
Group A PC1				
ST-MX	-0.17	-2.69	2.35	1.00
WT-MX	-0.29	-2.60	2.03	1.00
NT-MX	0.40	-1.90	2.70	1.00
AZ-MX	-0.19	-2.54	2.17	1.00
NM-MX	0.12	-2.16	2.40	1.00
OK-MX	0.63	-1.71	2.96	1.00
CO-MX	-0.91	-3.19	1.36	0.95
KS-MX	-0.82	-3.11	1.47	0.98
MO-MX	-0.04	-2.34	2.26	1.00
WT-ST	-0.11	-1.74	1.51	1.00
NT-ST	0.57	-1.03	2.18	0.98
AZ-ST	-0.02	-1.70	1.66	1.00
NM-ST	0.29	-1.28	1.86	1.00
OK-ST	0.80	-0.86	2.45	0.86
CO-ST	-0.74	-2.31	0.83	0.87
KS-ST	-0.65	-2.24	0.94	0.94
MO-ST	0.13	-1.48	1.73	1.00
NT-WT	0.69	-0.57	1.95	0.75
AZ-WT	0.10	-1.26	1.45	1.00
NM-WT	0.40	-0.81	1.62	0.99
OK-WT	0.91	-0.41	2.23	0.43
CO-WT	-0.63	-1.84	0.59	0.80
KS-WT	-0.54	-1.77	0.70	0.92
MO-WT	0.24	-1.02	1.50	1.00
AZ-NT	-0.59	-1.92	0.74	0.91
NM-NT	-0.28	-1.47	0.90	1.00
OK-NT	0.22	-1.07	1.51	1.00
CO-NT	-1.32	-2.50	-0.13	0.02
KS-NT	-1.22	-2.43	-0.02	0.04
MO-NT	-0.44	-1.68	0.79	0.97
NM-AZ	0.31	-0.98	1.59	1.00
OK-AZ	0.81	-0.57	2.20	0.66
CO-AZ	-0.73	-2.01	0.56	0.71

Table C4. (continued)

KS-AZ	-0.63	-1.94	0.67	0.86
MO-AZ	0.14	-1.18	1.47	1.00
OK-NM	0.51	-0.74	1.75	0.95
CO-NM	-1.03	-2.17	0.11	0.11
KS-NM	-0.94	-2.10	0.22	0.22
MO-NM	-0.16	-1.35	1.02	1.00
CO-OK	-1.54	-2.79	-0.29	<0.01
KS-OK	-1.45	-2.71	-0.18	0.01
MO-OK	-0.67	-1.96	0.62	0.80
KS-CO	0.09	-1.07	1.25	1.00
MO-CO	0.87	-0.31	2.06	0.35
MO-KS	0.78	-0.43	1.99	0.53
Group A PC2				
ST-MX	0.66	-1.85	3.18	1.00
WT-MX	-0.38	-2.69	1.94	1.00
NT-MX	-0.01	-2.31	2.28	1.00
AZ-MX	-0.46	-2.81	1.89	1.00
NM-MX	-1.25	-3.53	1.02	0.74
OK-MX	0.20	-2.13	2.53	1.00
CO-MX	-0.26	-2.53	2.01	1.00
KS-MX	0.05	-2.23	2.34	1.00
MO-MX	-0.19	-2.49	2.10	1.00
WT-ST	-1.04	-2.66	0.58	0.54
NT-ST	-0.68	-2.28	0.92	0.93
AZ-ST	-1.12	-2.80	0.56	0.48
NM-ST	-1.92	-3.48	-0.35	0.01
OK-ST	-0.46	-2.11	1.19	1.00
CO-ST	-0.92	-2.49	0.64	0.66
KS-ST	-0.61	-2.19	0.97	0.96
MO-ST	-0.86	-2.46	0.74	0.77
NT-WT	0.36	-0.89	1.62	0.99
AZ-WT	-0.08	-1.43	1.27	1.00
NM-WT	-0.88	-2.09	0.33	0.37
OK-WT	0.58	-0.73	1.89	0.91
CO-WT	0.11	-1.10	1.33	1.00
KS-WT	0.43	-0.80	1.66	0.98
MO-WT	0.18	-1.07	1.44	1.00

Table C4. (continued)

AZ-NT	-0.44	-1.77	0.88	0.98
NM-NT	-1.24	-2.42	-0.06	0.03
OK-NT	0.22	-1.07	1.50	1.00
CO-NT	-0.25	-1.43	0.93	1.00
KS-NT	0.07	-1.14	1.27	1.00
MO-NT	-0.18	-1.41	1.05	1.00
NM-AZ	-0.80	-2.08	0.49	0.59
OK-AZ	0.66	-0.72	2.04	0.86
CO-AZ	0.20	-1.09	1.48	1.00
KS-AZ	0.51	-0.79	1.82	0.96
MO-AZ	0.26	-1.06	1.59	1.00
OK-NM	1.46	0.21	2.70	0.01
CO-NM	0.99	-0.15	2.13	0.14
KS-NM	1.31	0.15	2.47	0.01
MO-NM	1.06	-0.12	2.24	0.12
CO-OK	-0.47	-1.71	0.78	0.97
KS-OK	-0.15	-1.41	1.12	1.00
MO-OK	-0.40	-1.69	0.89	0.99
KS-CO	0.32	-0.84	1.47	1.00
MO-CO	0.07	-1.12	1.25	1.00
MO-KS	-0.25	-1.45	0.95	1.00
Group B PC1				
ST-MX	-0.24	-2.71	2.22	1.00
WT-MX	0.12	-2.14	2.39	1.00
NT-MX	1.06	-1.19	3.31	0.87
AZ-MX	0.68	-1.62	2.99	0.99
NM-MX	0.23	-2.00	2.46	1.00
OK-MX	0.44	-1.85	2.72	1.00
CO-MX	-0.22	-2.45	2.01	1.00
KS-MX	0.97	-1.27	3.21	0.92
MO-MX	1.35	-0.91	3.60	0.64
WT-ST	0.37	-1.22	1.96	1.00
NT-ST	1.31	-0.26	2.88	0.19
AZ-ST	0.93	-0.72	2.57	0.71
NM-ST	0.48	-1.06	2.01	0.99
OK-ST	0.68	-0.93	2.30	0.93
CO-ST	0.03	-1.51	1.56	1.00

Table C4. (continued)

KS-ST	1.21	-0.34	2.76	0.26
MO-ST	1.59	0.02	3.16	0.04
NT-WT	0.94	-0.29	2.17	0.29
AZ-WT	0.56	-0.76	1.89	0.93
NM-WT	0.11	-1.08	1.30	1.00
OK-WT	0.32	-0.97	1.61	1.00
CO-WT	-0.34	-1.53	0.85	1.00
KS-WT	0.84	-0.36	2.05	0.42
MO-WT	1.22	-0.01	2.45	0.05
AZ-NT	-0.38	-1.68	0.92	0.99
NM-NT	-0.83	-1.99	0.33	0.38
OK-NT	-0.62	-1.89	0.64	0.84
CO-NT	-1.28	-2.44	-0.12	0.02
KS-NT	-0.09	-1.28	1.09	1.00
MO-NT	0.28	-0.92	1.49	1.00
NM-AZ	-0.45	-1.71	0.81	0.97
OK-AZ	-0.25	-1.60	1.11	1.00
CO-AZ	-0.90	-2.16	0.36	0.38
KS-AZ	0.28	-1.00	1.56	1.00
MO-AZ	0.66	-0.64	1.96	0.82
OK-NM	0.21	-1.01	1.43	1.00
CO-NM	-0.45	-1.56	0.67	0.95
KS-NM	0.74	-0.40	1.87	0.53
MO-NM	1.11	-0.05	2.27	0.07
CO-OK	-0.66	-1.88	0.57	0.77
KS-OK	0.53	-0.71	1.77	0.93
MO-OK	0.91	-0.36	2.17	0.38
KS-CO	1.18	0.05	2.32	0.03
MO-CO	1.56	0.40	2.72	<0.01
MO-KS	0.38	-0.80	1.56	0.99
Group B PC2				
ST-MX	1.29	-1.36	3.95	0.85
WT-MX	0.94	-1.49	3.38	0.96
NT-MX	0.51	-1.91	2.93	1.00
AZ-MX	0.58	-1.90	3.06	1.00
NM-MX	0.26	-2.14	2.66	1.00
OK-MX	0.81	-1.65	3.27	0.99

Table C4. (continued)

CO-MX	-0.02	-2.41	2.38	1.00
KS-MX	0.70	-1.71	3.11	0.99
MO-MX	0.21	-2.21	2.63	1.00
WT-ST	-0.35	-2.06	1.36	1.00
NT-ST	-0.78	-2.47	0.91	0.89
AZ-ST	-0.72	-2.49	1.05	0.95
NM-ST	-1.03	-2.69	0.62	0.58
OK-ST	-0.48	-2.22	1.25	1.00
CO-ST	-1.31	-2.96	0.34	0.24
KS-ST	-0.60	-2.26	1.07	0.98
MO-ST	-1.08	-2.77	0.60	0.54
NT-WT	-0.43	-1.76	0.89	0.99
AZ-WT	-0.37	-1.79	1.06	1.00
NM-WT	-0.68	-1.96	0.59	0.77
OK-WT	-0.13	-1.52	1.25	1.00
CO-WT	-0.96	-2.24	0.32	0.31
KS-WT	-0.24	-1.54	1.05	1.00
MO-WT	-0.73	-2.06	0.59	0.73
AZ-NT	0.06	-1.33	1.46	1.00
NM-NT	-0.25	-1.50	1.00	1.00
OK-NT	0.30	-1.06	1.66	1.00
CO-NT	-0.53	-1.78	0.72	0.93
KS-NT	0.19	-1.08	1.46	1.00
MO-NT	-0.30	-1.60	0.99	1.00
NM-AZ	-0.32	-1.67	1.04	1.00
OK-AZ	0.23	-1.22	1.69	1.00
CO-AZ	-0.59	-1.95	0.76	0.92
KS-AZ	0.12	-1.25	1.50	1.00
MO-AZ	-0.36	-1.76	1.03	1.00
OK-NM	0.55	-0.76	1.86	0.93
CO-NM	-0.28	-1.48	0.92	1.00
KS-NM	0.44	-0.78	1.66	0.98
MO-NM	-0.05	-1.30	1.20	1.00
CO-OK	-0.83	-2.14	0.48	0.57
KS-OK	-0.11	-1.45	1.22	1.00
MO-OK	-0.60	-1.96	0.76	0.91
KS-CO	0.72	-0.50	1.94	0.66

Table C4. (continued)

MO-CO	0.23	-1.02	1.48	1.00
MO-KS	-0.49	-1.76	0.78	0.96
Group B PC3				
ST-MX	0.36	-2.21	2.94	1.00
WT-MX	-0.15	-2.51	2.22	1.00
NT-MX	0.85	-1.50	3.20	0.97
AZ-MX	0.76	-1.65	3.16	0.99
NM-MX	0.44	-1.89	2.76	1.00
OK-MX	0.10	-2.29	2.48	1.00
CO-MX	0.28	-2.05	2.60	1.00
KS-MX	0.49	-1.85	2.83	1.00
MO-MX	0.31	-2.04	2.66	1.00
WT-ST	-0.51	-2.17	1.15	0.99
NT-ST	0.49	-1.15	2.13	0.99
AZ-ST	0.40	-1.32	2.11	1.00
NM-ST	0.07	-1.53	1.68	1.00
OK-ST	-0.27	-1.95	1.42	1.00
CO-ST	-0.08	-1.69	1.52	1.00
KS-ST	0.13	-1.49	1.75	1.00
MO-ST	-0.06	-1.69	1.58	1.00
NT-WT	1.00	-0.28	2.29	0.26
AZ-WT	0.91	-0.47	2.29	0.51
NM-WT	0.58	-0.65	1.82	0.87
OK-WT	0.25	-1.10	1.59	1.00
CO-WT	0.43	-0.81	1.67	0.98
KS-WT	0.64	-0.62	1.90	0.82
MO-WT	0.46	-0.83	1.74	0.98
AZ-NT	-0.10	-1.45	1.26	1.00
NM-NT	-0.42	-1.63	0.79	0.98
OK-NT	-0.76	-2.08	0.56	0.69
CO-NT	-0.57	-1.79	0.64	0.87
KS-NT	-0.36	-1.60	0.87	0.99
MO-NT	-0.55	-1.80	0.71	0.92
NM-AZ	-0.32	-1.64	0.99	1.00
OK-AZ	-0.66	-2.08	0.75	0.88
CO-AZ	-0.48	-1.79	0.83	0.97
KS-AZ	-0.27	-1.60	1.07	1.00

Table C4. (continued)

MO-AZ	-0.45	-1.81	0.90	0.99
OK-NM	-0.34	-1.61	0.93	1.00
CO-NM	-0.16	-1.32	1.01	1.00
KS-NM	0.05	-1.13	1.24	1.00
MO-NM	-0.13	-1.34	1.08	1.00
CO-OK	0.18	-1.09	1.46	1.00
KS-OK	0.39	-0.90	1.69	0.99
MO-OK	0.21	-1.11	1.53	1.00
KS-CO	0.21	-0.97	1.40	1.00
MO-CO	0.03	-1.18	1.24	1.00
MO-KS	-0.18	-1.42	1.05	1.00
Group B PC4				
ST-MX	0.29	-2.25	2.83	1.00
WT-MX	0.40	-1.94	2.73	1.00
NT-MX	-0.21	-2.52	2.11	1.00
AZ-MX	0.74	-1.63	3.11	0.99
NM-MX	0.34	-1.96	2.64	1.00
OK-MX	-0.29	-2.65	2.06	1.00
CO-MX	-0.13	-2.42	2.17	1.00
KS-MX	-0.63	-2.94	1.67	1.00
MO-MX	-0.59	-2.91	1.73	1.00
WT-ST	0.11	-1.53	1.75	1.00
NT-ST	-0.49	-2.11	1.12	0.99
AZ-ST	0.45	-1.24	2.15	1.00
NM-ST	0.05	-1.53	1.63	1.00
OK-ST	-0.58	-2.24	1.08	0.98
CO-ST	-0.41	-2.00	1.17	1.00
KS-ST	-0.92	-2.52	0.68	0.69
MO-ST	-0.88	-2.49	0.74	0.75
NT-WT	-0.60	-1.87	0.67	0.87
AZ-WT	0.35	-1.02	1.71	1.00
NM-WT	-0.06	-1.28	1.17	1.00
OK-WT	-0.69	-2.02	0.64	0.80
CO-WT	-0.52	-1.75	0.70	0.93
KS-WT	-1.03	-2.27	0.22	0.20
MO-WT	-0.99	-2.25	0.28	0.27
AZ-NT	0.95	-0.39	2.28	0.40

Table C4. (continued)

NM-NT	0.54	-0.65	1.74	0.89
OK-NT	-0.09	-1.39	1.21	1.00
CO-NT	0.08	-1.12	1.27	1.00
KS-NT	-0.43	-1.64	0.79	0.98
MO-NT	-0.38	-1.62	0.85	0.99
NM-AZ	-0.40	-1.70	0.90	0.99
OK-AZ	-1.03	-2.43	0.36	0.33
CO-AZ	-0.87	-2.16	0.43	0.48
KS-AZ	-1.37	-2.69	-0.06	0.03
MO-AZ	-1.33	-2.67	0.01	0.05
OK-NM	-0.63	-1.89	0.62	0.83
CO-NM	-0.47	-1.61	0.68	0.95
KS-NM	-0.97	-2.14	0.20	0.19
MO-NM	-0.93	-2.12	0.26	0.27
CO-OK	0.17	-1.09	1.42	1.00
KS-OK	-0.34	-1.62	0.94	1.00
MO-OK	-0.30	-1.60	1.00	1.00
KS-CO	-0.51	-1.68	0.66	0.92
MO-CO	-0.46	-1.66	0.73	0.96
MO-KS	0.04	-1.17	1.26	1.00
Group C PC1				
ST-MX	0.95	-1.70	3.60	0.98
WT-MX	1.01	-1.43	3.44	0.94
NT-MX	0.99	-1.43	3.41	0.94
AZ-MX	0.55	-1.92	3.03	1.00
NM-MX	0.88	-1.51	3.28	0.97
OK-MX	1.35	-1.10	3.80	0.74
CO-MX	0.36	-2.04	2.75	1.00
KS-MX	0.50	-1.91	2.90	1.00
MO-MX	0.52	-1.90	2.94	1.00
WT-ST	0.06	-1.65	1.77	1.00
NT-ST	0.04	-1.64	1.73	1.00
AZ-ST	-0.39	-2.16	1.37	1.00
NM-ST	-0.06	-1.71	1.59	1.00
OK-ST	0.40	-1.33	2.14	1.00
CO-ST	-0.59	-2.24	1.06	0.98
KS-ST	-0.45	-2.12	1.22	1.00

Table C4. (continued)

MO-ST	-0.42	-2.11	1.26	1.00
NT-WT	-0.02	-1.34	1.31	1.00
AZ-WT	-0.45	-1.88	0.97	0.99
NM-WT	-0.12	-1.40	1.15	1.00
OK-WT	0.34	-1.04	1.72	1.00
CO-WT	-0.65	-1.92	0.63	0.82
KS-WT	-0.51	-1.81	0.79	0.96
MO-WT	-0.48	-1.81	0.84	0.97
AZ-NT	-0.44	-1.83	0.96	0.99
NM-NT	-0.11	-1.35	1.14	1.00
OK-NT	0.36	-1.00	1.71	1.00
CO-NT	-0.63	-1.88	0.61	0.82
KS-NT	-0.49	-1.76	0.77	0.96
MO-NT	-0.47	-1.76	0.82	0.97
NM-AZ	0.33	-1.02	1.68	1.00
OK-AZ	0.79	-0.66	2.25	0.75
CO-AZ	-0.20	-1.55	1.16	1.00
KS-AZ	-0.06	-1.43	1.32	1.00
MO-AZ	-0.03	-1.43	1.37	1.00
OK-NM	0.46	-0.85	1.78	0.98
CO-NM	-0.53	-1.72	0.67	0.91
KS-NM	-0.39	-1.61	0.83	0.99
MO-NM	-0.36	-1.61	0.89	0.99
CO-OK	-0.99	-2.30	0.32	0.31
KS-OK	-0.85	-2.18	0.48	0.55
MO-OK	-0.83	-2.18	0.53	0.62
KS-CO	0.14	-1.08	1.36	1.00
MO-CO	0.16	-1.08	1.41	1.00
MO-KS	0.03	-1.24	1.29	1.00
Group C PC2				
ST-MX	0.59	-1.99	3.17	1.00
WT-MX	0.14	-2.23	2.51	1.00
NT-MX	0.52	-1.84	2.88	1.00
AZ-MX	0.78	-1.63	3.19	0.99
NM-MX	-0.14	-2.47	2.19	1.00
OK-MX	0.12	-2.27	2.51	1.00
CO-MX	0.41	-1.92	2.74	1.00

Table C4. (continued)

KS-MX	0.56	-1.78	2.90	1.00
MO-MX	1.09	-1.26	3.45	0.88
WT-ST	-0.45	-2.11	1.21	1.00
NT-ST	-0.07	-1.71	1.57	1.00
AZ-ST	0.19	-1.53	1.91	1.00
NM-ST	-0.73	-2.34	0.88	0.90
OK-ST	-0.47	-2.16	1.22	1.00
CO-ST	-0.17	-1.78	1.43	1.00
KS-ST	-0.03	-1.65	1.59	1.00
MO-ST	0.51	-1.14	2.15	0.99
NT-WT	0.38	-0.91	1.67	0.99
AZ-WT	0.64	-0.75	2.02	0.89
NM-WT	-0.28	-1.52	0.96	1.00
OK-WT	-0.02	-1.36	1.33	1.00
CO-WT	0.28	-0.97	1.52	1.00
KS-WT	0.42	-0.84	1.68	0.99
MO-WT	0.96	-0.33	2.24	0.33
AZ-NT	0.26	-1.10	1.62	1.00
NM-NT	-0.66	-1.88	0.55	0.75
OK-NT	-0.40	-1.72	0.92	0.99
CO-NT	-0.11	-1.32	1.11	1.00
KS-NT	0.04	-1.20	1.27	1.00
MO-NT	0.57	-0.68	1.83	0.89
NM-AZ	-0.92	-2.24	0.40	0.42
OK-AZ	-0.65	-2.07	0.76	0.89
CO-AZ	-0.36	-1.68	0.96	1.00
KS-AZ	-0.22	-1.55	1.12	1.00
MO-AZ	0.32	-1.04	1.68	1.00
OK-NM	0.26	-1.01	1.54	1.00
CO-NM	0.56	-0.61	1.72	0.87
KS-NM	0.70	-0.49	1.89	0.66
MO-NM	1.24	0.02	2.45	0.04
CO-OK	0.29	-0.98	1.57	1.00
KS-OK	0.44	-0.86	1.73	0.98
MO-OK	0.97	-0.35	2.29	0.34
KS-CO	0.14	-1.04	1.33	1.00
MO-CO	0.68	-0.53	1.89	0.72
MO-KS	0.54	-0.70	1.77	0.92

Table C5. Tukey's test table for lateral skull shape groups, between sexes.

	diff	lwr	upr	p adj
Group A PC1				
M-F	-0.05	-0.42	0.32	0.79
Group A PC2				
M-F	0.06	-0.31	0.43	0.74
Group B PC1				
M-F	-0.21	-0.57	0.16	0.26
Group B PC2				
M-F	-0.34	-0.73	0.05	0.09
Group B PC3				
M-F	-0.38	-0.76	-0.01	0.05
Group B PC4				
M-F	-0.31	-0.68	0.07	0.11
Group C PC1				
M-F	-0.15	-0.54	0.24	0.44
Group C PC2				
M-F	-0.23	-0.61	0.15	0.24

Table C6. Tukey's test table for lateral skull shape groups among sexes and populations.

	diff	lwr	upr	p adj
Group A PC1				
ST:F-MX:F	0.13	-4.03	4.29	1.00
WT:F-MX:F	0.53	-3.14	4.19	1.00
NT:F-MX:F	0.78	-2.85	4.41	1.00
AZ:F-MX:F	0.13	-3.59	3.85	1.00
NM:F-MX:F	1.27	-2.64	5.19	1.00
OK:F-MX:F	0.75	-3.04	4.55	1.00
CO:F-MX:F	-0.45	-4.25	3.34	1.00
KS:F-MX:F	-0.20	-3.80	3.40	1.00
MO:F-MX:F	0.57	-3.59	4.73	1.00
MX:M-MX:F	0.98	-3.82	5.78	1.00
ST:M-MX:F	0.44	-3.48	4.36	1.00
WT:M-MX:F	-0.19	-3.90	3.53	1.00
NT:M-MX:F	1.04	-2.68	4.76	1.00
AZ:M-MX:F	0.51	-3.28	4.31	1.00
NM:M-MX:F	0.43	-3.12	3.97	1.00
OK:M-MX:F	1.36	-2.31	5.02	1.00
CO:M-MX:F	-0.42	-3.97	3.14	1.00
KS:M-MX:F	-0.54	-4.26	3.17	1.00
MO:M-MX:F	0.42	-3.14	3.98	1.00
WT:F-ST:F	0.40	-2.37	3.17	1.00
NT:F-ST:F	0.65	-2.07	3.37	1.00
AZ:F-ST:F	<0.01	-2.84	2.84	1.00
NM:F-ST:F	1.15	-1.95	4.24	1.00
OK:F-ST:F	0.62	-2.32	3.56	1.00
CO:F-ST:F	-0.58	-3.52	2.36	1.00
KS:F-ST:F	-0.33	-3.01	2.35	1.00
MO:F-ST:F	0.44	-2.95	3.84	1.00
MX:M-ST:F	0.85	-3.31	5.01	1.00
ST:M-ST:F	0.31	-2.78	3.41	1.00
WT:M-ST:F	-0.31	-3.15	2.52	1.00
NT:M-ST:F	0.91	-1.93	3.75	1.00
AZ:M-ST:F	0.39	-2.55	3.32	1.00
NM:M-ST:F	0.30	-2.31	2.91	1.00

Table C6. (continued)

OK:M-ST:F	1.23	-1.54	4.00	0.98
CO:M-ST:F	-0.54	-3.17	2.08	1.00
KS:M-ST:F	-0.67	-3.51	2.17	1.00
MO:M-ST:F	0.29	-2.34	2.92	1.00
NT:F-WT:F	0.25	-1.63	2.14	1.00
AZ:F-WT:F	-0.40	-2.45	1.66	1.00
NM:F-WT:F	0.75	-1.65	3.15	1.00
OK:F-WT:F	0.22	-1.97	2.41	1.00
CO:F-WT:F	-0.98	-3.17	1.21	0.98
KS:F-WT:F	-0.73	-2.56	1.11	1.00
MO:F-WT:F	0.04	-2.73	2.82	1.00
MX:M-WT:F	0.45	-3.22	4.12	1.00
ST:M-WT:F	-0.08	-2.48	2.32	1.00
WT:M-WT:F	-0.71	-2.77	1.34	1.00
NT:M-WT:F	0.52	-1.54	2.57	1.00
AZ:M-WT:F	-0.01	-2.20	2.18	1.00
NM:M-WT:F	-0.10	-1.82	1.62	1.00
OK:M-WT:F	0.83	-1.13	2.79	0.99
CO:M-WT:F	-0.94	-2.70	0.81	0.91
KS:M-WT:F	-1.07	-3.13	0.98	0.93
MO:M-WT:F	-0.11	-1.86	1.65	1.00
AZ:F-NT:F	-0.65	-2.64	1.34	1.00
NM:F-NT:F	0.49	-1.85	2.83	1.00
OK:F-NT:F	-0.03	-2.16	2.10	1.00
CO:F-NT:F	-1.23	-3.36	0.90	0.84
KS:F-NT:F	-0.98	-2.74	0.78	0.87
MO:F-NT:F	-0.21	-2.93	2.51	1.00
MX:M-NT:F	0.20	-3.43	3.82	1.00
ST:M-NT:F	-0.34	-2.68	2.00	1.00
WT:M-NT:F	-0.97	-2.96	1.02	0.96
NT:M-NT:F	0.26	-1.73	2.25	1.00
AZ:M-NT:F	-0.27	-2.39	1.86	1.00
NM:M-NT:F	-0.36	-2.00	1.28	1.00
OK:M-NT:F	0.57	-1.31	2.46	1.00
CO:M-NT:F	-1.20	-2.87	0.48	0.50
KS:M-NT:F	-1.33	-3.31	0.66	0.63
MO:M-NT:F	-0.36	-2.03	1.31	1.00

Table C6. (continued)

NM:F-AZ:F	1.14	-1.34	3.62	0.98
OK:F-AZ:F	0.62	-1.66	2.90	1.00
CO:F-AZ:F	-0.58	-2.86	1.70	1.00
KS:F-AZ:F	-0.33	-2.27	1.60	1.00
MO:F-AZ:F	0.44	-2.40	3.28	1.00
MX:M-AZ:F	0.85	-2.87	4.56	1.00
ST:M-AZ:F	0.31	-2.17	2.79	1.00
WT:M-AZ:F	-0.32	-2.46	1.83	1.00
NT:M-AZ:F	0.91	-1.23	3.06	0.99
AZ:M-AZ:F	0.38	-1.89	2.66	1.00
NM:M-AZ:F	0.29	-1.54	2.12	1.00
OK:M-AZ:F	1.22	-0.83	3.28	0.80
CO:M-AZ:F	-0.55	-2.41	1.31	1.00
KS:M-AZ:F	-0.68	-2.82	1.47	1.00
MO:M-AZ:F	0.29	-1.57	2.15	1.00
OK:F-NM:F	-0.52	-3.12	2.07	1.00
CO:F-NM:F	-1.73	-4.32	0.87	0.63
KS:F-NM:F	-1.47	-3.77	0.82	0.70
MO:F-NM:F	-0.70	-3.80	2.40	1.00
MX:M-NM:F	-0.30	-4.22	3.62	1.00
ST:M-NM:F	-0.83	-3.60	1.94	1.00
WT:M-NM:F	-1.46	-3.94	1.02	0.82
NT:M-NM:F	-0.23	-2.71	2.25	1.00
AZ:M-NM:F	-0.76	-3.35	1.83	1.00
NM:M-NM:F	-0.85	-3.06	1.36	1.00
OK:M-NM:F	0.08	-2.32	2.48	1.00
CO:M-NM:F	-1.69	-3.92	0.54	0.39
KS:M-NM:F	-1.82	-4.30	0.66	0.45
MO:M-NM:F	-0.85	-3.09	1.38	1.00
CO:F-OK:F	-1.20	-3.60	1.20	0.95
KS:F-OK:F	-0.95	-3.03	1.13	0.98
MO:F-OK:F	-0.18	-3.12	2.76	1.00
MX:M-OK:F	0.23	-3.57	4.02	1.00
ST:M-OK:F	-0.31	-2.90	2.28	1.00
WT:M-OK:F	-0.94	-3.21	1.34	0.99
NT:M-OK:F	0.29	-1.99	2.57	1.00
AZ:M-OK:F	-0.24	-2.64	2.16	1.00

Table C6. (continued)

NM:M-OK:F	-0.33	-2.31	1.66	1.00
OK:M-OK:F	0.60	-1.59	2.80	1.00
CO:M-OK:F	-1.17	-3.17	0.84	0.83
KS:M-OK:F	-1.30	-3.57	0.98	0.85
MO:M-OK:F	-0.33	-2.34	1.68	1.00
KS:F-CO:F	0.25	-1.83	2.33	1.00
MO:F-CO:F	1.02	-1.92	3.96	1.00
MX:M-CO:F	1.43	-2.37	5.22	1.00
ST:M-CO:F	0.89	-1.70	3.49	1.00
WT:M-CO:F	0.26	-2.01	2.54	1.00
NT:M-CO:F	1.49	-0.78	3.77	0.66
AZ:M-CO:F	0.96	-1.44	3.36	0.99
NM:M-CO:F	0.88	-1.11	2.86	0.98
OK:M-CO:F	1.81	-0.38	4.00	0.25
CO:M-CO:F	0.04	-1.97	2.04	1.00
KS:M-CO:F	-0.09	-2.37	2.18	1.00
MO:M-CO:F	0.87	-1.14	2.88	0.99
MO:F-KS:F	0.77	-1.91	3.45	1.00
MX:M-KS:F	1.18	-2.42	4.78	1.00
ST:M-KS:F	0.64	-1.65	2.94	1.00
WT:M-KS:F	0.01	-1.92	1.95	1.00
NT:M-KS:F	1.24	-0.69	3.18	0.69
AZ:M-KS:F	0.71	-1.36	2.79	1.00
NM:M-KS:F	0.62	-0.95	2.20	1.00
OK:M-KS:F	1.56	-0.28	3.39	0.20
CO:M-KS:F	-0.22	-1.83	1.39	1.00
KS:M-KS:F	-0.35	-2.28	1.59	1.00
MO:M-KS:F	0.62	-0.99	2.23	1.00
MX:M-MO:F	0.41	-3.75	4.56	1.00
ST:M-MO:F	-0.13	-3.23	2.97	1.00
WT:M-MO:F	-0.76	-3.60	2.08	1.00
NT:M-MO:F	0.47	-2.37	3.31	1.00
AZ:M-MO:F	-0.06	-3.00	2.88	1.00
NM:M-MO:F	-0.15	-2.76	2.46	1.00
OK:M-MO:F	0.78	-1.99	3.56	1.00
CO:M-MO:F	-0.99	-3.62	1.64	1.00
KS:M-MO:F	-1.12	-3.96	1.72	1.00

Table C6. (continued)

MO:M-MO:F	-0.15	-2.78	2.48	1.00
ST:M-MX:M	-0.53	-4.45	3.39	1.00
WT:M-MX:M	-1.16	-4.88	2.55	1.00
NT:M-MX:M	0.07	-3.65	3.78	1.00
AZ:M-MX:M	-0.46	-4.26	3.33	1.00
NM:M-MX:M	-0.55	-4.10	2.99	1.00
OK:M-MX:M	0.38	-3.29	4.04	1.00
CO:M-MX:M	-1.39	-4.95	2.17	1.00
KS:M-MX:M	-1.52	-5.24	2.20	0.99
MO:M-MX:M	-0.56	-4.12	3.00	1.00
WT:M-ST:M	-0.63	-3.11	1.85	1.00
NT:M-ST:M	0.60	-1.88	3.08	1.00
AZ:M-ST:M	0.07	-2.52	2.66	1.00
NM:M-ST:M	-0.02	-2.23	2.19	1.00
OK:M-ST:M	0.91	-1.49	3.31	1.00
CO:M-ST:M	-0.86	-3.09	1.38	1.00
KS:M-ST:M	-0.99	-3.47	1.49	1.00
MO:M-ST:M	-0.02	-2.26	2.21	1.00
NT:M-WT:M	1.23	-0.92	3.38	0.85
AZ:M-WT:M	0.70	-1.58	2.98	1.00
NM:M-WT:M	0.61	-1.22	2.44	1.00
OK:M-WT:M	1.54	-0.51	3.60	0.41
CO:M-WT:M	-0.23	-2.09	1.63	1.00
KS:M-WT:M	-0.36	-2.51	1.79	1.00
MO:M-WT:M	0.61	-1.25	2.47	1.00
AZ:M-NT:M	-0.53	-2.81	1.75	1.00
NM:M-NT:M	-0.62	-2.45	1.21	1.00
OK:M-NT:M	0.31	-1.74	2.37	1.00
CO:M-NT:M	-1.46	-3.32	0.40	0.33
KS:M-NT:M	-1.59	-3.73	0.56	0.44
MO:M-NT:M	-0.62	-2.48	1.24	1.00
NM:M-AZ:M	-0.09	-2.07	1.89	1.00
OK:M-AZ:M	0.84	-1.35	3.03	1.00
CO:M-AZ:M	-0.93	-2.94	1.08	0.98
KS:M-AZ:M	-1.06	-3.34	1.22	0.97
MO:M-AZ:M	-0.09	-2.10	1.91	1.00
OK:M-NM:M	0.93	-0.79	2.65	0.90

Table C6. (continued)

CO:M-NM:M	-0.84	-2.32	0.64	0.86
KS:M-NM:M	-0.97	-2.80	0.86	0.92
MO:M-NM:M	<0.01	-1.49	1.48	1.00
CO:M-OK:M	-1.77	-3.52	-0.02	0.04
KS:M-OK:M	-1.90	-3.96	0.15	0.11
MO:M-OK:M	-0.93	-2.69	0.82	0.91
KS:M-CO:M	-0.13	-1.99	1.73	1.00
MO:M-CO:M	0.84	-0.68	2.35	0.89
MO:M-KS:M	0.97	-0.89	2.82	0.93
Group A PC2				
ST:F-MX:F	0.75	-3.40	4.90	1.00
WT:F-MX:F	-0.25	-3.91	3.40	1.00
NT:F-MX:F	0.37	-3.25	3.99	1.00
AZ:F-MX:F	-0.25	-3.96	3.45	1.00
NM:F-MX:F	-2.13	-6.04	1.78	0.90
OK:F-MX:F	-0.28	-4.07	3.50	1.00
CO:F-MX:F	-0.51	-4.29	3.28	1.00
KS:F-MX:F	0.16	-3.43	3.75	1.00
MO:F-MX:F	-0.18	-4.32	3.97	1.00
MX:M-MX:F	0.07	-4.72	4.86	1.00
ST:M-MX:F	0.66	-3.25	4.57	1.00
WT:M-MX:F	-0.44	-4.15	3.26	1.00
NT:M-MX:F	-0.47	-4.18	3.24	1.00
AZ:M-MX:F	-0.63	-4.42	3.15	1.00
NM:M-MX:F	-0.97	-4.51	2.57	1.00
OK:M-MX:F	0.59	-3.07	4.24	1.00
CO:M-MX:F	-0.11	-3.67	3.44	1.00
KS:M-MX:F	-0.02	-3.73	3.68	1.00
MO:M-MX:F	-0.16	-3.71	3.39	1.00
WT:F-ST:F	-1.00	-3.77	1.76	1.00
NT:F-ST:F	-0.38	-3.09	2.33	1.00
AZ:F-ST:F	-1.00	-3.84	1.83	1.00
NM:F-ST:F	-2.88	-5.97	0.21	0.10
OK:F-ST:F	-1.03	-3.97	1.90	1.00
CO:F-ST:F	-1.26	-4.19	1.67	0.99
KS:F-ST:F	-0.59	-3.27	2.09	1.00
MO:F-ST:F	-0.93	-4.31	2.46	1.00

Table C6. (continued)

MX:M-ST:F	-0.68	-4.83	3.47	1.00
ST:M-ST:F	-0.09	-3.18	3.00	1.00
WT:M-ST:F	-1.19	-4.03	1.64	0.99
NT:M-ST:F	-1.22	-4.05	1.62	0.99
AZ:M-ST:F	-1.38	-4.32	1.55	0.97
NM:M-ST:F	-1.72	-4.32	0.88	0.65
OK:M-ST:F	-0.16	-2.93	2.60	1.00
CO:M-ST:F	-0.86	-3.49	1.76	1.00
KS:M-ST:F	-0.77	-3.61	2.06	1.00
MO:M-ST:F	-0.91	-3.53	1.72	1.00
NT:F-WT:F	0.62	-1.26	2.51	1.00
AZ:F-WT:F	<0.01	-2.05	2.05	1.00
NM:F-WT:F	-1.87	-4.27	0.52	0.33
OK:F-WT:F	-0.03	-2.21	2.16	1.00
CO:F-WT:F	-0.25	-2.44	1.93	1.00
KS:F-WT:F	0.41	-1.41	2.24	1.00
MO:F-WT:F	0.08	-2.69	2.84	1.00
MX:M-WT:F	0.32	-3.33	3.98	1.00
ST:M-WT:F	0.92	-1.48	3.31	1.00
WT:M-WT:F	-0.19	-2.24	1.86	1.00
NT:M-WT:F	-0.21	-2.26	1.84	1.00
AZ:M-WT:F	-0.38	-2.56	1.81	1.00
NM:M-WT:F	-0.72	-2.43	1.00	0.99
OK:M-WT:F	0.84	-1.11	2.80	0.99
CO:M-WT:F	0.14	-1.61	1.89	1.00
KS:M-WT:F	0.23	-1.82	2.28	1.00
MO:M-WT:F	0.10	-1.65	1.85	1.00
AZ:F-NT:F	-0.62	-2.61	1.36	1.00
NM:F-NT:F	-2.50	-4.84	-0.16	0.02
OK:F-NT:F	-0.65	-2.78	1.47	1.00
CO:F-NT:F	-0.88	-3.00	1.24	0.99
KS:F-NT:F	-0.21	-1.96	1.54	1.00
MO:F-NT:F	-0.55	-3.26	2.17	1.00
MX:M-NT:F	-0.30	-3.92	3.32	1.00
ST:M-NT:F	0.29	-2.04	2.63	1.00
WT:M-NT:F	-0.81	-2.80	1.17	0.99
NT:M-NT:F	-0.84	-2.82	1.15	0.99

Table C6. (continued)

AZ:M-NT:F	-1.00	-3.13	1.12	0.97
NM:M-NT:F	-1.34	-2.98	0.30	0.26
OK:M-NT:F	0.22	-1.67	2.10	1.00
CO:M-NT:F	-0.48	-2.15	1.18	1.00
KS:M-NT:F	-0.39	-2.38	1.59	1.00
MO:M-NT:F	-0.53	-2.20	1.14	1.00
NM:F-AZ:F	-1.87	-4.35	0.60	0.39
OK:F-AZ:F	-0.03	-2.30	2.24	1.00
CO:F-AZ:F	-0.25	-2.53	2.02	1.00
KS:F-AZ:F	0.41	-1.52	2.34	1.00
MO:F-AZ:F	0.08	-2.76	2.91	1.00
MX:M-AZ:F	0.32	-3.39	4.03	1.00
ST:M-AZ:F	0.92	-1.56	3.39	1.00
WT:M-AZ:F	-0.19	-2.33	1.95	1.00
NT:M-AZ:F	-0.21	-2.35	1.93	1.00
AZ:M-AZ:F	-0.38	-2.65	1.89	1.00
NM:M-AZ:F	-0.72	-2.54	1.11	1.00
OK:M-AZ:F	0.84	-1.21	2.89	0.99
CO:M-AZ:F	0.14	-1.71	1.99	1.00
KS:M-AZ:F	0.23	-1.91	2.37	1.00
MO:M-AZ:F	0.10	-1.76	1.95	1.00
OK:F-NM:F	1.84	-0.74	4.43	0.50
CO:F-NM:F	1.62	-0.97	4.21	0.73
KS:F-NM:F	2.29	<0.01	4.58	0.05
MO:F-NM:F	1.95	-1.14	5.04	0.72
MX:M-NM:F	2.20	-1.71	6.11	0.87
ST:M-NM:F	2.79	0.03	5.56	0.05
WT:M-NM:F	1.68	-0.79	4.16	0.59
NT:M-NM:F	1.66	-0.81	4.13	0.62
AZ:M-NM:F	1.50	-1.09	4.08	0.84
NM:M-NM:F	1.16	-1.05	3.36	0.92
OK:M-NM:F	2.72	0.32	5.11	0.01
CO:M-NM:F	2.01	-0.21	4.24	0.13
KS:M-NM:F	2.10	-0.37	4.58	0.20
MO:M-NM:F	1.97	-0.26	4.20	0.15
CO:F-OK:F	-0.23	-2.62	2.17	1.00
KS:F-OK:F	0.44	-1.63	2.52	1.00

Table C6. (continued)

MO:F-OK:F	0.11	-2.83	3.04	1.00
MX:M-OK:F	0.35	-3.43	4.14	1.00
ST:M-OK:F	0.95	-1.64	3.53	1.00
WT:M-OK:F	-0.16	-2.43	2.11	1.00
NT:M-OK:F	-0.18	-2.45	2.09	1.00
AZ:M-OK:F	-0.35	-2.74	2.05	1.00
NM:M-OK:F	-0.69	-2.66	1.29	1.00
OK:M-OK:F	0.87	-1.32	3.06	1.00
CO:M-OK:F	0.17	-1.83	2.17	1.00
KS:M-OK:F	0.26	-2.01	2.53	1.00
MO:M-OK:F	0.13	-1.88	2.13	1.00
KS:F-CO:F	0.67	-1.40	2.74	1.00
MO:F-CO:F	0.33	-2.60	3.26	1.00
MX:M-CO:F	0.58	-3.21	4.36	1.00
ST:M-CO:F	1.17	-1.41	3.76	0.98
WT:M-CO:F	0.06	-2.21	2.34	1.00
NT:M-CO:F	0.04	-2.23	2.31	1.00
AZ:M-CO:F	-0.12	-2.52	2.27	1.00
NM:M-CO:F	-0.46	-2.44	1.52	1.00
OK:M-CO:F	1.10	-1.09	3.28	0.95
CO:M-CO:F	0.40	-1.61	2.40	1.00
KS:M-CO:F	0.49	-1.79	2.76	1.00
MO:M-CO:F	0.35	-1.65	2.36	1.00
MO:F-KS:F	-0.34	-3.01	2.34	1.00
MX:M-KS:F	-0.09	-3.68	3.50	1.00
ST:M-KS:F	0.50	-1.79	2.80	1.00
WT:M-KS:F	-0.60	-2.53	1.33	1.00
NT:M-KS:F	-0.63	-2.56	1.30	1.00
AZ:M-KS:F	-0.79	-2.87	1.28	1.00
NM:M-KS:F	-1.13	-2.70	0.44	0.49
OK:M-KS:F	0.43	-1.40	2.26	1.00
CO:M-KS:F	-0.27	-1.88	1.33	1.00
KS:M-KS:F	-0.18	-2.11	1.75	1.00
MO:M-KS:F	-0.32	-1.92	1.29	1.00
MX:M-MO:F	0.25	-3.90	4.39	1.00
ST:M-MO:F	0.84	-2.25	3.93	1.00
WT:M-MO:F	-0.27	-3.10	2.57	1.00

Table C6. (continued)

NT:M-MO:F	-0.29	-3.12	2.54	1.00
AZ:M-MO:F	-0.46	-3.39	2.48	1.00
NM:M-MO:F	-0.79	-3.40	1.81	1.00
OK:M-MO:F	0.76	-2.00	3.53	1.00
CO:M-MO:F	0.06	-2.56	2.69	1.00
KS:M-MO:F	0.15	-2.68	2.99	1.00
MO:M-MO:F	0.02	-2.60	2.64	1.00
ST:M-MX:M	0.59	-3.32	4.50	1.00
WT:M-MX:M	-0.51	-4.22	3.20	1.00
NT:M-MX:M	-0.54	-4.25	3.17	1.00
AZ:M-MX:M	-0.70	-4.49	3.08	1.00
NM:M-MX:M	-1.04	-4.58	2.50	1.00
OK:M-MX:M	0.52	-3.14	4.17	1.00
CO:M-MX:M	-0.18	-3.73	3.37	1.00
KS:M-MX:M	-0.09	-3.80	3.62	1.00
MO:M-MX:M	-0.23	-3.78	3.33	1.00
WT:M-ST:M	-1.11	-3.58	1.37	0.98
NT:M-ST:M	-1.13	-3.60	1.34	0.98
AZ:M-ST:M	-1.30	-3.88	1.29	0.95
NM:M-ST:M	-1.63	-3.84	0.57	0.43
OK:M-ST:M	-0.08	-2.47	2.32	1.00
CO:M-ST:M	-0.78	-3.01	1.45	1.00
KS:M-ST:M	-0.69	-3.16	1.79	1.00
MO:M-ST:M	-0.82	-3.05	1.41	1.00
NT:M-WT:M	-0.02	-2.16	2.12	1.00
AZ:M-WT:M	-0.19	-2.46	2.08	1.00
NM:M-WT:M	-0.53	-2.35	1.30	1.00
OK:M-WT:M	1.03	-1.02	3.08	0.95
CO:M-WT:M	0.33	-1.52	2.19	1.00
KS:M-WT:M	0.42	-1.72	2.56	1.00
MO:M-WT:M	0.29	-1.57	2.14	1.00
AZ:M-NT:M	-0.17	-2.44	2.11	1.00
NM:M-NT:M	-0.50	-2.33	1.32	1.00
OK:M-NT:M	1.05	-1.00	3.10	0.93
CO:M-NT:M	0.35	-1.50	2.21	1.00
KS:M-NT:M	0.44	-1.70	2.58	1.00
MO:M-NT:M	0.31	-1.54	2.16	1.00

Table C6. (continued)

NM:M-AZ:M	-0.34	-2.31	1.64	1.00
OK:M-AZ:M	1.22	-0.97	3.40	0.87
CO:M-AZ:M	0.52	-1.48	2.52	1.00
KS:M-AZ:M	0.61	-1.66	2.88	1.00
MO:M-AZ:M	0.48	-1.53	2.48	1.00
OK:M-NM:M	1.56	-0.16	3.27	0.13
CO:M-NM:M	0.86	-0.62	2.34	0.84
KS:M-NM:M	0.95	-0.88	2.77	0.93
MO:M-NM:M	0.81	-0.67	2.29	0.89
CO:M-OK:M	-0.70	-2.45	1.05	0.99
KS:M-OK:M	-0.61	-2.66	1.44	1.00
MO:M-OK:M	-0.74	-2.49	1.01	0.99
KS:M-CO:M	0.09	-1.76	1.94	1.00
MO:M-CO:M	-0.04	-1.56	1.47	1.00
MO:M-KS:M	-0.13	-1.99	1.72	1.00
Group B PC1				
ST:F-MX:F	-0.11	-4.17	3.96	1.00
WT:F-MX:F	0.26	-3.33	3.85	1.00
NT:F-MX:F	0.84	-2.71	4.39	1.00
AZ:F-MX:F	0.59	-3.05	4.23	1.00
NM:F-MX:F	0.43	-3.40	4.27	1.00
OK:F-MX:F	0.06	-3.66	3.77	1.00
CO:F-MX:F	-0.06	-3.77	3.66	1.00
KS:F-MX:F	0.59	-2.94	4.11	1.00
MO:F-MX:F	0.94	-3.13	5.01	1.00
MX:M-MX:F	-0.48	-5.18	4.21	1.00
ST:M-MX:F	-0.74	-4.57	3.10	1.00
WT:M-MX:F	-0.57	-4.21	3.06	1.00
NT:M-MX:F	0.79	-2.85	4.43	1.00
AZ:M-MX:F	0.26	-3.45	3.98	1.00
NM:M-MX:F	-0.13	-3.60	3.34	1.00
OK:M-MX:F	0.29	-3.30	3.88	1.00
CO:M-MX:F	-0.62	-4.10	2.86	1.00
KS:M-MX:F	0.95	-2.69	4.59	1.00
MO:M-MX:F	1.14	-2.35	4.62	1.00
WT:F-ST:F	0.37	-2.35	3.08	1.00
NT:F-ST:F	0.95	-1.71	3.61	1.00

Table C6. (continued)

AZ:F-ST:F	0.69	-2.08	3.47	1.00
NM:F-ST:F	0.54	-2.49	3.57	1.00
OK:F-ST:F	0.16	-2.71	3.04	1.00
CO:F-ST:F	0.05	-2.83	2.93	1.00
KS:F-ST:F	0.69	-1.93	3.32	1.00
MO:F-ST:F	1.05	-2.28	4.37	1.00
MX:M-ST:F	-0.38	-4.44	3.69	1.00
ST:M-ST:F	-0.63	-3.66	2.40	1.00
WT:M-ST:F	-0.47	-3.25	2.31	1.00
NT:M-ST:F	0.90	-1.88	3.67	1.00
AZ:M-ST:F	0.37	-2.51	3.25	1.00
NM:M-ST:F	-0.03	-2.58	2.53	1.00
OK:M-ST:F	0.40	-2.31	3.11	1.00
CO:M-ST:F	-0.51	-3.09	2.06	1.00
KS:M-ST:F	1.05	-1.72	3.83	1.00
MO:M-ST:F	1.24	-1.33	3.82	0.96
NT:F-WT:F	0.58	-1.27	2.43	1.00
AZ:F-WT:F	0.33	-1.68	2.34	1.00
NM:F-WT:F	0.17	-2.18	2.52	1.00
OK:F-WT:F	-0.20	-2.35	1.94	1.00
CO:F-WT:F	-0.32	-2.46	1.83	1.00
KS:F-WT:F	0.33	-1.47	2.12	1.00
MO:F-WT:F	0.68	-2.03	3.39	1.00
MX:M-WT:F	-0.74	-4.33	2.84	1.00
ST:M-WT:F	-1.00	-3.35	1.35	0.99
WT:M-WT:F	-0.83	-2.84	1.18	0.99
NT:M-WT:F	0.53	-1.48	2.54	1.00
AZ:M-WT:F	<0.01	-2.14	2.15	1.00
NM:M-WT:F	-0.39	-2.08	1.29	1.00
OK:M-WT:F	0.03	-1.89	1.95	1.00
CO:M-WT:F	-0.88	-2.59	0.84	0.94
KS:M-WT:F	0.69	-1.32	2.70	1.00
MO:M-WT:F	0.88	-0.84	2.59	0.94
AZ:F-NT:F	-0.25	-2.20	1.69	1.00
NM:F-NT:F	-0.41	-2.70	1.88	1.00
OK:F-NT:F	-0.79	-2.87	1.30	1.00
CO:F-NT:F	-0.90	-2.98	1.18	0.99

Table C6. (continued)

KS:F-NT:F	-0.26	-1.97	1.46	1.00
MO:F-NT:F	0.10	-2.57	2.76	1.00
MX:M-NT:F	-1.33	-4.88	2.22	1.00
ST:M-NT:F	-1.58	-3.87	0.71	0.57
WT:M-NT:F	-1.42	-3.36	0.53	0.47
NT:M-NT:F	-0.05	-2.00	1.89	1.00
AZ:M-NT:F	-0.58	-2.66	1.50	1.00
NM:M-NT:F	-0.97	-2.58	0.63	0.78
OK:M-NT:F	-0.55	-2.40	1.30	1.00
CO:M-NT:F	-1.46	-3.10	0.17	0.14
KS:M-NT:F	0.11	-1.84	2.05	1.00
MO:M-NT:F	0.29	-1.34	1.93	1.00
NM:F-AZ:F	-0.16	-2.58	2.27	1.00
OK:F-AZ:F	-0.53	-2.76	1.70	1.00
CO:F-AZ:F	-0.64	-2.87	1.58	1.00
KS:F-AZ:F	<0.01	-1.89	1.89	1.00
MO:F-AZ:F	0.35	-2.43	3.13	1.00
MX:M-AZ:F	-1.07	-4.71	2.57	1.00
ST:M-AZ:F	-1.33	-3.75	1.10	0.89
WT:M-AZ:F	-1.16	-3.26	0.94	0.88
NT:M-AZ:F	0.20	-1.90	2.30	1.00
AZ:M-AZ:F	-0.33	-2.55	1.90	1.00
NM:M-AZ:F	-0.72	-2.51	1.07	0.99
OK:M-AZ:F	-0.30	-2.31	1.71	1.00
CO:M-AZ:F	-1.21	-3.03	0.61	0.64
KS:M-AZ:F	0.36	-1.74	2.46	1.00
MO:M-AZ:F	0.55	-1.27	2.37	1.00
OK:F-NM:F	-0.38	-2.91	2.16	1.00
CO:F-NM:F	-0.49	-3.03	2.05	1.00
KS:F-NM:F	0.15	-2.09	2.40	1.00
MO:F-NM:F	0.51	-2.53	3.54	1.00
MX:M-NM:F	-0.92	-4.75	2.92	1.00
ST:M-NM:F	-1.17	-3.88	1.54	0.99
WT:M-NM:F	-1.01	-3.43	1.42	0.99
NT:M-NM:F	0.36	-2.07	2.78	1.00
AZ:M-NM:F	-0.17	-2.71	2.37	1.00
NM:M-NM:F	-0.56	-2.73	1.60	1.00

Table C6. (continued)

OK:M-NM:F	-0.14	-2.49	2.21	1.00
CO:M-NM:F	-1.05	-3.24	1.13	0.96
KS:M-NM:F	0.51	-1.91	2.94	1.00
MO:M-NM:F	0.70	-1.48	2.89	1.00
CO:F-OK:F	-0.11	-2.46	2.24	1.00
KS:F-OK:F	0.53	-1.50	2.56	1.00
MO:F-OK:F	0.88	-1.99	3.76	1.00
MX:M-OK:F	-0.54	-4.25	3.17	1.00
ST:M-OK:F	-0.80	-3.33	1.74	1.00
WT:M-OK:F	-0.63	-2.86	1.60	1.00
NT:M-OK:F	0.73	-1.50	2.96	1.00
AZ:M-OK:F	0.21	-2.14	2.55	1.00
NM:M-OK:F	-0.19	-2.13	1.75	1.00
OK:M-OK:F	0.24	-1.91	2.38	1.00
CO:M-OK:F	-0.68	-2.64	1.29	1.00
KS:M-OK:F	0.89	-1.34	3.12	0.99
MO:M-OK:F	1.08	-0.88	3.05	0.89
KS:F-CO:F	0.64	-1.39	2.68	1.00
MO:F-CO:F	0.99	-1.88	3.87	1.00
MX:M-CO:F	-0.43	-4.14	3.29	1.00
ST:M-CO:F	-0.68	-3.22	1.85	1.00
WT:M-CO:F	-0.52	-2.75	1.71	1.00
NT:M-CO:F	0.85	-1.38	3.07	1.00
AZ:M-CO:F	0.32	-2.03	2.67	1.00
NM:M-CO:F	-0.08	-2.01	1.86	1.00
OK:M-CO:F	0.35	-1.80	2.49	1.00
CO:M-CO:F	-0.56	-2.53	1.40	1.00
KS:M-CO:F	1.00	-1.22	3.23	0.98
MO:M-CO:F	1.19	-0.77	3.16	0.78
MO:F-KS:F	0.35	-2.27	2.98	1.00
MX:M-KS:F	-1.07	-4.59	2.45	1.00
ST:M-KS:F	-1.33	-3.57	0.92	0.82
WT:M-KS:F	-1.16	-3.05	0.73	0.76
NT:M-KS:F	0.20	-1.69	2.10	1.00
AZ:M-KS:F	-0.32	-2.36	1.71	1.00
NM:M-KS:F	-0.72	-2.26	0.82	0.97
OK:M-KS:F	-0.30	-2.09	1.50	1.00

Table C6. (continued)

CO:M-KS:F	-1.21	-2.78	0.37	0.37
KS:M-KS:F	0.36	-1.53	2.25	1.00
MO:M-KS:F	0.55	-1.03	2.13	1.00
MX:M-MO:F	-1.42	-5.49	2.65	1.00
ST:M-MO:F	-1.68	-4.71	1.35	0.88
WT:M-MO:F	-1.51	-4.29	1.27	0.90
NT:M-MO:F	-0.15	-2.93	2.63	1.00
AZ:M-MO:F	-0.68	-3.55	2.20	1.00
NM:M-MO:F	-1.07	-3.62	1.48	0.99
OK:M-MO:F	-0.65	-3.36	2.06	1.00
CO:M-MO:F	-1.56	-4.13	1.01	0.78
KS:M-MO:F	0.01	-2.77	2.79	1.00
MO:M-MO:F	0.20	-2.37	2.77	1.00
ST:M-MX:M	-0.26	-4.09	3.58	1.00
WT:M-MX:M	-0.09	-3.73	3.55	1.00
NT:M-MX:M	1.27	-2.37	4.91	1.00
AZ:M-MX:M	0.75	-2.97	4.46	1.00
NM:M-MX:M	0.35	-3.12	3.82	1.00
OK:M-MX:M	0.77	-2.81	4.36	1.00
CO:M-MX:M	-0.14	-3.62	3.35	1.00
KS:M-MX:M	1.43	-2.21	5.07	1.00
MO:M-MX:M	1.62	-1.86	5.10	0.97
WT:M-ST:M	0.17	-2.26	2.59	1.00
NT:M-ST:M	1.53	-0.90	3.95	0.72
AZ:M-ST:M	1.00	-1.54	3.54	1.00
NM:M-ST:M	0.61	-1.56	2.77	1.00
OK:M-ST:M	1.03	-1.32	3.38	0.99
CO:M-ST:M	0.12	-2.07	2.31	1.00
KS:M-ST:M	1.69	-0.74	4.11	0.55
MO:M-ST:M	1.88	-0.31	4.06	0.19
NT:M-WT:M	1.36	-0.74	3.46	0.68
AZ:M-WT:M	0.84	-1.39	3.06	1.00
NM:M-WT:M	0.44	-1.35	2.23	1.00
OK:M-WT:M	0.86	-1.15	2.88	0.99
CO:M-WT:M	-0.05	-1.87	1.77	1.00
KS:M-WT:M	1.52	-0.58	3.62	0.48
MO:M-WT:M	1.71	-0.11	3.53	0.09

Table C6. (continued)

AZ:M-NT:M	-0.53	-2.75	1.70	1.00
NM:M-NT:M	-0.92	-2.71	0.87	0.93
OK:M-NT:M	-0.50	-2.51	1.51	1.00
CO:M-NT:M	-1.41	-3.23	0.41	0.35
KS:M-NT:M	0.16	-1.94	2.26	1.00
MO:M-NT:M	0.35	-1.47	2.17	1.00
NM:M-AZ:M	-0.39	-2.33	1.54	1.00
OK:M-AZ:M	0.03	-2.12	2.17	1.00
CO:M-AZ:M	-0.88	-2.85	1.08	0.98
KS:M-AZ:M	0.68	-1.54	2.91	1.00
MO:M-AZ:M	0.87	-1.09	2.84	0.98
OK:M-NM:M	0.42	-1.26	2.11	1.00
CO:M-NM:M	-0.49	-1.94	0.96	1.00
KS:M-NM:M	1.08	-0.71	2.87	0.79
MO:M-NM:M	1.27	-0.18	2.72	0.17
CO:M-OK:M	-0.91	-2.63	0.80	0.91
KS:M-OK:M	0.66	-1.36	2.67	1.00
MO:M-OK:M	0.85	-0.87	2.56	0.95
KS:M-CO:M	1.57	-0.25	3.39	0.18
MO:M-CO:M	1.76	0.27	3.24	0.01
MO:M-KS:M	0.19	-1.63	2.01	1.00
Group B PC2				
ST:F-MX:F	1.99	-2.39	6.36	0.98
WT:F-MX:F	1.66	-2.20	5.52	0.99
NT:F-MX:F	1.25	-2.56	5.07	1.00
AZ:F-MX:F	1.77	-2.15	5.68	0.98
NM:F-MX:F	1.00	-3.13	5.12	1.00
OK:F-MX:F	2.00	-1.99	6.00	0.95
CO:F-MX:F	0.72	-3.27	4.71	1.00
KS:F-MX:F	1.41	-2.37	5.20	1.00
MO:F-MX:F	0.11	-4.26	4.49	1.00
MX:M-MX:F	1.14	-3.91	6.19	1.00
ST:M-MX:F	1.78	-2.34	5.91	0.99
WT:M-MX:F	1.34	-2.57	5.25	1.00
NT:M-MX:F	0.84	-3.07	4.76	1.00
AZ:M-MX:F	0.37	-3.62	4.36	1.00
NM:M-MX:F	0.79	-2.94	4.52	1.00

Table C6. (continued)

OK:M-MX:F	0.97	-2.89	4.82	1.00
CO:M-MX:F	0.49	-3.26	4.23	1.00
KS:M-MX:F	1.04	-2.87	4.95	1.00
MO:M-MX:F	0.92	-2.83	4.66	1.00
WT:F-ST:F	-0.33	-3.24	2.59	1.00
NT:F-ST:F	-0.73	-3.60	2.13	1.00
AZ:F-ST:F	-0.22	-3.21	2.77	1.00
NM:F-ST:F	-0.99	-4.25	2.27	1.00
OK:F-ST:F	0.02	-3.08	3.11	1.00
CO:F-ST:F	-1.27	-4.36	1.82	0.99
KS:F-ST:F	-0.57	-3.40	2.25	1.00
MO:F-ST:F	-1.87	-5.44	1.70	0.92
MX:M-ST:F	-0.85	-5.22	3.53	1.00
ST:M-ST:F	-0.20	-3.46	3.06	1.00
WT:M-ST:F	-0.65	-3.64	2.34	1.00
NT:M-ST:F	-1.14	-4.13	1.84	1.00
AZ:M-ST:F	-1.61	-4.71	1.48	0.93
NM:M-ST:F	-1.20	-3.95	1.54	0.99
OK:M-ST:F	-1.02	-3.94	1.90	1.00
CO:M-ST:F	-1.50	-4.27	1.27	0.90
KS:M-ST:F	-0.95	-3.94	2.04	1.00
MO:M-ST:F	-1.07	-3.84	1.69	1.00
NT:F-WT:F	-0.41	-2.39	1.58	1.00
AZ:F-WT:F	0.10	-2.06	2.27	1.00
NM:F-WT:F	-0.67	-3.19	1.86	1.00
OK:F-WT:F	0.34	-1.96	2.65	1.00
CO:F-WT:F	-0.94	-3.25	1.36	0.99
KS:F-WT:F	-0.25	-2.18	1.68	1.00
MO:F-WT:F	-1.55	-4.46	1.37	0.91
MX:M-WT:F	-0.52	-4.38	3.34	1.00
ST:M-WT:F	0.12	-2.40	2.65	1.00
WT:M-WT:F	-0.32	-2.49	1.84	1.00
NT:M-WT:F	-0.82	-2.98	1.34	1.00
AZ:M-WT:F	-1.29	-3.59	1.02	0.87
NM:M-WT:F	-0.88	-2.69	0.94	0.96
OK:M-WT:F	-0.69	-2.76	1.37	1.00
CO:M-WT:F	-1.17	-3.02	0.67	0.71

Table C6. (continued)

KS:M-WT:F	-0.62	-2.78	1.54	1.00
MO:M-WT:F	-0.75	-2.59	1.10	0.99
AZ:F-NT:F	0.51	-1.58	2.60	1.00
NM:F-NT:F	-0.26	-2.72	2.21	1.00
OK:F-NT:F	0.75	-1.49	2.99	1.00
CO:F-NT:F	-0.54	-2.77	1.70	1.00
KS:F-NT:F	0.16	-1.69	2.01	1.00
MO:F-NT:F	-1.14	-4.00	1.72	1.00
MX:M-NT:F	-0.11	-3.93	3.71	1.00
ST:M-NT:F	0.53	-1.93	2.99	1.00
WT:M-NT:F	0.08	-2.01	2.18	1.00
NT:M-NT:F	-0.41	-2.50	1.68	1.00
AZ:M-NT:F	-0.88	-3.12	1.36	1.00
NM:M-NT:F	-0.47	-2.19	1.26	1.00
OK:M-NT:F	-0.29	-2.27	1.70	1.00
CO:M-NT:F	-0.77	-2.53	0.99	0.99
KS:M-NT:F	-0.21	-2.30	1.88	1.00
MO:M-NT:F	-0.34	-2.10	1.42	1.00
NM:F-AZ:F	-0.77	-3.38	1.84	1.00
OK:F-AZ:F	0.24	-2.16	2.63	1.00
CO:F-AZ:F	-1.05	-3.44	1.35	0.99
KS:F-AZ:F	-0.35	-2.39	1.68	1.00
MO:F-AZ:F	-1.65	-4.64	1.33	0.88
MX:M-AZ:F	-0.63	-4.54	3.29	1.00
ST:M-AZ:F	0.02	-2.59	2.63	1.00
WT:M-AZ:F	-0.43	-2.69	1.83	1.00
NT:M-AZ:F	-0.92	-3.18	1.34	0.99
AZ:M-AZ:F	-1.39	-3.79	1.00	0.83
NM:M-AZ:F	-0.98	-2.91	0.95	0.94
OK:M-AZ:F	-0.80	-2.96	1.36	1.00
CO:M-AZ:F	-1.28	-3.24	0.68	0.66
KS:M-AZ:F	-0.73	-2.99	1.53	1.00
MO:M-AZ:F	-0.85	-2.81	1.11	0.99
OK:F-NM:F	1.01	-1.72	3.73	1.00
CO:F-NM:F	-0.28	-3.01	2.45	1.00
KS:F-NM:F	0.42	-2.00	2.84	1.00
MO:F-NM:F	-0.88	-4.14	2.38	1.00

Table C6. (continued)

MX:M-NM:F	0.14	-3.98	4.27	1.00
ST:M-NM:F	0.79	-2.13	3.70	1.00
WT:M-NM:F	0.34	-2.27	2.95	1.00
NT:M-NM:F	-0.15	-2.76	2.46	1.00
AZ:M-NM:F	-0.62	-3.35	2.10	1.00
NM:M-NM:F	-0.21	-2.54	2.12	1.00
OK:M-NM:F	-0.03	-2.55	2.50	1.00
CO:M-NM:F	-0.51	-2.86	1.84	1.00
KS:M-NM:F	0.04	-2.57	2.65	1.00
MO:M-NM:F	-0.08	-2.43	2.27	1.00
CO:F-OK:F	-1.29	-3.81	1.24	0.94
KS:F-OK:F	-0.59	-2.78	1.60	1.00
MO:F-OK:F	-1.89	-4.98	1.20	0.77
MX:M-OK:F	-0.86	-4.85	3.13	1.00
ST:M-OK:F	-0.22	-2.95	2.51	1.00
WT:M-OK:F	-0.67	-3.06	1.73	1.00
NT:M-OK:F	-1.16	-3.55	1.24	0.96
AZ:M-OK:F	-1.63	-4.16	0.89	0.68
NM:M-OK:F	-1.22	-3.30	0.87	0.83
OK:M-OK:F	-1.04	-3.34	1.27	0.98
CO:M-OK:F	-1.52	-3.63	0.60	0.49
KS:M-OK:F	-0.96	-3.36	1.43	0.99
MO:M-OK:F	-1.09	-3.20	1.03	0.93
KS:F-CO:F	0.70	-1.49	2.88	1.00
MO:F-CO:F	-0.60	-3.70	2.49	1.00
MX:M-CO:F	0.42	-3.57	4.42	1.00
ST:M-CO:F	1.07	-1.66	3.79	1.00
WT:M-CO:F	0.62	-1.78	3.02	1.00
NT:M-CO:F	0.13	-2.27	2.52	1.00
AZ:M-CO:F	-0.35	-2.87	2.18	1.00
NM:M-CO:F	0.07	-2.02	2.15	1.00
OK:M-CO:F	0.25	-2.06	2.55	1.00
CO:M-CO:F	-0.23	-2.34	1.88	1.00
KS:M-CO:F	0.32	-2.07	2.72	1.00
MO:M-CO:F	0.20	-1.91	2.31	1.00
MO:F-KS:F	-1.30	-4.12	1.52	0.98
MX:M-KS:F	-0.27	-4.06	3.51	1.00

Table C6. (continued)

ST:M-KS:F	0.37	-2.05	2.79	1.00
WT:M-KS:F	-0.08	-2.11	1.96	1.00
NT:M-KS:F	-0.57	-2.61	1.47	1.00
AZ:M-KS:F	-1.04	-3.23	1.14	0.97
NM:M-KS:F	-0.63	-2.29	1.03	1.00
OK:M-KS:F	-0.45	-2.38	1.48	1.00
CO:M-KS:F	-0.93	-2.62	0.77	0.89
KS:M-KS:F	-0.38	-2.41	1.66	1.00
MO:M-KS:F	-0.50	-2.19	1.19	1.00
MX:M-MO:F	1.03	-3.35	5.40	1.00
ST:M-MO:F	1.67	-1.59	4.93	0.94
WT:M-MO:F	1.22	-1.76	4.21	0.99
NT:M-MO:F	0.73	-2.26	3.72	1.00
AZ:M-MO:F	0.26	-2.83	3.35	1.00
NM:M-MO:F	0.67	-2.07	3.42	1.00
OK:M-MO:F	0.85	-2.06	3.77	1.00
CO:M-MO:F	0.37	-2.39	3.14	1.00
KS:M-MO:F	0.93	-2.06	3.91	1.00
MO:M-MO:F	0.80	-1.96	3.57	1.00
ST:M-MX:M	0.64	-3.48	4.77	1.00
WT:M-MX:M	0.20	-3.72	4.11	1.00
NT:M-MX:M	-0.30	-4.21	3.61	1.00
AZ:M-MX:M	-0.77	-4.76	3.22	1.00
NM:M-MX:M	-0.36	-4.08	3.37	1.00
OK:M-MX:M	-0.17	-4.03	3.68	1.00
CO:M-MX:M	-0.65	-4.40	3.09	1.00
KS:M-MX:M	-0.10	-4.01	3.81	1.00
MO:M-MX:M	-0.23	-3.97	3.52	1.00
WT:M-ST:M	-0.45	-3.05	2.16	1.00
NT:M-ST:M	-0.94	-3.55	1.67	1.00
AZ:M-ST:M	-1.41	-4.14	1.32	0.93
NM:M-ST:M	-1.00	-3.32	1.33	0.99
OK:M-ST:M	-0.82	-3.34	1.71	1.00
CO:M-ST:M	-1.30	-3.65	1.05	0.88
KS:M-ST:M	-0.75	-3.35	1.86	1.00
MO:M-ST:M	-0.87	-3.22	1.48	1.00
NT:M-WT:M	-0.49	-2.75	1.76	1.00

Table C6. (continued)

AZ:M-WT:M	-0.97	-3.36	1.43	0.99
NM:M-WT:M	-0.55	-2.48	1.37	1.00
OK:M-WT:M	-0.37	-2.53	1.79	1.00
CO:M-WT:M	-0.85	-2.81	1.11	0.99
KS:M-WT:M	-0.30	-2.56	1.96	1.00
MO:M-WT:M	-0.42	-2.38	1.53	1.00
AZ:M-NT:M	-0.47	-2.87	1.92	1.00
NM:M-NT:M	-0.06	-1.98	1.87	1.00
OK:M-NT:M	0.12	-2.04	2.28	1.00
CO:M-NT:M	-0.36	-2.31	1.60	1.00
KS:M-NT:M	0.20	-2.06	2.45	1.00
MO:M-NT:M	0.07	-1.88	2.03	1.00
NM:M-AZ:M	0.41	-1.67	2.50	1.00
OK:M-AZ:M	0.59	-1.71	2.90	1.00
CO:M-AZ:M	0.11	-2.00	2.23	1.00
KS:M-AZ:M	0.67	-1.73	3.06	1.00
MO:M-AZ:M	0.54	-1.57	2.66	1.00
OK:M-NM:M	0.18	-1.63	1.99	1.00
CO:M-NM:M	-0.30	-1.86	1.26	1.00
KS:M-NM:M	0.25	-1.67	2.18	1.00
MO:M-NM:M	0.13	-1.43	1.69	1.00
CO:M-OK:M	-0.48	-2.32	1.36	1.00
KS:M-OK:M	0.07	-2.09	2.23	1.00
MO:M-OK:M	-0.05	-1.90	1.79	1.00
KS:M-CO:M	0.55	-1.40	2.51	1.00
MO:M-CO:M	0.43	-1.17	2.03	1.00
MO:M-KS:M	-0.12	-2.08	1.83	1.00
Group B PC3				
ST:F-MX:F	0.39	-3.85	4.63	1.00
WT:F-MX:F	0.61	-3.14	4.35	1.00
NT:F-MX:F	1.11	-2.59	4.82	1.00
AZ:F-MX:F	1.03	-2.76	4.83	1.00
NM:F-MX:F	0.27	-3.73	4.27	1.00
OK:F-MX:F	1.77	-2.11	5.64	0.98
CO:F-MX:F	0.56	-3.31	4.43	1.00
KS:F-MX:F	0.98	-2.69	4.66	1.00
MO:F-MX:F	1.01	-3.23	5.26	1.00

Table C6. (continued)

MX:M-MX:F	0.52	-4.38	5.42	1.00
ST:M-MX:F	0.78	-3.22	4.78	1.00
WT:M-MX:F	-0.48	-4.28	3.31	1.00
NT:M-MX:F	1.12	-2.68	4.91	1.00
AZ:M-MX:F	1.00	-2.87	4.87	1.00
NM:M-MX:F	0.81	-2.81	4.43	1.00
OK:M-MX:F	-0.58	-4.33	3.16	1.00
CO:M-MX:F	0.53	-3.10	4.16	1.00
KS:M-MX:F	0.38	-3.41	4.18	1.00
MO:M-MX:F	0.48	-3.16	4.11	1.00
WT:F-ST:F	0.22	-2.61	3.05	1.00
NT:F-ST:F	0.72	-2.05	3.50	1.00
AZ:F-ST:F	0.65	-2.25	3.54	1.00
NM:F-ST:F	-0.11	-3.28	3.05	1.00
OK:F-ST:F	1.38	-1.62	4.38	0.98
CO:F-ST:F	0.17	-2.83	3.17	1.00
KS:F-ST:F	0.59	-2.15	3.33	1.00
MO:F-ST:F	0.63	-2.84	4.09	1.00
MX:M-ST:F	0.13	-4.11	4.37	1.00
ST:M-ST:F	0.39	-2.77	3.55	1.00
WT:M-ST:F	-0.87	-3.77	2.03	1.00
NT:M-ST:F	0.73	-2.17	3.63	1.00
AZ:M-ST:F	0.61	-2.39	3.61	1.00
NM:M-ST:F	0.42	-2.24	3.09	1.00
OK:M-ST:F	-0.97	-3.80	1.86	1.00
CO:M-ST:F	0.14	-2.54	2.83	1.00
KS:M-ST:F	-0.01	-2.90	2.89	1.00
MO:M-ST:F	0.09	-2.59	2.77	1.00
NT:F-WT:F	0.51	-1.42	2.43	1.00
AZ:F-WT:F	0.43	-1.67	2.53	1.00
NM:F-WT:F	-0.33	-2.78	2.12	1.00
OK:F-WT:F	1.16	-1.08	3.40	0.93
CO:F-WT:F	-0.05	-2.28	2.19	1.00
KS:F-WT:F	0.38	-1.50	2.25	1.00
MO:F-WT:F	0.41	-2.42	3.24	1.00
MX:M-WT:F	-0.09	-3.83	3.66	1.00
ST:M-WT:F	0.17	-2.27	2.62	1.00

Table C6. (continued)

WT:M-WT:F	-1.09	-3.19	1.01	0.93
NT:M-WT:F	0.51	-1.59	2.61	1.00
AZ:M-WT:F	0.39	-1.84	2.63	1.00
NM:M-WT:F	0.20	-1.55	1.96	1.00
OK:M-WT:F	-1.19	-3.19	0.81	0.80
CO:M-WT:F	-0.07	-1.86	1.71	1.00
KS:M-WT:F	-0.22	-2.32	1.87	1.00
MO:M-WT:F	-0.13	-1.92	1.66	1.00
AZ:F-NT:F	-0.08	-2.11	1.95	1.00
NM:F-NT:F	-0.84	-3.23	1.55	1.00
OK:F-NT:F	0.65	-1.52	2.82	1.00
CO:F-NT:F	-0.55	-2.73	1.62	1.00
KS:F-NT:F	-0.13	-1.92	1.66	1.00
MO:F-NT:F	-0.10	-2.88	2.68	1.00
MX:M-NT:F	-0.59	-4.30	3.11	1.00
ST:M-NT:F	-0.33	-2.72	2.06	1.00
WT:M-NT:F	-1.60	-3.62	0.43	0.32
NT:M-NT:F	<0.01	-2.02	2.03	1.00
AZ:M-NT:F	-0.11	-2.28	2.06	1.00
NM:M-NT:F	-0.30	-1.98	1.37	1.00
OK:M-NT:F	-1.70	-3.62	0.23	0.16
CO:M-NT:F	-0.58	-2.29	1.13	1.00
KS:M-NT:F	-0.73	-2.76	1.30	1.00
MO:M-NT:F	-0.64	-2.34	1.07	1.00
NM:F-AZ:F	-0.76	-3.29	1.77	1.00
OK:F-AZ:F	0.73	-1.59	3.06	1.00
CO:F-AZ:F	-0.48	-2.80	1.85	1.00
KS:F-AZ:F	-0.05	-2.03	1.92	1.00
MO:F-AZ:F	-0.02	-2.92	2.88	1.00
MX:M-AZ:F	-0.51	-4.31	3.28	1.00
ST:M-AZ:F	-0.25	-2.78	2.28	1.00
WT:M-AZ:F	-1.52	-3.71	0.67	0.56
NT:M-AZ:F	0.08	-2.11	2.27	1.00
AZ:M-AZ:F	-0.03	-2.36	2.29	1.00
NM:M-AZ:F	-0.22	-2.09	1.65	1.00
OK:M-AZ:F	-1.62	-3.72	0.48	0.36
CO:M-AZ:F	-0.50	-2.40	1.40	1.00

Table C6. (continued)

KS:M-AZ:F	-0.65	-2.84	1.54	1.00
MO:M-AZ:F	-0.56	-2.45	1.34	1.00
OK:F-NM:F	1.49	-1.15	4.14	0.86
CO:F-NM:F	0.28	-2.36	2.93	1.00
KS:F-NM:F	0.71	-1.64	3.05	1.00
MO:F-NM:F	0.74	-2.42	3.90	1.00
MX:M-NM:F	0.25	-3.75	4.25	1.00
ST:M-NM:F	0.51	-2.32	3.33	1.00
WT:M-NM:F	-0.76	-3.29	1.77	1.00
NT:M-NM:F	0.84	-1.69	3.37	1.00
AZ:M-NM:F	0.73	-1.92	3.37	1.00
NM:M-NM:F	0.54	-1.72	2.79	1.00
OK:M-NM:F	-0.86	-3.31	1.59	1.00
CO:M-NM:F	0.26	-2.02	2.54	1.00
KS:M-NM:F	0.11	-2.42	2.64	1.00
MO:M-NM:F	0.20	-2.08	2.48	1.00
CO:F-OK:F	-1.21	-3.66	1.24	0.95
KS:F-OK:F	-0.79	-2.91	1.34	1.00
MO:F-OK:F	-0.75	-3.75	2.25	1.00
MX:M-OK:F	-1.25	-5.12	2.63	1.00
ST:M-OK:F	-0.99	-3.63	1.66	1.00
WT:M-OK:F	-2.25	-4.57	0.07	0.07
NT:M-OK:F	-0.65	-2.97	1.67	1.00
AZ:M-OK:F	-0.77	-3.22	1.68	1.00
NM:M-OK:F	-0.96	-2.98	1.07	0.97
OK:M-OK:F	-2.35	-4.59	-0.11	0.03
CO:M-OK:F	-1.23	-3.28	0.81	0.79
KS:M-OK:F	-1.38	-3.71	0.94	0.80
MO:M-OK:F	-1.29	-3.34	0.76	0.73
KS:F-CO:F	0.42	-1.70	2.54	1.00
MO:F-CO:F	0.45	-2.55	3.45	1.00
MX:M-CO:F	-0.04	-3.91	3.83	1.00
ST:M-CO:F	0.22	-2.42	2.87	1.00
WT:M-CO:F	-1.04	-3.36	1.28	0.98
NT:M-CO:F	0.56	-1.77	2.88	1.00
AZ:M-CO:F	0.44	-2.01	2.89	1.00
NM:M-CO:F	0.25	-1.77	2.27	1.00

Table C6. (continued)

OK:M-CO:F	-1.14	-3.38	1.09	0.94
CO:M-CO:F	-0.03	-2.08	2.02	1.00
KS:M-CO:F	-0.18	-2.50	2.15	1.00
MO:M-CO:F	-0.08	-2.13	1.97	1.00
MO:F-KS:F	0.03	-2.71	2.77	1.00
MX:M-KS:F	-0.46	-4.13	3.21	1.00
ST:M-KS:F	-0.20	-2.55	2.14	1.00
WT:M-KS:F	-1.46	-3.44	0.51	0.43
NT:M-KS:F	0.14	-1.84	2.11	1.00
AZ:M-KS:F	0.02	-2.10	2.14	1.00
NM:M-KS:F	-0.17	-1.78	1.44	1.00
OK:M-KS:F	-1.57	-3.44	0.31	0.22
CO:M-KS:F	-0.45	-2.09	1.19	1.00
KS:M-KS:F	-0.60	-2.57	1.38	1.00
MO:M-KS:F	-0.50	-2.15	1.14	1.00
MX:M-MO:F	-0.49	-4.73	3.75	1.00
ST:M-MO:F	-0.23	-3.39	2.93	1.00
WT:M-MO:F	-1.50	-4.39	1.40	0.93
NT:M-MO:F	0.10	-2.79	3.00	1.00
AZ:M-MO:F	-0.01	-3.01	2.99	1.00
NM:M-MO:F	-0.20	-2.87	2.46	1.00
OK:M-MO:F	-1.60	-4.43	1.23	0.86
CO:M-MO:F	-0.48	-3.16	2.20	1.00
KS:M-MO:F	-0.63	-3.53	2.27	1.00
MO:M-MO:F	-0.54	-3.22	2.15	1.00
ST:M-MX:M	0.26	-3.74	4.26	1.00
WT:M-MX:M	-1.00	-4.80	2.79	1.00
NT:M-MX:M	0.60	-3.20	4.39	1.00
AZ:M-MX:M	0.48	-3.39	4.35	1.00
NM:M-MX:M	0.29	-3.33	3.91	1.00
OK:M-MX:M	-1.10	-4.85	2.64	1.00
CO:M-MX:M	0.01	-3.62	3.64	1.00
KS:M-MX:M	-0.14	-3.93	3.66	1.00
MO:M-MX:M	-0.04	-3.68	3.59	1.00
WT:M-ST:M	-1.26	-3.79	1.27	0.95
NT:M-ST:M	0.34	-2.19	2.87	1.00
AZ:M-ST:M	0.22	-2.43	2.87	1.00

Table C6. (continued)

NM:M-ST:M	0.03	-2.23	2.29	1.00
OK:M-ST:M	-1.36	-3.81	1.09	0.88
CO:M-ST:M	-0.25	-2.53	2.03	1.00
KS:M-ST:M	-0.40	-2.93	2.13	1.00
MO:M-ST:M	-0.30	-2.58	1.98	1.00
NT:M-WT:M	1.60	-0.59	3.79	0.46
AZ:M-WT:M	1.48	-0.84	3.81	0.70
NM:M-WT:M	1.29	-0.58	3.16	0.56
OK:M-WT:M	-0.10	-2.20	2.00	1.00
CO:M-WT:M	1.01	-0.88	2.91	0.91
KS:M-WT:M	0.86	-1.33	3.05	1.00
MO:M-WT:M	0.96	-0.94	2.86	0.94
AZ:M-NT:M	-0.12	-2.44	2.21	1.00
NM:M-NT:M	-0.31	-2.17	1.56	1.00
OK:M-NT:M	-1.70	-3.80	0.40	0.27
CO:M-NT:M	-0.58	-2.48	1.31	1.00
KS:M-NT:M	-0.73	-2.93	1.46	1.00
MO:M-NT:M	-0.64	-2.54	1.26	1.00
NM:M-AZ:M	-0.19	-2.21	1.83	1.00
OK:M-AZ:M	-1.58	-3.82	0.65	0.52
CO:M-AZ:M	-0.47	-2.52	1.58	1.00
KS:M-AZ:M	-0.62	-2.94	1.71	1.00
MO:M-AZ:M	-0.52	-2.57	1.53	1.00
OK:M-NM:M	-1.39	-3.15	0.36	0.31
CO:M-NM:M	-0.28	-1.79	1.23	1.00
KS:M-NM:M	-0.43	-2.30	1.44	1.00
MO:M-NM:M	-0.33	-1.85	1.18	1.00
CO:M-OK:M	1.12	-0.67	2.90	0.74
KS:M-OK:M	0.97	-1.13	3.06	0.98
MO:M-OK:M	1.06	-0.73	2.85	0.81
KS:M-CO:M	-0.15	-2.05	1.75	1.00
MO:M-CO:M	-0.05	-1.60	1.49	1.00
MO:M-KS:M	0.10	-1.80	1.99	1.00
Group B PC4				
ST:F-MX:F	-1.15	-5.33	3.04	1.00
WT:F-MX:F	-0.38	-4.08	3.31	1.00
NT:F-MX:F	-0.71	-4.36	2.95	1.00

Table C6. (continued)

AZ:F-MX:F	-0.47	-4.22	3.27	1.00
NM:F-MX:F	-0.17	-4.12	3.77	1.00
OK:F-MX:F	-1.19	-5.01	2.64	1.00
CO:F-MX:F	-0.56	-4.38	3.27	1.00
KS:F-MX:F	-1.59	-5.22	2.03	0.99
MO:F-MX:F	-1.04	-5.23	3.15	1.00
MX:M-MX:F	-1.91	-6.75	2.93	1.00
ST:M-MX:F	-0.35	-4.30	3.60	1.00
WT:M-MX:F	-0.77	-4.52	2.97	1.00
NT:M-MX:F	-1.80	-5.54	1.95	0.96
AZ:M-MX:F	0.11	-3.72	3.93	1.00
NM:M-MX:F	-0.74	-4.31	2.84	1.00
OK:M-MX:F	-1.29	-4.98	2.40	1.00
CO:M-MX:F	-1.29	-4.88	2.29	1.00
KS:M-MX:F	-1.58	-5.32	2.17	0.99
MO:M-MX:F	-1.65	-5.23	1.94	0.98
WT:F-ST:F	0.76	-2.03	3.56	1.00
NT:F-ST:F	0.44	-2.30	3.18	1.00
AZ:F-ST:F	0.68	-2.19	3.54	1.00
NM:F-ST:F	0.97	-2.15	4.09	1.00
OK:F-ST:F	-0.04	-3.00	2.92	1.00
CO:F-ST:F	0.59	-2.37	3.55	1.00
KS:F-ST:F	-0.45	-3.15	2.25	1.00
MO:F-ST:F	0.11	-3.31	3.53	1.00
MX:M-ST:F	-0.76	-4.95	3.42	1.00
ST:M-ST:F	0.80	-2.32	3.92	1.00
WT:M-ST:F	0.37	-2.49	3.23	1.00
NT:M-ST:F	-0.65	-3.51	2.21	1.00
AZ:M-ST:F	1.25	-1.71	4.21	0.99
NM:M-ST:F	0.41	-2.22	3.04	1.00
OK:M-ST:F	-0.14	-2.94	2.65	1.00
CO:M-ST:F	-0.14	-2.79	2.50	1.00
KS:M-ST:F	-0.43	-3.29	2.43	1.00
MO:M-ST:F	-0.50	-3.15	2.15	1.00
NT:F-WT:F	-0.32	-2.22	1.58	1.00
AZ:F-WT:F	-0.09	-2.16	1.98	1.00
NM:F-WT:F	0.21	-2.21	2.63	1.00

Table C6. (continued)

OK:F-WT:F	-0.80	-3.01	1.40	1.00
CO:F-WT:F	-0.17	-2.38	2.03	1.00
KS:F-WT:F	-1.21	-3.06	0.63	0.66
MO:F-WT:F	-0.66	-3.45	2.13	1.00
MX:M-WT:F	-1.53	-5.22	2.17	0.99
ST:M-WT:F	0.03	-2.38	2.45	1.00
WT:M-WT:F	-0.39	-2.46	1.68	1.00
NT:M-WT:F	-1.41	-3.48	0.66	0.59
AZ:M-WT:F	0.49	-1.72	2.70	1.00
NM:M-WT:F	-0.35	-2.09	1.38	1.00
OK:M-WT:F	-0.91	-2.88	1.07	0.98
CO:M-WT:F	-0.91	-2.67	0.86	0.93
KS:M-WT:F	-1.19	-3.26	0.88	0.84
MO:M-WT:F	-1.26	-3.03	0.50	0.50
AZ:F-NT:F	0.23	-1.77	2.24	1.00
NM:F-NT:F	0.53	-1.83	2.89	1.00
OK:F-NT:F	-0.48	-2.62	1.66	1.00
CO:F-NT:F	0.15	-2.00	2.29	1.00
KS:F-NT:F	-0.89	-2.66	0.88	0.95
MO:F-NT:F	-0.33	-3.08	2.41	1.00
MX:M-NT:F	-1.20	-4.86	2.45	1.00
ST:M-NT:F	0.36	-2.00	2.72	1.00
WT:M-NT:F	-0.07	-2.07	1.93	1.00
NT:M-NT:F	-1.09	-3.09	0.91	0.89
AZ:M-NT:F	0.81	-1.33	2.96	1.00
NM:M-NT:F	-0.03	-1.68	1.62	1.00
OK:M-NT:F	-0.59	-2.49	1.32	1.00
CO:M-NT:F	-0.59	-2.27	1.10	1.00
KS:M-NT:F	-0.87	-2.87	1.13	0.99
MO:M-NT:F	-0.94	-2.63	0.74	0.87
NM:F-AZ:F	0.30	-2.20	2.79	1.00
OK:F-AZ:F	-0.71	-3.01	1.58	1.00
CO:F-AZ:F	-0.09	-2.38	2.21	1.00
KS:F-AZ:F	-1.12	-3.07	0.83	0.84
MO:F-AZ:F	-0.57	-3.43	2.29	1.00
MX:M-AZ:F	-1.44	-5.18	2.31	1.00
ST:M-AZ:F	0.12	-2.37	2.62	1.00

Table C6. (continued)

WT:M-AZ:F	-0.30	-2.46	1.86	1.00
NT:M-AZ:F	-1.33	-3.49	0.84	0.76
AZ:M-AZ:F	0.58	-1.71	2.87	1.00
NM:M-AZ:F	-0.26	-2.11	1.58	1.00
OK:M-AZ:F	-0.82	-2.89	1.25	1.00
CO:M-AZ:F	-0.82	-2.69	1.05	0.99
KS:M-AZ:F	-1.10	-3.27	1.06	0.94
MO:M-AZ:F	-1.17	-3.05	0.70	0.73
OK:F-NM:F	-1.01	-3.62	1.60	1.00
CO:F-NM:F	-0.38	-2.99	2.23	1.00
KS:F-NM:F	-1.42	-3.73	0.89	0.76
MO:F-NM:F	-0.87	-3.99	2.26	1.00
MX:M-NM:F	-1.74	-5.68	2.21	0.99
ST:M-NM:F	-0.17	-2.96	2.62	1.00
WT:M-NM:F	-0.60	-3.10	1.90	1.00
NT:M-NM:F	-1.62	-4.12	0.87	0.67
AZ:M-NM:F	0.28	-2.33	2.89	1.00
NM:M-NM:F	-0.56	-2.79	1.67	1.00
OK:M-NM:F	-1.12	-3.53	1.30	0.98
CO:M-NM:F	-1.12	-3.37	1.13	0.95
KS:M-NM:F	-1.40	-3.90	1.10	0.87
MO:M-NM:F	-1.47	-3.72	0.78	0.66
CO:F-OK:F	0.63	-1.79	3.05	1.00
KS:F-OK:F	-0.41	-2.50	1.68	1.00
MO:F-OK:F	0.15	-2.82	3.11	1.00
MX:M-OK:F	-0.72	-4.55	3.10	1.00
ST:M-OK:F	0.84	-1.77	3.45	1.00
WT:M-OK:F	0.41	-1.88	2.71	1.00
NT:M-OK:F	-0.61	-2.91	1.68	1.00
AZ:M-OK:F	1.29	-1.13	3.71	0.91
NM:M-OK:F	0.45	-1.55	2.45	1.00
OK:M-OK:F	-0.11	-2.31	2.10	1.00
CO:M-OK:F	-0.11	-2.13	1.92	1.00
KS:M-OK:F	-0.39	-2.68	1.90	1.00
MO:M-OK:F	-0.46	-2.48	1.56	1.00
KS:F-CO:F	-1.04	-3.13	1.06	0.95
MO:F-CO:F	-0.48	-3.44	2.48	1.00

Table C6. (continued)

MX:M-CO:F	-1.35	-5.18	2.47	1.00
ST:M-CO:F	0.21	-2.40	2.82	1.00
WT:M-CO:F	-0.22	-2.51	2.08	1.00
NT:M-CO:F	-1.24	-3.53	1.05	0.90
AZ:M-CO:F	0.66	-1.75	3.08	1.00
NM:M-CO:F	-0.18	-2.17	1.82	1.00
OK:M-CO:F	-0.73	-2.94	1.47	1.00
CO:M-CO:F	-0.73	-2.76	1.29	1.00
KS:M-CO:F	-1.02	-3.31	1.28	0.98
MO:M-CO:F	-1.09	-3.11	0.93	0.90
MO:F-KS:F	0.55	-2.15	3.26	1.00
MX:M-KS:F	-0.32	-3.94	3.31	1.00
ST:M-KS:F	1.25	-1.07	3.56	0.90
WT:M-KS:F	0.82	-1.13	2.77	0.99
NT:M-KS:F	-0.20	-2.15	1.75	1.00
AZ:M-KS:F	1.70	-0.39	3.80	0.27
NM:M-KS:F	0.86	-0.73	2.45	0.90
OK:M-KS:F	0.30	-1.54	2.15	1.00
CO:M-KS:F	0.30	-1.32	1.93	1.00
KS:M-KS:F	0.02	-1.93	1.97	1.00
MO:M-KS:F	-0.05	-1.67	1.57	1.00
MX:M-MO:F	-0.87	-5.06	3.32	1.00
ST:M-MO:F	0.69	-2.43	3.81	1.00
WT:M-MO:F	0.27	-2.59	3.13	1.00
NT:M-MO:F	-0.76	-3.62	2.10	1.00
AZ:M-MO:F	1.15	-1.81	4.11	1.00
NM:M-MO:F	0.30	-2.32	2.93	1.00
OK:M-MO:F	-0.25	-3.04	2.54	1.00
CO:M-MO:F	-0.25	-2.90	2.40	1.00
KS:M-MO:F	-0.54	-3.40	2.33	1.00
MO:M-MO:F	-0.61	-3.25	2.04	1.00
ST:M-MX:M	1.56	-2.39	5.51	1.00
WT:M-MX:M	1.14	-2.61	4.88	1.00
NT:M-MX:M	0.11	-3.63	3.86	1.00
AZ:M-MX:M	2.02	-1.81	5.84	0.92
NM:M-MX:M	1.17	-2.40	4.75	1.00
OK:M-MX:M	0.62	-3.07	4.31	1.00

Table C6. (continued)

CO:M-MX:M	0.62	-2.97	4.20	1.00
KS:M-MX:M	0.33	-3.41	4.08	1.00
MO:M-MX:M	0.26	-3.32	3.85	1.00
WT:M-ST:M	-0.42	-2.92	2.07	1.00
NT:M-ST:M	-1.45	-3.95	1.05	0.83
AZ:M-ST:M	0.46	-2.16	3.07	1.00
NM:M-ST:M	-0.39	-2.61	1.84	1.00
OK:M-ST:M	-0.94	-3.36	1.47	1.00
CO:M-ST:M	-0.94	-3.19	1.31	0.99
KS:M-ST:M	-1.23	-3.72	1.27	0.96
MO:M-ST:M	-1.30	-3.55	0.95	0.84
NT:M-WT:M	-1.02	-3.19	1.14	0.97
AZ:M-WT:M	0.88	-1.41	3.17	1.00
NM:M-WT:M	0.04	-1.81	1.88	1.00
OK:M-WT:M	-0.52	-2.59	1.55	1.00
CO:M-WT:M	-0.52	-2.39	1.35	1.00
KS:M-WT:M	-0.80	-2.97	1.36	1.00
MO:M-WT:M	-0.87	-2.75	1.00	0.97
AZ:M-NT:M	1.90	-0.39	4.20	0.24
NM:M-NT:M	1.06	-0.78	2.91	0.84
OK:M-NT:M	0.51	-1.56	2.58	1.00
CO:M-NT:M	0.51	-1.37	2.38	1.00
KS:M-NT:M	0.22	-1.94	2.38	1.00
MO:M-NT:M	0.15	-1.72	2.02	1.00
NM:M-AZ:M	-0.84	-2.84	1.15	0.99
OK:M-AZ:M	-1.40	-3.61	0.81	0.72
CO:M-AZ:M	-1.40	-3.42	0.62	0.56
KS:M-AZ:M	-1.68	-3.98	0.61	0.45
MO:M-AZ:M	-1.75	-3.78	0.27	0.18
OK:M-NM:M	-0.56	-2.29	1.18	1.00
CO:M-NM:M	-0.56	-2.05	0.94	1.00
KS:M-NM:M	-0.84	-2.68	1.00	0.98
MO:M-NM:M	-0.91	-2.40	0.58	0.77
CO:M-OK:M	<0.01	-1.77	1.77	1.00
KS:M-OK:M	-0.28	-2.36	1.79	1.00
MO:M-OK:M	-0.36	-2.12	1.41	1.00
KS:M-CO:M	-0.28	-2.16	1.59	1.00

Table C6. (continued)

MO:M-CO:M	-0.35	-1.88	1.17	1.00
MO:M-KS:M	-0.07	-1.94	1.80	1.00
Group C PC1				
ST:F-MX:F	2.04	-2.33	6.41	0.97
WT:F-MX:F	2.42	-1.43	6.27	0.73
NT:F-MX:F	2.21	-1.60	6.02	0.84
AZ:F-MX:F	2.34	-1.57	6.25	0.80
NM:F-MX:F	2.11	-2.00	6.23	0.94
OK:F-MX:F	3.15	-0.84	7.13	0.32
CO:F-MX:F	1.53	-2.46	5.51	1.00
KS:F-MX:F	1.39	-2.39	5.17	1.00
MO:F-MX:F	1.25	-3.11	5.62	1.00
MX:M-MX:F	2.31	-2.73	7.36	0.98
ST:M-MX:F	2.15	-1.97	6.26	0.93
WT:M-MX:F	1.85	-2.05	5.76	0.97
NT:M-MX:F	2.06	-1.85	5.97	0.92
AZ:M-MX:F	0.92	-3.06	4.91	1.00
NM:M-MX:F	2.02	-1.70	5.74	0.90
OK:M-MX:F	2.08	-1.78	5.93	0.90
CO:M-MX:F	1.51	-2.23	5.25	0.99
KS:M-MX:F	2.07	-1.83	5.98	0.91
MO:M-MX:F	1.76	-1.98	5.50	0.97
WT:F-ST:F	0.38	-2.53	3.29	1.00
NT:F-ST:F	0.17	-2.69	3.03	1.00
AZ:F-ST:F	0.30	-2.68	3.28	1.00
NM:F-ST:F	0.07	-3.18	3.33	1.00
OK:F-ST:F	1.11	-1.98	4.19	1.00
CO:F-ST:F	-0.52	-3.60	2.57	1.00
KS:F-ST:F	-0.65	-3.47	2.17	1.00
MO:F-ST:F	-0.79	-4.35	2.78	1.00
MX:M-ST:F	0.27	-4.09	4.64	1.00
ST:M-ST:F	0.11	-3.15	3.36	1.00
WT:M-ST:F	-0.19	-3.17	2.80	1.00
NT:M-ST:F	0.02	-2.96	3.00	1.00
AZ:M-ST:F	-1.12	-4.21	1.97	1.00
NM:M-ST:F	-0.02	-2.76	2.72	1.00
OK:M-ST:F	0.04	-2.88	2.95	1.00

Table C6. (continued)

CO:M-ST:F	-0.53	-3.29	2.23	1.00
KS:M-ST:F	0.03	-2.95	3.02	1.00
MO:M-ST:F	-0.28	-3.04	2.49	1.00
NT:F-WT:F	-0.21	-2.19	1.77	1.00
AZ:F-WT:F	-0.08	-2.24	2.08	1.00
NM:F-WT:F	-0.31	-2.83	2.21	1.00
OK:F-WT:F	0.73	-1.58	3.03	1.00
CO:F-WT:F	-0.90	-3.20	1.41	1.00
KS:F-WT:F	-1.03	-2.96	0.89	0.91
MO:F-WT:F	-1.17	-4.08	1.75	0.99
MX:M-WT:F	-0.11	-3.96	3.74	1.00
ST:M-WT:F	-0.27	-2.80	2.25	1.00
WT:M-WT:F	-0.57	-2.72	1.59	1.00
NT:M-WT:F	-0.36	-2.52	1.80	1.00
AZ:M-WT:F	-1.50	-3.80	0.80	0.67
NM:M-WT:F	-0.40	-2.21	1.41	1.00
OK:M-WT:F	-0.34	-2.40	1.71	1.00
CO:M-WT:F	-0.91	-2.75	0.93	0.95
KS:M-WT:F	-0.35	-2.50	1.81	1.00
MO:M-WT:F	-0.66	-2.50	1.19	1.00
AZ:F-NT:F	0.13	-1.96	2.22	1.00
NM:F-NT:F	-0.10	-2.56	2.36	1.00
OK:F-NT:F	0.94	-1.30	3.17	0.99
CO:F-NT:F	-0.68	-2.92	1.55	1.00
KS:F-NT:F	-0.82	-2.67	1.03	0.98
MO:F-NT:F	-0.96	-3.81	1.90	1.00
MX:M-NT:F	0.10	-3.71	3.92	1.00
ST:M-NT:F	-0.06	-2.52	2.40	1.00
WT:M-NT:F	-0.35	-2.44	1.73	1.00
NT:M-NT:F	-0.15	-2.24	1.94	1.00
AZ:M-NT:F	-1.29	-3.52	0.95	0.84
NM:M-NT:F	-0.19	-1.91	1.53	1.00
OK:M-NT:F	-0.13	-2.12	1.85	1.00
CO:M-NT:F	-0.70	-2.46	1.06	1.00
KS:M-NT:F	-0.13	-2.22	1.95	1.00
MO:M-NT:F	-0.45	-2.20	1.31	1.00
NM:F-AZ:F	-0.23	-2.83	2.38	1.00

Table C6. (continued)

OK:F-AZ:F	0.81	-1.59	3.20	1.00
CO:F-AZ:F	-0.82	-3.21	1.58	1.00
KS:F-AZ:F	-0.95	-2.98	1.08	0.97
MO:F-AZ:F	-1.09	-4.07	1.90	1.00
MX:M-AZ:F	-0.03	-3.93	3.88	1.00
ST:M-AZ:F	-0.19	-2.80	2.41	1.00
WT:M-AZ:F	-0.49	-2.74	1.77	1.00
NT:M-AZ:F	-0.28	-2.54	1.98	1.00
AZ:M-AZ:F	-1.42	-3.81	0.97	0.81
NM:M-AZ:F	-0.32	-2.24	1.60	1.00
OK:M-AZ:F	-0.26	-2.42	1.90	1.00
CO:M-AZ:F	-0.83	-2.78	1.12	0.99
KS:M-AZ:F	-0.27	-2.52	1.99	1.00
MO:M-AZ:F	-0.58	-2.53	1.38	1.00
OK:F-NM:F	1.03	-1.69	3.76	1.00
CO:F-NM:F	-0.59	-3.31	2.14	1.00
KS:F-NM:F	-0.72	-3.14	1.69	1.00
MO:F-NM:F	-0.86	-4.11	2.40	1.00
MX:M-NM:F	0.20	-3.92	4.32	1.00
ST:M-NM:F	0.03	-2.88	2.94	1.00
WT:M-NM:F	-0.26	-2.86	2.35	1.00
NT:M-NM:F	-0.05	-2.66	2.55	1.00
AZ:M-NM:F	-1.19	-3.91	1.53	0.99
NM:M-NM:F	-0.09	-2.41	2.23	1.00
OK:M-NM:F	-0.04	-2.56	2.49	1.00
CO:M-NM:F	-0.60	-2.95	1.75	1.00
KS:M-NM:F	-0.04	-2.64	2.57	1.00
MO:M-NM:F	-0.35	-2.70	2.00	1.00
CO:F-OK:F	-1.62	-4.14	0.90	0.69
KS:F-OK:F	-1.76	-3.94	0.43	0.29
MO:F-OK:F	-1.89	-4.98	1.20	0.76
MX:M-OK:F	-0.83	-4.82	3.15	1.00
ST:M-OK:F	-1.00	-3.72	1.72	1.00
WT:M-OK:F	-1.29	-3.68	1.10	0.90
NT:M-OK:F	-1.09	-3.48	1.31	0.98
AZ:M-OK:F	-2.22	-4.75	0.30	0.15
NM:M-OK:F	-1.13	-3.21	0.96	0.90

Table C6. (continued)

OK:M-OK:F	-1.07	-3.37	1.23	0.97
CO:M-OK:F	-1.64	-3.75	0.47	0.35
KS:M-OK:F	-1.07	-3.46	1.32	0.98
MO:M-OK:F	-1.38	-3.49	0.73	0.66
KS:F-CO:F	-0.14	-2.32	2.05	1.00
MO:F-CO:F	-0.27	-3.36	2.82	1.00
MX:M-CO:F	0.79	-3.20	4.77	1.00
ST:M-CO:F	0.62	-2.10	3.34	1.00
WT:M-CO:F	0.33	-2.06	2.72	1.00
NT:M-CO:F	0.54	-1.86	2.93	1.00
AZ:M-CO:F	-0.60	-3.12	1.92	1.00
NM:M-CO:F	0.50	-1.59	2.58	1.00
OK:M-CO:F	0.55	-1.75	2.85	1.00
CO:M-CO:F	-0.02	-2.12	2.09	1.00
KS:M-CO:F	0.55	-1.84	2.94	1.00
MO:M-CO:F	0.24	-1.87	2.35	1.00
MO:F-KS:F	-0.14	-2.95	2.68	1.00
MX:M-KS:F	0.92	-2.86	4.71	1.00
ST:M-KS:F	0.76	-1.66	3.17	1.00
WT:M-KS:F	0.47	-1.57	2.50	1.00
NT:M-KS:F	0.67	-1.36	2.70	1.00
AZ:M-KS:F	-0.47	-2.65	1.72	1.00
NM:M-KS:F	0.63	-1.03	2.29	1.00
OK:M-KS:F	0.69	-1.24	2.61	1.00
CO:M-KS:F	0.12	-1.57	1.81	1.00
KS:M-KS:F	0.69	-1.35	2.72	1.00
MO:M-KS:F	0.37	-1.32	2.07	1.00
MX:M-MO:F	1.06	-3.31	5.43	1.00
ST:M-MO:F	0.89	-2.36	4.15	1.00
WT:M-MO:F	0.60	-2.38	3.58	1.00
NT:M-MO:F	0.81	-2.18	3.79	1.00
AZ:M-MO:F	-0.33	-3.42	2.76	1.00
NM:M-MO:F	0.77	-1.98	3.51	1.00
OK:M-MO:F	0.82	-2.09	3.73	1.00
CO:M-MO:F	0.26	-2.51	3.02	1.00
KS:M-MO:F	0.82	-2.16	3.80	1.00
MO:M-MO:F	0.51	-2.25	3.27	1.00

Table C6. (continued)

ST:M-MX:M	-0.17	-4.28	3.95	1.00
WT:M-MX:M	-0.46	-4.36	3.45	1.00
NT:M-MX:M	-0.25	-4.16	3.65	1.00
AZ:M-MX:M	-1.39	-5.38	2.60	1.00
NM:M-MX:M	-0.29	-4.02	3.43	1.00
OK:M-MX:M	-0.24	-4.09	3.61	1.00
CO:M-MX:M	-0.80	-4.54	2.94	1.00
KS:M-MX:M	-0.24	-4.14	3.67	1.00
MO:M-MX:M	-0.55	-4.29	3.19	1.00
WT:M-ST:M	-0.29	-2.89	2.31	1.00
NT:M-ST:M	-0.09	-2.69	2.52	1.00
AZ:M-ST:M	-1.22	-3.95	1.50	0.98
NM:M-ST:M	-0.13	-2.45	2.20	1.00
OK:M-ST:M	-0.07	-2.59	2.45	1.00
CO:M-ST:M	-0.64	-2.98	1.71	1.00
KS:M-ST:M	-0.07	-2.67	2.53	1.00
MO:M-ST:M	-0.38	-2.73	1.97	1.00
NT:M-WT:M	0.21	-2.05	2.46	1.00
AZ:M-WT:M	-0.93	-3.32	1.46	1.00
NM:M-WT:M	0.17	-1.76	2.09	1.00
OK:M-WT:M	0.22	-1.94	2.38	1.00
CO:M-WT:M	-0.34	-2.30	1.61	1.00
KS:M-WT:M	0.22	-2.04	2.48	1.00
MO:M-WT:M	-0.09	-2.04	1.86	1.00
AZ:M-NT:M	-1.14	-3.53	1.25	0.97
NM:M-NT:M	-0.04	-1.96	1.88	1.00
OK:M-NT:M	0.02	-2.14	2.18	1.00
CO:M-NT:M	-0.55	-2.50	1.40	1.00
KS:M-NT:M	0.01	-2.24	2.27	1.00
MO:M-NT:M	-0.30	-2.25	1.66	1.00
NM:M-AZ:M	1.10	-0.98	3.18	0.92
OK:M-AZ:M	1.15	-1.15	3.46	0.95
CO:M-AZ:M	0.59	-1.52	2.70	1.00
KS:M-AZ:M	1.15	-1.24	3.54	0.96
MO:M-AZ:M	0.84	-1.27	2.95	1.00
OK:M-NM:M	0.06	-1.75	1.87	1.00
CO:M-NM:M	-0.51	-2.07	1.05	1.00

Table C6. (continued)

KS:M-NM:M	0.05	-1.87	1.98	1.00
MO:M-NM:M	-0.26	-1.81	1.30	1.00
CO:M-OK:M	-0.57	-2.41	1.28	1.00
KS:M-OK:M	<0.01	-2.16	2.16	1.00
MO:M-OK:M	-0.31	-2.15	1.53	1.00
KS:M-CO:M	0.56	-1.39	2.52	1.00
MO:M-CO:M	0.25	-1.34	1.85	1.00
MO:M-KS:M	-0.31	-2.26	1.64	1.00
Group C PC2				
ST:F-MX:F	-0.87	-5.13	3.38	1.00
WT:F-MX:F	-0.50	-4.25	3.25	1.00
NT:F-MX:F	0.35	-3.36	4.06	1.00
AZ:F-MX:F	0.79	-3.02	4.59	1.00
NM:F-MX:F	-1.26	-5.27	2.75	1.00
OK:F-MX:F	-0.43	-4.31	3.46	1.00
CO:F-MX:F	-0.14	-4.02	3.74	1.00
KS:F-MX:F	-0.18	-3.86	3.51	1.00
MO:F-MX:F	0.49	-3.76	4.75	1.00
MX:M-MX:F	-1.35	-6.26	3.56	1.00
ST:M-MX:F	0.44	-3.57	4.45	1.00
WT:M-MX:F	-0.58	-4.38	3.23	1.00
NT:M-MX:F	-0.87	-4.67	2.94	1.00
AZ:M-MX:F	-0.76	-4.64	3.12	1.00
NM:M-MX:F	-0.70	-4.32	2.93	1.00
OK:M-MX:F	-0.64	-4.39	3.11	1.00
CO:M-MX:F	-0.31	-3.95	3.33	1.00
KS:M-MX:F	-0.02	-3.82	3.78	1.00
MO:M-MX:F	0.40	-3.24	4.05	1.00
WT:F-ST:F	0.37	-2.46	3.21	1.00
NT:F-ST:F	1.23	-1.56	4.01	0.99
AZ:F-ST:F	1.66	-1.24	4.57	0.85
NM:F-ST:F	-0.39	-3.56	2.78	1.00
OK:F-ST:F	0.45	-2.56	3.45	1.00
CO:F-ST:F	0.73	-2.27	3.74	1.00
KS:F-ST:F	0.70	-2.05	3.44	1.00
MO:F-ST:F	1.37	-2.11	4.84	1.00
MX:M-ST:F	-0.48	-4.73	3.78	1.00

Table C6. (continued)

ST:M-ST:F	1.31	-1.86	4.48	0.99
WT:M-ST:F	0.30	-2.61	3.20	1.00
NT:M-ST:F	0.01	-2.90	2.91	1.00
AZ:M-ST:F	0.12	-2.89	3.12	1.00
NM:M-ST:F	0.18	-2.49	2.85	1.00
OK:M-ST:F	0.24	-2.60	3.07	1.00
CO:M-ST:F	0.56	-2.13	3.25	1.00
KS:M-ST:F	0.85	-2.05	3.76	1.00
MO:M-ST:F	1.28	-1.41	3.97	0.97
NT:F-WT:F	0.85	-1.08	2.79	0.98
AZ:F-WT:F	1.29	-0.81	3.39	0.76
NM:F-WT:F	-0.76	-3.21	1.70	1.00
OK:F-WT:F	0.08	-2.17	2.32	1.00
CO:F-WT:F	0.36	-1.88	2.60	1.00
KS:F-WT:F	0.32	-1.55	2.20	1.00
MO:F-WT:F	1.00	-1.84	3.83	1.00
MX:M-WT:F	-0.85	-4.60	2.90	1.00
ST:M-WT:F	0.94	-1.52	3.39	1.00
WT:M-WT:F	-0.08	-2.18	2.03	1.00
NT:M-WT:F	-0.36	-2.46	1.74	1.00
AZ:M-WT:F	-0.25	-2.50	1.99	1.00
NM:M-WT:F	-0.20	-1.96	1.57	1.00
OK:M-WT:F	-0.14	-2.14	1.87	1.00
CO:M-WT:F	0.19	-1.60	1.99	1.00
KS:M-WT:F	0.48	-1.62	2.59	1.00
MO:M-WT:F	0.91	-0.89	2.70	0.94
AZ:F-NT:F	0.44	-1.60	2.47	1.00
NM:F-NT:F	-1.61	-4.01	0.79	0.62
OK:F-NT:F	-0.78	-2.95	1.40	1.00
CO:F-NT:F	-0.49	-2.67	1.69	1.00
KS:F-NT:F	-0.53	-2.33	1.27	1.00
MO:F-NT:F	0.14	-2.64	2.93	1.00
MX:M-NT:F	-1.70	-5.41	2.01	0.98
ST:M-NT:F	0.09	-2.31	2.48	1.00
WT:M-NT:F	-0.93	-2.96	1.10	0.98
NT:M-NT:F	-1.22	-3.25	0.82	0.80
AZ:M-NT:F	-1.11	-3.28	1.07	0.94

Table C6. (continued)

NM:M-NT:F	-1.05	-2.73	0.63	0.74
OK:M-NT:F	-0.99	-2.92	0.94	0.94
CO:M-NT:F	-0.66	-2.37	1.05	1.00
KS:M-NT:F	-0.37	-2.40	1.66	1.00
MO:M-NT:F	0.05	-1.66	1.76	1.00
NM:F-AZ:F	-2.05	-4.58	0.49	0.28
OK:F-AZ:F	-1.21	-3.54	1.12	0.93
CO:F-AZ:F	-0.93	-3.26	1.40	1.00
KS:F-AZ:F	-0.96	-2.94	1.01	0.96
MO:F-AZ:F	-0.29	-3.20	2.61	1.00
MX:M-AZ:F	-2.14	-5.94	1.67	0.87
ST:M-AZ:F	-0.35	-2.89	2.19	1.00
WT:M-AZ:F	-1.37	-3.56	0.83	0.74
NT:M-AZ:F	-1.65	-3.85	0.54	0.40
AZ:M-AZ:F	-1.54	-3.87	0.78	0.64
NM:M-AZ:F	-1.49	-3.36	0.39	0.31
OK:M-AZ:F	-1.43	-3.53	0.68	0.60
CO:M-AZ:F	-1.10	-3.00	0.80	0.84
KS:M-AZ:F	-0.81	-3.00	1.39	1.00
MO:M-AZ:F	-0.38	-2.29	1.52	1.00
OK:F-NM:F	0.83	-1.82	3.48	1.00
CO:F-NM:F	1.12	-1.53	3.77	0.99
KS:F-NM:F	1.08	-1.27	3.43	0.98
MO:F-NM:F	1.75	-1.42	4.92	0.88
MX:M-NM:F	-0.09	-4.10	3.92	1.00
ST:M-NM:F	1.70	-1.14	4.53	0.80
WT:M-NM:F	0.68	-1.85	3.22	1.00
NT:M-NM:F	0.39	-2.14	2.93	1.00
AZ:M-NM:F	0.50	-2.15	3.15	1.00
NM:M-NM:F	0.56	-1.70	2.82	1.00
OK:M-NM:F	0.62	-1.83	3.08	1.00
CO:M-NM:F	0.95	-1.34	3.23	0.99
KS:M-NM:F	1.24	-1.30	3.78	0.96
MO:M-NM:F	1.66	-0.62	3.95	0.47
CO:F-OK:F	0.29	-2.17	2.74	1.00
KS:F-OK:F	0.25	-1.88	2.38	1.00
MO:F-OK:F	0.92	-2.09	3.93	1.00

Table C6. (continued)

MX:M-OK:F	-0.92	-4.81	2.96	1.00
ST:M-OK:F	0.86	-1.79	3.52	1.00
WT:M-OK:F	-0.15	-2.48	2.18	1.00
NT:M-OK:F	-0.44	-2.77	1.89	1.00
AZ:M-OK:F	-0.33	-2.79	2.12	1.00
NM:M-OK:F	-0.27	-2.30	1.76	1.00
OK:M-OK:F	-0.21	-2.45	2.03	1.00
CO:M-OK:F	0.12	-1.94	2.17	1.00
KS:M-OK:F	0.41	-1.92	2.74	1.00
MO:M-OK:F	0.83	-1.22	2.88	0.99
KS:F-CO:F	-0.04	-2.16	2.09	1.00
MO:F-CO:F	0.63	-2.37	3.64	1.00
MX:M-CO:F	-1.21	-5.09	2.67	1.00
ST:M-CO:F	0.58	-2.08	3.23	1.00
WT:M-CO:F	-0.44	-2.77	1.89	1.00
NT:M-CO:F	-0.73	-3.05	1.60	1.00
AZ:M-CO:F	-0.62	-3.07	1.84	1.00
NM:M-CO:F	-0.56	-2.59	1.47	1.00
OK:M-CO:F	-0.50	-2.74	1.74	1.00
CO:M-CO:F	-0.17	-2.22	1.88	1.00
KS:M-CO:F	0.12	-2.21	2.45	1.00
MO:M-CO:F	0.54	-1.51	2.60	1.00
MO:F-KS:F	0.67	-2.07	3.42	1.00
MX:M-KS:F	-1.17	-4.86	2.51	1.00
ST:M-KS:F	0.61	-1.74	2.97	1.00
WT:M-KS:F	-0.40	-2.38	1.58	1.00
NT:M-KS:F	-0.69	-2.67	1.29	1.00
AZ:M-KS:F	-0.58	-2.71	1.55	1.00
NM:M-KS:F	-0.52	-2.13	1.09	1.00
OK:M-KS:F	-0.46	-2.34	1.41	1.00
CO:M-KS:F	-0.13	-1.78	1.51	1.00
KS:M-KS:F	0.16	-1.82	2.14	1.00
MO:M-KS:F	0.58	-1.07	2.23	1.00
MX:M-MO:F	-1.84	-6.10	2.41	0.99
ST:M-MO:F	-0.06	-3.23	3.11	1.00
WT:M-MO:F	-1.07	-3.98	1.83	1.00
NT:M-MO:F	-1.36	-4.26	1.55	0.97

Table C6. (continued)

AZ:M-MO:F	-1.25	-4.26	1.76	0.99
NM:M-MO:F	-1.19	-3.86	1.48	0.98
OK:M-MO:F	-1.13	-3.97	1.70	1.00
CO:M-MO:F	-0.80	-3.49	1.89	1.00
KS:M-MO:F	-0.51	-3.42	2.39	1.00
MO:M-MO:F	-0.09	-2.78	2.60	1.00
ST:M-MX:M	1.79	-2.22	5.80	0.98
WT:M-MX:M	0.77	-3.03	4.58	1.00
NT:M-MX:M	0.49	-3.32	4.29	1.00
AZ:M-MX:M	0.59	-3.29	4.48	1.00
NM:M-MX:M	0.65	-2.97	4.28	1.00
OK:M-MX:M	0.71	-3.04	4.46	1.00
CO:M-MX:M	1.04	-2.60	4.68	1.00
KS:M-MX:M	1.33	-2.47	5.14	1.00
MO:M-MX:M	1.75	-1.89	5.40	0.96
WT:M-ST:M	-1.01	-3.55	1.52	0.99
NT:M-ST:M	-1.30	-3.84	1.23	0.94
AZ:M-ST:M	-1.19	-3.85	1.46	0.98
NM:M-ST:M	-1.13	-3.40	1.13	0.95
OK:M-ST:M	-1.08	-3.53	1.38	0.99
CO:M-ST:M	-0.75	-3.03	1.54	1.00
KS:M-ST:M	-0.46	-2.99	2.08	1.00
MO:M-ST:M	-0.03	-2.32	2.25	1.00
NT:M-WT:M	-0.29	-2.48	1.91	1.00
AZ:M-WT:M	-0.18	-2.51	2.15	1.00
NM:M-WT:M	-0.12	-1.99	1.75	1.00
OK:M-WT:M	-0.06	-2.16	2.04	1.00
CO:M-WT:M	0.27	-1.63	2.17	1.00
KS:M-WT:M	0.56	-1.64	2.75	1.00
MO:M-WT:M	0.98	-0.92	2.88	0.93
AZ:M-NT:M	0.11	-2.22	2.44	1.00
NM:M-NT:M	0.17	-1.71	2.04	1.00
OK:M-NT:M	0.23	-1.88	2.33	1.00
CO:M-NT:M	0.55	-1.35	2.46	1.00
KS:M-NT:M	0.85	-1.35	3.04	1.00
MO:M-NT:M	1.27	-0.63	3.17	0.63
NM:M-AZ:M	0.06	-1.97	2.09	1.00

Table C6. (continued)

OK:M-AZ:M	0.12	-2.12	2.36	1.00
CO:M-AZ:M	0.45	-1.61	2.50	1.00
KS:M-AZ:M	0.74	-1.59	3.07	1.00
MO:M-AZ:M	1.16	-0.89	3.22	0.86
OK:M-NM:M	0.06	-1.70	1.82	1.00
CO:M-NM:M	0.39	-1.13	1.90	1.00
KS:M-NM:M	0.68	-1.19	2.55	1.00
MO:M-NM:M	1.10	-0.42	2.62	0.47
CO:M-OK:M	0.33	-1.46	2.12	1.00
KS:M-OK:M	0.62	-1.48	2.72	1.00
MO:M-OK:M	1.04	-0.75	2.84	0.83
KS:M-CO:M	0.29	-1.61	2.19	1.00
MO:M-CO:M	0.71	-0.84	2.27	0.98
MO:M-KS:M	0.42	-1.48	2.32	1.00

Table C7. List of loadings from the PCA of bioclimatic variables for PC1-PC10.

Bioclimatic Variable	PC1	PC2	PC3	PC4	PC5	PC6	PC7	PC8	PC9	PC10
bio1	0.02	-0.07	-0.28	0.11	-0.30	0.08	-0.13	-0.01	-0.09	0.02
bio2	<0.01	0.11	0.08	0.27	0.13	-0.24	-0.38	0.30	0.03	-0.25
bio3	<0.01	0.02	0.02	0.05	<0.01	-0.07	-0.06	<0.01	0.02	-0.06
bio4	-0.99	0.07	-0.03	0.04	-0.03	0.01	0.05	-0.02	0.01	<0.01
bio5	<0.01	<0.01	-0.22	0.30	-0.10	0.14	-0.21	0.25	0.21	0.18
bio6	0.03	-0.10	-0.27	0.03	-0.27	0.19	0.17	-0.13	0.30	0.04
bio7	-0.03	0.10	0.05	0.26	0.18	-0.05	-0.38	0.38	-0.09	0.14
bio8	0.01	-0.03	-0.02	-0.09	-0.50	-0.48	0.38	0.48	-0.31	-0.10
bio9	0.05	-0.04	0.21	0.81	-0.08	-0.08	0.31	-0.30	-0.05	-0.17
bio10	0.01	-0.06	-0.28	0.14	-0.26	0.14	-0.12	0.08	<0.01	0.08
bio11	0.03	-0.06	-0.27	0.14	-0.26	0.14	-0.11	0.08	-0.01	0.12
bio12	-0.07	-0.88	-0.12	<0.01	0.14	-0.18	-0.22	-0.14	-0.20	-0.13
bio13	<0.01	-0.11	0.06	0.04	0.13	0.46	0.19	0.21	-0.50	0.34
bio14	<0.01	-0.03	-0.07	-0.01	0.09	-0.14	0.02	0.05	-0.01	-0.03
bio15	<0.01	0.03	0.17	0.04	0.04	0.15	-0.03	0.04	-0.41	0.08
bio16	-0.02	-0.29	0.33	-0.01	-0.02	0.47	0.19	0.45	0.33	-0.43
bio17	<0.01	-0.12	-0.25	-0.04	0.28	-0.21	0.19	0.25	0.30	0.11
bio18	-0.03	-0.21	0.60	-0.06	-0.38	-0.14	-0.21	-0.04	0.27	0.52
bio19	<0.01	-0.12	-0.06	0.19	0.35	-0.17	0.39	0.13	0.18	0.46

Table C8. List of loadings from the PCA of bioclimatic variables for PC11-PC19.

Bioclimatic Variable	PC11	PC12	PC13	PC14	PC15	PC16	PC17	PC18	PC19
bio1	-0.26	-0.14	0.28	0.13	0.06	-0.76	0.03	-0.14	<0.01
bio2	0.15	-0.27	0.30	-0.35	0.45	0.08	<0.01	-0.15	<0.01
bio3	0.05	0.02	0.14	-0.09	0.01	-0.17	0.09	0.96	<0.01
bio4	-0.01	-0.01	0.01	-0.02	0.01	<0.01	-0.02	<0.01	<0.01
bio5	0.23	0.40	-0.30	-0.10	0.01	-0.09	-0.02	-0.01	0.58
bio6	0.22	0.18	-0.13	-0.39	0.29	-0.02	<0.01	-0.01	-0.58
bio7	0.01	0.21	-0.16	0.29	-0.27	-0.07	-0.02	<0.01	-0.58
bio8	0.10	0.13	-0.05	0.04	0.02	0.03	-0.01	<0.01	<0.01
bio9	<0.01	-0.12	-0.16	0.07	-0.08	-0.01	-0.02	-0.01	<0.01
bio10	-0.20	-0.21	0.06	0.12	-0.04	0.43	0.70	0.03	<0.01
bio11	-0.22	-0.18	0.22	-0.06	-0.20	0.38	-0.67	0.13	<0.01
bio12	0.07	0.12	-0.03	0.03	0.03	0.06	-0.02	<0.01	<0.01
bio13	0.43	-0.33	0.01	-0.10	0.05	-0.07	0.02	0.03	<0.01
bio14	-0.05	-0.09	<0.01	-0.66	-0.68	-0.14	0.16	-0.10	<0.01
bio15	-0.65	0.25	-0.27	-0.35	0.30	0.03	0.01	0.05	<0.01
bio16	-0.16	0.03	0.11	0.04	-0.09	-0.04	0.01	<0.01	<0.01
bio17	-0.22	-0.50	-0.50	0.06	0.13	-0.12	-0.08	0.10	<0.01
bio18	-0.02	-0.17	-0.04	-0.07	<0.01	-0.04	0.01	-0.01	<0.01
bio19	-0.16	0.28	0.52	<0.01	0.08	0.04	0.07	-0.04	<0.01

Table C9. Museum ID, locality information, assigned population, and sex for specimens included in this study.

Museum Short ID	Latitude	Longitude	STATE	County	Pop	sex
TJH 4001			Texas	Motley	OK	F
LACM 105224	27.01029	-101.8502	Coahuila	Cuatro	MX	M
CM 42842	26.99	-102.02	Coahuila	Cuatro	MX	M
KU 189151	38.38416667	-96.38277778	Kansas	Chase	KS	F
UCM 2534	38.44154	-103.225951	Colorado	Kiowa	CO	M
ASU 30633	31.58103	-109.25352	Arizona	Cochise	AZ	F
KU 342507	40.08751	-95.25092	Missouri	Holt	MO	M
UCM 2682			Colorado	Kiowa	CO	M
ASU 30155	31.59385	-109.23949	Arizona	Cochise	AZ	F
KU 84562	40.08751	-95.25092	Missouri	Holt	MO	M
OMNH 41962	35.05155182	-99.85707855	Oklahoma	Beckham	OK	F
OMNH 42782	35.8685	-99.6178	Oklahoma	Ellis	OK	M
OMNH 40305	34.899071	-98.778577	Oklahoma	Kiowa	OK	F
OMNH 27103	36.81193161	-99.81890106	Oklahoma	Harper	OK	M
OMNH 42783	35.89502	-99.73369	Oklahoma	Ellis	OK	M
TCWC 77557	33.68611389	-99.078925	Texas	Baylor	NT	F
TCWC 77549	33.75486667	-98.76916944	Texas	Archer	NT	M
TCWC 77545	33.95131389	-98.79122222	Texas	Wichita	NT	M
TCWC 82547	32.783877	-103.82285	New Mexico	Eddy	WT	F
TCWC 100333	33.57219	-98.84829	Texas	Archer	NT	F
TCWC 77558	33.66996389	-99.08716111	Texas	Baylor	NT	M
TCWC 77564	33.74261389	-98.96791944	Texas	Baylor	NT	M
KU 153053	37.07535	-98.98933	Kansas	Comanche	KS	F
KU 200736	40.08751	-95.25092	Missouri	Holt	MO	M
KU 189149	38.47805556	-98.63638889	Kansas	Barton	KS	M
KU 55285			Kansas	Franklin	KS	M
TCWC 93850	27.424158	-97.299107	Texas	Kleberg	ST	M
TCWC 100334	33.54152	-98.845436	Texas	Archer	NT	F
TCWC 77573	33.71611	-98.36222	Texas	Clay	NT	M
KU 200719	40.08751	-95.25092	Missouri	Holt	MO	M
KU 319083	38.47805556	-98.63638889	Kansas	Barton	KS	F
KU 152341	38.69666667	-98.25277778	Kansas	Ellsworth	KS	M
KU 189148	39.561707	-95.121837	Kansas	Atchison	KS	F
KU 189147			Kansas	Chase	KS	F
KU 84564	40.08751	-95.25092	Missouri	Holt	MO	M
KU 84566	40.08751	-95.25092	Missouri	Holt	MO	M

Table C9. (continued)

KU 84565	40.08751	-95.25092	Missouri	Holt	MO	M
KU 191979	38.66722222	-97.99805556	Kansas	Ellsworth	KS	M
KU 348940	37.7925	-97.8276	Kansas	Barton	KS	M
KU 191973	38.74222222	-97.98388889	Kansas	Ellsworth	KS	F
KU 84572	40.08751	-95.25092	Missouri	Holt	MO	M
KU 84573	40.08751	-95.25092	Missouri	Holt	MO	F
UCM 52026	38.247623	-103.516047	Colorado	Crowley	CO	M
UCM 25642	38.851817	-103.681799	Colorado	Lincoln	CO	M
TNHC 088027			Texas	Gaines	WT	F
TNHC 088023	33.643054	-103.374683	New Mexico	Roosevelt	WT	F
TNHC 088018	32.19053	-102.728899	Texas	Andrews	WT	F
TNHC 088022	32.175019	-102.765053	Texas	Andrews	WT	M
TNHC 33884	31.950577	-102.971581	Texas	Winkler	WT	F
OMNH 019664	36.97212982	-99.44739532	Oklahoma	Harper	OK	M
MSB 63046	35.12331	-106.8265	New Mexico	Bernalillo	NM	M
MSB 76465			New Mexico	Socorro	NM	M
MSB 52129	34.797498	-106.691526	New Mexico	Socorro	NM	M
MSB 30928	34.56167	-106.64966	New Mexico	Valencia	NM	F
MSB 55142	33.88437	-106.66453	New Mexico	Socorro	NM	F
MSB 56032	34.57441	-106.74889	New Mexico	Socorro	NM	M
MSB 55162	34.8135	-106.73352	New Mexico	Valencia	NM	M
MSB 19811	34.471669	-106.561839	New Mexico	Valencia	NM	M
MSB 52891	34.35021	-106.88378	New Mexico	Socorro	NM	F
KU 055282			Kansas	Franklin	KS	F
KU 342508	40.08751	-95.25092	Missouri	Holt	MO	F
KU 191974	38.66722222	-97.99805556	Kansas	Ellsworth	KS	M
TCWC 93898	27.41679	-97.30681	Texas	Kleberg	ST	F
TCWC 100736	31.421672	-102.832749	Texas	Ward	WT	M
TCWC 94857	32.9775925	-103.9385139	New Mexico	Chaves	WT	M
TCWC 77568	33.78260278	-98.84948056	Texas	Archer	NT	F
TCWC 22811	27.55218889	-97.24904444	Texas	Kleberg	ST	F
TCWC 93899	27.47374	-97.28467	Texas	Kleberg	ST	F
TCWC 93812	27.576453	-97.231297	Texas	Kleberg	ST	F
CM 52767	26.88	-102.08	Coahuila	Cuatro	MX	F
ASU 30584	31.548	-109.27892	Arizona	Cochise	AZ	F
ASU 30631	31.58554	-109.24867	Arizona	Cochise	AZ	M
ASU 30632	31.53366	-109.29297	Arizona	Cochise	AZ	M

Table C9. (continued)

ASU 30877	31.57661	-109.25665	Arizona	Cochise	AZ	M
ASU 30578	31.55488	-109.26717	Arizona	Cochise	AZ	M
ASU 30157	31.5415	-109.28622	Arizona	Cochise	AZ	M
ASU 10379	26.90842	-102.02839	Coahuila	Cuatro	MX	F
ASU 30626	31.58791	-109.24605	Arizona	Cochise	AZ	F
ASU 30169	31.55373	-109.26845	Arizona	Cochise	AZ	F
ASU 30583	31.59525	-109.23795	Arizona	Cochise	AZ	F
ASU 30636	31.55662	-109.26564	Arizona	Cochise	AZ	M
ASU 30163	31.59207	-109.24145	Arizona	Cochise	AZ	F
ASU 30637	31.57758	-109.25599	Arizona	Cochise	AZ	F
ASU 30624	31.57816	-109.2556	Arizona	Cochise	AZ	M
UCM 42373	38.849309	-103.485653	Colorado	Lincoln	CO	F
OMNH 42780	35.87393	-99.68023	Oklahoma	Ellis	OK	M
OMNH 42854	35.610067	-99.61686	Oklahoma	Roger Mills	OK	F
OMNH 13186	34.88505936	-98.70344543	Oklahoma	Kiowa	OK	F
OMNH 42853	35.610069	-99.631516	Oklahoma	Roger Mills	OK	F
OMNH 34833			Oklahoma	Harmon	OK	M
OMNH 27076	36.81222916	-99.90860748	Oklahoma	Harper	OK	M
TCWC 77556	33.64423889	-98.81751944	Texas	Archer	NT	M
TCWC 82548	33.76583333	-103.17	New Mexico	Roosevelt	WT	M
TCWC 77565	33.98162778	-99.15928611	Texas	Wilbarger	NT	M
TCWC 100218			Texas	Jim hogg	ST	M
TCWC 97771	27.09735	-98.589547	Texas	Jim hogg	ST	M
TCWC 77559	33.69943056	-98.47022222	Texas	Archer	NT	F
KU 340274	40.08751	-95.25092	Missouri	Holt	MO	M
KU 84569	40.08751	-95.25092	Missouri	Holt	MO	M
KU 52262	38.1477	-95.27608	Kansas	Anderson	KS	M
KU 340275	40.08751	-95.25092	Missouri	Holt	MO	F
TCWC 100693	31.464513	-102.90383	Texas	Ward	WT	M
TCWC 97997	32.12301	-102.72954	Texas	Andrews	WT	F
TCWC 94962	32.79278	-103.81867	New Mexico	Eddy	WT	M
TCWC 77566	34.01967222	-99.10693056	Texas	Wilbarger	NT	F
TCWC 100793	31.607877	-103.0255469	Texas	Ward	WT	M
TCWC 77552	33.64423889	-98.81751944	Texas	Archer	NT	F
TCWC 33390	27.09270556	-97.79047222	Texas	Kenedy	ST	M
UCM 61448	38.876849	-103.274135	Colorado	Lincoln	CO	M
UCM 42250	38.097606	-103.666042	Colorado	Otero	CO	M

Table C9. (continued)

UCM 19755	38.181948	-103.597668	Colorado	Crowley	CO	M
UCM 2684			Colorado	Kiowa	CO	F
UCM 19973	38.605775	-102.785973	Colorado	Cheyenne	CO	M
UCM 61452	38.328148	-103.488991	Colorado	Kiowa	CO	F
UCM 19754	38.827404	-103.102053	Colorado	Cheyenne	CO	M
UCM 61453	38.328148	-103.488991	Colorado	Kiowa	CO	M
UCM 61450	38.936619	-103.400884	Colorado	Lincoln	CO	M
UCM 19756	38.617647	-103.705508	Colorado	Lincoln	CO	F
TNHC 088019	32.512935	-102.226591	Texas	Andrews	WT	F
TNHC 090044	33.391852	-102.758624	Texas	Yoakum	WT	M
TNHC 090043	33.391852	-102.758624	Texas	Yoakum	WT	M
MSB 75546			New Mexico	Socorro	NM	M
MSB 72085	34.66126	-106.69221	New Mexico	Valencia	NM	M
MSB 53027	34.35019	-106.88379	New Mexico	Socorro	NM	M
MSB 54112	34.41017	-106.64492	New Mexico	Socorro	NM	M
MSB 75831			New Mexico	Bernalillo	NM	M
KU 191975	38.66722222	-97.99805556	Kansas	Ellsworth	KS	F
TCWC 33391	27.02583333	-98.20611	Texas	Brooks	ST	M
TCWC 77567	33.72915278	-98.69499444	Texas	Archer	NT	M
TCWC 93849	27.467322	-97.298854	Texas	Kleberg	WT	M

Code C1. This code performs Procrustes superimposition for dorsal and lateral skull landmarks by group, then ordinates that data. Univariate MANOVAs and Tukey's tests for shape, external measurements, and bioclimatic variables are also included, as is code for a correlation plot of all numerical and shape morphologic data.

```
#make sure to install required packages
library(devtools)
library(geomorph)
library(shapes)
library(ggplot2)
library(reshape2)
library(rgdal)
library(raster)
library(rgeos)
library(dplyr)
library(sp)
library(car)
library(phytools)
library(picante)
library(RColorBrewer)
library(ggbiplot)
library(corrplot)
getwd()
setwd("D:/Massasauga/")

dpygmy<-read.csv("Massasauga_DorsTPS_Data.csv", header=T)
head(dpygmy)

dlandmarks<-readland.tps("dorsalskullsistrurus.TPS")

###DORSAL###
plot(dlandmarks[,,1], xlim = c(0,600), ylim = c(0,600), cex=2)

text(dlandmarks[,,1], labels=1:22)
dA <- 1:3
dB <- 4:7
dC <- 8:18
dD <- 19:20

for(i in 2:length(dlandmarks[1,1,])){
  points(dlandmarks[,,i], col=i, cex=2)
}
```

```
proc<-gpagen(dlandmarks)
procA<-procGPA(dlandmarks[dA,,])
procB<-procGPA(dlandmarks[dB,,])
procC<-procGPA(dlandmarks[dC,,])
procD<-procGPA(dlandmarks[dD,,])

combo <- data.frame("A" = procA$stdscores, "B" = procB$stdscores, "C" =
procC$stdscores, "D" = procD$stdscores)
head(combo)

procA$percent
procB$percent
procC$percent
procD$percent

#par(cex=1.0)
#(pch = 16)
#par(col = "royalblue", bg="white")
plot(procA$mshape, xlab="X", ylab="Y")
text(procA$mshape,labels=1:3, pos = 2)
plot(procB$mshape, xlab="X", ylab="Y")
text(procB$mshape, labels=4:7, pos = 2)
plot(procC$mshape, xlab="X", ylab="Y")
text(procC$mshape, labels = 8:18, pos = )
plot(procD$mshape, xlab="X", ylab="Y")
text(procD$mshape, labels = 19:20, pos = )

plot(proc)
#plot(procD)

dpygmy$ssp=as.factor(dpygmy$ssp)
dpygmy$Pop=as.factor(dpygmy$Pop)

par(cex=1.0)
par(pch=16)
pal <- c("turquoise", "green", "blue", "darkorange1", "black", "yellow", "purple4", "red",
"darkred", "grey")
plot(procA$stdscores[,1], procA$stdscores[,2], xlab= "PC1", ylab="PC2", xlim=c(-2,
3.5), col = pal[dpygmy$Pop])
legend('bottomright', legend=levels(dpygmy$Pop), col = seq_along(dpygmy$Pop),
cex=1.0, pch=20)
text(procA$stdscores[,1], procA$stdscores[,2], labels = rownames(dpygmy), cex= 0.75)
```

```
pcaxis <- 2
sd_mag <- 3
plotRefToTarget(-sd_mag*sd(procA$scores[,pcaxis])*procA$pcar[,pcaxis] +
procA$mshape, sd_mag*sd(procA$scores[,pcaxis])*procA$pcar[,pcaxis] +
procA$mshape, method="vector")

pcaxis <- 2
sd_mag <- 3
plotRefToTarget(-sd_mag*sd(procB$scores[,pcaxis])*procB$pcar[,pcaxis] +
procB$mshape, sd_mag*sd(procB$scores[,pcaxis])*procB$pcar[,pcaxis] +
procB$mshape, method="vector")

pcaxis <- 3
sd_mag <- 3
plotRefToTarget(-sd_mag*sd(procC$scores[,pcaxis])*procC$pcar[,pcaxis] +
procC$mshape, sd_mag*sd(procC$scores[,pcaxis])*procC$pcar[,pcaxis] +
procC$mshape, method="vector")

tpsgrid(procA$rotated[,,10], procA$rotated[,,29], col=1, mag =1, cex = 3) #left to right
tpsgrid(procA$rotated[,,113], procA$rotated[,,54], col=1, mag =1, cex = 3) #max left to
right

tpsgrid(procA$rotated[,,113], procA$rotated[,,113], col=4, mag =1, cex = 3) #max left to
right
tpsgrid(procA$rotated[,,54], procA$rotated[,,54], col=4, mag =1, cex = 3) #max left to
right

tpsgrid(procA$rotated[,,1], procA$rotated[,,57], col=1, mag=1, cex=3) #bot to top
tpsgrid(procA$rotated[,,1], procA$rotated[,,1], col=4, mag=1, cex=3) #bot to top
tpsgrid(procA$rotated[,,57], procA$rotated[,,57], col=4, mag=1, cex=3) #bot to top


par(cex=1.0)
par(pch=16)
cols = c("deepskyblue", "orange", "gray", "darkgreen", "blue", "red", "black", "brown",
"yellow", "chartreuse" ,"gold1", "blueviolet", "orchid1", "hotpink", "darkblue", "cyan",
"wheat")
plot(procB$stdscores[,1], procB$stdscores[,2], xlab= "PC1", ylab="PC2", col=
dpygmy$Pop)
legend('bottomright', legend=levels(dpygmy$Pop), col = seq_along(dpygmy$Pop),
cex=1.0, pch=20)
text(procB$stdscores[,1], procB$stdscores[,2], cex= 0.75, labels = rownames(dpygmy))

tpsgrid(procB$rotated[,,4], procB$rotated[,,81], col=1, mag=1, cex=3)
```

```
tpsgrid(procB$rotated[,,107], procB$rotated[,,81], col=1, mag=1, cex=3) #PC1 Max
tpsgrid(procB$rotated[,,107], procB$rotated[,,107], col=3, mag=1, cex=3)
tpsgrid(procB$rotated[,,81], procB$rotated[,,81], col=3, mag=1, cex=3)

tpsgrid(procB$rotated[,,1], procB$rotated[,,93], col=1, mag=1, cex=3)
tpsgrid(procB$rotated[,,1], procB$rotated[,,1], col=3, mag=1, cex=3)
tpsgrid(procB$rotated[,,93], procB$rotated[,,93], col=3, mag=1, cex=3)

par(cex=1.0)
par(pch=16)
cols = c("deepskyblue", "orange", "gray", "darkgreen", "blue", "red", "black", "brown",
"yellow", "chartreuse" ,"gold1", "blueviolet", "orchid1", "hotpink", "darkblue", "cyan",
"wheat")
plot(procC$stdscores[,1], procC$stdscores[,2], xlab= "PC1", ylab="PC2", col=
dpygmy$Pop)
legend('bottomright', legend=levels(dpygmy$Pop), col = seq_along(dpygmy$Pop),
cex=1.0, pch=20)
text(procC$stdscores[,1], procC$stdscores[,2], cex= 0.75, labels = rownames(dpygmy))

plot(procC$stdscores[,3], procC$stdscores[,4], xlab= "PC3", ylab="PC4", col=
dpygmy$Pop)
legend('bottomright', legend=levels(dpygmy$Pop), col = seq_along(dpygmy$Pop),
cex=1.0, pch=20)
text(procC$stdscores[,3], procC$stdscores[,4], cex= 0.75, pos = 1, labels =
rownames(dpygmy))

tpsgrid(procC$rotated[,,55], procC$rotated[,,4], col=1, mag=1, cex=3)
tpsgrid(procC$rotated[,,55], procC$rotated[,,55], col=2, mag=1, cex=3)
tpsgrid(procC$rotated[,,4], procC$rotated[,,4], col=2, mag=1, cex=3)

#tpsgrid(procC$rotated[,,79], procC$rotated[,,63], col=1, mag=1, cex=3)
tpsgrid(procC$rotated[,,106], procC$rotated[,,93], col=1, mag=1, cex=3)
tpsgrid(procC$rotated[,,42], procC$rotated[,,35], col=1, mag=1, cex=3)
tpsgrid(procC$rotated[,,106], procC$rotated[,,106], col=2, mag=1, cex=3)
tpsgrid(procC$rotated[,,93], procC$rotated[,,93], col=2, mag=1, cex=3)
tpsgrid(procC$rotated[,,42], procC$rotated[,,42], col=2, mag=1, cex=3)
tpsgrid(procC$rotated[,,35], procC$rotated[,,35], col=2, mag=1, cex=3)


library(RColorBrewer)
dpygmy$Pop <- factor(dpygmy$Pop, levels = c("MX", "ST", "AZ", "WT", "NT", "NM",
"OK", "CO", "KS", "MO"), ordered = T)
pca_out <- cbind.data.frame(procC$stdscores[, 1:3], population = dpygmy$Pop)
```

```
p <- ggplot(pca_out, aes(x=PC1, y=PC3, color=population)) + geom_point(size = 4) +
scale_color_brewer(palette = "Set3")
p

############################
pal <- c("turquoise", "green", "blue", "darkorange1", "black", "yellow", "purple4", "red",
"darkred", "grey")


#Group A
plot(dpygmy$Longitude, procA$stdscores[,1], xlab="Longitude", xlim = c(-110, -90),
ylab="PC1", col=pal[dpygmy$Pop])
legend('bottomright', legend=levels(dpygmy$Pop), col = pal, cex=1.25, pch=16)
text(dpygmy$Longitude, procA$stdscores[,1], cex= 0.75, labels = rownames(dpygmy))

plot(dpygmy$Latitude, procA$stdscores[,1], xlab="Latitude", ylab="PC1", xlim= c(25,
45), col=pal[dpygmy$Pop])
legend('bottomright', legend=levels(dpygmy$Pop), col = pal, cex=1.0, pch=20)
text(dpygmy$Latitude, procA$stdscores[,1], cex= 0.75, labels = rownames(dpygmy))

plot(dpygmy$Longitude, procA$stdscores[,2], xlab="Longitude", ylab="PC2", xlim =
c(-110, -90), col=pal[dpygmy$Pop])
legend('bottomright', legend=levels(dpygmy$Pop), col = seq_along(dpygmy$Pop),
cex=1.0, pch=20)

plot(dpygmy$Latitude, procA$stdscores[,2], xlab="Latitude", ylab="PC2", xlim= c(24,
44), col=pal[dpygmy$Pop])
legend('bottomright', legend=levels(dpygmy$Pop), col = seq_along(dpygmy$Pop),
cex=1.0, pch=20)

#Group B
plot(dpygmy$Longitude, procB$stdscores[,1], xlab="Longitude", ylab="PC1", xlim =
c(-110, -90), col=pal[dpygmy$Pop])
legend('bottomright', legend=levels(dpygmy$Pop), col = seq_along(dpygmy$Pop),
cex=1.0, pch=20)

plot(dpygmy$Latitude, procB$stdscores[,1], xlab="Latitude", ylab="PC1", xlim= c(24,
44), col=pal[dpygmy$Pop])
legend('bottomright', legend=levels(dpygmy$Pop), col = seq_along(dpygmy$Pop),
cex=1.0, pch=20)

plot(dpygmy$Longitude, procB$stdscores[,2], xlab="Longitude", ylab="PC2", xlim =
c(-110, -90), col=pal[dpygmy$Pop])
```

```
legend('bottomright', legend=levels(dpygmy$Pop), col = seq_along(dpygmy$Pop),
cex=1.0, pch=20)

plot(dpygmy$Latitude, procB$stdscores[,2], xlab="Latitude", ylab="PC2", xlim= c(24,
44), col=pal[dpygmy$Pop])
legend('bottomright', legend=levels(dpygmy$Pop), col = seq_along(dpygmy$Pop),
cex=1.0, pch=20)

#Group C
plot(dpygmy$Longitude, procC$stdscores[,1], xlab="Longitude", ylab="PC1", xlim =
c(-110, -90), col=pal[dpygmy$Pop])
legend('bottomright', legend=levels(dpygmy$Pop), col = seq_along(dpygmy$Pop),
cex=1.0, pch=20)

plot(dpygmy$Latitude, procC$stdscores[,1], xlab="Latitude", ylab="PC1", xlim= c(24,
44), col=pal[dpygmy$Pop])
legend('bottomright', legend=levels(dpygmy$Pop), col = seq_along(dpygmy$Pop),
cex=1.0, pch=20)

plot(dpygmy$Longitude, procC$stdscores[,2], xlab="Longitude", ylab="PC2", xlim =
c(-110, -90), col=pal[dpygmy$Pop])
legend('bottomright', legend=levels(dpygmy$Pop), col = seq_along(dpygmy$Pop),
cex=1.0, pch=20)

plot(dpygmy$Latitude, procC$stdscores[,2], xlab="Latitude", ylab="PC2", xlim= c(24,
44), col=pal[dpygmy$Pop])
legend('bottomright', legend=levels(dpygmy$Pop), col = seq_along(dpygmy$Pop),
cex=1.0, pch=20)

plot(dpygmy$Longitude, procC$stdscores[,3], xlab="Longitude", ylab="PC3", xlim =
c(-110, -90), col=pal[dpygmy$Pop])
legend('bottomright', legend=levels(dpygmy$Pop), col = seq_along(dpygmy$Pop),
cex=1.0, pch=20)

plot(dpygmy$Latitude, procC$stdscores[,3], xlab="Latitude", ylab="PC3", xlim= c(24,
44), col=pal[dpygmy$Pop])
legend('bottomright', legend=levels(dpygmy$Pop), col = seq_along(dpygmy$Pop),
cex=1.0, pch=20)


dpygmy$Pop <- factor(dpygmy$Pop, levels = c("MX", "ST", "AZ", "WT", "NT", "NM",
"OK", "CO", "KS", "MO"), ordered = T)
BXPLT <- cbind.data.frame(procA$stdscores[, 1:2], population = dpygmy$Pop)
```

```
ggplot(data = BXPLT, aes(x = population, y = PC1)) + scale_fill_brewer(palette="Set3")
+ geom_boxplot(aes(fill =
population))+xlab("population")+theme(text=element_text(size=16))
ggplot(data = BXPLT, aes(x = population, y = PC2)) + scale_fill_brewer(palette="Set3")
+ geom_boxplot(aes(fill =
population))+xlab("population")+theme(text=element_text(size=16))

BXPLT <- cbind.data.frame(procB$stdscores[, 1:2], pop = dpygmy$Pop)
ggplot(data = BXPLT, aes(x = pop, y = PC1)) + scale_fill_brewer(palette="Set3") +
geom_boxplot(aes(fill = pop))+xlab("population")+theme(text=element_text(size=16))
ggplot(data = BXPLT, aes(x = pop, y = PC2)) + scale_fill_brewer(palette="Set3") +
geom_boxplot(aes(fill = pop))+xlab("population")+theme(text=element_text(size=16))

BXPLT <- cbind.data.frame(procC$stdscores[, 1:3], pop = dpygmy$Pop)
ggplot(data = BXPLT, aes(x = pop, y = PC1)) + scale_fill_brewer(palette="Set3") +
geom_boxplot(aes(fill = pop))+xlab("population")+theme(text=element_text(size=16))
ggplot(data = BXPLT, aes(x = pop, y = PC2)) + scale_fill_brewer(palette="Set3") +
geom_boxplot(aes(fill = pop))+xlab("population")+theme(text=element_text(size=16))
ggplot(data = BXPLT, aes(x = pop, y = PC3)) + scale_fill_brewer(palette="Set3") +
geom_boxplot(aes(fill = pop))+xlab("population")+theme(text=element_text(size=16))



BXPLT <- cbind.data.frame(procA$stdscores[, 1:2], sex = dpygmy$sex)
ggplot(data = BXPLT, aes(x = sex, y = PC1)) + scale_fill_brewer(palette="Set3") +
geom_boxplot(aes(fill = sex))+xlab("sex")+theme(text=element_text(size=16))
ggplot(data = BXPLT, aes(x = sex, y = PC2)) + scale_fill_brewer(palette="Set3") +
geom_boxplot(aes(fill = sex))+xlab("sex")+theme(text=element_text(size=16))

BXPLT <- cbind.data.frame(procB$stdscores[, 1:2], sex = dpygmy$sex)
ggplot(data = BXPLT, aes(x = sex, y = PC1)) + scale_fill_brewer(palette="Set3") +
geom_boxplot(aes(fill = sex))+xlab("sex")+theme(text=element_text(size=16))
ggplot(data = BXPLT, aes(x = sex, y = PC2)) + scale_fill_brewer(palette="Set3") +
geom_boxplot(aes(fill = sex))+xlab("sex")+theme(text=element_text(size=16))

BXPLT <- cbind.data.frame(procC$stdscores[, 1:3], sex = dpygmy$sex)
ggplot(data = BXPLT, aes(x = sex, y = PC1)) + scale_fill_brewer(palette="Set3") +
geom_boxplot(aes(fill = sex))+xlab("sex")+theme(text=element_text(size=16))
ggplot(data = BXPLT, aes(x = sex, y = PC2)) + scale_fill_brewer(palette="Set3") +
geom_boxplot(aes(fill = sex))+xlab("sex")+theme(text=element_text(size=16))
ggplot(data = BXPLT, aes(x = sex, y = PC3)) + scale_fill_brewer(palette="Set3") +
geom_boxplot(aes(fill = sex))+xlab("sex")+theme(text=element_text(size=16))
```

```
#ANOVA
#Group A
summary(aov(procA$stdscores[,1]~dpygmy$Pop*dpygmy$sex))
summary(aov(procA$stdscores[,2]~dpygmy$Pop*dpygmy$sex))
#Group B
summary(aov(procB$stdscores[,1]~dpygmy$Pop*dpygmy$sex))
summary(aov(procB$stdscores[,2]~dpygmy$Pop*dpygmy$sex))
#Group C
summary(aov(procC$stdscores[,1]~dpygmy$Pop*dpygmy$sex))
summary(aov(procC$stdscores[,2]~dpygmy$Pop*dpygmy$sex))
summary(aov(procC$stdscores[,3]~dpygmy$Pop*dpygmy$sex))

capture.output(summary(aov(procC$stdscores[,3]~dpygmy$Pop*dpygmy$sex)),
file="dc3")


tukey.test <- TukeyHSD(aov(procC$stdscores[,3]~dpygmy$Pop*dpygmy$sex))
tukey.test
#plot(tukey.test)
#summary(tukey.test)

capture.output(tukey.test, file="tukeydc3")


###DFA###
#function for creating a confusion matrix for the DFA results
confusion <- function(actual, predicted, names = NULL, prinit = T, prior = NULL) {
  if(is.null(names)) names <- levels(actual)
  tab <- table(actual, predicted)
  acctab <- t(apply(tab, 1, function(x)x/sum(x)))
  dimnames(acctab) <- list(Actual = names, Predicted = names)
  if(is.null(prior)) {
    relnum <- table(actual)
    prior <- relnum /sum(relnum)
    acc <- sum(tab[row(tab)==col(tab)])/sum(tab)
  } else {
    acc <- sum(prior*diag(acctab))
    names(prior) <- names
  }
  if(prinit) print(round(c("Overall accuracy" = acc, "Prior frequency" = prior), 4))
  if(prinit) {
    cat("\nConfusion matrix", "\n")
    print(round(acctab, 4))
```

```
  }
  invisible(acctab)
}

#below grabs  info (switch or add whatever is needed) fix later
getOption("max.print")

SVAL <- cbind.data.frame(pop = dpygmy$Pop, sex = dpygmy$sex, combo[,1:40])
DFA <- MASS::lda(SVAL$pop ~ ., data = SVAL[, c(3:6, 9:14, 17:36, 39:40)], CV = T)
confusion(SVAL$pop, DFA$class)

DFA2<- MASS::lda(SVAL$sex ~ ., data = SVAL[, c(3:4)], CV = T)
confusion(SVAL$sex, DFA2$class)


###END DORSAL#####################################################



###LATERAL#########################################################
lpygmy<-read.csv("Massasauga_TPS_Lat.csv", header=T)
head(lpygmy)

llandmarks<-readland.tps("LftLatskullsistrurus2.TPS")


plot(llandmarks[,,1], xlim = c(0,650), ylim = c(0,600), cex=2)


text(llandmarks[,,1], labels=1:22)
lA <- 1:3
lB <- 4:16
lC <- 17:22
lD <- 15:16
lE<-c(16,22)

for(i in 2:length(llandmarks[1,1,])){
  points(llandmarks[,,i], col=i, cex=2)
}

lproc<-gpagen(llandmarks)

#par(cex=1.0)
#par(pch = 16)
```

```
#par(col = "royalblue", bg="white")
#plot(lproc)

lprocA<-procGPA(llandmarks[lA,,])
lprocB<-procGPA(llandmarks[lB,,])
lprocC<-procGPA(llandmarks[lC,,])
#lprocD<-procGPA(llandmarks[lD,,])
#lprocE<-procGPA(llandmarks[lE,,])
#shapepca(proc_landmarks, pcno = c(1:2), type="v", mag = 2) #vector plots at 2x mag
(is that 2sd, or no?)

lcombo <- data.frame("A" = lprocA$stdscores, "B" = lprocB$stdscores, "C" =
lprocC$stdscores)
head(lcombo)

lprocA$percent
lprocB$percent
lprocC$percent

plot(lprocA$mshape, xlab="X", ylab="Y")
text(lprocA$mshape,labels=1:3)
plot(lprocB$mshape, xlab="X", ylab="Y")
text(lprocB$mshape, labels=4:16)
plot(lprocC$mshape, xlab="X", ylab="Y")
text(lprocC$mshape, labels = 17:22)


lpygmy$Pop=as.factor(lpygmy$Pop)

par(cex=1.0)
par(pch=16)
cols = c("deepskyblue", "orange", "gray", "darkgreen", "blue", "red", "black", "brown",
"yellow", "chartreuse" ,"gold1", "blueviolet", "orchid1", "hotpink", "darkblue", "cyan",
"wheat")
plot(lprocA$stdscores[,1], lprocA$stdscores[,2], xlab= "PC1", ylab="PC2", col=
lpygmy$Pop)
legend('bottomright', legend=levels(lpygmy$Pop), col = seq_along(lpygmy$Pop),
cex=1.0, pch=20)
text(lprocA$stdscores[,1], lprocA$stdscores[,2], cex= 0.75, labels = rownames(lpygmy))

pcaxis <- 2
sd_mag <- 3
```

```
plotRefToTarget(-sd_mag*sd(lprocA$scores[,pcaxis])*lprocA$pcar[,pcaxis] +
lprocA$mshape, sd_mag*sd(lprocA$scores[,pcaxis])*lprocA$pcar[,pcaxis] +
lprocA$mshape, method="vector")

pcaxis <- 4
sd_mag <- 3
plotRefToTarget(-sd_mag*sd(lprocB$scores[,pcaxis])*lprocB$pcar[,pcaxis] +
lprocB$mshape, sd_mag*sd(lprocB$scores[,pcaxis])*lprocB$pcar[,pcaxis] +
lprocB$mshape, method="vector")

pcaxis <- 2
sd_mag <- 3
plotRefToTarget(-sd_mag*sd(lprocC$scores[,pcaxis])*lprocC$pcar[,pcaxis] +
lprocC$mshape, sd_mag*sd(lprocC$scores[,pcaxis])*lprocC$pcar[,pcaxis] +
lprocC$mshape, method="vector")

tpsgrid(lprocA$rotated[,,35], lprocA$rotated[,,45], col=1, mag =1, cex = 3) #max
tpsgrid(lprocA$rotated[,,35], lprocA$rotated[,,33], col=1, mag =1, cex = 3) #left to right
tpsgrid(lprocA$rotated[,,35], lprocA$rotated[,,35], col=4, mag =1, cex = 3)
tpsgrid(lprocA$rotated[,,45], lprocA$rotated[,,45], col=4, mag =1, cex = 3)

tpsgrid(lprocA$rotated[,,49], lprocA$rotated[,,64], col=1, mag=1, cex=3) #bot to top
tpsgrid(lprocA$rotated[,,49], lprocA$rotated[,,26], col=1, mag=1, cex=3) #bot to top
tpsgrid(lprocA$rotated[,,49], lprocA$rotated[,,49], col=4, mag=1, cex=3)
tpsgrid(lprocA$rotated[,,64], lprocA$rotated[,,64], col=4, mag=1, cex=3)

par(cex=1.0)
par(pch=16)
cols = c("deepskyblue", "orange", "gray", "darkgreen", "blue", "red", "black", "brown",
"yellow", "chartreuse" ,"gold1", "blueviolet", "orchid1", "hotpink", "darkblue", "cyan",
"wheat")
plot(lprocB$stdscores[,1], lprocB$stdscores[,2], xlab= "PC1", ylab="PC2", col=
lpygmy$Pop)
legend('bottomright', legend=levels(lpygmy$Pop), col = seq_along(lpygmy$Pop),
cex=1.0, pch=20)
text(lprocB$stdscores[,1], lprocB$stdscores[,2], cex= 0.75, labels = rownames(lpygmy))

plot(lprocB$stdscores[,3], lprocB$stdscores[,4], xlab= "PC3", ylab="PC4", col=
lpygmy$Pop)
legend('bottomright', legend=levels(lpygmy$Pop), col = seq_along(lpygmy$Pop),
cex=1.0, pch=20)
text(lprocB$stdscores[,3], lprocB$stdscores[,4], cex= 0.75, labels = rownames(lpygmy))

tpsgrid(lprocB$rotated[,,1], lprocB$rotated[,,24], col=1, mag =1, cex = 3) #left to right
```

```
tpsgrid(lprocB$rotated[,,1], lprocB$rotated[,,1], col=2, mag =1, cex = 3)
tpsgrid(lprocB$rotated[,,24], lprocB$rotated[,,24], col=2, mag =1, cex = 3)

tpsgrid(lprocB$rotated[,,14], lprocB$rotated[,,69], col=1, mag=1, cex=3) #bot to top
tpsgrid(lprocB$rotated[,,14], lprocB$rotated[,,14], col=2, mag=1, cex=3) #bot to top
tpsgrid(lprocB$rotated[,,69], lprocB$rotated[,,69], col=2, mag=1, cex=3) #bot to top

tpsgrid(lprocB$rotated[,,54], lprocB$rotated[,,1], col=1, mag =1, cex = 3) #left to right
tpsgrid(lprocB$rotated[,,54], lprocB$rotated[,,54], col=2, mag =1, cex = 3) #left to right
tpsgrid(lprocB$rotated[,,1], lprocB$rotated[,,1], col=2, mag =1, cex = 3) #left to right

tpsgrid(lprocB$rotated[,,18], lprocB$rotated[,,53], col=1, mag=1, cex=3) #bot to top
tpsgrid(lprocB$rotated[,,18], lprocB$rotated[,,18], col=2, mag=1, cex=3) #bot to top
tpsgrid(lprocB$rotated[,,53], lprocB$rotated[,,53], col=2, mag=1, cex=3) #bot to top



par(cex=1.0)
par(pch=16)
cols = c("deepskyblue", "orange", "gray", "darkgreen", "blue", "red", "black", "brown",
"yellow", "chartreuse" ,"gold1", "blueviolet", "orchid1", "hotpink", "darkblue", "cyan",
"wheat")
plot(lprocC$stdscores[,1], lprocC$stdscores[,2], xlab= "PC1", ylab="PC2", col=
lpygmy$Pop)
legend('bottomright', legend=levels(lpygmy$Pop), col = seq_along(lpygmy$Pop),
cex=1.0, pch=20)
text(lprocC$stdscores[,1], lprocC$stdscores[,2], cex= 0.75, labels = rownames(lpygmy))

tpsgrid(lprocC$rotated[,,9], lprocC$rotated[,,59], col=1, mag =1, cex = 3) #left to right
tpsgrid(lprocC$rotated[,,1], lprocC$rotated[,,79], col=1, mag =1, cex = 3) #left to right
tpsgrid(lprocC$rotated[,,1], lprocC$rotated[,,1], col=3, mag =1, cex = 3) #left to right
tpsgrid(lprocC$rotated[,,79], lprocC$rotated[,,79], col=3, mag =1, cex = 3) #left to right



tpsgrid(lprocC$rotated[,,41], lprocC$rotated[,,85], col=1, mag=1, cex=3) #bot to top
tpsgrid(lprocC$rotated[,,41], lprocC$rotated[,,47], col=1, mag=1, cex=3) #bot to top
tpsgrid(lprocC$rotated[,,41], lprocC$rotated[,,41], col=3, mag=1, cex=3) #bot to top
tpsgrid(lprocC$rotated[,,47], lprocC$rotated[,,47], col=3, mag=1, cex=3) #bot to top

lpygmy$Pop <- factor(lpygmy$Pop, levels = c("MX", "ST", "AZ", "WT", "NT", "NM",
"OK", "CO", "KS", "MO"), ordered = T)
pca_out <- cbind.data.frame(lprocC$stdscores[, 1:2], population = lpygmy$Pop)
```

```
l <- ggplot(pca_out, aes(x=PC1, y=PC2, color=population)) + geom_point(size = 4) +
scale_color_brewer(palette = "Set3")
l


pal <- c("turquoise", "green", "blue", "darkorange1", "black", "yellow", "purple4", "red",
"darkred", "grey")



plot(lpygmy$Longitude, lprocA$stdscores[,1], xlab="Longitude", ylab="PC1", xlim =
c(-110, -90), col=pal[lpygmy$Pop])
legend('bottomright', legend=levels(lpygmy$Pop), col=pal, cex=1.0, pch=20)
text(lpygmy$Longitude, lprocA$stdscores[,1], cex= 0.75, labels = rownames(lpygmy))

plot(lpygmy$Latitude, lprocA$stdscores[,1], xlab="Latitude", ylab="PC1", xlim= c(24,
44), col=pal[lpygmy$Pop])
legend('bottomright', legend=levels(lpygmy$Pop), col = pal, cex=1.0, pch=20)
text(lpygmy$Latitude, lprocA$stdscores[,1], cex= 0.75, labels = rownames(lpygmy))

plot(lpygmy$Longitude, lprocA$stdscores[,2], xlab="Longitude", ylab="PC2", xlim =
c(-110, -90), col=pal[lpygmy$Pop])
legend('bottomright', legend=levels(lpygmy$Pop), col = seq_along(lpygmy$Pop),
cex=1.0, pch=20)

plot(lpygmy$Latitude, lprocA$stdscores[,2], xlab="Latitude", ylab="PC2", xlim= c(24,
44), col=pal[lpygmy$Pop])
legend('bottomright', legend=levels(lpygmy$Pop), col = seq_along(lpygmy$Pop),
cex=1.0, pch=20)

plot(lpygmy$Longitude, lprocB$stdscores[,1], xlab="Longitude", ylab="PC1", xlim =
c(-110, -90), col=pal[lpygmy$Pop])
legend('bottomright', legend=levels(lpygmy$Pop), col = seq_along(lpygmy$Pop),
cex=1.0, pch=20)

plot(lpygmy$Latitude, lprocB$stdscores[,1], xlab="Latitude", ylab="PC1", xlim= c(24,
44), col=pal[lpygmy$Pop])
legend('bottomright', legend=levels(lpygmy$Pop), col = seq_along(lpygmy$Pop),
cex=1.0, pch=20)

plot(lpygmy$Longitude, lprocB$stdscores[,2], xlab="Longitude", ylab="PC2", xlim =
c(-110, -90), col=pal[lpygmy$Pop])
```

```
legend('bottomright', legend=levels(lpygmy$Pop), col = seq_along(lpygmy$Pop),
cex=1.0, pch=20)

plot(lpygmy$Latitude, lprocB$stdscores[,2], xlab="Latitude", ylab="PC2", xlim= c(24,
44), col=pal[lpygmy$Pop])
legend('bottomright', legend=levels(lpygmy$Pop), col = seq_along(lpygmy$Pop),
cex=1.0, pch=20)

plot(lpygmy$Longitude, lprocB$stdscores[,3], xlab="Longitude", ylab="PC3", xlim =
c(-110, -90), col=pal[lpygmy$Pop])
legend('bottomright', legend=levels(lpygmy$Pop), col = seq_along(lpygmy$Pop),
cex=1.0, pch=20)

plot(lpygmy$Latitude, lprocB$stdscores[,3], xlab="Latitude", ylab="PC3", xlim= c(24,
44), col=pal[lpygmy$Pop])
legend('bottomright', legend=levels(lpygmy$Pop), col = seq_along(lpygmy$Pop),
cex=1.0, pch=20)

plot(lpygmy$Longitude, lprocB$stdscores[,4], xlab="Longitude", ylab="PC4", xlim =
c(-110, -90), col=pal[lpygmy$Pop])
legend('bottomright', legend=levels(lpygmy$Pop), col = seq_along(lpygmy$Pop),
cex=1.0, pch=20)

plot(lpygmy$Latitude, lprocB$stdscores[,4], xlab="Latitude", ylab="PC4", xlim= c(24,
44), col=pal[lpygmy$Pop])
legend('bottomright', legend=levels(lpygmy$Pop), col = seq_along(lpygmy$Pop),
cex=1.0, pch=20)

plot(lpygmy$Longitude, lprocC$stdscores[,1], xlab="Longitude", ylab="PC1", xlim =
c(-110, -90), col=pal[lpygmy$Pop])
legend('bottomright', legend=levels(lpygmy$Pop), col = seq_along(lpygmy$Pop),
cex=1.0, pch=20)

plot(lpygmy$Latitude, lprocC$stdscores[,1], xlab="Latitude", ylab="PC1", xlim= c(24,
44), col=pal[lpygmy$Pop])
legend('bottomright', legend=levels(lpygmy$Pop), col = seq_along(lpygmy$Pop),
cex=1.0, pch=20)

plot(lpygmy$Longitude, lprocC$stdscores[,2], xlab="Longitude", ylab="PC2", xlim =
c(-110, -90), col=pal[lpygmy$Pop])
legend('bottomright', legend=levels(lpygmy$Pop), col = seq_along(lpygmy$Pop),
cex=1.0, pch=20)
```

```
plot(lpygmy$Latitude, lprocC$stdscores[,2], xlab="Latitude", ylab="PC2", xlim= c(24, 44), col=pal[lpygmy$Pop])
legend('bottomright', legend=levels(lpygmy$Pop), col = seq_along(lpygmy$Pop), cex=1.0, pch=20)

BXPLT <- cbind.data.frame(lprocA$stdscores[, 1:2], pop = lpygmy$Pop)
ggplot(data = BXPLT, aes(x = pop, y = PC1)) + scale_fill_brewer(palette="Set3") +
geom_boxplot(aes(fill = pop))+xlab("population")+theme(text=element_text(size=16))
ggplot(data = BXPLT, aes(x = pop, y = PC2)) + scale_fill_brewer(palette="Set3") +
geom_boxplot(aes(fill = pop))+xlab("population")+theme(text=element_text(size=16))

BXPLT <- cbind.data.frame(lprocB$stdscores[, 1:4], pop = lpygmy$Pop)
ggplot(data = BXPLT, aes(x = pop, y = PC1)) + scale_fill_brewer(palette="Set3") +
geom_boxplot(aes(fill = pop))+xlab("population")+theme(text=element_text(size=16))
ggplot(data = BXPLT, aes(x = pop, y = PC2)) + scale_fill_brewer(palette="Set3") +
geom_boxplot(aes(fill = pop))+xlab("population")+theme(text=element_text(size=16))
ggplot(data = BXPLT, aes(x = pop, y = PC3)) + scale_fill_brewer(palette="Set3") +
geom_boxplot(aes(fill = pop))+xlab("population")+theme(text=element_text(size=16))
ggplot(data = BXPLT, aes(x = pop, y = PC4)) + scale_fill_brewer(palette="Set3") +
geom_boxplot(aes(fill = pop))+xlab("population")+theme(text=element_text(size=16))

lpygmy$Pop<- factor(lpygmy$Pop, levels = c("MX", "ST", "WT", "NT", "AZ", "NM", "OK", "CO", "KS", "MO"), ordered = T)
BXPLT <- cbind.data.frame(lprocC$stdscores[, 1:2], pop = lpygmy$Pop)
ggplot(data = BXPLT, aes(x = pop, y = PC1)) + scale_fill_brewer(palette="Set3") +
geom_boxplot(aes(fill = pop))+xlab("population")+theme(text=element_text(size=16))
ggplot(data = BXPLT, aes(x = pop, y = PC2)) + scale_fill_brewer(palette="Set3") +
geom_boxplot(aes(fill = pop))+xlab("population")+theme(text=element_text(size=16))

##
BXPLT <- cbind.data.frame(lprocA$stdscores[, 1:2], sex = lpygmy$sex)
ggplot(data = BXPLT, aes(x = sex, y = PC1)) + scale_fill_brewer(palette="Set3") +
geom_boxplot(aes(fill = sex))+xlab("sex")+theme(text=element_text(size=16))
ggplot(data = BXPLT, aes(x = sex, y = PC2)) + scale_fill_brewer(palette="Set3") +
geom_boxplot(aes(fill = sex))+xlab("sex")+theme(text=element_text(size=16))

BXPLT <- cbind.data.frame(lprocB$stdscores[, 1:4], sex = lpygmy$sex)
ggplot(data = BXPLT, aes(x = sex, y = PC1)) + scale_fill_brewer(palette="Set3") +
geom_boxplot(aes(fill = sex))+xlab("sex")+theme(text=element_text(size=16))
ggplot(data = BXPLT, aes(x = sex, y = PC2)) + scale_fill_brewer(palette="Set3") +
geom_boxplot(aes(fill = sex))+xlab("sex")+theme(text=element_text(size=16))
ggplot(data = BXPLT, aes(x = sex, y = PC3)) + scale_fill_brewer(palette="Set3") +
geom_boxplot(aes(fill = sex))+xlab("sex")+theme(text=element_text(size=16))
```

```
ggplot(data = BXPLT, aes(x = sex, y = PC4)) + scale_fill_brewer(palette="Set3") +
geom_boxplot(aes(fill = sex))+xlab("sex")+theme(text=element_text(size=16))

BXPLT <- cbind.data.frame(lprocC$stdscores[, 1:2], sex = lpygmy$sex)
ggplot(data = BXPLT, aes(x = sex, y = PC1)) + scale_fill_brewer(palette="Set3") +
geom_boxplot(aes(fill = sex))+xlab("sex")+theme(text=element_text(size=16))
ggplot(data = BXPLT, aes(x = sex, y = PC2)) + scale_fill_brewer(palette="Set3") +
geom_boxplot(aes(fill = sex))+xlab("sex")+theme(text=element_text(size=16))

#PCAL <- plotTangentSpace(lproc$coords, label = T, group = lpygmy$ssp, axis1=1,
axis2 = 2, legend=TRUE)
#PCAL$pc.summary
#PCAL$pc.scores[,1]

#PC1 changes, max and y=0
#tpsgrid(lproc$consensus, lproc$coords[,,75], col=1, mag =1.5, cex = 2.0)
#tpsgrid(lproc$consensus, lproc$coords[,,68], col=1, mag = 1, cex = 2.0)
#tpsgrid(lproc$coords[,,75], lproc$coords[,,68], col=1, mag =1, cex = 2.0)

#tpsgrid(lproc$consensus, lproc$coords[,,6], col=1, mag =1, cex = 2)
#tpsgrid(lproc$consensus, lproc$coords[,,68], col=1, mag = 1, cex = 2)

#PC2 changes, max and y=0
#tpsgrid(lproc$consensus, lproc$coords[,,1], col=1, mag =2, cex = 1.5)
#tpsgrid(lproc$consensus, lproc$coords[,,31], col=1, mag = 2, cex = 1.5)
#tpsgrid(lproc$coords[,,1], lproc$coords[,,31], col=1, mag = 1, cex = 2.0)

#tpsgrid(lproc$consensus, lproc$coords[,,78], col=1, mag =2, cex = 2)
#tpsgrid(lproc$consensus, lproc$coords[,,37], col=1, mag = 2, cex = 2)
#tpsgrid(lproc$coords[,,78], lproc$coords[,,37], col=1, mag = 2, cex = 2.0)



summary(aov(lprocA$stdscores[,1]~lpygmy$Pop*lpygmy$sex))
summary(aov(lprocA$stdscores[,2]~lpygmy$Pop*lpygmy$sex))

summary(aov(lprocB$stdscores[,1]~lpygmy$Pop*lpygmy$sex))
summary(aov(lprocB$stdscores[,2]~lpygmy$Pop*lpygmy$sex))
summary(aov(lprocB$stdscores[,3]~lpygmy$Pop*lpygmy$sex))
summary(aov(lprocB$stdscores[,4]~lpygmy$Pop*lpygmy$sex))

summary(aov(lprocC$stdscores[,1]~lpygmy$Pop*lpygmy$sex))
summary(aov(lprocC$stdscores[,2]~lpygmy$Pop*lpygmy$sex))
```

```
capture.output(summary(aov(lprocC$stdscores[,2]~lpygmy$Pop*lpygmy$sex)),
file="lc2")

tukey.test <- TukeyHSD(aov(lprocC$stdscores[,2]~lpygmy$Pop*lpygmy$sex))
tukey.test
#plot(tukey.test)
#summary(tukey.test)

capture.output(tukey.test, file="tukeylc2")

###boxplots###
#need to fix collection in excel#
#BXPLT <- cbind.data.frame(PCAL$pc.scores[, 1:2], collection = lpygmy$Collection)
#ggplot(data = BXPLT, aes(x = collection, y = PC1)) +
geom_boxplot()+xlab("Collection")+theme(text=element_text(size=16))
#ggplot(data = BXPLT, aes(x = collection, y = PC2)) +
geom_boxplot()+xlab("Collection")+theme(text=element_text(size=16))

#BXPLT <- cbind.data.frame(altPCAL$stdscores[, 1:2], ssp = lpygmy$ssp)
#ggplot(data = BXPLT, aes(x = ssp, y = PC1)) + scale_fill_brewer(palette="Accent") +
geom_boxplot(aes(fill = ssp))+xlab("subspecies")+theme(text=element_text(size=16))
#ggplot(data = BXPLT, aes(x = ssp, y = PC2)) + scale_fill_brewer(palette="Accent") +
geom_boxplot(aes(fill = ssp))+xlab("subspecies")+theme(text=element_text(size=16))

#BXPLT <- cbind.data.frame(altPCAL$stdscores[, 1:2], sex = lpygmy$sex)
#ggplot(data = BXPLT, aes(x = sex, y = PC1)) + scale_fill_brewer(palette="Set2") +
geom_boxplot(aes(fill = sex))+xlab("sex")+theme(text=element_text(size=16))
#ggplot(data = BXPLT, aes(x = sex, y = PC2)) + scale_fill_brewer(palette="Set2") +
geom_boxplot(aes(fill = sex))+xlab("sex")+theme(text=element_text(size=16))

#BXPLT <- cbind.data.frame(altPCAL$stdscores[, 1:2], pop = lpygmy$Pop)
#ggplot(data = BXPLT, aes(x = pop, y = PC1)) + scale_fill_brewer(palette="Set3") +
geom_boxplot(aes(fill = pop))+xlab("population")+theme(text=element_text(size=16))
#ggplot(data = BXPLT, aes(x = pop, y = PC2)) + scale_fill_brewer(palette="Set3") +
geom_boxplot(aes(fill = pop))+xlab("population")+theme(text=element_text(size=16))

#BXPLT <- cbind.data.frame(altPCAL$stdscores[, 1:2], pop = lpygmy$State)
#ggplot(data = BXPLT, aes(x = pop, y = PC1)) + scale_fill_brewer(palette="Paired") +
geom_boxplot()+xlab("state")+theme(text=element_text(size=16))
#ggplot(data = BXPLT, aes(x = pop, y = PC2)) + scale_fill_brewer(palette="Paired") +
geom_boxplot()+xlab("state")+theme(text=element_text(size=16))

###DFA### fix later
#function for creating a confusion matrix for the DFA results
```

```
confusion <- function(actual, predicted, names = NULL, prinit = T, prior = NULL) {
  if(is.null(names)) names <- levels(actual)
  tab <- table(actual, predicted)
  acctab <- t(apply(tab, 1, function(x)x/sum(x)))
  dimnames(acctab) <- list(Actual = names, Predicted = names)
  if(is.null(prior)) {
    relnum <- table(actual)
    prior <- relnum /sum(relnum)
    acc <- sum(tab[row(tab)==col(tab)])/sum(tab)
  } else {
    acc <- sum(prior*diag(acctab))
    names(prior) <- names
  }
  if(prinit) print(round(c("Overall accuracy" = acc, "Prior frequency" = prior), 4))
  if(prinit) {
    cat("\nConfusion matrix", "\n")
    print(round(acctab, 4))
  }
  invisible(acctab)
}

#below grabs  info (switch or add whatever is needed)
getOption("max.print")

SVAL <- cbind.data.frame(sex = lpygmy$sex, pop =  lpygmy$Pop, lcombo[, 1:44])

DFA<- MASS::lda(SVAL$sex ~ ., data = SVAL[, c(3:6,9:32,35:44)], CV = T)
confusion(SVAL$sex, DFA$class)

DFA2<- MASS::lda(SVAL$pop ~ ., data = SVAL[, c(3:6,9:32,35:44)], CV = T)
confusion(SVAL$pop, DFA2$class)



################################################

################################################
all.meas <- read.csv("Massasauga morphology data_CLEAN.csv", header = T)
#myData <- all.meas[-c(32, 34, 44, 64, 66, 68, 74, 102, 128), ] #removed specimens
without HW measurements
#all.meas <- myData[-c(32, 34, 44, 64, 66, 68, 74, 102, 128), ]
head(all.meas)

all.meas.dfa <- na.omit(all.meas[,c(6:27, 29, 34)])
```

```
################################################
################################################
################################################
all.meas$Museum.Short.ID <- as.character(all.meas$Museum.Short.ID)
combo <- combo[,c(1:2, 7:8, 15:17)]
dpygmy <- cbind(dpygmy, combo)

lcombo <- lcombo[,c(1:2, 7:10, 33:34)]
lpygmy <- cbind(lpygmy, lcombo)

dpygmy$Museum.Short.ID <- as.character(dpygmy$Museum.Short.ID)
lpygmy$Museum.Short.ID <- as.character(lpygmy$Museum.Short.ID)



cbind(all.meas$Museum.Short.ID,
dpygmy$Museum.Short.ID[match(all.meas$Museum.Short.ID,
dpygmy$Museum.Short.ID)])
cbind(all.meas$Museum.Short.ID,
lpygmy$Museum.Short.ID[match(all.meas$Museum.Short.ID,
lpygmy$Museum.Short.ID)])

#d_bagel <- cbind(all.meas, dpygmy[match(all.meas$Museum.Short.ID,
dpygmy$Museum.Short.ID), ])
bagel <- cbind(all.meas, dpygmy[match(all.meas$Museum.Short.ID,
dpygmy$Museum.Short.ID), ], lpygmy[match(all.meas$Museum.Short.ID,
lpygmy$Museum.Short.ID), ])
head(bagel)
bagel <- na.omit(bagel[,c(7:27, 29,56:62, 82:89)])
head(bagel)
################################################
################################################


all.meas2 <- na.omit(all.meas[,c(7:9,11:27, 29)]) #remove columns with NAs; remove 6
if cannot use categorical
head(all.meas2)


#all.meas <- all.meas[,c(-1,-23]
dim(all.meas2)
head(all.meas2)
#PCA
```

```
#desperate.meas <-read.csv("avg_median_meas.csv", header = T)
#head(desperate.meas)

#any(is.na(all.meas))
#any(is.na(desperate.meas))

all.meas.pca <- prcomp(all.meas2, center = TRUE, scale = TRUE)
summary(all.meas.pca)

#plot(desperate.meas.pca$x[,1], desperate.meas.pca$x[,2], col= c("cyan", "darkgreen",
"gray", "orange", "blue", "red", "black", "brown", "darkorchid1", "chartreuse4"
,"darkgoldenrod1", "blueviolet", "orchid1", "hotpink", "darkblue", "deepskyblue",
"burlywood4"))

ggbiplot(all.meas.pca, ellipses=T)
all.meas.pca$rotation
ggbiplot(all.meas.pca, choices=c(3,4))

#ANOVA
all.meas <- read.csv("Massasauga morphology data_CLEAN.csv", header = T)

summary(aov(all.meas$SVL~all.meas$Pop*all.meas$sex))
summary(aov(all.meas$Tail~all.meas$Pop*all.meas$sex))
summary(aov(all.meas$HL~all.meas$Pop*all.meas$sex))
summary(aov(all.meas$HW~all.meas$Pop*all.meas$sex))
summary(aov(all.meas$SL~all.meas$Pop*all.meas$sex))
summary(aov(all.meas$EPD~all.meas$Pop*all.meas$sex))
summary(aov(all.meas$ISD~all.meas$Pop*all.meas$sex))
summary(aov(all.meas$Eye~all.meas$Pop*all.meas$sex))
summary(aov(all.meas$BRW~all.meas$Pop*all.meas$sex))
summary(aov(all.meas$MBL~all.meas$Pop*all.meas$sex))
summary(aov(all.meas$MBI~all.meas$Pop*all.meas$sex))
summary(aov(all.meas$Vent~all.meas$Pop*all.meas$sex))
summary(aov(all.meas$SubC~all.meas$Pop*all.meas$sex))
summary(aov(all.meas$DSRN~all.meas$Pop*all.meas$sex))
summary(aov(all.meas$DSRM~all.meas$Pop*all.meas$sex))
summary(aov(all.meas$DSRC~all.meas$Pop*all.meas$sex))
summary(aov(all.meas$RFS~all.meas$Pop*all.meas$sex))
summary(aov(all.meas$SLab~all.meas$Pop*all.meas$sex))
summary(aov(all.meas$ILab~all.meas$Pop*all.meas$sex))
summary(aov(all.meas$DBB~all.meas$Pop*all.meas$sex))
summary(aov(all.meas$TB~all.meas$Pop*all.meas$sex))
summary(aov(all.meas$Vpat.~all.meas$Pop*all.meas$sex))
```

```
capture.output(summary(aov(all.meas$Vpat.~all.meas$Pop*all.meas$sex)),
file="VPAT")


confusion <- function(actual, predicted, names = NULL, prinit = T, prior = NULL) {
  if(is.null(names)) names <- levels(actual)
  tab <- table(actual, predicted)
  acctab <- t(apply(tab, 1, function(x)x/sum(x)))
  dimnames(acctab) <- list(Actual = names, Predicted = names)
  if(is.null(prior)) {
    relnum <- table(actual)
    prior <- relnum /sum(relnum)
    acc <- sum(tab[row(tab)==col(tab)])/sum(tab)
  } else {
    acc <- sum(prior*diag(acctab))
    names(prior) <- names
  }
  if(prinit) print(round(c("Overall accuracy" = acc, "Prior frequency" = prior), 4))
  if(prinit) {
    cat("\nConfusion matrix", "\n")
    print(round(acctab, 4))
  }
  invisible(acctab)
}

getOption("max.print")

SVAL <- cbind.data.frame(sex = all.meas.dfa$sex, pop =  all.meas.dfa$Pop,
all.meas.dfa[,c(2:23)])

DFA<- MASS::lda(SVAL$sex ~ ., data = SVAL[, 3:24], CV = T)
confusion(SVAL$sex, DFA$class)

DFA2<- MASS::lda(SVAL$pop ~ ., data = SVAL[, 3:24], CV = T)
confusion(SVAL$pop, DFA2$class)

####bioclim variables
bioclim <- raster::getData('worldclim', var="bio", res=2.5)

bc_points <- data.frame(raster::extract(bioclim, data.frame(lpygmy$Longitude,
lpygmy$Latitude)))
head(bc_points)
#bc_points <- na.omit(bc_points)
#sum(is.na(bc_points))
```

```
plot(log(bc_points$bio1), lprocB$stdscores[,1])
abline(lm(lprocC$stdscores[,1:2] ~ bc_points$bio1))
summary(lm(lprocC$stdscores[,1:2] ~ bc_points$bio1))

summary(lm(lprocA$stdscores[,1:2] ~ bc_points$bio4+bc_points$bio12))
summary(lm(lprocB$stdscores[,1:4] ~ bc_points$bio4+bc_points$bio12))
summary(lm(lprocC$stdscores[,1:2] ~ bc_points$bio4+bc_points$bio12))

capture.output(summary(lm(lprocA$stdscores[,1:2] ~
bc_points$bio4+bc_points$bio12)), file="biola")

bc_points2 <- data.frame(raster::extract(bioclim, data.frame(dpygmy$Longitude,
dpygmy$Latitude)))
head(bc_points2)

plot(log(bc_points2$bio1), procC$stdscores[,1])
abline(lm(procC$stdscores[,1] ~ bc_points2$bio1))


summary(lm(procA$stdscores[,1:2] ~ bc_points2$bio4+bc_points2$bio12))
summary(lm(procB$stdscores[,1:2] ~ bc_points2$bio4+bc_points2$bio12))
summary(lm(procC$stdscores[,1:3] ~ bc_points2$bio4+bc_points2$bio12))

capture.output(summary(lm(procC$stdscores[,1:3] ~
bc_points2$bio4+bc_points2$bio12)), file="biodc")



all.meas.redo <- read.csv("Massasauga morphology data_CLEAN.csv", header = T)
bc_points3 <- data.frame(raster::extract(bioclim, data.frame(all.meas.redo$Longitude,
all.meas.redo$Latitude)))
#(all.meas.redo[,7] + all.meas.redo[,8] + all.meas.redo[,9] + all.meas.redo[,10]
  # + all.meas.redo[,11] + all.meas.redo[,12] + all.meas.redo[,13] + all.meas.redo[,14] +
all.meas.redo[,15]
   #+ all.meas.redo[,16] + all.meas.redo[,17] + all.meas.redo[,18] + all.meas.redo[,19] +
all.meas.redo[,20]
  # + all.meas.redo[,21] + all.meas.redo[,22] + all.meas.redo[,23] + all.meas.redo[,24] +
all.meas.redo[,25]
  # + all.meas.redo[,26] + all.meas.redo[,27] + all.meas.redo[,29])

summary(lm(bc_points3$bio1 ~ all.meas.redo[,7] + all.meas.redo[,8] + all.meas.redo[,9]
+ all.meas.redo[,10]
```

```
        + all.meas.redo[,11] + all.meas.redo[,12] + all.meas.redo[,13] +
all.meas.redo[,14] + all.meas.redo[,15]
        + all.meas.redo[,16] + all.meas.redo[,17] + all.meas.redo[,18] +
all.meas.redo[,19] + all.meas.redo[,20]
        + all.meas.redo[,21] + all.meas.redo[,22] + all.meas.redo[,23] +
all.meas.redo[,24] + all.meas.redo[,25]
        + all.meas.redo[,26] + all.meas.redo[,27] + all.meas.redo[,29])) #7-29
summary(lm(bc_points3$bio2 ~ all.meas.redo[,7] + all.meas.redo[,8] + all.meas.redo[,9]
+ all.meas.redo[,10]
        + all.meas.redo[,11] + all.meas.redo[,12] + all.meas.redo[,13] +
all.meas.redo[,14] + all.meas.redo[,15]
        + all.meas.redo[,16] + all.meas.redo[,17] + all.meas.redo[,18] +
all.meas.redo[,19] + all.meas.redo[,20]
        + all.meas.redo[,21] + all.meas.redo[,22] + all.meas.redo[,23] +
all.meas.redo[,24] + all.meas.redo[,25]
        + all.meas.redo[,26] + all.meas.redo[,27] + all.meas.redo[,29])) #7-29
#summary(lm(bc_points3$bio3 ~ all.meas.redo[,29])) #7-29
summary(lm(bc_points3$bio4 ~ all.meas.redo[,7] + all.meas.redo[,8] + all.meas.redo[,9]
+ all.meas.redo[,10]
        + all.meas.redo[,11] + all.meas.redo[,12] + all.meas.redo[,13] +
all.meas.redo[,14] + all.meas.redo[,15]
        + all.meas.redo[,16] + all.meas.redo[,17] + all.meas.redo[,18] +
all.meas.redo[,19] + all.meas.redo[,20]
        + all.meas.redo[,21] + all.meas.redo[,22] + all.meas.redo[,23] +
all.meas.redo[,24] + all.meas.redo[,25]
        + all.meas.redo[,26] + all.meas.redo[,27] + all.meas.redo[,29])) #7-29
#summary(lm(bc_points3$bio5 ~ all.meas.redo[,29])) #7-29
summary(lm(bc_points3$bio6 ~ all.meas.redo[,7] + all.meas.redo[,8] + all.meas.redo[,9]
+ all.meas.redo[,10]
        + all.meas.redo[,11] + all.meas.redo[,12] + all.meas.redo[,13] +
all.meas.redo[,14] + all.meas.redo[,15]
        + all.meas.redo[,16] + all.meas.redo[,17] + all.meas.redo[,18] +
all.meas.redo[,19] + all.meas.redo[,20]
        + all.meas.redo[,21] + all.meas.redo[,22] + all.meas.redo[,23] +
all.meas.redo[,24] + all.meas.redo[,25]
        + all.meas.redo[,26] + all.meas.redo[,27] + all.meas.redo[,29])) #7-29
summary(lm(bc_points3$bio7 ~ all.meas.redo[,7] + all.meas.redo[,8] + all.meas.redo[,9]
+ all.meas.redo[,10]
        + all.meas.redo[,11] + all.meas.redo[,12] + all.meas.redo[,13] +
all.meas.redo[,14] + all.meas.redo[,15]
        + all.meas.redo[,16] + all.meas.redo[,17] + all.meas.redo[,18] +
all.meas.redo[,19] + all.meas.redo[,20]
        + all.meas.redo[,21] + all.meas.redo[,22] + all.meas.redo[,23] +
all.meas.redo[,24] + all.meas.redo[,25]
```

```
        + all.meas.redo[,26] + all.meas.redo[,27] + all.meas.redo[,29])) #7-29
#summary(lm(bc_points3$bio8 ~ all.meas.redo[,29])) #7-29
summary(lm(bc_points3$bio9 ~ all.meas.redo[,7] + all.meas.redo[,8] + all.meas.redo[,9]
+ all.meas.redo[,10]
        + all.meas.redo[,11] + all.meas.redo[,12] + all.meas.redo[,13] +
all.meas.redo[,14] + all.meas.redo[,15]
        + all.meas.redo[,16] + all.meas.redo[,17] + all.meas.redo[,18] +
all.meas.redo[,19] + all.meas.redo[,20]
        + all.meas.redo[,21] + all.meas.redo[,22] + all.meas.redo[,23] +
all.meas.redo[,24] + all.meas.redo[,25]
        + all.meas.redo[,26] + all.meas.redo[,27] + all.meas.redo[,29])) #7-29
#summary(lm(bc_points3$bio10 ~ all.meas.redo[,29])) #7-29
summary(lm(bc_points3$bio11 ~ all.meas.redo[,7] + all.meas.redo[,8] +
all.meas.redo[,9] + all.meas.redo[,10]
        + all.meas.redo[,11] + all.meas.redo[,12] + all.meas.redo[,13] +
all.meas.redo[,14] + all.meas.redo[,15]
        + all.meas.redo[,16] + all.meas.redo[,17] + all.meas.redo[,18] +
all.meas.redo[,19] + all.meas.redo[,20]
        + all.meas.redo[,21] + all.meas.redo[,22] + all.meas.redo[,23] +
all.meas.redo[,24] + all.meas.redo[,25]
        + all.meas.redo[,26] + all.meas.redo[,27] + all.meas.redo[,29])) #7-29
summary(lm(bc_points3$bio12 ~ all.meas.redo[,7] + all.meas.redo[,8] +
all.meas.redo[,9] + all.meas.redo[,10]
        + all.meas.redo[,11] + all.meas.redo[,12] + all.meas.redo[,13] +
all.meas.redo[,14] + all.meas.redo[,15]
        + all.meas.redo[,16] + all.meas.redo[,17] + all.meas.redo[,18] +
all.meas.redo[,19] + all.meas.redo[,20]
        + all.meas.redo[,21] + all.meas.redo[,22] + all.meas.redo[,23] +
all.meas.redo[,24] + all.meas.redo[,25]
        + all.meas.redo[,26] + all.meas.redo[,27] + all.meas.redo[,29])) #7-29
summary(lm(log(bc_points3$bio12) ~ all.meas.redo[,7] + all.meas.redo[,8] +
all.meas.redo[,9] + all.meas.redo[,10]
        + all.meas.redo[,11] + all.meas.redo[,12] + all.meas.redo[,13] +
all.meas.redo[,14] + all.meas.redo[,15]
        + all.meas.redo[,16] + all.meas.redo[,17] + all.meas.redo[,18] +
all.meas.redo[,19] + all.meas.redo[,20]
        + all.meas.redo[,21] + all.meas.redo[,22] + all.meas.redo[,23] +
all.meas.redo[,24] + all.meas.redo[,25]
        + all.meas.redo[,26] + all.meas.redo[,27] + all.meas.redo[,29]))
#summary(lm(bc_points3$bio13 ~ all.meas.redo[,29])) #7-29
#summary(lm(bc_points3$bio14 ~ all.meas.redo[,29])) #7-29
#summary(lm(bc_points3$bio15 ~ all.meas.redo[,29])) #7-29
summary(lm(bc_points3$bio16 ~ all.meas.redo[,7] + all.meas.redo[,8] +
all.meas.redo[,9] + all.meas.redo[,10]
```

```
        + all.meas.redo[,11] + all.meas.redo[,12] + all.meas.redo[,13] +
all.meas.redo[,14] + all.meas.redo[,15]
        + all.meas.redo[,16] + all.meas.redo[,17] + all.meas.redo[,18] +
all.meas.redo[,19] + all.meas.redo[,20]
        + all.meas.redo[,21] + all.meas.redo[,22] + all.meas.redo[,23] +
all.meas.redo[,24] + all.meas.redo[,25]
        + all.meas.redo[,26] + all.meas.redo[,27] + all.meas.redo[,29])) #7-29
#summary(lm(bc_points3$bio17 ~ all.meas.redo[,29])) #7-29
summary(lm(bc_points3$bio18 ~ all.meas.redo[,7] + all.meas.redo[,8] +
all.meas.redo[,9] + all.meas.redo[,10]
        + all.meas.redo[,11] + all.meas.redo[,12] + all.meas.redo[,13] +
all.meas.redo[,14] + all.meas.redo[,15]
        + all.meas.redo[,16] + all.meas.redo[,17] + all.meas.redo[,18] +
all.meas.redo[,19] + all.meas.redo[,20]
        + all.meas.redo[,21] + all.meas.redo[,22] + all.meas.redo[,23] +
all.meas.redo[,24] + all.meas.redo[,25]
        + all.meas.redo[,26] + all.meas.redo[,27] + all.meas.redo[,29])) #7-29
#summary(lm(bc_points3$bio19 ~ all.meas.redo[,29])) #7-29


capture.output(summary(lm(bc_points3$bio18 ~ all.meas.redo[,7] + all.meas.redo[,8] +
all.meas.redo[,9] + all.meas.redo[,10]
                + all.meas.redo[,11] + all.meas.redo[,12] + all.meas.redo[,13] +
all.meas.redo[,14] + all.meas.redo[,15]
                + all.meas.redo[,16] + all.meas.redo[,17] + all.meas.redo[,18] +
all.meas.redo[,19] + all.meas.redo[,20]
                + all.meas.redo[,21] + all.meas.redo[,22] + all.meas.redo[,23] +
all.meas.redo[,24] + all.meas.redo[,25]
                + all.meas.redo[,26] + all.meas.redo[,27] + all.meas.redo[,29])),
file="biopca1")
######

optional <- bc_points[,-c(4)]

all.bioclim.pca <- prcomp(bc_points)
optional.pca <- prcomp(optional)

ggbiplot(all.bioclim.pca, ellipses=T)
ggbiplot(all.bioclim.pca, choices=c(2,1))

ggbiplot(optional.pca, ellipses=T)
#Correlations
```

```
bagel <- na.omit(bagel[,c(7:9,11:27, 29)]) #remove columns with NAs; remove 6 if
cannot use categorical
head(all.meas)
acor <- cor(procA$stdscores, method = "pearson")
round(acor, 2)
bcor <- cor(procB$stdscores, method = "pearson")
round(bcor, 2)
ccor <- cor(procC$stdscores, method = "pearson")
round(bcor, 2)

lacor <- cor(lprocA$stdscores, method = "pearson")
round(acor, 2)
lbcor <- cor(lprocB$stdscores, method = "pearson")
round(bcor, 2)
lccor <- cor(lprocC$stdscores, method = "pearson")
round(bcor, 2)


col1<-colorRampPalette(c("purple", "white", "darkgreen"))
mcor <- cor(all.meas, method = "pearson")
round(mcor, 2)

corrplot(mcor, method="square", col=col1(10))

#run lines 706 to 735 and no other lines between there and here
hardcor <- cor(bagel, method = "pearson")
round(bagel, 2)
corrplot(hardcor, method = "square", type = 'lower', diag = FALSE, col=col1(10),
tl.cex=0.75, tl.col="black")
```

APPENDIX D

SUPPLEMENTAL MATERIAL FOR CHAPTER 5

Appendix D contents:

Table D1. Summary of statistics for phylogenetically informed ANOVAs between the first six PCs and individual substrate ecologies.

Foraging Habitat	Estimate	Std. Error	t	Pr (>|t|)
PC1				
Aquatic	-0.16	0.30	-0.53	0.60
Arboreal	0.55	0.48	1.13	0.26
Fossorial	1.11	0.30	3.76	<0.01
Semiaquatic	0.29	0.24	1.20	0.23
Semiarboreal	0.73	0.38	1.92	0.06
Semifossorial	0.92	0.26	3.51	<0.01
Terrestrial	0.57	0.25	2.27	0.03
PC2				
Aquatic	0.05	0.33	0.15	0.88
Arboreal	-0.12	0.54	-0.23	0.82
Fossorial	0.72	0.33	2.17	0.03
Semiaquatic	0.21	0.27	0.79	0.43
Semiarboreal	0.02	0.43	0.05	0.96
Semifossorial	1.05	0.29	3.59	<0.01
Terrestrial	0.30	0.28	1.09	0.28
PC3				
Aquatic	-0.07	0.45	-0.17	0.87
Arboreal	0.83	0.71	1.17	0.25
Fossorial	0.61	0.48	1.26	0.21
Semiaquatic	0.10	0.45	-0.50	0.62
Semiarboreal	0.09	0.58	0.16	0.87
Semifossorial	-0.34	0.44	-0.77	0.45
Terrestrial	-0.11	0.44	-0.25	0.81
PC4				
Aquatic	0.61	0.46	1.32	0.19
Arboreal	-0.28	0.76	-0.37	0.71
Fossorial	-0.03	0.46	-0.07	0.94

Table D1. (continued)

Semiaquatic	-0.31	0.38	-0.83	0.41
Semiarboreal	-0.27	0.60	-0.46	0.65
Semifossorial	-0.49	0.41	-1.18	0.24
Terrestrial	-0.24	0.39	-0.63	0.53
PC5				
Aquatic	-0.12	0.46	-0.25	0.80
Arboreal	-1.07	0.73	-1.47	0.15
Fossorial	0.10	0.48	0.22	0.83
Semiaquatic	-0.79	0.42	-1.87	0.07
Semiarboreal	0.59	0.59	1.01	0.31
Semifossorial	0.27	0.44	0.61	0.54
Terrestrial	-0.57	0.43	-1.33	0.19
PC6				
Aquatic	-0.70	0.38	-1.83	0.07
Arboreal	-1.12	0.62	-1.82	0.07
Fossorial	0.28	0.39	0.71	0.48
Semiaquatic	0.16	0.34	0.49	0.62
Semiarboreal	0.71	0.49	1.44	0.15
Semifossorial	-0.07	0.35	-0.19	0.85
Terrestrial	0.22	0.34	0.65	0.52
PC1-PC6				
Aquatic	-0.38	1.05	-0.37	0.72
Arboreal	-1.23	1.69	-0.72	0.47
Fossorial	2.55	1.08	2.37	0.02
Semiaquatic	-0.64	0.92	-0.69	0.49
Semiarboreal	1.83	1.34	1.36	0.18
Semifossorial	1.56	0.97	1.60	0.11
Terrestrial	0.07	0.94	0.08	0.94

Table D2. Results of MANOVA statistical models for PCs 1-6 and bioclimatic variables.

Bioclimatic Variable	F	df	p	Adj. R^2
Mean Annual Temperature				
PC 1-6	1629	4565	<0.01	0.68
PC1	343	4570	<0.01	0.07
PC2	945.1	4570	<0.01	0.17
PC3	1754	4570	<0.01	0.28
PC4	260.7	4570	<0.01	0.05
PC5	1653	4570	<0.01	0.27
PC6	6565	4570	<0.01	0.59
Mean Diurnal Range				
PC 1-6	698	4565	<0.01	0.48
PC1	142.4	4570	<0.01	0.03
PC2	1.81	4570	0.18	<0.01
PC3	0.27	4570	0.60	<0.01
PC4	0.19	4570	0.66	<0.01
PC5	1591	4570	<0.01	0.26
PC6	2698	4570	<0.01	0.37
Isothermality				
PC 1-6	1103	4565	<0.01	0.59
PC1	499.6	4570	<0.01	0.10
PC2	308.9	4570	<0.01	0.06
PC3	261.1	4570	<0.01	0.05
PC4	670.4	4570	<0.01	0.13
PC5	1194	4570	<0.01	0.21
PC6	4485	4570	<0.01	0.50
Temp. Seasonality		4570		
PC 1-6	704.9	4565	<0.01	0.48
PC1	576.8	4570	<0.01	0.11
PC2	627.5	4570	<0.01	0.12
PC3	494.3	4570	<0.01	0.10
PC4	1320	4570	<0.01	0.22
PC5	524.5	4570	<0.01	0.10
PC6	2154	4570	<0.01	0.32
Max. Temp. of Warmest Month				
PC 1-6	1838	4565	<0.01	0.71

Table D2. (continued)

PC1	217.4	4570	<0.01	0.05
PC2	499.8	4570	<0.01	0.10
PC3	917.1	4570	<0.01	0.17
PC4	5.857	4570	0.02	<0.01
PC5	3362	4570	<0.01	0.42
PC6	9170	4570	<0.01	0.67
Min. Temp. of Coldest Month				
PC 1-6	1386	4565	<0.01	0.65
PC1	541.1	4570	<0.01	0.11
PC2	1086	4570	<0.01	0.19
PC3	1368	4570	<0.01	0.23
PC4	744.4	4570	<0.01	0.14
PC5	1325	4570	<0.01	0.22
PC6	5256	4570	<0.01	0.53
Temp. Annual Range				
PC 1-6	466	4565	<0.01	0.38
PC1	426.3	4570	<0.01	0.09
PC2	736.9	4570	<0.01	0.14
PC3	673.3	4570	<0.01	0.13
PC4	1498	4570	<0.01	0.25
PC5	125.9	4570	<0.01	0.03
PC6	854	4570	<0.01	0.16
Mean Temp. of Wettest Quarter				
PC 1-6	193.5	4565	<0.01	0.20
PC1	13.34	4570	<0.01	<0.01
PC2	40.03	4570	<0.01	0.01
PC3	371.5	4570	<0.01	0.07
PC4	102.7	4570	<0.01	0.02
PC5	132.1	4570	<0.01	0.03
PC6	345.5	4570	<0.01	0.07
Mean Temp. of Driest Quarter				
PC 1-6	638.5	4565	<0.01	0.46
PC1	525.1	4570	<0.01	0.10
PC2	513.1	4570	<0.01	0.10
PC3	595.3	4570	<0.01	0.12
PC4	751.9	4570	<0.01	0.14
PC5	651.8	4570	<0.01	0.12
PC6	2509	4570	<0.01	0.35

Table D2. (continued)

Mean Temp. of Warmest Quarter				
PC 1-6	1200	4565	<0.01	0.61
PC1	145.8	4570	<0.01	0.03
PC2	630.7	4570	<0.01	0.12
PC3	1536	4570	<0.01	0.25
PC4	12.18	4570	<0.01	<0.01
PC5	1718	4570	<0.01	0.27
PC6	4768	4570	<0.01	0.51
Mean Temp. of Coldest Quarter				
PC 1-6	1627	4565	<0.01	0.68
PC1	510.9	4570	<0.01	0.10
PC2	971.1	4570	<0.01	0.18
PC3	1393	4570	<0.01	0.23
PC4	596.1	4570	<0.01	0.12
PC5	1510	4570	<0.01	0.25
PC6	6524	4570	<0.01	0.59
Log Annual Precipitation				
PC 1-6	367.5	4565	<0.01	0.32
PC1	0.61	4570	0.43	<0.01
PC2	585.9	4570	<0.01	0.11
PC3	315.7	4570	<0.01	0.06
PC4	491.3	4570	<0.01	0.10
PC5	301.2	4570	<0.01	0.06
PC6	115.9	4570	<0.01	0.02
Log Precip. of Wettest Month				
PC 1-6	319.5	4565	<0.01	0.29
PC1	7.81	4570	0.01	<0.01
PC2	407.2	4570	<0.01	0.08
PC3	157.2	4570	<0.01	0.03
PC4	487.6	4570	<0.01	0.10
PC5	266.3	4570	<0.01	0.05
PC6	142.3	4570	<0.01	0.03
Log Precip. of Driest Month				
PC 1-6	298.2	4565	<0.01	0.28
PC1	6.921	4570	0.01	<0.01
PC2	351.6	4570	<0.01	0.07
PC3	319	4570	<0.01	0.07

Table D2. (continued)

PC4	183.4	4570	<0.01	0.04
PC5	409.3	4570	<0.01	0.08
PC6	176.7	4570	<0.01	0.04
Log Precip. Seasonality				
PC 1-6	107.7	4565	<0.01	0.12
PC1	101.3	4570	<0.01	0.02
PC2	323.3	4570	<0.01	0.07
PC3	394.4	4570	<0.01	0.08
PC4	85.84	4570	<0.01	0.02
PC5	50.3	4570	<0.01	0.01
PC6	4.063	4570	0.04	<0.01
Log Precip. of Wettest Quarter				
PC 1-6	334.8	4565	<0.01	0.30
PC1	8.3	4570	<0.01	<0.01
PC2	376.2	4570	<0.01	0.08
PC3	123.4	4570	<0.01	0.03
PC4	469.5	4570	<0.01	0.09
PC5	318.2	4570	<0.01	0.06
PC6	205.	4570	<0.01	0.04
Log Precip. of Driest Quarter				
PC 1-6	319.3	4565	<0.01	0.29
PC1	1.439	4570	0.23	<0.01
PC2	409.8	4570	<0.01	0.08
PC3	369.3	4570	<0.01	0.07
PC4	236.1	4570	<0.01	0.05
PC5	426.8	4570	<0.01	0.09
PC6	153.8	4570	<0.01	0.03
Log Precip. of Warmest Quarter				
PC 1-6	322.3	4565	<0.01	0.30
PC1	186.7	4570	<0.01	0.04
PC2	127.1	4570	<0.01	0.03
PC3	121.7	4570	<0.01	0.03
PC4	8.521	4570	<0.01	<0.01
PC5	467.5	4570	<0.01	0.09
PC6	371.4	4570	<0.01	0.07

Table D2. (continued)

Log Precip. of Coldest Quarter				
PC 1-6	337.4	4565	<0.01	0.31
PC1	109.4	4570	<0.01	0.02
PC2	455.6	4570	<0.01	0.09
PC3	308.6	4570	<0.01	0.06
PC4	1129	4570	<0.01	0.20
PC5	315.4	4570	<0.01	0.06
PC6	37.28	4570	<0.01	0.01

Table D3. Results of univariate MANOVA statistical models for PCs 1-6 and altitude, ecological domain, ecological province, and vegetation cover.

Environmental Factor	Df	Pillai	approx F	num Df	den Df	Pr(>F)
Altitude						
Intercept	1.00	0.75	2191.25	6.00	4385.00	<0.01
PC 1-6	1.00	0.03	18.96	6.00	4385.00	<0.01
Residuals	439<0.01					
Domain						
Intercept	1.00	0.80	2902.50	6.00	4383.00	<0.01
PC 1-6	3.00	0.41	114.43	18.00	13155.00	<0.01
Residuals	4388.00					
Province						
Intercept	1.00	0.85	3986.00	6.00	4338.00	<0.01
PC 1-6	48.00	1.02	18.50	288.00	26058.00	<0.01
Residuals	4343.00					
Vegetation Cover						
Intercept	1.00	0.81	3019.27	6.00	4365.00	<0.01
PC 1-6	21.00	0.54	20.54	126.00	2622<0.01	<0.01
Residuals	437<0.01					

Table D4. Results of univariate MANOVA statistical models for individual PCs and altitude, ecological domain, ecological province, and vegetation cover.

Environmental factor	F	p	Adj. R^2
Altitude			
PC1	1.585 on 1 & 4390 df	0.21	<0.01
PC2	21.09 on 1 & 4390 df	<0.01	<0.01
PC3	0.6731 on 1 & 4390 df	0.41	<0.01
PC4	45.82 on 1 & 4390 df	<0.01	0.01
PC5	16.42 on 1 & 4390 df	<0.01	<0.01
PC6	14.32 on 1 & 4390 df	<0.01	<0.01
Domain			
PC1	89.64 on 3 & 4388 df	<0.01	0.06
PC2	156.6 on 3 & 4388 df	<0.01	0.10
PC3	280.5 on 3 & 4388 df	<0.01	0.16
PC4	55.81 on 3 & 4388 df	<0.01	0.04
PC5	128.9 on 3 & 4388 df	<0.01	0.08
PC6	400.5 on 3 & 4388 df	<0.01	0.21
Province			
PC1	17.15 on 48 and 4343 df	<0.01	0.15
PC2	21.94 on 48 and 4343 df	<0.01	0.19
PC3	30.11 on 48 and 4343 df	<0.01	0.24
PC4	8.259 on 48 and 4343 df	<0.01	0.07
PC5	53.66 on 48 and 4343 df	<0.01	0.37
PC6	120.6 on 48 and 4343 df	<0.01	0.57
Vegetation Cover			
PC1	19.74 on 21 and 4370 df	<0.01	0.08
PC2	26.86 on 21 and 4370 df	<0.01	0.11
PC3	44.94 on 21 and 4370 df	<0.01	0.17
PC4	8.978 on 21 and 4370 df	<0.01	0.04
PC5	37.7 on 21 and 4370 df	<0.01	0.15
PC6	94.79 on 21 and 4370 df	<0.01	0.31

Table D5. List of taxa with assigned substrate use ecology.

Genus	Species	Family	Subfamily	Substrate
Agkistrodon	*Agkistrodon contortrix*	Viperidae	Crotalinae	Terrestrial
Agkistrodon	*Agkistrodon piscivorus*	Viperidae	Crotalinae	Semiaquatic
Arizona	*Arizona elegans*	Colubridae	Colubrinae	Semifossorial
Bogertophis	*Bogertophis subocularis*	Colubridae	Colubrinae	Terrestrial
Carphophis	*Carphophis amoenus*	Colubridae	Dipsadinae	Fossorial
Cemophora	*Cemophora coccinea*	Colubridae	Colubrinae	Fossorial
Charina	*Charina bottae*	Charinidae	Charininae	Semifossorial
Chilomeniscus	*Chilomeniscus stramineus*	Colubridae	Colubrinae	Fossorial
Chionactis	*Chionactis occipitalis*	Colubridae	Colubrinae	Fossorial
Clonophis	*Clonophis kirtlandi*	Colubridae	Natricinae	Semiaquatic
Coluber	*Coluber constrictor*	Colubridae	Colubrinae	Semiarboreal
Contia	*Contia tenuis*	Colubridae	Dipsadinae	Semifossorial
Crotalus	*Crotalus adamanteus*	Viperidae	Crotalinae	Terrestrial
Crotalus	*Crotalus atrox*	Viperidae	Crotalinae	Terrestrial
Crotalus	*Crotalus cerastes*	Viperidae	Crotalinae	Terrestrial
Crotalus	*Crotalus helleri*	Viperidae	Crotalinae	Terrestrial
Crotalus	*Crotalus horridus*	Viperidae	Crotalinae	Terrestrial
Crotalus	*Crotalus lepidus*	Viperidae	Crotalinae	Terrestrial
Crotalus	*Crotalus mitchellii*	Viperidae	Crotalinae	Terrestrial
Crotalus	*Crotalus molossus*	Viperidae	Crotalinae	Terrestrial
Crotalus	*Crotalus oreganus*	Viperidae	Crotalinae	Terrestrial
Crotalus	*Crotalus ruber*	Viperidae	Crotalinae	Terrestrial
Crotalus	*Crotalus scutulatus*	Viperidae	Crotalinae	Terrestrial
Crotalus	*Crotalus tigris*	Viperidae	Crotalinae	Terrestrial
Crotalus	*Crotalus viridis*	Viperidae	Crotalinae	Terrestrial
Crotalus	*Crotalus willardi*	Viperidae	Crotalinae	Terrestrial
Diadophis	*Diadophis punctatus*	Colubridae	Dipsadinae	Semifossorial
Drymarchon	*Drymarchon couperi*	Colubridae	Colubrinae	Terrestrial
Drymobius	*Drymobius margaritiferus*	Colubridae	Colubrinae	Arboreal
Farancia	*Farancia abacura*	Colubridae	Dipsadinae	Semiaquatic
Farancia	*Farancia erytrogramma*	Colubridae	Dipsadinae	Aquatic
Ficimia	*Ficimia streckeri*	Colubridae	Colubrinae	Fossorial
Gyalopion	*Gyalopion canum*	Colubridae	Colubrinae	Fossorial
Heterodon	*Heterodon nasicus*	Colubridae	Dipsadinae	Semifossorial
Heterodon	*Heterodon platirhinos*	Colubridae	Dipsadinae	Semifossorial

Table D5. (continued)

Heterodon	*Heterodon simus*	Colubridae	Dipsadinae	Semifossorial
Hypsiglena	*Hypsiglena torquata*	Colubridae	Dipsadinae	Terrestrial
Lampropeltis	*Lampropeltis alterna*	Colubridae	Colubrinae	Terrestrial
Lampropeltis	*Lampropeltis calligaster*	Colubridae	Colubrinae	Semifossorial
Lampropeltis	*Lampropeltis elapsoides*	Colubridae	Colubrinae	Semifossorial
Lampropeltis	*Lampropeltis extenuata*	Colubridae	Colubrinae	Fossorial
Lampropeltis	*Lampropeltis getula*	Colubridae	Colubrinae	Terrestrial
Lampropeltis	*Lampropeltis nigra*	Colubridae	Colubrinae	Terrestrial
Lampropeltis	*Lampropeltis pyromelana*	Colubridae	Colubrinae	Terrestrial
Lampropeltis	*Lampropeltis triangulum*	Colubridae	Colubrinae	Semifossorial
Lampropeltis	*Lampropeltis zonata*	Colubridae	Colubrinae	Terrestrial
Lichanura	*Lichanura roseofusca*	Charinidae	Charininae	Semifossorial
Lichanura	*Lichanura trivirgata*	Charinidae	Charininae	Semifossorial
Masticophis	*Masticophis bilineatus*	Colubridae	Colubrinae	Semiarboreal
Masticophis	*Masticophis flagellum*	Colubridae	Colubrinae	Semiarboreal
Masticophis	*Masticophis fuliginosus*	Colubridae	Colubrinae	Semiarboreal
Masticophis	*Masticophis lateralis*	Colubridae	Colubrinae	Semiarboreal
Masticophis	*Masticophis taeniatus*	Colubridae	Colubrinae	Arboreal
Micruroides	*Micruroides euryxanthus*	Elapidae	Elapinae	Fossorial
Micrurus	*Micrurus fulvius*	Elapidae	Elapinae	Fossorial
Micrurus	*Micrurus tener*	Elapidae	Elapinae	Fossorial
Nerodia	*Nerodia cyclopion*	Colubridae	Natricinae	Aquatic
Nerodia	*Nerodia erythrogaster*	Colubridae	Natricinae	Semiaquatic
Nerodia	*Nerodia fasciata*	Colubridae	Natricinae	Aquatic
Nerodia	*Nerodia floridana*	Colubridae	Natricinae	Aquatic
Nerodia	*Nerodia harteri*	Colubridae	Natricinae	Aquatic
Nerodia	*Nerodia paucimaculata*	Colubridae	Natricinae	Aquatic
Nerodia	*Nerodia rhombifer*	Colubridae	Natricinae	Semiaquatic
Nerodia	*Nerodia sipedon*	Colubridae	Natricinae	Aquatic
Nerodia	*Nerodia taxispilota*	Colubridae	Natricinae	Aquatic
Opheodrys	*Opheodrys aestivus*	Colubridae	Colubrinae	Arboreal
Opheodrys	*Opheodrys vernalis*	Colubridae	Colubrinae	Semiarboreal
Oxybelis	*Oxybelis aeneus*	Colubridae	Colubrinae	Arboreal
Pantherophis	*Pantherophis bairdi*	Colubridae	Colubrinae	Arboreal
Pantherophis	*Pantherophis emoryi*	Colubridae	Colubrinae	Terrestrial
Pantherophis	*Pantherophis guttatus*	Colubridae	Colubrinae	Terrestrial
Pantherophis	*Pantherophis obsoletus*	Colubridae	Colubrinae	Arboreal

Table D5. (continued)

Pantherophis	*Pantherophis vulpinus*	Colubridae	Colubrinae	Terrestrial
Pelamis	*Pelamis platura*	Elapidae	Hydrophiinae	Aquatic
Phyllorhynchus	*Phyllorhynchus browni*	Colubridae	Colubrinae	Fossorial
Phyllorhynchus	*Phyllorhynchus decurtatus*	Colubridae	Colubrinae	Fossorial
Pituophis	*Pituophis catenifer*	Colubridae	Colubrinae	Semifossorial
Pituophis	*Pituophis melanoleucas*	Colubridae	Colubrinae	Semifossorial
Pituophis	*Pituophis melanoleucus*	Colubridae	Colubrinae	Semifossorial
Pituophis	*Pituophis sayi*	Colubridae	Colubrinae	Semifossorial
Regina	*Regina grahamii*	Colubridae	Natricinae	Aquatic
Regina	*Regina septemvittata*	Colubridae	Natricinae	Semiaquatic
Rena	*Rena dulcis*	Leptotyphlopidae	Leptotyphlopinae	Fossorial
Rena	*Rena humilis*	Leptotyphlopidae	Leptotyphlopinae	Fossorial
Rhadinaea	*Rhadinaea flavilata*	Colubridae	Colubrinae	Terrestrial
Rhinocheilus	*Rhinocheilus lecontei*	Colubridae	Colubrinae	Semifossorial
Salvadora	*Salvadora grahamiae*	Colubridae	Colubrinae	Semiarboreal
Salvadora	*Salvadora hexalepis*	Colubridae	Colubrinae	Semiarboreal
Seminatrix	*Seminatrix pygaea*	Colubridae	Natricinae	Aquatic
Senticolis	*Senticolis triaspis*	Colubridae	Colubrinae	Semiarboreal
Sistrurus	*Sistrurus catenatus*	Viperidae	Crotalinae	Terrestrial
Sistrurus	*Sistrurus miliarius*	Viperidae	Crotalinae	Terrestrial
Sonora	*Sonora semiannulata*	Colubridae	Colubrinae	Semifossorial
Storeria	*Storeria dekayi*	Colubridae	Natricinae	Terrestrial
Storeria	*Storeria occipitomaculata*	Colubridae	Natricinae	Terrestrial
Tantilla	*Tantilla coronata*	Colubridae	Colubrinae	Semifossorial
Tantilla	*Tantilla gracilis*	Colubridae	Colubrinae	Semifossorial
Tantilla	*Tantilla hobartsmithi*	Colubridae	Colubrinae	Semifossorial
Tantilla	*Tantilla nigriceps*	Colubridae	Colubrinae	Semifossorial
Tantilla	*Tantilla planiceps*	Colubridae	Colubrinae	Fossorial
Tantilla	*Tantilla relicta*	Colubridae	Colubrinae	Fossorial
Thamnophis	*Thamnophis brachystoma*	Colubridae	Natricinae	Terrestrial
Thamnophis	*Thamnophis butleri*	Colubridae	Natricinae	Terrestrial
Thamnophis	*Thamnophis cyrtopsis*	Colubridae	Natricinae	Terrestrial
Thamnophis	*Thamnophis elegans*	Colubridae	Natricinae	Terrestrial
Thamnophis	*Thamnophis eques*	Colubridae	Natricinae	Terrestrial
Thamnophis	*Thamnophis hammondii*	Colubridae	Natricinae	Aquatic
Thamnophis	*Thamnophis marcianus*	Colubridae	Natricinae	Semiaquatic
Thamnophis	*Thamnophis ordinoides*	Colubridae	Natricinae	Terrestrial

Table D5. (continued)

Thamnophis	*Thamnophis proximus*	Colubridae	Natricinae	Semiaquatic
Thamnophis	*Thamnophis radix*	Colubridae	Natricinae	Terrestrial
Thamnophis	*Thamnophis rufipunctatus*	Colubridae	Natricinae	Aquatic
Thamnophis	*Thamnophis sauritus*	Colubridae	Natricinae	Semiaquatic
Thamnophis	*Thamnophis sirtalis*	Colubridae	Natricinae	Semiaquatic
Trimorphodon	*Trimorphodon biscutatus*	Colubridae	Colubrinae	Terrestrial
Trimorphodon	*Trimorphodon lambda*	Colubridae	Colubrinae	Terrestrial
Tropidoclonion	*Tropidoclonion lineatum*	Colubridae	Natricinae	Semifossorial
Virginia	*Virginia striatula*	Colubridae	Natricinae	Semifossorial
Virginia	*Virginia valeriae*	Colubridae	Natricinae	Semifossorial

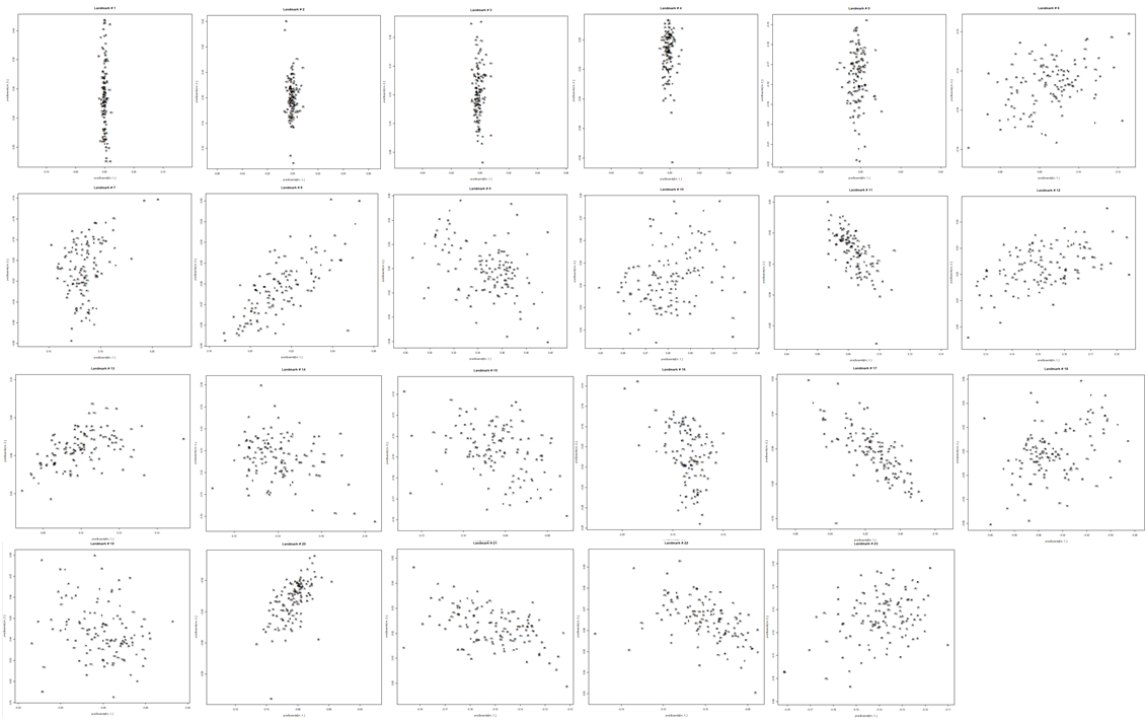

Figure D1. Distributions of each individual landmark for 119 snake species after aggregation of data.

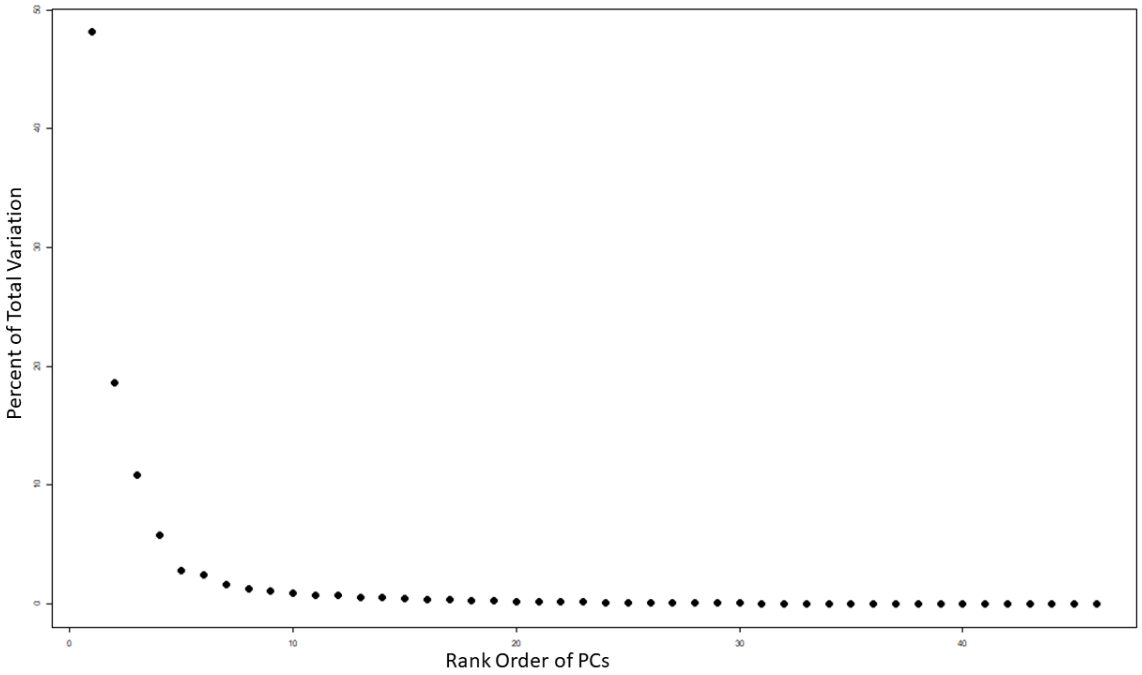

Figure D2. Plot of the percent of morphological variation represented by each PC.

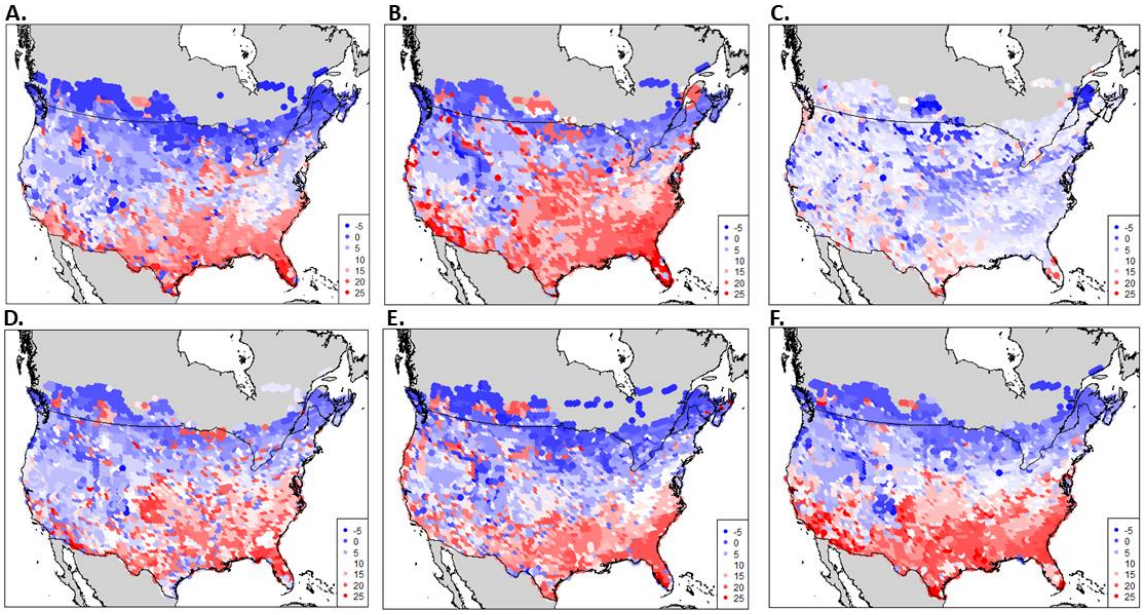

Figure D3. Projection of maximum likelihood MAT over geographic space, based on community snake vertebral shape. Letters correspond with the first six PCs in numerical order.

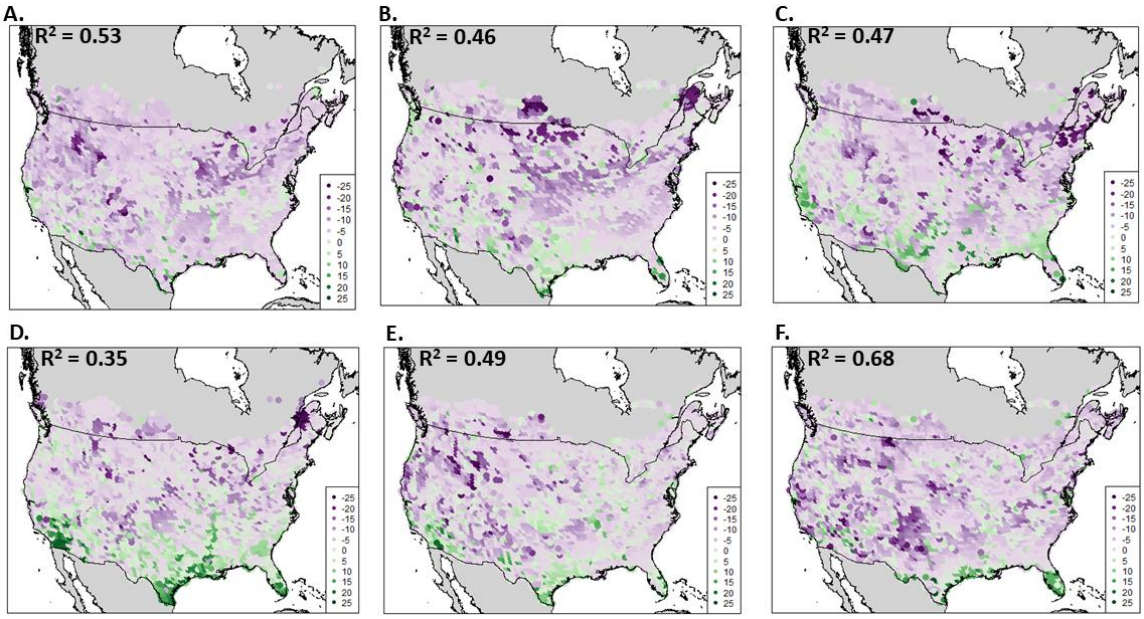

Figure D4. Projection of anomaly values between actual and predicted MAT over geographic space, based on community snake vertebral shape. Letters correspond with the first six PCs in numerical order.

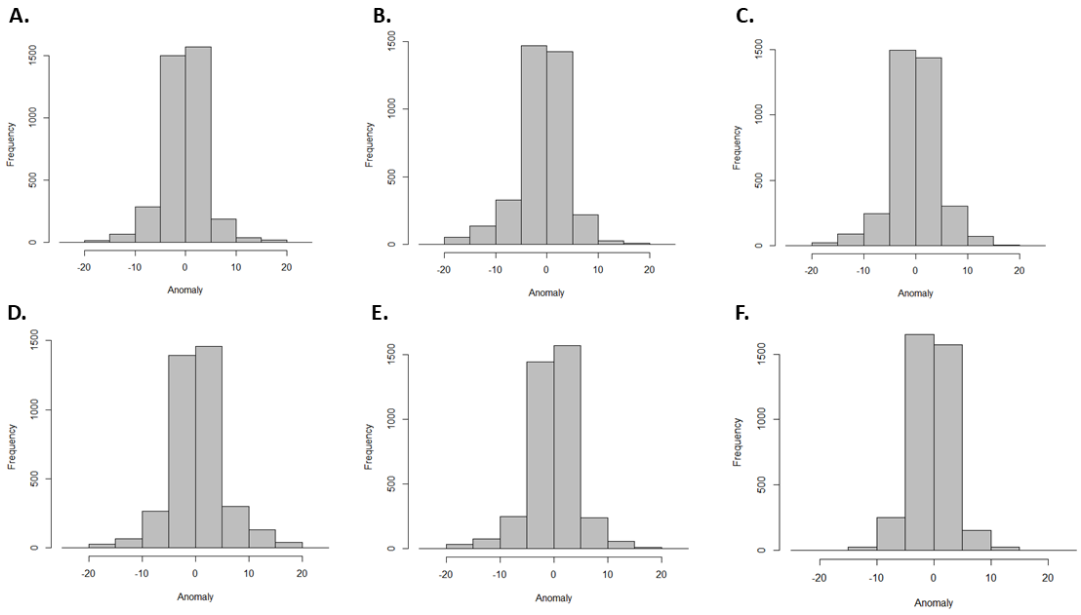

Figure D5. Anomaly histograms showing the frequency of overpredictions and underpredictions at intervals of 5ºC. Letters correspond with the first six PCs in numerical order.

Code D1. This code applies Procrustes superimposition to landmark data, then ordinates it. Univariate MANOVAs and linear correlations can be run for shape data and environmental variables. Additionally, new code for determining the geography of morphology, ecometric spaces, maximum likelihood projections of ecometric space, and anomaly maps is introduced in the latter portions of the code.

```
#make sure to install required packages
library(geomorph)
library(shapes)
library(ggplot2)
library(reshape2)
library(rgdal)
library(raster)
library(rgeos)
library(dplyr)
library(sp)
library(car)
library(phytools)
library(picante)
library(caper)
library(geiger)
library(nlme)
library(phytools)
getwd()
setwd("D:/extant_snake_ecometrics/")

snakemorph<-read.csv("Delimit_Dissertation_Table.csv", header=T)
head(snakemorph)
dim(snakemorph) #504 by 10
snakeco<-read.csv("NAlist_MCAlist.csv", header=T)
head(snakeco)
phy<-read.tree("phy.txt")
plot(phy)

#where x = number of specimens; y = ???
landmarks<-readland.tps("fullantmorph.TPS")
landmarks<-landmarks[-24,,]
dim(landmarks) #23 2 504.. matrix w/ 23 rows and 1008 coulumns
#landmarks2<-readland.tps("ant_extant_ecometric.TPS")
#landmarks2<-landmarks[-24,,]

options(max.print=100000)
NAm_snakemorph <- snakemorph %>%
  filter (Region == "NAm")
NAm_ID <- NAm_snakemorph[,1]
```

```
# landmarks<-
landmarks[,,c(1,2,10,15,16,17,18,22,24,25,26,27,29,30,31,33,34,35,37,47,48,49,50,51,5
4,55,56,57,60,65,66,68,70,72,73,74,75,76,77,78,80,81,82,86,87,88,89,90,
#               91,93,96,97,98,99,100,101,103, 106, 107, 110,111, 112, 113, 114, 115,
116, 117, 118, 119, 120, 121, 122,
#               123, 125, 130, 131, 132, 133, 134, 135, 136, 137, 138, 139,140, 141, 142,
143, 144, 145, 146, 147, 148, 149, 150, 151,
#               152, 153, 154, 155, 156, 157, 158, 159, 160, 161, 162, 163,164, 165, 166,
167, 168, 169, 170, 171, 172, 173, 174, 175,
#               176, 177, 178, 179, 180, 181, 182, 183, 184, 185, 186, 187,188, 189, 190,
191, 192, 193, 194, 195, 196, 197, 198, 199,
#               200, 201, 202, 203, 204, 205, 206, 207, 208, 209, 210, 211,212, 213, 214,
215, 216, 217, 218, 221, 222, 223, 224, 225,
#               226, 227, 228, 229, 230, 231, 232, 233, 234, 235, 236, 237,250, 251, 252,
253, 254, 255,256, 257, 258, 259, 260, 261,
#               262, 263, 264, 265, 266, 267, 268, 269, 271, 272, 273, 274,275, 276, 280,
281, 282, 283, 284, 285, 286, 287, 288, 292,
#               293, 294, 295, 296, 297, 298, 299, 300, 301, 302, 303, 304,305, 306, 307,
308, 309, 310, 314, 318, 319, 320, 326, 327,
#               328, 329, 330, 331, 332, 333, 334, 335, 336, 337, 338, 339,340, 341, 342,
343, 344, 345, 347, 348, 349, 350, 351, 352,
#               353, 354, 355, 356,357, 358, 359, 360, 361, 362, 363, 364,365, 366, 367,
368, 369, 370, 371, 372, 373, 374, 375, 376,
#               377, 380, 381, 382,383, 384, 385, 386, 387, 388, 389, 390,391, 392, 393,
394, 395, 396, 397, 398, 399, 400, 401, 402,
#               403, 404, 405, 406, 408, 409, 410, 411, 412, 413, 414, 415,
#               416, 417, 418, 419, 420, 421, 422, 423, 424, 425, 426, 427,
#               428, 429, 430, 431, 432, 433, 434, 435, 436, 437, 438, 439,
#               440, 441, 442, 443, 444, 445, 446, 447, 448, 449, 452, 453,
#               457, 458, 460, 461, 463, 464, 465, 466,467, 468, 469, 470,
#               472, 474, 475, 476, 478, 479, 481, 482, 484, 485, 486, 487,
#               489, 490, 491, 492, 493, 494, 496, 497, 498, 499, 500, 501,502, 503, 504)]

landmarks<-landmarks[,,snakemorph$Region == "NAm"] #what does this do? How
does landmarks link to snakemorph?
dim(landmarks) #now is 23 2 396... 23 rows 1398 columns



plot(landmarks[,,1], xlim = c(0,3000), ylim = c(0,3000), cex=2)

for(i in 2:length(landmarks[1,1,])){
  points(landmarks[,,i], col=i, cex=2)
}
```

```
proc<-gpagen(landmarks)

dev.off()
plot(proc$consensus, xlab="X", ylab="Y", cex=2, pch=19)
text(proc$consensus,labels=1:23, pos = 2)


par(cex=0.5)
#par(pch=20, col = "royalblue", bg="white")
plot(proc$coords[,1,1],proc$coords[,2,1], xlim = c(-0.45, 0.45), ylim = c(-0.35, 0.5),
xaxs="i", yaxs="i", col = "lightgray", cex = 2, pch = 16)
for(i in 2:length(proc$coords[1,1,])){
  points(proc$coords[,1,i],proc$coords[,2,i], col="lightgray", cex=2, pch=16)
}
points(proc$consensus[,1],proc$consensus[,2], col = "black", cex = 3, pch = 16)

############################
#Aggregate same species together
length(unique(NAm_snakemorph$Species))
ag_X <- aggregate(t(proc$coords[,1,]),by=list(NAm_snakemorph$Species),
FUN="mean") #gets the mean spatial point?
ag_Y <- aggregate(t(proc$coords[,2,]),by=list(NAm_snakemorph$Species),
FUN="mean") #119 species

#reduced landmarks
r_landmarks <- array(NA, dim = c(23,2,length(unique(NAm_snakemorph$Species))))
r_landmarks[,1,] <- t(ag_X[,2:24]) #what if you kept the species column? These are
unique species. Rownames sorta thing.
r_landmarks[,2,] <- t(ag_Y[,2:24])
dim(r_landmarks) #122 columns. Same as length(unique(NAm_snakemorph$Species))

plot(r_landmarks[,,1], cex=2)

for(i in 2:length(r_landmarks[1,1,])){
  points(r_landmarks[,,i], col=i, cex=2)
}

proc<-gpagen(r_landmarks)

plot(proc$coords[,1,1],proc$coords[,2,1], xlim = c(-0.45, 0.45), ylim = c(-0.35, 0.5),
xaxs="i", yaxs="i", col = "lightgray", cex = 2, pch = 16)
for(i in 2:length(proc$coords[1,1,])){
  points(proc$coords[,1,i],proc$coords[,2,i], col="lightgray", cex=2, pch=16)
```

```
}
points(proc$consensus[,1],proc$consensus[,2], col = "black", cex = 3, pch = 16)

#what if you were to re-add the NAm_snakemorph$Species back to the r_landmarks?

NAm_snakemorph <- NAm_snakemorph[!duplicated(NAm_snakemorph$Species),]
#r_landmarks has the unique Species
NAm_snakemorph <-
NAm_snakemorph[order(match(NAm_snakemorph$Species,ag_X[,1])),] #BOOM this
orders the column based on matching rownames with ag_X (Peter)
#write.csv(NAm_snakemorph, file="USA_snakeslist.csv")

##############################


for(lm in 1:23){
  plot(proc$coords[lm,1,], proc$coords[lm,2,], xlim =
c(min(proc$coords[lm,1,]),max(proc$coords[lm,1,])), ylim =
c(min(proc$coords[lm,2,]),max(proc$coords[lm,2,])), main = paste("Landmark #", lm),
asp = 1)
  text(proc$coords[lm,1,], proc$coords[lm,2,], labels =
1:length(NAm_snakemorph$Species))
}


proc_landmarks <- procGPA(r_landmarks)
#shapepca(proc_landmarks, pcno = c(1), type="v") #vector plots at 2x mag (is that 2sd,
or no?)

proc_landmarks$percent
NAm_snakemorph$Substrate <- factor(NAm_snakemorph$Substrate, levels =
c("Aquatic", "Semiaquatic", "Arboreal", "Semiarboreal", "Fossorial", "Semifossorial",
"Terrestrial"), ordered = T)
ecology <- NAm_snakemorph$Substrate

plot(proc_landmarks$stdscores[,1], proc_landmarks$stdscores[,2], xlab = "PC1", ylab=
"PC2", col = NAm_snakemorph$Substrate, cex= 2,  pch = 16)
legend('bottomright', legend = levels(NAm_snakemorph$Substrate), col =
seq_along(NAm_snakemorph$Substrate), cex=0.55, pch=16)
text(proc_landmarks$stdscores[,1], proc_landmarks$stdscores[,2],
labels=rownames(NAm_snakemorph), cex=2)


library(RColorBrewer)
```

```
NAm_snakemorph$Substrate <- factor(NAm_snakemorph$Substrate, levels =
c("Aquatic", "Semiaquatic", "Arboreal", "Semiarboreal", "Fossorial", "Semifossorial",
"Terrestrial"), ordered = F)
pca_out <- cbind.data.frame(proc_landmarks$stdscores[, 1:6], Ecology =
NAm_snakemorph$Substrate)
p <- ggplot(pca_out, aes(x=PC1, y=PC2, shape = Ecology, color=Ecology)) +
scale_shape_manual(values=c(17, 17, 15, 15, 18, 18, 16)) + geom_point(size = 4) +
scale_color_brewer(palette = "Paired")
p<-p+theme(axis.text=element_text(size=14), axis.title=element_text(size=16,
face="bold"))
p


#Connect trees to species
NAm_snakemorph$Species<-gsub(" ", "_", NAm_snakemorph$Species)
rownames(proc_landmarks$stdscores) <- NAm_snakemorph$Species


family <- NAm_snakemorph$Family
species <- NAm_snakemorph$Species

dataframe <- data.frame(ecology, family, species, proc_landmarks$stdscores)


#remove node labels
phy$node.label<-NULL


comparative_data <- comparative.data(phy, dataframe, names.col = species)

plot(comparative_data$phy, show.tip.label = T, cex=.75)

#phy.data <- match.phylo.data(phy, data.frame(ecology, family,
proc_landmarks$stdscores))
#plot(phy.data$phy)

#plot the percent contribution of each PC axis to the total variation in the dataset
#barplot(round(proc_landmarks$percent[1:20],2),names.arg =
colnames(proc_landmarks$stdscores)[1:20])

#pick the top 85% explained variance, PC1-6
pgls_model <- pgls(PC1+PC2+PC3+PC4+PC5+PC6~ecology, data = comparative_data,
lambda = "ML")
anova_all <- anova(pgls_model) #look at overall signal
```

```
anova_all
sum_anova_all <- summary(pgls_model)#look at specific ecological signal
sum_anova_all
#coef(pgls_model)
#capture.output(anova_all, file="pgls_all")
#capture.output(sum_anova_all, file="pgls_all_sum")

pgls_model1 <- pgls(PC1~ecology, data = comparative_data, lambda = "ML")
anova1 <- anova(pgls_model1) #look at overall signal
anova1
sum_anova1 <- summary(pgls_model1)#look at specific ecological signal
sum_anova1
#capture.output(anova1, file="pgls_1")
#capture.output(sum_anova1, file="pgls_1_sum")

pgls_model2 <- pgls(PC2~ecology, data = comparative_data, lambda = "ML")
anova2 <- anova(pgls_model2) #look at overall signal
anova2
sum_anova2 <- summary(pgls_model2) #look at specific ecological signal
sum_anova2
#capture.output(anova2, file="pgls_2")
#capture.output(sum_anova2, file="pgls_2_sum")

pgls_model3 <- pgls(PC3~ecology, data = comparative_data, lambda = "ML")
anova3 <- anova(pgls_model3) #look at overall signal
anova3
sum_anova3 <- summary(pgls_model3) #look at specific ecological signal
sum_anova3
#capture.output(anova3, file="pgls_3")
#capture.output(sum_anova3, file="pgls_3_sum")

pgls_model4 <- pgls(PC4~ecology, data = comparative_data, lambda = "ML")
anova4 <- anova(pgls_model4) #look at overall signal
anova4
sum_anova4 <- summary(pgls_model4) #look at specific ecological signal
sum_anova4
#capture.output(anova4, file="pgls_4")
#capture.output(sum_anova4, file="pgls_4_sum")

pgls_model5 <- pgls(PC5~ecology, data = comparative_data, lambda = "ML")
anova5 <- anova(pgls_model5) #look at overall signal
anova5
sum_anova5 <- summary(pgls_model5) #look at specific ecological signal
sum_anova5
```

```
#capture.output(anova5, file="pgls_5")
#capture.output(sum_anova5, file="pgls_5_sum")

pgls_model6 <- pgls(PC6~ecology, data = comparative_data, lambda = "ML")
anova6 <- anova(pgls_model6) #look at overall signal
anova6
sum_anova6 <- summary(pgls_model6) #look at specific ecological signal
sum_anova6
#capture.output(anova6, file="pgls_6")
#capture.output(sum_anova6, file="pgls_6_sum")

#MANOVA
regr.ecology<-lm(proc_landmarks$stdscores[,1:6]~ecology)
summary(regr.ecology)
capture.output(summary(regr.ecology), file="regrecology")
#anova.phy1<-phylANOVA(phy.data$phy, phy.data$data$ecology,
as.numeric(phy.data$data$PC1))
#anova.phy2<-phylANOVA(phy.data$phy, phy.data$data$ecology,
as.numeric(phy.data$data$PC2))
#anova.phy3<-phylANOVA(phy.data$phy, phy.data$data$ecology,
as.numeric(phy.data$data$PC3))
#anova.phy4<-phylANOVA(phy.data$phy, phy.data$data$ecology,
as.numeric(phy.data$data$PC4))
#anova.phy5<-phylANOVA(phy.data$phy, phy.data$data$ecology,
as.numeric(phy.data$data$PC5))
#anova.phy6<-phylANOVA(phy.data$phy, phy.data$data$ecology,
as.numeric(phy.data$data$PC6))

#t(cbind(anova.phy1$Pf, anova.phy2$Pf, anova.phy3$Pf,
anova.phy4$Pf,anova.phy5$Pf, anova.phy6$Pf))

#regr.family<-lm(proc_landmarks$stdscores[,1:6]~family)
#summary(regr.family)

##____________
#subset.by <- family == "Colubridae"
#data.sub.col <- data.frame("ecology" = ecology[subset.by], "family" =
family[subset.by],  proc_landmarks$stdscores[subset.by,])

#phy.data.col <- match.phylo.data(phy, data.sub.col)
#just retype first part for results
#anova.phy.col1 <- phylANOVA(phy.data.col$phy, phy.data.col$data[,1],
as.numeric(phy.data.col$data[,3]), nsim = 1000)
```

```
#anova.phy.col2 <- phylANOVA(phy.data.col$phy, phy.data.col$data[,1],
as.numeric(phy.data.col$data[,4]))
#anova.phy.col3 <- phylANOVA(phy.data.col$phy, phy.data.col$data[,1],
as.numeric(phy.data.col$data[,5]))
#anova.phy.col4 <- phylANOVA(phy.data.col$phy, phy.data.col$data[,1],
as.numeric(phy.data.col$data[,6]))
#anova.phy.col5 <- phylANOVA(phy.data.col$phy, phy.data.col$data[,1],
as.numeric(phy.data.col$data[,7]))
#anova.phy.col6 <- phylANOVA(phy.data.col$phy, phy.data.col$data[,1],
as.numeric(phy.data.col$data[,8]))
#t(cbind(anova.phy1$Pf, anova.phy2$Pf, anova.phy3$Pf,
anova.phy4$Pf,anova.phy5$Pf, anova.phy6$Pf))

########defunct section; fix later
#subset.by <- family == "Colubridae: Dipsadinae"
#data.sub.dip <- data.frame("ecology" = ecology[subset.by], "family" =
family[subset.by], PCA$pc.scores[subset.by,])
#phy.data.dip <- match.phylo.data(phy, data.sub.dip)
#anova.phy.dip1 <- phylANOVA(phy.data.dip$phy, phy.data.dip$data[,1],
as.numeric(phy.data.dip$data[,3]), nsim = 1000)
#anova.phy.dip2 <- phylANOVA(phy.data.dip$phy, phy.data.dip$data[,1],
as.numeric(phy.data.dip$data[,4]), nsim = 1000)
#anova.phy.dip3 <- phylANOVA(phy.data.dip$phy, phy.data.dip$data[,1],
as.numeric(phy.data.dip$data[,5]), nsim = 1000)
#anova.phy.dip4 <- phylANOVA(phy.data.dip$phy, phy.data.dip$data[,1],
as.numeric(phy.data.dip$data[,6]), nsim = 1000)
#anova.phy.dip5 <- phylANOVA(phy.data.dip$phy, phy.data.dip$data[,1],
as.numeric(phy.data.dip$data[,7]), nsim = 1000)
#anova.phy.dip6 <- phylANOVA(phy.data.dip$phy, phy.data.dip$data[,1],
as.numeric(phy.data.dip$data[,8]), nsim = 1000)

#subset.by <- family == "Colubridae: Natricinae"
#data.sub.nat <- data.frame("ecology" = ecology[subset.by], "family" =
family[subset.by], PCA$pc.scores[subset.by,])
#phy.data.nat <- match.phylo.data(phy, data.sub.nat)
#anova.phy.nat1 <- phylANOVA(phy.data.nat$phy, phy.data.nat$data[,1],
as.numeric(phy.data.nat$data[,3]), nsim = 1000)
#anova.phy.nat2 <- phylANOVA(phy.data.nat$phy, phy.data.nat$data[,1],
as.numeric(phy.data.nat$data[,4]), nsim = 1000)
#anova.phy.nat3 <- phylANOVA(phy.data.nat$phy, phy.data.nat$data[,1],
as.numeric(phy.data.nat$data[,5]), nsim = 1000)
#anova.phy.nat4 <- phylANOVA(phy.data.nat$phy, phy.data.nat$data[,1],
as.numeric(phy.data.nat$data[,6]), nsim = 1000)
```

```
#anova.phy.nat5 <- phylANOVA(phy.data.nat$phy, phy.data.nat$data[,1],
as.numeric(phy.data.nat$data[,7]), nsim = 1000)
#anova.phy.nat6 <- phylANOVA(phy.data.nat$phy, phy.data.nat$data[,1],
as.numeric(phy.data.nat$data[,8]), nsim = 1000)

#subset.by <- family == "Viperidae"
#data.sub.vip <- data.frame("ecology" = ecology[subset.by], "family" =
family[subset.by], PCA$pc.scores[subset.by,])
#phy.data.vip <- match.phylo.data(phy, data.sub.vip)
#anova.phy.vip1 <- phylANOVA(phy.data.vip$phy, phy.data.vip$data[,1],
as.numeric(phy.data.vip$data[,3]), nsim = 1000)
#anova.phy.vip2 <- phylANOVA(phy.data.vip$phy, phy.data.vip$data[,1],
as.numeric(phy.data.vip$data[,4]), nsim = 1000)
#anova.phy.vip3 <- phylANOVA(phy.data.vip$phy, phy.data.vip$data[,1],
as.numeric(phy.data.vip$data[,5]), nsim = 1000)
#anova.phy.vip4 <- phylANOVA(phy.data.vip$phy, phy.data.vip$data[,1],
as.numeric(phy.data.vip$data[,6]), nsim = 1000)
#anova.phy.vip5 <- phylANOVA(phy.data.vip$phy, phy.data.vip$data[,1],
as.numeric(phy.data.vip$data[,7]), nsim = 1000)
#anova.phy.vip6 <- phylANOVA(phy.data.vip$phy, phy.data.vip$data[,1],
as.numeric(phy.data.vip$data[,8]), nsim = 1000)
##_______________

#tpsgrid(-proc$consensus, -proc$coords[,,5])#########

#tpsgrid(-proc$consensus, -proc$coords[,,1])

#tpsgrid(-3*sd(proc_landmarks$scores[,1])*proc_landmarks$pcar[,1] +
proc_landmarks$mshape, 2*sd(proc_landmarks$scores[,1])*proc_landmarks$pcar[,1] +
proc_landmarks$mshape)#2 std dev from mean in each direction

#tpsgrid(proc_landmarks$mshape,
3*sd(proc_landmarks$scores[,1])*proc_landmarks$pcar[,1] +
proc_landmarks$mshape)#2 std dev from mean in one direction

#which axis to model?
pcaxis <- 1
sd_mag <- 3
tpsgrid(-sd_mag*sd(proc_landmarks$scores[,pcaxis])*proc_landmarks$pcar[,pcaxis] +
proc_landmarks$mshape,
sd_mag*sd(proc_landmarks$scores[,pcaxis])*proc_landmarks$pcar[,pcaxis] +
proc_landmarks$mshape, opt = 1)

dev.off()
```

```
pcaxis <- 1
sd_mag <- 3
plotRefToTarget(-
sd_mag*sd(proc_landmarks$scores[,pcaxis])*proc_landmarks$pcar[,pcaxis] +
proc_landmarks$mshape,
sd_mag*sd(proc_landmarks$scores[,pcaxis])*proc_landmarks$pcar[,pcaxis] +
proc_landmarks$mshape, method="vector")

#adjust the values below to show extremes of shape for different PCs
#PC1
#par(col="grey", bg="white")
#tpsgrid(-proc$consensus, -proc$coords[,,70], col = 1, mag =1, cex = 2.5)
#tpsgrid(-proc$consensus, -proc$coords[,,29], col=1, mag = 1, cex = 2.5)
#tpsgrid(-proc$coords[,,70], -proc$coords[,,29], col=1, mag=1,cex=2.5) #max distance
#tpsgrid(-proc$coords[,,70], -proc$coords[,,28], col=1, mag=1,cex=2.5) #at zero

#PC2
#tpsgrid(-proc$coords[,,79], -proc$coords[,,30], col = 1, mag = 1, cex = 2.5) #at zero
#tpsgrid(-proc$coords[,,79], -proc$coords[,,5], col = 1, mag = 1, cex = 2.5) #max
distance

#PC3
#tpsgrid(-proc$coords[,,35], -proc$coords[,,24], col = 1, mag = 1, cex = 2.5) #max
distance
#tpsgrid(-proc$coords[,,91],- proc$coords[,,24], col = 1, mag = 1, cex = 2.5) #same y

#PC4
#tpsgrid(-proc$coords[,,22], -proc$coords[,,68], col =1, mag = 1, cex = 2.5) #at zero
#tpsgrid(-proc$coords[,,29], -proc$coords[,,68], col = 1, mag = 1, cex = 2.5) #max
distance

#PC5
#tpsgrid(-proc$coords[,,40], -proc$coords[,,16], col = 1, mag = 1, cex = 2.5) #max
distance
#tpsgrid(-proc$coords[,,62], -proc$coords[,,16], col = 1, mag = 1, cex = 2.5) #same y

#PC6
#tpsgrid(-proc$coords[,,41], -proc$coords[,,105], col = 1, mag = 1, cex = 2.5) #at zero
#tpsgrid(-proc$coords[,,1], -proc$coords[,,105], col = 1, mag = 1, cex = 2.5) #max
distance

#do boxplots for for all six PC scores individually; add splines in illustrator
```

```
NAm_snakemorph$Substrate <- factor(NAm_snakemorph$Substrate, levels =
c("Aquatic", "Semiaquatic", "Arboreal", "Semiarboreal", "Fossorial", "Semifossorial",
"Terrestrial"), ordered = T)

BXPLT <- cbind.data.frame(proc_landmarks$stdscores[, 1:6], Ecology =
NAm_snakemorph$Substrate)

ggplot(data = BXPLT, aes(x = Ecology, y = PC1)) + geom_boxplot(aes(fill =
Ecology))+xlab("Ecology")+ scale_fill_brewer(palette = "Paired") +
theme(text=element_text(size=20, face="bold"), axis.text.x = element_text(angle=90))
ggplot(data = BXPLT, aes(x = Ecology, y = PC2)) + geom_boxplot(aes(fill =
Ecology))+xlab("Ecology")+ scale_fill_brewer(palette = "Paired") +
theme(text=element_text(size=20, face="bold"), axis.text.x = element_text(angle=90))
ggplot(data = BXPLT, aes(x = Ecology, y = PC3)) + geom_boxplot(aes(fill =
Ecology))+xlab("Ecology")+ scale_fill_brewer(palette = "Paired") +
theme(text=element_text(size=20, face="bold"), axis.text.x = element_text(angle=90))
ggplot(data = BXPLT, aes(x = Ecology, y = PC4)) + geom_boxplot(aes(fill =
Ecology))+xlab("Ecology")+ scale_fill_brewer(palette = "Paired") +
theme(text=element_text(size=20, face="bold"), axis.text.x = element_text(angle=90))
ggplot(data = BXPLT, aes(x = Ecology, y = PC5)) + geom_boxplot(aes(fill =
Ecology))+xlab("Ecology")+ scale_fill_brewer(palette = "Paired") +
theme(text=element_text(size=20, face="bold"), axis.text.x = element_text(angle=90))
ggplot(data = BXPLT, aes(x = Ecology, y = PC6)) + geom_boxplot(aes(fill =
Ecology))+xlab("Ecology")+ scale_fill_brewer(palette = "Paired") +
theme(text=element_text(size=20, face="bold"), axis.text.x = element_text(angle=90))

#MLT <- melt(BXPLT, id.var = "Ecology")
#ggplot(data = MLT, aes(x = Ecology, y = value)) + geom_boxplot(aes(fill = variable))


#####CODE FOR GEOGRAPHY OF MORPHOLOGY AND ECOMETRICS#####

admin0_poly <- readOGR("ne_10m_admin_0_countries",
layer="ne_10m_admin_0_countries")
summary(admin0_poly)
na <- admin0_poly[admin0_poly$CONTINENT == "North America", ]
usa <- admin0_poly[admin0_poly$ADMIN == "United States of America" |
admin0_poly$ADMIN == "Canada", ]

na_proj4string <- "+proj=laea +lon_0=-100 +lat_0=50 +x_0=0 +y_0=0 +ellps=WGS84
+datum=WGS84 +units=m +no_defs"
na_crs <- CRS(na_proj4string)
na_proj <-spTransform(na, na_crs)
usa_proj <-spTransform(usa, na_crs)
```

```
na_bb <- as(extent(-5000000,5000000,-4510000,4480000), "SpatialPolygons")
proj4string(na_bb) <- na_proj4string

na_bb <- gBuffer(na_bb, byid=TRUE, width=0)
na_proj <- gSimplify(na_proj, tol = <0.01001)
na_proj <- gBuffer(na_proj, byid=TRUE, width=0)
na_proj <- gIntersection(na_proj, byid=TRUE, na_bb)

NApoints <- read.csv("NA50kmPoints.csv", header=T)
bioclim<-read.csv("BioclimVariables.csv", header=T) #variables are WorlClim
BIO12=Annual Precip, BIO1=Annual Temp
veggie<-read.csv("WilmottPrecipTempMatthewsVegCover.csv", header=T)
province<-read.csv("DomainProvinceAltitude.csv", header=T)
NApoints <- cbind(ID = 1:9699, NApoints, bioclim[,2:20])
NApoints_vp <- merge(NApoints, veggie, by.x = "GLOBALID", by.y = "GlobalID")
NApoints_vp <- merge(NApoints_vp, province, by.x = "GLOBALID", by.y =
"GlobalID")

head(NApoints)

NApoints_sp <- SpatialPointsDataFrame(data.frame(NApoints$Longitude,
NApoints$Latitude), NApoints, proj4string = CRS("+proj=longlat +datum=WGS84"))
NApoints_sp_proj <-spTransform(NApoints_sp, na_crs)

NApoints_sp_vp <- SpatialPointsDataFrame(data.frame(NApoints_vp$Longitude,
NApoints_vp$Latitude), NApoints_vp, proj4string = CRS("+proj=longlat
+datum=WGS84"))
NApoints_sp_vp_proj <- spTransform(NApoints_sp_vp, na_crs)

snakegeo<-read.csv("USA_snake_geog2.csv", header=T)
head(snakegeo)
dim(NAm_snakemorph)
dim(proc_landmarks$stdscores)

#this is where the bioclim variables are linked to the snake data table
temp <- left_join(snakegeo, NApoints, by = c("ID"))

snakegeo_sp <- SpatialPointsDataFrame(data.frame(snakegeo$long, snakegeo$lat),
temp, proj4string = CRS("+proj=longlat +datum=WGS84"))
snakegeo_sp_proj <- spTransform(snakegeo_sp, na_crs)

link <- !is.na(over(snakegeo_sp_proj, as(usa_proj, "SpatialPolygons")))#replace
usa_proj with na_proj to get entire  continent
```

```
snakegeo_sp_proj_mod <- snakegeo_sp_proj[link,]

#this is where veg + prov are linked to the snake data table
#vegproj <- left_join(snakegeo, NApoints_vp, by = c("ID"))

#snakegeo_sp_vp <- SpatialPointsDataFrame(data.frame(snakegeo$long, snakegeo$lat),
vegproj, proj4string = CRS("+proj=longlat +datum=WGS84"))
#snakegeo_sp_vp_proj <- spTransform(snakegeo_sp_vp,na_crs)

#link2 <- !is.na(over(snakegeo_sp_vp_proj, as(usa_proj, "SpatialPolygons")))

#snakegeo_sp_vp_proj_mod <- snakegeo_sp_vp_proj[link2,]

#################################################################
temp_range<-1+max(NApoints_sp_proj$BIO1, na.rm=T)-
min(NApoints_sp_proj$BIO1, na.rm=T)
colfunc<-colorRampPalette(c("darkblue", "blue", "grey", "yellow",
"red"))(temp_range)[1+NApoints_sp_proj$BIO1-min(NApoints_sp_proj$BIO1,
na.rm=T)]
h <- hist(NApoints_sp_proj$BIO1, main = "", xlab = "Mean Annual Temperature", col =
"gray",
breaks = 5)
plot(NApoints_sp_proj, col=colfunc, pch = 16, main = "Mean Annual Temperature
(Degrees Celsius)")
box()
legend("bottomright", legend = h$breaks, pch = 16, col =
colorRampPalette(c("darkblue", "blue", "yellow", "orange", "red"))(length(h$breaks)),
cex = 0.5)

precip_range<-1+max(log(NApoints_sp_proj$BIO12), na.rm=T)-
min(log(NApoints_sp_proj$BIO12), na.rm=T)
colfunc_precip<-colorRampPalette(c("brown",
"green"))(precip_range)[1+log(NApoints_sp_proj$BIO12)-
min(log(NApoints_sp_proj$BIO12), na.rm=T)]
h2<-hist(log(NApoints_sp_proj$BIO12), breaks = 5, col = "gray")
plot(NApoints_sp_proj, col = colfunc_precip, pch = 16, main = "Annual Precipitation
(mm)")
box()
legend("bottomright", legend = round(exp(h2$breaks)), pch = 16, col =
colorRampPalette(c("brown", "green"))(length(h2$breaks)), cex = 0.5)

UID <- snakegeo_sp_proj_mod[!duplicated(snakegeo_sp_proj_mod$ID),1:3]
logAP <- log(NApoints$BIO12 + 1)
```

```
#UID2 <- snakegeo_sp_vp_proj_mod[!duplicated(snakegeo_sp_vp_proj_mod$ID),1:3]

#richness
richness <- unlist(lapply(UID$ID, function (x) sum(snakegeo_sp_proj_mod$ID == x)))
h_rich <- hist(richness, breaks = 10)
h_rich$breaks[1] <- 1
colfunc<-colorRampPalette(c("blue", "yellow", "red"))(max(richness))[richness]
plot(snakegeo_sp_proj_mod, pch = 16, cex = 0.01, ylim=c(20,30))
plot(na_proj, add = T, col = "lightgray")
points(UID[,1:2], col = colfunc, pch = 16, cex = 0.75)
plot(na_proj, add = T)
box()
title("Richness")
legend("bottomright",  legend = h_rich$breaks, pch = 16, col =
colorRampPalette(c("blue", "yellow", "red"))(length(h_rich$breaks)), cex = 0.70)

#GEOGRAPHY OF MORPHOLOGY

breaks <- c(-2.5, -2.0, -1.5, -1.0, -.50, 0, 0.5, 1, 1.5, 2.0, 2.5) #equal breaks for colors
#breaksrange <- (max(breaks, na.rm = T) - min(breaks, na.rm = T))

NAm_snakemorph$Species <- gsub("_", " ", NAm_snakemorph$Species)

ecometric_pc1 <- unlist(lapply(1:length(UID$ID), function(x)
mean(proc_landmarks$stdscores[NAm_snakemorph$Species %in%
snakegeo[snakegeo$ID  %in% UID$ID[x],4],1], na.rm = T )))
tmp <- (ecometric_pc1 - min(ecometric_pc1, na.rm = T)) * 100 #0-195.9
#tmp <- (ecometric_pc1 - min(ecometric_pc1, na.rm = T))
h_tmp <- hist((tmp/100) + min(ecometric_pc1, na.rm = T), breaks = breaks)
colfunc<-colorRampPalette(c("blue","white", "yellow"))(max(tmp, na.rm = T))[tmp]
plot(snakegeo_sp_proj_mod, pch = 16, cex = 0.01)
plot(na_proj, add = T, col = "lightgray")
points(UID[,1:2], col = colfunc, pch = 16, cex = 1.5)
plot(na_proj, add = T)
box()
title("Ecometric PC1")
legend("bottomright", legend =h_tmp$breaks, pch = 16, col =
colorRampPalette(c("blue", "white", "yellow"))(length(breaks)), cex = 1.5)

ecometric_pc2 <- unlist(lapply(1:length(UID$ID), function(x)
mean(proc_landmarks$stdscores[NAm_snakemorph$Species %in%
snakegeo[snakegeo$ID  %in% UID$ID[x],4],2], na.rm = T )))
tmp2 <- (ecometric_pc2 - min(ecometric_pc2, na.rm = T)) * 100 #0-258.10
```

```
h_tmp <- hist((tmp2/100) + min(ecometric_pc2, na.rm = T), breaks = breaks)
colfunc<-colorRampPalette(c("blue","white", "yellow"))(max(tmp2, na.rm = T))[tmp2]
plot(snakegeo_sp_proj_mod, pch = 16, cex = 0.01)
plot(na_proj, add = T, col = "lightgray")
points(UID[,1:2], col = colfunc, pch = 16, cex = 1.5)
plot(na_proj, add = T)
box()
title("Ecometric PC2")
legend("bottomright", legend = h_tmp$breaks, pch = 16, col =
colorRampPalette(c("blue","white", "yellow"))(length(h_tmp$breaks)), cex = 1.5)

ecometric_pc3 <- unlist(lapply(1:length(UID$ID), function(x)
mean(proc_landmarks$stdscores[NAm_snakemorph$Species %in%
snakegeo[snakegeo$ID  %in% UID$ID[x],4],3], na.rm = T )))
tmp3 <- (ecometric_pc3 - min(ecometric_pc3, na.rm = T)) * 100 #0-206.5
h_tmp <- hist((tmp3/100) + min(ecometric_pc3, na.rm = T), breaks = breaks)
colfunc<-colorRampPalette(c("blue","white", "yellow"))(max(tmp3, na.rm = T))[tmp3]
plot(snakegeo_sp_proj_mod, pch = 16, cex = 0.01)
plot(na_proj, add = T, col = "lightgray")
points(UID[,1:2], col = colfunc, pch = 16, cex = 1.5)
plot(na_proj, add = T)
box()
title("Ecometric PC3")
legend("bottomright", legend = h_tmp$breaks, pch = 16, col =
colorRampPalette(c("blue","white", "yellow"))(length(h_tmp$breaks)), cex = 1.5)

ecometric_pc4 <- unlist(lapply(1:length(UID$ID), function(x)
mean(proc_landmarks$stdscores[NAm_snakemorph$Species %in%
snakegeo[snakegeo$ID  %in% UID$ID[x],4],4], na.rm = T )))
tmp4 <- (ecometric_pc4 - min(ecometric_pc4, na.rm = T)) * 100 #0-271.8
h_tmp <- hist((tmp4/100) + min(ecometric_pc4, na.rm = T), breaks = breaks)
colfunc<-colorRampPalette(c("blue","white", "yellow"))(max(tmp4, na.rm = T))[tmp4]
plot(snakegeo_sp_proj_mod, pch = 16, cex = 0.01)
plot(na_proj, add = T, col = "lightgray")
points(UID[,1:2], col = colfunc, pch = 16, cex = 1.5)
plot(na_proj, add = T)
box()
title("Ecometric PC4")
legend("bottomright", legend = h_tmp$breaks, pch = 16, col =
colorRampPalette(c("blue","white", "yellow"))(length(h_tmp$breaks)), cex = 1.5)

ecometric_pc5 <- unlist(lapply(1:length(UID$ID), function(x)
mean(proc_landmarks$stdscores[NAm_snakemorph$Species %in%
snakegeo[snakegeo$ID  %in% UID$ID[x],4],5], na.rm = T )))
```

```
tmp5 <- (ecometric_pc5 - min(ecometric_pc5, na.rm = T)) * 100 #0-326.2
h_tmp <- hist((tmp5/100) + min(ecometric_pc5, na.rm = T), breaks = breaks)
colfunc<-colorRampPalette(c("blue","white", "yellow"))(max(tmp5, na.rm = T))[tmp5]
plot(snakegeo_sp_proj_mod, pch = 16, cex = 0.01)
plot(na_proj, add = T, col = "lightgray")
points(UID[,1:2], col = colfunc, pch = 16, cex = 1.5)
plot(na_proj, add = T)
box()
title("Ecometric PC5")
legend("bottomright", legend = h_tmp$breaks, pch = 16, col =
colorRampPalette(c("blue","white", "yellow"))(length(h_tmp$breaks)), cex = 1.5)

ecometric_pc6 <- unlist(lapply(1:length(UID$ID), function(x)
mean(proc_landmarks$stdscores[NAm_snakemorph$Species %in%
snakegeo[snakegeo$ID  %in% UID$ID[x],4],6], na.rm = T )))
tmp6 <- (ecometric_pc6 - min(ecometric_pc6, na.rm = T)) * 100 #0-367.7
h_tmp <- hist((tmp6/100) + min(ecometric_pc6, na.rm = T), breaks = breaks)
colfunc<-colorRampPalette(c("blue","white", "yellow"))(max(tmp6, na.rm = T))[tmp6]
plot(snakegeo_sp_proj_mod, pch = 16, cex = 0.01)
plot(na_proj, add = T, col = "lightgray")
points(UID[,1:2], col = colfunc, pch = 16, cex = 1.5)
plot(na_proj, add = T)
box()
title("Ecometric PC6")
legend("bottomright", legend = h_tmp$breaks, pch = 16, col =
colorRampPalette(c("blue","white", "yellow"))(length(h_tmp$breaks)), cex = 1.5)


#########################################################################
#
#Ecometric code ####################################
#########################################################################
#

#Multivariate regression of ecometric shapes and climate
#ecobind[,1] is PC1, etc.
ecobind <- cbind(ecometric_pc1[richness >= 1], ecometric_pc2[richness >= 1],
ecometric_pc3[richness >= 1], ecometric_pc4[richness >= 1], ecometric_pc5[richness
>= 1], ecometric_pc6[richness >= 1])

model_pc_all <- lm(log(NApoints_sp$BIO19+1)[UID$ID][richness >= 1] ~
ecobind[,6])
anova <- anova(model_pc_all)
anova
```

```
summary <- summary(model_pc_all)
summary


#capture.output(anova, file="bio1_6")
#capture.output(summary, file="bio1_sum6")


######################################################################


#MANOVA with ecometrics shapes and veg/province
f_domain <- factor(NApoints_sp_vp$Domain)
n_domain <- as.numeric(f_domain)
domain <- NApoints_sp_vp$Domain
domain

f_prov <- factor(NApoints_sp_vp$Province)
n_prov <- as.numeric(f_prov)
ecoregion <- NApoints_sp_vp$Province
ecoregion

f_veg <- factor(NApoints_sp_vp$VegDescrip)
n_veg <- as.numeric(f_veg)
veg <- NApoints_sp_vp$VegDescrip
vegcov

alt <- NApoints_sp_vp$altitude

#all PC
ecobind <- cbind(ecometric_pc1[richness >= 1], ecometric_pc2[richness >= 1],
ecometric_pc3[richness >= 1], ecometric_pc4[richness >= 1], ecometric_pc5[richness
>= 1], ecometric_pc6[richness >= 1])

model_pc_all <- lm(n_domain[UID$ID][richness >= 1] ~ ecobind[,1])
anova <- anova(model_pc_all)
anova
summary <- summary(model_pc_all)
summary

model_pc_all <- lm(n_prov[UID$ID][richness >= 1] ~ ecobind)
anova(model_pc_all)
summary(model_pc_all)
```

```
model_pc_all <- lm(n_veg[UID$ID][richness >= 1] ~ ecobind)
anova(model_pc_all)
summary(model_pc_all)

#each PC
#model_pc_all <- lm(ecobind ~ NApoints_vp$Domain[UID$ID][richness >= 1])
#anova <- anova(model_pc_all)
#anova
#summary <- summary(model_pc_all)
#summary

#capture.output(anova, file="domain_16")
#capture.output(summary, file="domain_sum_16")

#model_pc_all <- lm(ecobind ~ NApoints_vp$Province[UID$ID][richness >= 1])
#anova <- anova(model_pc_all)
#anova
#summary <- summary(model_pc_all)
#summary
#capture.output(anova, file="province_16")
#capture.output(summary, file="province_sum_16")

#model_pc_all <- lm(ecobind ~ NApoints_vp$VegDescrip[UID$ID][richness >= 1])
#anova <-anova(model_pc_all)
#anova
#summary <- summary(model_pc_all)
#summary
#capture.output(anova, file="veg_16")
#capture.output(summary, file="veg_sum_16")

#model_pc_all <- lm(ecobind ~ NApoints_vp$altitude[UID$ID][richness >= 1])
#anova <- anova(model_pc_all)
#anova
#summary <- summary(model_pc_all)
#summary
#capture.output(anova, file="alti_16")
#capture.output(summary, file="alti_sum_16")


#logistic regression with ecometric shapes and veg/province
#install.packages("nnet")
#library(nnet)

###veg
```

```
#f_veg <- as.factor(NApoints_vp$VegDescrip)
#model_pc_all <- multinom(f_veg[UID$ID][richness >= 1] ~
cbind(ecometric_pc1[richness >= 1], ecometric_pc2[richness >= 1],
ecometric_pc3[richness >= 1], ecometric_pc4[richness >= 1], ecometric_pc5[richness
>= 1], ecometric_pc6[richness >= 1]))
#summary(model_pc_all)

#z <- summary(model_pc_all)$coefficients/summary(model_pc_all)$standard.errors

#2-tailed z test
#ztest <- (1 - pnorm(abs(z), 0,1))*2
#ztest

#predicted probabilities
#head(prob <- fitted(model_pc_all))

###Prov
#f_prov <- as.factor(NApoints_vp$Province)
#model_pc_all <- multinom(f_prov[UID$ID][richness >= 1] ~
cbind(ecometric_pc1[richness >= 1], ecometric_pc2[richness >= 1],
ecometric_pc3[richness >= 1], ecometric_pc4[richness >= 1], ecometric_pc5[richness
>= 1], ecometric_pc6[richness >= 1]))
#summary(model_pc_all)

#z <- summary(model_pc_all)$coefficients/summary(model_pc_all)$standard.errors

#2-tailed z test
#ztest <- (1 - pnorm(abs(z), 0,1))*2
#ztest

#predicted probabilities
#head(prob <- fitted(model_pc_all))

###Dom
#f_dom <- as.factor(NApoints_vp$Domain)
#model_pc_all <- multinom(f_dom[UID$ID][richness >= 1] ~
cbind(ecometric_pc1[richness >= 1], ecometric_pc2[richness >= 1],
ecometric_pc3[richness >= 1], ecometric_pc4[richness >= 1], ecometric_pc5[richness
>= 1], ecometric_pc6[richness >= 1]))
#summary(model_pc_all)

#z <- summary(model_pc_all)$coefficients/summary(model_pc_all)$standard.errors

#2-tailed z test
```

```
#test <- (1 - pnorm(abs(z), 0,1))*2
#ztest

#predicted probabilities
#head(prob <- fitted(model_pc_all))
#############################################################################
#

#############################################################################
#
#Ecometric and climate linear model
#scatterplot of variables


#pc1
model_pc1 <- lm(NApoints$BIO1[UID$ID][richness >= 1] ~ ecometric_pc1[richness
>=1])
summary(model_pc1)

#scatterplot of variables
#plot(ecometric_pc1[richness >= 1], NApoints$BIO1[UID$ID][richness >= 1], ylab =
"MAT", xlab ="ecometric_pc1", pch = 16, col = "gray")
#abline(model_pc1, col = "red", lwd=4)
#curve(model_pc1$coefficients[1] + model_pc1$coefficients[2] * x, col = "red", lwd =
4, add = T)
#significant but low R2 -- is this a body size or phylogenetic indirect relationship

#pc2
model_pc2 <- lm(NApoints$BIO1[UID$ID][richness >= 1] ~ ecometric_pc2[richness
>= 1])
summary(model_pc2)

#pc3
model_pc3 <- lm(NApoints$BIO1[UID$ID][richness >= 1] ~ ecometric_pc3[richness
>= 1])
summary(model_pc3)

#pc4
model_pc4 <- lm(NApoints$BIO1[UID$ID][richness >= 1] ~ ecometric_pc4[richness
>= 1])
summary(model_pc4)

#pc5
```

```
model_pc5 <- lm(NApoints$BIO1[UID$ID][richness >= 1] ~ ecometric_pc5[richness
>= 1])
summary(model_pc5)



#pc6
model_pc6 <- lm(NApoints$BIO1[UID$ID][richness >= 1] ~ ecometric_pc6[richness
>= 1])
summary(model_pc6)


#Ecometric and Precipitation Linear Model
#NApoints$BIO12 instead of logAP to take out log
#pc1

model_pc1 <- lm(logAP[UID$ID][richness >= 1] ~ ecometric_pc1[richness >= 1])
summary(model_pc1)

#scatterplot of variables
plot(ecometric_pc1[richness >= 1], logAP[UID$ID][richness >= 1], ylab = "log AP",
xlab ="ecometric_pc1", pch = 16, col = "gray")
abline(model_pc1, col = "red", lwd=4)
curve(model_pc1$coefficients[1] + model_pc1$coefficients[2] * x, col = "red", lwd = 4,
add = T)

#pc2
#model_pc2 <- lm(NApoints$BIO12[UID$ID][richness >= 1] ~ ecometric_pc2[richness
>= 1])
model_pc2 <- lm(logAP[UID$ID][richness >= 1] ~ ecometric_pc2[richness >= 1])
summary(model_pc2)


#pc3
model_pc3 <- lm(logAP[UID$ID][richness >= 1] ~ ecometric_pc3[richness >= 1])
summary(model_pc3)

#pc4
model_pc4 <- lm(logAP[UID$ID][richness >= 1] ~ ecometric_pc4[richness >= 1])
summary(model_pc4)

#pc5
model_pc5 <- lm(logAP[UID$ID][richness >= 1] ~ ecometric_pc5[richness >= 1])
summary(model_pc5)
```

```
#pc6
model_pc6 <- lm(logAP[UID$ID][richness >= 1] ~ ecometric_pc6[richness >= 1])
summary(model_pc6)

#########################################################################
#
#anova/manova
#########################################################################
#


#########################################################################
#
#Most likely temp given mean and stdev of ecometric pc 1 ###############
#########################################################################
#
#maximum likelihood estimation

##Case study code

#Species lists for case studies

#Rio Grande New Mexico

nm19_splist<-
names(proc_landmarks$stdscores[c(11,25,42,83,50,77,91,34,14,3,86,105,108,114,104,3
7,99),1])

nm20_splist <- names(proc_landmarks$stdscores[c(11, 25, 42, 83, 50, 77, 34, 14, 3, 105,
108, 114, 99),1])

#eastern TX

ltx_splist <- names(proc_landmarks$stdscores[c(11, 30, 42, 50, 59, 94, 95, 34, 2, 72, 58,
66, 110, 1),1])

udtx_splist <- names(proc_landmarks$stdscores[c(11, 35, 50, 55, 59, 94, 95, 34, 72, 58,
66, 1, 110, 39, 119, 97),1])

uctx_splist <- names(proc_landmarks$stdscores[c(11, 35, 50, 59, 94, 34, 72, 3, 66, 1),1])

#Jackson-Pulaski Fish and Wildlife Refuge, Indiana (Lawing et al., 2012)
```

```
in30_splist <- names(proc_landmarks$stdscores[c(11, 35, 67, 73, 77, 91, 94, 45, 64, 110,
114, 111, 113),1])

in20_splist <- names(proc_landmarks$stdscores[c(11, 35, 73, 77, 94, 45, 64, 110, 114,
113),1])



#Fort Riley Military Reservation, Kansas (Lawing et al., 2012)

frk30_splist <- names(proc_landmarks$stdscores[c(5, 11, 17, 35, 42, 77, 81, 94, 34, 72,
27, 45, 64, 110, 114, 1, 70, 39, 111, 117, 97, 99),1])

frk90_splist <- names(proc_landmarks$stdscores[c(11, 42, 77, 94, 34, 72, 27, 45, 64,
110, 114, 1, 70, 39, 117, 97, 99),1])

#University of Kansas Natural History Reservation (Lawing et al., 2012)

uks40_splist <- names(proc_landmarks$stdscores[c(11, 17, 77, 94, 72, 27, 45, 64, 114,
39),1])

uks20_splist <- names(proc_landmarks$stdscores[c(94, 72, 27, 45, 64, 114),1])

casestudy <- function(splist, pcscores, pcnumber, mbreaks, sdbreaks){
  cs<-pcscores[splist,pcnumber]
  cs_mean <- mean(cs)
  cs_sd <- sd(cs)
  mean_bincode <- .bincode(cs_mean, breaks = mbreaks)
  sd_bincode <- .bincode(cs_sd, breaks = sdbreaks)
  return(list(mean = cs_mean, sd = cs_sd, mean_bincode = mean_bincode,
sd_bincode=sd_bincode))
}

#nm19_cs <- casestudy(nm19_splist, proc_landmarks$stdscores, 1, mbrks1,sdbrks1)



#PC1 MAT
#stdev variable
sd_ecometric_pc1 <- unlist(lapply(1:length(UID$ID), function(x)
sd(proc_landmarks$stdscores[NAm_snakemorph$Species %in% snakegeo[snakegeo$ID
%in% UID$ID[x],4],1], na.rm = T )))

#bins 25x25 community level trait distrib
mtemp1 <- range(ecometric_pc1, na.rm = T)
```

```
sdtemp1 <- range(sd_ecometric_pc1, na.rm = T)

#break points for mean and stdev
mbrks1 <- seq(mtemp1[1], mtemp1[2], diff(mtemp1)/25)
sdbrks1 <- seq(sdtemp1[1], sdtemp1[2], diff(sdtemp1)/25)

#assign bin codes
mbc1 <- .bincode(ecometric_pc1, breaks = mbrks1)
sdbc1 <- .bincode(sd_ecometric_pc1, breaks = sdbrks1)

#calc temp for each bin
#mean
#obj <- array(NA,dim = c(25,25))
#for(i in 1:25){
  #for(j in 1:25){
   # dat <- round(NApoints$BIO1[UID$ID][which(mbc1==i & sdbc1==j)])
   # obj[26 - j,i] <- mean(dat, na.rm = T)
 # }
#}

#Maxlike
mod <- list()
obj <- array(NA,dim = c(25,25))
for(i in 1:25){
  for(j in 1:25){
    if(sum(mbc1 == i & sdbc1 == j, na.rm = T) != 0){
      dat <- NApoints$BIO1[UID$ID][which(mbc1 ==i & sdbc1 ==j)]
      mod[[i]] <- density(dat[!is.na(dat)], bw = 1)
      obj[26 - j,i] <- mod[[i]]$x[which.max(mod[[i]]$y)]
    }
  }
}

#make a raster
r1 <- raster(extent(0,25,0,25), resolution = 1)
#set the values to the obj
r1 <- setValues(r1,obj)

#set colors for all MAT plots
change_breaks <- 10
color_r <- colorRampPalette(c("darkblue", "blue","grey","yellow",
"red"))(change_breaks*round((maxValue(r1) + 0.50) - (minValue(r1) - 0.50)))

#make an empty plot
```

```
plot(0:25, 0:25, type = "n", xlim = c(0,25), ylim = c(0,25),
    xaxs = "i", yaxs = "i", asp = 1, axes = F, xlab ="Mean PC1", ylab="Std. Dev.PC1")
#add the rectangle/box
rect(0, 0, 25, 25, lwd = 3)
#add the raster data
plot(r1, col = color_r, add = T)
lines (x = c(8.3, 8.3), y = c(0, 25))
lines (x = c(16.6, 16.6), y = c(0, 25))
lines(x = c(0, 25), y = c(8.3, 8.3))
lines(x = c(0, 25), y = c(16.6, 16.6))
axis(side = 2, at = c(0, 8.3, 16.6, 25), labels = c(0.02, 0.49, 0.96, 1.43), line = -3)
axis(side = 1, at = c(0, 8.3, 16.6, 25), labels = c(-1.34, -0.69, -0.03, 0.63))

#this is the mean
#rect(13, 10, 14, 11, lwd = 4)
#box()

#for case studies

#New Mexico
cs <- casestudy(nm19_splist, proc_landmarks$stdscores, pcnumber = 1, mbrks1,
sdbrks1)
#rect(cs$mean_bincode-1, cs$sd_bincode-1, cs$mean_bincode, cs$sd_bincode, lwd = 4)
cs2 <- casestudy(nm20_splist, proc_landmarks$stdscores, pcnumber = 1, mbrks1,
sdbrks1)
#rect(cs2$mean_bincode-1, cs2$sd_bincode-1, cs2$mean_bincode, cs2$sd_bincode, lwd
= 4)
arrows(cs$mean_bincode-0.5, cs$sd_bincode-0.5, cs2$mean_bincode-0.5,
cs2$sd_bincode-0.5, length = 0.10,lwd = 4)

#uks
cs <- casestudy(uks40_splist, proc_landmarks$stdscores, pcnumber = 1, mbrks1,
sdbrks1)
cs2 <- casestudy(uks20_splist, proc_landmarks$stdscores, pcnumber = 1, mbrks1,
sdbrks1)
arrows(cs$mean_bincode-0.5, cs$sd_bincode-0.5, cs2$mean_bincode-0.5,
cs2$sd_bincode-0.5, length = 0.10,lwd = 4)

#frk
cs <- casestudy(frk30_splist, proc_landmarks$stdscores, pcnumber = 1, mbrks1,
sdbrks1)
cs2 <- casestudy(frk90_splist, proc_landmarks$stdscores, pcnumber = 1, mbrks1,
sdbrks1)
```

```
arrows(cs$mean_bincode-0.5, cs$sd_bincode-0.5, cs2$mean_bincode-0.5,
cs2$sd_bincode-0.5, length = 0.10,lwd = 4)

#in
cs <- casestudy(in30_splist, proc_landmarks$stdscores, pcnumber = 1, mbrks1, sdbrks1)
cs2 <- casestudy(in20_splist, proc_landmarks$stdscores, pcnumber = 1, mbrks1,
sdbrks1)
arrows(cs$mean_bincode-0.5, cs$sd_bincode-0.5, cs2$mean_bincode-0.5,
cs2$sd_bincode-0.5, length = 0.10,lwd = 4)

#tx
cs <- casestudy(ltx_splist, proc_landmarks$stdscores, pcnumber = 1, mbrks1, sdbrks1)
cs2 <- casestudy(udtx_splist, proc_landmarks$stdscores, pcnumber = 1, mbrks1,
sdbrks1)
cs3 <- casestudy(uctx_splist, proc_landmarks$stdscores, pcnumber = 1, mbrks1,
sdbrks1)
arrows(cs$mean_bincode-0.5, cs$sd_bincode-0.5, cs2$mean_bincode-0.5,
cs2$sd_bincode-0.5, length = 0.10,lwd = 4)
arrows(cs2$mean_bincode-0.5, cs2$sd_bincode-0.5, cs3$mean_bincode-0.5,
cs3$sd_bincode-0.5, length = 0.10,lwd = 4)

#grab all the data for that box
dat <- round(NApoints$BIO1[UID$ID][which(mbc1==11 & sdbc1==13)])

#plot the kernel density with gaussian kernel, bandwidth = 1
mod <- density(dat, bw = 1)
plot(mod, ylim = c(0,1), col = "darkblue", lwd = 2)
polygon(mod$x, mod$y, col = "skyblue")

#####
modmax <- array(NA, dim = length(sd_ecometric_pc1)) #this should only be the length
of the # of geographic points that have snakes
mod <- list()
for(i in 1:length(sd_ecometric_pc1)){
  if(!(is.na(mbc1[i]) | is.na(sdbc1[i]))){
    dat <- round(NApoints$BIO1[UID$ID][which(mbc1==mbc1[i] & sdbc1==sdbc1[i])])
#(mbc1==mbc1[i] & sdbc1==sdbc1[i] & mbc2==mbc2[i] $ sdbc2==sdbc2[i])]) to add
additional PCs
    if(sum(!is.na(dat)) > 0) {
      mod[[i]] <- density(dat[!is.na(dat)], bw = 1)
      modmax[i] <- mod[[i]]$x[which.max(mod[[i]]$y)]
  }}}
modmax<-round(modmax)
cutoff<-1
```

```
#calculate maximum likelihood for all bins; cutoff >1 species for snakes

h <- hist(NApoints$BIO1[UID$ID], main = "", xlab = "Mean Annual Temperature", col
= "gray", breaks = 5)

#plot maximum likelihood temperature from ecometric
tmp <- (modmax - min(modmax, na.rm = T)) * 100
colfunc<-colorRampPalette(c("blue", "white", "red"))(max(tmp, na.rm = T))[tmp]
plot(snakegeo_sp_proj_mod, pch = 16, cex = 0.01)
plot(na_proj, add = T, col = "lightgray")
points(UID[,1:2], col = colfunc, pch = 16, cex = 1)
plot(na_proj, add = T)
box()
title("Ecometric Temperature PC1")
legend("bottomright", legend = h$breaks, pch = 16, col = colorRampPalette(c("blue",
"white", "red"))(length(h$breaks)), cex = .75)

#plot actual temperature for comparison
tmp <- (bioclim$BIO1[UID$ID] - min(bioclim$BIO1[UID$ID], na.rm = T))
colfunc<-colorRampPalette(c("blue", "white", "red"))(max(tmp, na.rm = T))[tmp]
plot(snakegeo_sp_proj_mod, pch = 16, cex = 0.01)
plot(na_proj, add = T, col = "lightgray")
points(UID[,1:2], col = colfunc, pch = 16, cex = 1)
plot(na_proj, add = T)
box()
title("Mean Annual Temperature")
legend("bottomright", legend = h$breaks, pch = 16, col = colorRampPalette(c("blue",
"white", "red"))(length(h$breaks)), cex = 0.75)


#plot anomaly to visualize differences
abreaks <- c(-25, -20, -15, -10, -5, 0, 5, 10, 15, 20, 25) #equal breaks for colors
anom1 <- NApoints$BIO1[UID$ID] - modmax
h_anom1 <- hist(anom1, main = "", xlab = "Anomaly", col = "gray", breaks = abreaks)
tmp1 <- (anom1 - min(anom1, na.rm = T))

color_a<-colorRampPalette(brewer.pal(10, "PRGn"))(max(tmp1, na.rm = T))[tmp1]

plot(snakegeo_sp_proj_mod, pch = 16, cex = 0.01)
plot(na_proj, add = T, col = "lightgray")
points(UID[,1:2], col = color_a, pch = 16, cex = 1.25)
plot(na_proj, add = T)
box()
title("MAT Anomaly PC1")
```

```
legend("bottomright", legend = h_anom1$breaks, pch = 16, col =
colorRampPalette(brewer.pal(10, "PRGn"))(length(h_anom1$breaks)), cex = .75)

#correlation between real temp and max like temp
tempcor <- cor(bioclim$BIO1[UID$ID], modmax, use = "pairwise.complete.obs",
method = "pearson")
tempcor^2 #this is the R-squared (amount of explained variance of the expected from the
observed)

#PC2 MAT
#stdev variable
sd_ecometric_pc2 <- unlist(lapply(1:length(UID$ID), function(x)
sd(proc_landmarks$stdscores[NAm_snakemorph$Species %in% snakegeo[snakegeo$ID
%in% UID$ID[x],4],2], na.rm = T )))

#bins 25x25 community level trait distrib
mtemp2 <- range(ecometric_pc2, na.rm = T)
sdtemp2 <- range(sd_ecometric_pc2, na.rm = T)

#break points for mean and stdev
mbrks2 <- seq(mtemp2[1], mtemp2[2], diff(mtemp2)/25)
sdbrks2 <- seq(sdtemp2[1], sdtemp2[2], diff(sdtemp2)/25)

#assign bin codes
mbc2 <- .bincode(ecometric_pc2, breaks = mbrks2)
sdbc2 <- .bincode(sd_ecometric_pc2, breaks = sdbrks2)

#calc temp for each bin
#mean
#obj <- array(NA,dim = c(25,25))
#for(i in 1:25){
 # for(j in 1:25){
  #  dat <- round(NApoints$BIO1[UID$ID][which(mbc2==i & sdbc2==j)])
   # obj[26 - j,i] <- mean(dat, na.rm = T)
  #}
#}

#Maxlike
mod <- list()
obj <- array(NA,dim = c(25,25))
for(i in 1:25){
  for(j in 1:25){
    if(sum(mbc2 == i & sdbc2 == j, na.rm = T) != 0){
      dat <- NApoints$BIO1[UID$ID][which(mbc2 ==i & sdbc2 ==j)]
```

```
      mod[[i]] <- density(dat[!is.na(dat)], bw = 1)
      obj[26 - j,i] <- mod[[i]]$x[which.max(mod[[i]]$y)]
    }
  }
}
#make a raster
r <- raster(extent(0,25,0,25), resolution = 1)
#set the values to the obj
r <- setValues(r,obj)
change_breaks <- 10

#make an empty plot
plot(0:25, 0:25, type = "n", xlim = c(0,25), ylim = c(0,25),
     xaxs = "i", yaxs = "i", asp = 1, axes = F, xlab ="mean PC2", ylab="Std. Dev. PC2")
#add the rectangle/box
rect(0, 0, 25, 25, lwd = 3)
#add the raster data
plot(r, col = color_r, add = T)
lines (x = c(8.3, 8.3), y = c(0, 25))
lines (x = c(16.6, 16.6), y = c(0, 25))
lines(x = c(0, 25), y = c(8.3, 8.3))
lines(x = c(0, 25), y = c(16.6, 16.6))
axis(side = 2, at = c(0.0, 8.3, 16.6, 25), labels = c(0.02, 0.75, 1.48, 2.21), line = -3)
axis(side = 1, at = c(0.0, 8.3, 16.6, 25), labels = c(-1.12, -0.25, 0.61, 1.47))

#this is for the means
#rect(9, 8, 10, 9, lwd = 4)
#box()


#for case studies

#New Mexico
cs <- casestudy(nm19_splist, proc_landmarks$stdscores, pcnumber = 2, mbrks2,
sdbrks2)
#rect(cs$mean_bincode-1, cs$sd_bincode-1, cs$mean_bincode, cs$sd_bincode, lwd = 4)
cs2 <- casestudy(nm20_splist, proc_landmarks$stdscores, pcnumber = 2, mbrks2,
sdbrks2)
#rect(cs2$mean_bincode-1, cs2$sd_bincode-1, cs2$mean_bincode, cs2$sd_bincode, lwd
= 4)
arrows(cs$mean_bincode-0.5, cs$sd_bincode-0.5, cs2$mean_bincode-0.5,
cs2$sd_bincode-0.5, length = 0.10,lwd = 4)

#uks
```

```
cs <- casestudy(uks40_splist, proc_landmarks$stdscores, pcnumber = 2, mbrks2,
sdbrks2)
cs2 <- casestudy(uks20_splist, proc_landmarks$stdscores, pcnumber = 2, mbrks2,
sdbrks2)
arrows(cs$mean_bincode-0.5, cs$sd_bincode-0.5, cs2$mean_bincode-0.5,
cs2$sd_bincode-0.5, length = 0.10,lwd = 4)

#frk
cs <- casestudy(frk30_splist, proc_landmarks$stdscores, pcnumber = 2, mbrks2,
sdbrks2)
cs2 <- casestudy(frk90_splist, proc_landmarks$stdscores, pcnumber = 2, mbrks2,
sdbrks2)
arrows(cs$mean_bincode-0.5, cs$sd_bincode-0.5, cs2$mean_bincode-0.5,
cs2$sd_bincode-0.5, length = 0.10,lwd = 4)

#in
cs <- casestudy(in30_splist, proc_landmarks$stdscores, pcnumber = 2, mbrks2, sdbrks2)
cs2 <- casestudy(in20_splist, proc_landmarks$stdscores, pcnumber = 2, mbrks2,
sdbrks2)
arrows(cs$mean_bincode-0.5, cs$sd_bincode-0.5, cs2$mean_bincode-0.5,
cs2$sd_bincode-0.5, length = 0.10,lwd = 4)

#tx
cs <- casestudy(ltx_splist, proc_landmarks$stdscores, pcnumber = 2, mbrks2, sdbrks2)
cs2 <- casestudy(udtx_splist, proc_landmarks$stdscores, pcnumber = 2, mbrks2,
sdbrks2)
cs3 <- casestudy(uctx_splist, proc_landmarks$stdscores, pcnumber = 2, mbrks2,
sdbrks2)
arrows(cs$mean_bincode-0.5, cs$sd_bincode-0.5, cs2$mean_bincode-0.5,
cs2$sd_bincode-0.5, length = 0.10,lwd = 4)
arrows(cs2$mean_bincode-0.5, cs2$sd_bincode-0.5, cs3$mean_bincode-0.5,
cs3$sd_bincode-0.5, length = 0.10,lwd = 4)


#grab all the data for that box
dat <- round(NApoints$BIO1[UID$ID][which(mbc2==13 & sdbc2==11)])

#plot the kernel density with gaussian kernel, bandwidth = 1
mod <- density(dat, bw = 1, na.rm = TRUE)
plot(mod, ylim = c(0,1), col = "darkblue", lwd = 2)
polygon(mod$x, mod$y, col = "skyblue")

#####
```

```
modmax <- array(NA, dim = length(sd_ecometric_pc2)) #this should only be the length
of the # of geographic points that have snakes
mod <- list()
for(i in 1:length(sd_ecometric_pc2)){
  if(!(is.na(mbc2[i]) | is.na(sdbc2[i]))){
    dat <- round(NApoints$BIO1[UID$ID][which(mbc2==mbc2[i] & sdbc2==sdbc2[i])])
    if(sum(!is.na(dat)) > 0) {
      mod[[i]] <- density(dat[!is.na(dat)], bw = 1)
      modmax[i] <- mod[[i]]$x[which.max(mod[[i]]$y)]
    }}}
modmax<-round(modmax)
cutoff<-1
#calculate maximum likelihood for all bins; cutoff >1 species for snakes

h <- hist(NApoints$BIO1[UID$ID], main = "", xlab = "Mean Annual Temperature", col
= "gray", breaks = 5)

#plot maximum likelihood temperature from ecometric
tmp <- (modmax - min(modmax, na.rm = T)) * 100
colfunc<-colorRampPalette(c("blue", "white", "red"))(max(tmp, na.rm = T))[tmp]
plot(snakegeo_sp_proj_mod, pch = 16, cex = 0.01)
plot(na_proj, add = T, col = "lightgray")
points(UID[,1:2], col = colfunc, pch = 16, cex = 1.25)
plot(na_proj, add = T)
box()
title("Ecometric Temperature PC2")
legend("bottomright", legend = h$breaks, pch = 16, col = colorRampPalette(c("blue",
"white", "red"))(length(h$breaks)), cex = .75)

#plot actual temperature for comparison
tmp <- (bioclim$BIO1[UID$ID] - min(bioclim$BIO1[UID$ID], na.rm = T))
colfunc<-colorRampPalette(c("blue", "green", "yellow","orange", "red"))(max(tmp,
na.rm = T))[tmp]
plot(snakegeo_sp_proj_mod, pch = 16, cex = 0.01)
plot(na_proj, add = T, col = "lightgray")
points(UID[,1:2], col = colfunc, pch = 16, cex = 0.75)
plot(na_proj, add = T)
box()
title("Mean Annual Temperature")
legend("bottomright", legend = h$breaks, pch = 16, col = colorRampPalette(c("blue",
"green", "yellow","orange", "red"))(length(h$breaks)), cex = 0.75)

#plot anomaly to visualize differences
anom <- NApoints$BIO1[UID$ID] - modmax
```

```
h_anom <- hist(anom, main = "", xlab = "Anomaly", col = "gray", breaks = abreaks)
tmp <- (anom - min(anom, na.rm = T))

colfunc<-colorRampPalette(brewer.pal(10, "PRGn"))(max(tmp, na.rm = T))[tmp]

plot(snakegeo_sp_proj_mod, pch = 16, cex = 0.01)
plot(na_proj, add = T, col = "lightgray")
points(UID[,1:2], col = colfunc, pch = 16, cex = 1.25)
plot(na_proj, add = T)
box()
title("MAT Anomaly PC2")
legend("bottomright", legend = h_anom$breaks, pch = 16, col =
colorRampPalette(brewer.pal(10, "PRGn"))(length(h_anom$breaks)), cex = .75)

tempcor <- cor(bioclim$BIO1[UID$ID], modmax, use = "pairwise.complete.obs",
method = "pearson")
tempcor^2

#PC3 MAT
#stdev variable
sd_ecometric_pc3 <- unlist(lapply(1:length(UID$ID), function(x)
sd(proc_landmarks$stdscores[NAm_snakemorph$Species %in% snakegeo[snakegeo$ID
%in% UID$ID[x],4],3], na.rm = T )))

#bins 25x25 community level trait distrib
mtemp3 <- range(ecometric_pc3, na.rm = T)
sdtemp3 <- range(sd_ecometric_pc3, na.rm = T)

#break points for mean and stdev
mbrks3 <- seq(mtemp3[1], mtemp3[2], diff(mtemp3)/25)
sdbrks3 <- seq(sdtemp3[1], sdtemp3[2], diff(sdtemp3)/25)

#assign bin codes
mbc3 <- .bincode(ecometric_pc3, breaks = mbrks3)
sdbc3 <- .bincode(sd_ecometric_pc3, breaks = sdbrks3)

#calc temp for each bin
#mean
#obj <- array(NA,dim = c(25,25))
#for(i in 1:25){
#  for(j in 1:25){
#    dat <- round(NApoints$BIO1[UID$ID][which(mbc3==i & sdbc3==j)])
#    obj[26 - j,i] <- mean(dat, na.rm = T)
#  }
```

```
#}

#Maxlike
mod <- list()
obj <- array(NA,dim = c(25,25))
for(i in 1:25){
  for(j in 1:25){
    if(sum(mbc3 == i & sdbc3 == j, na.rm = T) != 0){
      dat <- NApoints$BIO1[UID$ID][which(mbc3 ==i & sdbc3 ==j)]
      mod[[i]] <- density(dat[!is.na(dat)], bw = 1)
      obj[26 - j,i] <- mod[[i]]$x[which.max(mod[[i]]$y)]
    }
  }
}
#make a raster
r <- raster(extent(0,25,0,25), resolution = 1)
#set the values to the obj
r <- setValues(r,obj)
change_breaks <- 10

#make an empty plot
plot(0:25, 0:25, type = "n", xlim = c(0,25), ylim = c(0,25),
     xaxs = "i", yaxs = "i", asp = 1, axes = F, xlab ="mean PC3", ylab="Std. Dev. PC3")
#add the rectangle/box
rect(0, 0, 25, 25, lwd = 3)
#add the raster data
plot(r, col = color_r, add = T)
lines (x = c(8.3, 8.3), y = c(0, 25))
lines (x = c(16.6, 16.6), y = c(0, 25))
lines(x = c(0, 25), y = c(8.3, 8.3))
lines(x = c(0, 25), y = c(16.6, 16.6))
axis(side = 2, at = c(0.0, 8.3, 16.6, 25), labels = c(<0.01, 0.60, 1.20, 1.80), line=-3)
axis(side = 1, at = c(0.0, 8.3, 16.6, 25), labels = c(-1.12, -0.43, 0.26, 0.95))

#this is mean = 3.1, 12, and sd = 1.08, 10
#rect(9, 7, 10, 8, lwd = 4)
#box()

#for case studies

#New Mexico
cs <- casestudy(nm19_splist, proc_landmarks$stdscores, pcnumber = 3, mbrks3,
sdbrks3)
#rect(cs$mean_bincode-1, cs$sd_bincode-1, cs$mean_bincode, cs$sd_bincode, lwd = 4)
```

```
cs2 <- casestudy(nm20_splist, proc_landmarks$stdscores, pcnumber = 3, mbrks3,
sdbrks3)
#rect(cs2$mean_bincode-1, cs2$sd_bincode-1, cs2$mean_bincode, cs2$sd_bincode, lwd
= 4)
arrows(cs$mean_bincode-0.5, cs$sd_bincode-0.5, cs2$mean_bincode-0.5,
cs2$sd_bincode-0.5, length = 0.10,lwd = 4)

#uks
cs <- casestudy(uks40_splist, proc_landmarks$stdscores, pcnumber = 3, mbrks3,
sdbrks3)
cs2 <- casestudy(uks20_splist, proc_landmarks$stdscores, pcnumber = 3, mbrks3,
sdbrks3)
arrows(cs$mean_bincode-0.5, cs$sd_bincode-0.5, cs2$mean_bincode-0.5,
cs2$sd_bincode-0.5, length = 0.10,lwd = 4)

#frk
cs <- casestudy(frk30_splist, proc_landmarks$stdscores, pcnumber = 3, mbrks3,
sdbrks3)
cs2 <- casestudy(frk90_splist, proc_landmarks$stdscores, pcnumber = 3, mbrks3,
sdbrks3)
arrows(cs$mean_bincode-0.5, cs$sd_bincode-0.5, cs2$mean_bincode-0.5,
cs2$sd_bincode-0.5, length = 0.10,lwd = 4)

#in
cs <- casestudy(in30_splist, proc_landmarks$stdscores, pcnumber = 3, mbrks3, sdbrks3)
cs2 <- casestudy(in20_splist, proc_landmarks$stdscores, pcnumber = 3, mbrks3,
sdbrks3)
arrows(cs$mean_bincode-0.5, cs$sd_bincode-0.5, cs2$mean_bincode-0.5,
cs2$sd_bincode-0.5, length = 0.10,lwd = 4)

#tx
cs <- casestudy(ltx_splist, proc_landmarks$stdscores, pcnumber = 3, mbrks3, sdbrks3)
cs2 <- casestudy(udtx_splist, proc_landmarks$stdscores, pcnumber = 3, mbrks3,
sdbrks3)
cs3 <- casestudy(uctx_splist, proc_landmarks$stdscores, pcnumber = 3, mbrks3,
sdbrks3)
arrows(cs$mean_bincode-0.5, cs$sd_bincode-0.5, cs2$mean_bincode-0.5,
cs2$sd_bincode-0.5, length = 0.10,lwd = 4)
arrows(cs2$mean_bincode-0.5, cs2$sd_bincode-0.5, cs3$mean_bincode-0.5,
cs3$sd_bincode-0.5, length = 0.10,lwd = 4)
rect(10, 13, 11,14, lwd = 4)

#grab all the data for that box
dat <- round(NApoints$BIO1[UID$ID][which(mbc3==12 & sdbc3==10)])
```

```
#plot the kernel density with gaussian kernel, bandwidth = 1
mod <- density(dat, bw = 1)
plot(mod, ylim = c(0,1), col = "darkblue", lwd = 2)
polygon(mod$x, mod$y, col = "skyblue")

#####
modmax <- array(NA, dim = length(sd_ecometric_pc3)) #this should only be the length
of the # of geographic points that have snakes
mod <- list()
for(i in 1:length(sd_ecometric_pc3)){
  if(!(is.na(mbc3[i]) | is.na(sdbc3[i]))){
    dat <- round(NApoints$BIO1[UID$ID][which(mbc3==mbc3[i] & sdbc3==sdbc3[i])])
    if(sum(!is.na(dat)) > 0) {
      mod[[i]] <- density(dat[!is.na(dat)], bw = 1)
      modmax[i] <- mod[[i]]$x[which.max(mod[[i]]$y)]
    }}}
modmax<-round(modmax)
cutoff<-1
#calculate maximum likelihood for all bins; cutoff >3 species for snakes

h <- hist(NApoints$BIO1[UID$ID], main = "", xlab = "Mean Annual Temperature", col
= "gray", breaks = 5)

#plot maximum likelihood temperature from ecometric
tmp <- (modmax - min(modmax, na.rm = T)) * 100
colfunc<-colorRampPalette(c("blue","white", "red"))(max(tmp, na.rm = T))[tmp]
plot(snakegeo_sp_proj_mod, pch = 16, cex = 0.01)
plot(na_proj, add = T, col = "lightgray")
points(UID[,1:2], col = colfunc, pch = 16, cex = 1.25)
plot(na_proj, add = T)
box()
title("Ecometric Temperature PC3")
legend("bottomright", legend = h$breaks, pch = 16, col = colorRampPalette(c("blue",
"white", "red"))(length(h$breaks)), cex = .75)

#plot actual temperature for comparison
tmp <- (bioclim$BIO1[UID$ID] - min(bioclim$BIO1[UID$ID], na.rm = T))
colfunc<-colorRampPalette(c("blue", "green", "yellow","orange", "red"))(max(tmp,
na.rm = T))[tmp]
plot(snakegeo_sp_proj_mod, pch = 16, cex = 0.01)
plot(na_proj, add = T, col = "lightgray")
points(UID[,1:2], col = colfunc, pch = 16, cex = 0.75)
plot(na_proj, add = T)
```

```
box()
title("Mean Annual Temperature")
legend("bottomright", legend = h$breaks, pch = 16, col = colorRampPalette(c("blue",
"green", "yellow","orange", "red"))(length(h$breaks)), cex = 0.75)

#plot anomaly to visualize differences
anom <- NApoints$BIO1[UID$ID] - modmax
h_anom <- hist(anom, main = "", xlab = "Anomaly", col = "gray", breaks = abreaks)
tmp <- (anom - min(anom, na.rm = T))

colfunc<-colorRampPalette(brewer.pal(10, "PRGn"))(max(tmp, na.rm = T))[tmp]

plot(snakegeo_sp_proj_mod, pch = 16, cex = 0.01)
plot(na_proj, add = T, col = "lightgray")
points(UID[,1:2], col = colfunc, pch = 16, cex = 1.25)
plot(na_proj, add = T)
box()
title("MAT Anomaly PC3")
legend("bottomright", legend = h_anom$breaks, pch = 16, col =
colorRampPalette(brewer.pal(10, "PRGn"))(length(h_anom$breaks)), cex = .75)

tempcor <- cor(bioclim$BIO1[UID$ID], modmax, use = "pairwise.complete.obs",
method = "pearson")
tempcor^2

#PC4 MAT
#stdev variable
sd_ecometric_pc4 <- unlist(lapply(1:length(UID$ID), function(x)
sd(proc_landmarks$stdscores[NAm_snakemorph$Species %in% snakegeo[snakegeo$ID
%in% UID$ID[x],4],4], na.rm = T )))

#bins 25x25 community level trait distrib
mtemp4 <- range(ecometric_pc4, na.rm = T)
sdtemp4 <- range(sd_ecometric_pc4, na.rm = T)

#break points for mean and stdev
mbrks4 <- seq(mtemp4[1], mtemp4[2], diff(mtemp4)/25)
sdbrks4 <- seq(sdtemp4[1], sdtemp4[2], diff(sdtemp4)/25)

#assign bin codes
mbc4 <- .bincode(ecometric_pc4, breaks = mbrks4)
sdbc4 <- .bincode(sd_ecometric_pc4, breaks = sdbrks4)

#calc temp for each bin
```

```
#mean
#obj <- array(NA,dim = c(25,25))
#for(i in 1:25){
 # for(j in 1:25){
  #  dat <- round(NApoints$BIO1[UID$ID][which(mbc4==i & sdbc4==j)])
   # obj[26 - j,i] <- mean(dat, na.rm = T)
  #}
#}

#Maxlike
mod <- list()
obj <- array(NA,dim = c(25,25))
for(i in 1:25){
  for(j in 1:25){
    if(sum(mbc4 == i & sdbc4 == j, na.rm = T) != 0){
      dat <- NApoints$BIO1[UID$ID][which(mbc4 ==i & sdbc4 ==j)]
      mod[[i]] <- density(dat[!is.na(dat)], bw = 1)
      obj[26 - j,i] <- mod[[i]]$x[which.max(mod[[i]]$y)]
    }
  }
}
#make a raster
r <- raster(extent(0,25,0,25), resolution = 1)
#set the values to the obj
r <- setValues(r,obj)
change_breaks <- 10

#make an empty plot
plot(0:25, 0:25, type = "n", xlim = c(0,25), ylim = c(0,25),
     xaxs = "i", yaxs = "i", asp = 1, axes = F, xlab ="mean PC4", ylab="Std. Dev. PC4")
#add the rectangle/box
rect(0, 0, 25, 25, lwd = 3)
#add the raster data
plot(r, col = color_r, add = T)
lines (x = c(8.3, 8.3), y = c(0, 25))
lines (x = c(16.6, 16.6), y = c(0, 25))
lines(x = c(0, 25), y = c(8.3, 8.3))
lines(x = c(0, 25), y = c(16.6, 16.6))
axis(side = 2, at = c(0.0, 8.3, 16.6, 25), labels = c(<0.01, 0.55, 1.09, 1.63), line = -3)
axis(side = 1, at = c(0.0, 8.3, 16.6, 25), labels = c(-1.77, -0.87, 0.04, 0.95))

#this is mean = 3.1, 12, and sd = 1.08, 10
#rect(8, 10, 9, 11, lwd = 4)
#box()
```

```
#for case studies

#New Mexico
cs <- casestudy(nm19_splist, proc_landmarks$stdscores, pcnumber = 4, mbrks4,
sdbrks4)
#rect(cs$mean_bincode-1, cs$sd_bincode-1, cs$mean_bincode, cs$sd_bincode, lwd = 4)
cs2 <- casestudy(nm20_splist, proc_landmarks$stdscores, pcnumber = 4, mbrks4,
sdbrks4)
#rect(cs2$mean_bincode-1, cs2$sd_bincode-1, cs2$mean_bincode, cs2$sd_bincode, lwd
= 4)
arrows(cs$mean_bincode-0.5, cs$sd_bincode-0.5, cs2$mean_bincode-0.5,
cs2$sd_bincode-0.5, length = 0.10,lwd = 4)

#uks
cs <- casestudy(uks40_splist, proc_landmarks$stdscores, pcnumber = 4, mbrks4,
sdbrks4)
cs2 <- casestudy(uks20_splist, proc_landmarks$stdscores, pcnumber = 4, mbrks4,
sdbrks4)
arrows(cs$mean_bincode-0.5, cs$sd_bincode-0.5, cs2$mean_bincode-0.5,
cs2$sd_bincode-0.5, length = 0.10,lwd = 4)

#frk
cs <- casestudy(frk30_splist, proc_landmarks$stdscores, pcnumber = 4, mbrks4,
sdbrks4)
cs2 <- casestudy(frk90_splist, proc_landmarks$stdscores, pcnumber = 4, mbrks4,
sdbrks4)
arrows(cs$mean_bincode-0.5, cs$sd_bincode-0.5, cs2$mean_bincode-0.5,
cs2$sd_bincode-0.5, length = 0.10,lwd = 4)

#in
cs <- casestudy(in30_splist, proc_landmarks$stdscores, pcnumber = 4, mbrks4, sdbrks4)
cs2 <- casestudy(in20_splist, proc_landmarks$stdscores, pcnumber = 4, mbrks4,
sdbrks4)
arrows(cs$mean_bincode-0.5, cs$sd_bincode-0.5, cs2$mean_bincode-0.5,
cs2$sd_bincode-0.5, length = 0.10,lwd = 4)

#tx
cs <- casestudy(ltx_splist, proc_landmarks$stdscores, pcnumber = 4, mbrks4, sdbrks4)
cs2 <- casestudy(udtx_splist, proc_landmarks$stdscores, pcnumber = 4, mbrks4,
sdbrks4)
cs3 <- casestudy(uctx_splist, proc_landmarks$stdscores, pcnumber = 4, mbrks4,
sdbrks4)
```

```
arrows(cs$mean_bincode-0.5, cs$sd_bincode-0.5, cs2$mean_bincode-0.5,
cs2$sd_bincode-0.5, length = 0.10,lwd = 4)
arrows(cs2$mean_bincode-0.5, cs2$sd_bincode-0.5, cs3$mean_bincode-0.5,
cs3$sd_bincode-0.5, length = 0.10,lwd = 4)


#grab all the data for that box
dat <- round(NApoints$BIO1[UID$ID][which(mbc4==12 & sdbc4==10)])
#dat <- na.omit(dat)
#plot the kernel density with gaussian kernel, bandwidth = 1
mod <- density(dat, bw = 1)
plot(mod, ylim = c(0,1), col = "darkblue", lwd = 2)
polygon(mod$x, mod$y, col = "skyblue")

#####
modmax <- array(NA, dim = length(sd_ecometric_pc4)) #this should only be the length
of the # of geographic points that have snakes
mod <- list()
for(i in 1:length(sd_ecometric_pc4)){
  if(!(is.na(mbc4[i]) | is.na(sdbc4[i]))){
    dat <- round(NApoints$BIO1[UID$ID][which(mbc4==mbc4[i] & sdbc4==sdbc4[i])])
    if(sum(!is.na(dat)) > 0) {
    mod[[i]] <- density(dat[!is.na(dat)], bw = 1)
    modmax[i] <- mod[[i]]$x[which.max(mod[[i]]$y)]
  }}}
modmax<-round(modmax)
cutoff<-1

#calculate maximum likelihood for all bins; cutoff >3 species for snakes

h <- hist(NApoints$BIO1[UID$ID], main = "", xlab = "Mean Annual Temperature", col
= "gray", breaks = 5)

#plot maximum likelihood temperature from ecometric
tmp <- (modmax - min(modmax, na.rm = T)) * 100
colfunc<-colorRampPalette(c("blue", "white", "red"))(max(tmp, na.rm = T))[tmp]
plot(snakegeo_sp_proj_mod, pch = 16, cex = 0.01)
plot(na_proj, add = T, col = "lightgray")
points(UID[,1:2], col = colfunc, pch = 16, cex = 1.25)
plot(na_proj, add = T)
box()
title("Ecometric Temperature PC4")
legend("bottomright", legend = h$breaks, pch = 16, col = colorRampPalette(c("blue",
"white", "red"))(length(h$breaks)), cex = .75)
```

```
#plot actual temperature for comparison
tmp <- (bioclim$BIO1[UID$ID] - min(bioclim$BIO1[UID$ID], na.rm = T))
colfunc<-colorRampPalette(c("blue", "green", "yellow","orange", "red"))(max(tmp,
na.rm = T))[tmp]
plot(snakegeo_sp_proj_mod, pch = 16, cex = 0.01)
plot(na_proj, add = T, col = "lightgray")
points(UID[,1:2], col = colfunc, pch = 16, cex = 0.75)
plot(na_proj, add = T)
box()
title("Mean Annual Temperature")
legend("bottomright", legend = h$breaks, pch = 16, col = colorRampPalette(c("blue",
"green", "yellow","orange", "red"))(length(h$breaks)), cex = 0.75)

#plot anomaly to visualize differences
anom <- NApoints$BIO1[UID$ID] - modmax
h_anom <- hist(anom, main = "", xlab = "Anomaly", col = "gray", breaks = abreaks)
tmp <- (anom - min(anom, na.rm = T))

colfunc<-colorRampPalette(brewer.pal(10, "PRGn"))(max(tmp, na.rm = T))[tmp]

plot(snakegeo_sp_proj_mod, pch = 16, cex = 0.01)
plot(na_proj, add = T, col = "lightgray")
points(UID[,1:2], col = colfunc, pch = 16, cex = 1.25)
plot(na_proj, add = T)
box()
title("MAT Anomaly PC4")
legend("bottomright", legend = h_anom$breaks, pch = 16, col =
colorRampPalette(brewer.pal(10, "PRGn"))(length(h_anom$breaks)), cex = .75)

tempcor <- cor(bioclim$BIO1[UID$ID], modmax, use = "pairwise.complete.obs",
method = "pearson")
tempcor^2

#PC5 MAT
#stdev variable
sd_ecometric_pc5 <- unlist(lapply(1:length(UID$ID), function(x)
sd(proc_landmarks$stdscores[NAm_snakemorph$Species %in% snakegeo[snakegeo$ID
%in% UID$ID[x],4],5], na.rm = T )))

#bins 25x25 community level trait distrib
mtemp5 <- range(ecometric_pc5, na.rm = T)
sdtemp5 <- range(sd_ecometric_pc5, na.rm = T)
```

```
#break points for mean and stdev
mbrks5 <- seq(mtemp5[1], mtemp5[2], diff(mtemp5)/25)
sdbrks5 <- seq(sdtemp5[1], sdtemp5[2], diff(sdtemp5)/25)

#assign bin codes
mbc5 <- .bincode(ecometric_pc5, breaks = mbrks5)
sdbc5 <- .bincode(sd_ecometric_pc5, breaks = sdbrks5)

#calc temp for each bin
#mean
#obj <- array(NA,dim = c(25,25))
#for(i in 1:25){
#  for(j in 1:25){
#    dat <- round(NApoints$BIO1[UID$ID][which(mbc5==i & sdbc5==j)])
#    obj[26 - j,i] <- mean(dat, na.rm = T)
#  }
#}

#Maxlike
mod <- list()
obj <- array(NA,dim = c(25,25))
for(i in 1:25){
  for(j in 1:25){
    if(sum(mbc5 == i & sdbc5 == j, na.rm = T) != 0){
      dat <- NApoints$BIO1[UID$ID][which(mbc5 ==i & sdbc5 ==j)]
      mod[[i]] <- density(dat[!is.na(dat)], bw = 1)
      obj[26 - j,i] <- mod[[i]]$x[which.max(mod[[i]]$y)]
    }
  }
}
#make a raster
r <- raster(extent(0,25,0,25), resolution = 1)
#set the values to the obj
r <- setValues(r,obj)
change_breaks <- 10

#make an empty plot
plot(0:25, 0:25, type = "n", xlim = c(0,25), ylim = c(0,25),
     xaxs = "i", yaxs = "i", asp = 1, axes = F, xlab ="Mean PC5", ylab="Std. Dev. PC5")
#add the rectangle/box
rect(0, 0, 25, 25, lwd = 3)
#add the raster data
plot(r, col = color_r, add = T)
lines (x = c(8.3, 8.3), y = c(0, 25))
```

```
lines (x = c(16.6, 16.6), y = c(0, 25))
lines(x = c(0, 25), y = c(8.3, 8.3))
lines(x = c(0, 25), y = c(16.6, 16.6))
axis(side = 2, at = c(0.0, 8.3, 16.6, 25), labels = c(<0.01, 0.87, 1.74, 2.61), line = -3)
axis(side = 1, at = c(0.0, 8.3, 16.6, 25), labels = c(-1.47, -0.38, 0.71, 1.80))

#this is mean = 3.1, 12, and sd = 1.08, 10
#rect(11, 10, 12, 11, lwd = 4)
#box()

#for case studies

#New Mexico
cs <- casestudy(nm19_splist, proc_landmarks$stdscores, pcnumber = 5, mbrks5,
sdbrks5)
#rect(cs$mean_bincode-1, cs$sd_bincode-1, cs$mean_bincode, cs$sd_bincode, lwd = 4)
cs2 <- casestudy(nm20_splist, proc_landmarks$stdscores, pcnumber = 5, mbrks5,
sdbrks5)
#rect(cs2$mean_bincode-1, cs2$sd_bincode-1, cs2$mean_bincode, cs2$sd_bincode, lwd
= 4)
arrows(cs$mean_bincode-0.5, cs$sd_bincode-0.5, cs2$mean_bincode-0.5,
cs2$sd_bincode-0.5, length = 0.10,lwd = 4)

#uks
cs <- casestudy(uks40_splist, proc_landmarks$stdscores, pcnumber = 5, mbrks5,
sdbrks5)
cs2 <- casestudy(uks20_splist, proc_landmarks$stdscores, pcnumber = 5, mbrks5,
sdbrks5)
arrows(cs$mean_bincode-0.5, cs$sd_bincode-0.5, cs2$mean_bincode-0.5,
cs2$sd_bincode-0.5, length = 0.10,lwd = 4)

#frk
cs <- casestudy(frk30_splist, proc_landmarks$stdscores, pcnumber = 5, mbrks5,
sdbrks5)
cs2 <- casestudy(frk90_splist, proc_landmarks$stdscores, pcnumber = 5, mbrks5,
sdbrks5)
arrows(cs$mean_bincode-0.5, cs$sd_bincode-0.5, cs2$mean_bincode-0.5,
cs2$sd_bincode-0.5, length = 0.10,lwd = 4)

#in
cs <- casestudy(in30_splist, proc_landmarks$stdscores, pcnumber = 5, mbrks5, sdbrks5)
cs2 <- casestudy(in20_splist, proc_landmarks$stdscores, pcnumber = 5, mbrks5,
sdbrks5)
```

```
arrows(cs$mean_bincode-0.5, cs$sd_bincode-0.5, cs2$mean_bincode-0.5,
cs2$sd_bincode-0.5, length = 0.10,lwd = 4)

#tx
cs <- casestudy(ltx_splist, proc_landmarks$stdscores, pcnumber = 5, mbrks5, sdbrks5)
cs2 <- casestudy(udtx_splist, proc_landmarks$stdscores, pcnumber = 5, mbrks5,
sdbrks5)
cs3 <- casestudy(uctx_splist, proc_landmarks$stdscores, pcnumber = 5, mbrks5,
sdbrks5)
arrows(cs$mean_bincode-0.5, cs$sd_bincode-0.5, cs2$mean_bincode-0.5,
cs2$sd_bincode-0.5, length = 0.10,lwd = 4)
arrows(cs2$mean_bincode-0.5, cs2$sd_bincode-0.5, cs3$mean_bincode-0.5,
cs3$sd_bincode-0.5, length = 0.10,lwd = 4)


#grab all the data for that box
dat <- round(NApoints$BIO1[UID$ID][which(mbc5==12 & sdbc5==11)])
dat <- na.omit(dat)
#plot the kernel density with gaussian kernel, bandwidth = 1
mod <- density(dat, bw = 1)
plot(mod, ylim = c(0,1), col = "darkblue", lwd = 2)
polygon(mod$x, mod$y, col = "skyblue")


#####
modmax <- array(NA, dim = length(sd_ecometric_pc5)) #this should only be the length
of the # of geographic points that have snakes
mod <- list()
for(i in 1:length(sd_ecometric_pc5)){
  if(!(is.na(mbc5[i]) | is.na(sdbc5[i]))){
    dat <- round(NApoints$BIO1[UID$ID][which(mbc5==mbc5[i] & sdbc5==sdbc5[i])])
    if(sum(!is.na(dat)) > 0) {
     mod[[i]] <- density(dat[!is.na(dat)], bw = 1)
    modmax[i] <- mod[[i]]$x[which.max(mod[[i]]$y)]
  }}}
modmax<-round(modmax)
cutoff<-1

#calculate maximum likelihood for all bins; cutoff >3 species for snakes

h <- hist(NApoints$BIO1[UID$ID], main = "", xlab = "Mean Annual Temperature", col
= "gray", breaks = 5)

#plot maximum likelihood temperature from ecometric
```

```
tmp <- (modmax - min(modmax, na.rm = T)) * 100
colfunc<-colorRampPalette(c("blue","white", "red"))(max(tmp, na.rm = T))[tmp]
plot(snakegeo_sp_proj_mod, pch = 16, cex = 0.01)
plot(na_proj, add = T, col = "lightgray")
points(UID[,1:2], col = colfunc, pch = 16, cex = 1.25)
plot(na_proj, add = T)
box()
title("Ecometric Temperature PC5")
legend("bottomright", legend = h$breaks, pch = 16, col = colorRampPalette(c("blue",
"white", "red"))(length(h$breaks)), cex = .75)

#plot actual temperature for comparison
tmp <- (bioclim$BIO1[UID$ID] - min(bioclim$BIO1[UID$ID], na.rm = T))
colfunc<-colorRampPalette(c("blue", "green", "yellow","orange", "red"))(max(tmp,
na.rm = T))[tmp]
plot(snakegeo_sp_proj_mod, pch = 16, cex = 0.01)
plot(na_proj, add = T, col = "lightgray")
points(UID[,1:2], col = colfunc, pch = 16, cex = 0.75)
plot(na_proj, add = T)
box()
title("Mean Annual Temperature")
legend("bottomright", legend = h$breaks, pch = 16, col = colorRampPalette(c("blue",
"green", "yellow","orange", "red"))(length(h$breaks)), cex = 0.75)


#plot anomaly to visualize differences
anom <- NApoints$BIO1[UID$ID] - modmax
h_anom <- hist(anom, main = "", xlab = "Anomaly", col = "gray", breaks = abreaks)
tmp <- (anom - min(anom, na.rm = T))

colfunc<-colorRampPalette(brewer.pal(10, "PRGn"))(max(tmp, na.rm = T))[tmp]

plot(snakegeo_sp_proj_mod, pch = 16, cex = 0.01)
plot(na_proj, add = T, col = "lightgray")
points(UID[,1:2], col = colfunc, pch = 16, cex = 1.25)
plot(na_proj, add = T)
box()
title("MAT Anomaly PC5")
legend("bottomright", legend = h_anom$breaks, pch = 16, col =
colorRampPalette(brewer.pal(10, "PRGn"))(length(h_anom$breaks)), cex = .75)

tempcor <- cor(bioclim$BIO1[UID$ID], modmax, use = "pairwise.complete.obs",
method = "pearson")
tempcor^2
```

```
#PC6 MAT
#stdev variable
sd_ecometric_pc6 <- unlist(lapply(1:length(UID$ID), function(x)
sd(proc_landmarks$stdscores[NAm_snakemorph$Species %in% snakegeo[snakegeo$ID
%in% UID$ID[x],4],6], na.rm = T )))

#bins 25x25 community level trait distrib
mtemp6 <- range(ecometric_pc6, na.rm = T)
sdtemp6 <- range(sd_ecometric_pc6, na.rm = T)

#break points for mean and stdev
mbrks6 <- seq(mtemp6[1], mtemp6[2], diff(mtemp6)/25)
sdbrks6 <- seq(sdtemp6[1], sdtemp6[2], diff(sdtemp6)/25)

#assign bin codes
mbc6 <- .bincode(ecometric_pc6, breaks = mbrks6, include.lowest=T)
sdbc6 <- .bincode(sd_ecometric_pc6, breaks = sdbrks6, include.lowest=T)
#mbc6[mbc6<1] <- NA
#sdbc6[sdbc6<1] <- NA
#cutoff <- 1
#calc temp for each bin
#Mean
#obj <- array(NA,dim = c(25,25))
#for(i in 1:25){
#  for(j in 1:25){
#    dat <- round(NApoints$BIO1[UID$ID][which(mbc6==i & sdbc6==j)])
#    obj[26 - j,i] <- mean(dat, na.rm = T)
#  }
#}

#Maxlike
mod <- list()
obj <- array(NA,dim = c(25,25))
for(i in 1:25){
  for(j in 1:25){
    if(sum(mbc6 == i & sdbc6 == j, na.rm = T) != 0){
      dat <- NApoints$BIO1[UID$ID][which(mbc6 ==i & sdbc6 ==j)]
      mod[[i]] <- density(dat[!is.na(dat)], bw = 1)
      obj[26 - j,i] <- mod[[i]]$x[which.max(mod[[i]]$y)]
    }
  }
}
#make a raster
```

```
r <- raster(extent(0,25,0,25), resolution = 1)
#set the values to the obj
r <- setValues(r,obj)
change_breaks <- 10

#make an empty plot
plot(0:25, 0:25, type = "n", xlim = c(0,25), ylim = c(0,25),
    xaxs = "i", yaxs = "i", asp = 1, axes = F, xlab ="Mean PC6", ylab="Std. Dev. PC6")
#add the rectangle/box
rect(0, 0, 25, 25, lwd = 3)
#add the raster data
plot(r, col = color_r, add = T)
lines (x = c(8.3, 8.3), y = c(0, 25))
lines (x = c(16.6, 16.6), y = c(0, 25))
lines(x = c(0, 25), y = c(8.3, 8.3))
lines(x = c(0, 25), y = c(16.6, 16.6))
axis(side = 2, at = c(0.0, 8.3, 16.6, 25), labels = c(0.02, 0.88, 1.74, 2.60), line = -3)
axis(side = 1, at = c(0.0, 8.3, 16.6, 25), labels = c(-1.73, -0.50, 0.73, 1.96))

#this is for the mean values
#rect(16, 8, 17, 9, lwd = 4)
#box()

#for case studies

#New Mexico
cs <- casestudy(nm19_splist, proc_landmarks$stdscores, pcnumber = 6, mbrks6,
sdbrks6)
#rect(cs$mean_bincode-1, cs$sd_bincode-1, cs$mean_bincode, cs$sd_bincode, lwd = 4)
cs2 <- casestudy(nm20_splist, proc_landmarks$stdscores, pcnumber = 6, mbrks6,
sdbrks6)
#rect(cs2$mean_bincode-1, cs2$sd_bincode-1, cs2$mean_bincode, cs2$sd_bincode, lwd
= 4)
arrows(cs$mean_bincode-0.5, cs$sd_bincode-0.5, cs2$mean_bincode-0.5,
cs2$sd_bincode-0.5, length = 0.10,lwd = 4)



#uks
cs <- casestudy(uks40_splist, proc_landmarks$stdscores, pcnumber = 6, mbrks6,
sdbrks6)
cs2 <- casestudy(uks20_splist, proc_landmarks$stdscores, pcnumber = 6, mbrks6,
sdbrks6)
```

```
arrows(cs$mean_bincode-0.5, cs$sd_bincode-0.5, cs2$mean_bincode-0.5,
cs2$sd_bincode-0.5, length = 0.10,lwd = 4)

#frk
cs <- casestudy(frk30_splist, proc_landmarks$stdscores, pcnumber = 6, mbrks6,
sdbrks6)
cs2 <- casestudy(frk90_splist, proc_landmarks$stdscores, pcnumber = 6, mbrks6,
sdbrks6)
arrows(cs$mean_bincode-0.5, cs$sd_bincode-0.5, cs2$mean_bincode-0.5,
cs2$sd_bincode-0.5, length = 0.10,lwd = 4)
rect(17, 11, 18, 12, lwd = 4)

#in
cs <- casestudy(in30_splist, proc_landmarks$stdscores, pcnumber = 6, mbrks6, sdbrks6)
cs2 <- casestudy(in20_splist, proc_landmarks$stdscores, pcnumber = 6, mbrks6,
sdbrks6)
arrows(cs$mean_bincode-0.5, cs$sd_bincode-0.5, cs2$mean_bincode-0.5,
cs2$sd_bincode-0.5, length = 0.10,lwd = 4)

#tx
cs <- casestudy(ltx_splist, proc_landmarks$stdscores, pcnumber = 6, mbrks6, sdbrks6)
cs2 <- casestudy(udtx_splist, proc_landmarks$stdscores, pcnumber = 6, mbrks6,
sdbrks6)
cs3 <- casestudy(uctx_splist, proc_landmarks$stdscores, pcnumber = 6, mbrks6,
sdbrks6)
arrows(cs$mean_bincode-0.5, cs$sd_bincode-0.5, cs2$mean_bincode-0.5,
cs2$sd_bincode-0.5, length = 0.10,lwd = 4)
arrows(cs2$mean_bincode-0.5, cs2$sd_bincode-0.5, cs3$mean_bincode-0.5,
cs3$sd_bincode-0.5, length = 0.10,lwd = 4)
rect(16, 11, 17, 12, lwd = 4)

#grab all the data for that box
dat <- round(NApoints$BIO1[UID$ID][which(mbc6==16 & sdbc6==12)])
dat <- na.omit(dat)
#plot the kernel density with gaussian kernel, bandwidth = 1
mod <- density(dat, bw = 1)
plot(mod, ylim = c(0,1), col = "darkblue", lwd = 2)
polygon(mod$x, mod$y, col = "skyblue")


#####
modmax <- array(NA, dim = length(sd_ecometric_pc6))  #this should only be the length
of the # of geographic points that have snakes
mod <- list()
```

```
for(i in 1:length(sd_ecometric_pc6)){
  if(!(is.na(mbc6[i]) | is.na(sdbc6[i]))){
    dat <- round(NApoints$BIO1[UID$ID][which(mbc6==mbc6[i] & sdbc6==sdbc6[i])])
    if(sum(!is.na(dat)) > 0) {
    mod[[i]] <- density(dat[!is.na(dat)], bw = 1)
    modmax[i] <- mod[[i]]$x[which.max(mod[[i]]$y)]
  }}}
modmax<-round(modmax)
cutoff<-1
#calculate maximum likelihood for all bins; cutoff >3 species for snakes

h <- hist(NApoints$BIO1[UID$ID], main = "", xlab = "Mean Annual Temperature", col
= "gray", breaks = 5)

#plot maximum likelihood temperature from ecometric
tmp <- (modmax - min(modmax, na.rm = T)) * 100
colfunc<-colorRampPalette(c("blue", "white", "red"))(max(tmp, na.rm = T))[tmp]
plot(snakegeo_sp_proj_mod, pch = 16, cex = 0.01)
plot(na_proj, add = T, col = "lightgray")
points(UID[,1:2], col = colfunc, pch = 16, cex = 1.25)
plot(na_proj, add = T)
box()
title("Ecometric Temperature PC6")
legend("bottomright", legend = h$breaks, pch = 16, col = colorRampPalette(c("blue",
"white", "red"))(length(h$breaks)), cex = .75)

#plot actual temperature for comparison
tmp <- (bioclim$BIO1[UID$ID] - min(bioclim$BIO1[UID$ID], na.rm = T))
colfunc<-colorRampPalette(c("blue", "green", "yellow","orange", "red"))(max(tmp,
na.rm = T))[tmp]
plot(snakegeo_sp_proj_mod, pch = 16, cex = 0.01)
plot(na_proj, add = T, col = "lightgray")
points(UID[,1:2], col = colfunc, pch = 16, cex = 0.75)
plot(na_proj, add = T)
box()
title("Mean Annual Temperature")
legend("bottomright", legend = h$breaks, pch = 16, col = colorRampPalette(c("blue",
"green", "yellow","orange", "red"))(length(h$breaks)), cex = 0.75)

#plot anomaly to visualize differences
anom <- bioclim$BIO1[UID$ID] - modmax
h_anom <- hist(anom, main = "", xlab = "Anomaly", col = "gray", breaks = abreaks)
tmp <- (anom - min(anom, na.rm = T))
```

```
colfunc<-colorRampPalette(brewer.pal(10, "PRGn"))(max(tmp, na.rm = T))[tmp]

plot(snakegeo_sp_proj_mod, pch = 16, cex = 0.01)
plot(na_proj, add = T, col = "lightgray")
points(UID[,1:2], col = colfunc, pch = 16, cex = 1.25)
plot(na_proj, add = T)
box()
title("MAT Anomaly PC6")
legend("bottomright", legend = h_anom$breaks, pch = 16, col =
colorRampPalette(brewer.pal(10, "PRGn"))(length(h_anom$breaks)), cex = .75)

tempcor <- cor(bioclim$BIO1[UID$ID], modmax, use = "pairwise.complete.obs",
method = "pearson")
tempcor^2

#PC 1&6 MAT
modmax <- array(NA, dim = length(sd_ecometric_pc6)) #this should only be the length
of the # of geographic points that have snakes
mod <- list()
for(i in 1:length(sd_ecometric_pc6)){
  if(!(is.na(mbc6[i]) | is.na(sdbc6[i]))){
    dat <- round(NApoints$BIO1[UID$ID][which(mbc1==mbc1[i] & sdbc1==sdbc1[i] &
mbc6==mbc6[i] & sdbc6 ==sdbc6[i])]) #add additional PCs
    if(sum(!is.na(dat)) > 0) {
      mod[[i]] <- density(dat[!is.na(dat)], bw = 1)
      modmax[i] <- mod[[i]]$x[which.max(mod[[i]]$y)]
    }}}
for(i in 1:length(sd_ecometric_pc1)){
  if(!(is.na(mbc1[i]) | is.na(sdbc1[i]))){
    dat <- round(NApoints$BIO1[UID$ID][which(mbc1==mbc1[i] & sdbc1==sdbc1[i] &
mbc6==mbc6[i] & sdbc6 ==sdbc6[i])]) #add additional PCs
    if(sum(!is.na(dat)) > 0) {
      mod[[i]] <- density(dat[!is.na(dat)], bw = 1)
      modmax[i] <- mod[[i]]$x[which.max(mod[[i]]$y)]
    }}}
modmax<-round(modmax)
cutoff<-1
#calculate maximum likelihood for all bins; cutoff >3 species for snakes

h <- hist(NApoints$BIO1[UID$ID], main = "", xlab = "Mean Annual Temperature", col
= "gray", breaks = 10)


#plot maximum likelihood temperature from ecometric
```

```
tmp <- (modmax - min(modmax, na.rm = T)) * 100
colfunc<-colorRampPalette(c("blue", "white", "red"))(max(tmp, na.rm = T))[tmp]
plot(snakegeo_sp_proj_mod, pch = 16, cex = 0.01)
plot(na_proj, add = T, col = "lightgray")
points(UID[,1:2], col = colfunc, pch = 16, cex = 1.0)
plot(na_proj, add = T)
box()
title("Ecometric Temperature PCs 1&6")
legend("bottomright", legend = h$breaks, pch = 16, col = colorRampPalette(c("blue",
"white", "red"))(length(h$breaks)), cex = .75)

#plot actual temperature for comparison
tmp <- (bioclim$BIO1[UID$ID] - min(bioclim$BIO1[UID$ID], na.rm = T))
colfunc<-colorRampPalette(c("blue", "green", "yellow","orange", "red"))(max(tmp,
na.rm = T))[tmp]
plot(snakegeo_sp_proj_mod, pch = 16, cex = 0.01)
plot(na_proj, add = T, col = "lightgray")
points(UID[,1:2], col = colfunc, pch = 16, cex = 0.75)
plot(na_proj, add = T)
box()
title("Mean Annual Temperature")
legend("bottomright", legend = h$breaks, pch = 16, col = colorRampPalette(c("blue",
"green", "yellow","orange", "red"))(length(h$breaks)), cex = 0.75)

#plot anomaly to visualize differences
anom <- NApoints$BIO1[UID$ID] - modmax
h_anom <- hist(anom, main = "", xlab = "Anomaly", col = "gray", breaks = abreaks)
tmp <- (anom - min(anom, na.rm = T))

colfunc<-colorRampPalette(brewer.pal(10, "PRGn"))(max(tmp, na.rm = T))[tmp]

plot(snakegeo_sp_proj_mod, pch = 16, cex = 0.01)
plot(na_proj, add = T, col = "lightgray")
points(UID[,1:2], col = colfunc, pch = 16, cex = 1.0)
plot(na_proj, add = T)
box()
title("MAT Anomaly  PC1 & PC6")
legend("bottomright", legend = h_anom$breaks, pch = 16, col =
colorRampPalette(brewer.pal(10, "PRGn"))(length(h_anom$breaks)), cex = .75)

tempcor <- cor(bioclim$BIO1[UID$ID], modmax, use = "pairwise.complete.obs",
method = "pearson")
tempcor^2
```

```
#PC2 and PC6
modmax <- array(NA, dim = length(sd_ecometric_pc6)) #this should only be the length
of the # of geographic points that have snakes
mod <- list()
for(i in 1:length(sd_ecometric_pc6)){
  if(!(is.na(mbc6[i]) | is.na(sdbc6[i]))){
    dat <- round(NApoints$BIO1[UID$ID][which(mbc2==mbc2[i] & sdbc2==sdbc2[i] &
mbc6==mbc6[i] & sdbc6 ==sdbc6[i])]) #add additional PCs
    if(sum(!is.na(dat)) > 0) {
      mod[[i]] <- density(dat[!is.na(dat)], bw = 1)
      modmax[i] <- mod[[i]]$x[which.max(mod[[i]]$y)]
    }}}
for(i in 1:length(sd_ecometric_pc2)){
  if(!(is.na(mbc2[i]) | is.na(sdbc2[i]))){
    dat <- round(NApoints$BIO1[UID$ID][which(mbc2==mbc2[i] & sdbc2==sdbc2[i] &
mbc6==mbc6[i] & sdbc6 ==sdbc6[i])]) #add additional PCs
    if(sum(!is.na(dat)) > 0) {
      mod[[i]] <- density(dat[!is.na(dat)], bw = 1)
      modmax[i] <- mod[[i]]$x[which.max(mod[[i]]$y)]
    }}}
modmax<-round(modmax)
cutoff<-1
#calculate maximum likelihood for all bins; cutoff >3 species for snakes

h <- hist(NApoints$BIO1[UID$ID], main = "", xlab = "Mean Annual Temperature", col
= "gray", breaks = 10)

#plot maximum likelihood temperature from ecometric
tmp <- (modmax - min(modmax, na.rm = T)) * 100
colfunc<-colorRampPalette(c("blue", "white", "red"))(max(tmp, na.rm = T))[tmp]
plot(snakegeo_sp_proj_mod, pch = 16, cex = 0.01)
plot(na_proj, add = T, col = "lightgray")
points(UID[,1:2], col = colfunc, pch = 16, cex = 1.0)
plot(na_proj, add = T)
box()
title("Ecometric Temperature PC2 & PC6")
legend("bottomright", legend = h$breaks, pch = 16, col = colorRampPalette(c("blue",
"white", "red"))(length(h$breaks)), cex = .75)

#plot actual temperature for comparison
tmp <- (bioclim$BIO1[UID$ID] - min(bioclim$BIO1[UID$ID], na.rm = T))
colfunc<-colorRampPalette(c("blue", "green", "yellow","orange", "red"))(max(tmp,
na.rm = T))[tmp]
plot(snakegeo_sp_proj_mod, pch = 16, cex = 0.01)
```

```
plot(na_proj, add = T, col = "lightgray")
points(UID[,1:2], col = colfunc, pch = 16, cex = 0.75)
plot(na_proj, add = T)
box()
title("Mean Annual Temperature")
legend("bottomright", legend = h$breaks, pch = 16, col = colorRampPalette(c("blue",
"green", "yellow","orange", "red"))(length(h$breaks)), cex = 0.75)

#plot anomaly to visualize differences
anom <- NApoints$BIO1[UID$ID] - modmax
h_anom <- hist(anom, main = "", xlab = "Anomaly", col = "gray", breaks = abreaks)
tmp <- (anom - min(anom, na.rm = T))

colfunc<-colorRampPalette(brewer.pal(10, "PRGn"))(max(tmp, na.rm = T))[tmp]

plot(snakegeo_sp_proj_mod, pch = 16, cex = 0.01)
plot(na_proj, add = T, col = "lightgray")
points(UID[,1:2], col = colfunc, pch = 16, cex = 1.0)
plot(na_proj, add = T)
box()
title("MAT Anomaly  PC2 & PC6")
legend("bottomright", legend = h_anom$breaks, pch = 16, col =
colorRampPalette(brewer.pal(10, "PRGn"))(length(h_anom$breaks)), cex = .75)

tempcor <- cor(bioclim$BIO1[UID$ID], modmax, use = "pairwise.complete.obs",
method = "pearson")
tempcor^2

#PC 3&6 MAT
modmax <- array(NA, dim = length(sd_ecometric_pc6)) #this should only be the length
of the # of geographic points that have snakes
mod <- list()
for(i in 1:length(sd_ecometric_pc6)){
  if(!(is.na(mbc6[i]) | is.na(sdbc6[i]))){
    dat <- round(NApoints$BIO1[UID$ID][which(mbc3==mbc3[i] & sdbc3==sdbc3[i] &
mbc6==mbc6[i] & sdbc6 ==sdbc6[i])]) #add additional PCs
    if(sum(!is.na(dat)) > 0) {
      mod[[i]] <- density(dat[!is.na(dat)], bw = 1)
      modmax[i] <- mod[[i]]$x[which.max(mod[[i]]$y)]
    }}}
for(i in 1:length(sd_ecometric_pc3)){
  if(!(is.na(mbc3[i]) | is.na(sdbc3[i]))){
    dat <- round(NApoints$BIO1[UID$ID][which(mbc3==mbc3[i] & sdbc3==sdbc3[i] &
mbc6==mbc6[i] & sdbc6 ==sdbc6[i])]) #add additional PCs
```

```
   if(sum(!is.na(dat)) > 0) {
     mod[[i]] <- density(dat[!is.na(dat)], bw = 1)
     modmax[i] <- mod[[i]]$x[which.max(mod[[i]]$y)]
   }}}
modmax<-round(modmax)
cutoff<-1
#calculate maximum likelihood for all bins; cutoff >3 species for snakes

h <- hist(NApoints$BIO1[UID$ID], main = "", xlab = "Mean Annual Temperature", col
= "gray", breaks = 10)

#plot maximum likelihood temperature from ecometric
tmp <- (modmax - min(modmax, na.rm = T)) * 100
colfunc<-colorRampPalette(c("blue","white", "red"))(max(tmp, na.rm = T))[tmp]
plot(snakegeo_sp_proj_mod, pch = 16, cex = 0.01)
plot(na_proj, add = T, col = "lightgray")
points(UID[,1:2], col = colfunc, pch = 16, cex = 1.0)
plot(na_proj, add = T)
box()
title("Ecometric Temperature PC3 & PC6")
legend("bottomright", legend = h$breaks, pch = 16, col = colorRampPalette(c("blue",
"white", "red"))(length(h$breaks)), cex = .75)

#plot actual temperature for comparison
tmp <- (bioclim$BIO1[UID$ID] - min(bioclim$BIO1[UID$ID], na.rm = T))
colfunc<-colorRampPalette(c("blue", "green", "yellow","orange", "red"))(max(tmp,
na.rm = T))[tmp]
plot(snakegeo_sp_proj_mod, pch = 16, cex = 0.01)
plot(na_proj, add = T, col = "lightgray")
points(UID[,1:2], col = colfunc, pch = 16, cex = 0.75)
plot(na_proj, add = T)
box()
title("Mean Annual Temperature")
legend("bottomright", legend = h$breaks, pch = 16, col = colorRampPalette(c("blue",
"green", "yellow","orange", "red"))(length(h$breaks)), cex = 0.75)

#plot anomaly to visualize differences
anom <- NApoints$BIO1[UID$ID] - modmax
h_anom <- hist(anom, main = "", xlab = "Anomaly", col = "gray", breaks = abreaks)
tmp <- (anom - min(anom, na.rm = T))

colfunc<-colorRampPalette(brewer.pal(10, "PRGn"))(max(tmp, na.rm = T))[tmp]

plot(snakegeo_sp_proj_mod, pch = 16, cex = 0.01)
```

```
plot(na_proj, add = T, col = "lightgray")
points(UID[,1:2], col = colfunc, pch = 16, cex = 1.0)
plot(na_proj, add = T)
box()
title("MAT Anomaly  PC3 & PC6")
legend("bottomright", legend = h_anom$breaks, pch = 16, col =
colorRampPalette(brewer.pal(10, "PRGn"))(length(h_anom$breaks)), cex = .75)

tempcor <- cor(bioclim$BIO1[UID$ID], modmax, use = "pairwise.complete.obs",
method = "pearson")
tempcor^2

#PC 4&6 MAT

modmax <- array(NA, dim = length(sd_ecometric_pc6)) #this should only be the length
of the # of geographic points that have snakes
mod <- list()
for(i in 1:length(sd_ecometric_pc6)){
  if(!(is.na(mbc6[i]) | is.na(sdbc6[i]))){
    dat <- round(NApoints$BIO1[UID$ID][which(mbc4==mbc4[i] & sdbc4==sdbc4[i] &
mbc6==mbc6[i] & sdbc6 ==sdbc6[i])]) #add additional PCs
    if(sum(!is.na(dat)) > 0) {
      mod[[i]] <- density(dat[!is.na(dat)], bw = 1)
      modmax[i] <- mod[[i]]$x[which.max(mod[[i]]$y)]
    }}}
for(i in 1:length(sd_ecometric_pc4)){
  if(!(is.na(mbc4[i]) | is.na(sdbc4[i]))){
    dat <- round(NApoints$BIO1[UID$ID][which(mbc4==mbc4[i] & sdbc4==sdbc4[i] &
mbc6==mbc6[i] & sdbc6 ==sdbc6[i])]) #add additional PCs
    if(sum(!is.na(dat)) > 0) {
      mod[[i]] <- density(dat[!is.na(dat)], bw = 1)
      modmax[i] <- mod[[i]]$x[which.max(mod[[i]]$y)]
    }}}
modmax<-round(modmax)
cutoff<-1
#calculate maximum likelihood for all bins; cutoff >3 species for snakes

h <- hist(NApoints$BIO1[UID$ID], main = "", xlab = "Mean Annual Temperature", col
= "gray", breaks = 10)

#plot maximum likelihood temperature from ecometric
tmp <- (modmax - min(modmax, na.rm = T)) * 100
colfunc<-colorRampPalette(c("blue","white", "red"))(max(tmp, na.rm = T))[tmp]
plot(snakegeo_sp_proj_mod, pch = 16, cex = 0.01)
```

```
plot(na_proj, add = T, col = "lightgray")
points(UID[,1:2], col = colfunc, pch = 16, cex = 1.0)
plot(na_proj, add = T)
box()
title("Ecometric Temperature PC4 & PC6")
legend("bottomright", legend = h$breaks, pch = 16, col = colorRampPalette(c("blue",
"white", "red"))(length(h$breaks)), cex = .75)

#plot actual temperature for comparison
tmp <- (bioclim$BIO1[UID$ID] - min(bioclim$BIO1[UID$ID], na.rm = T))
colfunc<-colorRampPalette(c("blue", "green", "yellow","orange", "red"))(max(tmp,
na.rm = T))[tmp]
plot(snakegeo_sp_proj_mod, pch = 16, cex = 0.01)
plot(na_proj, add = T, col = "lightgray")
points(UID[,1:2], col = colfunc, pch = 16, cex = 0.75)
plot(na_proj, add = T)
box()
title("Mean Annual Temperature")
legend("bottomright", legend = h$breaks, pch = 16, col = colorRampPalette(c("blue",
"green", "yellow","orange", "red"))(length(h$breaks)), cex = 0.75)

#plot anomaly to visualize differences
anom <- NApoints$BIO1[UID$ID] - modmax
h_anom <- hist(anom, main = "", xlab = "Anomaly", col = "gray", breaks = abreaks)
tmp <- (anom - min(anom, na.rm = T))

colfunc<-colorRampPalette(brewer.pal(10, "PRGn"))(max(tmp, na.rm = T))[tmp]

plot(snakegeo_sp_proj_mod, pch = 16, cex = 0.01)
plot(na_proj, add = T, col = "lightgray")
points(UID[,1:2], col = colfunc, pch = 16, cex = 1.0)
plot(na_proj, add = T)
box()
title("MAT Anomaly  PC4 & PC6")
legend("bottomright", legend = h_anom$breaks, pch = 16, col =
colorRampPalette(brewer.pal(10, "PRGn"))(length(h_anom$breaks)), cex = .75)

tempcor <- cor(bioclim$BIO1[UID$ID], modmax, use = "pairwise.complete.obs",
method = "pearson")
tempcor^2

#PC5 and PC6
modmax <- array(NA, dim = length(sd_ecometric_pc6)) #this should only be the length
of the # of geographic points that have snakes
```

```
mod <- list()
for(i in 1:length(sd_ecometric_pc6)){
  if(!(is.na(mbc6[i]) | is.na(sdbc6[i]))){
    dat <- round(NApoints$BIO1[UID$ID][which(mbc5==mbc5[i] & sdbc5==sdbc5[i] &
mbc6==mbc6[i] & sdbc6 ==sdbc6[i])]) #add additional PCs
    if(sum(!is.na(dat)) > 0) {
      mod[[i]] <- density(dat[!is.na(dat)], bw = 1)
      modmax[i] <- mod[[i]]$x[which.max(mod[[i]]$y)]
    }}}
for(i in 1:length(sd_ecometric_pc5)){
  if(!(is.na(mbc5[i]) | is.na(sdbc5[i]))){
    dat <- round(NApoints$BIO1[UID$ID][which(mbc5==mbc5[i] & sdbc5==sdbc5[i] &
mbc6==mbc6[i] & sdbc6 ==sdbc6[i])]) #add additional PCs
    if(sum(!is.na(dat)) > 0) {
      mod[[i]] <- density(dat[!is.na(dat)], bw = 1)
      modmax[i] <- mod[[i]]$x[which.max(mod[[i]]$y)]
    }}}
modmax<-round(modmax)
cutoff<-1
#calculate maximum likelihood for all bins; cutoff >3 species for snakes

h <- hist(NApoints$BIO1[UID$ID], main = "", xlab = "Mean Annual Temperature", col
= "gray", breaks = 10)

#plot maximum likelihood temperature from ecometric
tmp <- (modmax - min(modmax, na.rm = T)) * 100
colfunc<-colorRampPalette(c("blue", "white", "red"))(max(tmp, na.rm = T))[tmp]
plot(snakegeo_sp_proj_mod, pch = 16, cex = 0.01)
plot(na_proj, add = T, col = "lightgray")
points(UID[,1:2], col = colfunc, pch = 16, cex = 1.0)
plot(na_proj, add = T)
box()
title("Ecometric Temperature PCs 5&6")
legend("bottomright", legend = h$breaks, pch = 16, col = colorRampPalette(c("blue",
"white", "red"))(length(h$breaks)), cex = .75)

#plot actual temperature for comparison
tmp <- (bioclim$BIO1[UID$ID] - min(bioclim$BIO1[UID$ID], na.rm = T))
colfunc<-colorRampPalette(c("blue", "green", "yellow","orange", "red"))(max(tmp,
na.rm = T))[tmp]
plot(snakegeo_sp_proj_mod, pch = 16, cex = 0.01)
plot(na_proj, add = T, col = "lightgray")
points(UID[,1:2], col = colfunc, pch = 16, cex = 0.75)
```

```
plot(na_proj, add = T)
box()
title("Mean Annual Temperature")
legend("bottomright", legend = h$breaks, pch = 16, col = colorRampPalette(c("blue",
"green", "yellow","orange", "red"))(length(h$breaks)), cex = 0.75)

#plot anomaly to visualize differences
anom <- NApoints$BIO1[UID$ID] - modmax
h_anom <- hist(anom, main = "", xlab = "Anomaly", col = "gray", breaks = abreaks)
tmp <- (anom - min(anom, na.rm = T))

colfunc<-colorRampPalette(brewer.pal(10, "PRGn"))(max(tmp, na.rm = T))[tmp]

plot(snakegeo_sp_proj_mod, pch = 16, cex = 0.01)
plot(na_proj, add = T, col = "lightgray")
points(UID[,1:2], col = colfunc, pch = 16, cex = 1.0)
plot(na_proj, add = T)
box()
title("MAT Anomaly  PC5 & PC6")
legend("bottomright", legend = h_anom$breaks, pch = 16, col =
colorRampPalette(brewer.pal(10, "PRGn"))(length(h_anom$breaks)), cex = .75)

tempcor <- cor(bioclim$BIO1[UID$ID], modmax, use = "pairwise.complete.obs",
method = "pearson")
tempcor^2
```